



**US Army Corps
of Engineers**
Waterways Experiment
Station

Technical Report EL-95-34
December 1995

Effect of Soil Composition on Complex Dielectric Properties

by John O. Curtis, Charles A. Weiss, Jr., Joel B. Everett

DTIC QUALITY INSPECTED 5

Approved For Public Release; Distribution Is Unlimited

19960229 089

Prepared for U.S. Army Corps of Engineers Research
and Development Directorate

DTIC QUALITY INSPECTED 5

The contents of this report are not to be used for advertising, publication, or promotional purposes. Citation of trade names does not constitute an official endorsement or approval of the use of such commercial products.



PRINTED ON RECYCLED PAPER

Effect of Soil Composition on Complex Dielectric Properties

by John O. Curtis, Charles A. Weiss, Jr., Joel B. Everett

U.S. Army Corps of Engineers
Waterways Experiment Station
3909 Halls Ferry Road
Vicksburg, MS 39180-6199

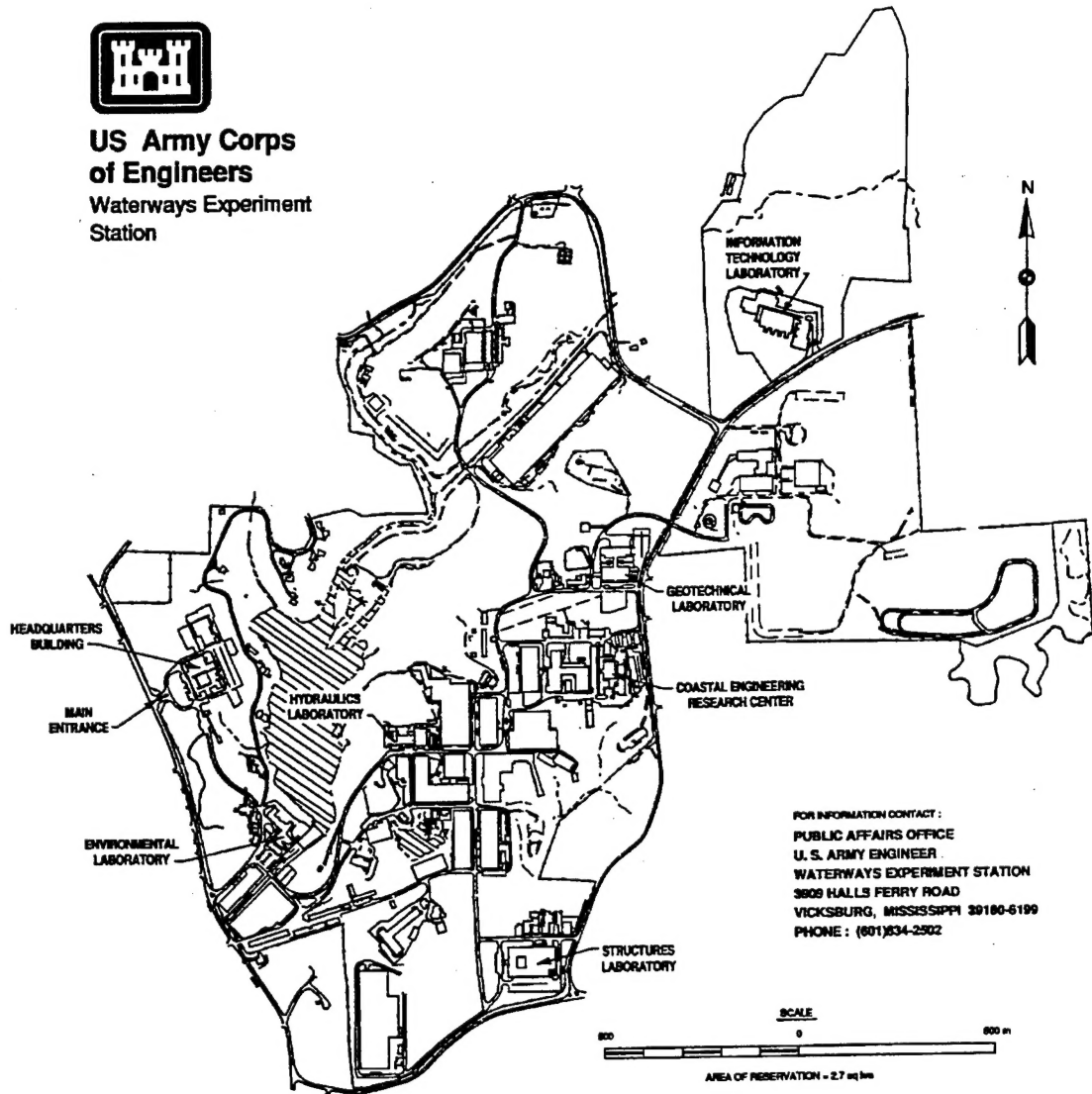
Final report

Approved for public release; distribution is unlimited

Prepared for U.S. Army Corps of Engineers Research
and Development Directorate
Washington, DC 20314-1000



**US Army Corps
of Engineers**
Waterways Experiment
Station



Waterways Experiment Station Cataloging-in-Publication Data

Curtis, John O.

Effect of soil composition on complex dielectric properties / by John O. Curtis, Charles A. Weiss, Jr., Joel B. Everett ; prepared for U.S. Army Corps of Engineers Research and Development Directorate.

283 p. : ill. ; 28 cm. -- (Technical report ; EL-95-34)

Includes bibliographic references.

1. Dielectric measurements. 2. Soils -- Composition. 3. Soils -- Testing. I. Weiss, Charles A. II. Everett, Joel B. III. United States. Army. Corps of Engineers. IV. U.S. Army Engineer Waterways Experiment Station. V. Environmental Laboratory (U.S. Army Engineer Waterways Experiment Station) VI. United States. Army. Corps of Engineers. Research and Development Directorate. VII. Title. VIII. Series: Technical report (U.S. Army Engineer Waterways Experiment Station) ; EL-95-34.

TA7 W34 no.EL-95-34

Contents

Preface	vi
1—Introduction	1
Motivation for Study	1
Supporting Studies	2
Fundamental Relationships	3
Microwave Loss Mechanisms	6
Ionic conductivity	6
Free water relaxation	6
Bound water relaxation	8
Maxwell-Wagner effect	8
Study Objectives	8
2—Experimental Technique for Measuring Complex Dielectric Constants	9
Governing Equation	10
Calibration Procedure	11
Data Collection Procedure	12
Procedure Validation	15
3—Characterization of Soils	19
Physical Properties	19
Soil Chemistry	21
Laboratory procedures	21
Phase composition and shape parameters	23
Bulk chemical composition	28
Chemistry and electrical conductivity	30
4—Analyses of Representative Data	31
Dispersive Behavior	31
Sand	41
Silt	42
Clay	43
A hypothetical sensor design	43
Moisture Effects	44
5—Summary of Observations and Conclusions	54

References	56
Appendix A: Data Collection and Data Presentation Software	A1
Appendix B: Electrical Properties of Soils Plotted Against Frequency ...	B1
Appendix C: Electrical Properties of Soils Plotted Against Volumetric Moisture Content	C1
SF 298	

List of Figures

Figure 1. Dielectric loss mechanisms for heterogeneous moist materials	7
Figure 2. Dielectric property measurement apparatus block diagram	9
Figure 3. Brass square cross-section coaxial sample holders	10
Figure 4. Filling a sample holder with soil/water mixture	13
Figure 5. Sample holder placed in sink/source with cables attached ...	14
Figure 6. Complex dielectric constant for air, 100-mm holder	15
Figure 7. Complex dielectric constant for pure water, 20 °C, 100-mm holder	16
Figure 8. Complex dielectric constant for pure water, 20 °C, 15-mm holder	17
Figure 9. Soil gradation curves	20
Figure 10. Electrical properties of a sand	32
Figure 11. Electrical properties of a silt	35
Figure 12. Electrical properties of a clay	38
Figure 13. Electrical properties of all soils at 78 MHz	45
Figure 14. A bilinear fit to permittivity data collected at 78 MHz, 20 °C	48
Figure 15. Least square polynomial fits to permittivity data collected at 78 MHz, 20 °C	49
Figure 16. Permittivity mixing model applied to a sand, 78 MHz, 20 °C	52
Figure 17. Permittivity mixing model applied to a silt, 78 MHz, 20 °C	53
Figure 18. Permittivity mixing model applied to a clay, 78 MHz, 20 °C	53

List of Tables

Table 1.	Physical Characteristics of Soil Samples	19
Table 2.	Measured Concentrations of Mineral Phases With Associated Precision Using Quantitative X-ray Diffraction Data . .	23
Table 3.	Results of Chemical Analyses for Individual Particles for Selected Samples Using Standardless EDX Analysis on SEM	24
Table 4.	Mineral Phases Assemblages Given in Table 2 Adjusted to 100 Percent	26
Table 5.	Average Sphericity and Roundness for Samples Examined in This Study	27
Table 6.	Results of Chemical Analyses for Bulk Samples A Through L	28
Table 7.	Stoichiometries Used to Calculate Chemical Compositions Based on Adjusted Phase Assemblages From Table 4	29
Table 8.	Calculated Chemical Compositions of Samples A Through L Based on Normalized Quantitative X-ray Diffraction Data and Stoichiometries for Mineral Phases as Indicated in Table 7	29

Preface

The report herein represents one in a series of reports that document the results of a basic research project entitled "In-Situ Obstacle Discrimination" (project number 61102/AT22), which has been funded by the U.S. Army Corps of Engineers Research and Development Directorate in Washington, DC. The primary goal of this study is to gain a fundamental understanding of the mechanisms associated with the propagation of electromagnetic energy through soils and how those phenomena affect the detectability of objects buried beneath the surface.

Dr. John O. Curtis, Environmental Engineering Division (EED), Environmental Laboratory (EL), U.S. Army Engineer Waterways Experiment Station (WES), had overall responsibility for the conduct of this effort and was the primary author for this report. He also developed the experimental procedure used in this study and conducted the dielectric data analyses. Dr. Charles Weiss, Concrete Technology Division, Structures Laboratory, WES, was responsible for the petrographic analyses of the 12 soils and made use of numerous laboratory and analytical tools to determine the chemical compositions of the soils. Mr. Joel Everett, EED, conducted all of the dielectric property measurements and created the initial database of raw results. Soil samples were obtained from the Soil Test Facility, Geotechnical Laboratory, WES, where many of the physical characteristics were also identified. Soil specific surface measurements were conducted by the Quantachrome Corporation in Syosset, NY.

This study was under the direct supervision of Dr. Raymond L. Montgomery, Chief, EED, and Dr. John Harrison, Director, EL.

At the time of publication of this report, Director of WES was Dr. Robert W. Whalin. Commander was COL Bruce K. Howard, EN.

This report should be cited as follows:

Curtis, J. O., Weiss, C. A., Jr., and Everett, J. B. (1995).
"Effect of soil composition on complex dielectric properties,"
U.S. Army Engineer Waterways Experiment Station, Vicksburg,
MS.

*The contents of this report are not to be used for advertising, publication,
or promotional purposes. Citation of trade names does not constitute an
official endorsement or approval of the use of such commercial products.*

1 Introduction

Motivation for Study

The need to characterize conditions and to locate anomalies beneath the terrain surface is driven by numerous scenarios that originate in both the military and private sectors. Soldiers in the battlefield need to locate and neutralize buried land mines. They often need to know the location and extent of tunnel systems used by the enemy. Military training sites require frequent searches for unexploded ordnance (UXO) to ensure the safety of the troops. Military bases that are scheduled for return to private use must be cleared of UXO. Chemical contaminant burial or dump sites at both military and non-military sites throughout the world must be located and cleaned up. The extent of subsurface contamination at burial or dump sites, or even storage sites, where the containers have leaked must be known before that site can be remediated. Civilian construction activities can be made safer if onsite personnel have an accurate picture of subsurface conditions including utility lines, cavities, and the depth to the water table.

One of the most effective ways of safely probing beneath the terrain surface to detect anomalies is through the use of active electromagnetic systems such as ground-penetrating radars that typically operate in 100-MHz to 1-GHz frequency range (although numerous applications exist outside of this range). Of vital importance, then, is the need to understand how the electromagnetic waves will be attenuated through the subsurface material and how fast they will travel. The former factor determines, when coupled with the sensitivity of the receiver and the electrical properties of material, the depth at which an anomaly can be detected. The latter factor is particularly important for accurately determining the depth to the anomaly and for synthetic aperture processing of data, where keeping track of the phase of the waves is of paramount importance.

Being able to predict the performance of active electromagnetic systems as tools for probing subsurface soil conditions requires knowledge of the complex propagation constants of the soils (to be discussed in the following section) and how they are affected by moisture, temperature, dry density, chemical composition of the soils, specific surface, grain-size distributions, etc. The electrical properties of the soil-water-air-organics mixture define

both the phase velocity and attenuation information that is required. If one can develop an adequate database of electrical properties for a broad range of soil types, moisture conditions, temperatures, etc., researchers and designers can make informed decisions regarding how to optimize a system for a particular problem. One of the objectives of this project is to develop such a database. Hopefully, these data will complement other published results. While spotty data exist at high frequencies, there have been thorough studies conducted below the range of these measurements (Campbell 1990).

Supporting Studies

The volumetric moisture content has clearly been shown to be one of the dominant factors in controlling the electrical properties of soils over a broad range of frequencies (Curtis 1993a,b,c). Within certain frequency ranges, other important elements affecting the electrical conductivity of soils include the mineralogic composition, the type of clay minerals present, and possibly other factors such as sample dry density.

An excellent set of soil electromagnetic property measurements were conducted at the United States Army Electronics Command at Fort Monmouth, New Jersey, during the late 1960s and early 1970s (Hulse, Walker, and Pearce 1969; Walker, Pearce, and Hulse 1969; Walker 1970; Hulse, Walker, and Pearce 1972; and Hulse and Walker 1972). These measurements covered the frequency range of 50 to 500 MHz and were motivated by the search for ways to effectively detect enemy tunnels in the Vietnam theater.

One of the conclusions of these studies was that soils containing high concentrations of smectite group minerals were observed to have higher conductivities than those not containing smectite (or expandable clays), primarily because smectite group minerals have abundant structural water. These researchers even attempted to develop an empirical relationship that associates electrical behavior to geochemical composition. For example, in the southern Atlantic and southeastern areas of the United States, the conductivity of the soils (σ) at frequencies less than 100 MHz was related to the ratio of montmorillonite, a smectite group mineral, to kaolinite (m/k) and the clastic, fraction by weight (c) by the following empirical relationship (Hulse, Walker, and Pearce 1972):

$$\sigma = 1 + 8.4 (m/k)^{2.3} - 0.1 c,$$

Clastic fraction was not defined by the authors but is assumed to represent the weight fraction of the soil containing mineral and rock fragments. The units of conductivity are mmhos/meter. No allowance was made in the above relationship for moisture content. The researchers did comment, however, that they expected each clay mineral or soil system to have its own unique conductivity dependence on moisture content. Obviously, determination of the

hydrous phases, especially hydrated clays, is going to be important to the understanding of the electrical properties of soils.

Another excellent source of both electrical and magnetic properties of soils is the United States Geological Survey in Denver, CO. Since the late 1970s, numerous measurements made there and by colleagues at the nearby Colorado School of Mines in Golden, CO, have been conducted as part of an overall effort to use geophysical methods for subsurface characterization. Some of this work represents summaries of measurement programs that support larger field tests (Olhoeft and Capron 1993). Other studies reported in the literature focus on the physics of electromagnetic propagation through soils and the chemistry of soil/water/organic/air mixtures that produce losses in the propagating signals (Olhoeft 1985, 1987; Olhoeft and King 1991; Olhoeft and Capron 1994). The results of these studies will be compared with the results of the current effort in a later chapter.

Another source of information on the electromagnetic properties of soils comes from research conducted at the University of California at Davis since the late 1960s. Experiments and modeling conducted by this organization vary from electrical analogues used in an empirical fashion to duplicate low-frequency measurement results (Smith 1971) to sophisticated analytical models used to help predict geophysical properties of soils based on electromagnetic measurements (Smith and Arulanandan 1981; Arulanandan 1991, 1994).

The final source of supporting data and models (although certainly not meaning to say that this list is all inclusive) is the microwave measurement program led by Professor Fawwaz Ulaby, first at the University of Kansas during the early 1980s, and then at the University of Michigan. Although a great deal of the work conducted by this group focuses on radar terrain reflectances, some very significant dielectric data for moist soils were collected using both coaxial devices and free-space measurement systems (Hallikainen et al. 1985). An attempt was also made by this group to develop models for predicting dielectric properties that were both theoretical and semiempirical (Dobson et al. 1985).

Fundamental Relationships

The relationships that follow will be useful in interpreting the experimental results as will be discussed in a later chapter. Supporting references include Jackson (1975), Stratton (1941), and Bohren and Huffman (1983).

For these derivations, plane harmonic wave propagation is assumed in a lossy, nonmagnetic, unbounded medium. Therefore, one may assume that the amplitude function may be written:

$$e^{i(kx - \omega t)}$$

where

i = symbol designating an imaginary quantity $= \sqrt{-1}$

$$k = \beta + i\alpha = \omega N/c \quad (1)$$

= complex propagation constant

β = phase constant

α = amplitude attenuation factor

ω = radial frequency

N = complex index of refraction

c = velocity of light in a vacuum

x = a space coordinate

t = time

Furthermore,

$$N^2 = \epsilon = \epsilon' + i\epsilon'' \quad (2)$$

where, as stated earlier, ϵ is the relative complex dielectric constant, which, along with the electrical conductivity from Ohm's Law, represents the electrical properties of the medium. The interpretation of these properties as used in this study is that the conductivity, σ , accounts for current due to free charged particle motion, while the imaginary part of the complex dielectric constant, ϵ'' , accounts for displacement current losses (those due to the electric polarization of the medium). When both conduction and displacement currents are considered, one finds two terms in Ampere's law for current flow that represent losses (or a shift in phase), one containing the electrical conductivity and one containing the imaginary part of the dielectric constant. While these two terms account for different loss mechanisms, most researchers use only one term or the other to identify losses, with many users preferring to deal with the concept of electrical conductivity. In MKS units, the relationship between the two quantities is taken to be

$$\sigma + \epsilon'' \epsilon_0 \omega \quad (3)$$

where the units of conductivity are mhos/meter (or siemens/meter) and ϵ_0 is the permittivity of free space (8.85×10^{-12} farads/meter). However, in the development of the fundamental relationships used to interpret laboratory data,

it was found more convenient to account for the dispersive properties of the medium completely by the complex dielectric constant (implicit in Equation 2). When electrical conductivity is desired, Equation 3 will be utilized.

Combining the square of Equation 1 with Equation 2 and equating real and imaginary components result in two algebraic equations that relate the amplitude attenuation factor and phase constant to the complex dielectric constant:

$$\beta^2 - \alpha^2 = \frac{\omega^2}{c^2} \epsilon'$$

and

$$\alpha\beta = \frac{\omega^2 \epsilon''}{2c^2}$$

Solving these equations for the amplitude attenuation factor and for the phase constant results in the following expressions:

$$\alpha = \frac{\omega}{c} \left[\frac{\epsilon'}{2} \left[\sqrt{1 + \left[\frac{\epsilon''}{\epsilon'} \right]^2} - 1 \right] \right]^{1/2} \quad (4)$$

and

$$\beta = \frac{\omega}{c} \left[\frac{\epsilon'}{2} \left[\sqrt{1 + \left[\frac{\epsilon''}{\epsilon'} \right]^2} + 1 \right] \right]^{1/2} \quad (5)$$

The ϵ''/ϵ' ratio is also referred to as the loss tangent. Some researchers prefer to work with the electrical conductivity (Equation 3) in place of the dielectric loss term.

Plane waves of constant phase (but not necessarily energy or signal) will propagate with a velocity

$$v = \frac{\omega}{\beta} = c \left[\frac{\epsilon'}{2} \left[\sqrt{1 + \left[\frac{\epsilon''}{\epsilon'} \right]^2} + 1 \right] \right]^{-1/2} \quad (6)$$

The power intensity of the plane electromagnetic wave decreases exponentially with depth of penetration by the factor, $e^{-2\alpha x}$, or, in one unit of distance traveled, a decrease of $e^{-2\alpha}$. Power attenuation expressed in decibels per meter can then be written as:

$$PL = -8.6859 \frac{\omega}{c} \left[\frac{\epsilon'}{2} \left[\sqrt{1 + \left[\frac{\epsilon''}{\epsilon'} \right]^2} - 1 \right] \right]^{1/2} \quad (7)$$

Microwave Loss Mechanisms

Before examining the data collected in this study, reviewing several of the mechanisms that can contribute to the loss in energy of propagating electromagnetic waves would be helpful. The best single source of information on this topic is found in a textbook by J. B. Hasted (Hasted 1973). In particular, one of his figures, reproduced here in Figure 1, attempts to qualitatively identify the relative magnitudes and approximate spectral range for several loss mechanisms. The following paragraphs briefly describe those mechanisms that apply to moist soils and that cover the range of frequencies of this study and may prove to be helpful in interpreting much of the data.

Ionic conductivity

The most dominant loss mechanism in moist heterogeneous materials at low frequencies is that due to ionic conductivity, the $\sigma/(\epsilon_0\omega)$ term in Equation 3. Ionic conductivity results when salts in the soil are dissolved by water and a path is available through the pore spaces for these ions to travel when subjected to an external electric field. Therefore, low-frequency ionic conductivity in moist soils has to be related in some way to the degree of saturation and how the pore spaces fill with water.

Free water relaxation

Individual water molecules can be considered to be electric dipoles. In the presence of an oscillating electric field, the dipoles will try to align themselves with the field. If pure water was placed between the charged surfaces of a parallel-plate capacitor, the effect would be an enhancement of the capacitance

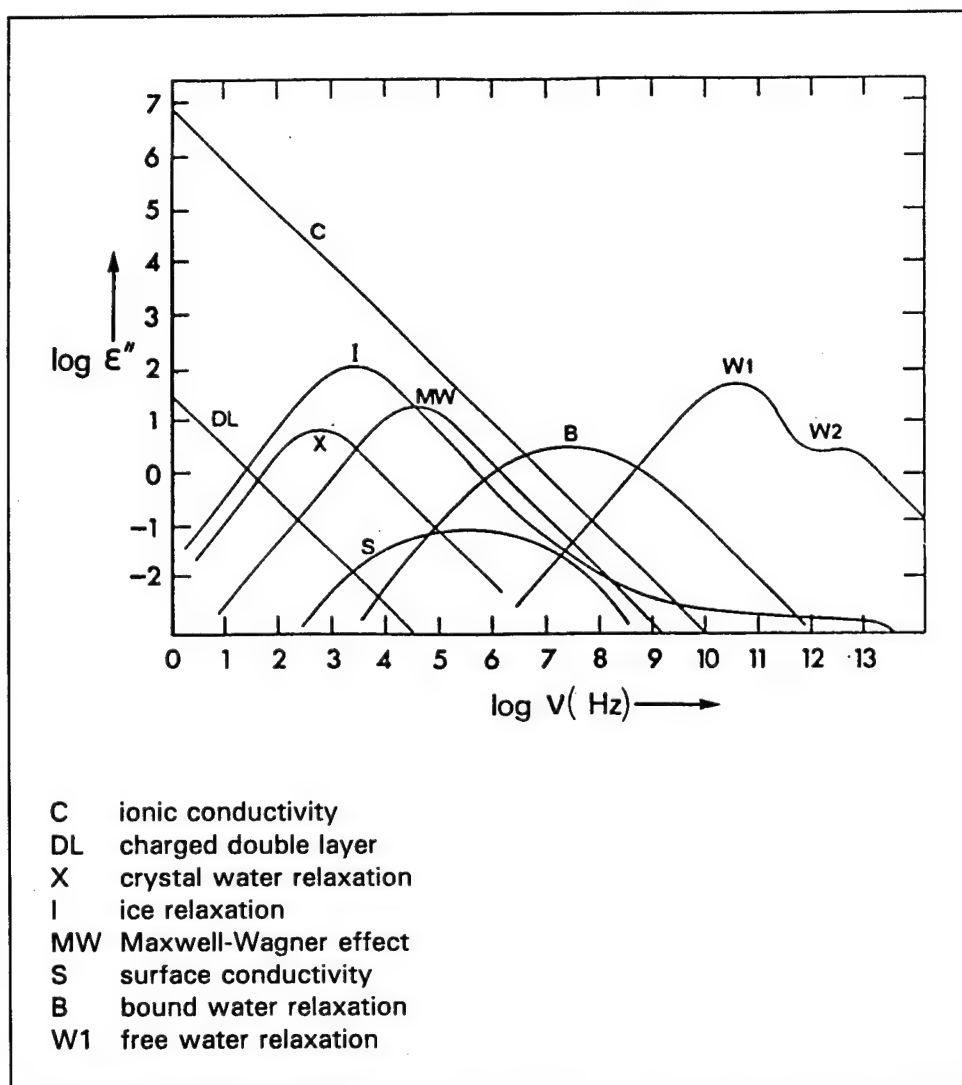


Figure 1. Dielectric loss mechanisms for heterogeneous moist materials (from Hasted 1973)

of the system due to the alignment of these dipoles and the effective reduction of the electric field (voltage difference) between the plates. This capacitive enhancement is measured by the real part of the complex dielectric constant (also referred to as the permittivity of the material). At low frequencies, the permittivity of pure water is about 80 times that of air or a vacuum).

As one increases the frequency of the oscillating field, the dipoles are forced to rotate more and more quickly. At some frequency, the dipoles will start to lag behind the forcing field due to rotational inertia and viscosity. At this point, the permittivity of the substance starts to decrease, and the imaginary part of the dielectric constant starts to increase to reflect the increasing lag between the electric field and the orientation of the water dipole. As the frequency of the field further increases, the dipoles get to the point where they do not respond to the field at all, resulting in minimum values for both the

real and imaginary parts of the complex dielectric constant. This behavior is referred to as anomalous dispersion ("dispersion" being the change in properties with frequency). It is also referred to as a relaxation phenomenon with regard to the measure of the dipole's ability to return to its equilibrium position, or "relax," after the removal of an electric field.

Bound water relaxation

Experimental evidence exists (Muir 1954; Hoekstra and Delaney 1974) that indicates a lowering of the frequency at which maximum relaxation losses occur in water that is bound to solid particle surfaces. Physically this makes sense if one thinks of the water to solid attraction as a kind of added viscosity. Hall and Rose (1978) proposed bound water relaxation as the dominant loss mechanism in carefully prepared kaolinite clays in the 10- to 100-kHz range of the spectrum; however, their conclusions seem to contradict the observations of other researchers.

Maxwell-Wagner effect

Another loss mechanism often referred to in the literature as a dominant mechanism at radio frequencies is one termed the Maxwell-Wagner effect (Campbell 1988; Bidadi, Schroeder, and Pinnavaia 1988). It originates in the experimental observation that there is dispersion in a suspension of conducting particles in nonconducting dielectric media much like that observed in a parallel-plate capacitor filled with two different dielectrics. The Maxwell-Wagner effect is seen as an accumulation of charge at the interface of dissimilar materials during the flow of current through heterogeneous material due to a discontinuity in dielectric constant values. This charge buildup is time-dependent and results in dispersion as the frequency of the alternating current increases to a point where the buildup and relaxation cannot keep up.

Study Objectives

The objectives of this study are to describe a laboratory procedure for measuring the complex dielectric constant of a material (in this case, moist soils) and to report the results of those measurements on a large number of samples in various forms including conductivity, loss tangent, normalized phase velocity, and power loss using the relationships presented above. As will be seen in a later chapter, these parameters are a strong function of signal frequency, moisture content, and, in some instances, soil composition. Sample temperature (above the freezing point for the water in the soil) will be found to be a much weaker contributor to the dielectric response of moist soils. The results of the present study will try to delineate those soils in which the greatest attenuation of electromagnetic power, based on their mineralogy and chemical composition, will occur.

2 Experimental Technique for Measuring Complex Dielectric Constants

The apparatus used to collect complex dielectric constant data is a modification of an earlier system developed at the U.S. Army Engineer Waterways Experiment Station (WES) (Curtis 1993b) and is shown in block diagram form in Figure 2. The system is built around a Hewlett Packard 8510C Vector Network Analyzer, which controls a synthesized source and an S-parameter test set. Specialized flexible cables connect the test set to unique coaxial sample holders that were developed at WES. The holders (shown in Figure 3) were machined from brass stock and have a cross section of 7.5 by 7.5 mm. Sample holders were manufactured with both 15- and 100-mm-length cavities to ensure that valid data could be collected at the extremes of the frequency sweep. Connection to the test set cables is made through SMA connectors on the ends of the sample holders and a pair of 3.5-mm adapters. The complete apparatus and the methodology under which it was operated are somewhat similar to those reported in another recent study of the electrical properties of soils (Wensink 1993).

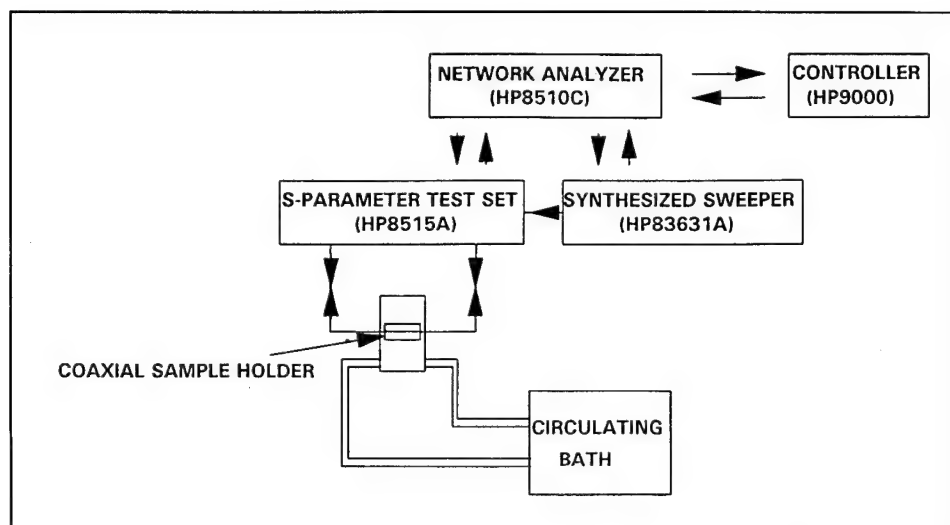


Figure 2. Dielectric property measurement apparatus block diagram

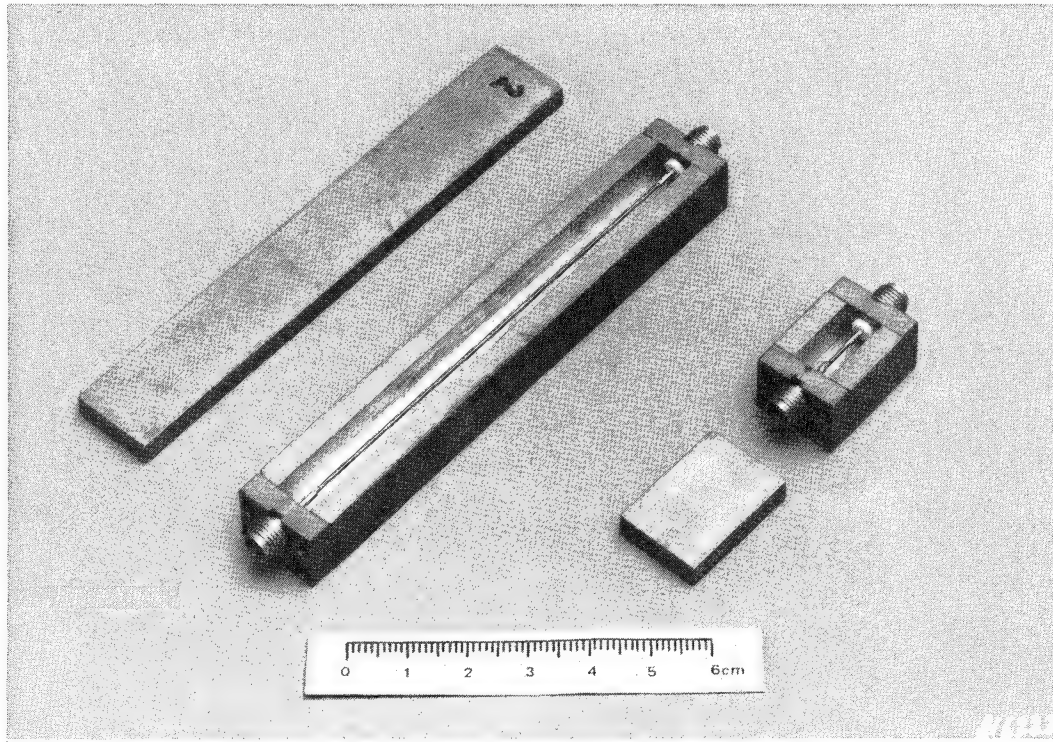


Figure 3. Brass square cross-section coaxial sample holders

Control of the network analyzer measurement system, creation of raw data files, and plotting of complex dielectric constants are accomplished by an HP-9000-362 instrument controller. A copy of the WES-developed code, written in HP BASIC, can be found in Appendix A. Further processing and display of data took place on an off-line PC using the SAS software system (SAS Institute, Inc. 1988).

Governing Equation

The synthesized source has the capability of generating signals that span a 45-MHz to 26.5-GHz range. Complex reflection and transmission coefficients (S_{11} and S_{21} , respectively) are measured by the test set. Assuming plane wave behavior within nonmagnetic samples, one can show that the relative complex dielectric constant (ϵ) can be calculated from the following governing equation (Curtis 1993b):

$$\cos \left[\omega d \frac{\sqrt{\epsilon}}{c} \right] = \frac{1 + (S_{21})^2 - (S_{11})^2}{2S_{21}} \quad (8)$$

where d is the length of the sample.

The right-hand side of this equation is a vector in complex space that rotates about the origin as frequency changes. As it crosses the real axis, both on the positive side and on the negative side, it passes through or near branch cuts for the inverse cosine function (Abramowitz and Stegun 1972), leading to instabilities in the calculation of the argument on the left. As will be seen later, plots of the real part of the complex dielectric constant against frequency take on the characteristics of anomalous dispersion (Jackson 1975) at these points where the complex vector approaches the real axis.

A physical description of what is happening within the test sample at these points of instability may best be demonstrated when one attempts to measure the response of the empty sample holder; i.e., a measurement of the complex dielectric constant of air. The relative constant for air has a real part equal to unity and an imaginary part equal to zero. One can then rewrite the argument of the cosine function in the governing equation as a function of wavelength and sample cavity length by setting the dielectric constant to unity and substituting the definition of frequency in terms of wave velocity and wavelength

$$\frac{\omega d \sqrt{\epsilon}}{c} = \pi \left[\frac{d}{\lambda/2} \right]$$

At the same time, experimental results show that the complex vector from the right-hand side of Equation 8 rotates through the real axis on both sides with a value of nearly unity. Now the inverse cosine function evaluated at unity is $2k\pi$, and the function evaluated at negative unity is $(\pi + 2k\pi)$. In other words, every integer multiple of π is accounted for. Then the argument of the cosine function can be set equal to an integer multiple, n , of π , leading to the conclusion that as the complex vector crosses the real axis,

$$d = n(\lambda/2)$$

Therefore, the instability in the calculation of complex dielectric properties takes place whenever the sample contains an integer multiple of half wavelengths.

Calibration Procedure

Prior to collecting data on moist soil samples, a full 2-port calibration was performed using an HP85052B, 3.5-mm Calibration Kit. Under normal conditions, each calibration would hold for several hours before instrumentation drift would force the system out of acceptable limits. The limits were defined by the amplitude and phase measurements made when the two S-parameter test cables were directly connected. A calibration was considered to be valid when the amplitude did not vary more than 0.1 db over the entire range of frequencies, and when the phase did not vary more than 1 deg over the frequency range.

As described elsewhere (Curtis 1993b), one other correction had to be made to the data, even after a successful calibration, before correct values of the dielectric constant could be computed. Because of the requirements for adapters between the sample holder SMA connectors and the S-parameter test set cables and because of the existence of the SMA connectors, themselves, an electrical delay had to be added to each parameter (S_{11} and S_{21}) to account for the additional electrical path length between the calibration planes at the ends of the cables and the surface of the sample. For these measurements, the necessary electrical delay for each parameter was found to be 270 picoseconds.

Data Collection Procedure

All of the soils used in this study were organic-matter free and had been processed for ease of handling (oven-dried, pulverized, and screened to remove large grains). Sample preparation began by mixing sufficient deionized, distilled water and soil in a plastic bag to provide a mixture that was nearly saturated. The bag was sealed and left several days to ensure adequate time for adsorption of the water to soil particle surfaces. While it might be useful to establish a target gravimetric moisture content (weight of water/weight of dry solid), sample preparation procedure would not ensure that the same gravimetric moisture could be achieved in the sample holder. Furthermore, volumetric moisture (volume of water/volume of sample), which is the most meaningful measure of moisture for interpreting the dielectric properties of mixtures, can not be controlled at all by this experimental procedure.

Once the soil/water mixtures had been properly cured, the mixture was "spooned" into both the 15-mm and the 100-mm sample holders (Figure 4). Removal of most, if not all, air pockets was accomplished by tamping the mixture with the sharp end of the sample preparation tool and by gently striking the sample holder against a flat surface. A sharp knife edge was used to flatten the sample surface and clear the upper edge of the sample holder of particles. The covers were placed on the sample holders, and a careful measurement of the combined holder and sample mass was made (the empty sample holder mass was known). While it was not possible to ensure that both the 15-mm and the 100-mm samples possessed the same volumetric moisture, approximately the same mechanical effort was made to prepare each sample. Actual differences in sample dry density (weight of dry solid/volume of sample) and their effect on dielectric properties will be discussed in a later chapter.

As soon as the soil/water mixture was placed in the two holders and weighed, the holders were placed into the heat sink/source (Figure 5), which had been brought to a specified temperature, usually 10 °C. The cables from the S-parameter test set were then attached, and the cover of the sink/source was tightened. A Caron Model 2065 Refrigerated and Heated Circulating

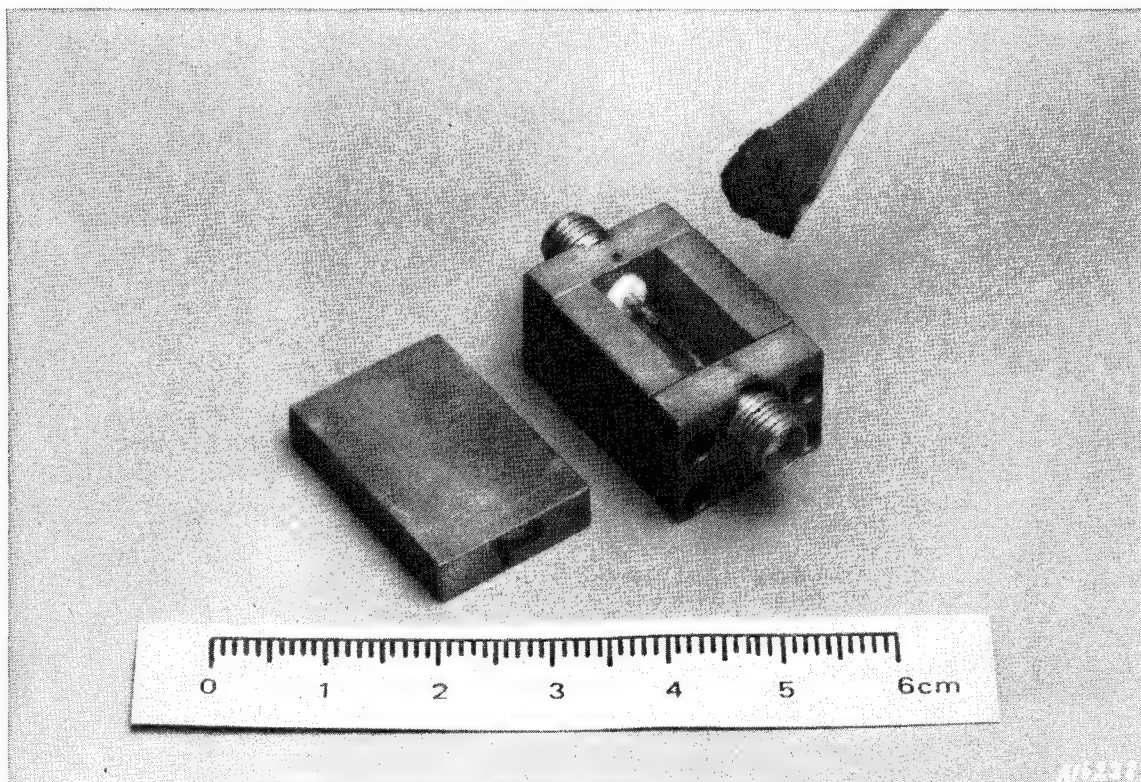


Figure 4. Filling a sample holder with soil/water mixture

Bath was used to circulate an antifreeze solution through the sink/source. Once any required temperature was achieved in the Caron bath, the sample was allowed to reach thermal equilibrium by waiting at least 10 min before a measurement was made.

Collection of complex reflection and transmission data and subsequent calculation of complex dielectric constants at each desired temperature (10, 20, 30, and 40 °C) were achieved by interactively executing the code contained in Appendix A. The entire frequency range of 45 MHz to 26.5 GHz was divided into 800 steps. At each frequency step, the S_{11} and S_{21} data collected represent an average of 64 readings. Following a frequency sweep for whichever sample holder (either the 15-mm or the 100-mm holder) was connected to the S-parameter test set, the cables were disconnected and moved to the other holder and another sweep of frequencies was executed. After measurements were made at one temperature setting, a new sample temperature was selected on the Caron circulating bath control panel, and another set of measurements was made after thermal equilibrium was allowed to be achieved. As long as the sample had reached thermal equilibrium, the stepped-frequency measurements made in this study were highly repeatable. A separate data file was created for each sample holder and at each temperature. A complete set of measurements on a pair of samples at all four temperatures took 3 to 4 hr.

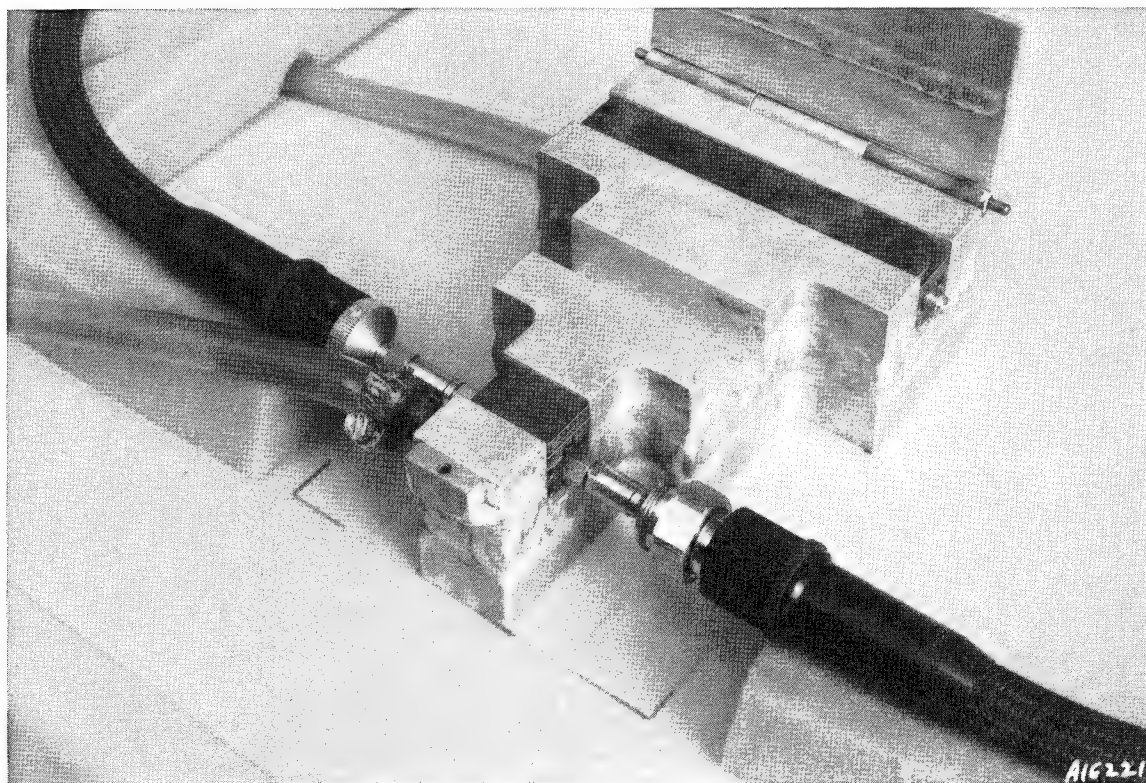


Figure 5. Sample holder placed in sink/source with cables attached

If only one moisture content condition was desired, the sample holders were removed from the sink/source as soon as the last temperature measurements had been completed and were weighed again to determine how much, if any, moisture has been lost during the measurement procedure. Then the samples were scraped and flushed from the holders into separate containers whose empty weight was known, the samples were dried in an oven for 24 hr, and the dry solid weight of each sample was determined. This allows for an after-the-fact determination of sample volumetric moisture, gravimetric moisture, and dry sample density, the relationship among these parameters being:

$$\text{volumetric moisture} = \text{gravimetric moisture} * \text{dry soil density}$$

For soils that did not have a high clay mineral content, it was often possible to collect data at different moisture contents by partially drying each sample after a complete set of temperature measurements. This was accomplished by either exposing the sample to the air for a period of several hours or by heating the sample holder with a hair dryer to evaporate some of the moisture. Assuming that one has the same volumetric moisture content in each pair of sample holders during the first set of measurements, and knowing the volume of each sample holder, one can attempt to achieve similar moisture contents in the two holders by monitoring the weight of each sample holder during the drying process. This technique for controlling moisture contents without disturbing the samples was not very successful. With hindsight, it is probably

better to make up different moisture content samples than to try to control the drying process. Furthermore, there is no assurance that the samples possessed a uniform distribution of moisture after being partially dried, and the impact of nonuniform moisture distribution on measurement results is very difficult to predict (a model might consist of both series and parallel capacitances whose weighting factors are a function of how the sample dries).

Procedure Validation

As an example of the results generated by this experimental procedure, consider the measurement results shown in Figure 6. These data are for an empty 100-mm sample holder, thus representing a measurement of the complex dielectric constant for air. Note that the experimental results are very close to the theoretical results of a real part equal to unity and an imaginary part equal to zero. Note also the frequencies at which the calculation

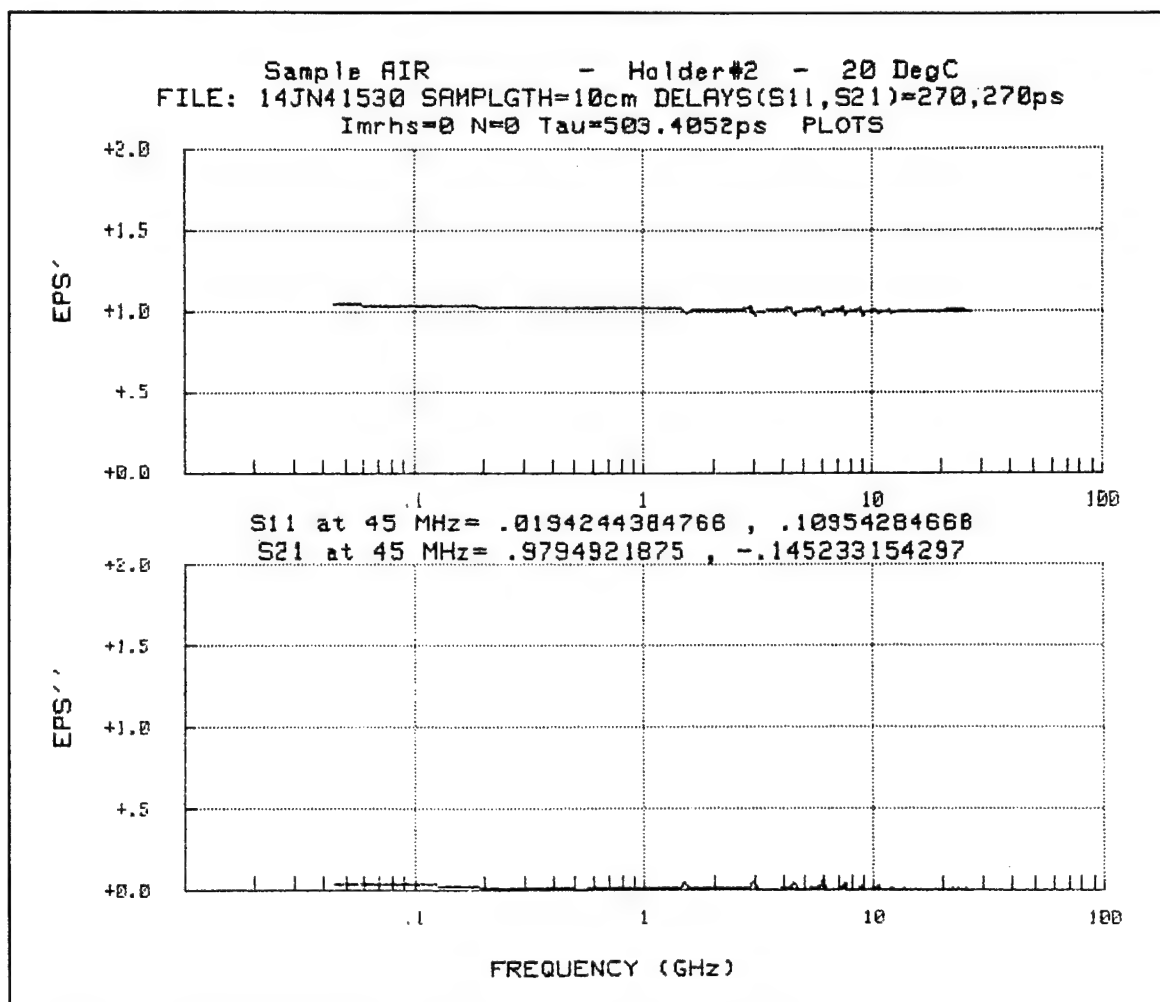


Figure 6. Complex dielectric constant for air, 100-mm holder

instability shows up as anomalous dispersions. Calculations verify that these unstable points occur at frequencies where an integer number of half wave-lengths exist in the sample holder.

Similar results are shown in Figures 7 and 8 for measurements on distilled, deionized water at 20 °C, Figure 7 being for a sample length of 100 mm and Figure 8 being for a sample length of 15 mm. Low-frequency results for the long sample holder match published data on fresh water (Ray 1972) quite well up to a frequency value of around 3 GHz. Short sample holder results represent a pretty good match to the expected behavior of water at 20 °C at the highest frequencies.

These data demonstrate several points that need to be made. The first is that the shorter sample holder is required to obtain data at the highest frequencies for very moist samples due to the attenuation of the signal through the longer sample length. However, the limit of system sensitivity (about -90 db)

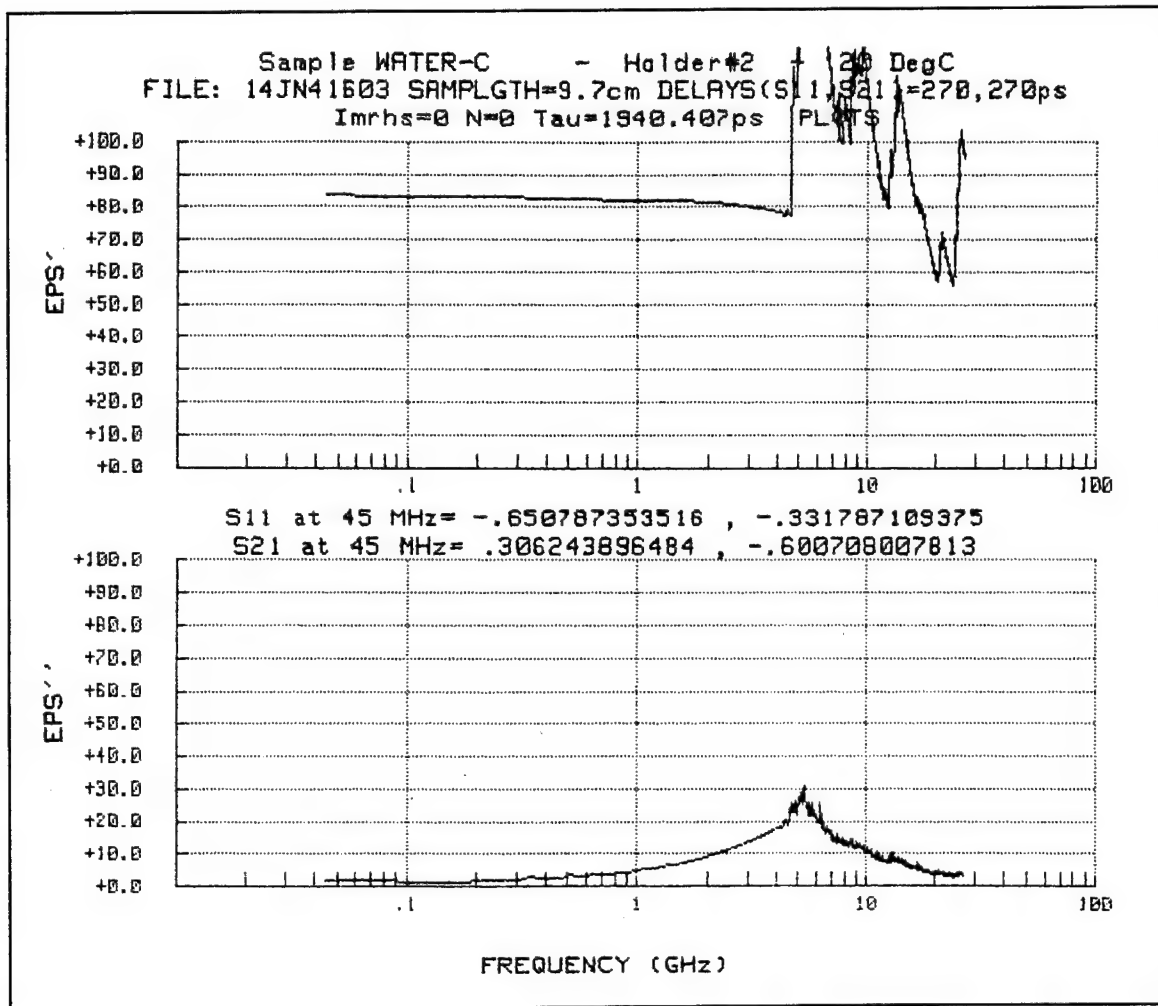


Figure 7. Complex dielectric constant for pure water, 20 °C, 100-mm holder

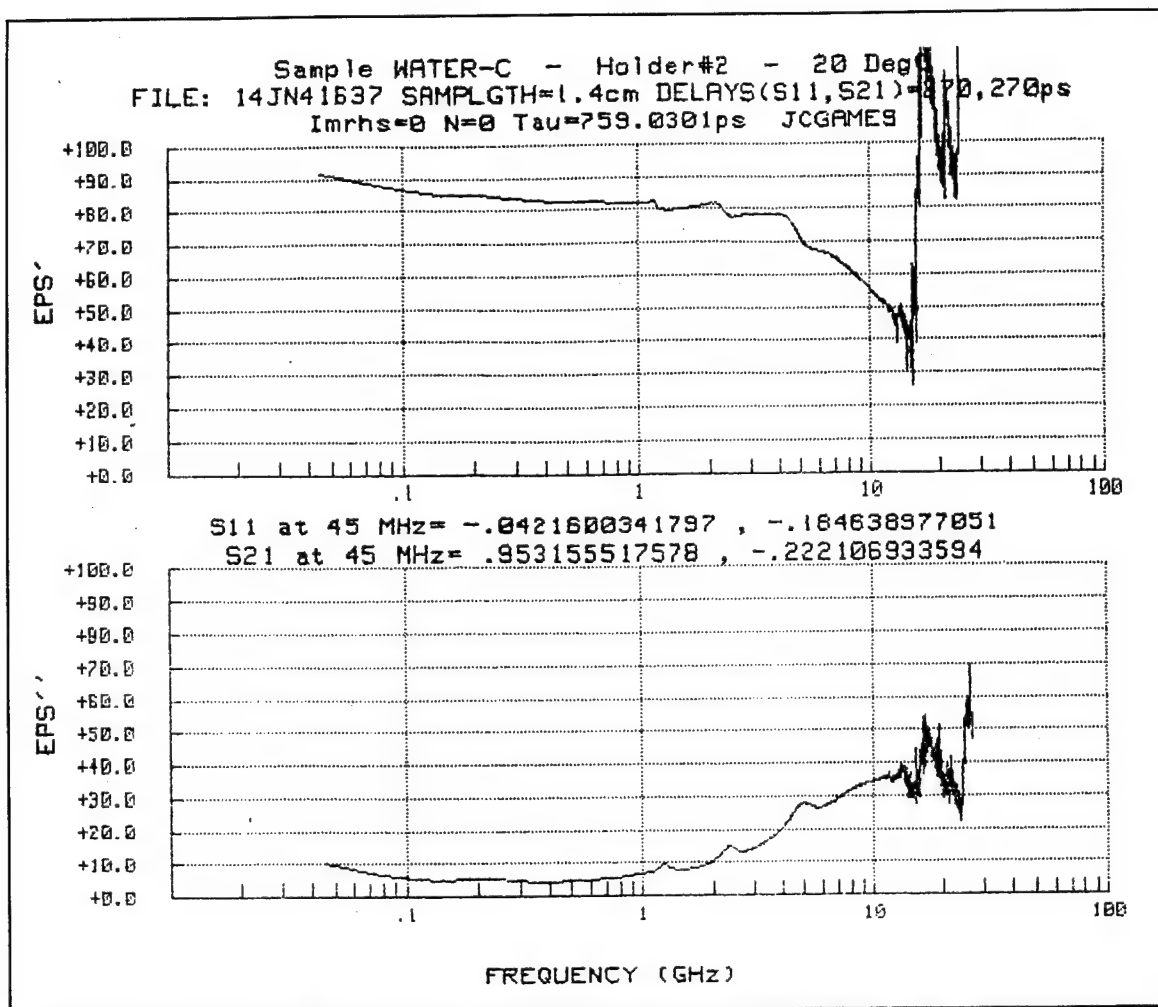


Figure 8. Complex dielectric constant for pure water, 20 °C, 15-mm holder

for the transmission parameter, S_{21} , is reached even for a 15-mm-length sample of water.

A second conclusion that can be drawn from these data is that, given comparable sample dry densities and volumetric moistures, the short sample holder gives results that deviate from the long holder measurements at low frequencies. This can be due to at least two possible factors. One is that the system may be incapable of accurately measuring phase shifts for lossy materials in the short holders; however, this can not be because measurements of the empty holder are quite accurate. The other is that during the calculation of dielectric constants, one encounters from Equation 7 a constant factor of the speed of light divided by the product of the sample length and test frequency. This constant must be squared. At the low end of the frequency sweep with the shorter sample holder, this factor squared has a value of 6,177.2; whereas, for the longer sample holder, the squared factor has a value of 119.7, over 50 times smaller. It is entirely possible that the calculations of

the complex dielectric constant are made more sensitive at low frequencies by the large constant factor associated with the short sample holder.

Regardless of why the 15-mm sample holders have difficulty reproducing known results at low frequencies, the fact remains that they do. As a result of this observation and the fact that moist sample attenuation will very likely be too high to obtain useful data at high frequencies from the 100-mm holder, all of the complex dielectric data reported in a later chapter were screened in the following way. All data reported at frequencies below 3 GHz were collected from the 100-mm holder; most data above 3 GHz came from the 15-mm holder because of the unpredictable attenuation of the signal at these frequencies in the long samples; the only exceptions were for measurements made on so-called "dry" soils using the 100-mm holder. While an effort was made to produce moist soil samples of comparable volumetric moisture in both holder sizes, the truth is that there will be different volumetric moistures associated with high- and low-frequency data. It is also possible that dry soil density for each sample will be different, and it may be possible to examine the impact of that variable.

The text on Figures 7 and 8 indicates sample lengths of 97 mm and 14 mm, respectively. These lengths represent a final calibration adjustment through the calculation of the complex dielectric constant that results in the best match to accepted values for water. There is some physical basis for using sample lengths in the calculations that are shorter than the cavity length in that the SMA connectors have dielectric sleeves around the center conductor that extend a short distance into the sample cavity. An analytical effort to model the true sample holder geometry and to predict an effective sample length is beyond the scope of this project.

3 Characterization of Soils

Physical Properties

Table 1 is a summary of the physical properties of 12 different soils chosen for this study. These soils, provided by the Soil Test Facility of the Geotechnical Laboratory at WES, were selected to span the gamut of grain-size distributions that might occur in nature and include such extremes as poorly graded clean sand to "fat" clays. Among the entries found in Table 1 are three columns referred to as "Percent Sand," "Percent Silt," and "Percent Clay." These numbers were arrived at by inspection of Figure 9, which contains all of the gradation curves for these 12 soils. Sand was taken to be the percent (by weight) of whatever material did not pass the number 200 sieve. Clay content represents the percent of material whose particles exhibited an equivalent size of less than $2\ \mu\text{m}$ (Mitchell 1993). The last column of Table 1 is a record of sample specific surfaces, measured by Quantachrome Corporation in Syosset, NY, using nitrogen gas sorption techniques (krypton gas was used for soil "I" because of its extremely low specific surface).

Table 1
Physical Characteristics of Soil Samples

Sample	Description (Unified Soil Classification System)	(by weight)			Liquid Limit	Plastic Limit	Specific Gravity	Specific Surface m^2/g
		Percent Sand	Percent Silt	Percent Clay				
A	Clay (CH), Light Gray	2	22	76	289	39	2.34	25.97
B	Sand (SP), Light Gray	98	2	0	--	--	2.62	0.66
C	Silty Sand (SM), Brown	88	8	4	--	--	2.64	3.64
D	Silty Sand, (SM), Reddish Brown	77	9	14	--	--	2.66	15.01
E	Clayey Silt (ML), Brown	TR	93	7	32	24	2.59	13.89
F	Clay (CH), Gray	1	48	51	68	21	2.73	33.34
G	Clayey Sand (SC), Dark Brown	55	32	13	38	17	2.66	33.18
H	Clay (CH), Gray	2	64	34	61	20	2.74	40.49
I	Sand (SP), White	100	0	0	--	--	2.67	0.03
J	Silt (ML), White	0	46	54	47	30	2.61	9.29
K	Clayey Silt (ML), Brown; Trace of Sand	4	89	7	27	22	2.71	12.5
L	Sand (SP), Brown	99	1	0	--	--	2.66	0.31

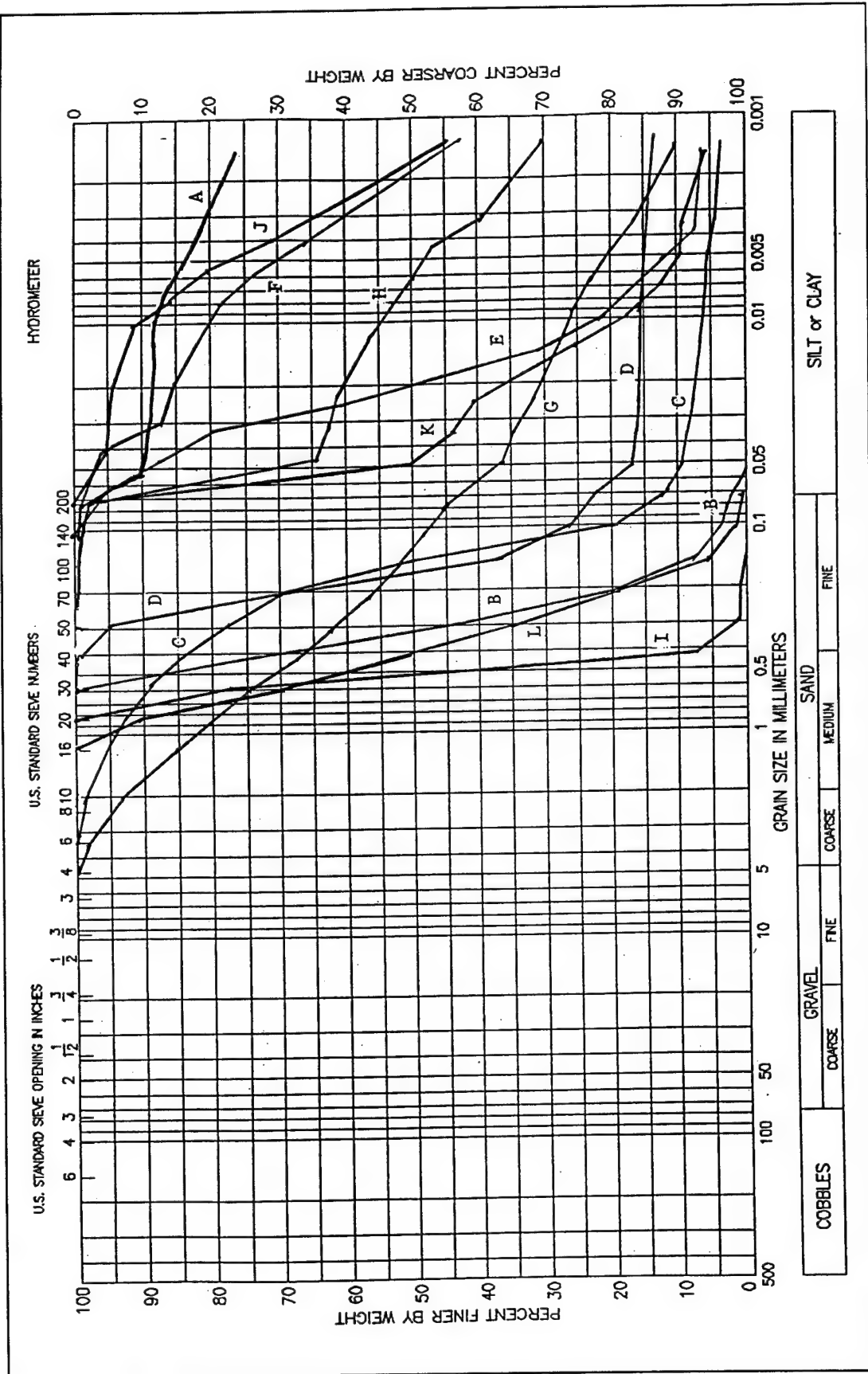


Figure 9. Soil gradation curves

Soil Chemistry

As stated in the Introduction, soil chemistry has to be one of the primary factors in determining the electrical behavior of the soil/water/air mixtures found in nature. The following paragraphs outline a number of soil chemistry investigations conducted within the Petrography and Chemistry Group of the Structures Laboratory at WES. The objective of these studies was to identify sample mineralogy, chemical composition, and particle shape characteristics that might influence the electrical response of moistened soils.

Laboratory procedures

Qualitative X-ray diffraction (XRD) was used to determine the mineralogy of each sample and also to estimate the quantity of each mineral present. The equipment used in this analysis was a Philips APD1700 Version 4.0 Automated Powder Diffractometer system driven by a Digital Equipment Corporation (DEC) VAX 3100 computer. In preparation for X-ray diffraction of the bulk samples as random powder mounts (a sample with random crystal orientations), a portion of each sample was ground in a mortar and pestle to pass through a 45- μm (No. 325) mesh sieve. To determine if clays were present, a slurry of the powder with water was made, suspended on a substrate, and dried overnight; X-ray diffraction patterns were collected on these oriented samples. To determine if the clays were expandable, X-ray diffraction patterns were collected after exposure to an ethylene glycol atmosphere overnight at room temperature.

Random powder mounts were prepared for quantitative X-ray diffraction (QXRD) analyses. Five standards were made using the phases found in the samples and an internal standard (CeO_2). The procedure used to quantify bulk powders using internal standards is given in many sources (Klug and Alexander 1974; Bertin 1975). The standards were used to obtain calibration coefficients for the intensity of a reference peak for each mineral as a function of the proportion of that mineral. These coefficients were used to calculate mineral concentrations. Each sample was analyzed twice, and the results were averaged.

Scanning electron microscopy coupled with energy-dispersive X-ray (EDX) chemical analysis also was used in this study to identify any additional phases present in a form or amount not detectable by X-ray diffraction analysis. This was accomplished by examining the morphology and determining the chemical composition for individual particles. The equipment used was a Hitachi S2500 scanning electron microscope (SEM) with an EDX windowless detector linked to a SUN SPARCstation IPC running the IMIX analysis software (Princeton Gamma-Tech, Princeton, NJ).

Visual examination of each sample was done to verify the QXRD results. In this examination, a portion of each soil was placed on a glass slide, immersed in oil (refractive index, $n = 1.544$), covered with a cover slip, and

examined using a Nikon petrographic microscope. Verification of the QXRD results was done on Samples B, C, D, G, and K. This procedure consisted of scanning the slide sample under the petrographic microscope along parallel tracks and visually identifying the type of mineral grains within the field of view until a total of 200 grains had been identified and tabulated. Samples A, E, F, and H could not be point-counted because the particle grains were agglomerations of various minerals. Samples I and J was virtually monomineralic, and these samples also were not counted.

Computer-based image analysis was used to characterize the size and shape parameters of each soil. In this analysis, a portion of each sample is photographed, digitized, and analyzed for sphericity and roundness. Particles that were touching the edge of the image or touching another particle were not analyzed. Organic debris such as seen in sample C also were ignored. The equipment used in this analysis included a Kodak Eikonix scanner connected to a DEC VAXstation II/GPX computer. The data were collected and analyzed using the Icometrics version 3.0 software package (Everest Technologies 1991).

Differential scanning calorimetric measurements were made to ascertain the presence of hydrous phases. The equipment used was a Perkin-Elmer DSC7 differential scanning calorimeter (DSC). The DSC measures the amount of energy absorbed or evolved by the sample. In these analyses, 10 mg of each sample was placed in an aluminum pan, covered with an aluminum lid, and heated from 20 to 200 °C at a rate of 10 °C/min.

The presence of the acid-soluble carbonate minerals calcite and dolomite was determined by dissolution in HCl. In this procedure, 5.0 g of sample was put into 100 mL of a 10-percent solution of HCl (by volume) and then stirred continuously at room temperature for at least 1 hr. The sample was then filtered, dried, and weighed. The result reported for this procedure is the percent weight loss subsequent to treatment. The resultant sample was examined using XRD to verify that the carbonate phases had been removed.

Bulk chemical composition of each sample was determined using an energy-dispersive X-ray analyzer. The samples were prepared by making a pellet using a portion of the <45- μ m fraction and a methylcellulose binder. The equipment used was a Fisons-Kevex 771 EDX chemical analyzer for bulk samples running the XRF Toolbox II version 4.4 software on a Visions 486 computer. These analyses were made using the EXACT analysis procedure (Fisons-Kevex 1990) and a plastic clay standard (Source Reference Material from NIST, SRM 98b). In this procedure, the standard is analyzed and the intensity obtained for each element is calibrated to the known chemical composition. Subsequent analysis of each sample is given relative to the intensities for the standard.

Phase composition and shape parameters

The results of qualitative X-ray diffraction were used to select standards for quantitative mineralogic determinations. All phases were incorporated in the QXRD analysis with the exception of cristobalite, which was present in sample A. Due to the lack of a suitable standard of cristobalite the quantity of this mineral was estimated at 15 percent of the total based on the peak height of the bulk pattern. Results of QXRD are given in Table 2. Several factors could contribute to the totals deviating from 100 percent. These factors could include the presence of additional phases or poorly crystalline phases not identified by XRD, differences in extent or perfection of crystallinity between minerals in the samples and in the standards, differences in total chemical composition between samples and standards, and associated error in the technique.

Table 2
Measured Concentrations of Mineral Phases With Associated Precision Using Quantitative X-ray Diffraction Data

Sample	A ¹		B		C		D		E		F	
	Conc. %	Prec. abs	Conc. %	Prec. abs	Conc. %	Prec. abs	Conc. %	Prec. abs	Conc. %	Prec. abs	Conc. %	Prec. abs
Quartz	3.1	1.9	100.7	19.3	92.3	17.6	56.7	11.2	49.9	9.8	27.7	5.8
Smectite	25.6	2.2							14.7	1.4	4.1	1.3
Calcite	0.2	0.1					0.2	0.0				
K-Feldspar	1.5	0.4	33.2	8.4	1.2	0.3	4.3	1.1	5.1	1.3	0.3	0.1
Na-Plagioclase	0.9	0.1	9.0	0.5					3.1	0.2		
Mica			0.1	0.0					0.2	0.0	0.1	0.0
Kaolinite					1.2	0.3	3.0	0.4	1.7	0.3	4.6	0.4
Dolomite									2.2	0.1		
Total	31.3		143.0		94.7		64.2		76.9		36.8	

Sample	G		H		I		J		K		L	
	Conc. %	Prec. abs	Conc. %	Prec. abs	Conc. %	Prec. abs	Conc. %	Prec. abs	Conc. %	Prec. abs	Conc. %	Prec. abs
Quartz	28.0	5.8	32.9	6.8	113.9	21.3	1.0	0.9	40.8	8.1	135.1	25.3
Smectite	3.1	1.0	22.1	1.8								
Calcite	0.2	0.0							2.1	0.1		
K-Feldspar	5.1	1.3	1.4	0.4					2.5	0.7	1.3	0.4
Na-Plagioclase	3.0	0.2	2.6	0.1					2.2	0.1		
Mica			0.1	0.0					0.2	0.0		
Kaolinite	0.5	0.2	1.3	0.3			95.2	3.8	1.3	0.3		
Dolomite					0.1	0.0			12.8	0.3		
Total	39.9		60.4		114.0		96.2		61.9		136.4	

¹ Cristobalite also was present in this sample, but was omitted from the quantitative analysis because a suitable standard could not be obtained.

The large error associated with the quartz measurement could explain some of these discrepancies, but even assuming that all of the error is associated with this measurement, the totals either are too high or too low. Also, it is unlikely that an error in the calibration constant calculated from the standards would manifest itself in overestimation of quartz in some samples, while underestimating it in the others.

Because the method used for QXRD is based on the individual peaks of XRD patterns of minerals, variation in crystallinity and resulting peak heights will be manifested in the quantitative results. For example, if a given mineral sample is more perfectly crystalline than the standard, then an equal amount of that mineral in the sample will be overestimated in the analysis. This may explain the overestimation of quartz in some of the samples.

Differences in total chemical composition between the minerals in the samples and those of the standards may account for much of the error in the analyses. For example, the smectite standard used was an Fe-poor Ca montmorillonite. If the smectite in the samples either contained more Fe or had some substitution of Na for Ca in the clay interlayer, this would lead to errors in the quantitative analysis. The difficulties associated with quantification of clay minerals are discussed by Zussman (1967).

To verify the presence of Fe and a variable interlayer cation content in the structure of the montmorillonite, EDX standardless analysis of individual particles was undertaken. The results of these analyses are given in Table 3. The chemical analyses for samples A, F, G, and H are typical for those samples and have similar chemical compositions to dioctahedral smectites. The analysis for sample J is representative of a kaolinite. It is given as a contrast to the smectite analyses. From these analyses, it is obvious that the smectites have abundant structural Fe and a variable interlayer cation content. These results support the idea that the smectites were underrepresented in the QXRD analysis because the clays were so different chemically.

Table 3
Results of Chemical Analyses for Individual Particles for Selected
Samples Using Standardless EDX Analysis on SEM

Composition	A	F	G	H	J
SiO ₂	68.3	65.4	59.0	66.8	55.2
Al ₂ O ₃	23.1	27.8	30.8	23.0	43.8
MgO	3.8	0.8	1.1	3.2	0
Na ₂ O	2.8	0	0	0	0
CaO	0	0.12	0.7	0.6	0
K ₂ O	0.2	2.1	1.4	1.4	0.1
Fe ₂ O ₃	1.8	3.5	6.7	4.7	0
TiO ₂	0	0.1	0.4	0.3	0.9

Energy-dispersive chemical analyses of individual smectite particles from samples A, E, F, G, and H indicate that the smectites in these samples have abundant structural Fe and variable amounts of Na, Ca, and K in their structures. Compositional differences seem to explain much of the inconsistencies in the results, as those samples (A, E, F, G, and H) containing smectite have some of the lowest totals in Table 2. Note that the samples that did not contain smectite had totals either close to or greater than 100 percent (Table 2: Samples B, C, I, J, and L). The low totals in Table 2 for Samples D and K, which have little or no smectite, appear to be attributable to other errors, such as differences in perfection of crystallinity. No additional phases were indicated by observations using the SEM.

Results of the quantitative analyses in Table 2 were adjusted to account for the discrepancies discussed previously. These adjusted compositions are given in Table 4. For those samples with smectite present (A, E, F, G, and H), all of the difference from 100 percent was attributed to smectite. For these samples, no other phases were adjusted. For the rest of the samples, the phase compositions were normalized to 100 percent. For samples C and J, which were already close to 100 percent, this had little effect on the amount of each mineral. For samples D and K, which had totals further from 100 percent, this effectively increased the amount of quartz in each sample by 26 to 32 percent, but had smaller effect on the less abundant phases. For samples B, I, and L, which had totals over 100 percent, this diminished the amount of quartz by 14 to 36 percent. This overestimation of quartz in the original quantitative analysis indicates that the quartz standard used probably had a less perfect crystallinity than the quartz in samples B, I, and L.

The visual examination of these samples using the petrographic microscope was done to corroborate the XRD results. Examination of samples I and L indicated that both were virtually all quartz. In agreement with the XRD results, a trace of carbonate was observed in sample I. Sample L had a trace of feldspar. These results confirm that QXRD overestimated the amount of quartz in these samples. Furthermore, the results of point-counting sample B gave 52.5-percent quartz, 45.5-percent feldspar, and 2-percent mica. This result corroborates the amount of feldspar as determined by QXRD and that the amount of quartz is overestimated.

Visual examination of samples A, E, F, G, and H confirmed the presence of clay minerals. The clay particles in these samples were brownish colored. The type of clay mineral could not be identified by this examination. As noted previously, samples A, E, F, and H could not be counted, but one sample containing clay, sample G, was counted. The point-count for sample G was 36-percent quartz, 47-percent clay, 3.5-percent carbonate, 12.5-percent feldspar, and 1-percent mica (percent of one type of mineral grain out of total grains counted). These results compare favorably with the adjusted QXRD results (Table 4). Although all the samples containing clay could not be counted, this one result confirms that the QXRD underestimated the amount of expandable clays. Furthermore, the brownish color of the clays indicates the presence of Fe in the structure.

Table 4
Mineral Phases Assemblages Given in Table 2 Adjusted to
100 Percent¹

Sample	A	B	C	D	E	F	G	H	I	J	K	L
Quartz	3	71	98	89	50	28	28	33	100	1	67	99
Smectite	80	0	0	0	38	67	64	62	0	0	TR	0
Calcite	TR ²	0	0	TR	0	0	TR	0	0	0	3	0
K-Feldspar	1	23	1	6	5	TR	5	1	0	0	3	1
Na-Plagioclase	1	6	0	0	3	0	3	2	0	0	3	0
Mica	0	TR	0	0	TR	TR	0	TR	0	0	TR	0
Kaolinite	0	0	1	5	2	5	TR	1	0	99	2	0
Dolomite	0	0	0	0	2	0	0	0	TR	0	21	0
Cristobalite	15 ³	0	0	0	0	0	0	0	0	0	0	0

¹ Sample total may not sum to 100 percent due to truncation errors.

² TR indicates a trace amount (<1 percent) of this mineral present.

³ This amount is estimated.

Quantitative X-ray diffraction analysis, along with adjustments described in the preceding paragraphs, provided reasonable phase assemblages for samples in this study (Table 4). Using these data, classification of the soil samples can be made that support the classifications made by the Soil Test Facility. Sample A is a smectite bentonite soil; sample B is a quartzofeldspathic soil; samples C, D, and L are quartzose soils; samples E, F, G, and H are soils rich in quartz and smectite; sample I is virtually a pure quartz sand; sample J is a kaolinitic soil, and sample K is a carbonaceous quartzose soil.

Because the presence of hydrous phases is an important factor in the measured electrical conductivity of soil, differential scanning calorimetry was used to verify the presence of these phases. Expandable clays, such as smectites, have water that surround (hydrate) cations within their structure, which is released upon heating at about 100 °C (Mackenzie 1957). This loss of water is manifested as a peak due to the endothermic reaction. The DSC result for sample A clearly shows a peak at 97 °C, which is ascribed to the loss of hydration water. The peak area in this region of the scan is directly related to the amount of adsorbed water in a sample. As previously noted, samples rich in smectite and hydration water are likely to have higher conductivities. Because this sample had the largest peak due to loss of water and contained the most smectite, it probably would have the highest conductivity in a "dry" state. Other samples (E, F, G, and H) also have peaks in this region due to loss of hydration water. These samples also should have higher electrical conductivities than the rest of the samples devoid of hydration water. None of the other samples had any peaks in this region. These results agree with the XRD results that smectite is present in samples A, E, F, G, and H.

Sample J, which was primarily kaolinite, did not disperse properly in the oil and, therefore, was not counted. However, as already discussed, EDX analysis on the SEM indicated that the chemical composition of nearly all the particles is as found in Table 3.

For samples C, D, and K, there was good agreement between the point-count results and the adjusted QXRD results (Table 4). The point-count result for sample C was 90-percent quartz, 9-percent feldspar, 0.5-percent mica, and 1-percent clay. The point-count for sample D was 87-percent quartz, 8-percent clay, 3.5-percent feldspar, 0.5-percent mica, and 1-percent carbonate. Again, the amount of carbonate as determined by dissolution in HCl (0.5 wt. percent) agrees with the point-count and the QXRD results. The point-count for sample K was 54-percent quartz, 30.5-percent carbonate, 12-percent feldspar, 1.5-percent mica, and 2-percent clay. Probably due to errors in counting, the amount of carbonate by point-count was slightly higher than the adjusted QXRD value (24 percent). The amount of carbonate yielded during the dissolution in HCl was 22.7 wt. percent, in agreement with the adjusted QXRD results.

Sphericity and roundness were calculated from data obtained using image analysis of each soil (Table 5). Roundness relates to the angularity of particles. When the curvature or angles of the corners of a solid approach that of the radius of the inscribed circle, it has a roundness approaching 1. Sphericity states quantitatively how nearly equal the three dimensions of a particle are (Folk 1968). Samples J and K were omitted because they were too fine grained. Values for sphericity and roundness for these soils range from 0.4 to 0.8 (Table 5). These parameters were calculated from the data obtained from the image analysis software. The sphericity and roundness values are based on the analysis of particles with defined sphericity and roundness values (Krumbein and Sloss 1963). Although the spread in values for sphericity and roundness is small, small changes in these values have a great effect on the shape characteristics of the particles. Sample I, which is virtually all quartz, has the largest sphericity (0.8) and roundness (0.6) values. Copies of the images used for this analysis are on file and available on request.

Table 5
Average Sphericity and Roundness for Samples Examined in This Study

Sample	A	B	C	D	E	F	G	H	I	J	K	L
Average Sphericity	0.6	0.7	0.6	0.7	0.6	0.6	0.7	0.6	0.8	--	--	0.7
Average Roundness	0.4	0.5	0.4	0.4	0.4	0.4	0.5	0.5	0.6	--	--	0.5

Bulk chemical composition

Bulk chemical analyses for these samples are given in Table 6. Totals for most of the samples are close to 100 percent. The low totals for samples E and K are attributed to the presence of dolomite and/or calcite as a component. The low totals are a consequence of the inability of the energy-dispersive chemical analyzer to detect the presence of carbonate, which is an important component in these samples.

Composition	A	B	C	D	E	F	G	H	I	J	K	L
SiO ₂	74.3	83.6	91.9	85.9	73.8	68.6	75.4	73.9	80.3	57.4	60.2	99.8
Al ₂ O ₃	19.7	11.7	5.5	13.1	11.5	24.7	15.5	18.3	2.6	42.2	9.6	3.5
MgO	1.9	0.3	0.2	0.3	0.9	1.4	0.6	1.5	0.0	0.4	2.2	0.1
Na ₂ O	3.2	3.2	0.5	0.0	1.1	1.3	1.4	1.3	0.3	0.0	1.5	0.2
P ₂ O ₅	0.6	0.6	0.4	0.2	0.3	0.6	0.1	0.7	0.4	0.1	0.6	0.3
CaO	1.3	0.7	0.1	0.1	1.0	0.5	0.6	0.8	0.1	0.1	4.6	0.1
K ₂ O	0.3	1.8	0.1	0.5	1.0	1.2	1.4	1.2	0.0	0.1	0.7	0.2
Fe ₂ O ₃	3.7	0.4	0.8	2.2	3.3	5.0	3.5	4.4	0.1	0.5	2.7	0.2
TiO ₂	0.2	0.2	0.6	0.3	0.7	0.8	0.5	0.7	0.1	1.9	0.6	0.2
MnO	0.0	0.0	0.0	0.0	0.1	0.1	0.0	0.1	0.0	0.0	0.1	0.0
Total	105.0	102.4	99.9	102.6	93.6	104.1	99.0	102.7	84.0	102.6	82.7	104.5

Although sample I also has dolomite as a constituent, there is probably not enough present to account for the disparity observed. This interpretation is corroborated by the low concentrations of CaO and MgO (Table 6) and the loss of merely 0.26 wt. percent carbonate by dissolution in HCl. The X-ray diffraction results indicate that quartz is virtually the only crystalline phase in this sample, and the chemical composition indicates a predominance of SiO₂. There is currently no satisfactory explanation for the low compositional total for sample I.

The hypothesis that the normalized phase assemblages from Table 4 are consistent with the bulk chemical compositions was tested to check the assumptions made during QXRD. To do this, the normalized phase assemblages were used to back-calculate bulk chemical compositions. A chemical composition for each sample was calculated from the amount of each phase given in Table 4 and stoichiometries for the mineral phases indicated in Table 7. The results of these calculations are shown in Table 8. In this exercise, the amount of each phase with a concentration less than 1 percent was assumed to be 0. Comparing data in Tables 6 and 8, the compositions calculated from the adjusted phase assemblages agree reasonably well with the results of the bulk chemical analyses.

Table 7
Stoichiometries Used to Calculate Chemical Compositions Based on Adjusted Phase Assemblages From Table 4

Quartz	SiO ₂
Smectite	Ca _{0.25} Na _{0.17} [(Al _{2.88} Fe ³⁺ _{0.68} Mg _{0.47})(Si _{7.71} Al _{0.29})O ₂₀ (OH) ₄]
Calcite	CaCO ₃
K-Feldspar	KAlSi ₃ O ₈
Na-Plagioclase	Na _{0.8} Ca _{0.1} AlSi ₃ O ₈
Mica	K ₂ Al ₄ (Si ₆ Al ₂)O ₂₀ (OH) ₄
Kaolinite	Al ₄ Si ₄ O ₁₀ (OH) ₈
Dolomite	CaMg(CO ₃) ₂
Cristobalite	SiO ₂

Table 8
Calculated Chemical Compositions of Samples A Through L Based on Normalized Quantitative X-ray Diffraction Data (Table 3) and Stoichiometries for Mineral Phases as Indicated in Table 7

Composition	A	B	C	D	E	F	G	H	I	J	K	L
SiO ₂	68	90	99	95	80	72	73	74	100	47	72	100
Al ₂ O ₃	18	5	1	3	10	16	15	15	0	39	2	0
MgO	2	0	0	0	1	2	2	2	0	0	5	0
Na ₂ O	1	1	0	0	1	0	1	1	0	0	0	0
P ₂ O ₅	0	0	0	0	0	0	0	0	0	0	0	0
CaO	2	0	0	0	1	1	1	1	0	0	8	0
K ₂ O	0	4	0	1	1	0	1	0	0	0	1	0
Fe ₂ O ₃	6	0	0	0	3	5	5	4	0	0	0	0
TiO ₂	0	0	0	0	0	0	0	0	0	0	0	0
MnO	0	0	0	0	0	0	0	0	0	0	0	0
H ₂ O	4	0	0	1	2	4	3	3	0	14	0	0
CO ₂	0	0	0	0	1	0	0	0	0	0	11	0
Total	101	100	100	100	100	100	101	100	100	100	99	100

Measured and calculated compositions of those samples with smectite in them (A, E, F, G, and H) agree closely. The good agreement between the measured and calculated chemical compositions for sample A also probably means that the estimated amount of cristobalite was not excessive. For

samples B, C, D, and K, the predicted amount of SiO_2 in each sample exceeds the amount measured. It is probable that the amount of quartz was overestimated by the normalization technique used. Other normalization schemes, such as keeping the amount of quartz fixed and varying the other phases, are unsuitable because this would elevate the concentrations of the other cations above the amounts actually measured. The technique used is imperfect, but gives a justifiable fit between predicted and measured compositions.

These soil chemistry analyses reveal a serious problem with interpreting the results of previous studies of the electrical behavior of soils. At best, these earlier efforts characterized the physical properties of the soils being studied, perhaps listing percentages of sand, silt, and clay, as was done in Table 1. Using these physical properties would result in materials E and J being classified as silts and giving no indication of the existence and character of any clay minerals that may be present. Table 4, on the other hand, clearly shows that Soil E contains a significant amount of expandable clay minerals, which will strongly affect its electrical behavior. In the same way, Soil J is shown to be pure kaolinite, a nonexpandable clay mineral, a clay mineral, nevertheless, whose surface chemistry is quite different from that of quartz, and whose electrical behavior is likely to be different from quartz.

Chemistry and electrical conductivity

Because the electrical conductivity of soils is strongly controlled by the amount of water and because the amount of water that can be adsorbed by soil particles is greatest for smectite clays, estimates of the electrical conductivities of these soils can be made using the soil chemistry information presented above. Sample A, which has the most adsorbed water and the greatest amount of smectite, should provide some of the highest low-frequency conductivities that will be measured using the apparatus described in the preceding chapter. The other samples (E, F, G, and H) with observable water of hydration and abundant smectite concentration also should provide higher electrical conductivities than the remainder of the samples whose smectite content is low or nonexistent.

4 Analyses of Representative Data

Well over 500 measurements of complex dielectric constant versus frequency were collected for the 12 soils described in the previous chapter. Data were recorded using samples at four different temperatures (10, 20, 30, and 40 °C) and several moisture contents. All of the data appear in the Appendixes B and C, first plotted against frequency and then plotted against moisture content at fixed frequencies. This chapter contains samples of those data that will be examined closely in an attempt to draw general conclusions about the electrical behavior of soils as a function of physical and chemical properties and to begin to explore the possibilities for modeling such behavior. Data presented in this section are for measurements made at a single temperature of 20 °C. An examination of all of the data reveal only a small effect due to changes in sample temperature over this entire temperature range, an observation that has already been reported elsewhere (Curtis 1993c).

Dispersive Behavior

Examples of how electrical properties of these soils change with frequency are shown in Figures 10-12, which contain experimental results for Soil B (a sand), Soil K (a silt), and Soil H (an expandable clay). For each soil, the figures contain plots of the real and imaginary parts of the relative complex dielectric constant, the electrical conductivity of the soil/water/air mixture calculated from Equation 3, the loss tangent (the ratio of the imaginary to the real part of the complex dielectric constant), the phase velocity of the plane wave calculated from Equation 6 and normalized to the speed of light in a vacuum, and, finally, the loss in power of the propagating plane wave expressed in decibels/meter and calculated from Equation 7.

As mentioned earlier, very little soil dispersion data exist from other sources that cover a broad range of frequencies and that are supported with adequate physical property descriptions to allow for proper comparisons. Nevertheless, there appears to be good correlation between the data collected for this study and that reported elsewhere wherever supporting information is

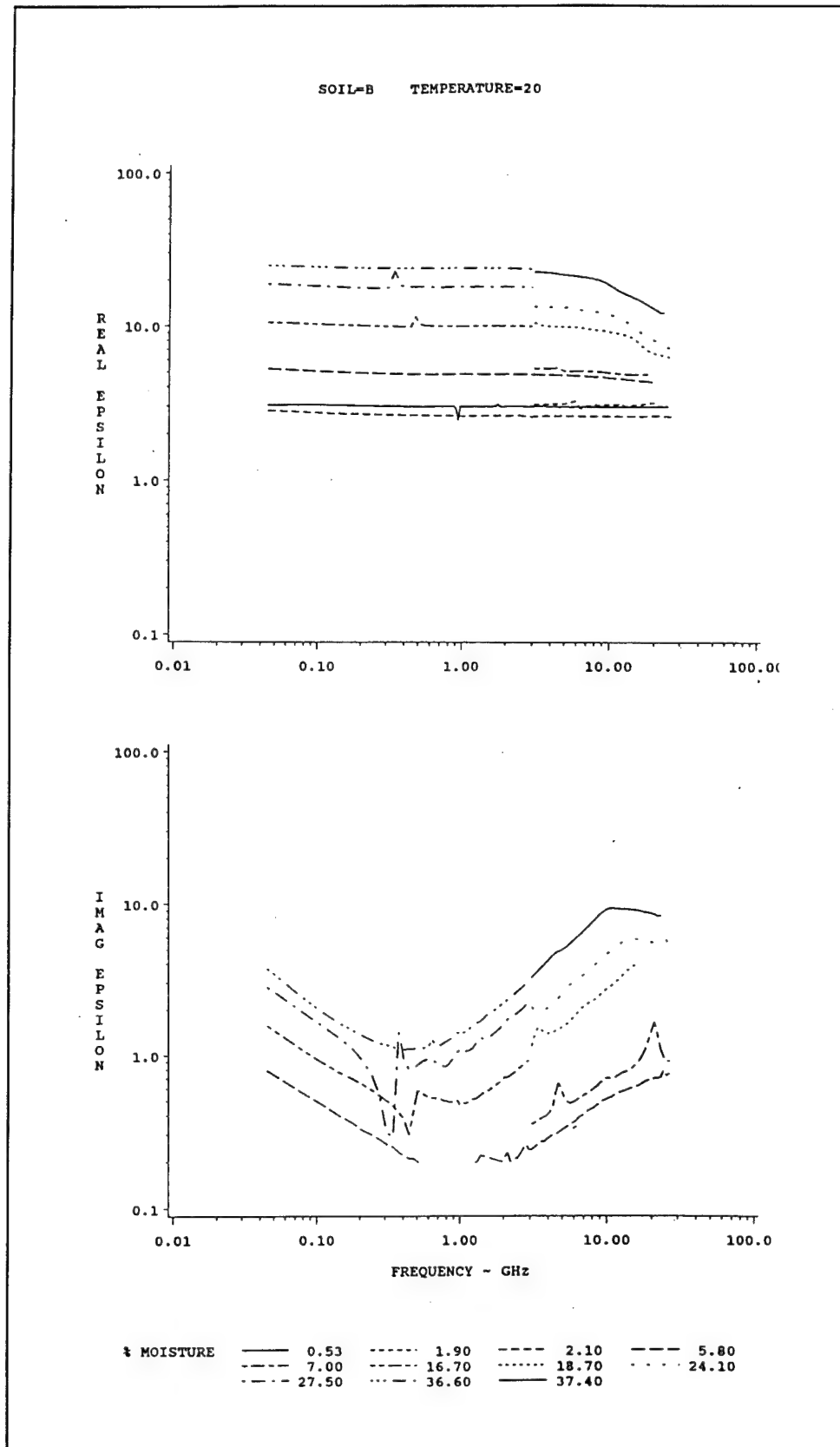


Figure 10. Electrical properties of a sand (Sheet 1 of 3)

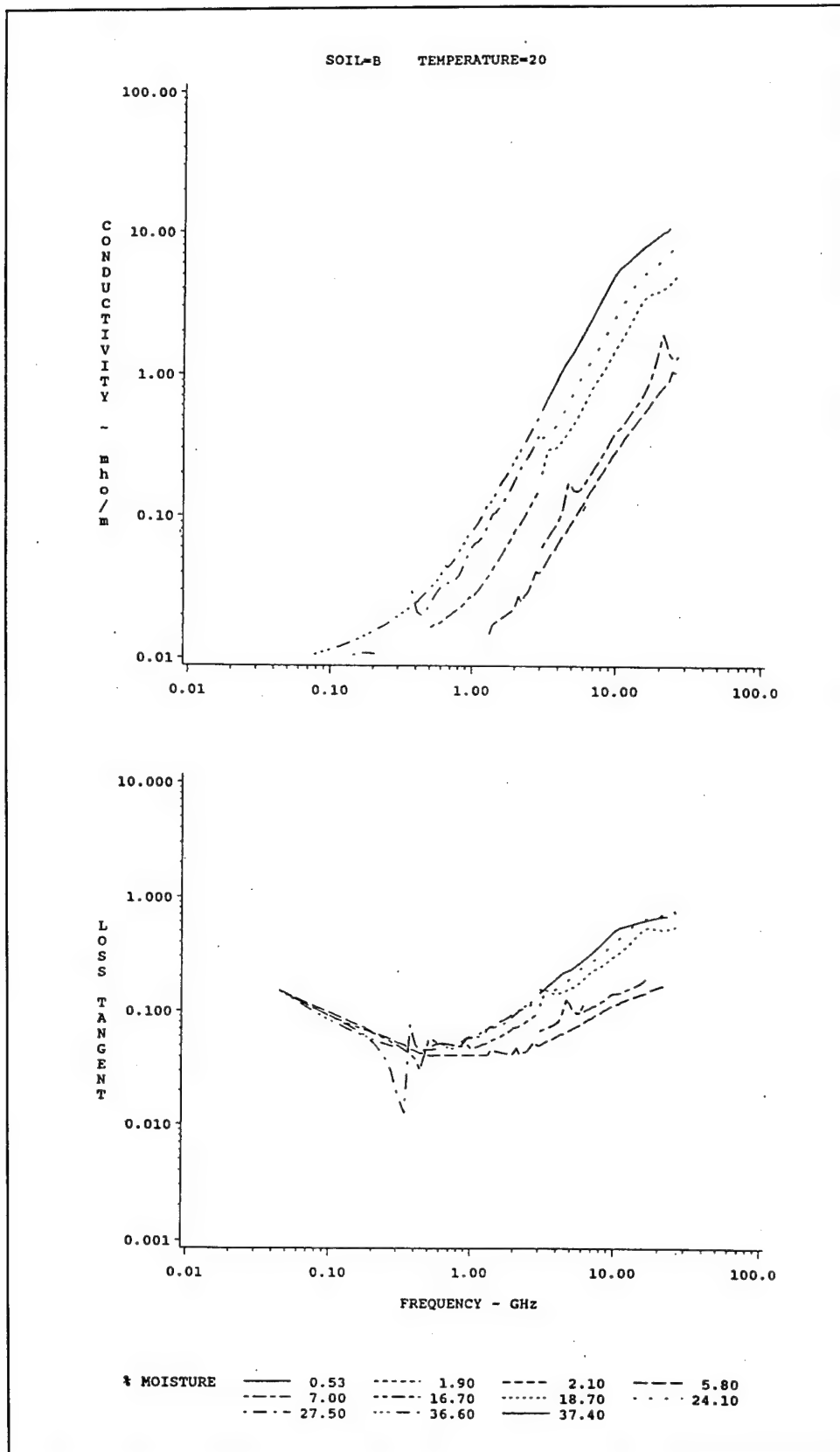


Figure 10. (Sheet 2 of 3)

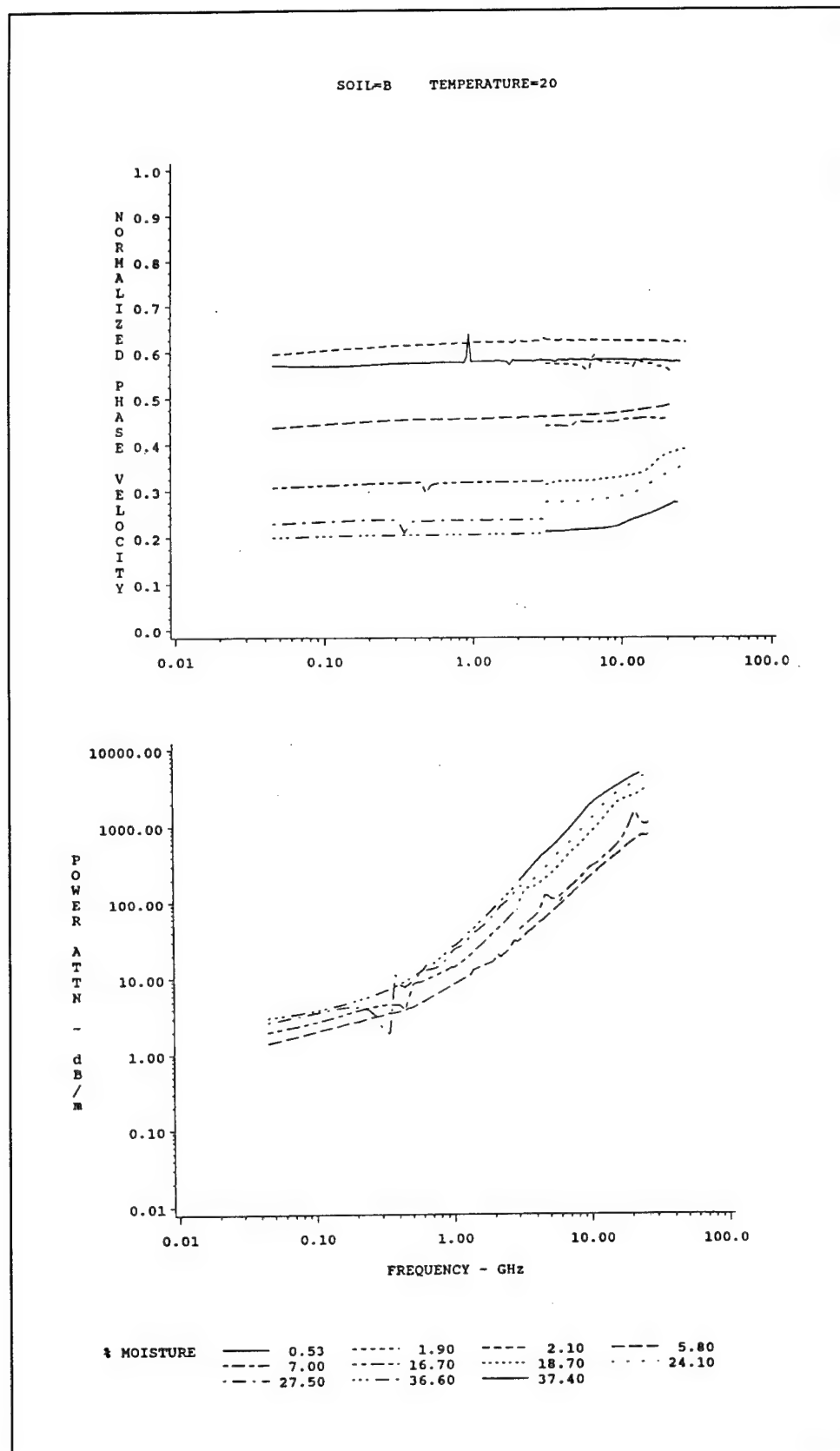


Figure 10. (Sheet 3 of 3)

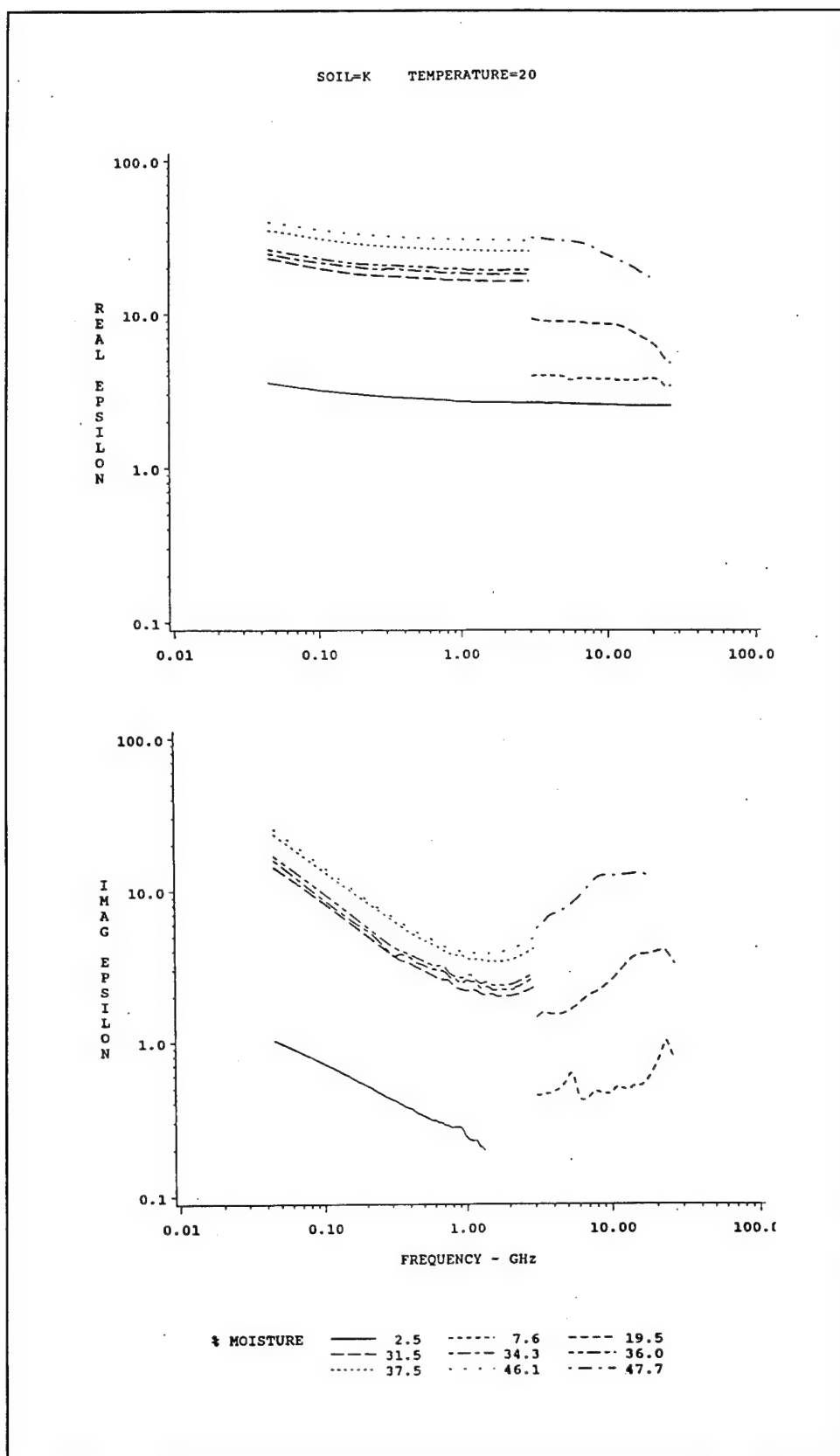


Figure 11. Electrical properties of a silt (Sheet 1 of 3)

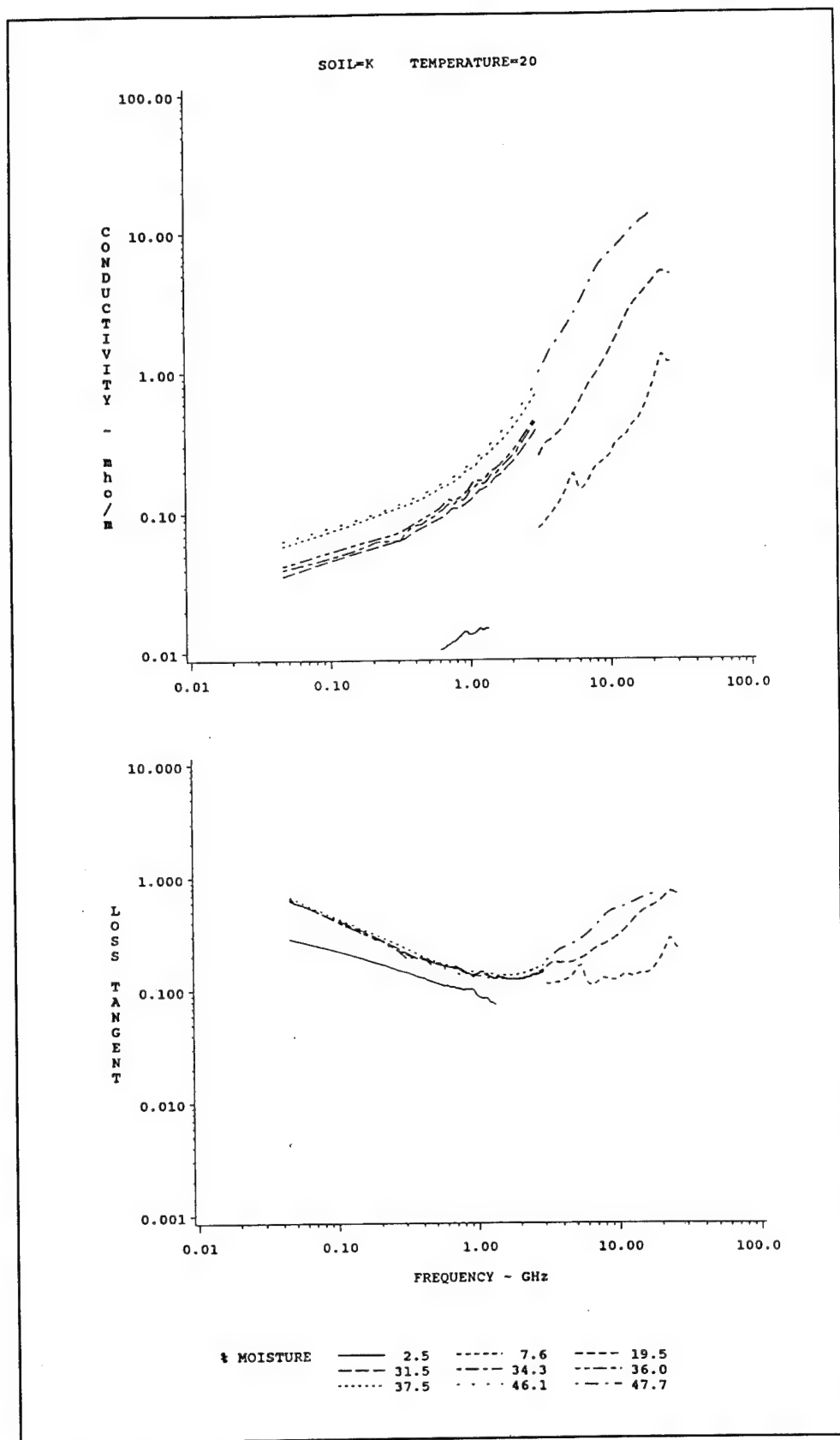


Figure 11. (Sheet 2 of 3)

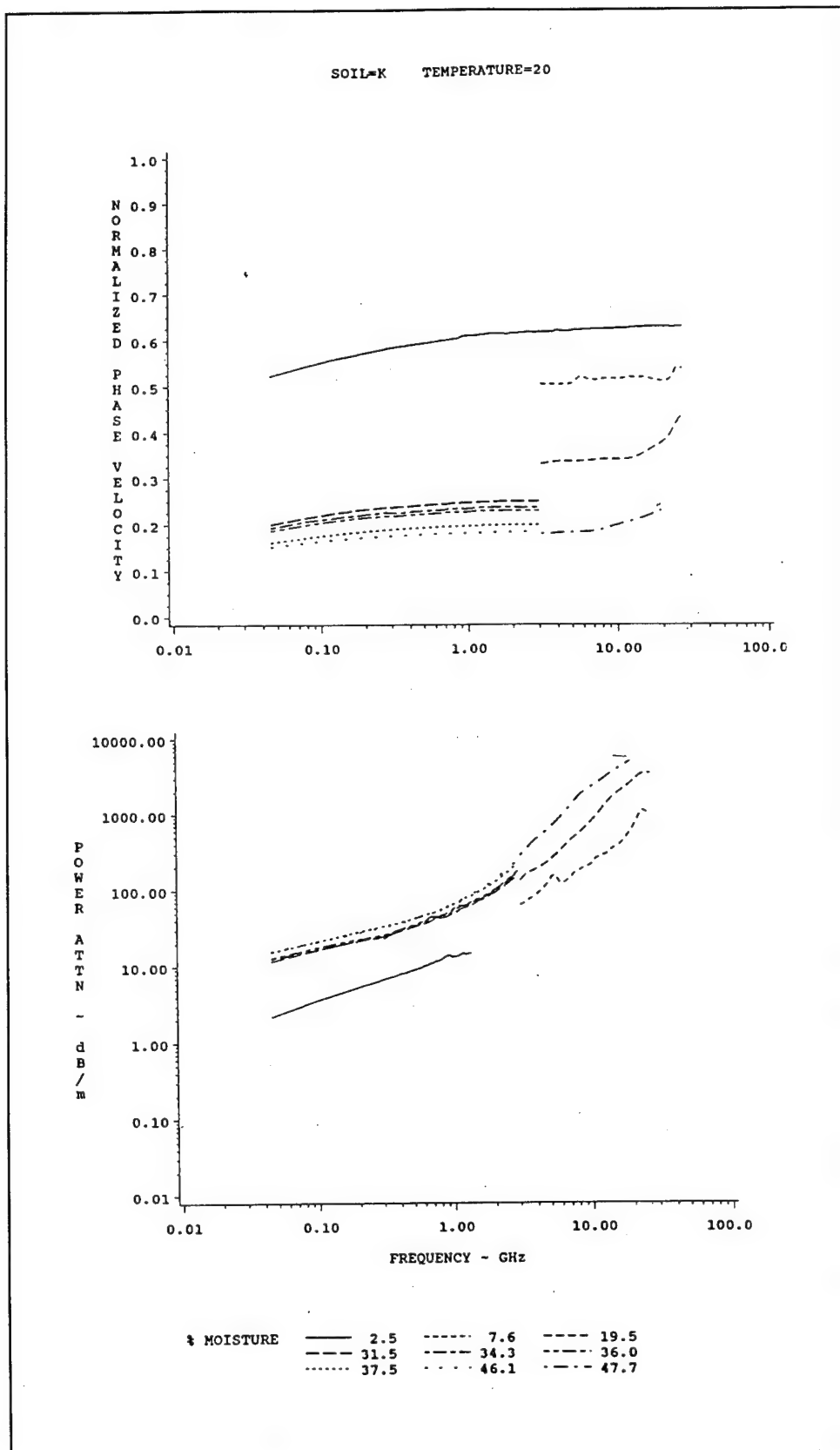


Figure 11. (Sheet 3 of 3)

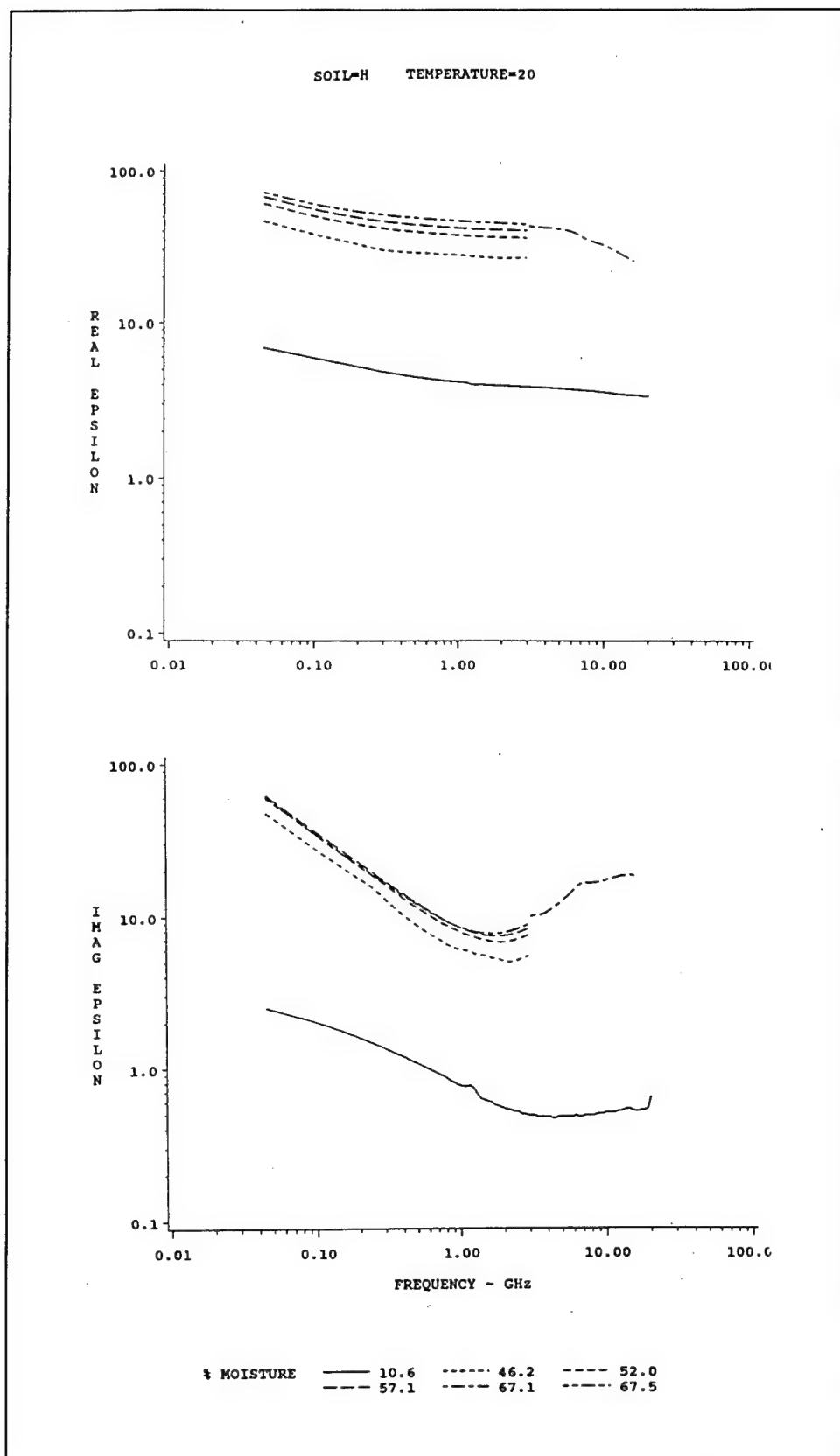


Figure 12. Electrical properties of a clay (Sheet 1 of 3)

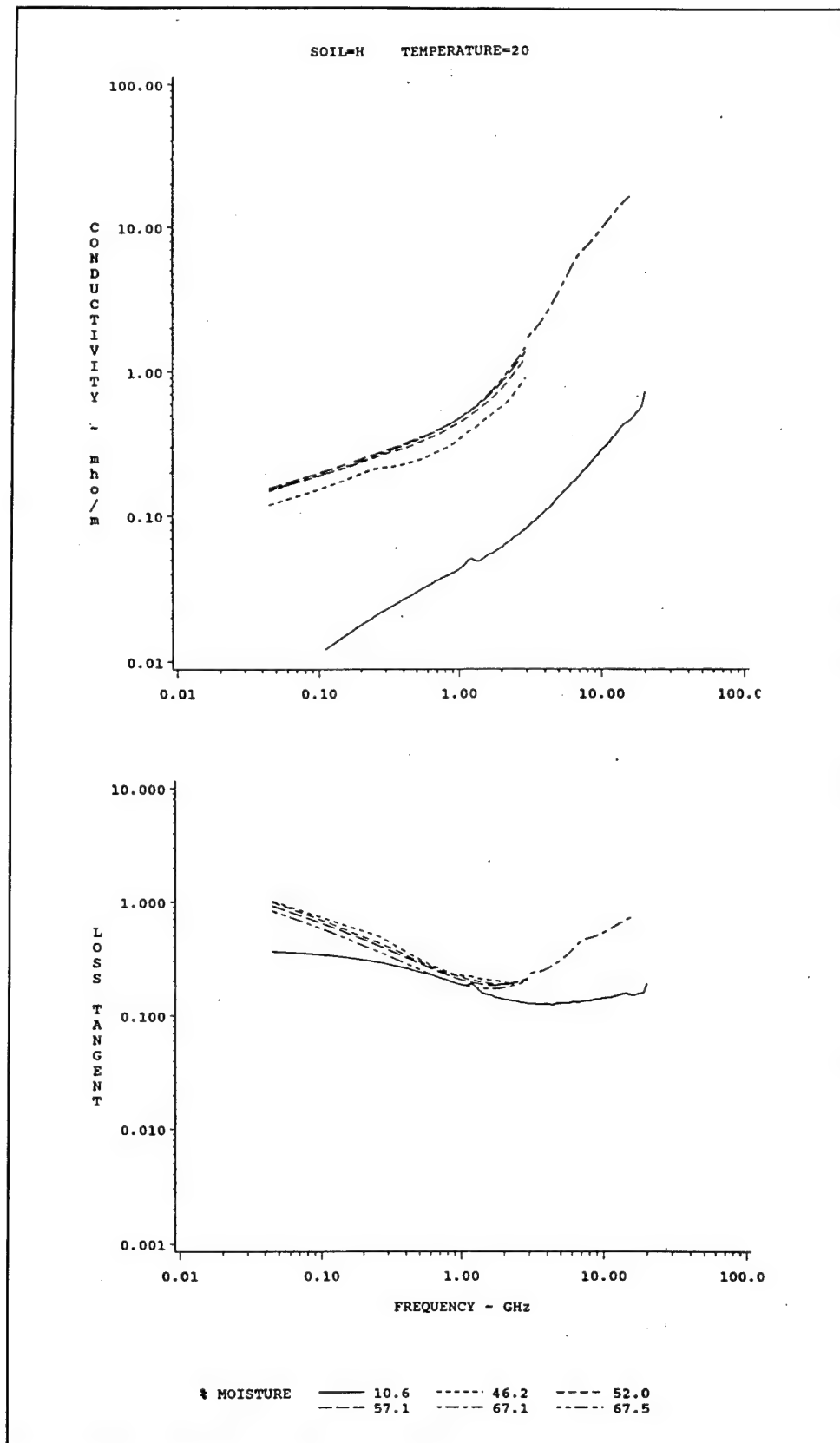


Figure 12. (Sheet 2 of 3)

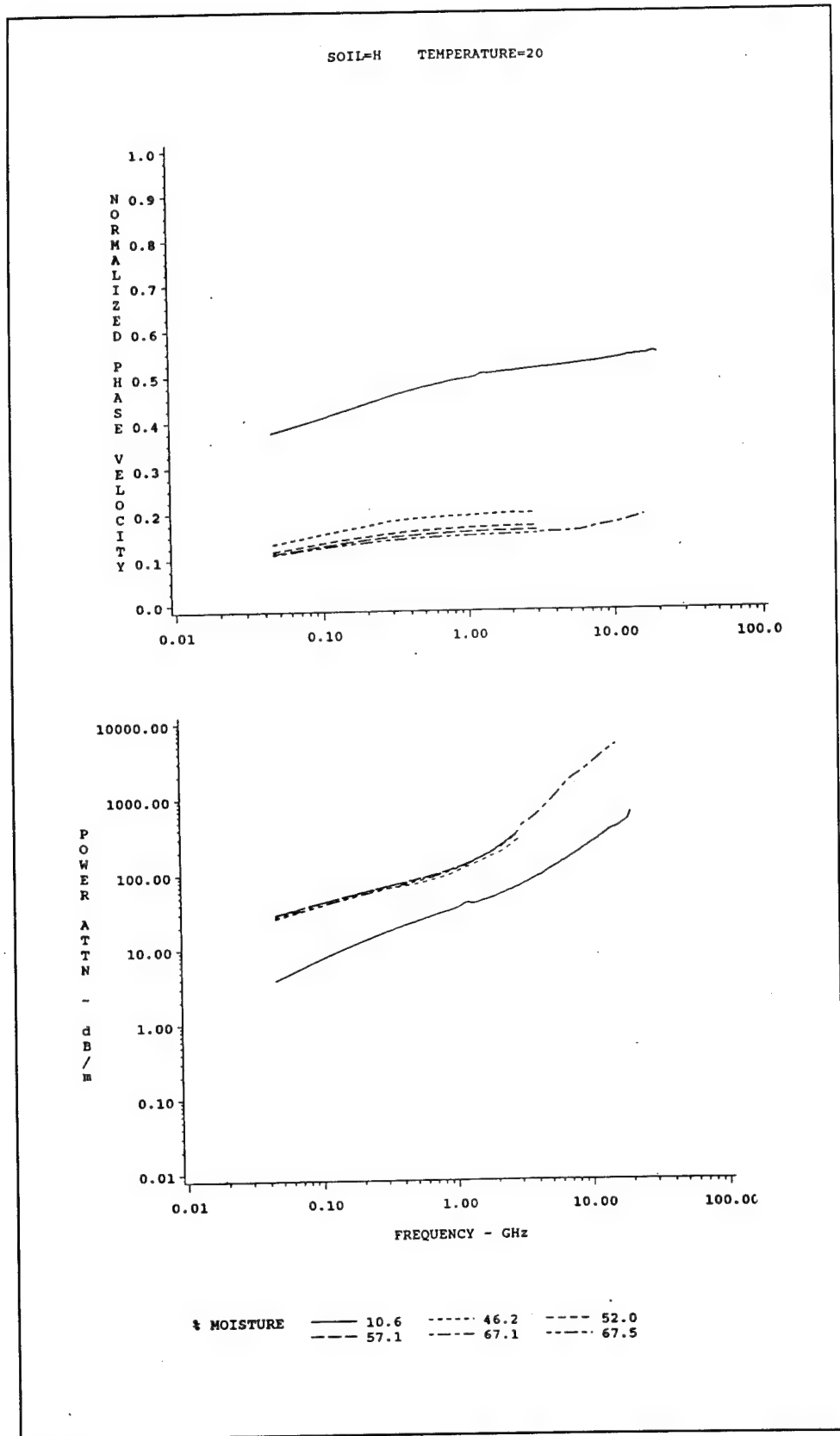


Figure 12. (Sheet 3 of 3)

adequate (Hulse, Walker, and Pearce 1969; Walker, Pearce, and Hulse 1969; Delaney and Arcone 1982; Hallikainen et al. 1985).

Sand

Consider first the data and calculated parameters shown on Figure 10 for the representative sand. The first thing to note is the very strong dependence of permittivity (the real part of the complex dielectric constant) on volumetric moisture content. The greater the amount of water, the greater is the number of electric dipoles (water molecules) available for orientation in the oscillating electric field; hence, the greater is the permittivity. This strong association with moisture will be examined more closely in a following section dealing with mixing model predictions for the permittivity.

Examination of the plots of the imaginary part of the dielectric constant reveals more than one loss mechanism in the soil/water/air mixtures (Hasted 1973). As discussed in the Introduction, low-frequency losses may be attributed to conductivity due to the generation of ions resulting from the combination of water and ionic compounds (salts) in the soil. Water used for these studies is distilled and deionized. Data shown in the next section reveals that the water, by itself, does not exhibit low-frequency losses. Salts from the soil must be going into solution with the added water.

Low-frequency losses may also be attributed to the Maxwell-Wagner effect, in which effective polarization occurs because of charge buildup on particle surfaces in the mixture having dissimilar dielectric properties. Which mechanism is dominant is unclear for the simple reason that dielectric property measurements were not made at frequencies low enough to determine whether or not losses are anomalous in nature (characteristic of Maxwell-Wagner effects). Anomalous dispersion, as used in this document, refers to a decrease in permittivity with increasing frequency accompanied by a maxima in the imaginary part of the dielectric constant.

Some authors have effectively argued that the Maxwell-Wagner effect is dominant in soils or other heterogeneous mixtures at these low frequencies (Smith 1971; Bidadi, Schroeder, and Pinnavaia 1988). In a recent study that made use of laboratory procedures similar to the ones used here, one researcher published data on the dielectric response of natural soils between 1 and 50 MHz that clearly shows a Maxwell-Wagner-like anomalous dispersion although he never referred to it as such (Wensink 1993). However, if an anomalous dispersion such as the Maxwell-Wagner effect was playing a part in the low-frequency response of this sand, one would expect to see a decrease in permittivity along with a decrease in the imaginary dielectric constant as frequency increased. This trend is not observed in the sand.

High-frequency losses are undoubtedly due to the classical Debye relaxation of either free water or bound water molecule dipoles (Debye 1929; Hasted 1973). Because this sand is relatively free of clay minerals, its

high-frequency response is probably dominated by free water in the soil/water/air mixture.

Although the imaginary part of the complex dielectric constant is associated with a shift in phase of a propagating electromagnetic and, hence, is related to losses in the mixture, the true measure of loss has to be that part of the complex propagation constant referred to as the amplitude attenuation factor (Equation 4). Whereas the imaginary part of the dielectric constant indicates an optimum range of frequencies (200 to 1,000 MHz) in which losses are minimized, an examination of the power attenuation calculations clearly indicates that losses increase steadily with frequency. This is because the increase in frequency is the dominant term in Equation 7.

Phase-velocity calculations provide a first order approximation to signal arrival times. This would be very important in an iterative scheme for processing ground-penetrating sensor data using synthetic aperture techniques. Clearly, phase velocity is a strong function of the permittivity of the mixture.

Silt

Figure 11 contains data and calculated parameters for a typical silt at a sample temperature of 20 °C. Two significant differences between silt and sand results are apparent when comparisons are made at similar moisture contents. The first is that the permittivity of the silt/water/air mixture is not a constant over a broad range of frequencies as was true for the sand. This indicates that as frequency drops, the mixture polarizes more easily. The observed behavior is compatible with an anomalous dispersion model, leading once again to the concept of the Maxwell-Wagner effect. An increased amount of charged particles are available in this silt due to the interaction of water and the dolomite contained in the soil. It would be the movement of these ions within the quartz matrix that leads to charge accumulation at particle boundaries and its subsequent relaxation.

At similar volumetric moisture contents, the imaginary part of the dielectric constant is greater in the silt than in the sand by a factor of about five at low frequencies. Although the data are not as complete, there appears to be little difference between this silt and sand at the high-frequency end of the spectrum. This is probably as it should be, because the mechanism for high-frequency loss is dipole relaxation of water molecules. If the amount of water is basically the same, and if there is no reason to believe that the water molecules are being constrained in the silt any more than they are in the sand (each soil has about the same quantity of quartz), then the behavior of the two soil/water/air mixtures in the high-frequency region should be similar.

Phase velocities in the silt are more dependent on frequency than for the sand. Power attenuation in the silt is greater at low frequencies than it is in the sand by a factor of about five, while attenuation in the two soil/water/air mixtures at high frequencies is about the same.

Clay

Figure 12 shows results for a soil that contains a large amount of expandable clay minerals. Although there is only a limited amount of high-frequency data for this soil, there is enough along with the low-frequency results to draw several conclusions. The first is that at low frequencies, similar moisture content samples of the carbonaceous silt and this particular clay have pretty much the same complex dielectric response. The imaginary part of the constant for the clay is about twice the magnitude of that for the silt at 45 MHz. The permittivity of the clay falls off more quickly with increasing frequency than it does for the silt, indicating a stronger anomalous dispersion in the clay than in the silt. It is highly probable that this dispersion is enhanced in the clay due to its higher specific surface. If the dispersion mechanism is relaxation of charges built up on solid particle surfaces, and there is more surface area for charge buildup in the clay, then it seems reasonable that the dispersion will be more pronounced in the clay.

At high-moisture contents, it appears that all three representative soils have similar dielectric response. This could be explained by assuming that most of the water in the soils is "free" and that the dielectric response of the mixture is dominated by the dipole relaxation of the "free" water molecules.

At low-moisture contents, there is clearly a difference in the dielectric response of the soils due to how the water and soil are combined. At volumetric moistures less than 10 percent, the sand/water/air mixture shows the classical dipole relaxation of water; hence, in the sand, most of the water must be free to react to the electric field. In the silt, there is some indication of free-water relaxation, although it is not as pronounced as in the sand. As for the representative clay, a measurement made for what was thought to be dry soil (air dried) and which turned out to be about 10-percent volumetric water shows a low-frequency loss having a character different from that of the other soils and virtually no dipole relaxation at high frequencies. The water in the so-called dry clay must be bound to the clay particles, probably within the clay interlayer spacing as water of hydration (Mitchell 1993), but not so much that it cannot respond to the applied electric field. The best interpretation of low-moisture content data is that the clay exhibits bound-water relaxation (Hasted 1973).

Results of calculations of the effective conductivity, phase velocity, and power attenuation are simply reflections of the dielectric property measurements. Signal attenuation (power) in this clay will be about two times the attenuation of the silt at the lowest measurement frequencies.

A hypothetical sensor design

The power attenuation curves can be useful as a tool for conducting a first order design of a ground-penetrating electromagnetic sensor. For example, the sensitivity of a receiver is such that it can detect signals (power levels) that

are 50 db less than the transmitted signal. Furthermore, one wishes to detect a signal from a buried object whose reflected signal is 10 db less than that of the incident wave. Finally, the sensor operates at a frequency of 500 MHz and suffers no loss in signal power at the air/ground interface.

The calculated power attenuation curves for the representative sand and the associated range of moisture levels indicate that the soil could attenuate the signal by as much as 10 db per meter of travel distance for a volumetric moisture content of about 35 percent. One could then estimate that the sensor would be able to detect the buried object at depths up to 2 m (greater depths for dryer sand).

Applying the same parameters to the design of a sensor that might operate in the representative silt, one discovers a maximum attenuation of about 30 db per meter. The buried object discussed above would not be found below a depth of about two-thirds of a meter at high moisture contents.

With respect to the representative clay, one could interpolate the calculated attenuation curves to say that power attenuation at 500 MHz and about 35-percent volumetric moisture occurs at a level of about 40 db per meter of travel distance. The end result of the design calculation is that the particular buried object could be "seen" in the clay at a depth of no more than one-half meter.

Of course, these example designs are for an operating frequency of 500 MHz, somewhat midrange within the normal operating bands of ground-penetrating radars. Lower frequency systems would be able to penetrate much further into soils. Although the data from which these values of attenuation were calculated were collected from mixtures of soil and distilled, deionized water, which has a low-frequency behavior much different from fresh water or brine, there is a clear indication that in the normal range of operations of ground-penetrating radars (< 1 GHz), a signal should be able to penetrate almost any soil to a shallow depth of less than 1 m if signal strength and sensitivity are both adequate. For dry sandy soils, measurable signal penetration could be several meters or more.

Moisture Effects

From the representative data shown in the previous section, one immediately recognizes the very strong dependence of dielectric properties on volumetric moisture content. Plotting electrical properties versus moisture content at some frequency of interest and a known sample temperature will provide further insight into the dielectric response of soil/water/air mixtures. Consider Figure 13, which contains data and calculation results for all of the soils plotted at 78 MHz and at 20 °C. Although low-frequency electrical data are the least predictable because of great variation in the loss term, several useful observations can still be made.

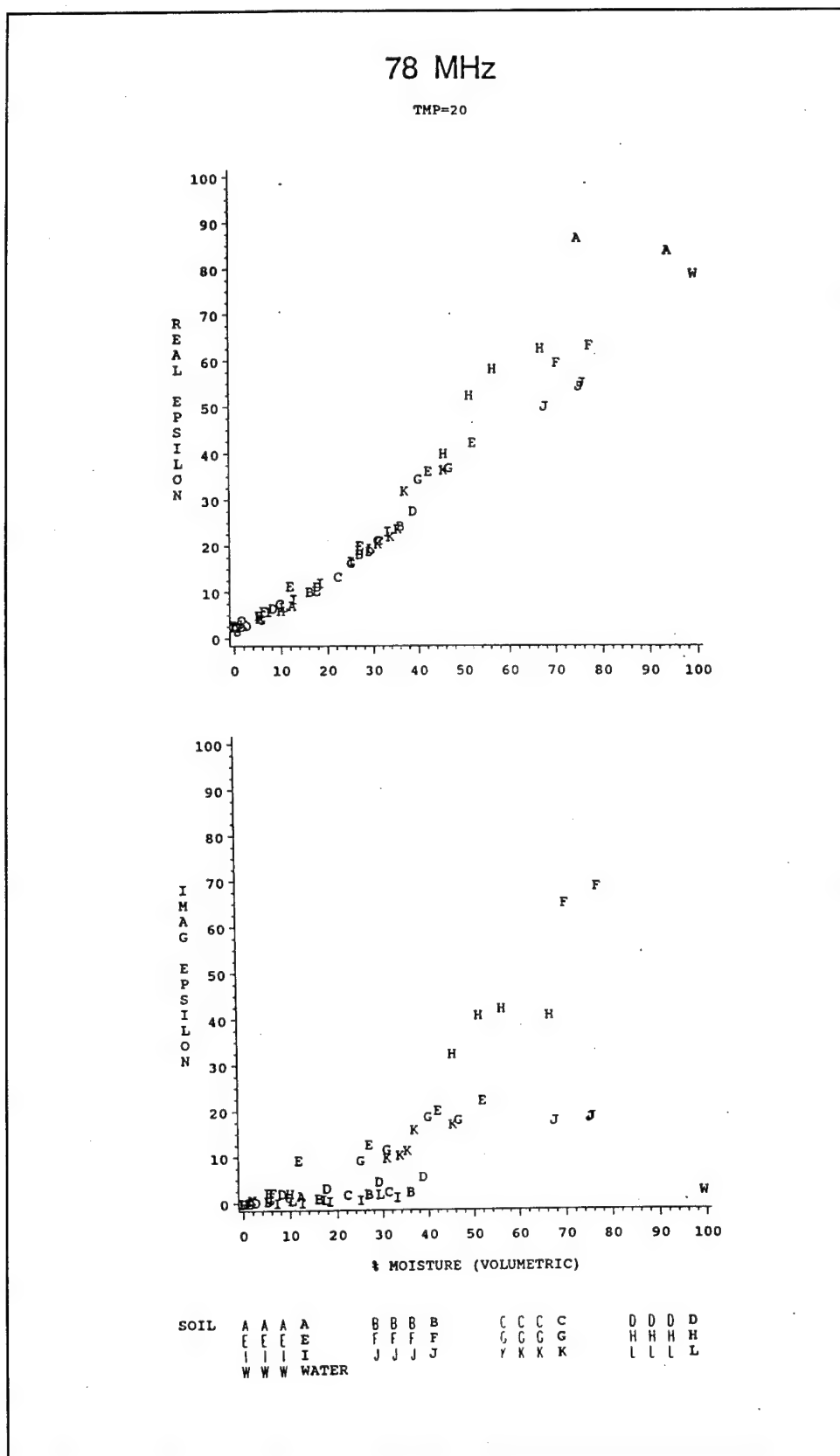


Figure 13. Electrical properties of all soils at 78 MHz (Sheet 1 of 3)

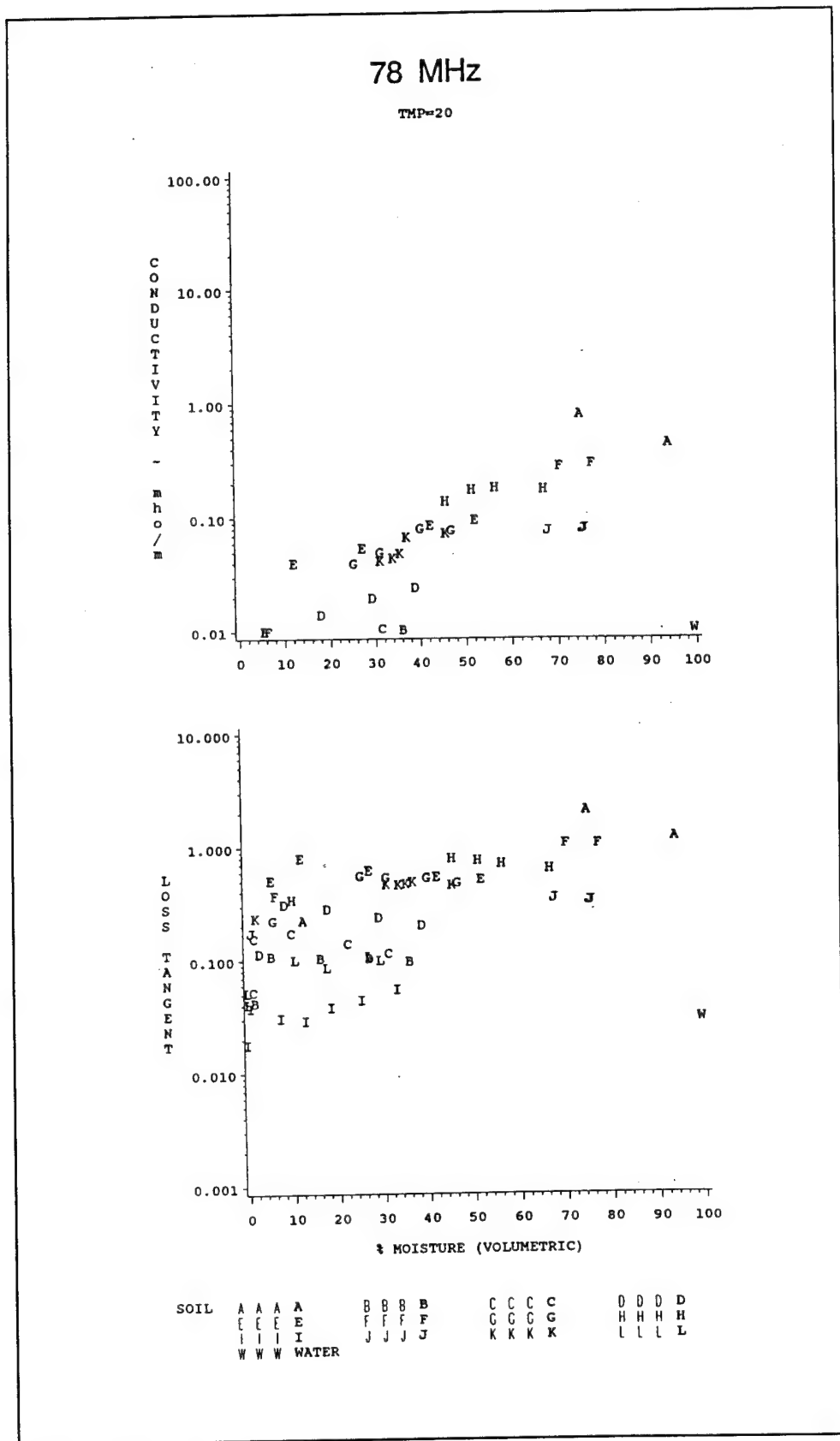


Figure 13. (Sheet 2 of 3)

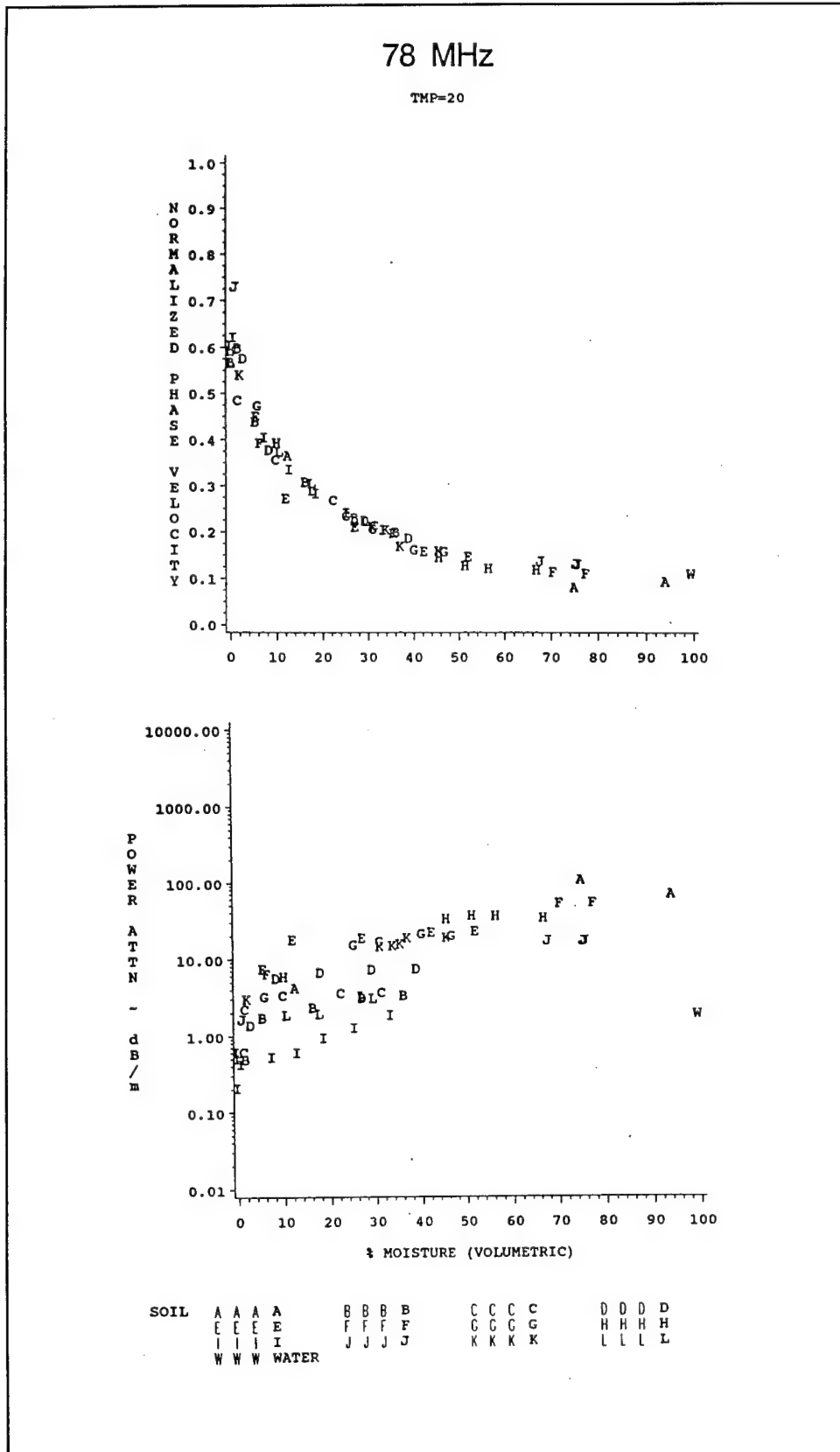


Figure 13. (Sheet 3 of 3)

Note, first of all, that capacitive properties of the soils (the real part of the dielectric constant) and their normalized phase velocities hint at a material-independent response when considered as a function of volumetric moisture content. Other data in Appendix C for higher frequencies show an even stronger relationship between permittivity and volumetric moisture content. This is particularly useful if one considers using microwave sensor technology to measure moisture in the soil.

The real part of the dielectric constant at this frequency varies nonlinearly with moisture just as has been reported elsewhere (Wang and Schmutge 1980). One could also easily imagine a bilinear fit to these data, which could be interpreted through the use of electrical analogues as a change from a model of series capacitors to one of parallel capacitors at some critical moisture content (Wang and Schmutge 1980; Campbell 1988; Curtis 1993c). These models reflect the creation of long-range electrical paths in the soil/water/air mixture at the critical moisture content and above. For the 78-MHz data, a bilinear fit (by inspection) would result in a critical moisture content of about 24 percent as shown Figure 14.

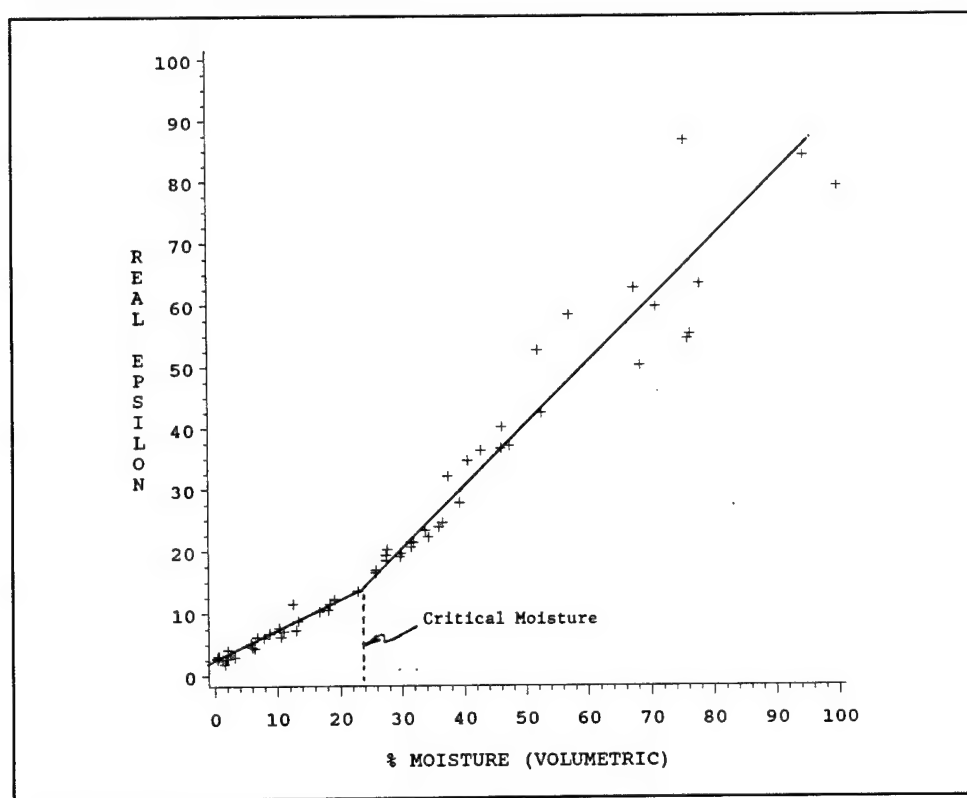


Figure 14. A bilinear fit to permittivity data collected at 78 MHz, 20 °C

One could easily use standard statistical techniques to perform least-squares fits to such data as is shown in Figure 15, where one second-order polynomial fit of all data at 20 °C is compared with a similar fit of data having less than 36-percent moisture by volume. Because natural soils normally do not exhibit

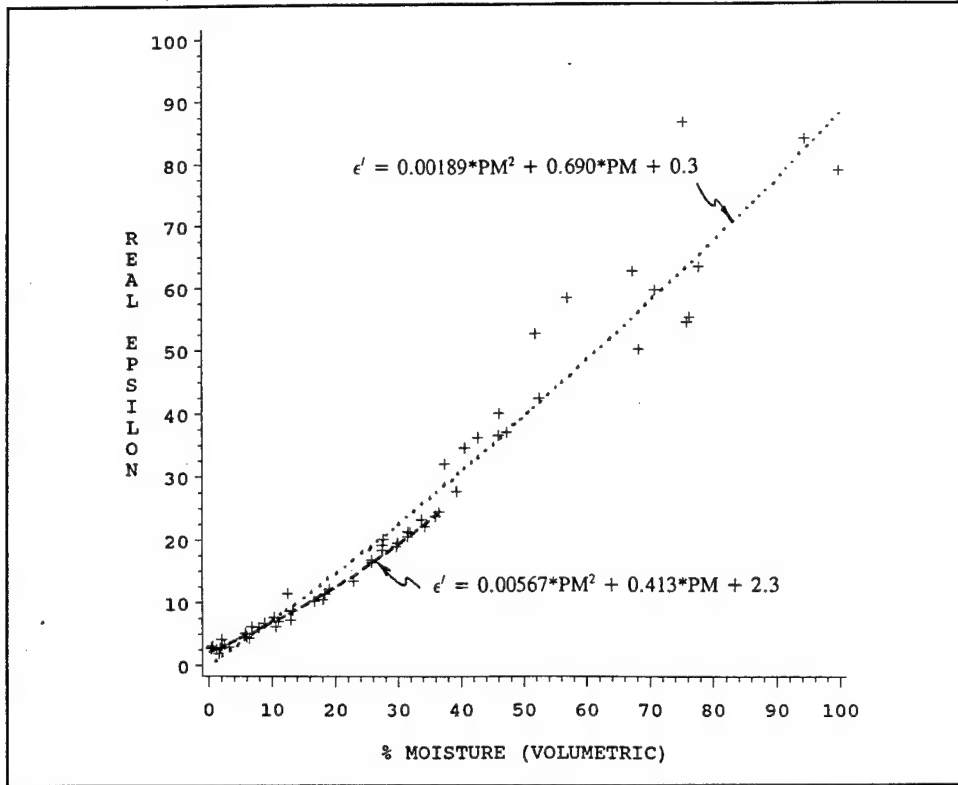


Figure 15. Least square polynomial fits to permittivity data collected at 78 MHz, 20 °C

volumetric moistures higher than this level, the latter fit would be a very good representation of the permittivity-volumetric moisture relationship for soil/water/air mixtures at 78 MHz and 20 °C.

Another option for fitting a model to the permittivity-moisture content data in Figure 13 is an exponential relationship

$$\epsilon'_{\text{mixture}} = \epsilon'_{\text{dry soil}} e^{k \cdot MC}$$

where MC is the moisture content expressed as a decimal. Within these constraints, the constant factor, k , is

$$k = \ln \left[\frac{\epsilon'_{\text{water}}}{\epsilon'_{\text{dry soil}}} \right]$$

which, for the data shown in Figure 13, have a value of about 3.45. Checking the midpoint of the exponential model fit, one sees that the model predicts a permittivity of about 14, whereas the data show an average value on the order of 35. An exponential model is not adequate for the composite data.

Only permittivity data collected at very low frequencies and high-moisture contents exhibited any sort of variance about the means at those moistures. Note also that all of the soils whose permittivities did not exhibit predictable behavior were soils that contained a reasonably large amount of the expandable clay mineral, smectite. Because permittivity is a result of polarization phenomena within the soil/water/air mixture, something is different about what causes polarization in the smectitic soils as opposed to other soil types. In sandy soils with little or no clay content, polarization is controlled by rotation of the "free" water dipoles. As was argued in the previous section, wet silts and clays are both likely to contain ions that effectively produce polarization by charge accumulation on soil particle surfaces. It was further argued that some other mechanism had to be responsible for the enhanced permittivity in the smectitic soils, clearly evident in the measurements of so-called dry soil. All sources seem to point to the response of water molecules that are bound to the clay mineral particles, and whose resonant frequency (inverse of relaxation time) is on the order of 100 MHz (Hasted 1973).

Another useful observation from the data shown in Figure 13 can be made from the power attenuation plot. About an order of magnitude difference in power attenuation at any moisture content over the range of soil types as well as an expected increase in attenuation with increasing moisture is first of all seen. The upper bound of these data could be used as a conservative design parameter for a given ground-penetrating radar system, from which one might conclude that power loss in nearly dry soils is on the order of a few decibels/meter, while saturated soils may result in 40 to 50 db/meter of loss. Data in the appendixes indicate even higher losses at some frequencies.

Because of the strong correlation between soil/water/air mixture permittivities and volumetric moisture demonstrated by the composite data, one might be strongly tempted to utilize a permittivity-mixing model based on electrical analogues for the physical mixtures. In other words, one could equate the permittivity of each component in the mixture to the capacitance of a simple parallel plate capacitor. These capacitors could be arranged in a series circuit, a parallel circuit, or in a more complex configuration. The effective capacitance of the combined elements would represent the permittivity of the mixture. The most general form of such a mixture model, as it applies to mixtures of dry soil, pure water, and air, is (Curtis, In Preparation):

$$\epsilon_{mixture}^k = \delta_{soil} \epsilon_{soil}^k + \delta_{water} \epsilon_{water}^k + \delta_{air} \epsilon_{air}^k$$

where the subscripted deltas represent volume fractions of the components and the primed notation for the real part of the dielectric constant has been dropped. One implicit assumption to this kind of model is that each of the constituent materials do not lose their individual capacitive properties. In other words, there can be no chemical interaction among the mixture components that changes their respective dielectric responses. The mixing law exponent, k , takes on the special values of $+1$ if the electrical paths through the

mixture components are parallel to each other and -1 if the current is forced to pass through each component in a series arrangement.

Such a model cannot, however, be applied to the composite data shown in Figure 13 for the following reasons. First of all, if one wished to fit a single mixing model to the composite data, the volume fraction for water would have to vary from 0.0 to 1.0. What meaning, then, could be given to the volume fraction of the dry soil element or to that for air? Most of the samples from which the composite data are derived had different solid fractions. In fact, high moisture content in these data is synonymous with low solid fractions. Even if some kind of average solid fraction was chosen for all soil types, the model would still fail at high-moisture contents because of the physical constraint that the sum of the volume fractions must be equal to unity.

The only sensible way to use a mixing model like that above is to apply it to a series of mixtures whose solid fraction remains fixed and whose water fraction is allowed to vary. The maximum allowable moisture fraction would then be limited to the conditions for saturation.

Fortunately, a number of the data points collected for this study do represent measurements made of samples that were first tested at near-saturation conditions and then dried and retested without disturbing the physical sample. In fact, each of the soils whose dispersion curves were shown in the previous section were examined this way. It should be possible, then, to test the hypothesis that a dielectric mixing model such as that shown above is useful for predicting the permittivity of mixtures at other moisture contents.

The application of the generalized mixing model to establish the mixing law exponents for each soil type requires that one additional factor be taken into account. For so-called dry soil samples, the permittivity measurement is really a measurement of a mixture containing dry solid material and air. The model must apply for this condition as well. What is required, then, is that a value for permittivity for the dry solid component be chosen to force the model to generate the correct "dry" soil measurement result. Actually, this solid fraction permittivity is calculated for each value of the mixing exponent using the measured dry solid fraction, an air volume fraction that is one minus the dry solid fraction, and an appropriate dry soil mixture permittivity. The results of calculating solid fraction permittivities using this technique are very much in line with published data on rocks and compressed soils (Nelson, Lindroth, and Blake 1989; Ulaby et al. 1990).

Figures 16, 17, and 18 show the results of fitting the generalized mixing model at 78 MHz and 20 °C to the volume fraction parameters associated with the measurements of soils B, K, and H, respectively. The permittivity of pure water was taken to be 78.96; solid fractions were 0.627 for soil B, 0.531 for soil K, and 0.32 for soil H. Superimposed on the calculated mixture model responses for various values of the mixing exponent are the measured data for the soil/water/air mixtures.

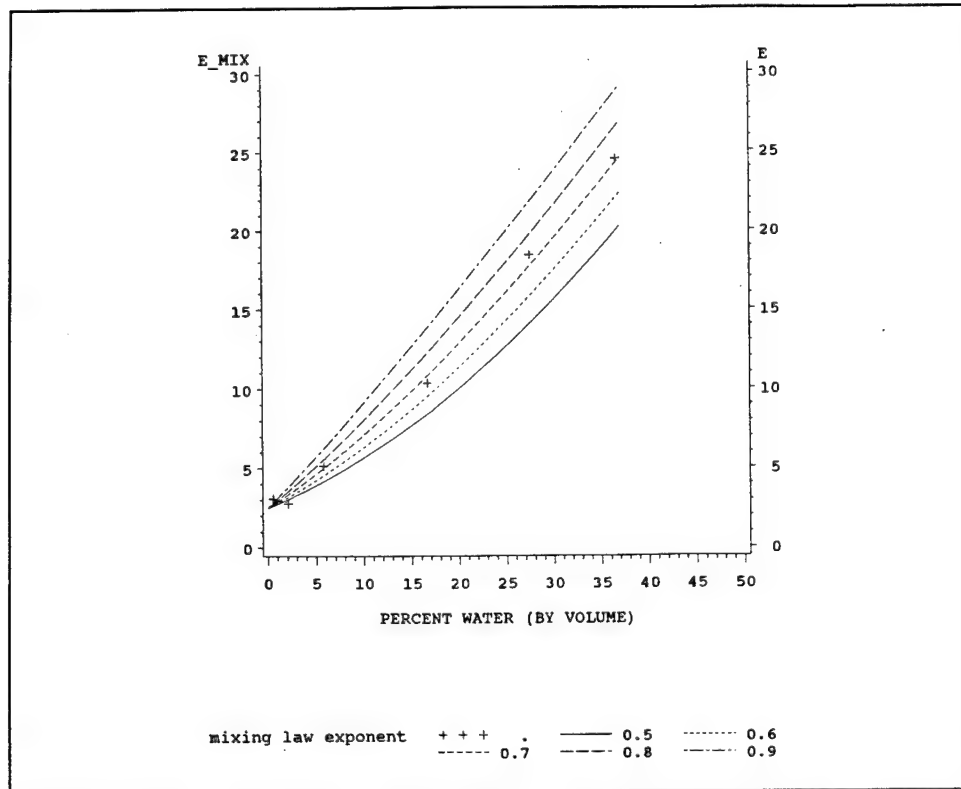


Figure 16. Permittivity mixing model applied to a sand, 78 MHz, 20 °C

Conclusions that can be drawn from Figures 16-18 include the following statements. First of all, the mixing model exponents are clearly material dependent. One could argue that this observation is misleading because samples were measured at different dry densities. Unfortunately, there was no control over this variable, and the concern cannot be addressed.

Another conclusion is that the only decent correlation between data and models was for the sandy soil, B. Neither the silt data nor the expandable clay soil data were well represented by a single mixing exponent. One possible explanation is the possibility of chemical reactions within the silt and clay due to the addition of water. As noted in an earlier section, chemical reactions could account for unexpected low-frequency permittivity and conductivity results, and would be in direct conflict with the model assumption that each component of the mixture retain its unique dielectric properties.

Because of the extreme variability of dry soil densities in the real world along with the fact that water and some soil minerals combine to produce unpredictable dielectric responses, it seems unlikely that any advantage can be realized from trying to fit a generalized mixing model to permittivity-moisture content data.

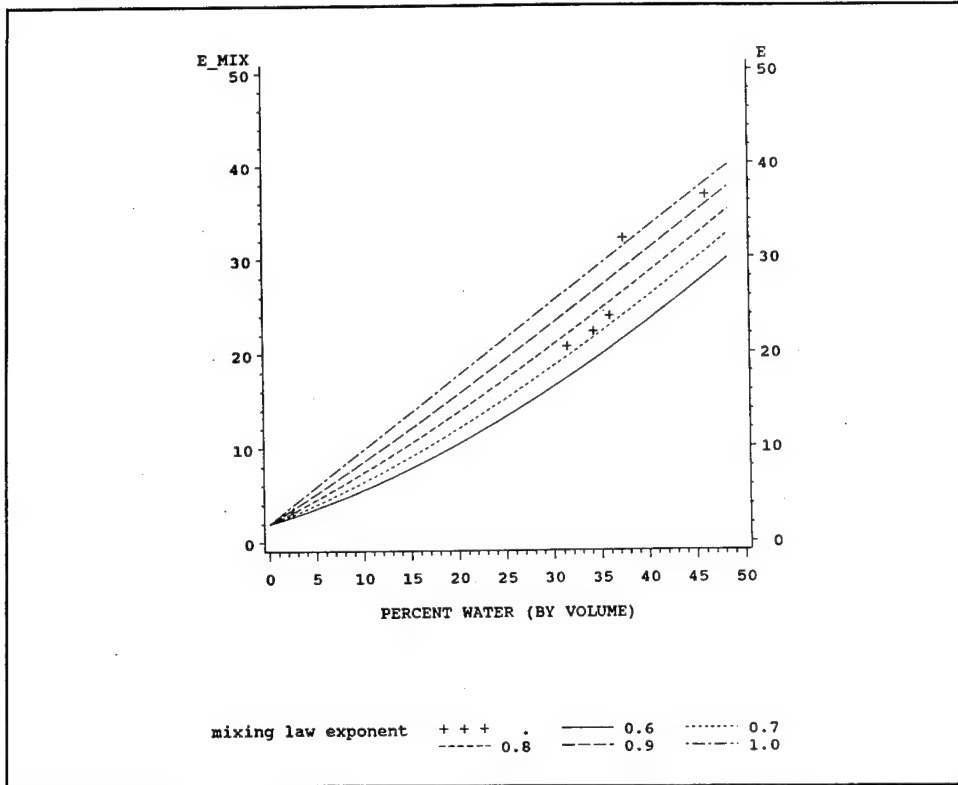


Figure 17. Permittivity mixing model applied to a silt, 78 MHz, 20 °C

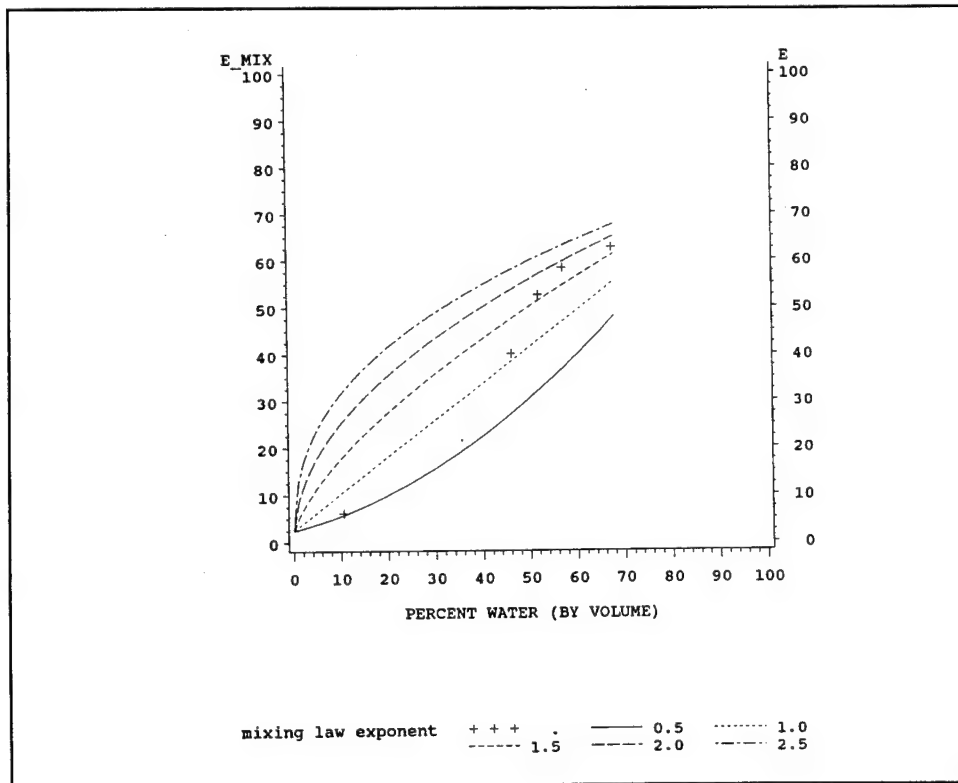


Figure 18. Permittivity mixing model applied to a clay, 78 MHz, 20 °C

5 Summary of Observations and Conclusions

Broadband (45 MHz to 26.5 GHz) complex dielectric property measurements were made for 12 different soils having a wide spectrum of physical and chemical properties. Data were collected at numerous volumetric moisture contents and at four distinct temperatures (10, 20, 30, and 40 °C). Presentation of the data was made in various forms including not only values of the measured complex dielectric constant, but also computed values of conductivity, loss tangent, normalized phase velocity, and power attenuation for idealized plane wave propagation. These data were plotted against frequency for each temperature and each sample volumetric moisture and against moisture content at fixed frequencies, and correlated well with limited data available elsewhere in the literature.

Dispersion data revealed separate low-frequency and high-frequency loss mechanisms (a rough division between low- and high-frequency behavior being about 1 GHz). High-frequency losses are attributed to free-water molecule dipole relaxation and appear to be independent of soil type. Low-frequency losses seem to be associated with the movement of ions in the soil/water/air mixtures that, due to the presence of a solid matrix, result in charge accumulation on particle surfaces and an effective polarization and relaxation. Measurements were not made at frequencies sufficiently low to separate the contribution of this effect (known as Maxwell-Wagner) from pure ionic conduction. The soils containing expandable clay minerals demonstrate another loss mechanism at low frequencies; namely, bound water relaxation due to the presence of water of hydration. Low-frequency losses are definitely related to the chemistry of the soil through either the generation of ions by salts within the soil or by the presence of water within the soil mineral crystals due to hydration. Physical properties (dry density, moisture content, grain-size distributions, specific surface, etc.), alone, are not sufficient to predict the electrical response of all soils.

The permittivity of soil/water/air mixtures is independent of soil type at higher frequencies when considered as a function of volumetric moisture content. Even at the lower frequencies examined in this study, a good fit to the permittivity data can be made by a bilinear function with a break at about 24-percent volumetric moisture. Very effective models for predicting

permittivity can also be generated by least-square polynomial fits over a reasonable range of moisture values. Exponential models do not predict permittivity if fitted to the entire range of moistures.

Electrical analogues can be used to generate permittivity mixture models for data in which the moisture content was allowed to vary for a fixed volume fraction of solid particles. Arguments are given regarding why these models cannot be applied to the composite data for all soil types. The mixture models appear to be effective only for soils in which chemical reactions (ionization, effective bonding of water by various mechanisms) have not taken place. Electrical analogues must be used very cautiously when attempting to model the dielectric response of moist soils.

As with any useful study, attempting to answer one set of questions generates another. More experiments are needed to better understand the effect of variable mineralogy, chemical composition, particle size, and water content on the dielectric properties of soils. The following suggestions are made for future studies.

- a. To assess the effect of particle size as well as to address questions of varying sample dry density, a number of samples of the same soil type could be prepared for testing by selectively screening the soil to produce samples with different, but nearly uniform, particle sizes.
- b. To address the structural and chemical effects of expandable clays on the permittivity of the soil/water/air mixture, soil samples could be prepared so that each contains a different smectitic clay mineral.
- c. To eliminate the concern that different cations could accumulate different amounts of hydration water, which, in turn, affects the dielectric properties of the sample, homoionic clays could be used in future studies.
- d. Soil mixtures containing varying amounts of a pure sand, a pure silt, and a pure clay could be developed and tested to more clearly determine the interrelationships of idealized mixture components on the dielectric properties of the mixture.
- e. To better understand the effects of mineralogy, monomineralic samples could be prepared for testing.
- f. All of the measurements made in this study were done on samples prepared with pure distilled, deionized water. The effect of increased ion availability could be studied by preparing samples with fresh water and with brackish water.
- g. A clearer picture of the low-frequency loss mechanisms could be developed by extending these measurements to lower frequencies. This would, however, require a new set of instrumentation.

References

- Abramowitz, M., and Stegun, I. E., ed. (1972). *Handbook of mathematical functions*. Applied Mathematics Series - 55, National Bureau of Standards, Washington, DC.
- Arulanandan, K. (1991). "Dielectric method for prediction of porosity of saturated soil," *Journal of Geotechnical Engineering*, ASCE 117(2), 319-330.
- _____. (1994). "Geophysical characterization of sites." *Proceedings of XIII ICSMFE, New Delhi, India*. 81-90.
- Bertin, E. P. (1975). *Principles and practice of X-ray spectrometric analysis*. Plenum Press, New York.
- Bidadi, H., Schroeder, P. A., and Pinnavaia, T. J. (1988). "Dielectric properties of montmorillonite clay films: Effects of water and layer charge reduction," *Journal of Physics and Chemistry of Solids* 49(12), 1435-1440.
- Bohren, C. F., and Huffman, D. R. (1983). *Absorption and scattering of light by small particles*. John Wiley and Sons, New York.
- Campbell, J. E. (1988). "Dielectric properties of moist soils at RF and microwave frequencies," Ph.D. diss., Dartmouth College, Hanover, NH.
- _____. (1990). "Dielectric properties and influence of conductivity in soils at one to fifty megahertz," *Soil Science Society of America Journal* 54, 332-341.
- Curtis, J. O. (1993a). "Microwave dielectric behavior of soils, Report 1: Summary of related research and applications," Technical Report EL-93-25, U.S. Army Engineer Waterways Experiment Station, Vicksburg, MS.
- _____. (1993b). "Microwave dielectric behavior of soils, Report 2: A unique coaxial measurement apparatus," Technical Report EL-93-25, U.S. Army Engineer Waterways Experiment Station, Vicksburg, MS.

- Curtis, J. O. (1993c). "Microwave dielectric behavior of soils, Report 3: Measurements and modeling," Technical Report EL-93-25, U.S. Army Engineer Waterways Experiment Station, Vicksburg, MS.
- _____. "Broadband electrical response of organic contaminants and contaminant/soil mixtures," Technical Report in preparation, U.S. Army Engineer Waterways Experiment Station, Vicksburg, MS.
- Debye, P. (1929). *Polar molecules*. Dover Publications, Inc., New York.
- Delaney, A. J., and Arcone, S. A. (1982). "Laboratory measurements of soil electric properties between 0.1 and 5 GHz," CRREL Report 82-10, U.S. Army Engineer Cold Regions Research and Engineering Laboratory, Hanover, NH.
- Dobson, M. C., Ulaby, F. T., Hallikainen, M. T., and El-Rayes, M. A. (1985). "Microwave dielectric behavior of wet soil—Part II: Dielectric mixing models," *Transactions on Geoscience and Remote Sensing* GE-23(1), 35-46.
- Everest Technologies. (1991). *Icometrics (TM) Version 3.0 user's guide*. Houston, TX.
- Fisons-Kevex. (1990). *Kevex XRF Toolbox II reference manual*. Valencia, CA.
- Folk, R. L. (1968). *Petrology of sedimentary rocks*. Hemphill's, Austin, TX.
- Hall, P. G., and Rose, M. A. (1978). "Dielectric properties of water adsorbed by kaolinite," *Journal of the Chemical Society of London, Faraday Transactions* 174, 1221-1233.
- Hallikainen, M. T., Ulaby, F. T., Dobson, M. C., El-Rayes, M. A., and Wu, L. (1985). "Microwave dielectric behavior of wet soil — Part I: Empirical models and experimental observations," *Transactions on Geoscience and Remote Sensing* GE-23(1), 25-34.
- Hasted, J. B. (1973). *Aqueous dielectrics*. Chapman and Hall, London.
- Hoekstra, P., and Delaney, A. (1974). "Dielectric properties of soils at UHF and microwave frequencies," *Journal of Geophysical Research* 79(11), 1699-1708.
- Hulse, W. H., and Walker, J. W. (1972). "Electromagnetic properties of soils at three test sites near Fort Monmouth, New Jersey," Technical Report 4063, U.S. Army Electronics Command, Fort Monmouth, NJ.

- Hulse, W. H., Walker, J. W., and Pearce, D. C. (1969). "Electrical properties of selected Vietnam soils," Technical Report 3097, U.S. Army Electronics Command, Fort Monmouth, NJ.
- _____. (1972). "Electrical conductivity studies of the soils of the Middle Atlantic Region: Virginia," Technical Report 3564, U.S. Army Electronics Command, Fort Monmouth, NJ.
- Jackson, J. D. (1975). *Classical electrodynamics*. 2nd ed., John Wiley and Sons, Inc., New York.
- Klug, H. P., and Alexander, L. E. (1974). *X-ray diffraction procedures for polycrystalline and amorphous materials*. Wiley-Interscience, New York.
- Krumbein, W. C., and Sloss, L. L. (1963). *Stratigraphy and sedimentation*. 2nd ed., W. H. Freeman and Co, San Francisco, CA.
- Mackenzie, R. C. (1957). *The differential thermal investigation of clays*. Mineralogical Society, London.
- Mitchell, J. K. (1993). *Fundamentals of soil behavior*. 2nd ed., John Wiley and Sons, Inc., New York.
- Muir, J. (1954). "Dielectric loss in water films adsorbed by some silicate clay minerals," Chemical Society of London, *Faraday Transactions* 50, 249-254.
- Nelson, S. O., Lindroth, D. P., and Blake, R. L. (1989). "Dielectric properties of selected minerals at 1 to 22 GHz," *Geophysics* 54(10), 1344-1349.
- Olhoeft, G. R. (1985). "Low-frequency electrical properties," *Geophysics* 50(12), 2492-2503.
- _____. (1987). "Electrical properties from 10^{-3} to 10^{+9} Hz—physics and chemistry." *Proceedings of the 2nd international symposium on the physics and chemistry of porous media, Ridgefield, CT, October, 1986*. American Institute of Physics Conference Proceedings 154, 281-298.
- Olhoeft, G. R., and Capron, D. E. (1993). "Laboratory measurements of the radiofrequency electrical and magnetic properties of soils from near Yuma, Arizona," U. S. Geological Survey, Open File Report 93-701.
- _____. (1994). "Petrophysical causes of electromagnetic dispersion." *Proceedings of the fifth international conference on ground penetrating radar, Kitchener, Ontario, Canada, June, 1994*.

- Olhoeft, G. R., and King, T. V. V. (1991). "Mapping subsurface organic compounds noninvasively by their reactions with clays." *Proceedings of the U.S. Geological Survey Toxic Substance Hydrology Program, Monterey, CA, March, 1991*. U.S. Geological Survey Water Resources Investigation Report 91-4034.
- Ray, P. S. (1972). "Broadband complex refractive indices of ice and water," *Applied Optics* 11(8), 1836-1844.
- SAS Institute, Inc. (1988). *SAS/GRAPH User's Guide, Release 6.03 Edition*, Cary, NC.
- Smith, S. S. (1971). "Soil characterization by radio frequency electrical dispersion," Ph.D. diss., University of California, Davis.
- Smith, S. S., and Arulanandan, K. (1981). "Relationship of electrical dispersion to soil properties," *Journal of the Geotechnical Engineering Division*, ASCE 107(GT5), 591-604.
- Stratton, J. A. (1941). *Electromagnetic theory*. McGraw-Hill Book Company, New York.
- Ulaby, F. T., Bengal, T. H., Dobson, M. C., East, J. R., Garvin, J. B., and Evans, D. L. (1990). "Microwave dielectric properties of dry rocks," *IEEE Transactions on Geoscience and Remote Sensing* 28(3), 325-336.
- Walker, J. W. (1970). "Comparative study of the electromagnetic properties of some lateritic soils of Vietnam," Technical Report 3263, U.S. Army Electronics Command, Fort Monmouth, NJ.
- Walker, J. W., Pearce, D. C., and Hulse, W. H. (1969). "Soil conductivity and attenuation at selected tunnel simulation sites—Virginia, North Carolina and Texas," Technical Report 3109, U.S. Army Electronics Command, Fort Monmouth, NJ.
- Wang, J. R., and Schmugge, T. J. (1980). "An empirical model for the complex dielectric permittivity of soils as a function of water content," *IEEE Transactions on Geoscience and Remote Sensing* GE-18(4), 288-295.
- Wensink, W. A. (1993). "Dielectric properties of wet soils in the frequency range 1-3000 MHz," *Geophysical Prospecting* 41, 671-696.
- Zussman, J. (1967). *Physical methods in determinative mineralogy*. Academic Press Inc., London.

Appendix A

Data Collection and Data Presentation Software

The first two codes contained in this appendix are written in Hewlett Packard BASIC and are used in an interactive manner on an HP9000/362 data controller. The first code instructs an HP8510C Network Analyzer System to collect data, stores raw data (in the form of complex S-parameters) on the HP9000/362, and produces color, annotated graphs of the measured complex dielectric constant versus frequency. It is also used to retrieve existing data files for further study. The second code reads existing binary S-parameter files and writes ASCII files containing real and imaginary components of the complex dielectric constants to DOS-formatted diskettes.

The other codes are written in the SAS language (SAS Institute, Inc. 1988)¹ and are used for creating SAS data files and generating the plots contained in this report. The third listing is the program that creates the SAS data set that provides input to all other operations. The fourth listing is the code that plots data and calculated results versus frequency (Appendix B), and the fifth code plots data and calculated results versus moisture content (Appendix C).

¹ References cited in this appendix are located at the end of the main text.

Data Collection Program

```

10 | PROGRAM NAME: EPS12   3 MAR 94
20 |
30 | A MULTIPURPOSE CODE FOR 1) COLLECTING COAXIAL REFLECTION AND
40 | TRANSMISSION DATA AND CALCULATING BOTH THE REAL AND IMAGINARY
50 | PARTS OF THE COMPLEX DIELECTRIC CONSTANT, OR 2) DISPLAYING
60 | THE RESULTS OF PREVIOUSLY COLLECTED DATA
70 |
80 | USES THE HP9000 ACS ALGORITHM WITH SIGN ADJUSTMENTS
90 |
100 | OPTION BASE 1
110 | COMPLEX S11(1:801),S21(1:801),Rhs,Lhs,Rt,Eps
120 | INTEGER Preamble,Bytes,Hldrnum,Temper,Hldr_tmp,Temper_tmp
130 | DIM Ttl$(60),Secline$(80),Epsp(1:801),Epspp(1:801)
140 |
150 | GOSUB Init_vars
160 | GOSUB System_setup
170 | WHILE 1
180 |   GOSUB Main_menu
190 |   GOSUB Plot_data
200 |   PAUSE
210 |   INPUT "1) PRINTER    2) PLOTTER  : ",Plt$
220 |   IF Plt$ = "2" THEN
230 |     GOSUB Copy_data
240 |     GOSUB Plot_data
250 |   END IF
260 |   IF Plt$ = "1" THEN
270 |     GOSUB Plot_data
280 |     GOSUB Print_to_701
290 |     GOSUB Copy_data
300 |   END IF
310 |   PRINTER IS CRT
320 |   PLOTTER IS CRT,"INTERNAL"
330 |   CLEAR SCREEN
340 |   KEY LABELS ON
350 |   LOCAL @Nwa
360 | END WHILE
370 | STOP
380 | Main_menu: |*****
390 | REPEAT
400 |   PRINTER IS CRT
410 |   BEEP 2000,,2
420 |   CLEAR SCREEN
430 |   PRINT
440 |   PRINT
450 |   PRINT "  FILENAME : ",Namef$
460 |   PRINT "  _____ "
470 |   PRINT
480 |   PRINT
490 |   PRINT "  N,TAU = ",N1st,Tau
500 |   PRINT
510 |   PRINT
520 |   PRINT "  MAX & MIN VALUE OF EPSP = ",MAX(Epsp(*)),MIN(Epsp(*))
530 |   PRINT "  MAX & MIN VALUE OF EPSPP = ",MAX(Epspp(*)),MIN(Epspp(*))
540 |   PRINT
550 |   PRINT
560 |   PRINT
570 |   PRINT " 1) ENTER SAMPLE HEADER DATA    : ",Ttl$
580 |   PRINT " 2) CHANGE PLOT SCALE - MIN MAX TICK : ",Wmin,Wmax,Ytick

```

```

590 PRINT " 3) CHANGE ELECTRICAL DELAYS - S11 S21 :",Ed11,Ed21,"ps"
600 PRINT " 4) CHANGE CUT-OFF VALUE          :",lmrhs
610 PRINT " 5) CHANGE SAMPLE LENGTH          :",D,"cm"
620 PRINT " 6) FILE MANAGEMENT MENU - PERM RTRV  :",Dirperm$,Dirrecv$
630 PRINT " 7) MAKE ANOTHER MEASUREMENT"
640 PRINT " 8) EXIT PROGRAM"
650 Sel1=0
660 INPUT "SELECT : ",Sel1
670 SELECT Sel1
680 CASE 1
690 GOSUB Menu3
700 CASE 2
710 INPUT "INPUT PLOT SCALE MINIMUM, MAXIMUM, AND TICK MARK INCRE-
MENTS",Wmin,Wmax,Ytick
720 CASE 3
730 INPUT "INPUT ELECTRICAL DELAYS S11,S21 (ps) :",Ed11,Ed21
740 OUTPUT @Nwa;"S11:ELED";Ed11;"ps;"
750 OUTPUT @Nwa;"S21:ELED";Ed21;"ps;"
760 GOSUB Get_data
770 GOSUB Compute_eps
780 CASE 4
790 INPUT "INPUT THE CUTOFF VALUE :",lmrhs
800 GOSUB Get_data
810 GOSUB Compute_eps
820 CASE 5
830 INPUT "ENTER THE SAMPLE LENGTH (cm) ? ",D
840 GOSUB Get_data
850 GOSUB Compute_eps
860 CASE 6
870 GOSUB Menu2
880 CASE 7
890 GOSUB Get_newfile
900 GOSUB Get_data
910 GOSUB Compute_eps
920 CASE 8
930 STOP
940 END SELECT
950 UNTIL Sel1=0
960 RETURN
970 Menu2: |*****
980 REPEAT
990 CLEAR SCREEN
1000 PRINT
1010 PRINT " 1) RETRIEVE AN EXISTING FILE          :"
1020 PRINT " 2) CHANGE DIRECTORY NAME FOR EXISTING FILE :",Dirrecv$
1030 PRINT
1040 PRINT " 3) SAVE FILE IN PERMANENT DIRECTORY          :"
1050 PRINT " 4) CHANGE PERMANENT DIRECTORY NAME          :",Dirperm$
1060 PRINT " 5) CREATE PERMANENT DIRECTORY"
1070 PRINT " 6) DELETE FILE FROM PERMANENT DIRECTORY"
1080 PRINT
1090 PRINT " 7) CLEAR TEMPORARY DIRECTORY          : DATATEMP"
1100 Sel2=0
1110 INPUT "SELECT : ",Sel2
1120 SELECT Sel2
1130 CASE 1
1140 GOSUB Get_oldfile
1150 GOSUB Get_data
1160 GOSUB Compute_eps
1170 Sel2=0
1180 CASE 2
1190 CAT Dirroot$
1200 INPUT "ENTER DIRECTORY NAME FOR EXISTING FILE :",Dirrecv$
1210 CASE 3
1220 GOSUB Copy_data

```

```

1230 CASE 4
1240 CAT Dirroot$
1250 LINPUT "ENTER PERMANENT DIRECTORY NAME :",Dirperm$
1260 CASE 5
1270 CAT Dirroot$
1280 LINPUT "ENTER PERMANENT DIRECTORY NAME :",Dirperm$
1290 ON ERROR GOTO 1270
1300 CREATE DIR Dirroot$&"\"&Dirperm$
1310 CREATE DIR Dirroot$&"\"&Dirperm$&"RAW"
1320 OFF ERROR
1330 CASE 6
1340 CAT Dirroot$&"\"&Dirperm$
1350 LINPUT "ENTER FILENAME TO DELETE :",Del$
1360 ON ERROR GOTO 1340
1370 PURGE Dirroot$&"\"&Dirperm$&"\"&Del$
1380 PURGE Dirroot$&"\"&Dirperm$&"RAW\"&Del$&"R"
1390 OFF ERROR
1400 CASE 7
1410 CAT Dirroot$&"\"&Dirtemp$
1420 LINPUT "CLEAR THIS DIRECTORY (Y/N) : ",Del$
1430 IF Del$="Y" THEN
1440 PURGE Dirroot$&"\"&Dirtemp$&"RAW/"
1450 PURGE Dirroot$&"\"&Dirtemp$&"/*"
1460 CREATE DIR Dirroot$&"\"&Dirtemp$&"RAW"
1470 END IF
1480 END SELECT
1490 UNTIL Sel2=0
1500 RETURN
1510 Menu3: !*****
1520 REPEAT
1530 CLEAR SCREEN
1540 PRINT
1550 PRINT " HEADER DATA :",Ttl$
1560 PRINT " _____ "
1570 PRINT
1580 PRINT " 1) SAMPLE          :",Samp$
1590 PRINT " 2) HOLDER NUMBER     :",Hldrnum
1600 PRINT " 3) TEMPERATURE (DEGREES C) :",Temper
1610 PRINT
1620 PRINT " 4) INPUT OWN TITLE "
1630 Sel3=0
1640 INPUT "SELECT : ",Sel3
1650 SELECT Sel3
1660 CASE 1
1670 LINPUT "INPUT SAMPLE LABEL :",Samp$
1680 CASE 2
1690 INPUT "INPUT HOLDER NUMBER :",Hldrnum
1700 CASE 3
1710 INPUT "INPUT TEMPERATURE (Degrees C) :",Temper
1720 CASE 4
1730 LINPUT "INPUT A TITLE FOR THE PLOT :",Ttl$
1740 Sel3=0
1750 END SELECT
1760 IF Sel3<>0 THEN Ttl$="Sample "&Samp$&" - Holder#"&VAL$(Hldrnum)&" - "&VAL$(Temper)&" DegC"
1770 UNTIL Sel3=0
1780 RETURN
1790 Get_newfile: !*****
1800 I
1810 I PREPARE TO MAKE A NEW SET OF MEASUREMENTS
1820 I
1830 REPEAT
1840 Dup_filename=0
1850 Fd$=DATE$(TIMEDATE)
1860 Ft$=TIME$(TIMEDATE)
1870 Nameold$=Namef$

```

```

1880 Namef$ = Fd$(1,2)&UPC$(Fd$(4,4))&UPC$(Fd$(6,6))&Fd$(11,11)&Ft$(1,2)&Ft$(4,5)
1890 Namer$ = Namef$&"R"
1900 IF Nameold$ = Namef$ THEN
1910 PRINT
1920 PRINT "DUPLICATE FILES EXIST -- PLEASE WAIT !!!"
1930 WAIT 5
1940 Dup_filename = 1
1950 END IF
1960 UNTIL Dup_filename = 0
1970 CLEAR SCREEN
1980 PRINT
1990 PRINT " ***** MAKING 8510 MEASUREMENT *****"
2000 PRINT
2010 PRINT " PLEASE WAIT !!!!!"
2020 OUTPUT @Nwa;"WAIT;SING;"
2030 OUTPUT @Nwa;"WAIT;S11:ELED";Ed11;"ps;"
2040 OUTPUT @Nwa;"WAIT;S21:ELED";Ed21;"ps;"
2050 OUTPUT @Nwa;"WAIT;S11;FORM3;OUTPDATA;"
2060 ENTER @Nwa_data;Preamble;Bytes
2070 M=Bytes/16
2080 REDIM S11(1:M),S21(1:M)
2090 ENTER @Nwa_data;S11(*)
2100 OUTPUT @Nwa;"WAIT;S21;FORM3;OUTPDATA;"
2110 ENTER @Nwa_data;Preamble;Bytes;S21(*)
2120 CREATE BDAT Dirroot$&"\"&Dirtemp$&"\"&Namef$,1,Hdr_lgth+(Bytes*2)
2130 ASSIGN @F1 TO Dirroot$&"\"&Dirtemp$&"\"&Namef$;FORMAT OFF
2140 OUTPUT @F1 USING "10A";Namef$,Samp$
2150 OUTPUT @F1;D,Hldnum,Temper,Ed11,Ed21,lmrhs,Preamble,Bytes
2160 OUTPUT @F1;S11(*),S21(*)
2170 ASSIGN @F1 TO *
2180 OUTPUT @Nwa;"WAIT;S11;FORM3;OUTPRAW1;"
2190 ENTER @Nwa_data;Preamble;Bytes,S11(*)
2200 OUTPUT @Nwa;"WAIT;S21;FORM3;OUTPRAW2;"
2210 ENTER @Nwa_data;Preamble;Bytes;S21(*)
2220 CREATE BDAT Dirroot$&"\"&Dirtemp$&"RAW\"&Namer$,1,Hdr_lgth+(Bytes*2)
2230 ASSIGN @F1 TO Dirroot$&"\"&Dirtemp$&"RAW\"&Namer$;FORMAT OFF
2240 OUTPUT @F1 USING "10A";Namer$,Samp$
2250 OUTPUT @F1;D,Hldnum,Temper,Ed11,Ed21,lmrhs,Preamble,Bytes
2260 OUTPUT @F1;S11(*),S21(*)
2270 ASSIGN @F1 TO *
2280 RETURN
2290 Get_oldfile: !*****
2300 !
2310 ! RETRIEVE AN EXISTING DATA FILE FOR FURTHER ANALYSIS
2320 !
2330 CAT Dirroot$&"\"&Dirrecv$
2340 BEEP 4000,.2
2350 INPUT "WHAT IS THE NAME OF THE EXISTING DATA FILE?",Namef$
2360 ON ERROR GOTO 2330
2370 ASSIGN @F1 TO Dirroot$&"\"&Dirrecv$&"\"&Namef$;FORMAT OFF
2380 OFF ERROR
2390 ENTER @F1 USING "10A";Nameold$,Samp$
2400 ENTER @F1;D,Hldnum,Temper,Ed11,Ed21,lmrhs,Preamble,Bytes
2410 Ttl$ = "Sample "&Samp$&" - Holder# "&VAL$(Hldnum)&" - "&VAL$(Temper)&"
DegC"
2420 M=Bytes/16
2430 PRINT
2440 PRINT "NUMBER OF DATA POINTS IN FILE =",M
2450 REDIM S11(1:M),S21(1:M)
2460 ENTER @F1;S11(*),S21(*)
2470 ASSIGN @F1 TO *
2480 OUTPUT @Nwa;"WAIT;S11:ELED";Ed11;"ps;"
2490 OUTPUT @Nwa;"WAIT;S21:ELED";Ed21;"ps;"
2500 Last=LEN(Namef$)
2510 IF Namef$(Last,Last)="R" THEN

```

```

2520  Namer$ = Namef$
2530  Namef$[Last,Last] = ""
2540  Namef$ = TRIM$(Namef$)
2550  PRINT
2560  PRINT "    LOADING RAW DATA FILE: ",Namer$
2570  PRINT "MUST LOAD CORRESPONDING CALIBRATION FILE ON 8510"
2580  PRINT
2590  PRINT "    --- PRESS CONTINUE WHEN READY ----"
2600  PAUSE
2610  PRINT
2620  PRINT "LOADING RAW DATA FILE ....."
2630  OUTPUT @Nwa;"WAIT;HOLD;S11;FORM3;INPURAW1;"
2640  OUTPUT @Nwa_data;Preamble,Bytes,S11(*)
2650  OUTPUT @Nwa;"WAIT;S21;FORM3;INPURAW2;"
2660  OUTPUT @Nwa_data;Preamble,Bytes,S21(*)
2670  ELSE
2680  OUTPUT @Nwa;"WAIT;HOLD;S11;FORM3;INPUDATA;"
2690  OUTPUT @Nwa_data;Preamble,Bytes,S11(*)
2700  OUTPUT @Nwa;"WAIT;S21;FORM3;INPUDATA;"
2710  OUTPUT @Nwa_data;Preamble,Bytes,S21(*)
2720  END IF
2730  ASSIGN @F1 TO *
2740  RETURN
2750  Get_data: !*****
2760  ! ESTIMATE THE INITIAL 'N' VALUE FOR COMPUTING THE CORRECT PHASE ANGLE
2770  PLOTTER IS CRT,"INTERNAL"
2780  OUTPUT @Nwa;"WAIT;S11;WAIT;AUTO;"
2790  OUTPUT @Nwa;"S21;DELA;"
2800  OUTPUT @Nwa;"WAIT;MARK1";Fi;"
2810  OUTPUT @Nwa;"OUTPMARK;"
2820  ENTER @Nwa;Tau,Dummy
2830  N=INT(Tau*Fi)
2840  IF N<0 THEN N=0
2850  IF N>99 THEN N=99
2860  OUTPUT @Nwa;"WAIT;REIP;WAIT;AUTO;ENTO"
2870  !
2880  ! LOAD THE DATA INTO COMPLEX ARRAYS ON THE 330 FOR FURTHER PROCESSING
2890  !
2900  OUTPUT @Nwa;"WAIT;S11;FORM3;OUTPFORM;"
2910  ENTER @Nwa_data;Preamble;Bytes;S11(*)
2920  OUTPUT @Nwa;"WAIT;S21;FORM3;OUTPFORM;"
2930  ENTER @Nwa_data;Preamble;Bytes;S21(*)
2940  RETURN
2950  Compute_eps: !*****
2960  ! CALCULATE THE COMPLEX DIELECTRIC CONSTANT
2970  C=3.E+10
2980  RAD
2990  PRINTER IS CRT
3000  N1st=N
3010  Anglel=0.
3020  FOR I=1 TO Np
3030  Rhs=(1+S21(I))*S21(I)-S11(I)*S11(I)/(2*S21(I))
3040  IF ABS(Rhs)>1.E+6 THEN GOTO 3220
3050  IF ABS(IMAG(Rhs))<Imrhs THEN Rhs=CMPLX(REAL(Rhs),0)
3060  Lhs=ACS(Rhs)
3070  Lhs=CMPLX(REAL(Lhs),ABS(IMAG(Lhs)))
3080  IF IMAG(Rhs)<0 THEN Lhs=CMPLX(2*PI-REAL(Lhs),IMAG(Lhs))
3090  Angle=REAL(Lhs)
3100  IF I=1 THEN GOTO 3130
3110  IF ABS(Angle-Anglel)<4.5 THEN GOTO 3130
3120  N=N+1
3130  Lhs=CMPLX(REAL(Lhs)+N*2*PI,IMAG(Lhs))
3140  ! PRINT USING "DDDD,5(2X,SDDD.DDD),2X,DDD";I,Rhs,Lhs,Angle,N
3150  Anglel=Angle
3160  Rhs=Lhs*Lhs
3170  Radfreq=2*PI*(Fi+(I-1)*(Ff-Fi)/(Np-1))

```

```

3180 Fact=C/(Radfreq*D)
3190 Epsp(I)=Fact*Fact*REAL(Rhs)
3200 Epspp(I)=Fact*Fact*IMAG(Rhs)
3210 I PRINT Epsp(I),Epspp(I)
3220 NEXT I
3230 RETURN
3240 Plot_data: I*****
3250 I
3260 I PLOT THE RESULTS
3270 I
3280 GINIT
3290 PRINTER IS CRT
3300 PLOTTER IS CRT,"INTERNAL"
3310 IF Plt$="2" THEN
3320 PRINTER IS 705
3330 PLOTTER IS 705,"HPGL"
3340 END IF
3350 GRAPHICS ON
3360 CLEAR SCREEN
3370 Plt$="0"
3380 X_gdu_max=100*MAX(1,RATIO)
3390 Y_gdu_max=100*MAX(1,1/RATIO)
3400 Xmax=X_gdu_max*1.0
3410 Ymax=Y_gdu_max*1.0
3420 LORG 6
3430 CSIZE 3.0
3440 PEN 6
3450 MOVE Xmax*.5,Ymax
3460 LABEL Ttl$
3470 Secline$="FILE: "&Namef$&" SAMPLGTH="&VAL$(D)&"cm DE-
LAYS(S11,S21)="&VAL$(Ed11)&","&VAL$(Ed21)&"ps"
3480 MOVE Xmax*.5,Ymax*.97
3490 LABEL Secline$
3500 Secline$="Imrhs="&VAL$(Imrhs)&" N="&VAL$(N1st)&" Tau="&VAL$(Tau/1.0E-12)-
&"ps "&Dirperm$
3510 MOVE Xmax*.5,Ymax*.94
3520 LABEL Secline$
3525 MOVE Xmax*.5,.51*Ymax
3526 DIM Spar$(80)
3527 Spar$="S11 at 45 MHz="&VAL$(REAL(S11(1)))&","&VAL$(IMAG(S11(1)))
3528 LABEL Spar$
3529 MOVE Xmax*.5,.48*Ymax
3531 Spar$="S21 at 45 MHz="&VAL$(REAL(S21(1)))&","&VAL$(IMAG(S21(1)))
3532 LABEL Spar$
3533 DEG
3540 LDIR 90
3550 MOVE Xmax*.04,Ymax*.75
3560 LABEL "EPS"
3570 MOVE Xmax*.04,Ymax*.3
3580 LABEL "EPS'"
3590 LORG 4
3600 LDIR 0
3610 KEY LABELS OFF
3620 MOVE Xmax*.5,0
3630 LABEL "FREQUENCY (GHz)"
3640 VIEWPORT .15*Xmax,.9*Xmax,.55*Ymax,.90*Ymax
3650 GOSUB Plot_axes
3660 FOR I=1 TO Np
3670 IF ABS(Epsp(I))<.001 THEN GOTO 3710
3680 X=LGT(Fi+(I-1)*(Ff-Fi)/(Np-1))
3690 PEN 2
3700 PLOT X,Epsp(I)
3710 NEXT I
3770 VIEWPORT .15*Xmax,.9*Xmax,.1*Ymax,.45*Ymax
3780 GOSUB Plot_axes

```

```

3790 FOR I=1 TO Np
3800 X=LGT(Fi + (I-1)*(Ff-Fi)/(Np-1))
3810 PEN 2
3820 PLOT X,Epspp(I)
3830 NEXT I
3840 RETURN
3850 Plot_axes: !*****
3860 WINDOW 7,11,Wmin,Wmax
3870 PEN 5
3880 AXES 1,Ytick,7,0,1,1,2
3890 LINE TYPE 4,2
3900 GRID 1,Ytick,7,0,1,1,2
3910 LINE TYPE 1,5
3920 CLIP OFF
3930 CSIZE 2.5,.5
3940 LORG 6
3950 FOR I=8 TO 11
3960 MOVE I,-.2*Ytick
3970 LABEL USING "#,K";(10^I)/1.E+9
3980 FOR J=2 TO 9
3990 Jtick=LGT(J)
4000 MOVE I-1+Jtick,Wmin
4010 PEN 5
4020 PLOT I-1+Jtick,.04*(Wmax-Wmin),-1
4030 NEXT J
4040 NEXT I
4050 LORG 8
4060 FOR I=Wmin TO Wmax STEP Ytick
4070 MOVE 6.85,I
4080 LABEL USING "#,SDDD.D";I
4090 NEXT I
4100 PENUP
4110 RETURN
4120 Print_to_701: !*****
4130 ! THESE 4 LINES MARKS START OF NOISE & PRINTS 8510 SCREEN TO XL300.
4140 OUTPUT @Nwa;"WAIT;OUTPERRO;"
4150 ENTER @Nwa_data;Preamble
4160 OUTPUT @Nwa;"WAIT;S12;WAIT;AUTO;WAIT;MARK1;TARV -80;MARKTARG;"
4170 OUTPUT @Nwa;"WAIT;ENTO;PRINALL;"
4180 LOADSUB ALL FROM "/UTILITIES/GDUMP_C"
4190 Gdump_colored(CRT,701,"NORMAL",180,"OFF")
4200 PRINTER IS 701
4210 PRINT CHR$(12)
4220 PRINTER IS CRT
4230 Plt$="0"
4240 BEEP 2000,.2
4250 PRINT "PRINT COMPLETE"
4260 RETURN
4270 Copy_data: !*****
4280 OUTPUT @Nwa;"WAIT;S11;FORM3;OUTPDATA;"
4290 ENTER @Nwa_data;Preamble,Bytes,S11(*)
4300 OUTPUT @Nwa;"WAIT;S21;FORM3;OUTPDATA;"
4310 ENTER @Nwa_data;Preamble,Bytes,S21(*)
4320 Namer$=Namef$&"R"
4330 ON ERROR GOTO 4360
4340 PURGE Dirroot$&"/"&Dirperm$&"/"&Namef$
4350 PURGE Dirroot$&"/"&Dirperm$&"/RAW/"&Namer$
4360 OFF ERROR
4370 CREATE BDAT Dirroot$&"/"&Dirperm$&"/"&Namef$,1,Hdr_lgth+(Bytes*2)
4380 ASSIGN @F1 TO Dirroot$&"/"&Dirperm$&"/"&Namef$;FORMAT OFF
4390 OUTPUT @F1 USING "10A";Namef$,Samp$
4400 OUTPUT @F1;D,Hldnum,Temp,Ed11,Ed21,Imrhs,Preamble,Bytes
4410 OUTPUT @F1;S11(*),S21(*)
4420 OUTPUT @Nwa;"WAIT;S11;FORM3;OUTPRAW1;"
4430 ENTER @Nwa_data;Preamble,Bytes,S11(*)
4440 OUTPUT @Nwa;"WAIT;S21;FORM3;OUTPRAW2;"

```



```

4450 ENTER @Nwa_data:Preamble,Bytes,S21(*)
4460 CREATE BDAT Dirroot$&"/" &Dirperm$&"/RAW/" &Namer$,1,Hdr_lgth+(Bytes*2)
4470 ASSIGN @F1 TO Dirroot$&"/" &Dirperm$&"/RAW/" &Namer$;FORMAT OFF
4480 OUTPUT @F1 USING "10A";Namer$,Samp$
4490 OUTPUT @F1;D,Hldnum,Temper,Ed11,Ed21,lmrhs,Preamble,Bytes
4500 OUTPUT @F1;S11(*),S21(*)
4510 ASSIGN @F1 TO "
4520 RETURN
4530 System_setup: !*****
4540 WILDCARDS DOS
4550 REDIM S11(1:Num_data_pts),S21(1:Num_data_pts)
4560 FOR I=1 TO Num_data_pts
4570   S21(I)=1.0
4580 NEXT I
4590 ASSIGN @Nwa TO 716
4600 ASSIGN @Nwa_data TO 716;FORMAT OFF
4610 LOCAL @Nwa
4620 PRINTER IS CRT
4630 GINIT
4640 PLOTTER IS CRT,"INTERNAL"
4650 GRAPHICS ON
4660 ASSIGN @Hpib TO 7
4670 REMOTE @Hpib
4680 ABORT @Hpib
4690 CLEAR @Nwa
4700 CLEAR 717
4710 CLEAR SCREEN
4720 BEEP 2000,.2
4730 PRINT "NUMBER OF DATA POINTS =",Num_data_pts
4740 INPUT "ENTER INSTRUMENT STATE NUMBER TO RECALL :",Instr_num
4750 IF Instr_num<>0 THEN
4760   PRINT
4770   PRINT "WAIT - MAKING INITIAL MEASUREMENT FOR INST#",Instr_num
4780   OUTPUT @Nwa;"WAIT;RECA"&VAL$(Instr_num)&";"
4790   OUTPUT @Nwa;"WAIT;S11;ELED";Ed11;"ps;"
4800   OUTPUT @Nwa;"WAIT;S21;ELED";Ed21;"ps;WAIT;ENTO;"
4810   OUTPUT @Nwa;"WAIT;SING;WAIT;HOLD;"
4820 END IF
4830 RETURN
4840 Init_vars: !*****
4850 Num_data_pts=801   ! # OF 8510 DATA POINTS
4860 PRINT "NUMBER OF DATA POINTS IS",Num_data_pts
4870 INPUT "INPUT A NEW NUMBER OF POINTS",Num_data_pts
4880 Samp$="AIR"       ! SAMPLE NAME
4890 PRINT "MEASUREMENT DESCRIPTION IS",Samp$
4900 INPUT "INPUT A NEW DESCRIPTION",Samp$
4910 D=10.0           ! HOLDER LENGTH
4920 PRINT "HOLDER LENGTH IS",D," CM"
4930 INPUT "INPUT A NEW HOLDER LENGTH",D
4940 Hldnum=2          ! HOLDER NUMBER
4950 PRINT "HOLDER NUMBER IS",Hldnum
4960 INPUT "INPUT A NEW HOLDER NUMBER",Hldnum
4970 Temper=22         ! TEMPERATURE
4980 PRINT "SAMPLE TEMPERATURE IS",Temper," DEG C"
4990 INPUT "INPUT A NEW SAMPLE TEMPERATURE",Temper
5000 Ed11=270.0       ! S11 DELAY
5010 PRINT "S11 DELAY IS",Ed11," PICOSECONDS"
5020 INPUT "INPUT A NEW S11 DELAY",Ed11
5030 Ed21=270.0       ! S21 DELAY
5040 PRINT "S21 DELAY IS",Ed21," PICOSECONDS"
5050 INPUT "INPUT A NEW S21 DELAY",Ed21
5060 lmrhs=0.          ! CUT-OFF VALUE
5070 Ttl$="Sample "&Samp$&" - Holder#"&VAL$(Hldnum)&" - "&VAL$(Temper)&"
    DegC"           ! TITLE ON PLOTS
5080 Hdr_string1=10    ! EVEN NUMBER OF CHARS

```

```

5090 Hdr_string2=10      I EVEN NUMBER OF CHARS
5100 Hdr_strings=(4+Hdr_string1)+(4+Hdr_string2)
5110 Hdr_integers=4      I # OF INTEGERS IN HEADER
5120 Hdr_floats=4        I # OF FLOATS IN HEADER
5130 Hdr_lgth=Hdr_strings+(Hdr_integers*2)+(Hdr_floats*8)
5140 Wmin=0              I MINIMUM PLOT SCALE
5150 Wmax=2.0            I MAXIMUM PLOT SCALE
5160 Ytick=.5            I TICK MARKS
5170 Dirroot$="/EPS/DATA" I ROOT DIRECTORY OF DATA
5180 Dirperm$="PLOTS"     I PERMANENT DIRECTORY, SAVED WHEN PLOTTED
5190 Dirrecv$="DATATEMP" I DIRECTORY OF EXISTING FILES TO RECEIVE
5200 Dirtemp$="DATATEMP" I ALL MEASUREMENTS MADE SAVED HERE
5210 Fi=4.5E+7           I START FREQUENCY
5220 Ff=2.65E+10         I STOP FREQUENCY
5230 Np=Num_data_pts     I # OF 8510 DATA POINTS
5240 RETURN
5250 Errs: PRINT "*****"
5260 PRINT " UNEXPECTED ERROR #",ERRN," AT LINE#",ERRLN
5270 PRINT " PRESS CONTINUE OR RESET"
5280 PAUSE
5290 ERROR RETURN
5300 END

```

Program for Producing ASCII Data Files

```

10  I PROGRAM MAKEASCII - THIS PROGRAM READS S11 & S21 CORRECTED
20  I          DATA FILES, CALCULATES EP' & EP'', AND
30  I          STORES DATA IN ASCII TO DOS FLOPPY DISK.
40  OPTION BASE 1
50  COMPLEX S11(1:801),S21(1:801),Rhs,Lhs,Rt,Eps
60  INTEGER Preamble,Bytes,Hldnum,Temper,Phscorr,Stat1,Stat2
70  REAL Fq,Fq1,Fq2,Fqstep,Fq1lg,Fq2lg,Steplg
80  DIM Tt$(60),Secline$(60),Epsp(1:801),Epspp(1:801),Idx(1:801),Ep(1:801),Epp(1:801),Fr-
eq(1:801)
90  I
100 WILDCARDS DOS
110 Instr_num=1      I INSTRUMENT STATE NUMBER
120 Num_data_pts=801 I NUMBER OF DATA POINTS
130 IF Num_data_pts<>801 THEN
140   REDIM S11(1:Num_data_pts),S21(1:Num_data_pts)
150   REDIM Epsp(1:Num_data_pts),Epspp(1:Num_data_pts)
160 END IF
170 D=10.0
180 Ed11=270
190 Ed21=270
200 lmrhs=0
210 Fi=4.5E+7
220 Ff=2.65E+10
230 Np=Num_data_pts
240 ASSIGN @Nwa TO 716
250 ASSIGN @Nwa_data TO 716;FORMAT OFF
260 LOCAL @Nwa
270 PRINTER IS CRT
280 GINIT
290 PLOTTER IS CRT,"INTERNAL"
300 GRAPHICS ON
310 Total_pts=100
320 REDIM Idx(1:Total_pts),Ep(1:Total_pts),Epp(1:Total_pts),Freq(1:Total_pts)
330 Fq1=1.00399375E+9
340 Fq2=2.65E+10
350 Fqstep=(Ff-Fi)/(Num_data_pts-1)
360 Idx_start=(Fq1-Fi)/Fqstep+1
370 Ptslg=Total_pts-Idx_start
380 Fq1lg=LGT(Fq1)
390 Fq2lg=LGT(Fq2)
400 Steplg=(Fq2lg-Fq1lg)/Ptslg
410 FOR I=1 TO Idx_start
420   Idx(I)=I
430 NEXT I
440 J=Idx_start
450 K=Idx_start+1
460 FOR Fq=Fq1 TO Fq2 STEP Fqstep
470   J=J+1
480   IF (10^(Fq1lg+(Steplg*(K-Idx_start))))<Fq THEN
490     Idx(K)=J-1
500     K=K+1
510   END IF
520 NEXT Fq
530 I
540 ASSIGN @Hpib TO 7
550 REMOTE @Hpib
560 ABORT @Hpib
570 CLEAR @Nwa
580 CLEAR 717

```

```

590 OUTPUT @Nwa;"WAIT;RECA"&VAL$(Instr_num)&";" I RECALL INSTRUMENT STATE
600 |-----
610 CLEAR SCREEN
620 LINPUT "ENTER FILENAME FOR DATA TO DISKETTE : ",Ascname$
621 LINPUT "ENTER FILENAME FOR FREQUENCIES TO DISKETTE : ",Frqname$
630 CREATE Ascname$&":DOS,1400",1
640 ASSIGN @F2 TO Ascname$&":DOS,1400";FORMAT OFF
641 CREATE Frqname$&":DOS,1400",1
642 ASSIGN @F3 TO Frqname$&":DOS,1400";FORMAT OFF
650 Cntsaved=0
660 |-----
670 BEEP 4000,.2
680 CLEAR SCREEN
690 CAT "/EPS/DATA"
700 LINPUT "ENTER DIRECTORY NAME FROM ABOVE : ",Dirname$
710 CLEAR SCREEN
720 ON ERROR GOTO 1470
730 CAT "/EPS/DATA/"&Dirname$;NO HEADER,COUNT Num_files
740 OFF ERROR
770 ALLOCATE Filebuffer$(1:Num_files)[20]
780 CAT "/EPS/DATA/"&Dirname$ TO Filebuffer$(*);NAMES
781 MAT SORT Filebuffer$(*)
790 CLEAR SCREEN
791 PRINT USING "20A,/" ;Filebuffer$(*)
796 PRINT "PRESS CONTINUE"
797 PAUSE
800 FOR I=1 TO 2
810 IF I=2 THEN PRINTER IS 701
820 PRINT USING "/,@,#"
830 PRINT USING "14A,#" ;Ascname$
840 PRINT "DIR      FILE      SAMP  LGTH  #    MC    TMP"
850 PRINT "-----"
860 PRINTER IS CRT
870 NEXT I
880 FOR Cnt=1 TO Num_files
890 BEEP 2000,.2
900 Fmt1: IMAGE 2D,2X,4A,2D,4X,12A,14A,#
910 PRINTER IS 701
920 PRINT USING Fmt1;Cnt,"OF",Num_files,Dirname$,Filebuffer$(Cnt)
930 PRINTER IS CRT
940 PRINT USING Fmt1;Cnt,"OF",Num_files,Dirname$,Filebuffer$(Cnt)
941 IF Filebuffer$(Cnt)[1,3]="RAW" THEN GOTO 2100
950 I LINPUT "CONVERT FILE (N=NO Q=QUIT B=BACK) ? ",Sel$
960 I IF Sel$="Q" THEN STOP
970 I IF Sel$="N" OR Sel$="B" THEN
980 I PRINTER IS 701
990 I PRINT
1000 I PRINTER IS CRT
1010 I PRINT
1020 I IF Sel$="B" THEN Cnt=Cnt-2
1030 I GOTO 2100
1040 I END IF
1050 Cntsaved=Cntsaved+1
1060 Namef$=Filebuffer$(Cnt)
1070 ON ERROR GOTO Errs
1080 ASSIGN @F1 TO "/EPS/DATA/"&Dirname$&"/"&Namef$;FORMAT OFF
1090 OFF ERROR
1091 Last_samp$=Samp$
1100 ENTER @F1 USING "10A";Namef$,Samp$
1110 ENTER @F1;D,Hldnum,Temp,Ed11,Ed21,Imrhs,Preamble,Bytes
1120 M=Bytes/16
1130 REDIM S11(1:M),S21(1:M)
1140 ENTER @F1;S11(*),S21(*)
1150 ASSIGN @F1 TO *
1160 Fmt4: IMAGE 8A,2D.D,#
1170 PRINTER IS 701

```

```

1180 PRINT USING Fmt4;Samp$,D
1190 PRINTER IS CRT
1200 PRINT USING Fmt4;Samp$,D
1201 BEEP 3000,.2
1202 INPUT "MC?",Mc
1210 IF D=5.0 OR Samp$(1,3)="AIR" THEN
1220   Mc=0
1221   Last_samp_air=1
1230 ELSE
1240 IF Samp$(1,5)="WATER" OR Samp$(1,3)="H2O" THEN
1250   Mc=100
1260 ELSE
1261 IF Last_samp_air OR Last_samp$ <> Samp$ THEN
1263   BEEP 3000,.2
1300   INPUT "MC FOR 1.4cm?",Mc1
1303   IF Mc1=999 THEN STOP
1310   INPUT "MC FOR 9.7cm?",Mc2
1341   END IF
1343   IF D=1.4 OR D=1.5 THEN Mc=Mc1
1345   IF D=9.7 OR D=10.0 THEN Mc=Mc2
1350   END IF
1351   Last_samp_air=0
1360   END IF
1370 Fmt2: IMAGE 6D,7D.D,7D,4D
1380 PRINTER IS 701
1390 PRINT USING Fmt2;Hldnum,Mc,Temper,Cntsaved
1400 PRINTER IS CRT
1410 PRINT USING Fmt2;Hldnum,Mc,Temper,Cntsaved
1420 OUTPUT @Nwa;"WAIT;HOLD;S11;FORM3;INPUdata;"
1430 OUTPUT @Nwa_data;Preamble,Bytes,S11(*)
1440 OUTPUT @Nwa;"WAIT;S21;FORM3;INPUdata;"
1450 OUTPUT @Nwa_data;Preamble,Bytes,S21(*)
1460 |
1470 | ESTIMATE THE INITIAL 'N' VALUE FOR COMPUTING THE CORRECT PHASE ANGLE
1480 |
1490 PLOTTER IS CRT,"INTERNAL"
1500 OUTPUT @Nwa;"WAIT;S11;WAIT;AUTO;"
1510 OUTPUT @Nwa;"S21;DELA;"
1520 OUTPUT @Nwa;"WAIT;MARK1";Fi;"
1530 OUTPUT @Nwa;"OUTPMARK;"
1540 ENTER @Nwa;Tau,Dummy
1550 N=INT(Tau*Fi)
1560 IF N<0 THEN N=0
1570 IF N>99 THEN N=99
1580 OUTPUT @Nwa;"WAIT;REIP;WAIT;AUTO;ENTO"
1590 |
1600 | LOAD THE DATA INTO COMPLEX ARRAYS ON THE 330 FOR FURTHER PROCESSING
1610 |
1620 OUTPUT @Nwa;"WAIT;S11;FORM3;OUTPFORM;"
1630 ENTER @Nwa_data;Preamble;Bytes;S11(*)
1640 OUTPUT @Nwa;"WAIT;S21;FORM3;OUTPFORM;"
1650 ENTER @Nwa_data;Preamble;Bytes;S21(*)
1660 |
1670 | CALCULATE THE COMPLEX DIELECTRIC CONSTANT
1680 |
1690 C=3.E+10
1700 RAD
1710 PRINTER IS CRT
1720 N1st=N
1730 Angle1=0.
1731 PRINT "WARNING !!!!!!!!!!!!!!!"
1732 PRINT "RESETTING SAMPLE LENGTHS TO 1.4 cm AND 9.7 cm"
1733 IF D=1.5 THEN D=1.4
1734 IF D=10. THEN D=9.7
1740 FOR I=1 TO Np

```

```

1750 Rhs = (1 + S21(I) * S21(I) - S11(I) * S11(I)) / (2 * S21(I))
1760 IF ABS(Rhs) > 1.E + 6 THEN GOTO 1940
1770 IF ABS(IMAG(Rhs)) < Imrhs THEN Rhs = CMPLX(REAL(Rhs), 0)
1780 Lhs = ACS(Rhs)
1790 Lhs = CMPLX(REAL(Lhs), ABS(IMAG(Lhs)))
1800 IF IMAG(Rhs) < 0 THEN Lhs = CMPLX(2 * PI - REAL(Lhs), IMAG(Lhs))
1810 Angle = REAL(Lhs)
1820 IF I = 1 THEN GOTO 1850
1830 IF ABS(Angle - AngleI) < 4.5 THEN GOTO 1850
1840 N = N + 1
1850 Lhs = CMPLX(REAL(Lhs) + N * 2 * PI, IMAG(Lhs))
1860 I PRINT USING "DDDD,5(2X,SDDD.DDD),2X,DDD"; I, Rhs, Lhs, Angle, N
1870 AngleI = Angle
1880 Rhs = Lhs * Lhs
1890 Radfreq = 2 * PI * (Fi + (I - 1) * (Ff - Fi) / (Np - 1))
1900 Fact = C / (Radfreq * D)
1910 Epsp(I) = Fact * Fact * REAL(Rhs)
1920 Epspp(I) = Fact * Fact * IMAG(Rhs)
1930 I PRINT I, Epsp(I), Epspp(I)
1940 NEXT I
1950 I
1960 FOR I = 1 TO Total_pts
1962 Freq(I) = (Fi + ((Idx(I) - 1) * Fqstep)) / 1.0E + 9
1970 Ep(I) = Epsp(Idx(I))
1980 Epp(I) = Epspp(Idx(I))
1990 IF I = 1 THEN GOTO 2020
1991 IF Ep(I) > 999 THEN Ep(I) = 999
1992 IF Epp(I) > 999 THEN Epp(I) = 999
2000 I IF ABS(Ep(I) - Ep(I - 1)) > 2 THEN Ep(I) = 999
2010 I IF ABS(Epp(I) - Epp(I - 1)) > 2 THEN Epp(I) = 999
2020 I
2030 I PRINTER IS 701
2040 I PRINT Idx(I), I, Ep(I), Epp(I)
2050 I PRINTER IS CRT
2060 NEXT I
2070 Fmt3: IMAGE K, /, K, /, K, /, K, /, K, /, K
2080 OUTPUT @F2 USING Fmt3; Name$, Samp$, D, Hldnum, Mc, Temper
2090 OUTPUT @F2 USING "3D.DD, /"; Ep(*), Epp(*)
2095 IF Cntsavd = 1 THEN OUTPUT @F3 USING "2D.3D, /"; Freq(*)
2100 NEXT Cnt
2110 PRINT
2120 PRINT "FINISHED DIRECTORY ", Dirname$, " PRESS CONTINUE FOR MORE DIRECTO-
RIES"
2130 PAUSE
2140 DEALLOCATE Filebuffer$(*)
2150 GOTO 670
2160 STOP
2170 Errs: I
2180 PRINT "*****"
2190 IF ERRN = 54 THEN
2200 PRINT " NO COPY - FILE ALREADY EXIST!"
2210 ELSE
2220 PRINT " UNEXPECTED ERROR #", ERRN, " AT LINE#", ERRLN
2230 END IF
2240 PRINT " PRESS CONTINUE OR RESET"
2250 PAUSE
2260 ERROR RETURN
2270 END

```

SAS Data File Creation Code

```
•
• program 'makesd5'
•;
libname eps 'c:\sas_win\aug93\';
data eps.aug93_5;
  infile "aug93\aug93_5";
  input date $10. material $10. holder hldnum moisture
        temp e1-e100 ep1-ep100;
  array e{100} e1-e100;
  array ep{100} ep1-ep100;
  do i = 1 to 100;
    if e{i}=999 then e{i}=.;
    if ep{i}=999 then ep{i}=.;
    if holder=1.4 and i<54 then do;
      e{i}=.;
      ep{i}=.;
    end;
    if holder=9.7 and i>53 and moisture>13 then do;
      e{i}=.;
      ep{i}=.;
    end;
  end;
  drop i;
run;
proc printto new print='aug93\aug93_5.prn';
  options ps=54;
run;
proc print;
  var date material holder hldnum moisture temp;
run;
```

SAS Code for Generating Frequency Plots

```

*
* program "plotallf", directory "aug93"
* ;
*
* "powattn" is power loss -20log10(exp(-1/skin depth)) in dB/meter
*
* "phasevel" is the phase velocity = radial frequency/beta
*
* "sigma" is the electrical conductivity in mho/m and is calculated
* by the formula: epspp*radial freq*free space permittivity
*
* "losstan" is the loss tangent defined as epspp/eps
* ;
libname eps 'c:\sas_win\aug93\';
data plt_tmp;
  set eps.aug93_5;
  array e{100} e1-e100;
  array ep{100} ep1-ep100;
  array f{100} (.045,.078,.111,.144,.177,.210,.243,.276,.310,.343,
    .376,.409,.442,.475,.508,.541,.574,.607,.640,.673,.706,.739,.773,
    .806,.839,.872,.905,.938,.971,1.004,1.07,1.103,1.169,1.235,1.269,
    1.335,1.401,1.467,1.533,1.632,1.698,1.765,1.864,1.963,2.029,2.128,
    2.228,2.36,2.459,2.558,2.691,2.823,2.955,3.087,3.253,3.418,3.550,
    3.749,3.914,4.112,4.311,4.509,4.708,4.939,5.171,5.435,5.667,5.964,
    6.229,6.526,6.857,7.188,7.519,7.882,8.246,8.643,9.073,9.503,9.933,
    10.429,10.925,11.454,11.983,12.545,13.173,13.802,14.43,15.124,
    15.852,16.612,17.406,18.233,19.126,20.019,20.978,22.003,23.061,
    24.152,25.310,26.5);
  if material ^= 'AIR';
  drop date hldrnum;
  do i = 1 to 100;
    epsp = e{i};
    epspp = ep{i};
    if epspp < 0.2 then epspp = 0.;
    freq = f{i};
    powattn = .;
    phasevel = .;
    sigma = epspp * 2 * 3.14159 * freq * 0.00885;
    losstan = epspp / epsp;
    if epsp = 999 then losstan = .;
    phasevel = 1 / (sqrt((epsp * (sqrt(1 + (epspp / epsp) ** 2) + 1)) / 2));
    if epsp = 999 then phasevel = .;
    if epspp = 0 then go to skip;
    if epspp = . or epsp = . then go to skip;
    num = 3e8 / (freq * 1e9);
    powattn = num / (2 * 3.14159 * sqrt((epsp * (sqrt(1 + (epspp / epsp) ** 2) - 1)) / 2));
    powattn = -1 / powattn;
    powattn = -20 * log10(exp(powattn));
    skip: tmp = temp;
    output;
  end;
  drop e1-e100 ep1-ep100 f1-f100 i num;
run;
* ;
proc sort;
  by material temp descending holder moisture;
run;
* ;
options reset = all device = hpljs3;
title1 h = 2 ' ';
title3 ' ' a = 90 ' ' a = -90 ' ' ;
footnote h = 6 ' ' ;

```



```

axis1 length=13 cm logbase=10 order=(.01 .1 1 10 100);
axis2 length=13 cm logbase=10 order=(.1 1 10 100);
axis3 length=13 cm logbase=10 order=(.001 .01 .1 1 10);
axis4 length=13 cm order=(0 to 1 by .1);
axis5 length=13 cm logbase=10 order=(.01 .1 1 10 100 1000 10000);
symbol1 l=1 i=j w=2;
symbol2 l=2 i=j w=2;
symbol3 l=3 i=j w=2;
symbol4 l=4 i=j w=2;
symbol5 l=8 i=j w=2;
symbol6 l=14 i=j w=2;
symbol7 l=33 i=j w=2;
symbol8 l=35 i=j w=2;
symbol9 l=41 i=j w=2;
symbol10 l=43 i=j w=2;
symbol11 l=1 i=j w=2;
symbol12 l=2 i=j w=2;
*;
proc gplot data=plt_tmp;
by material temp;
plot epsp*freq=moisture /haxis=axis1 vaxis=axis2;
label epsp='REAL EPSILON';
label freq='FREQUENCY ~ GHz';
label temp=' TEMPERATURE';
label moisture='% MOISTURE';
label material='SOIL';
run;
*;
proc gplot data=plt_tmp;
by material temp;
plot epspp*freq=moisture /haxis=axis1 vaxis=axis2;
label epspp='IMAG EPSILON';
label freq='FREQUENCY ~ GHz';
label temp=' TEMPERATURE';
label moisture='% MOISTURE';
label material='SOIL';
run;
*;
proc gplot data=plt_tmp;
by material temp;
plot sigma*freq=moisture /haxis=axis1 vaxis=axis1;
label sigma='CONDUCTIVITY ~ mho/m';
label freq='FREQUENCY ~ GHz';
label temp=' TEMPERATURE';
label moisture='% MOISTURE';
label material='SOIL';
run;
*;
proc gplot data=plt_tmp;
by material temp;
plot losstan*freq=moisture /haxis=axis1 vaxis=axis3;
label losstan='LOSS TANGENT';
label freq='FREQUENCY ~ GHz';
label temp=' TEMPERATURE';
label moisture='% MOISTURE';
label material='SOIL';
run;
*;
proc gplot data=plt_tmp;
by material temp;
plot phasevel*freq=moisture /haxis=axis1 vaxis=axis4;
label phasevel='NORMALIZED PHASE VELOCITY';
label freq='FREQUENCY ~ GHz';
label temp=' TEMPERATURE';
label moisture='% MOISTURE';

```

```

label material = 'SOIL';
run;
*;
proc gplot data = plt_tmp;
by material temp;
plot powattn*freq = moisture /haxis = axis1 vaxis = axis5;
label powattn = 'POWER ATTN ~ dB/m';
label freq = 'FREQUENCY ~ GHz';
label temp = 'TEMPERATURE';
label moisture = '% MOISTURE';
label material = 'SOIL';
run;

```

SAS Code for Generating Moisture Content Plots

```

*
* program "plotallm", directory "aug93"
*
*
* "powattn" is power loss -20log10(exp(-1/skin depth)) in dB/meter
*
* "phasevel" is the phase velocity = radial frequency/beta
*
* "sigma" is the electrical conductivity in mho/m and is calculated
* by the formula: epspp*radial freq*free space permittivity
*
* "losstan" is the loss tangent defined as epspp/eps
*
libname eps 'c:\sas_win\aug93\';
data plt_tmp;
  set eps.aug93_5;
  array f{100} (.045,.078,.111,.144,.177,.210,.243,.276,.310,.343,
.376,.409,.442,.475,.508,.541,.574,.607,.640,.673,.706,.739,.773,
.806,.839,.872,.905,.938,.971,1.004,1.07,1.103,1.169,1.235,1.269,
1.335,1.401,1.467,1.533,1.632,1.698,1.765,1.864,1.963,2.029,2.128,
2.228,2.36,2.459,2.558,2.691,2.823,2.955,3.087,3.253,3.418,3.550,
3.749,3.914,4.112,4.311,4.509,4.708,4.939,5.171,5.435,5.667,5.964,
6.229,6.526,6.857,7.188,7.519,7.882,8.246,8.643,9.073,9.503,9.933,
10.429,10.925,11.454,11.983,12.545,13.173,13.802,14.43,15.124,
15.852,16.612,17.406,18.233,19.126,20.019,20.978,22.003,23.061,
24.152,25.310,26.5);
  if material='AIR';
  drop date holder hldnum temp;
  epsp=e2;
  epspp=ep2;
  freq=0.078;
  powattn=.;
  phasevel=.;
  sigma=epspp*2*3.14159*freq*0.00885;
  losstan=epspp/eps;
  if epsp=999 then losstan=.;
  phasevel=1/(sqrt((epsp*(sqrt(1+(epspp/eps)**2)+1))/2));
  if epsp=999 then phasevel=.;
  if epspp=0 then go to skip;
  if epspp=. or epsp=. then go to skip;
  num=3e8/(freq*1e9);
  powattn=num/(2*3.14159*sqrt((epsp*(sqrt(1+(epspp/eps)**2)-1))/2));
  powattn=-1/powattn;
  powattn=-20*log10(exp(powattn));
  skip: tmp=temp;
  output;
  drop e1-e100 ep1-ep100 f1-f100 i num;
run;
*
proc sort;
  by tmp material moisture;
run;
*
goptions reset=all device=hpljs3;
title1 h=2'';
title2 j=c h=2 f=swiss '78 MHz';
title3 '' a=90'' a=-90'';
footnote h=6'';
axis1 length=13 cm order=(0 to 100 by 10);
axis2 length=13 cm order=(0 to 100 by 10);
axis3 length=13 cm logbase=10 order=(.001 .01 .1 1 10);
axis4 length=13 cm order=(0 to 1 by .1);

```

```

axis5 length = 13 cm logbase = 10 order = (.01 .1 1 10 100 1000 10000);
axis6 length = 13 cm logbase = 10 order = (.01 .1 1 10 100);
symbol1 v = A;
symbol2 v = B;
symbol3 v = C;
symbol4 v = D;
symbol5 v = E;
symbol6 v = F;
symbol7 v = G;
symbol8 v = H;
symbol9 v = I;
symbol10 v = J;
symbol11 v = K;
symbol12 v = L;
symbol13 v = W;
*;
proc gplot data = plt_tmp;
  by tmp;
  plot epsp*moisture = material /haxis = axis1 vaxis = axis2;
  label epsp = 'REAL EPSILON';
  label freq = 'FREQUENCY ~ GHz';
  label temp = 'TEMPERATURE';
  label moisture = '% MOISTURE (VOLUMETRIC)';
  label material = 'SOIL';
run;
*;
proc gplot data = plt_tmp;
  by tmp;
  plot epspp*moisture = material /haxis = axis1 vaxis = axis2;
  label epspp = 'IMAG EPSILON';
  label freq = 'FREQUENCY ~ GHz';
  label temp = 'TEMPERATURE';
  label moisture = '% MOISTURE (VOLUMETRIC)';
  label material = 'SOIL';
run;
*;
proc gplot data = plt_tmp;
  by tmp;
  plot sigma*moisture = material /haxis = axis1 vaxis = axis6;
  label sigma = 'CONDUCTIVITY ~ mho/m';
  label freq = 'FREQUENCY ~ GHz';
  label temp = 'TEMPERATURE';
  label moisture = '% MOISTURE (VOLUMETRIC)';
  label material = 'SOIL';
run;
*;
proc gplot data = plt_tmp;
  by tmp;
  plot losstan*moisture = material /haxis = axis1 vaxis = axis3;
  label losstan = 'LOSS TANGENT';
  label freq = 'FREQUENCY ~ GHz';
  label temp = 'TEMPERATURE';
  label moisture = '% MOISTURE (VOLUMETRIC)';
  label material = 'SOIL';
run;
*;
proc gplot data = plt_tmp;
  by tmp;
  plot phasevel*moisture = material /haxis = axis1 vaxis = axis4;
  label phasevel = 'NORMALIZED PHASE VELOCITY';
  label freq = 'FREQUENCY ~ GHz';
  label temp = 'TEMPERATURE';
  label moisture = '% MOISTURE (VOLUMETRIC)';
  label material = 'SOIL';
run;
*;

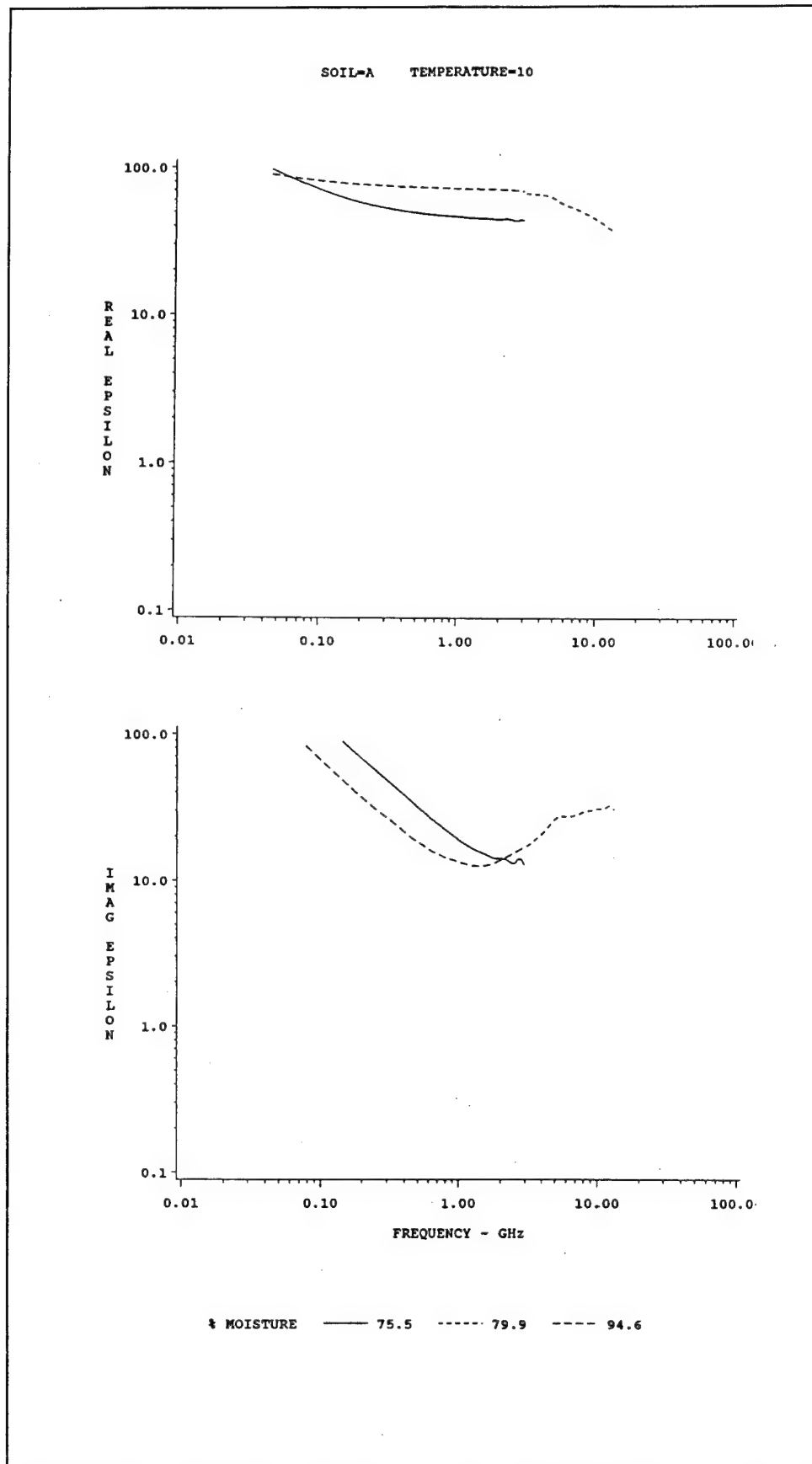
```

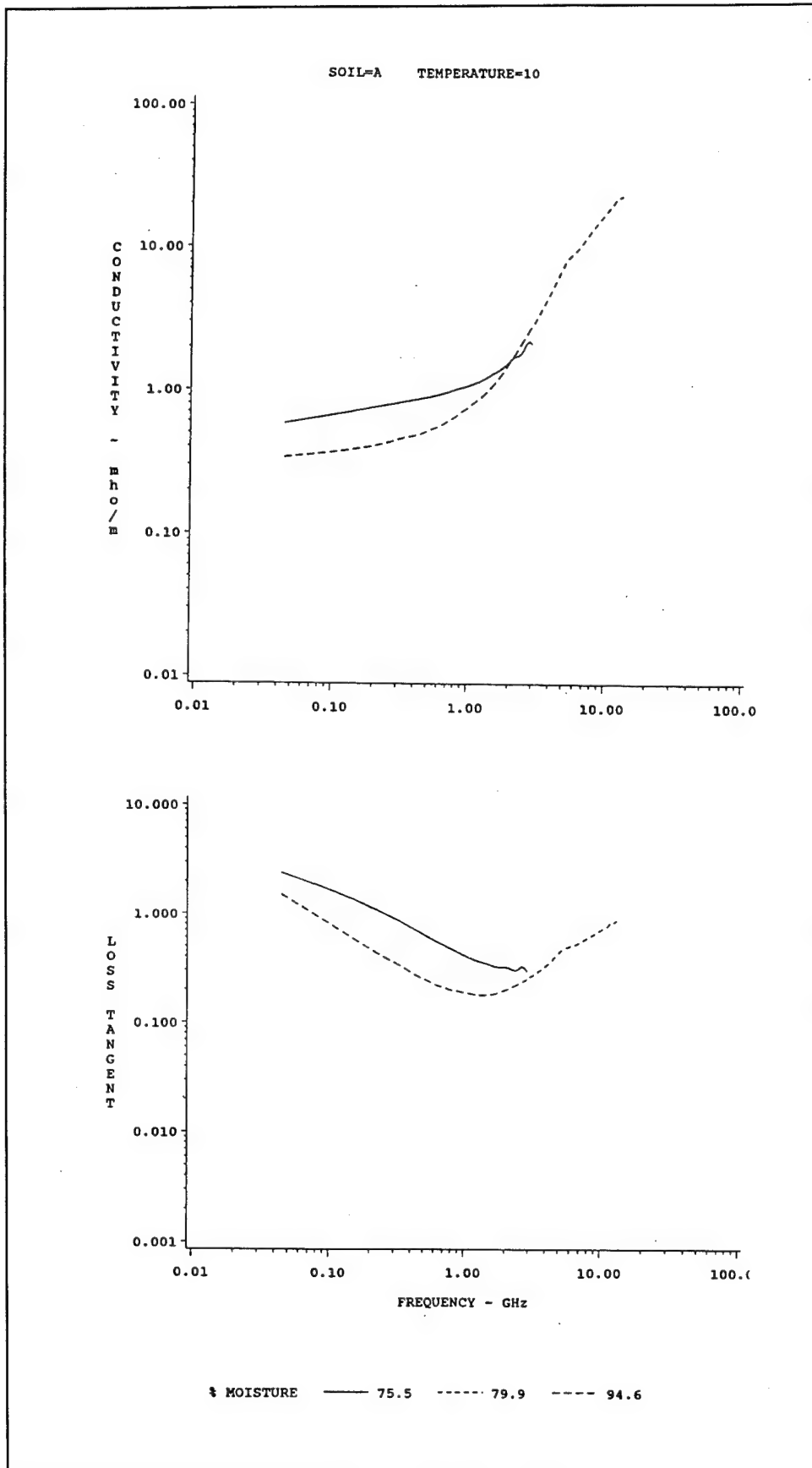
```
proc gplot data=plt_tmp;  
  by tmp;  
  plot powattn*moisture=material /haxis=axis1 vaxis=axis5;  
  label powattn='POWER ATTN ~ dB/m';  
  label freq='FREQUENCY ~ GHz';  
  label temp=' TEMPERATURE';  
  label moisture='% MOISTURE (VOLUMETRIC)';  
  label material='SOIL';  
run;
```

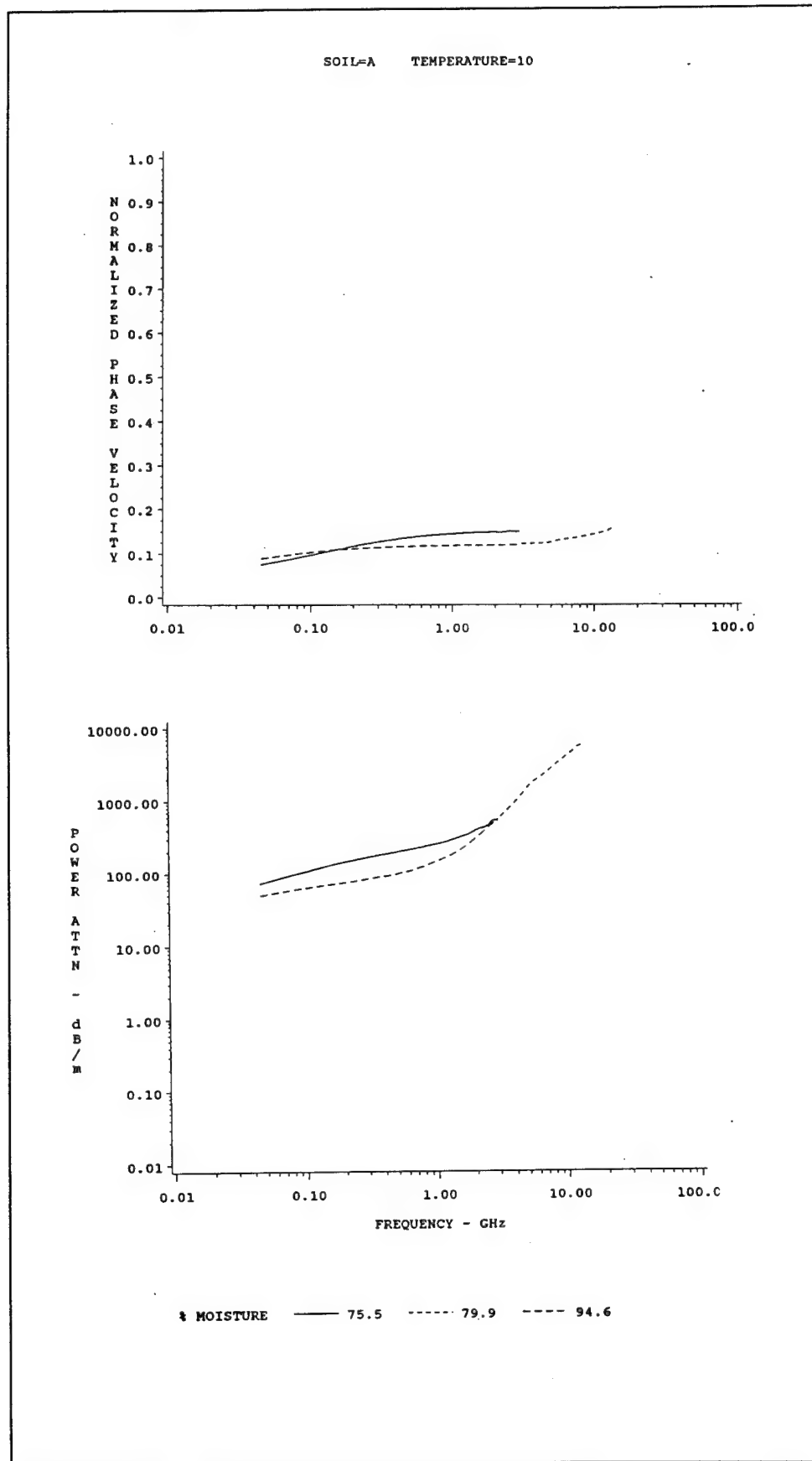
:

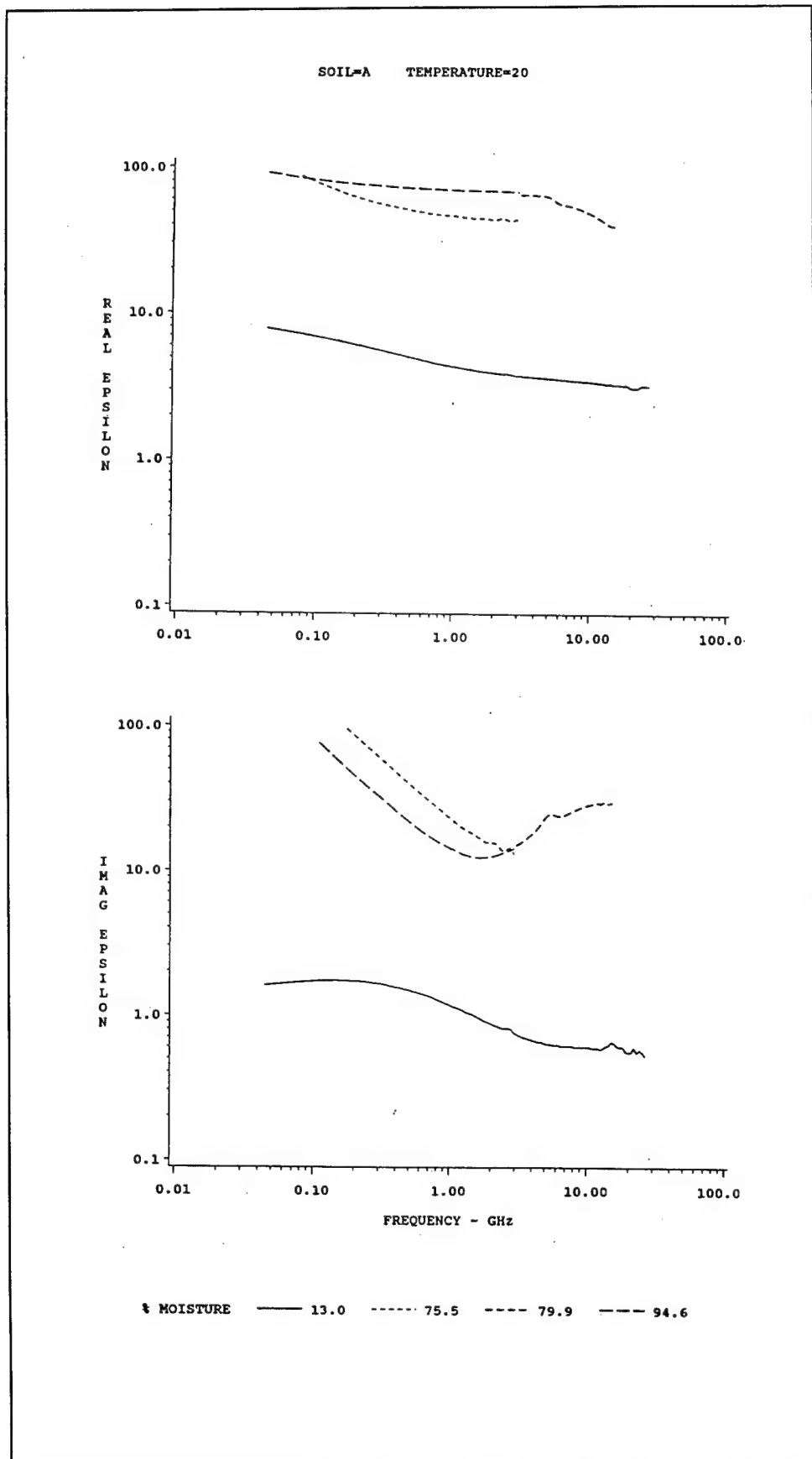
Appendix B

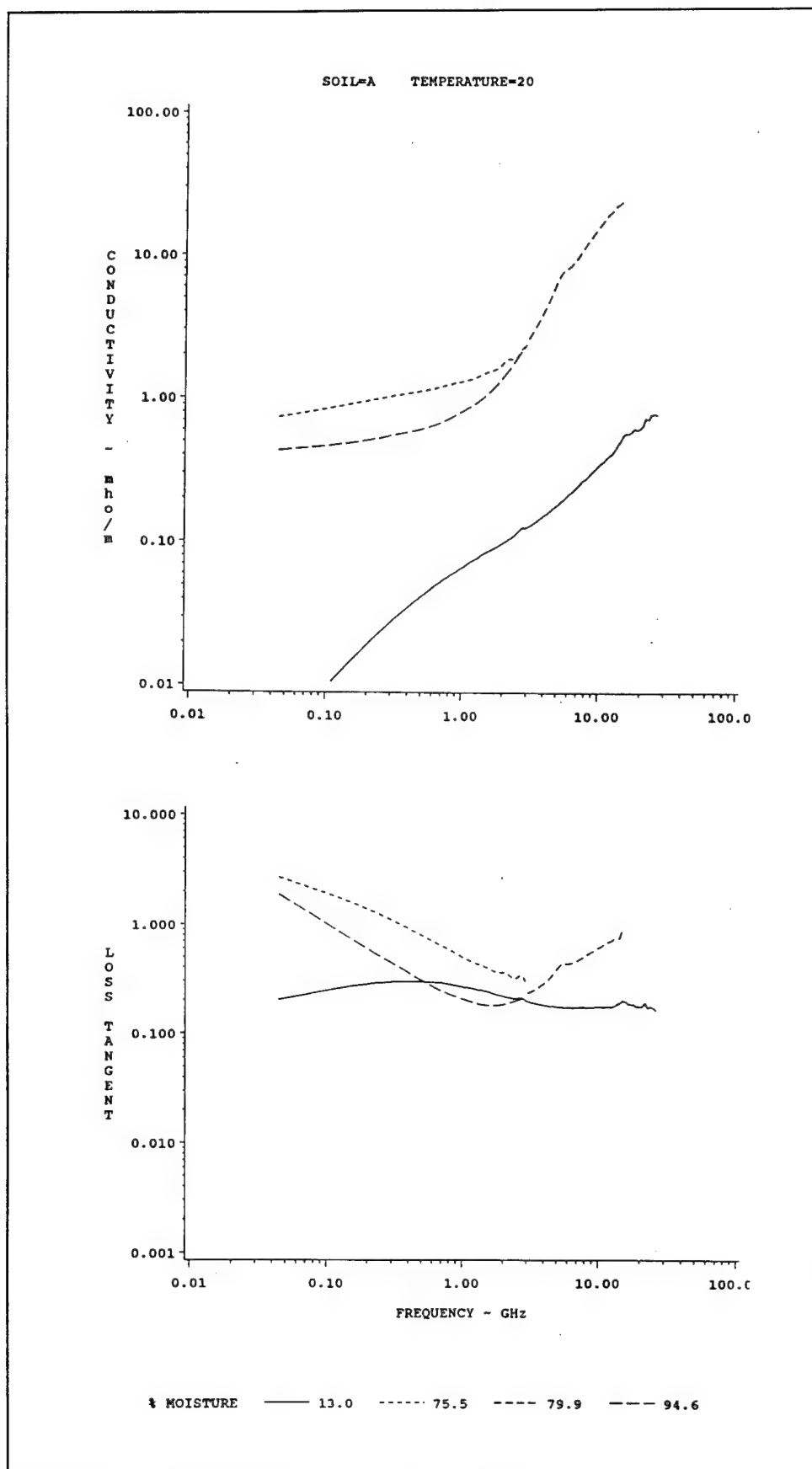
Electrical Properties of Soils Plotted Against Frequency

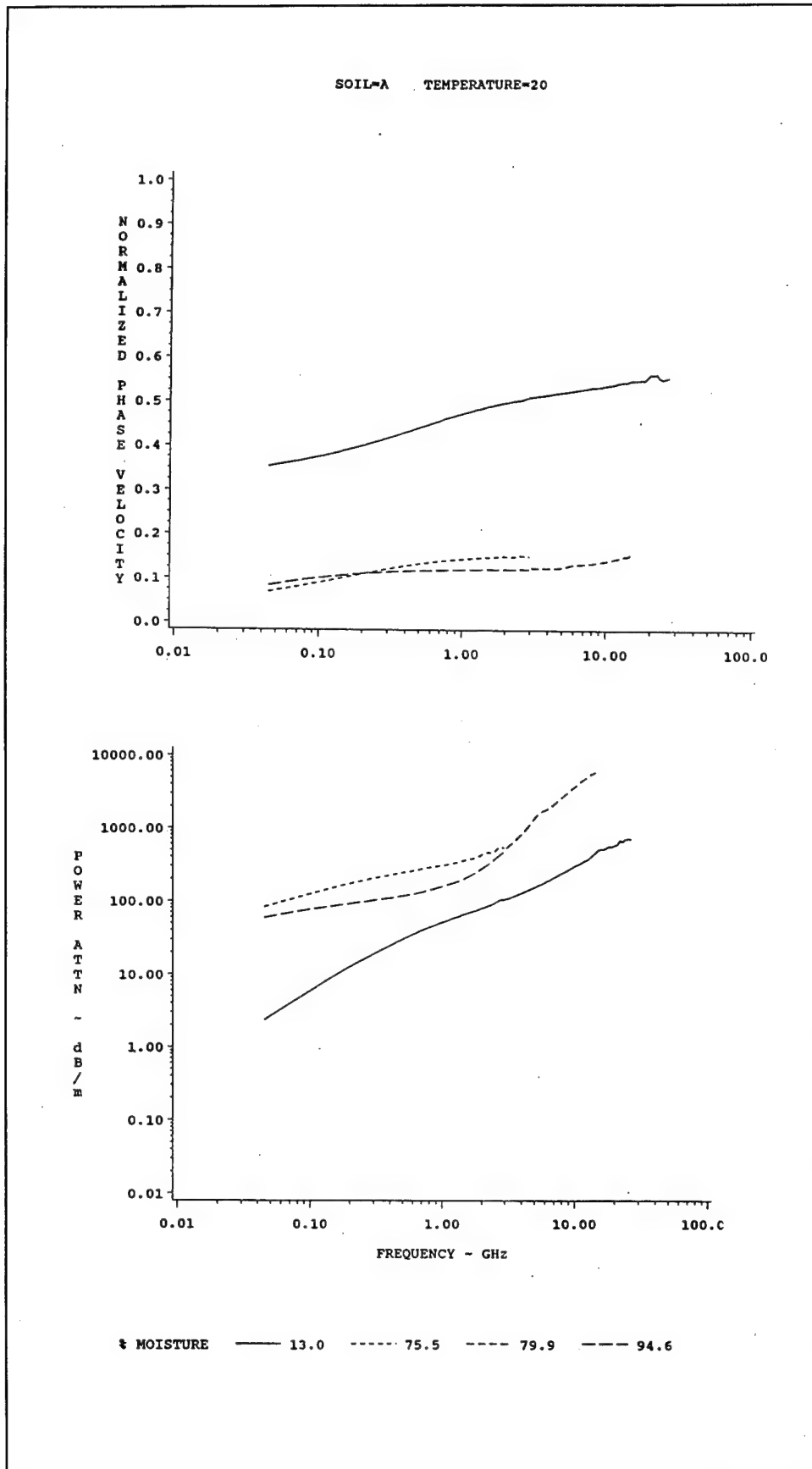


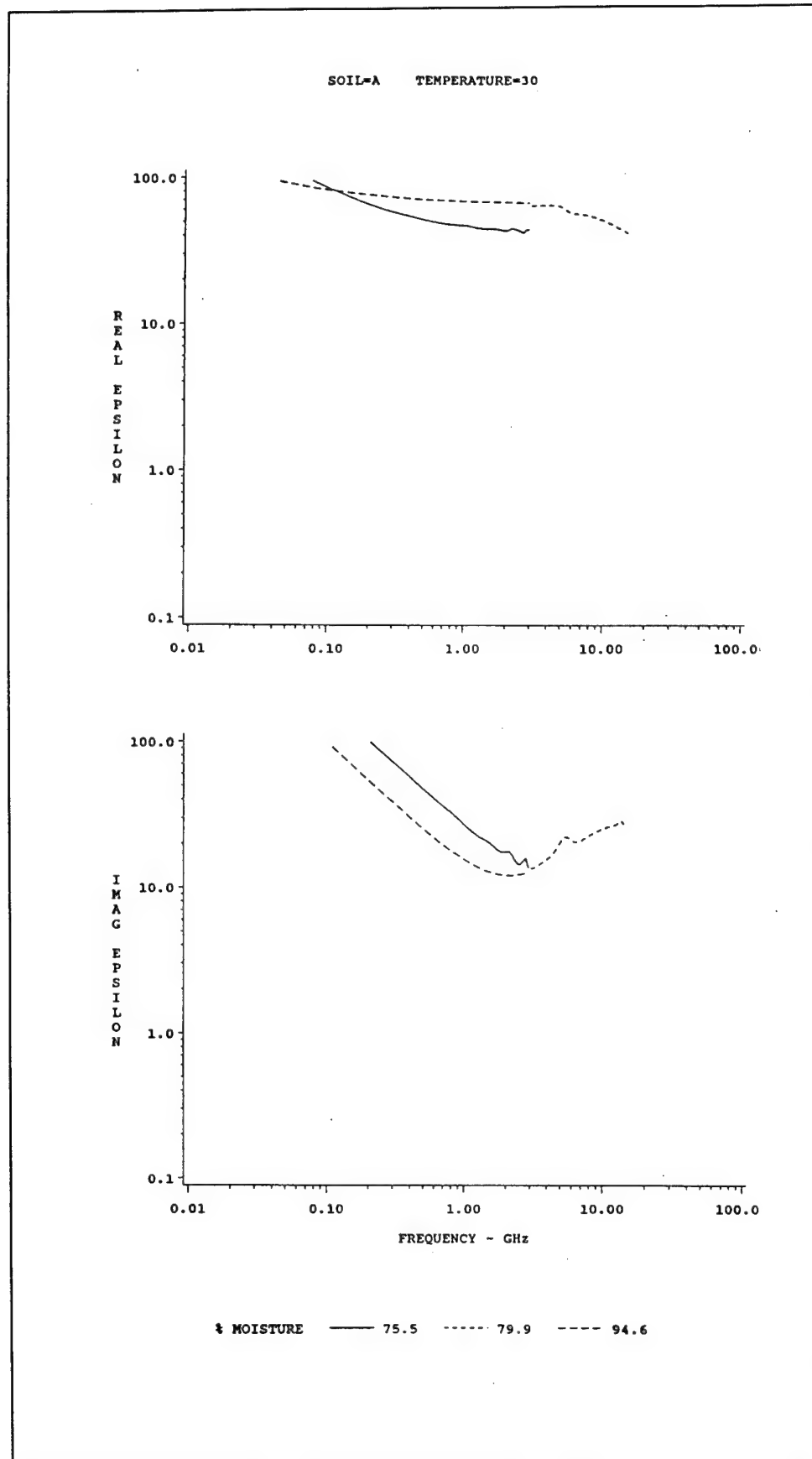


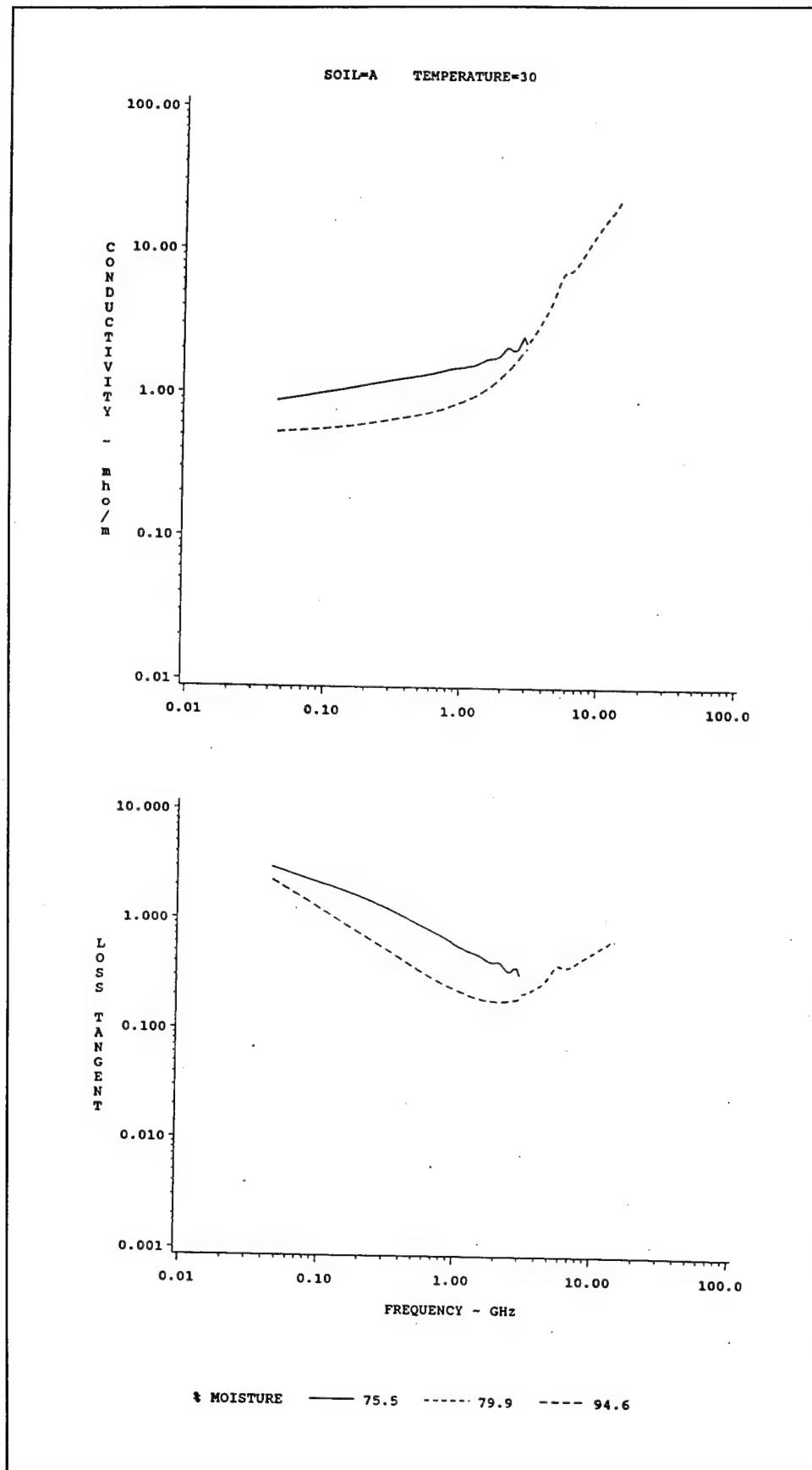


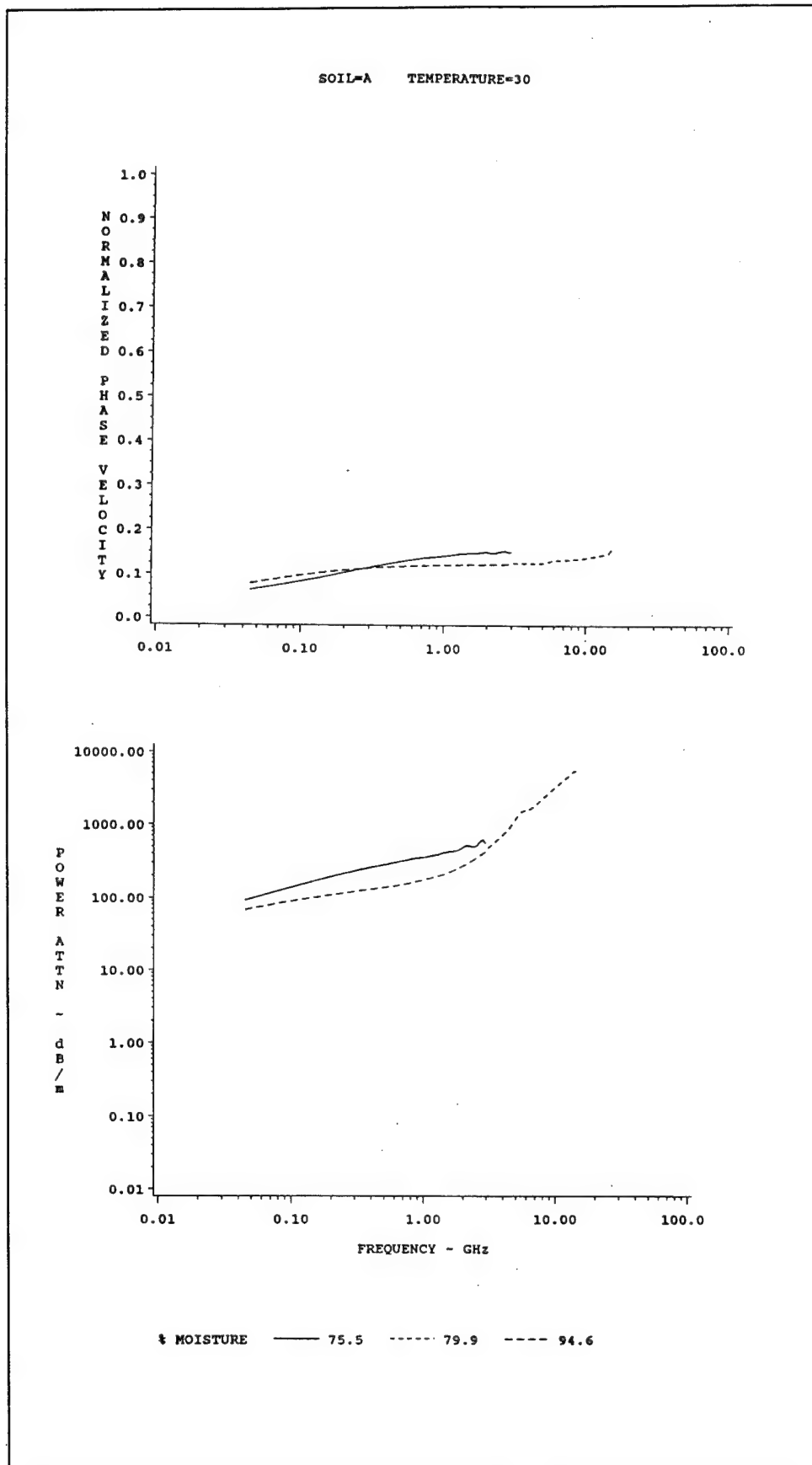


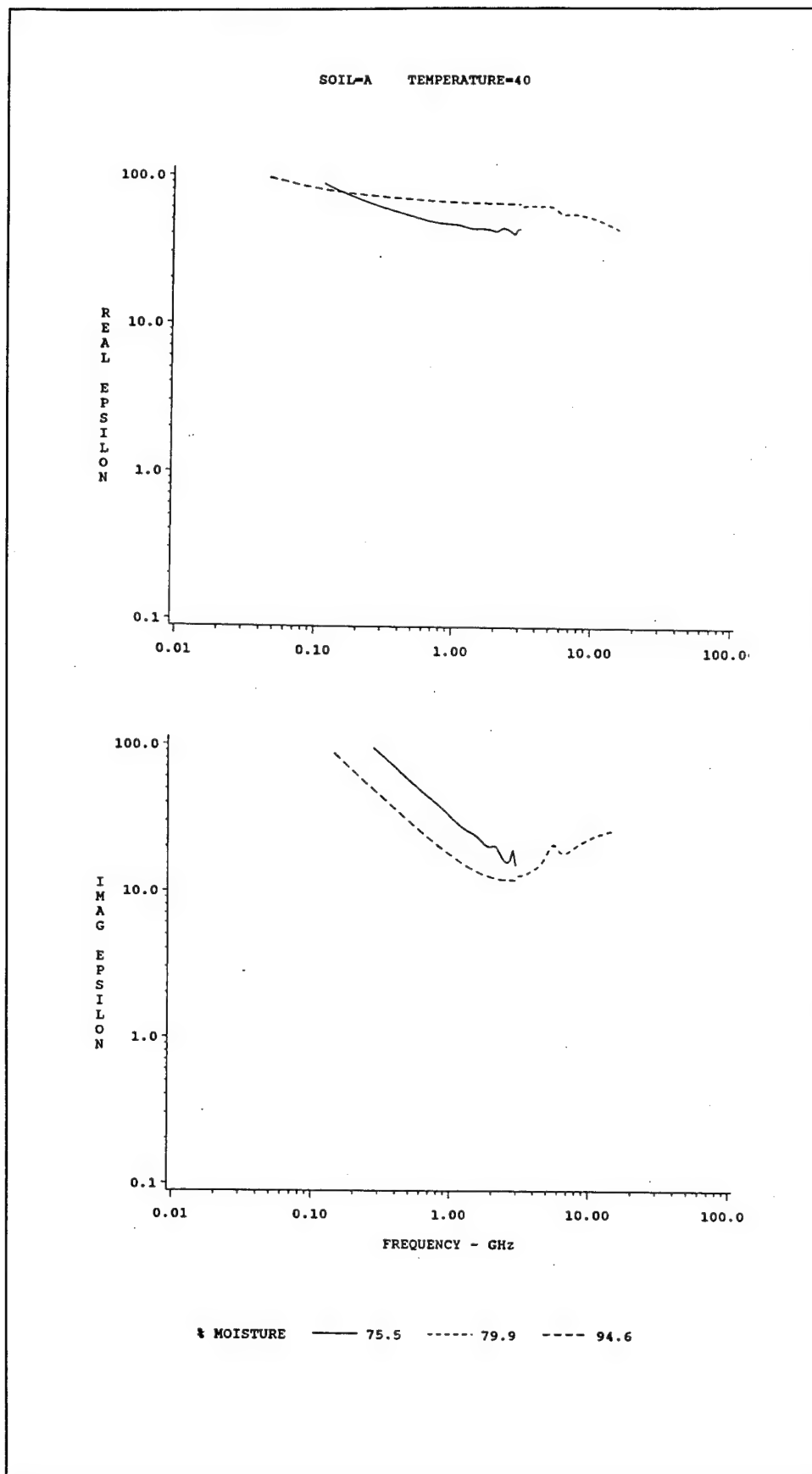


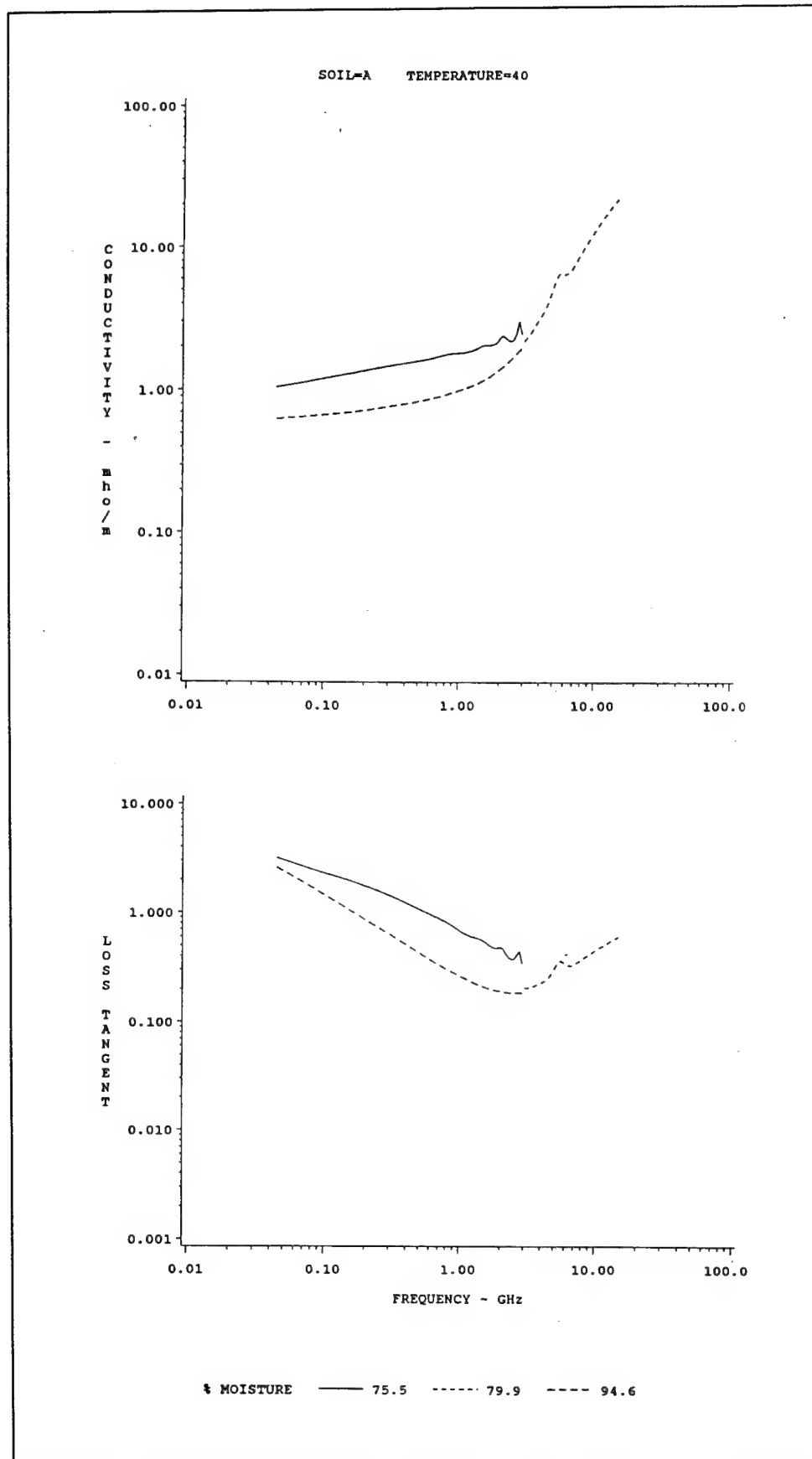


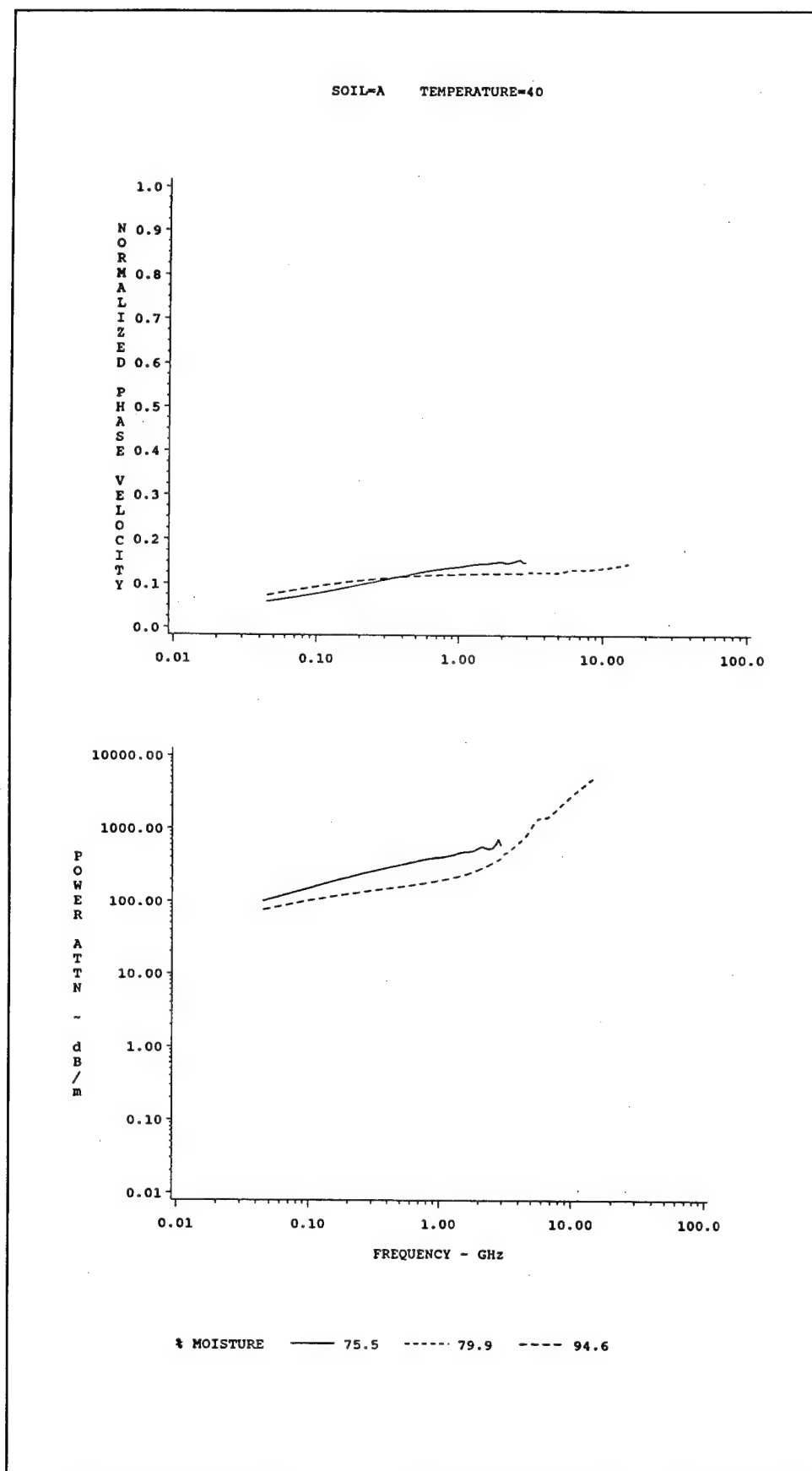


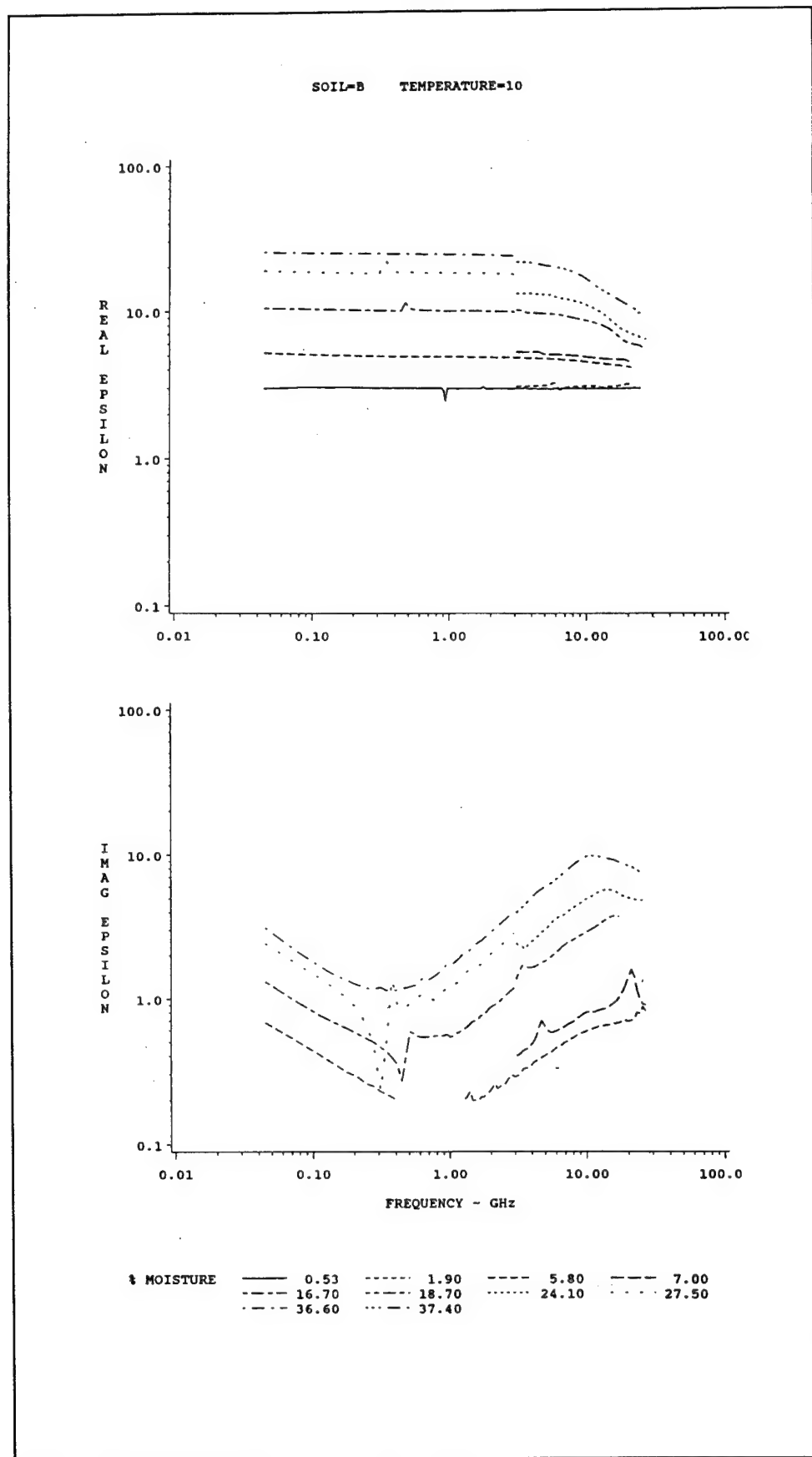


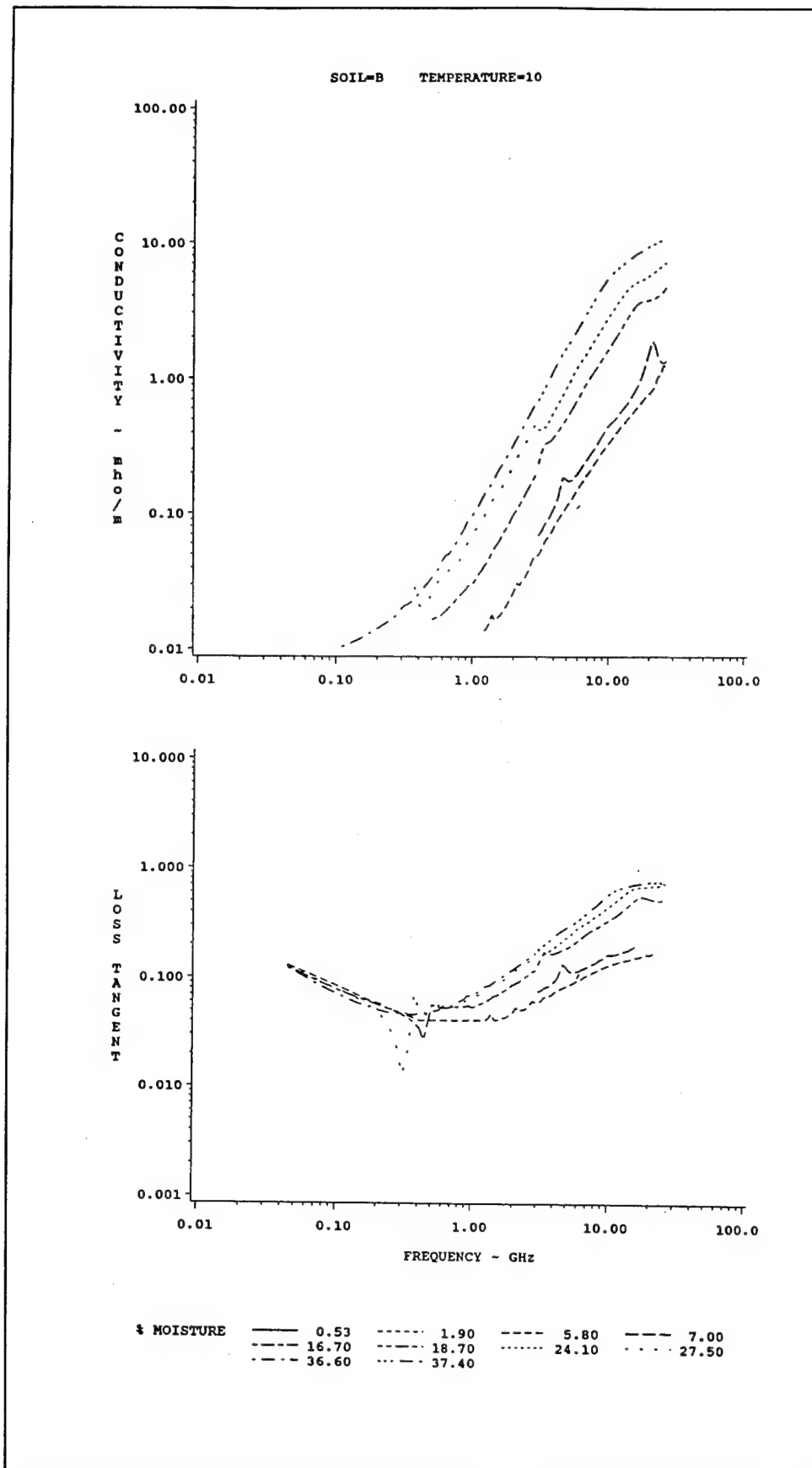


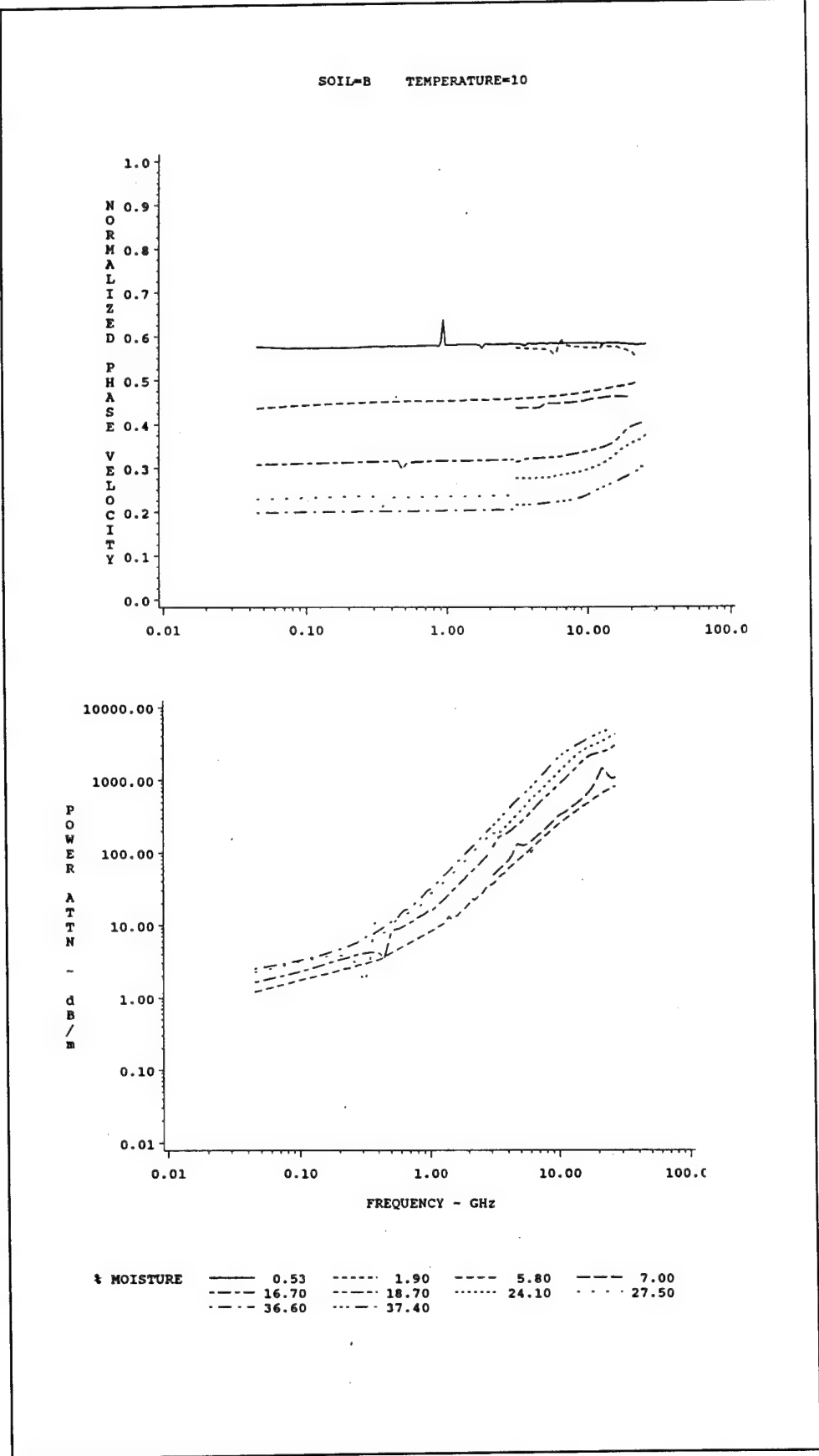




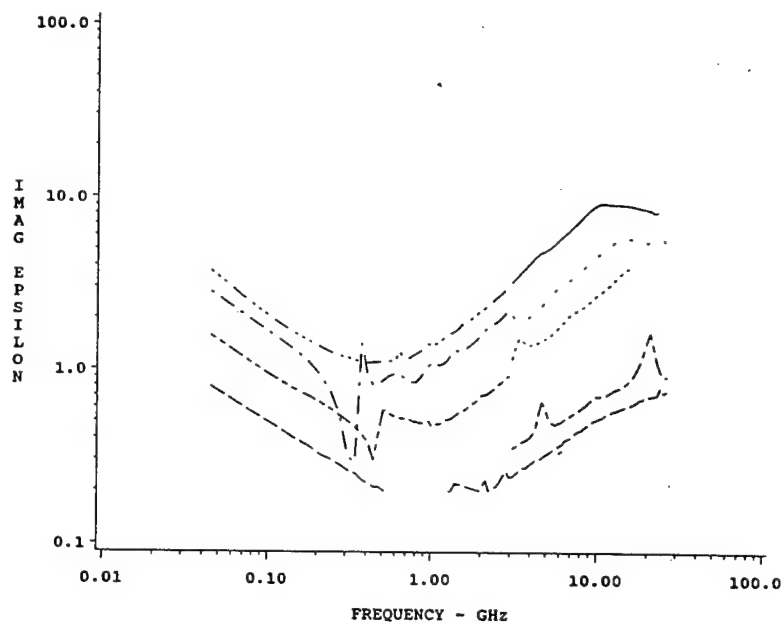
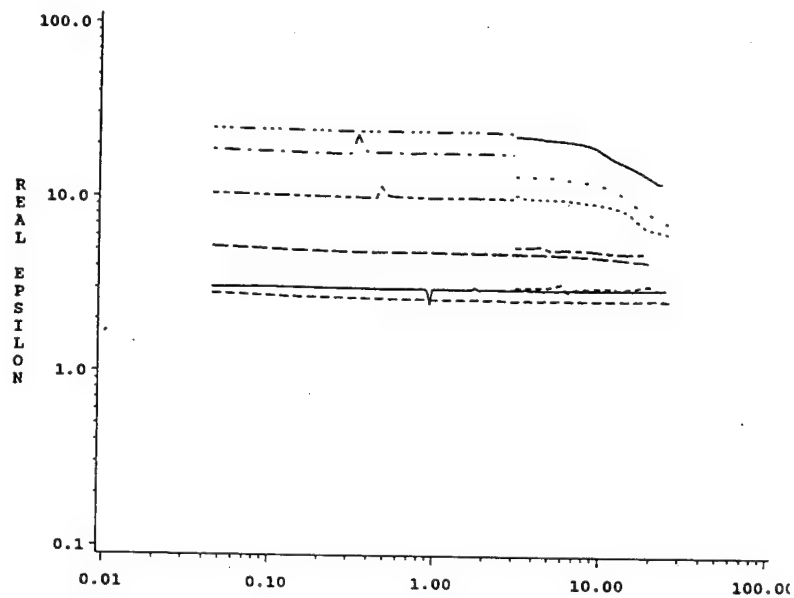




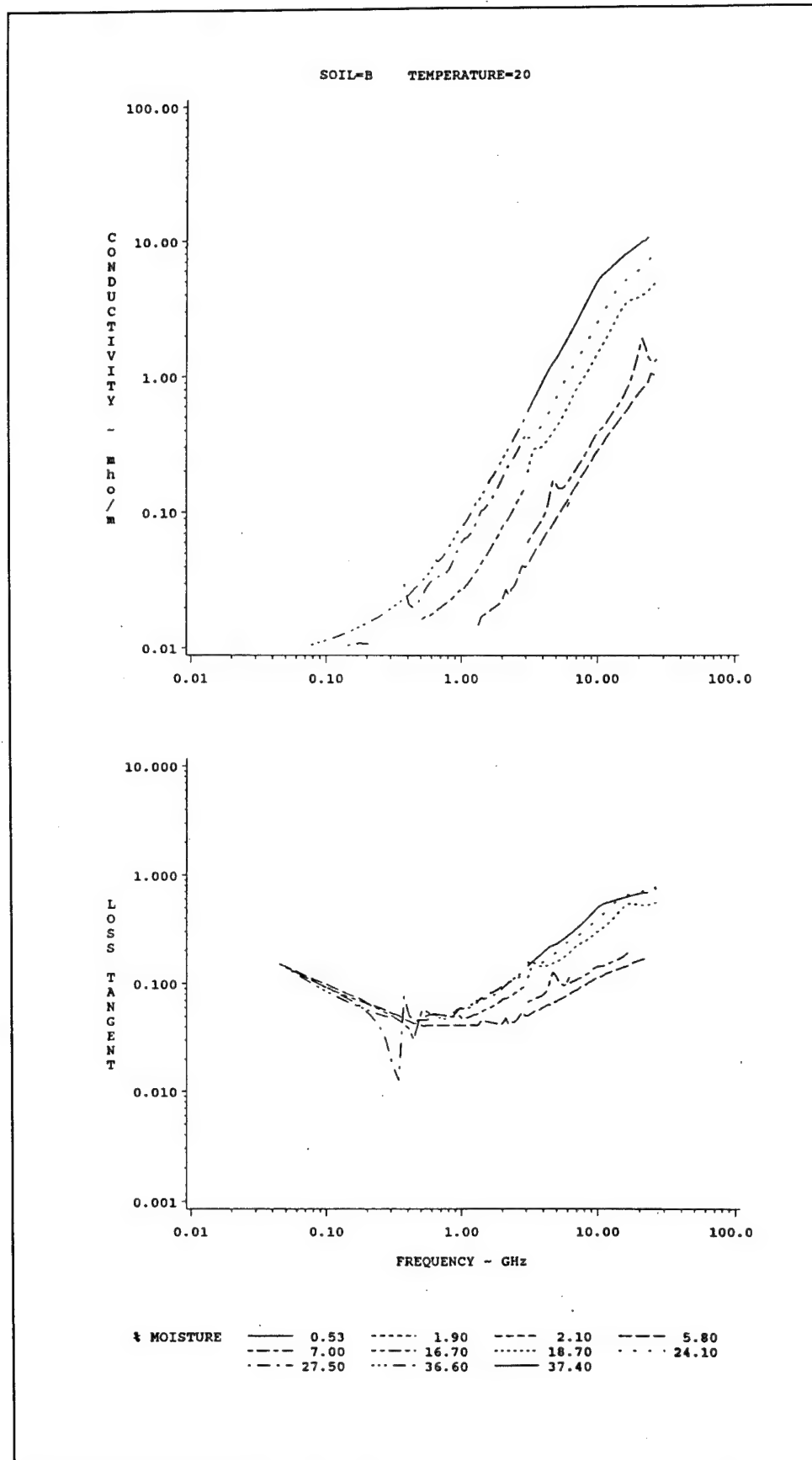




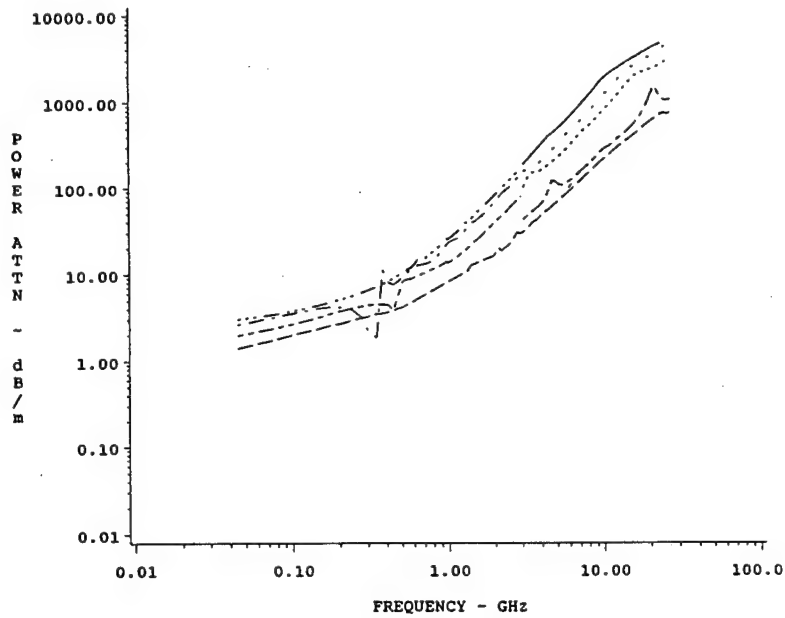
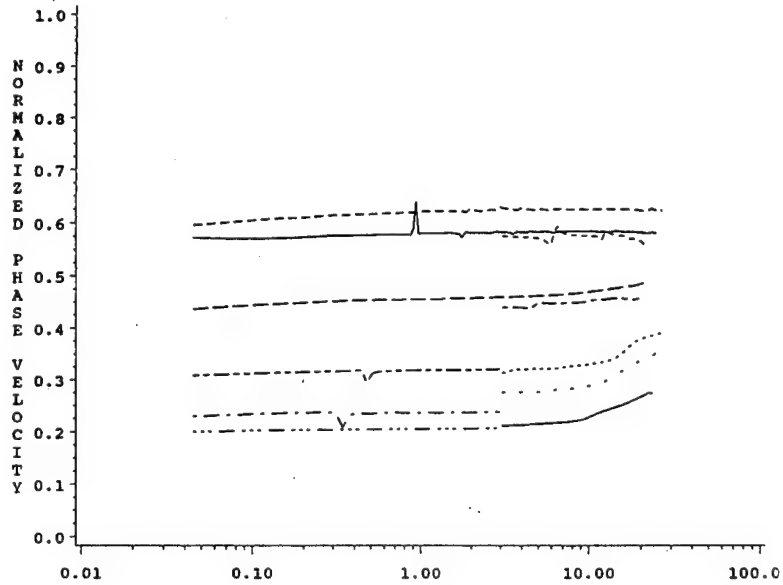
SOIL=B TEMPERATURE=20



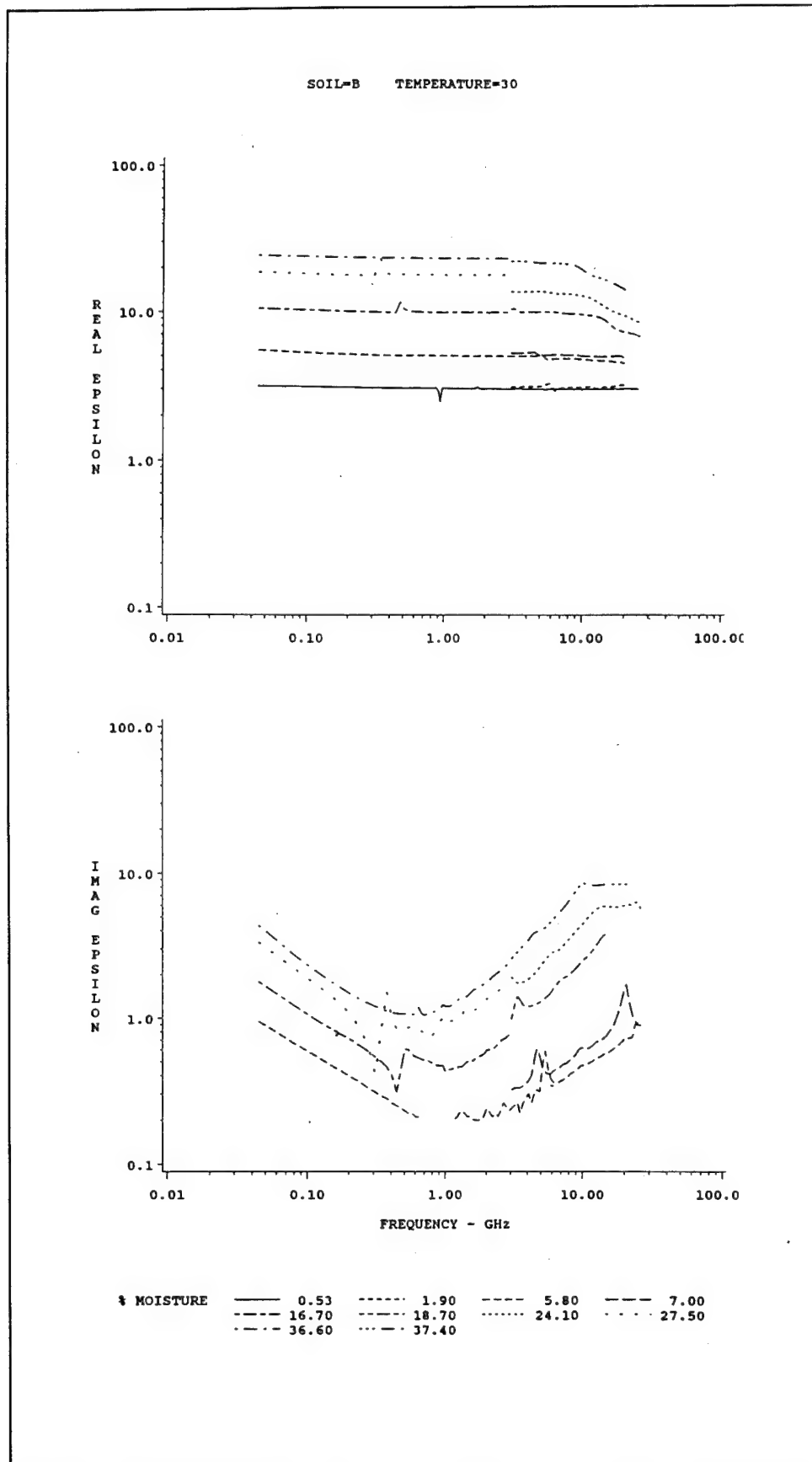
MOISTURE	0.53	1.90	2.10	5.80
	7.00	16.70	18.70	24.10
	27.50	36.60	37.40	

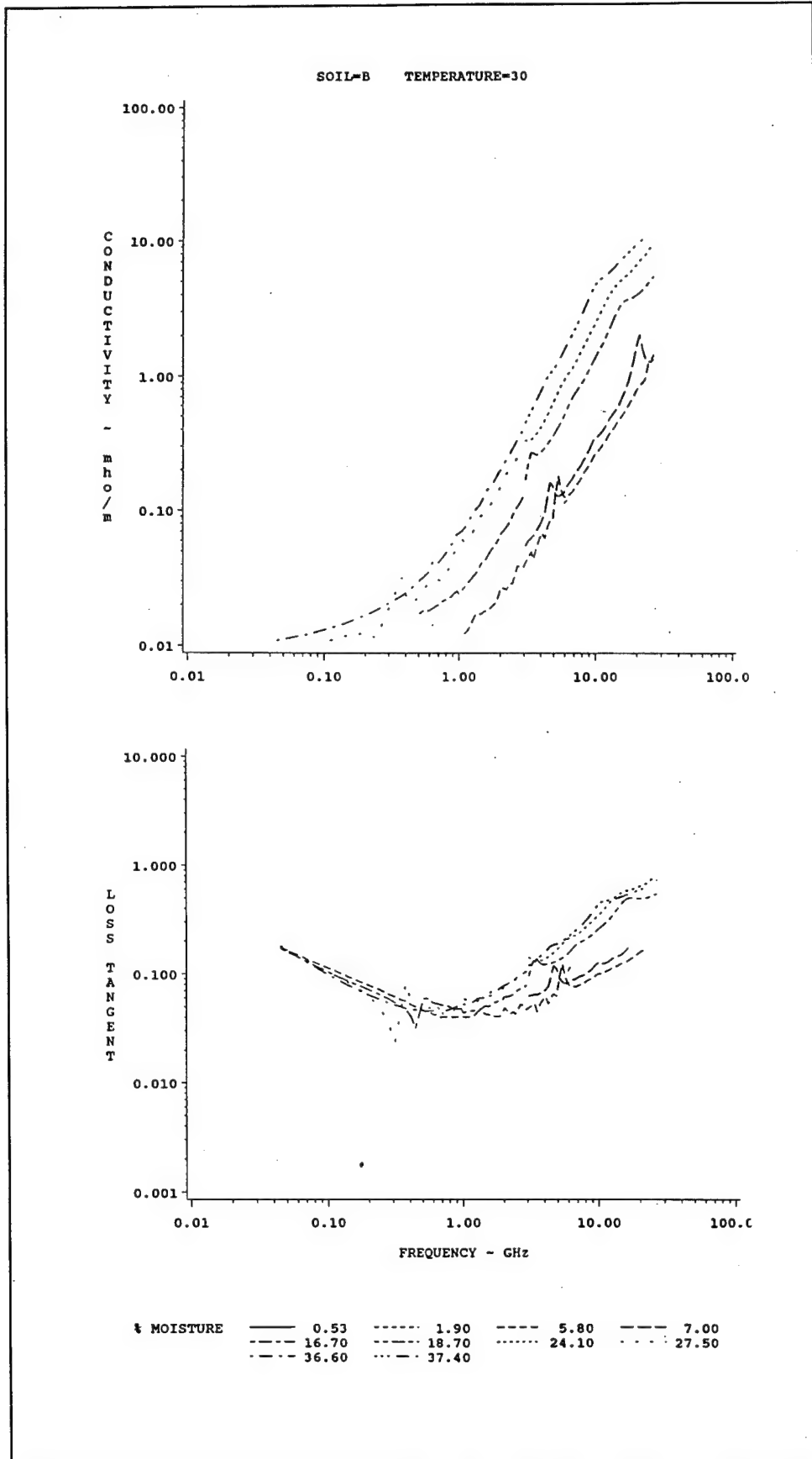


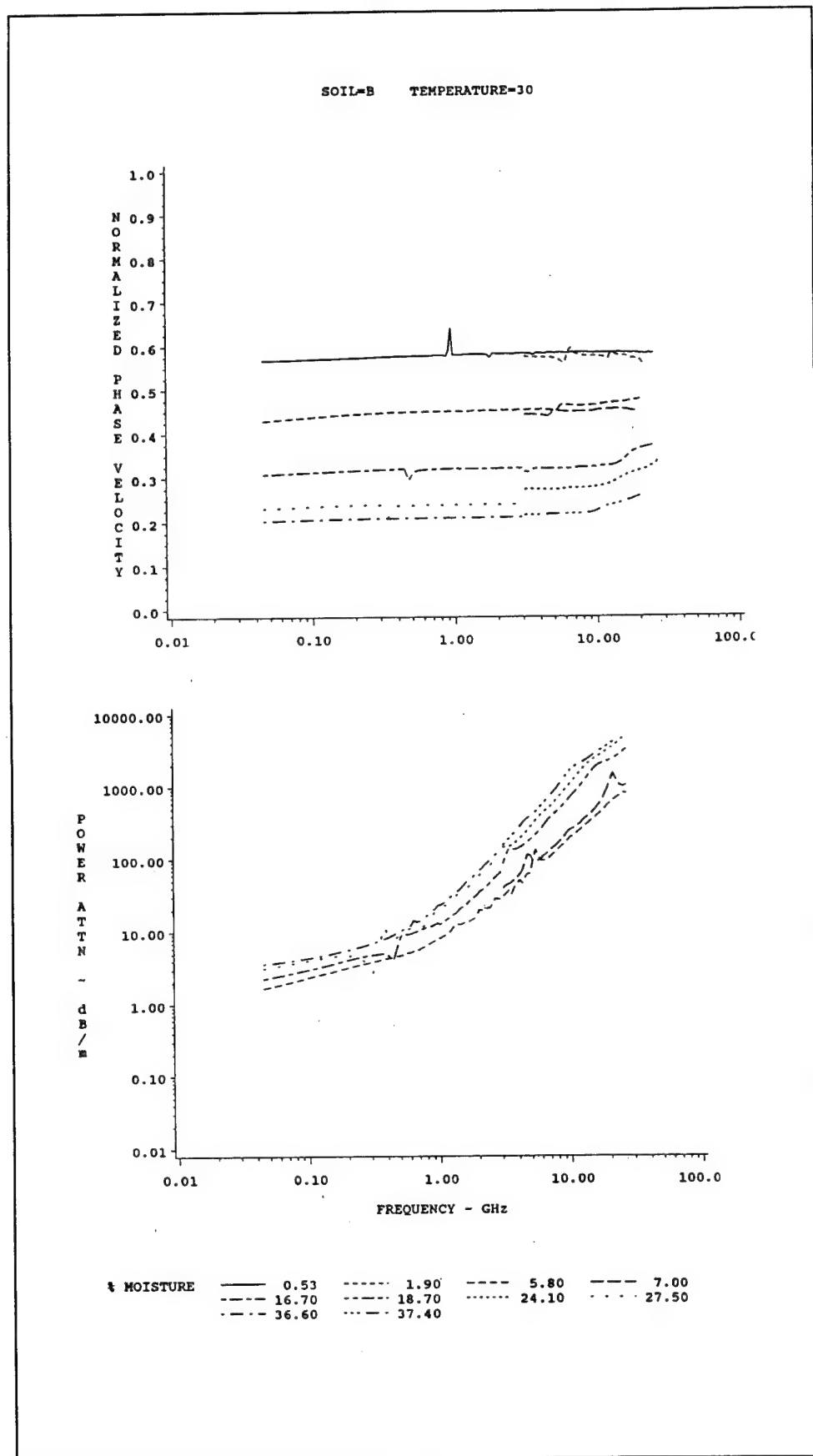
SOIL-B TEMPERATURE=20

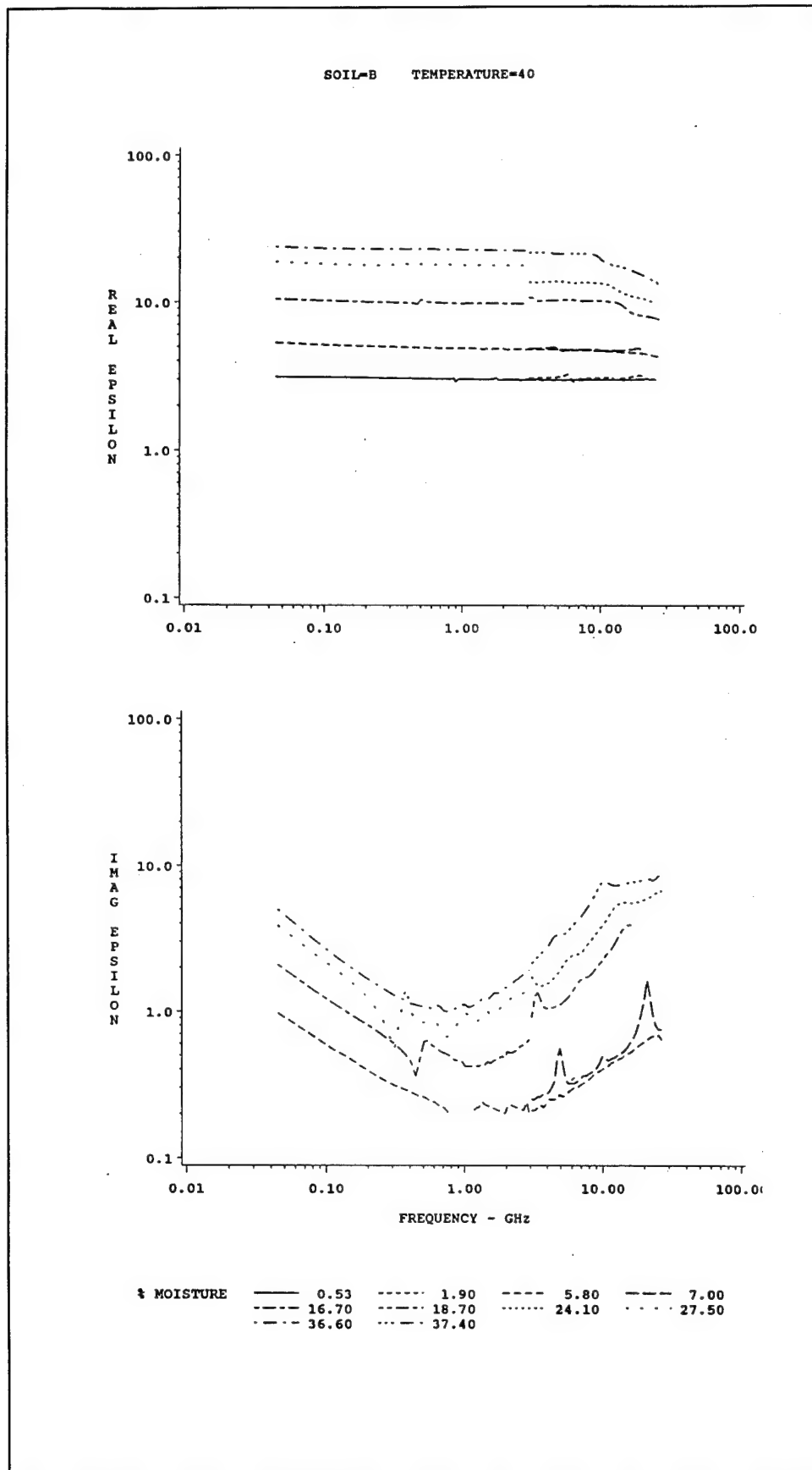


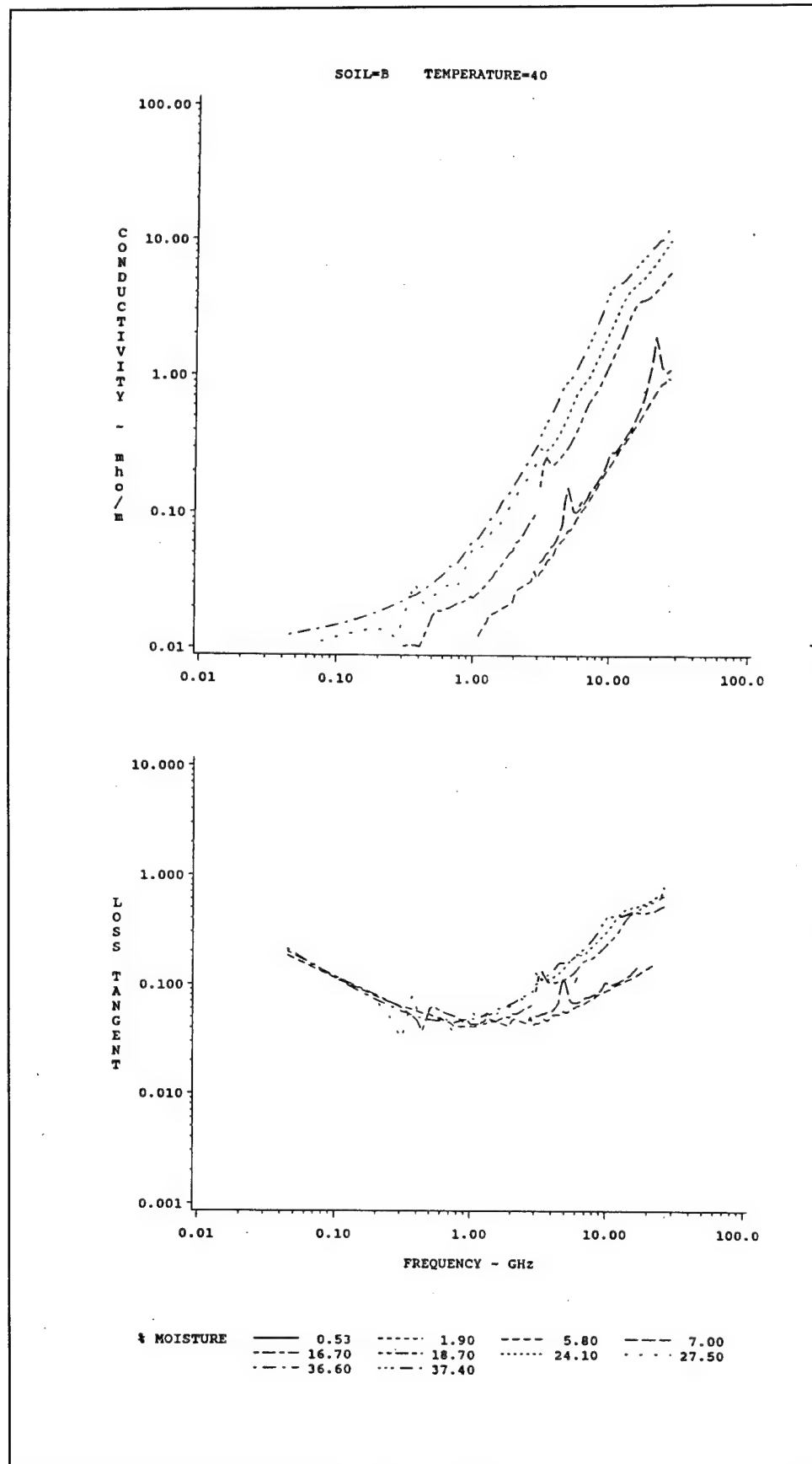
* MOISTURE	0.53	1.90	2.10	5.80
	7.00	16.70	18.70	24.10
	27.50	36.60	37.40	



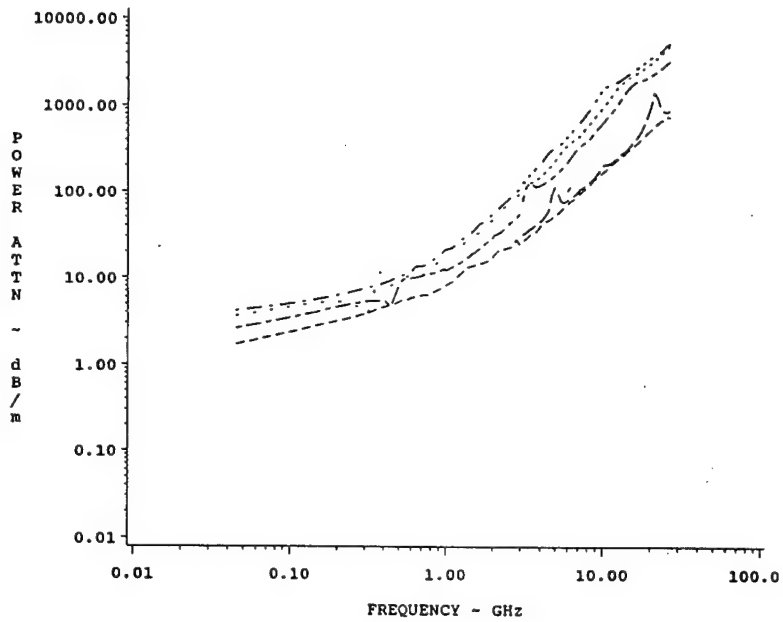
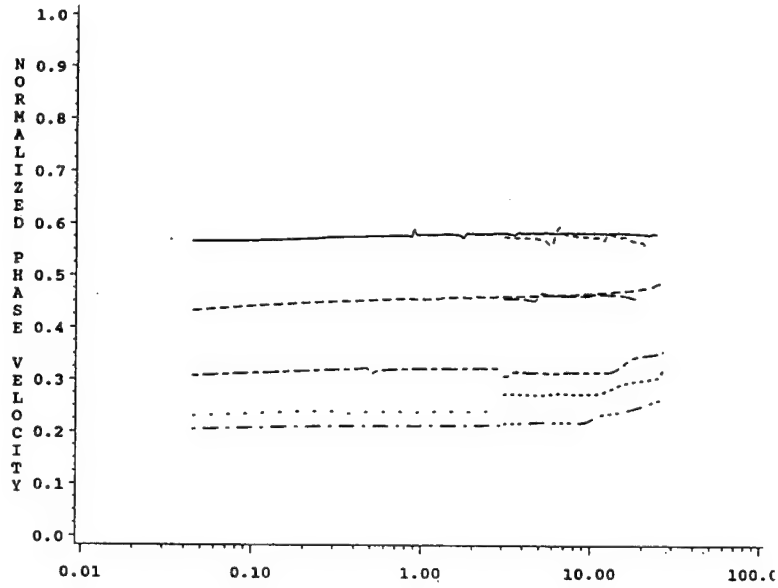




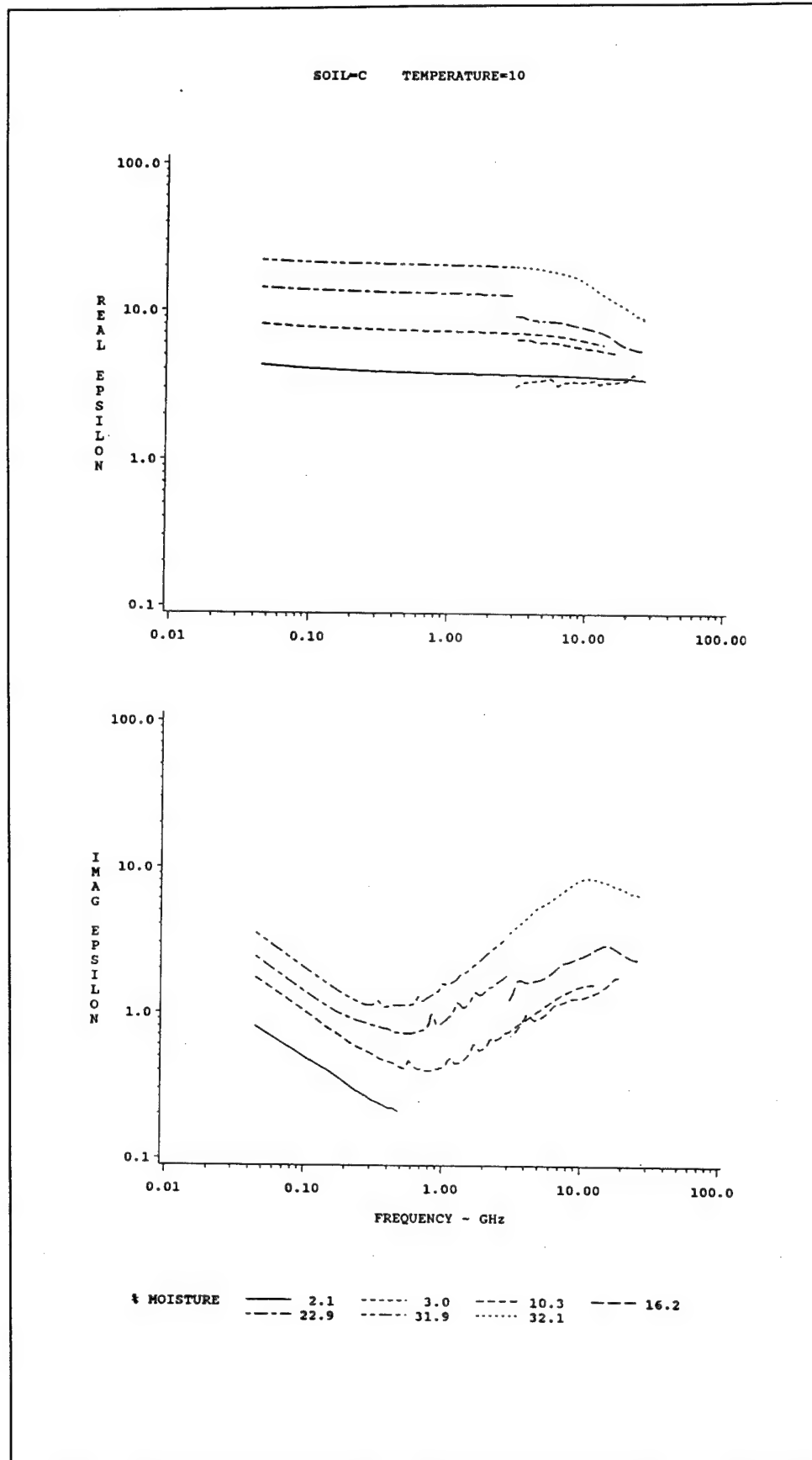


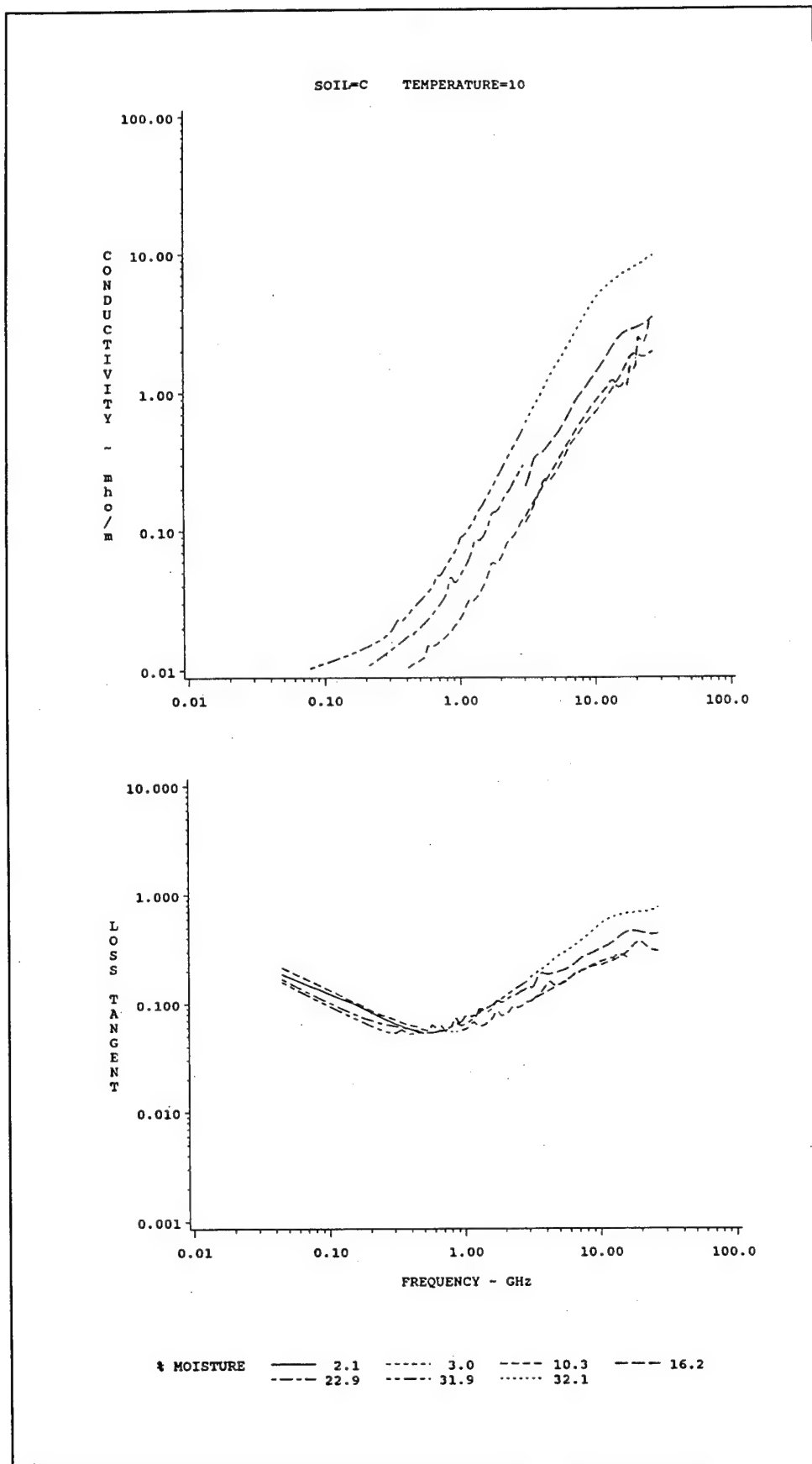


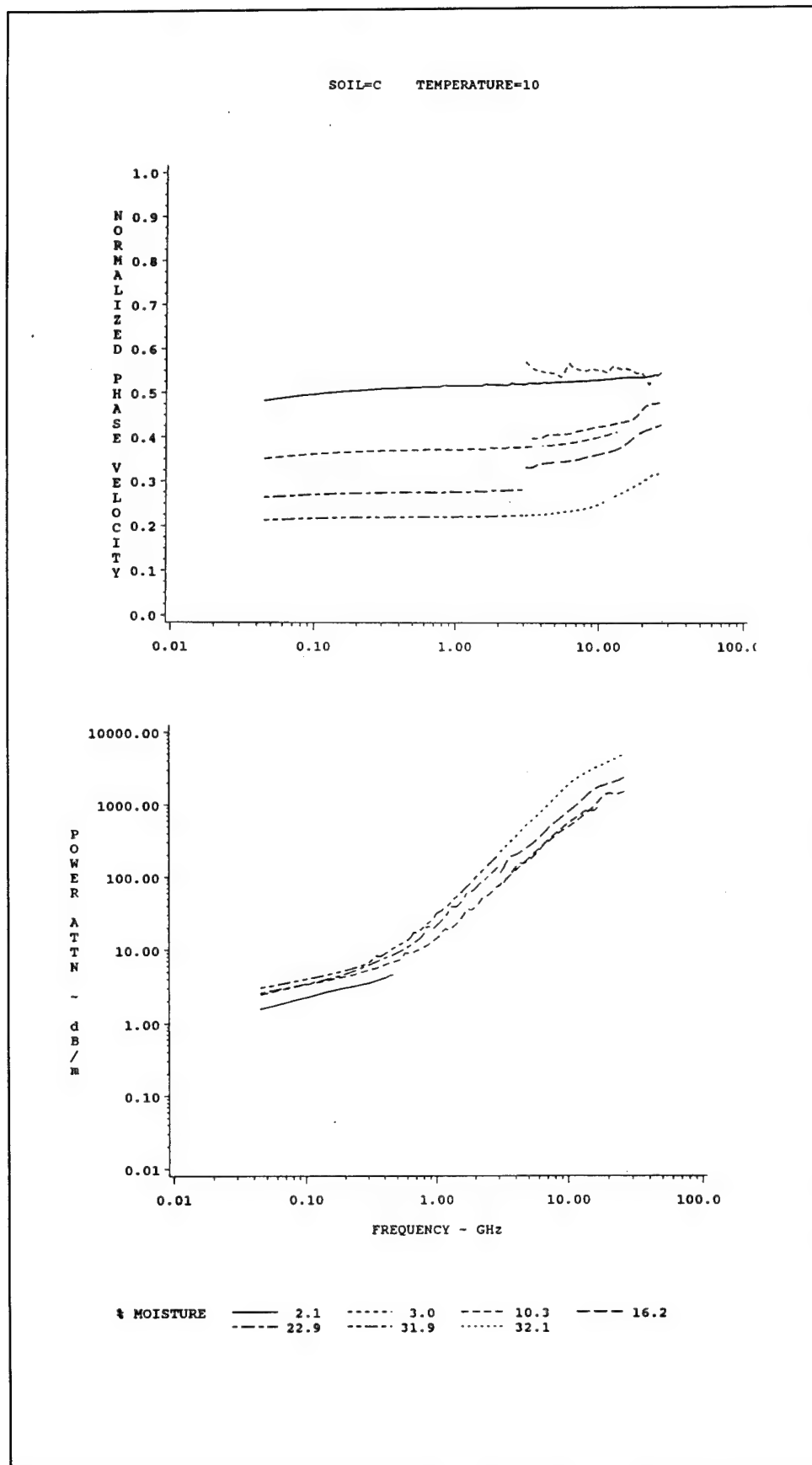
SOIL-B TEMPERATURE=40

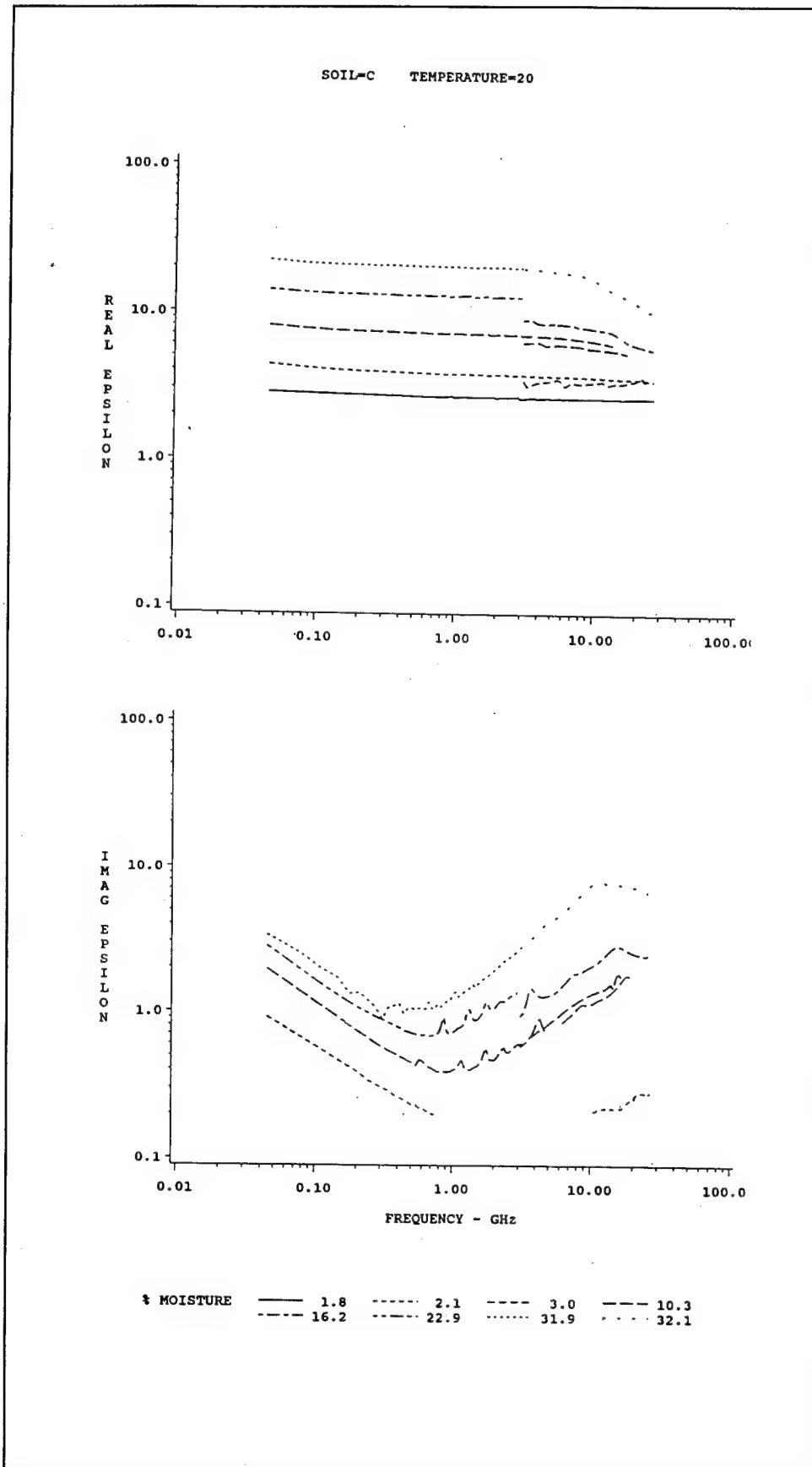


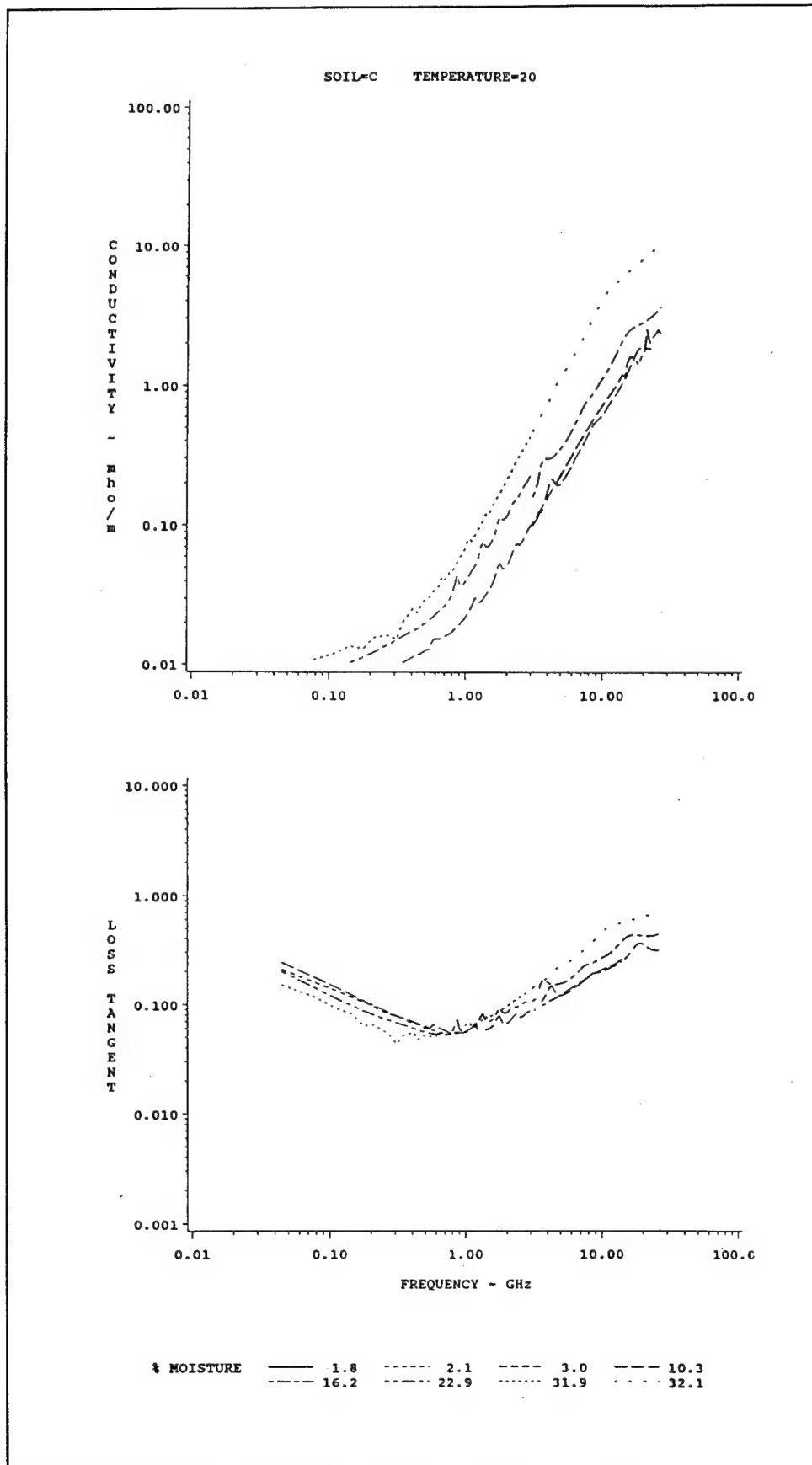
% MOISTURE	0.53	1.90	5.80	7.00
	16.70	18.70	24.10	27.50
	36.60	37.40		

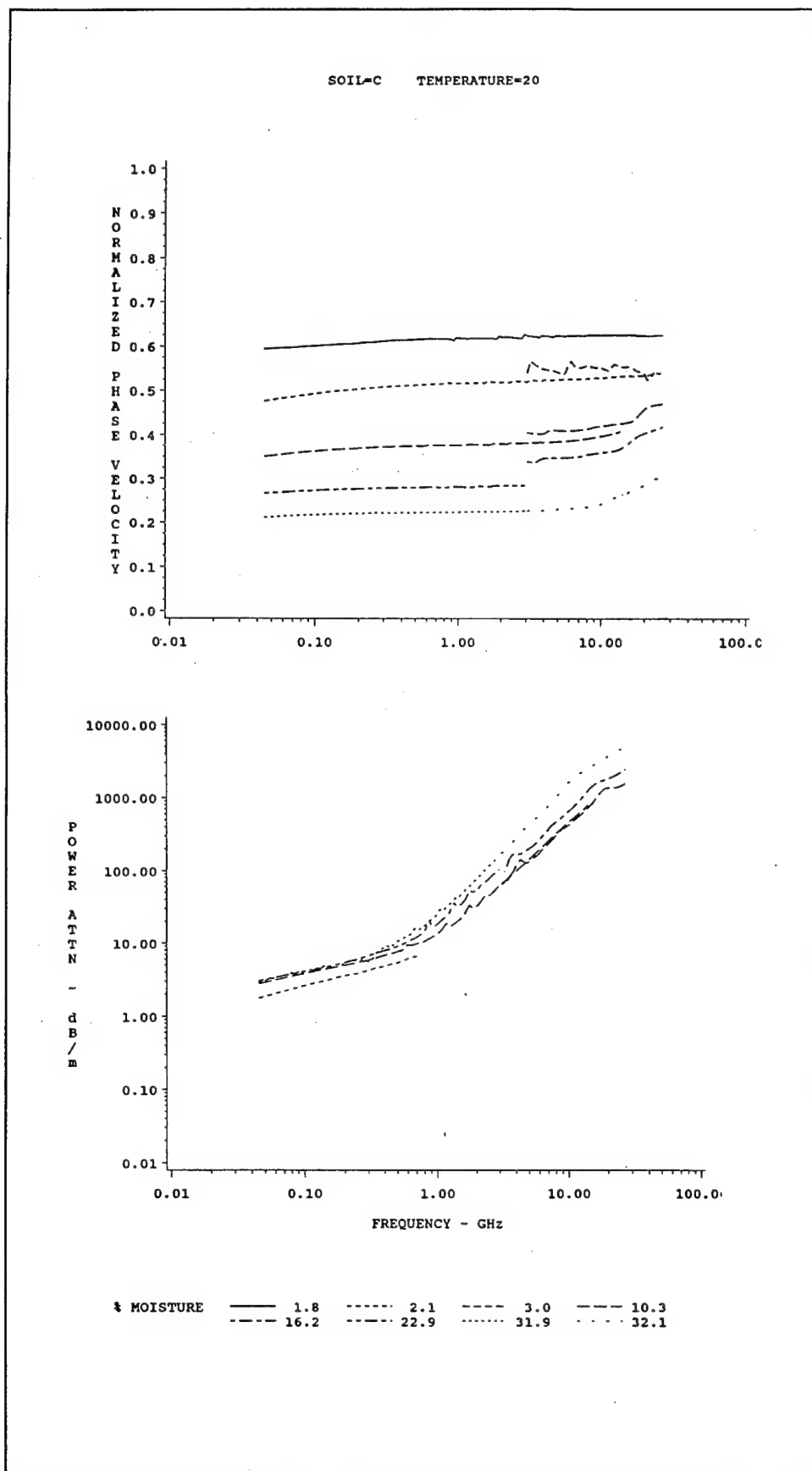


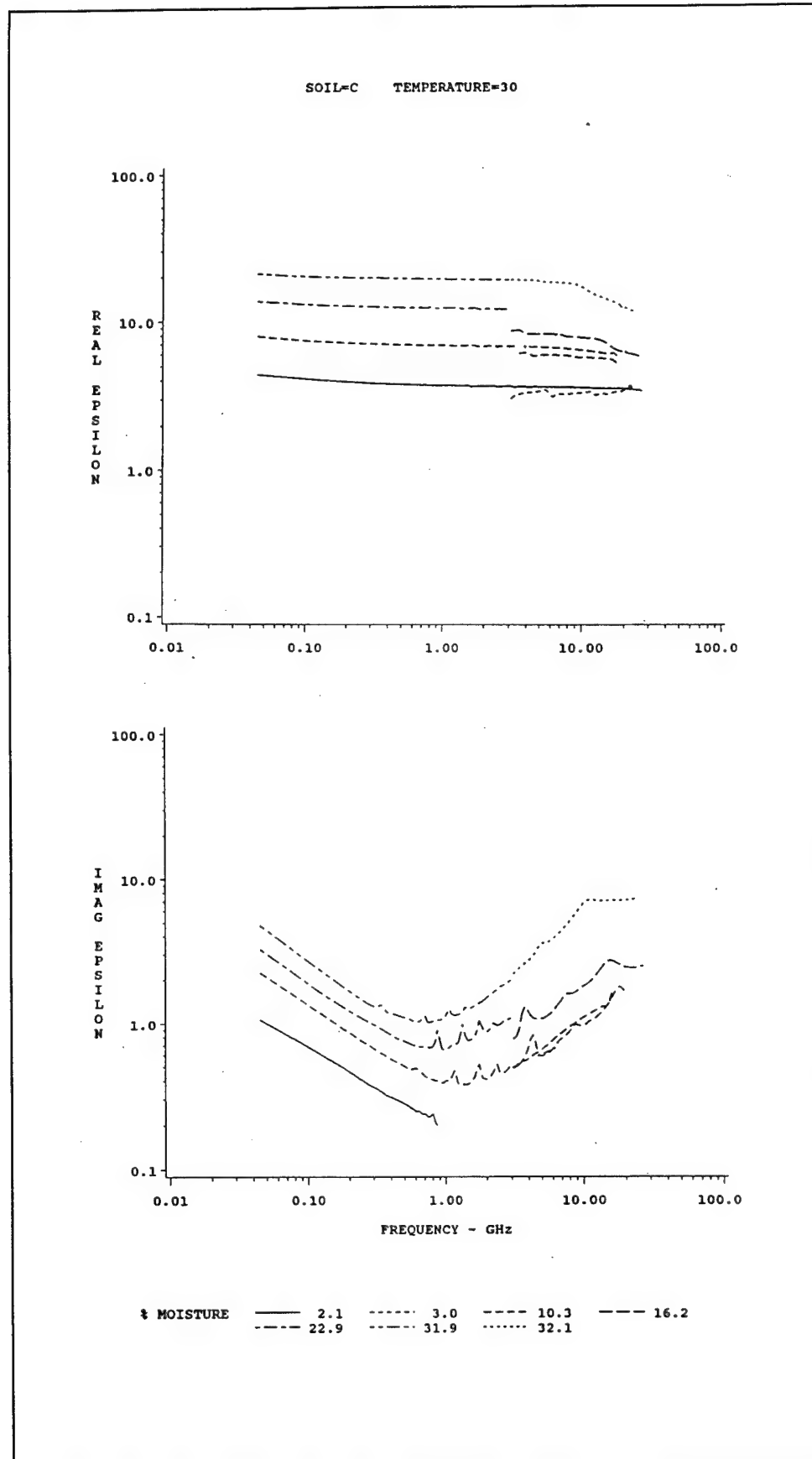


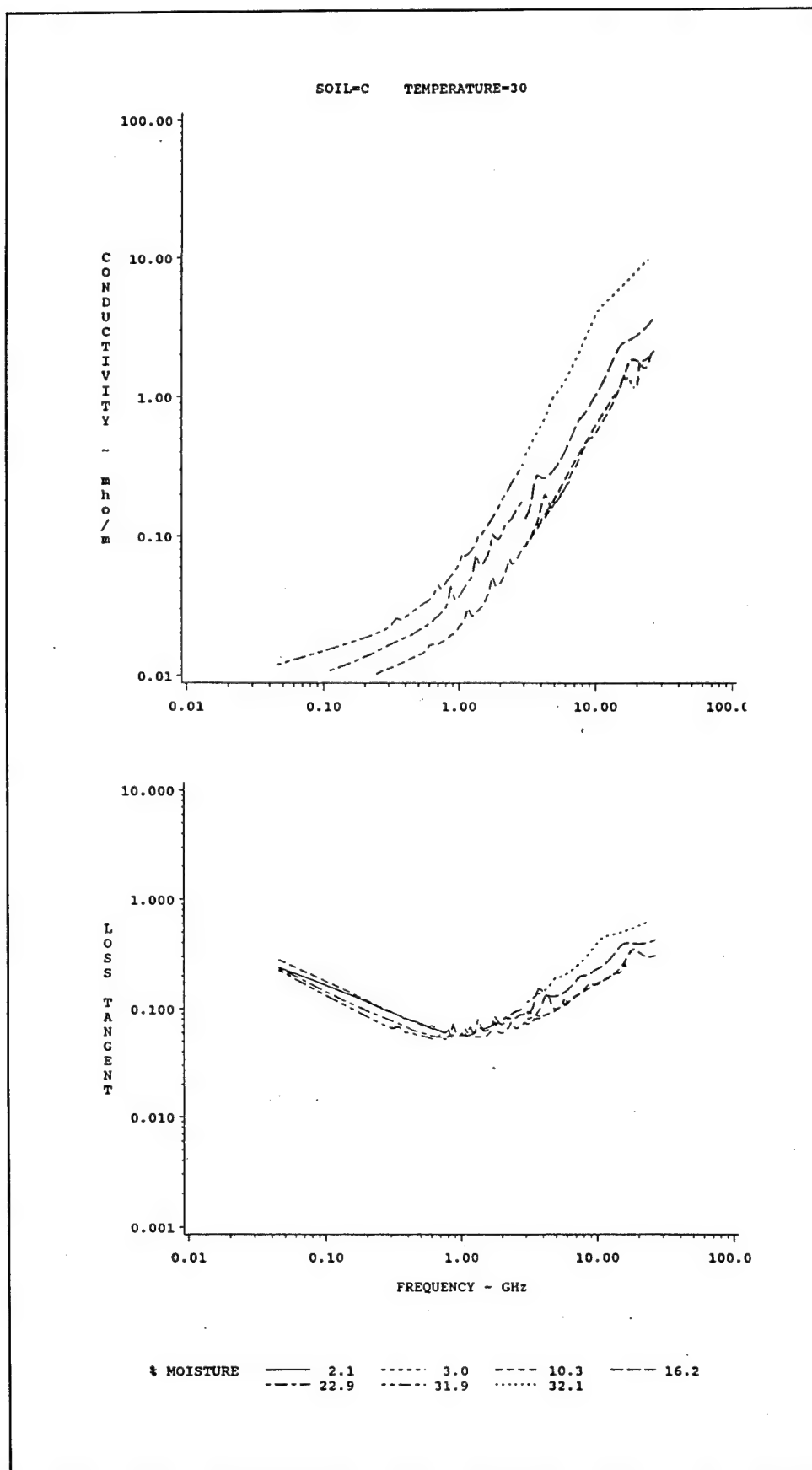


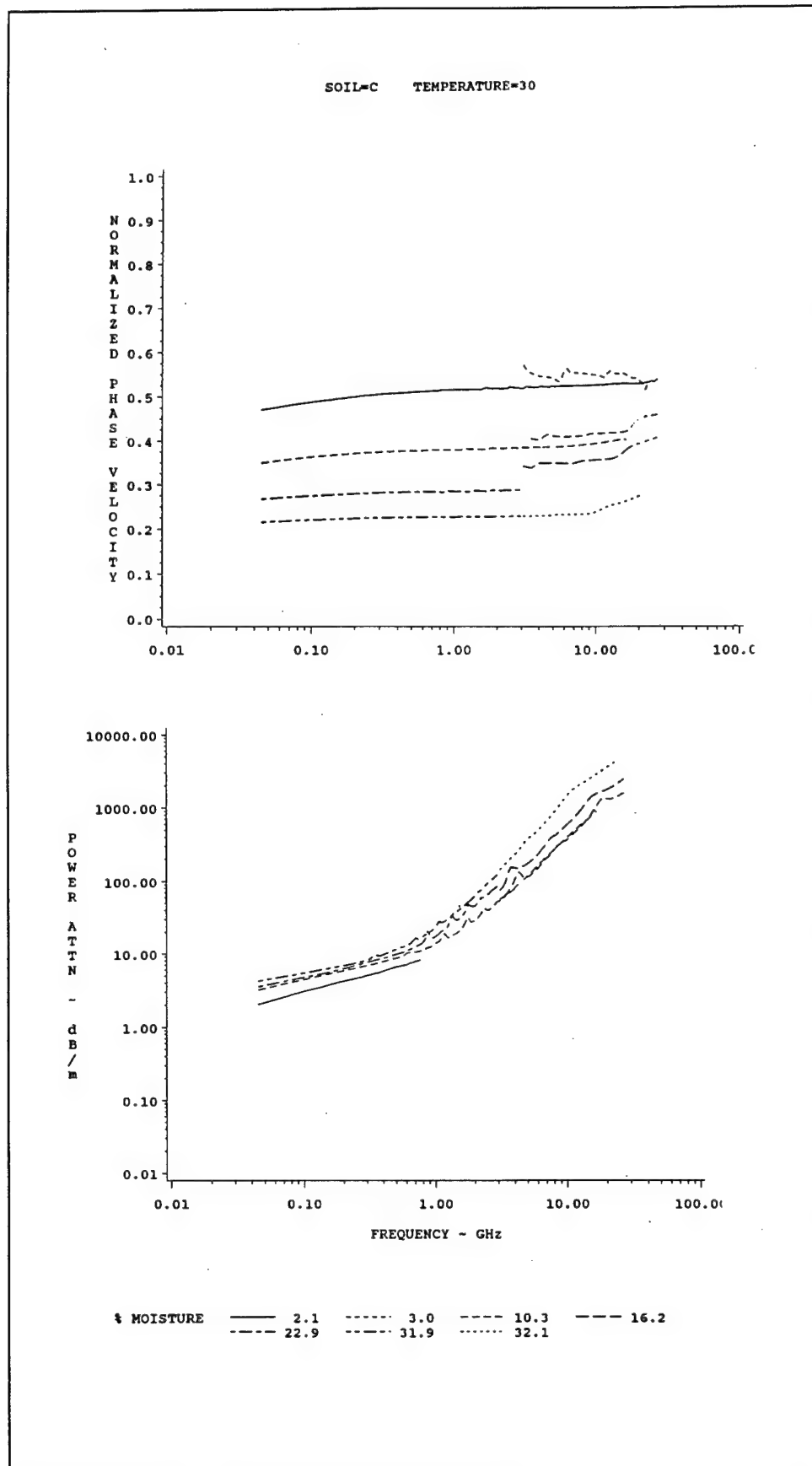


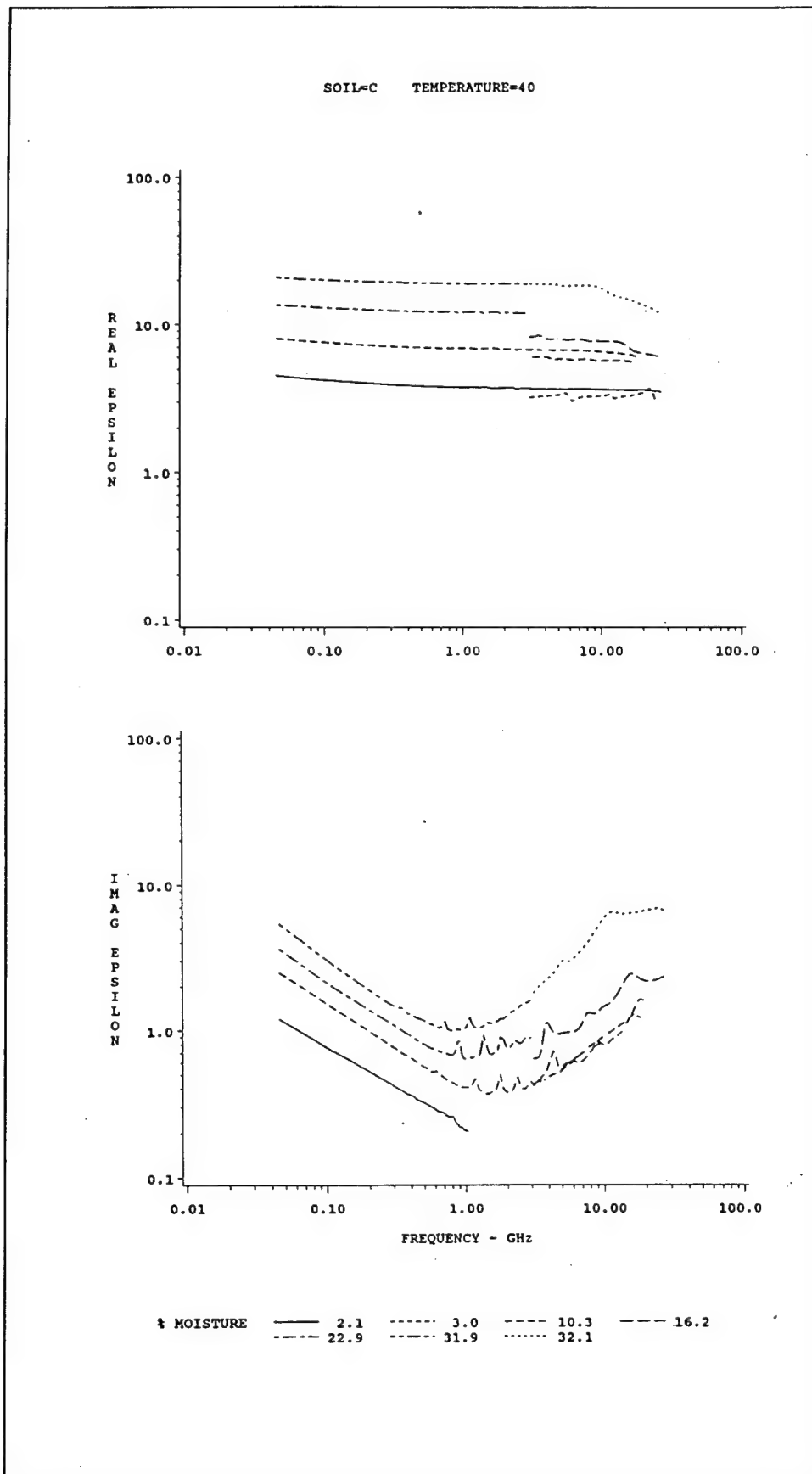


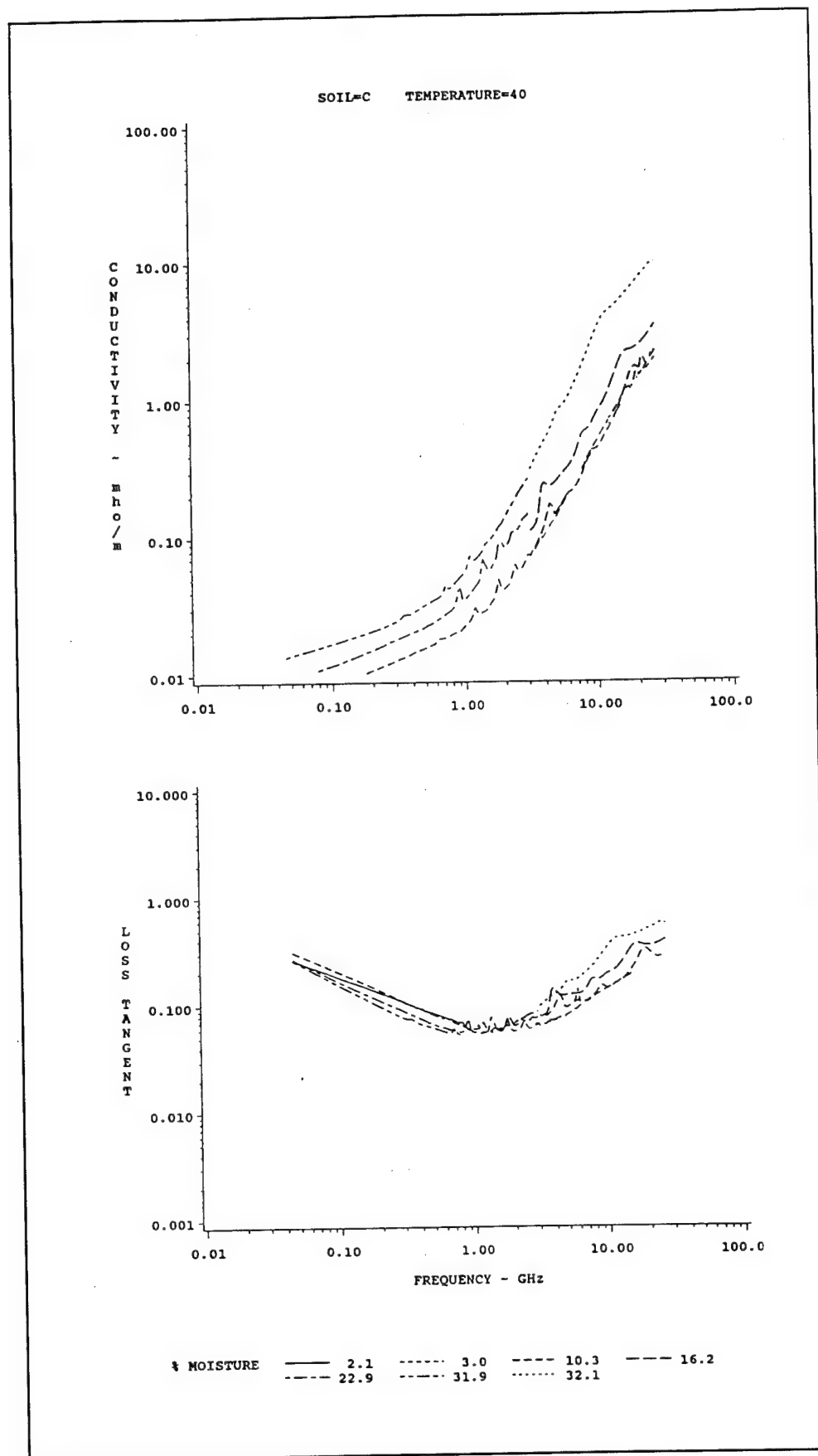


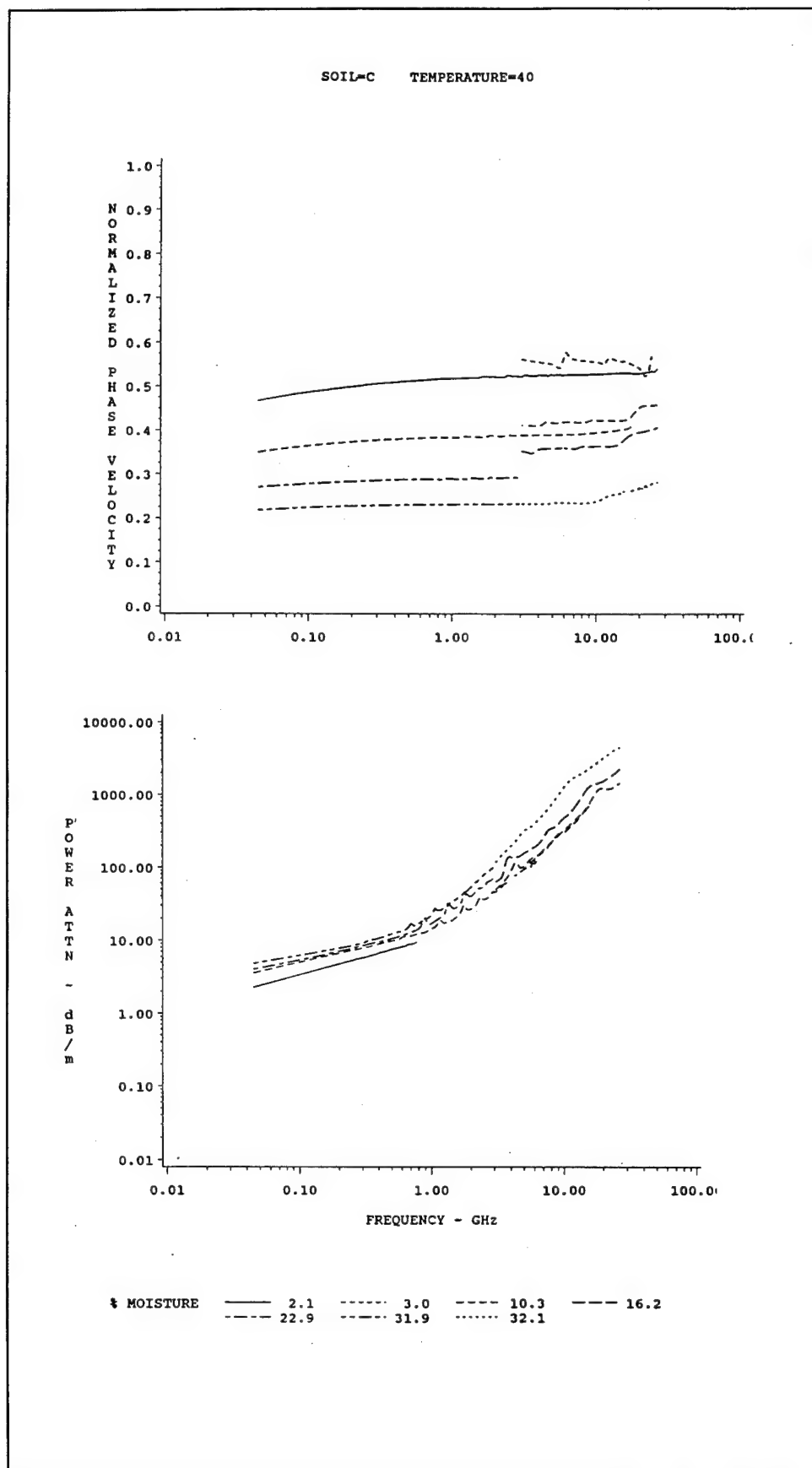


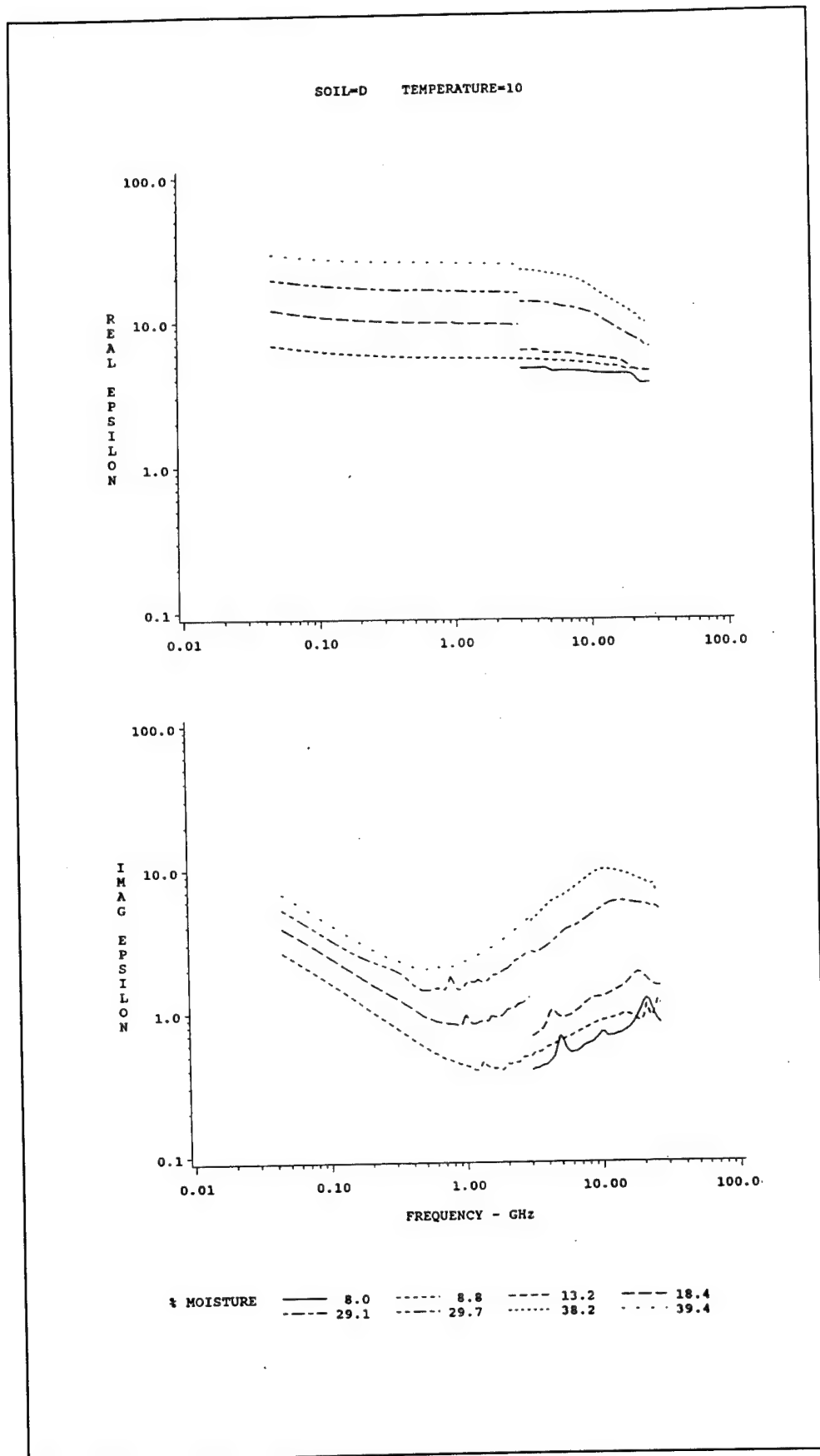


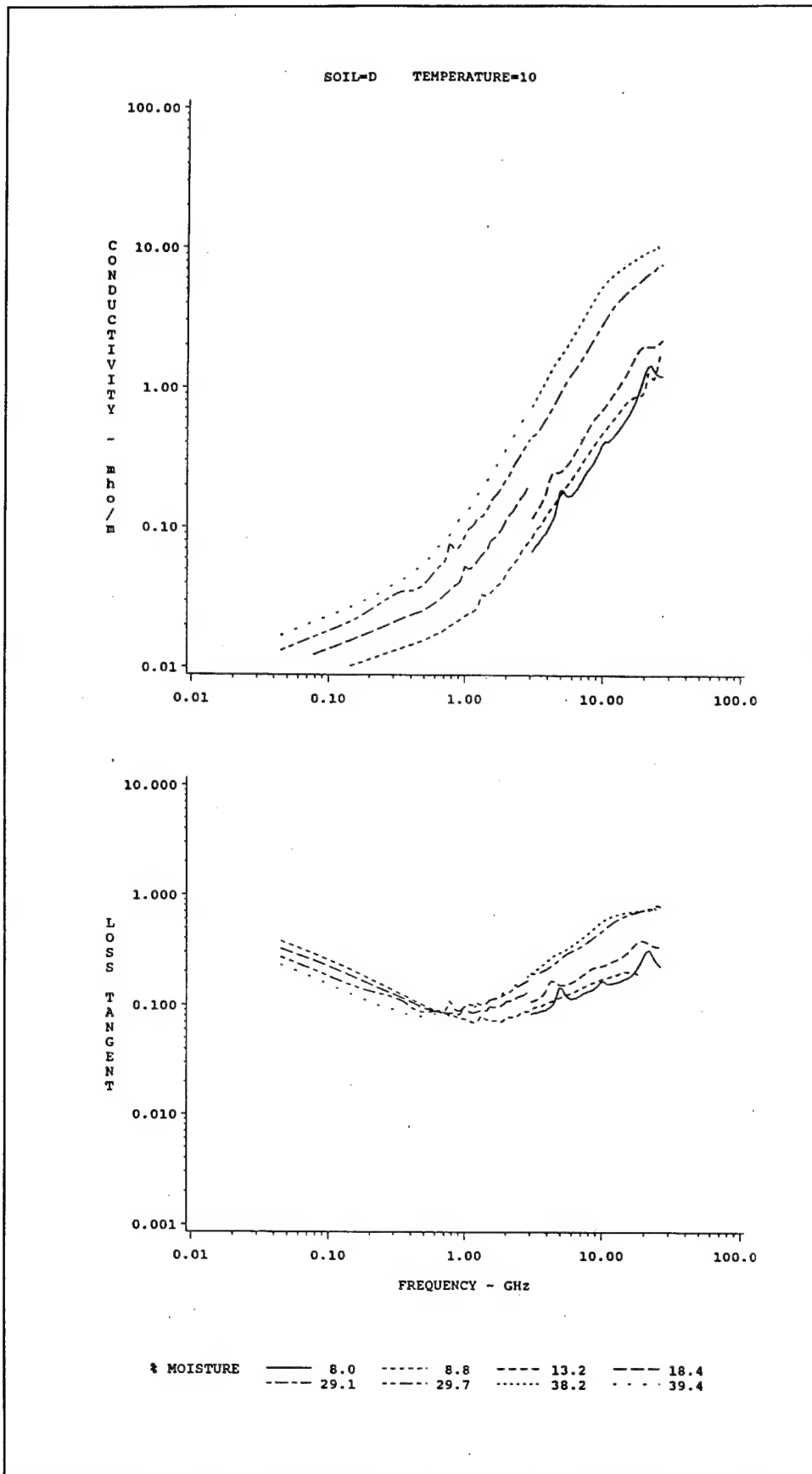


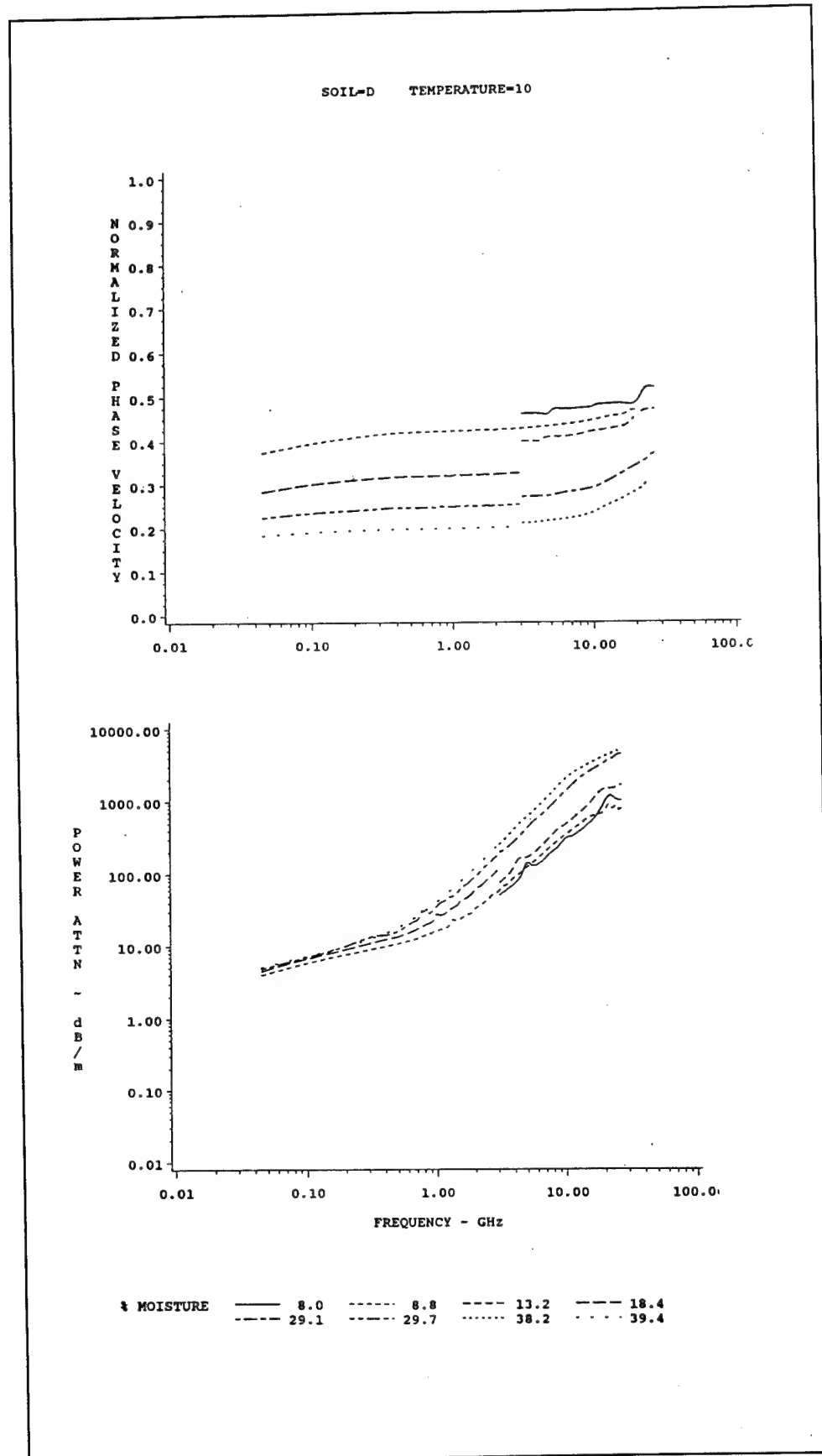


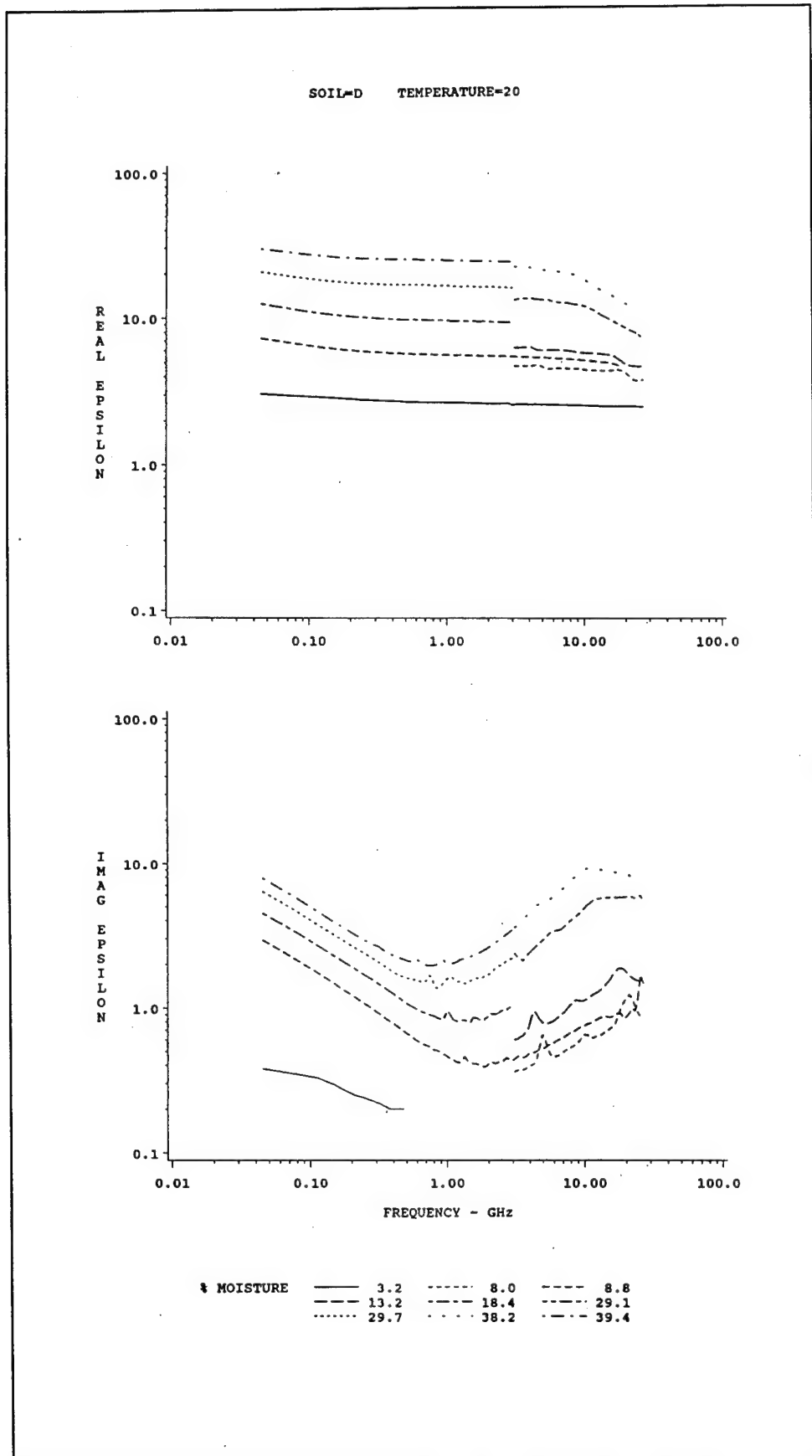


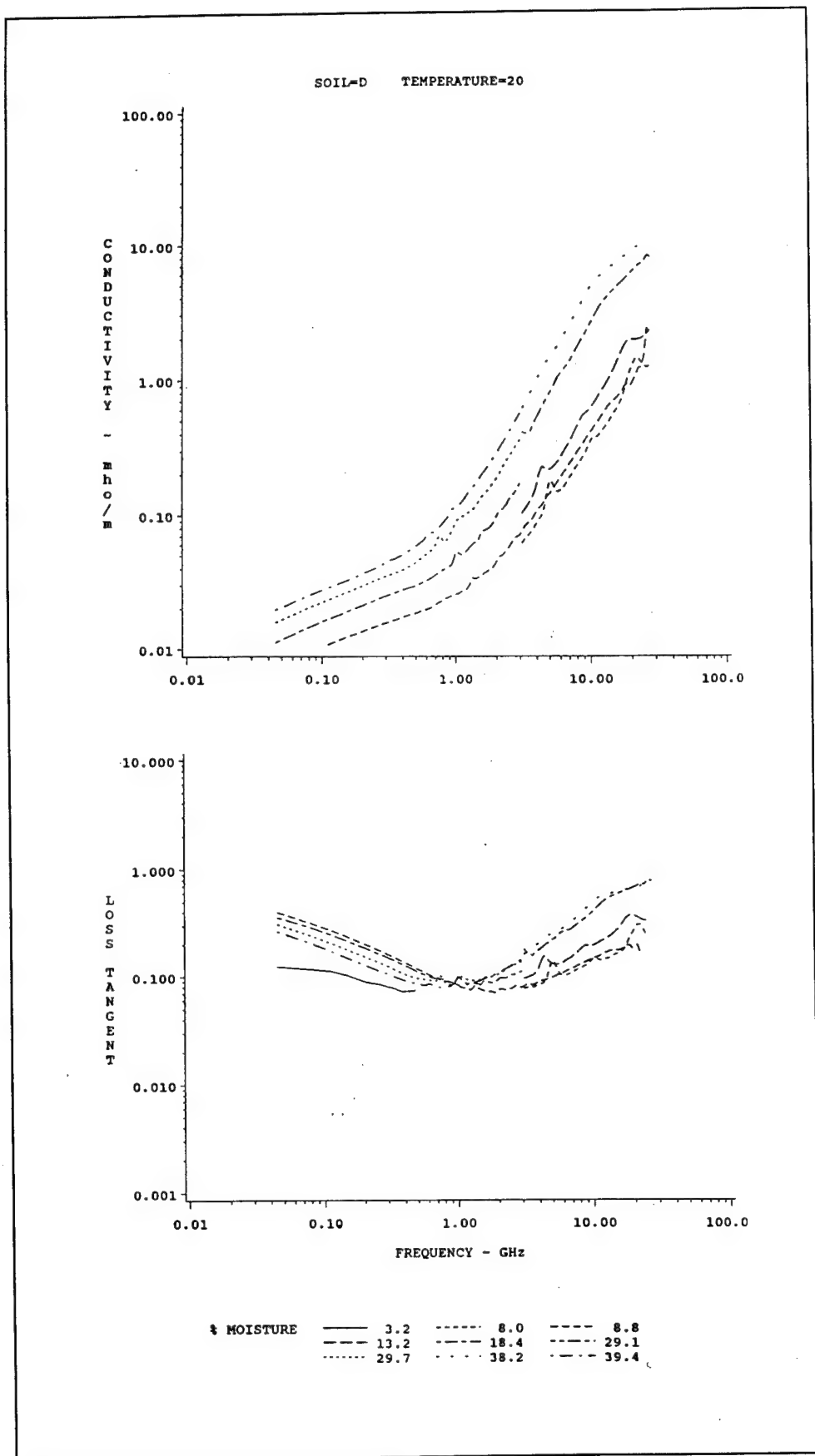


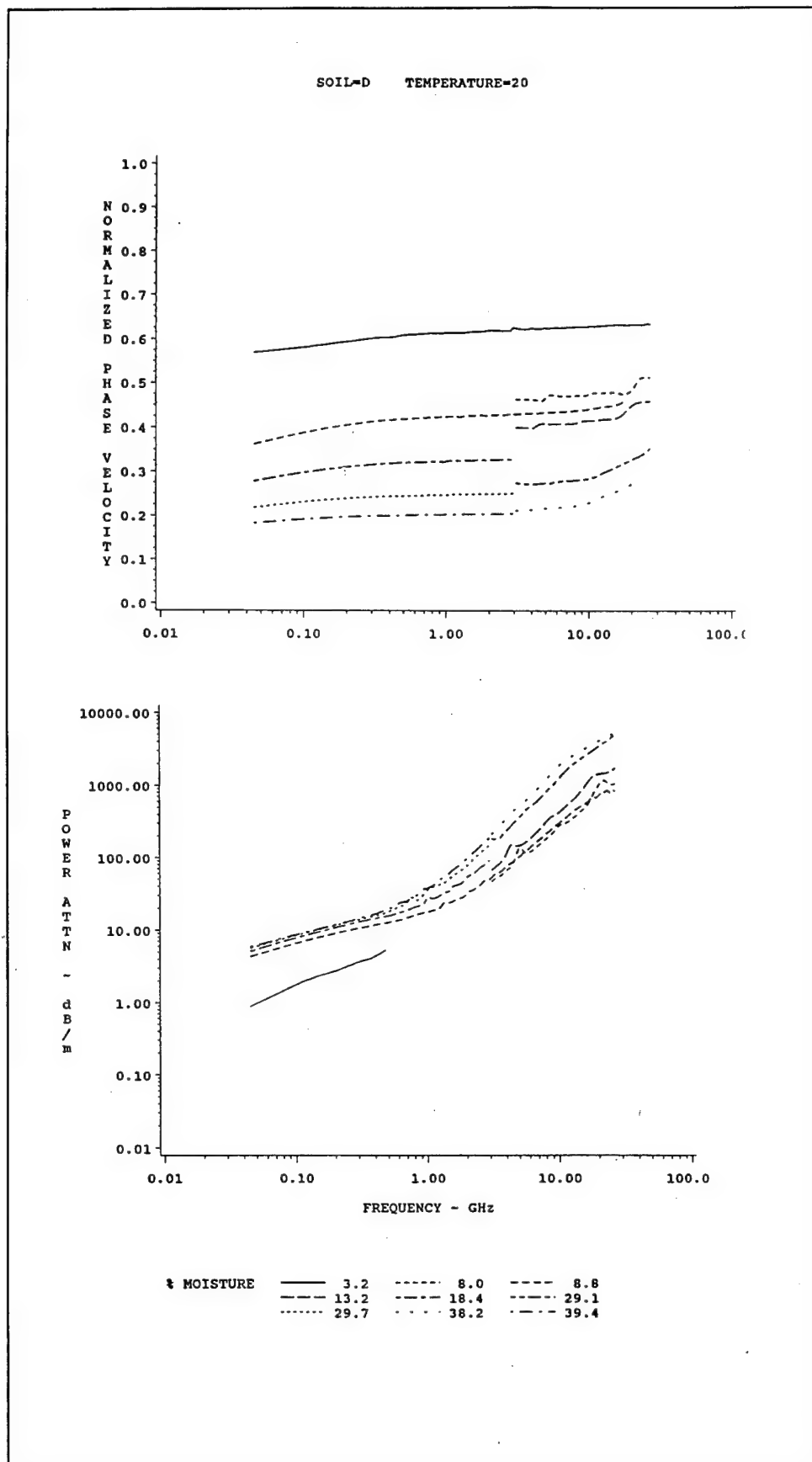


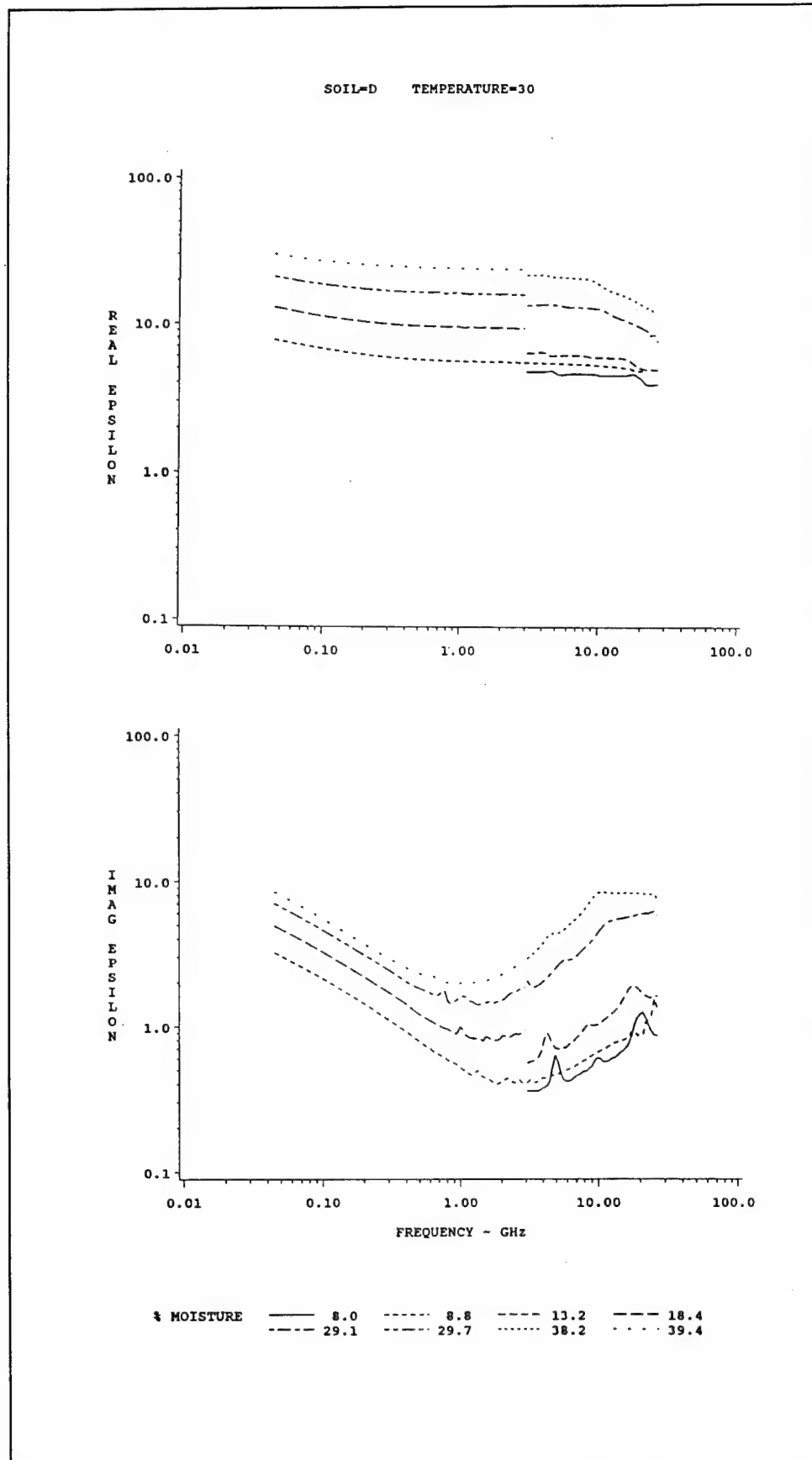


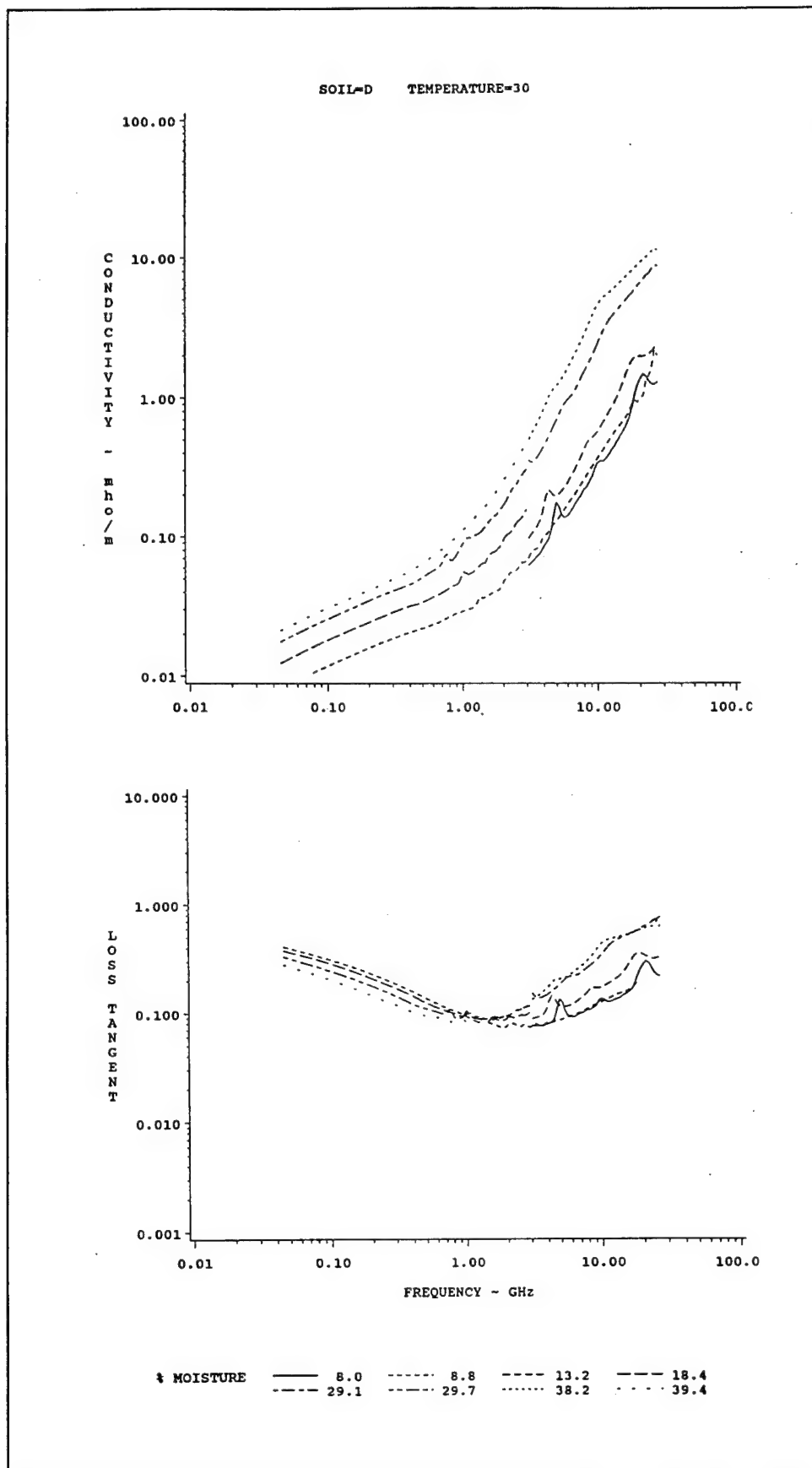


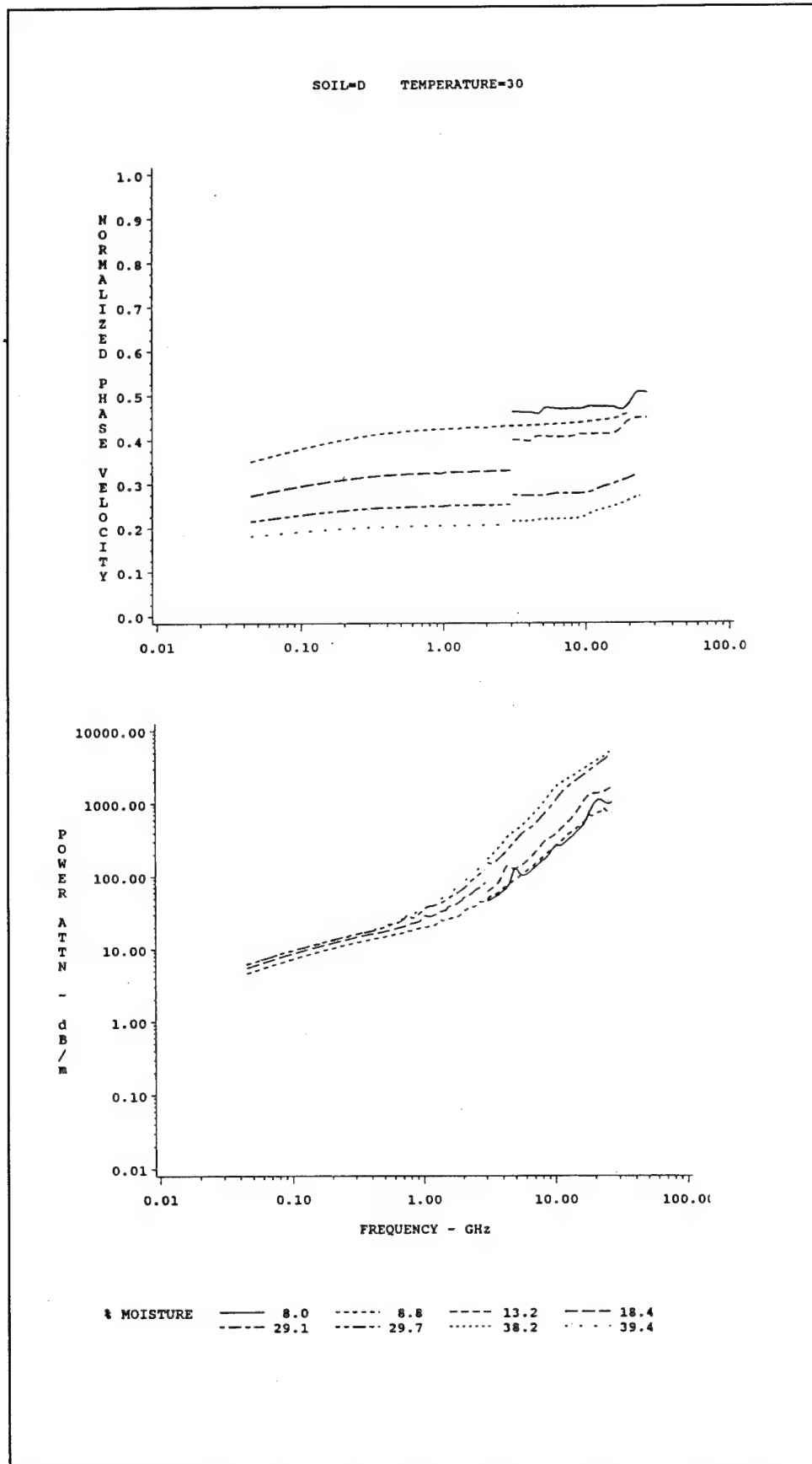




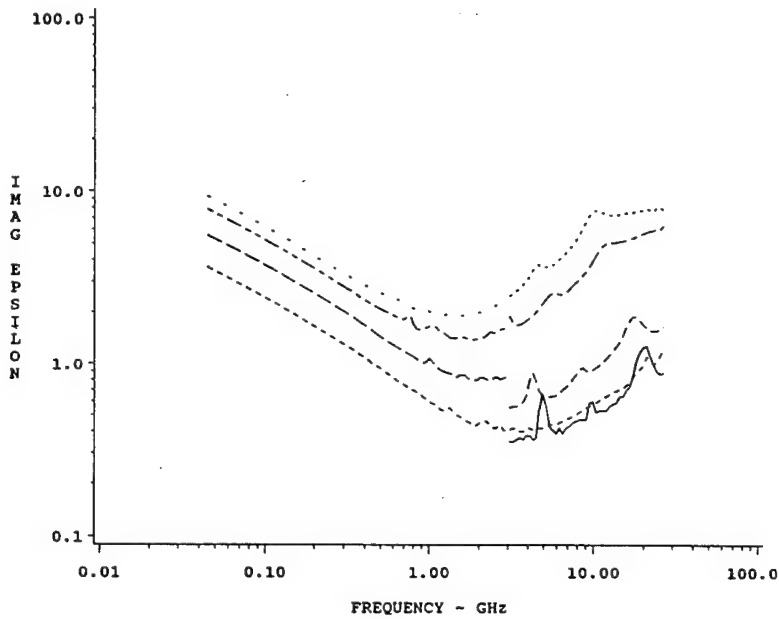
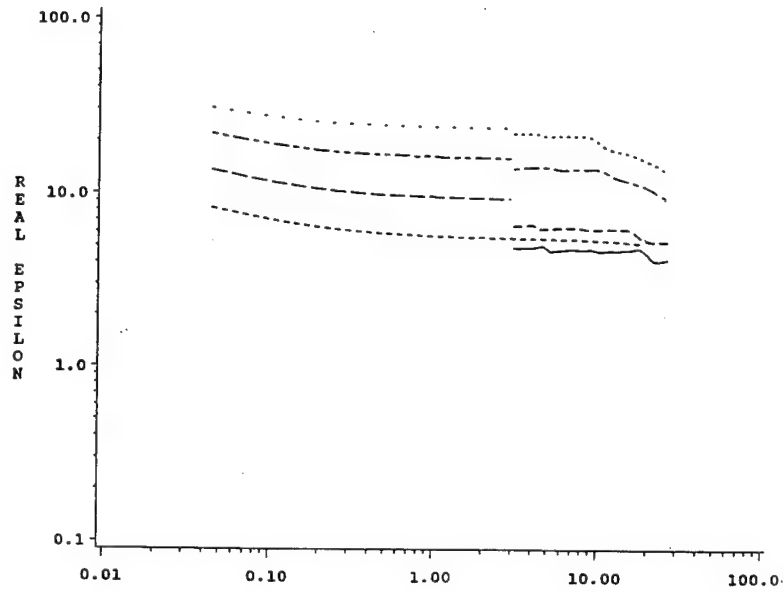




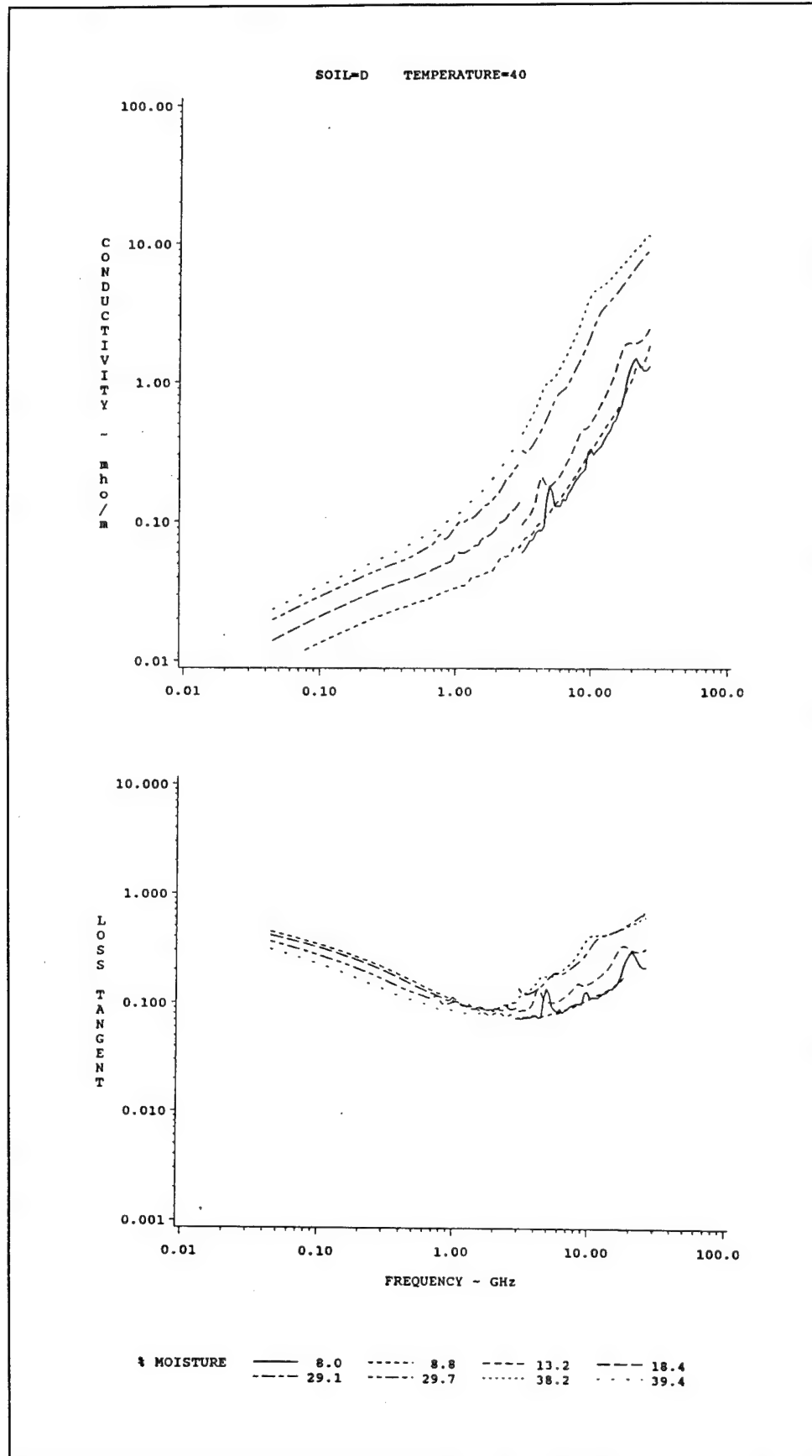




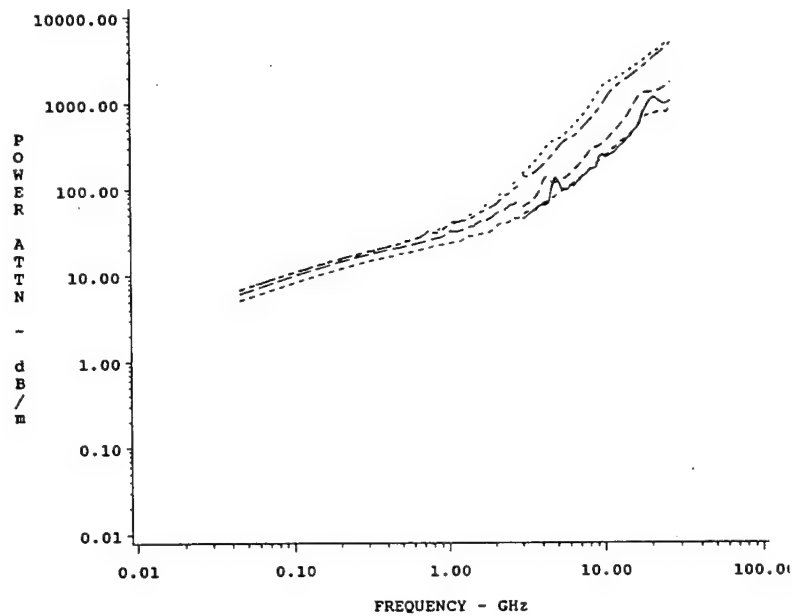
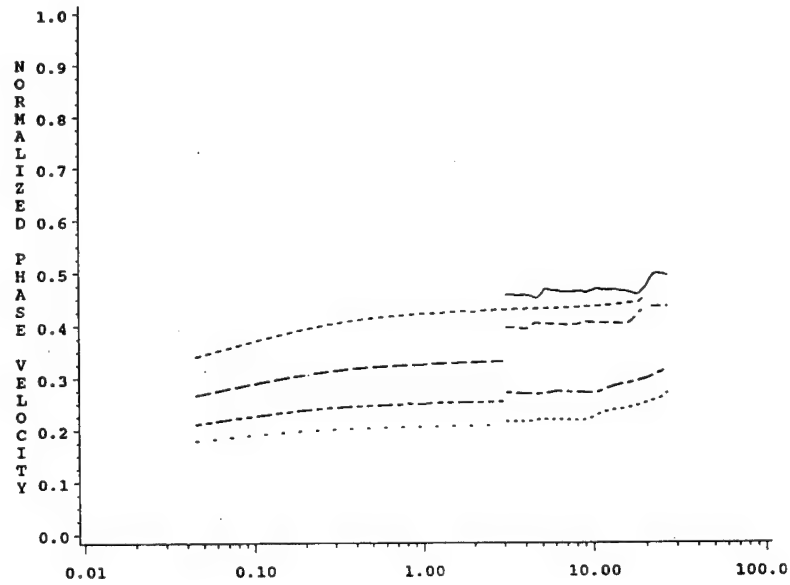
SOIL-D TEMPERATURE=40



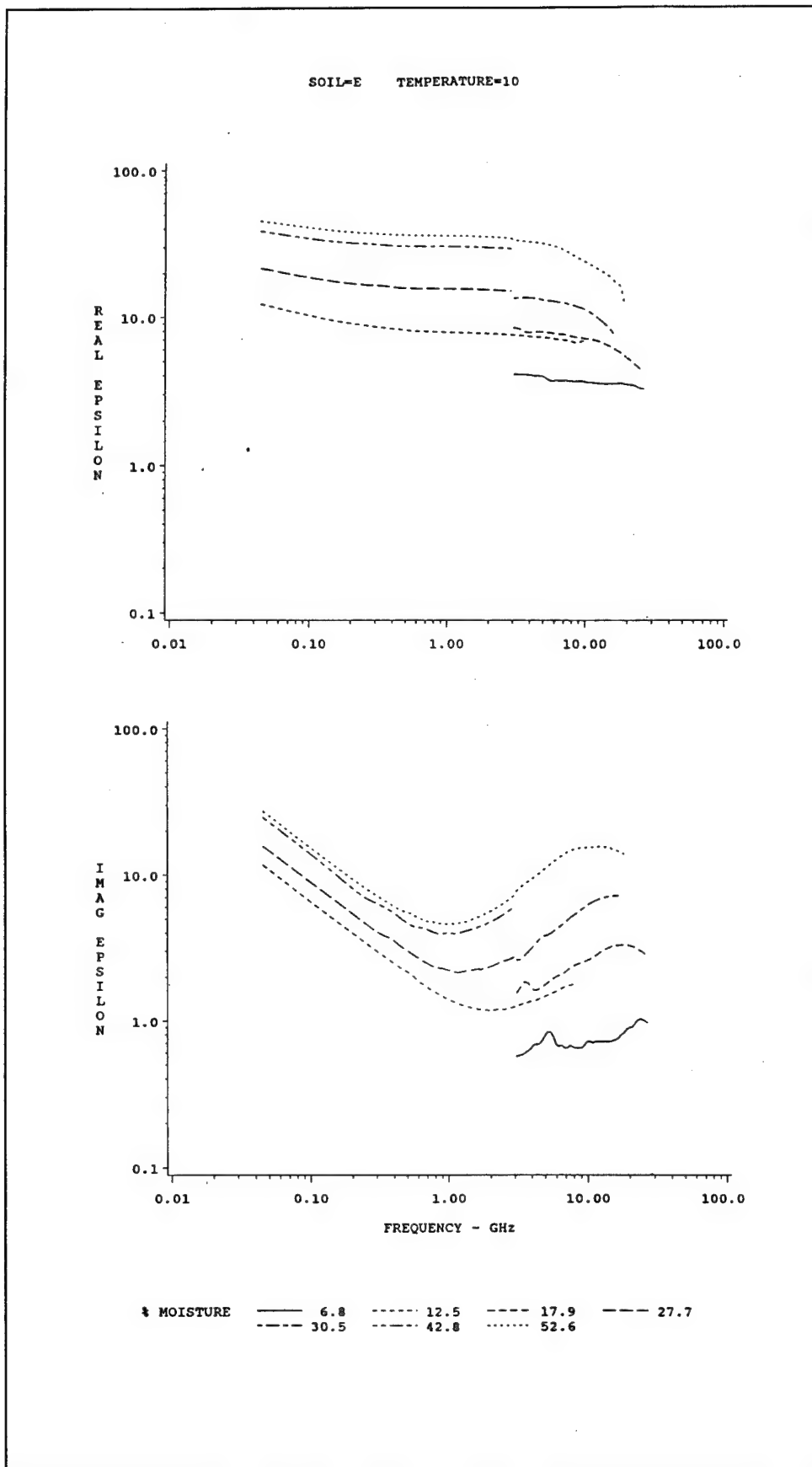
% MOISTURE ——— 8.0 - - - 8.8 - - - 13.2 - - - 18.4
 - - - 29.1 - - - 29.7 - - - 38.2 - - - 39.4

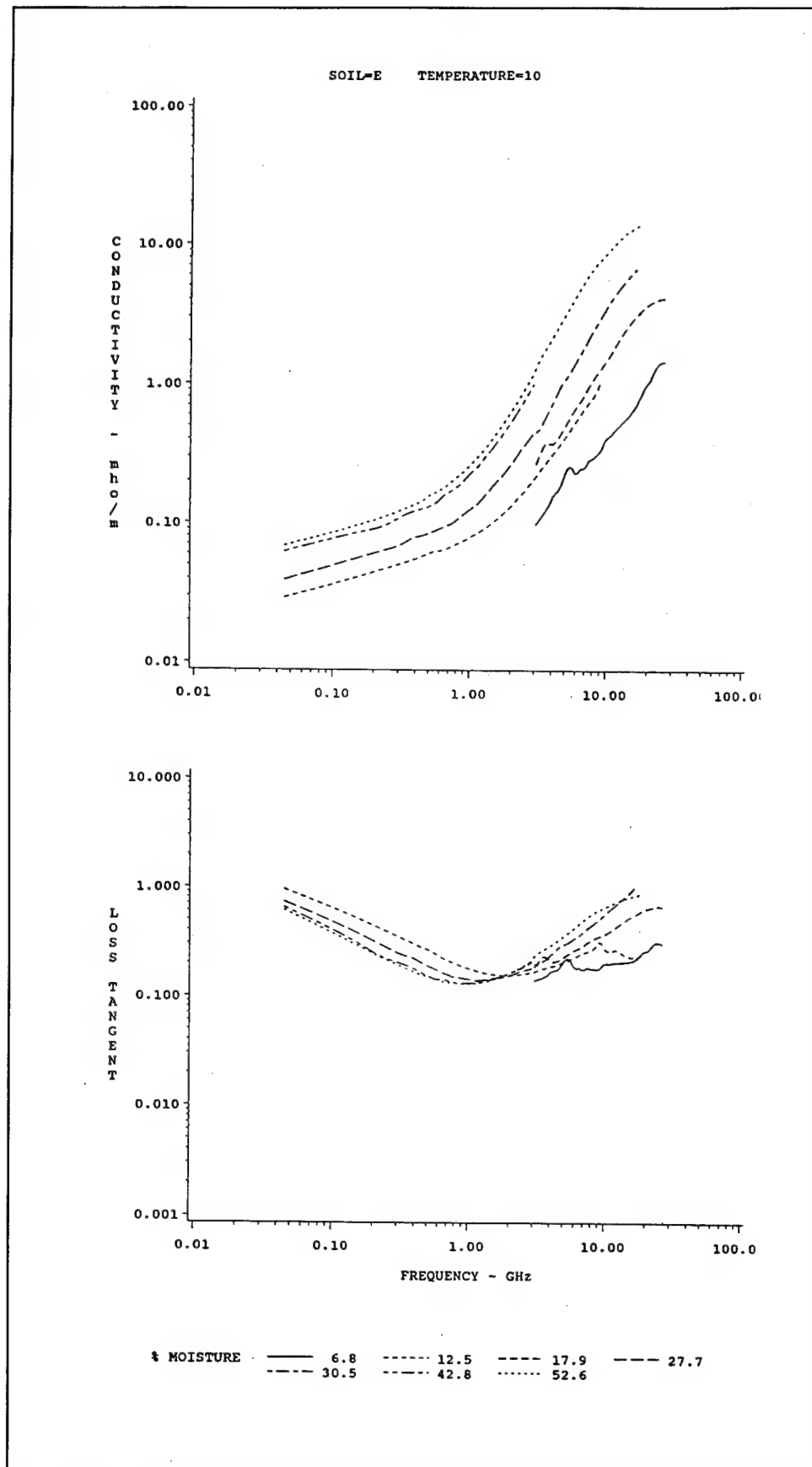


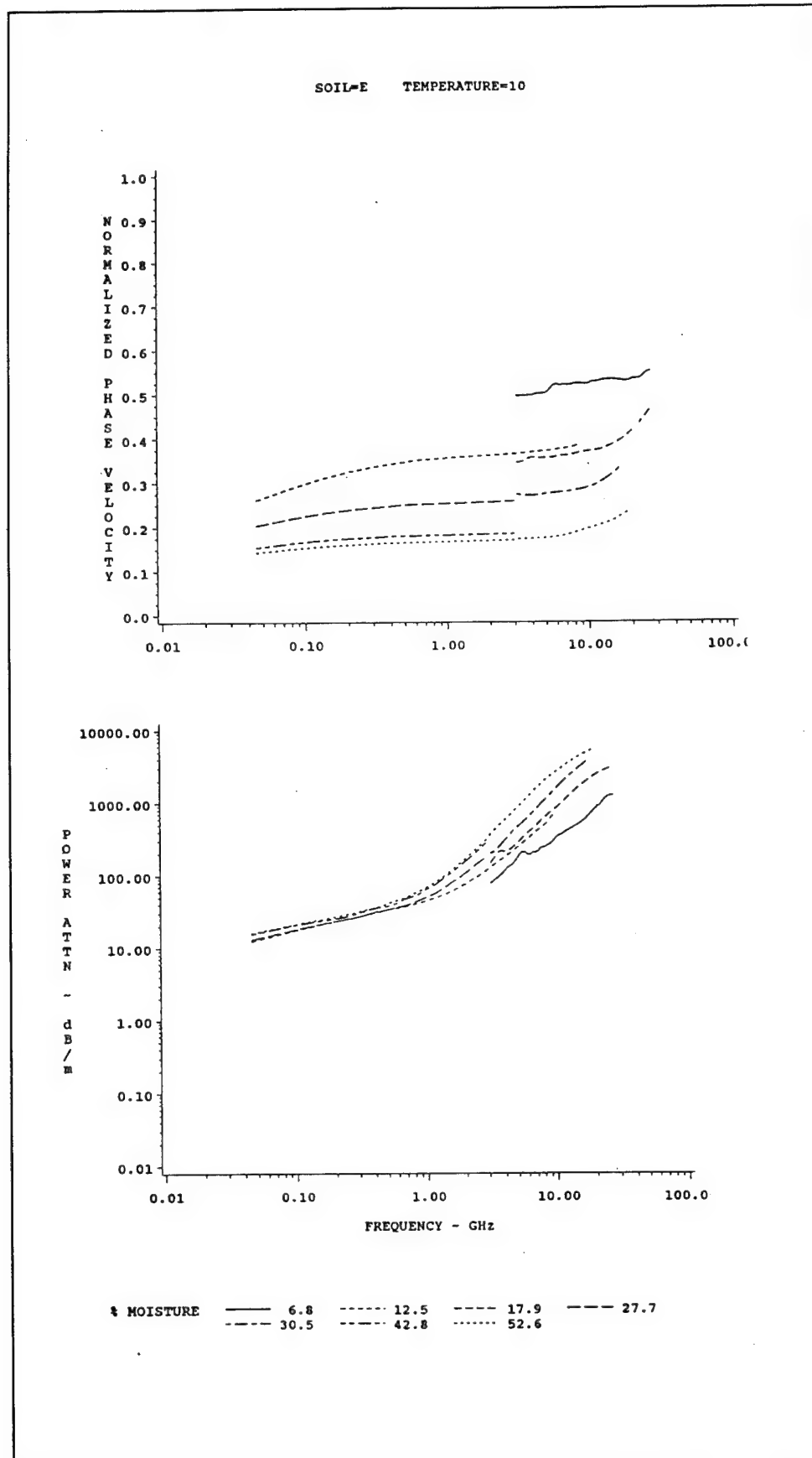
SOIL=D TEMPERATURE=40

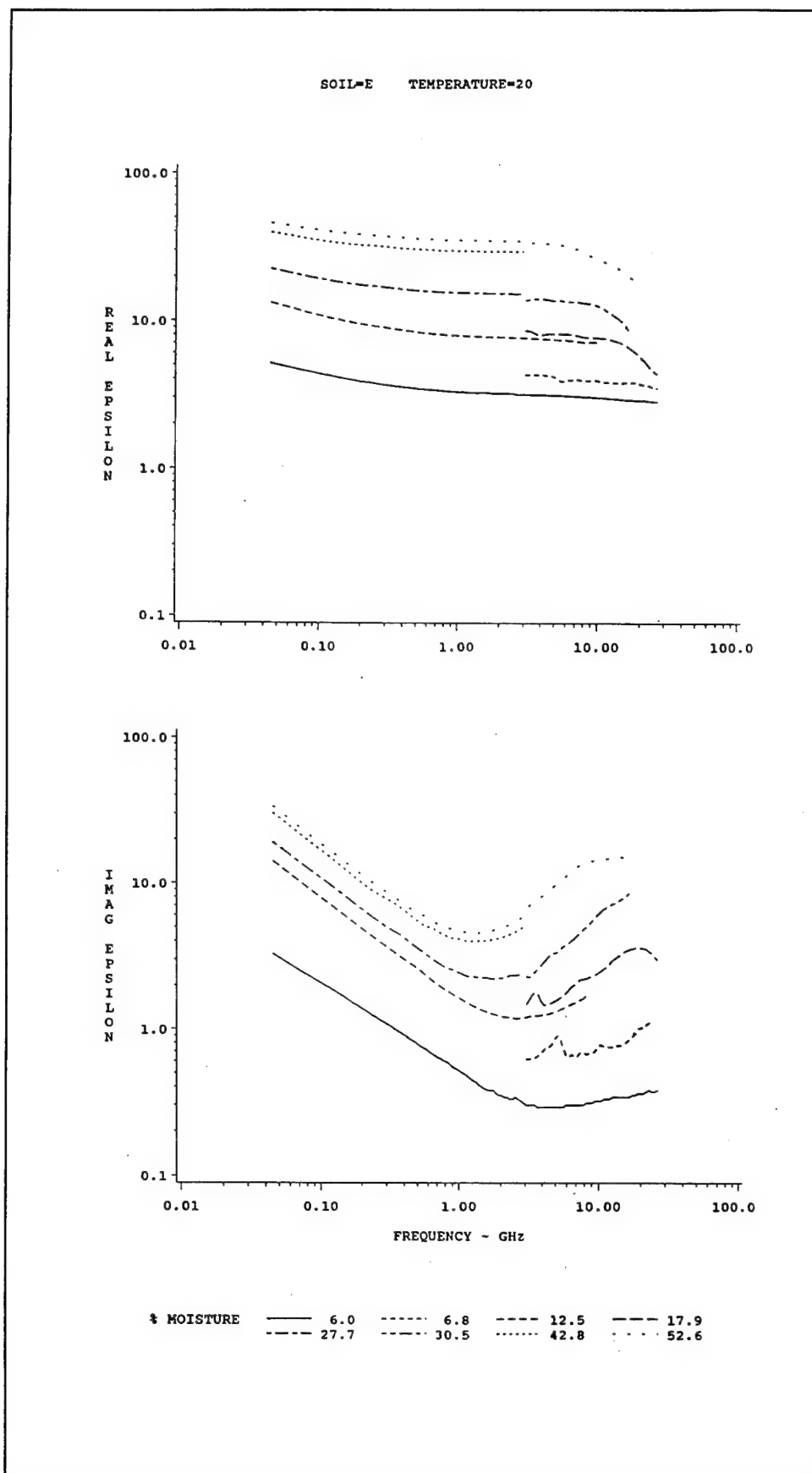


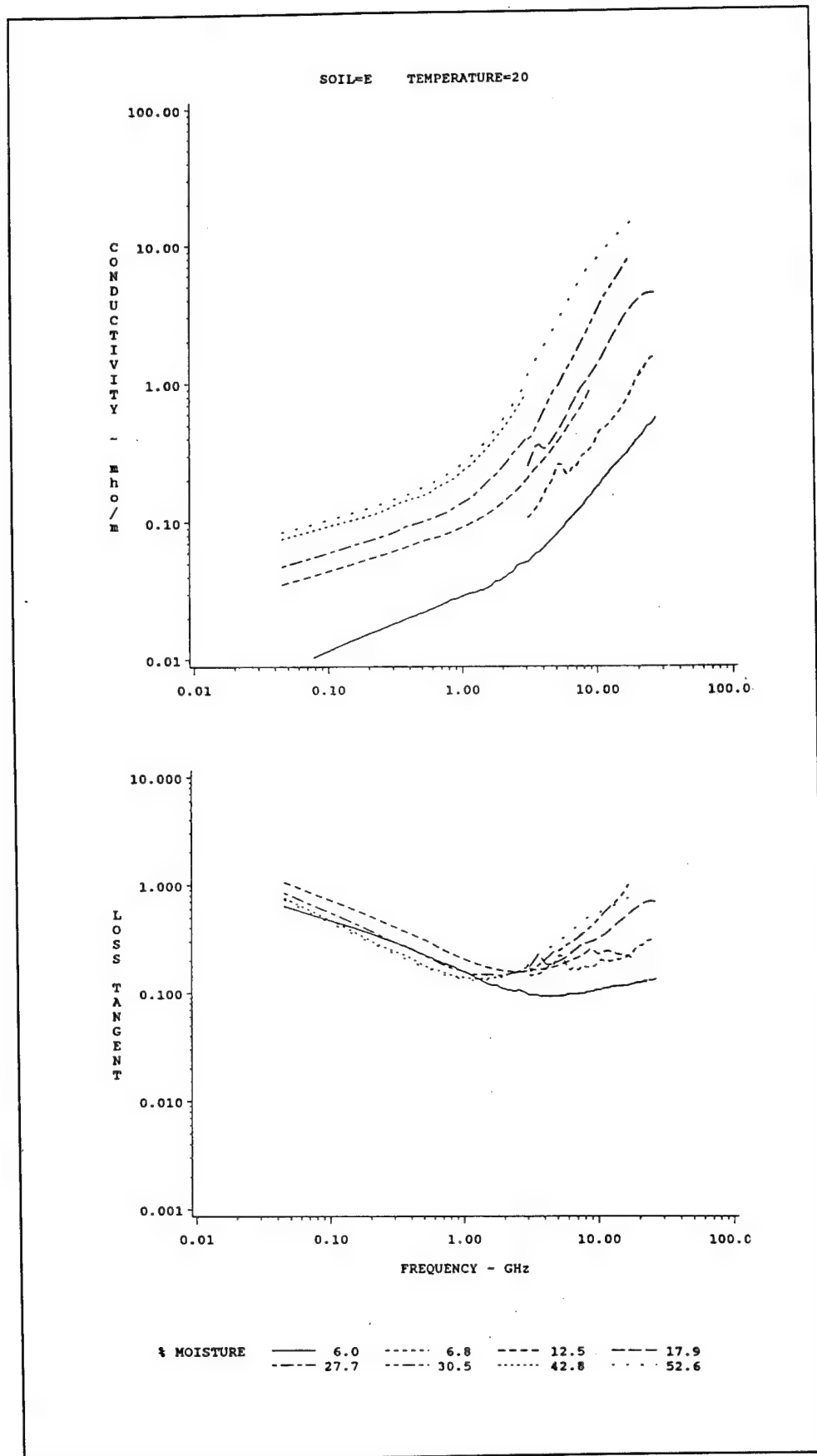
% MOISTURE ——— 8.0 - - - - 8.8 - . - . 13.2 - - - - 18.4
 - - - - 29.1 - . - . 29.7 38.2 - . - . 39.4

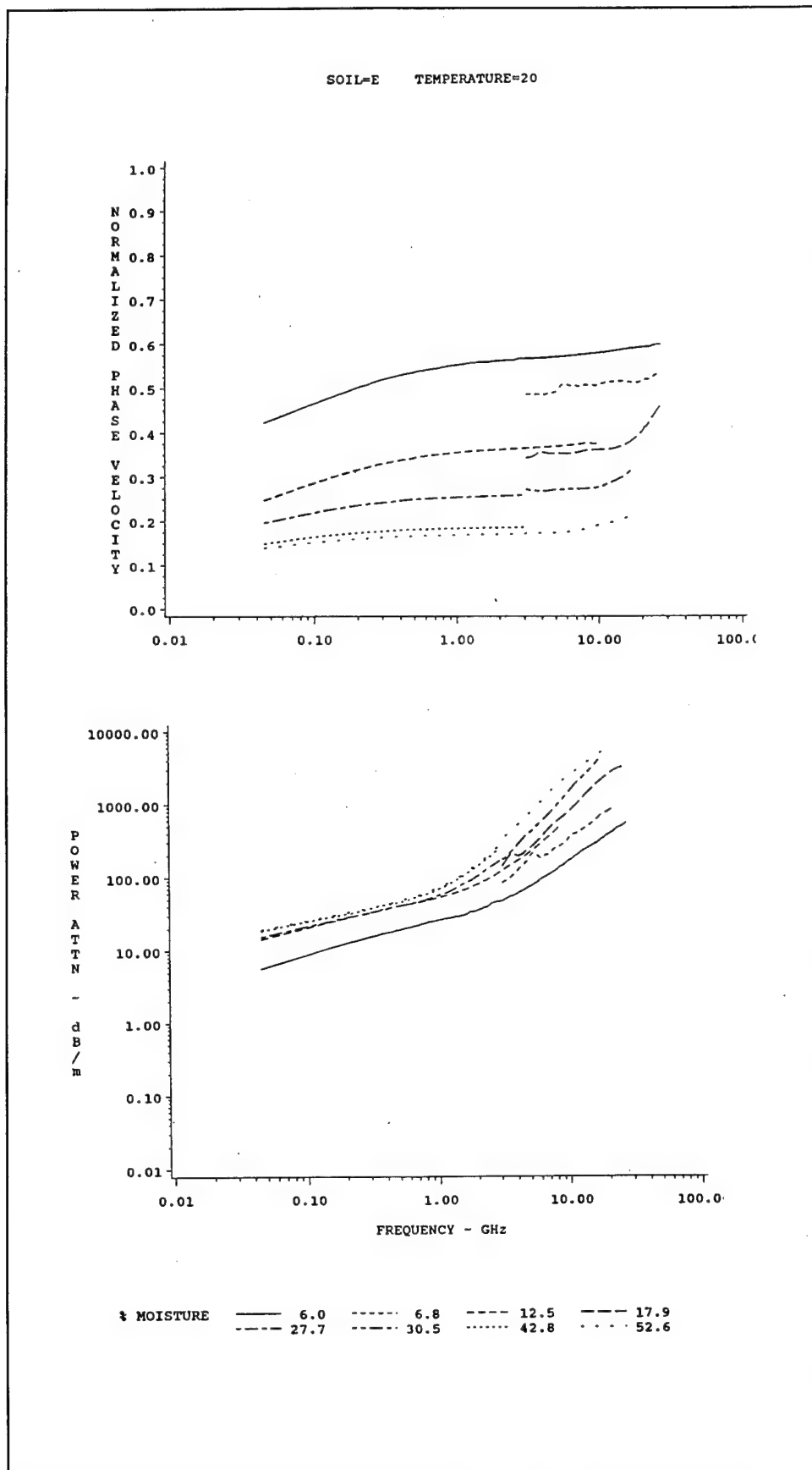


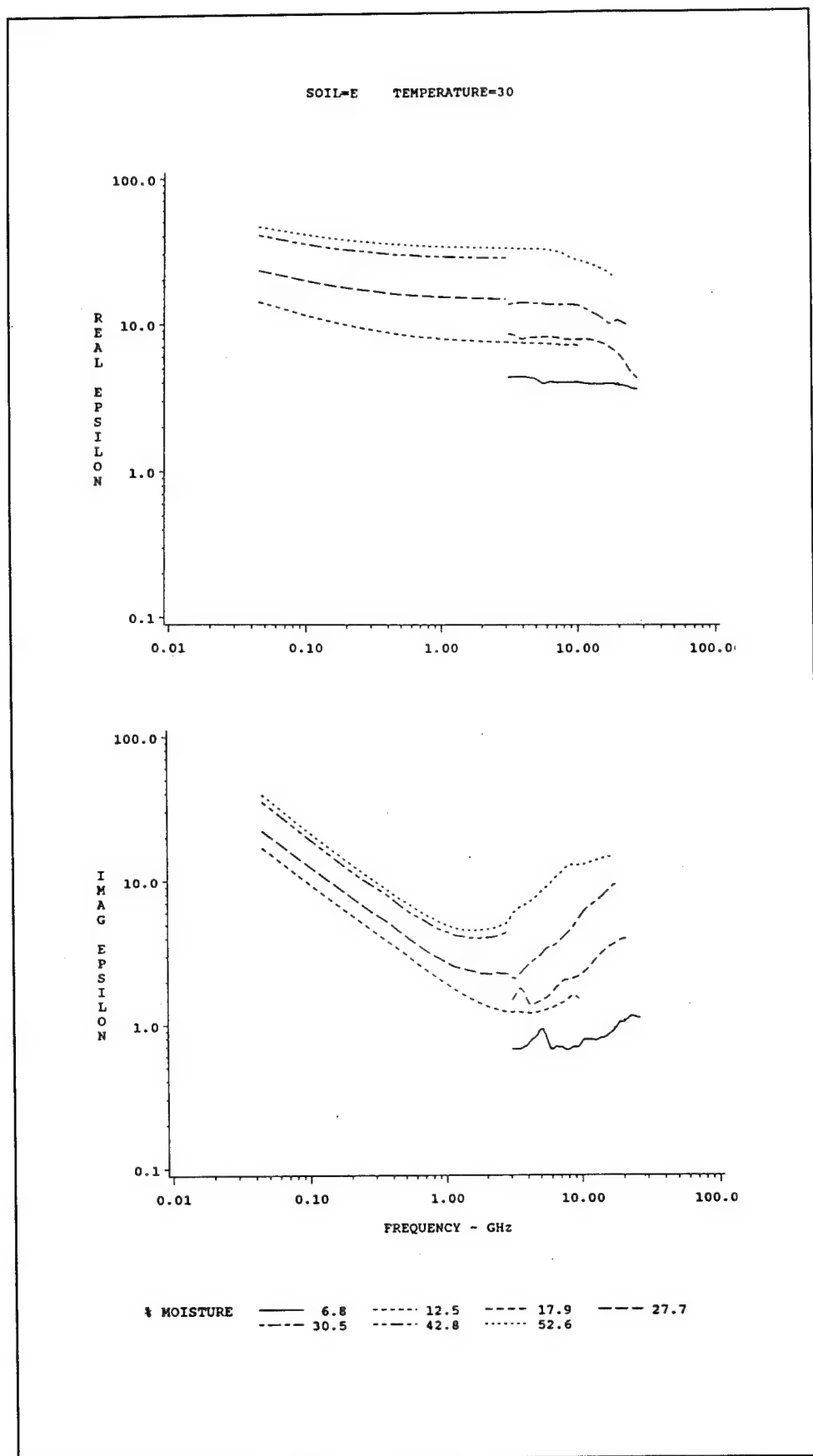


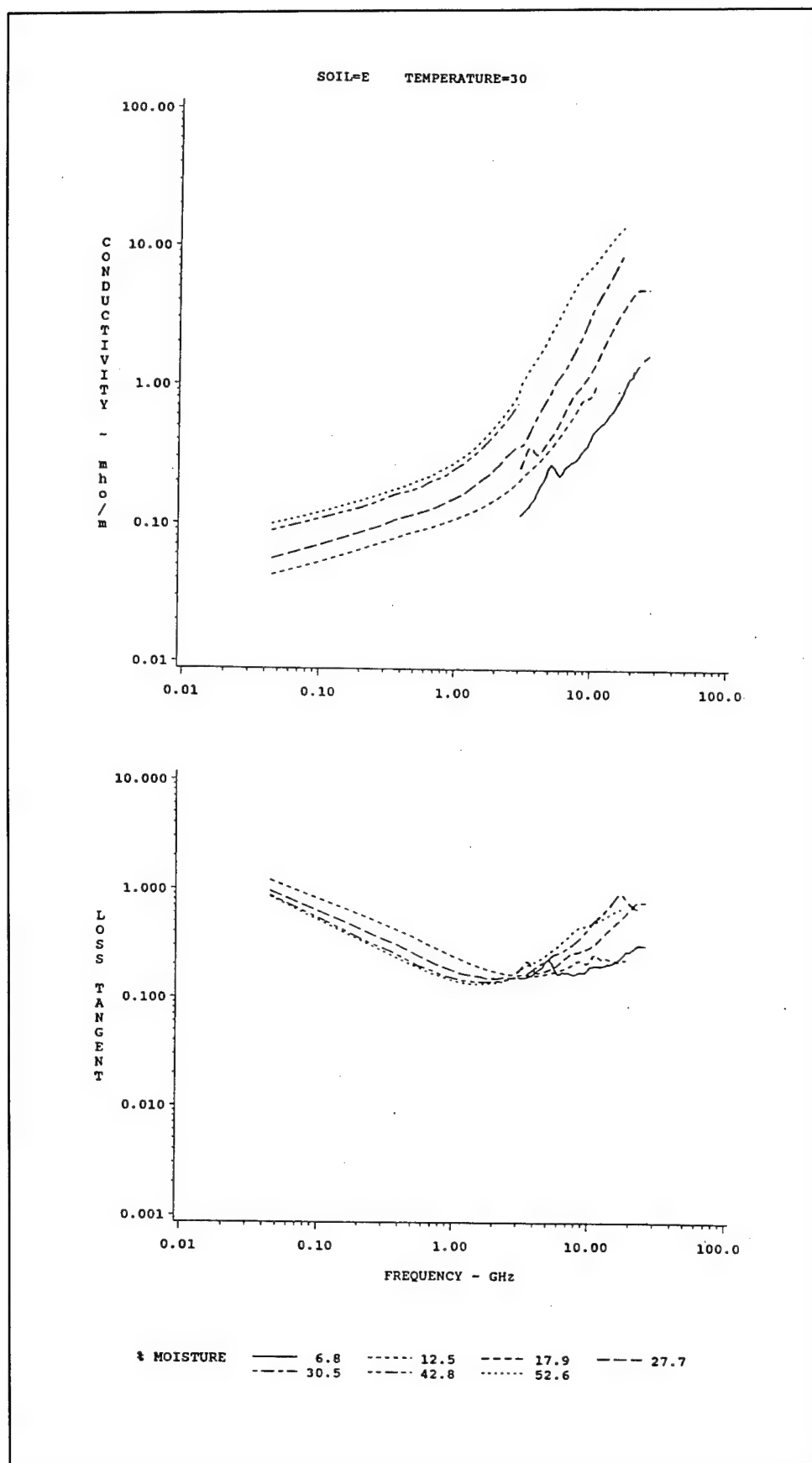




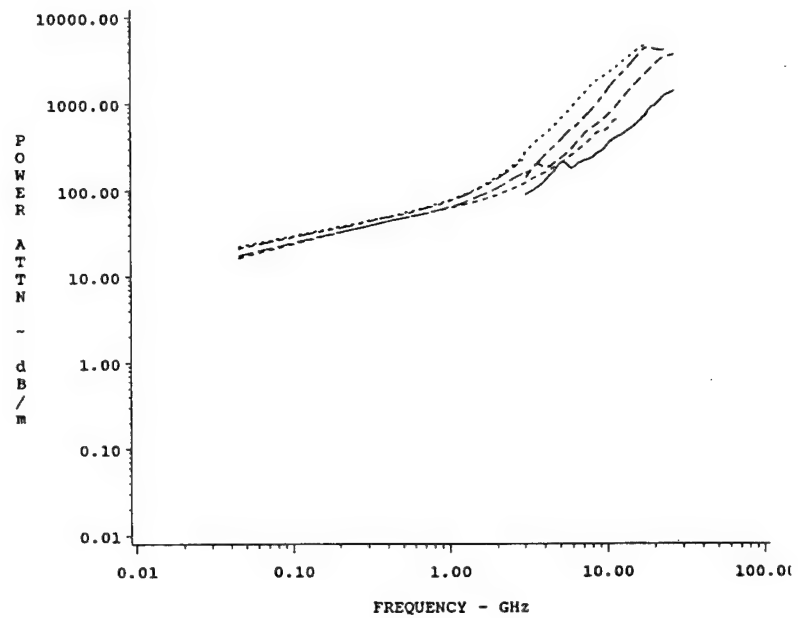
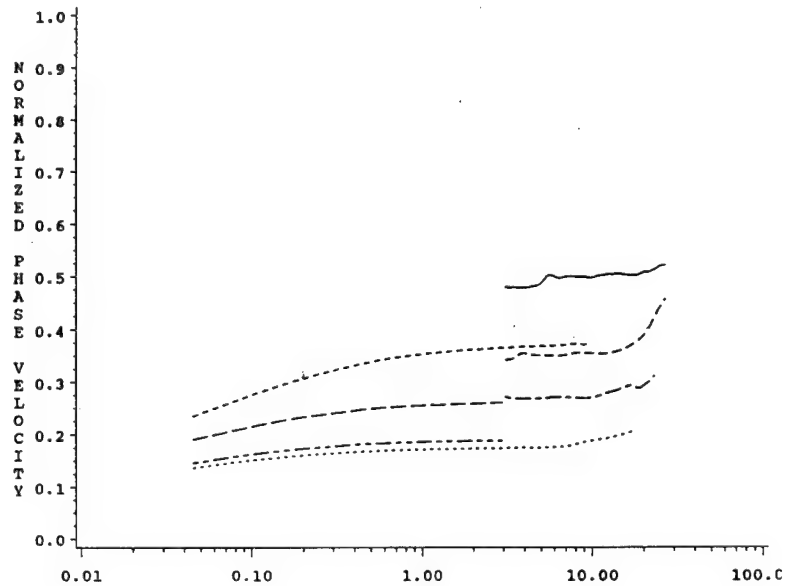




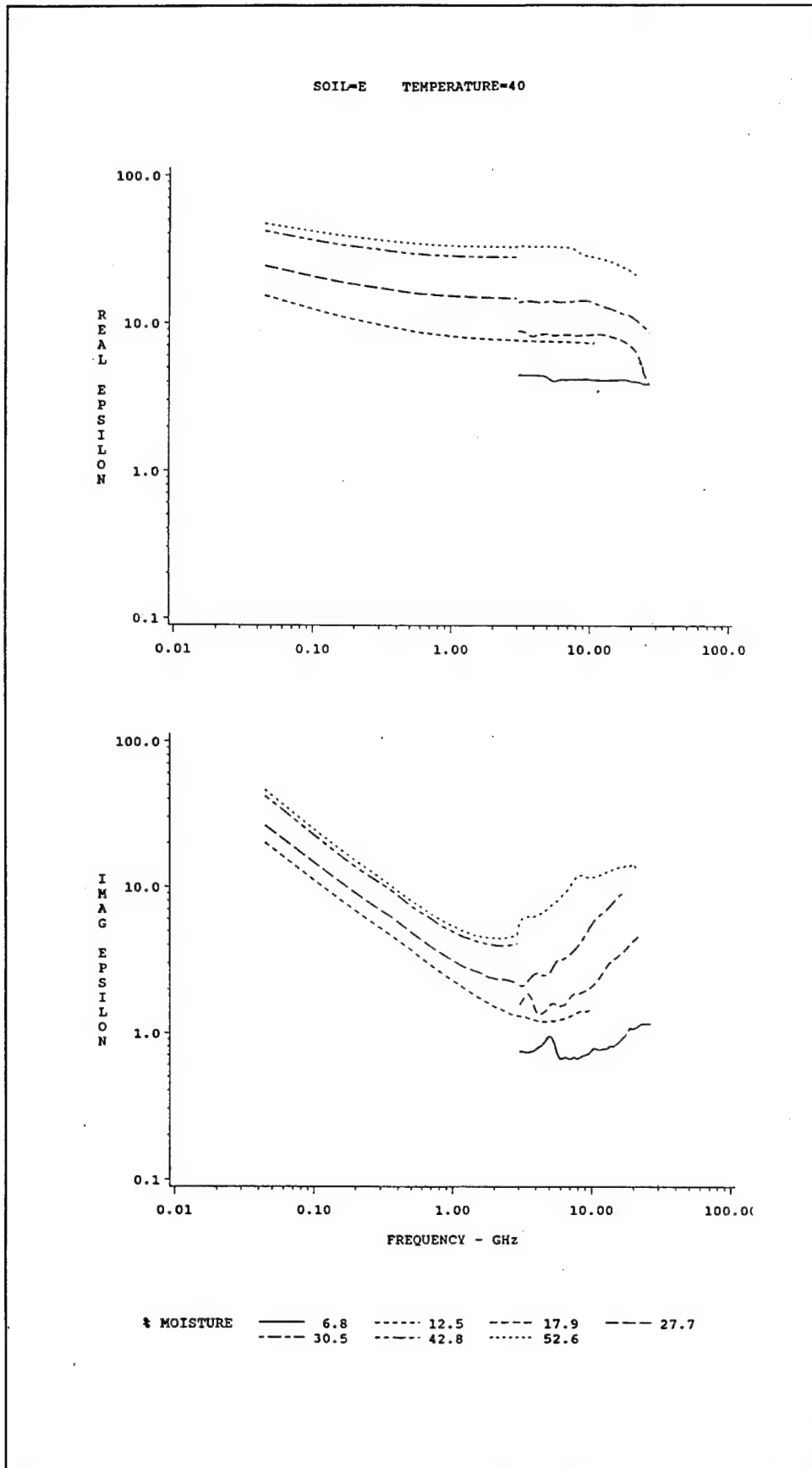


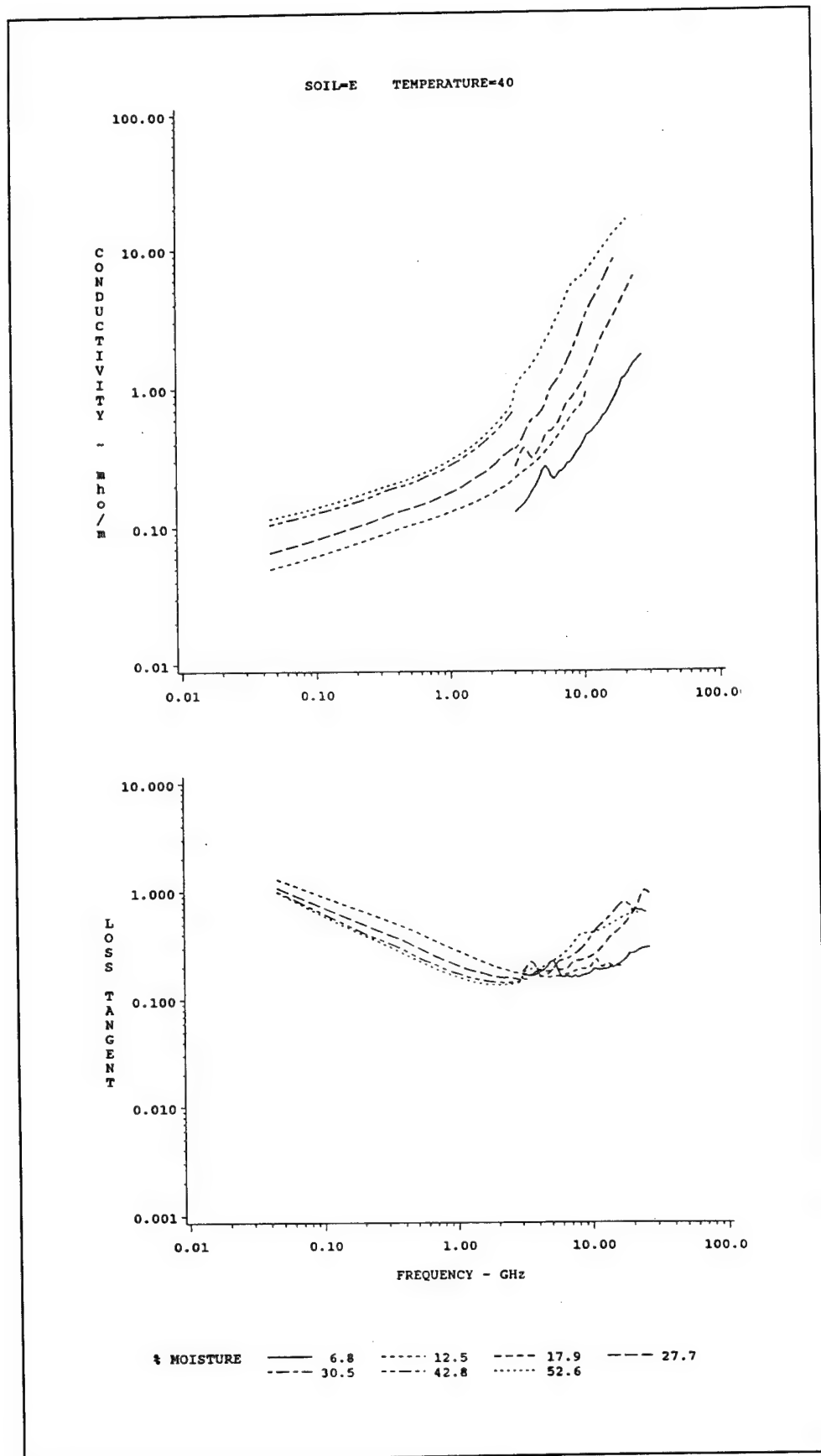


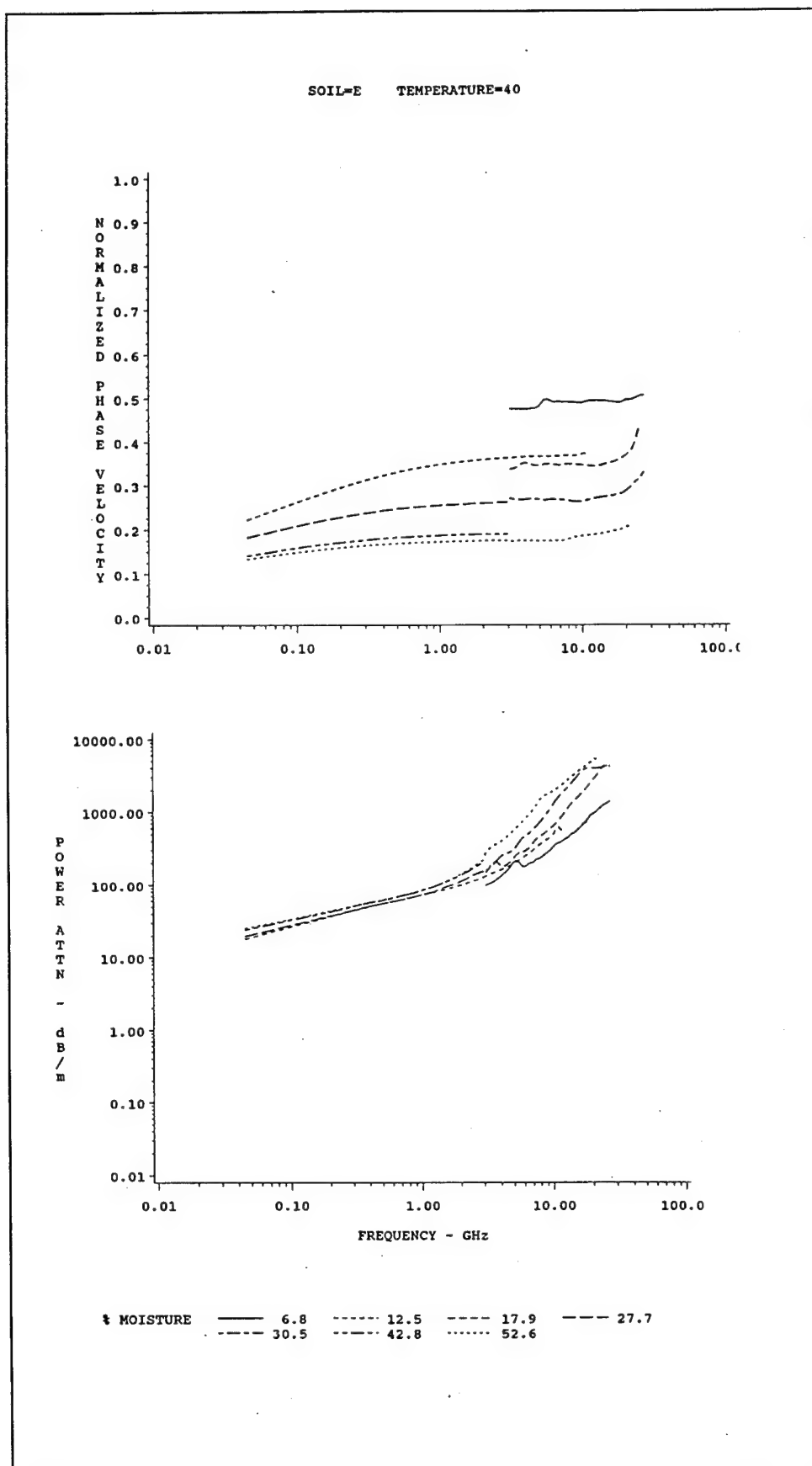
SOIL=E TEMPERATURE=30

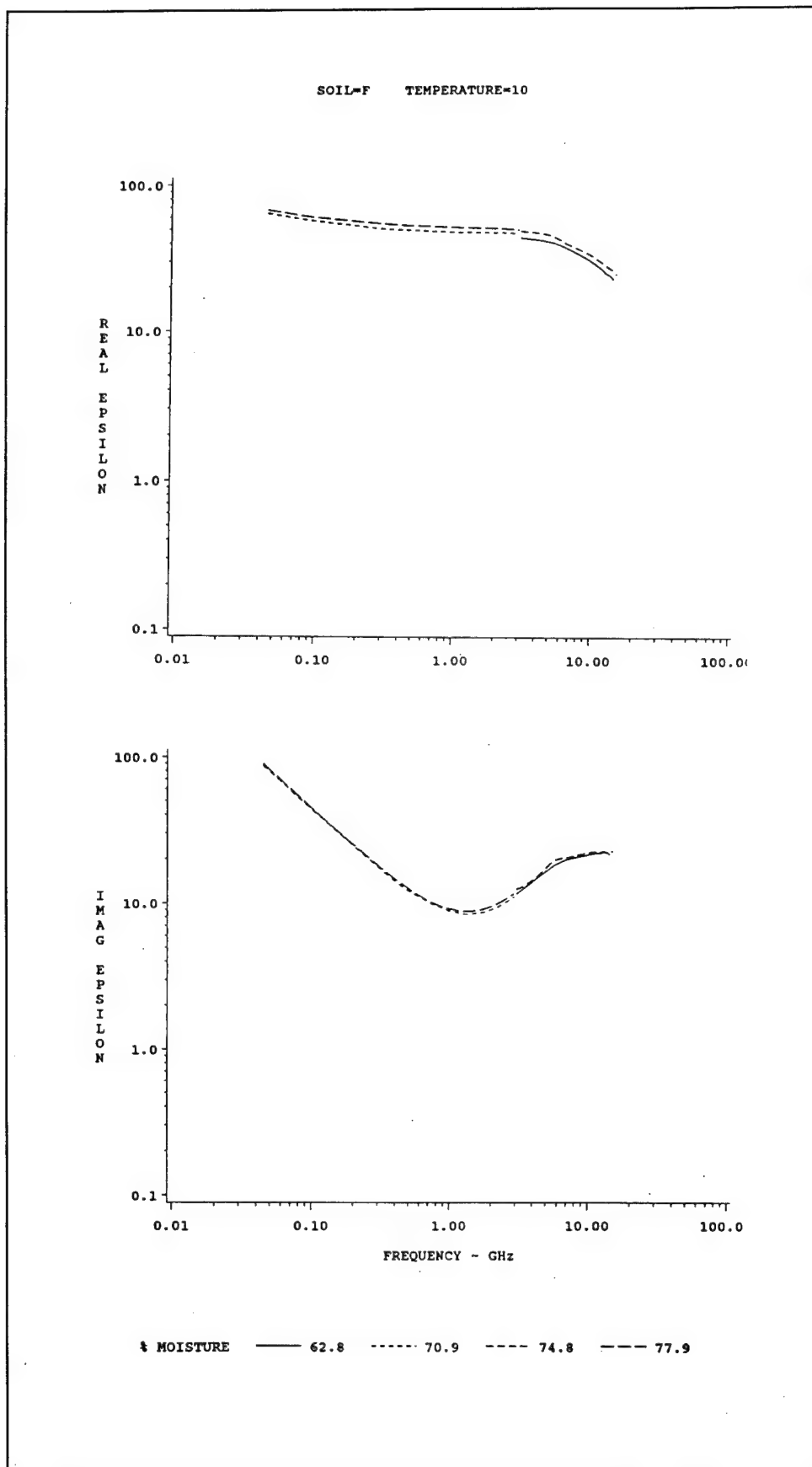


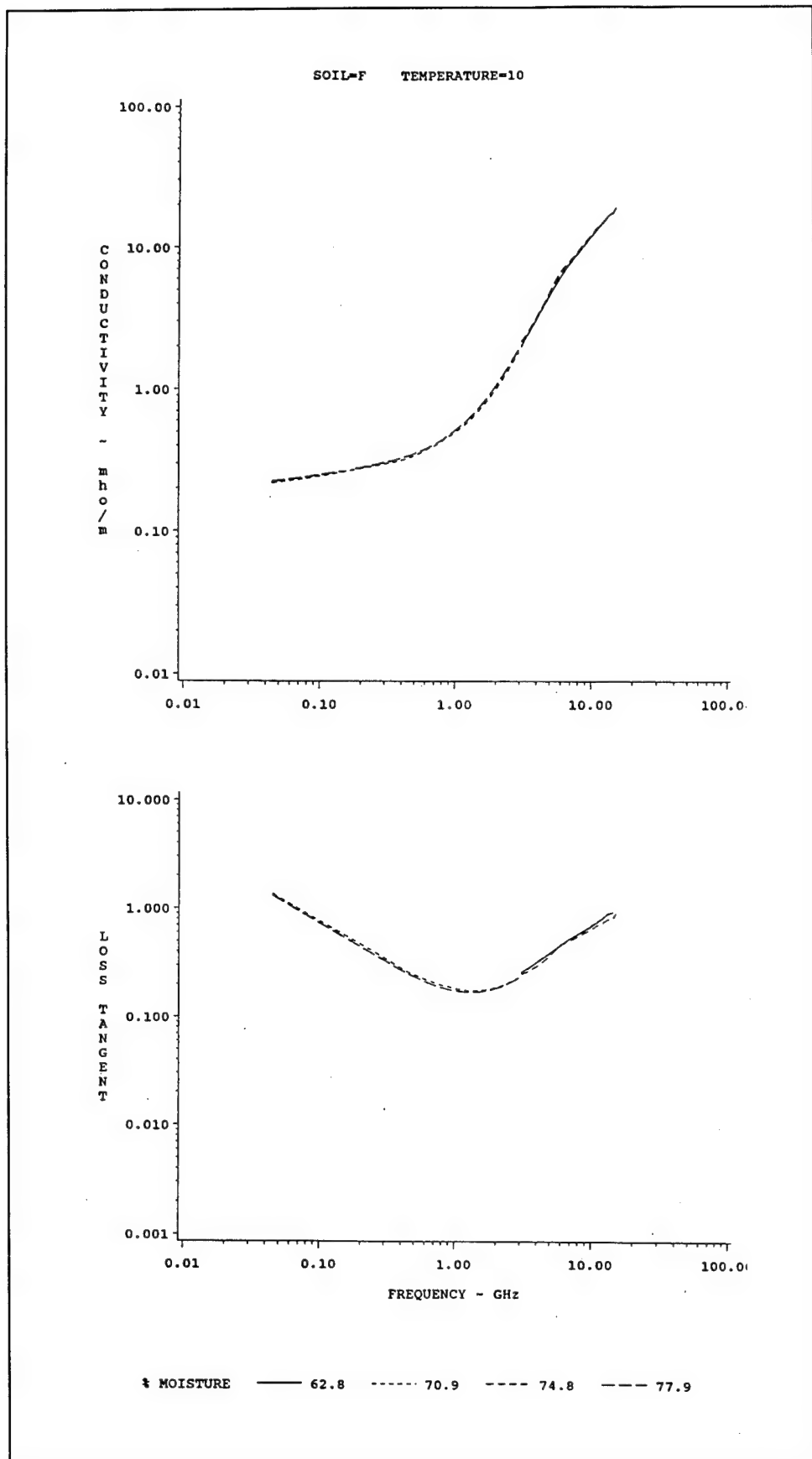
% MOISTURE ——— 6.8 - - - 12.5 . . . 17.9 - · - 27.7
 - - - 30.5 . . . 42.8 . . . 52.6

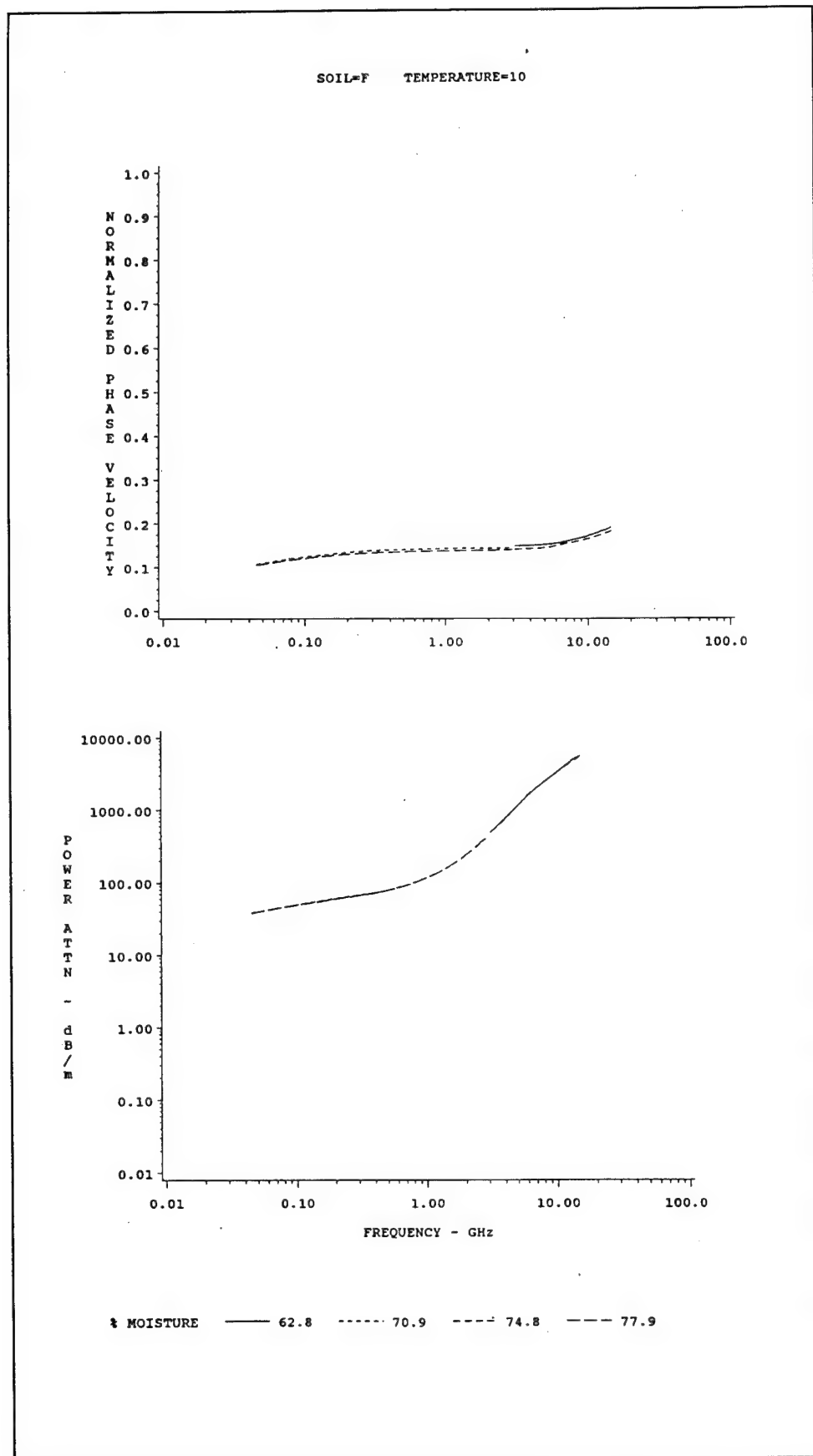


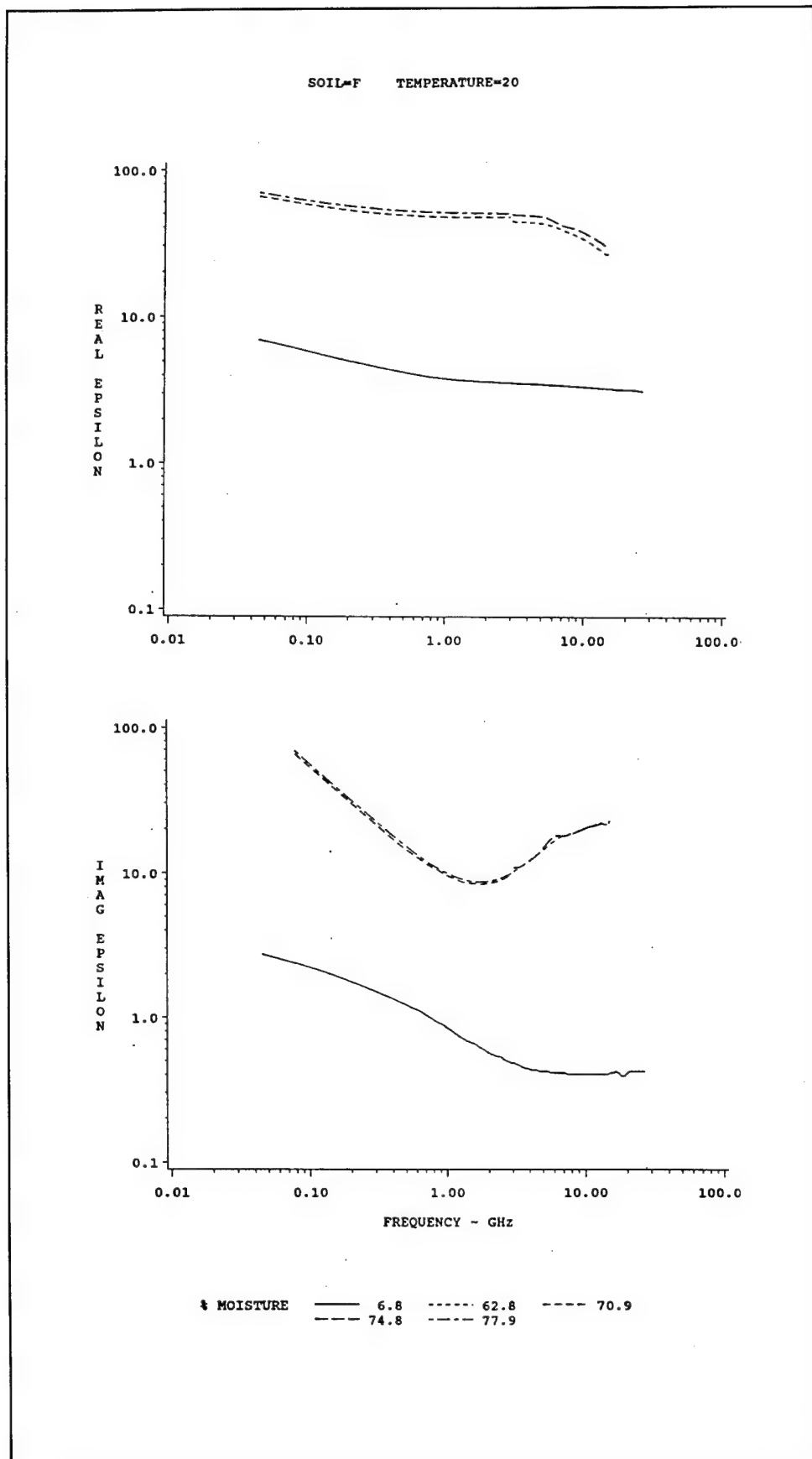


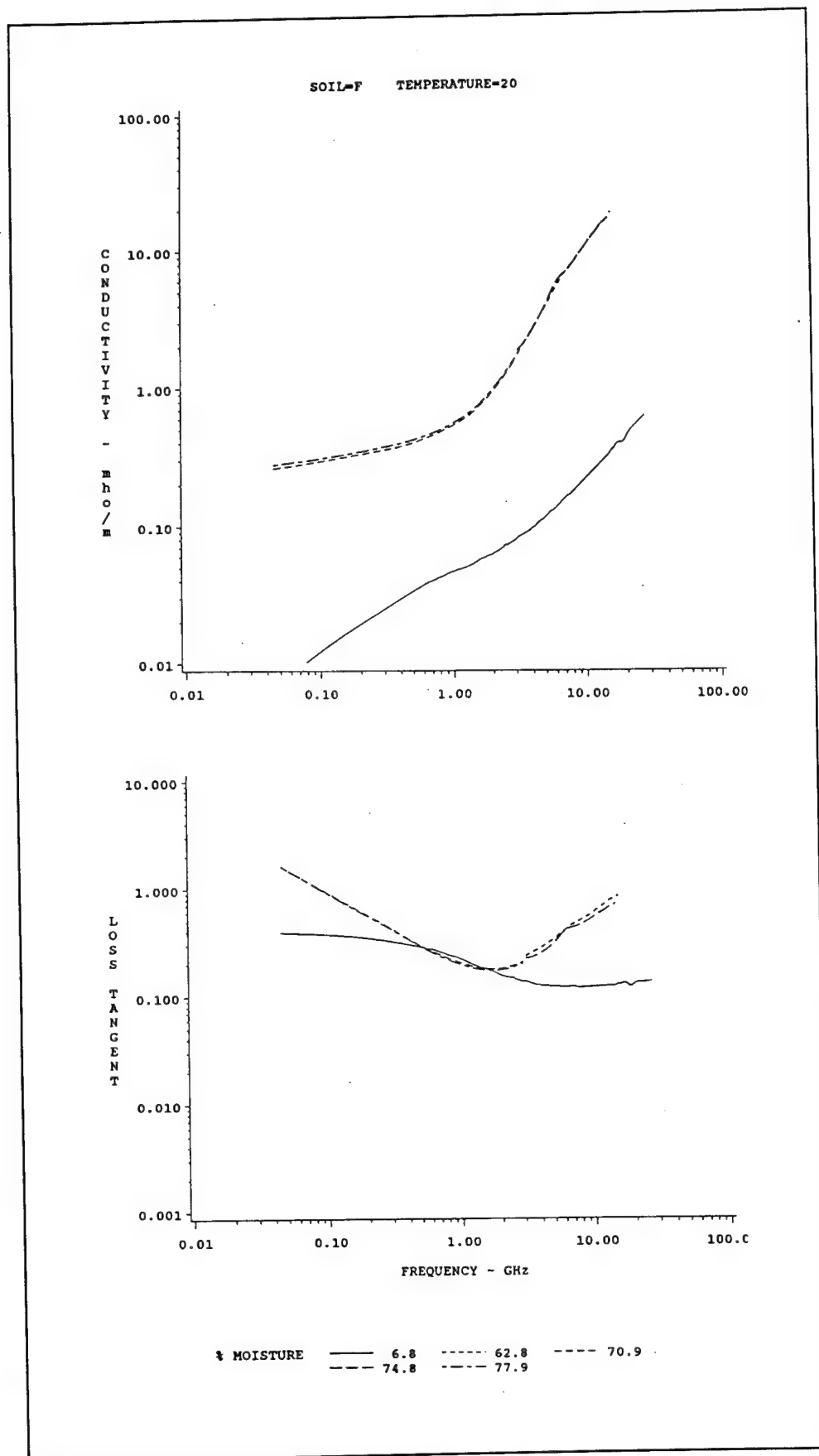


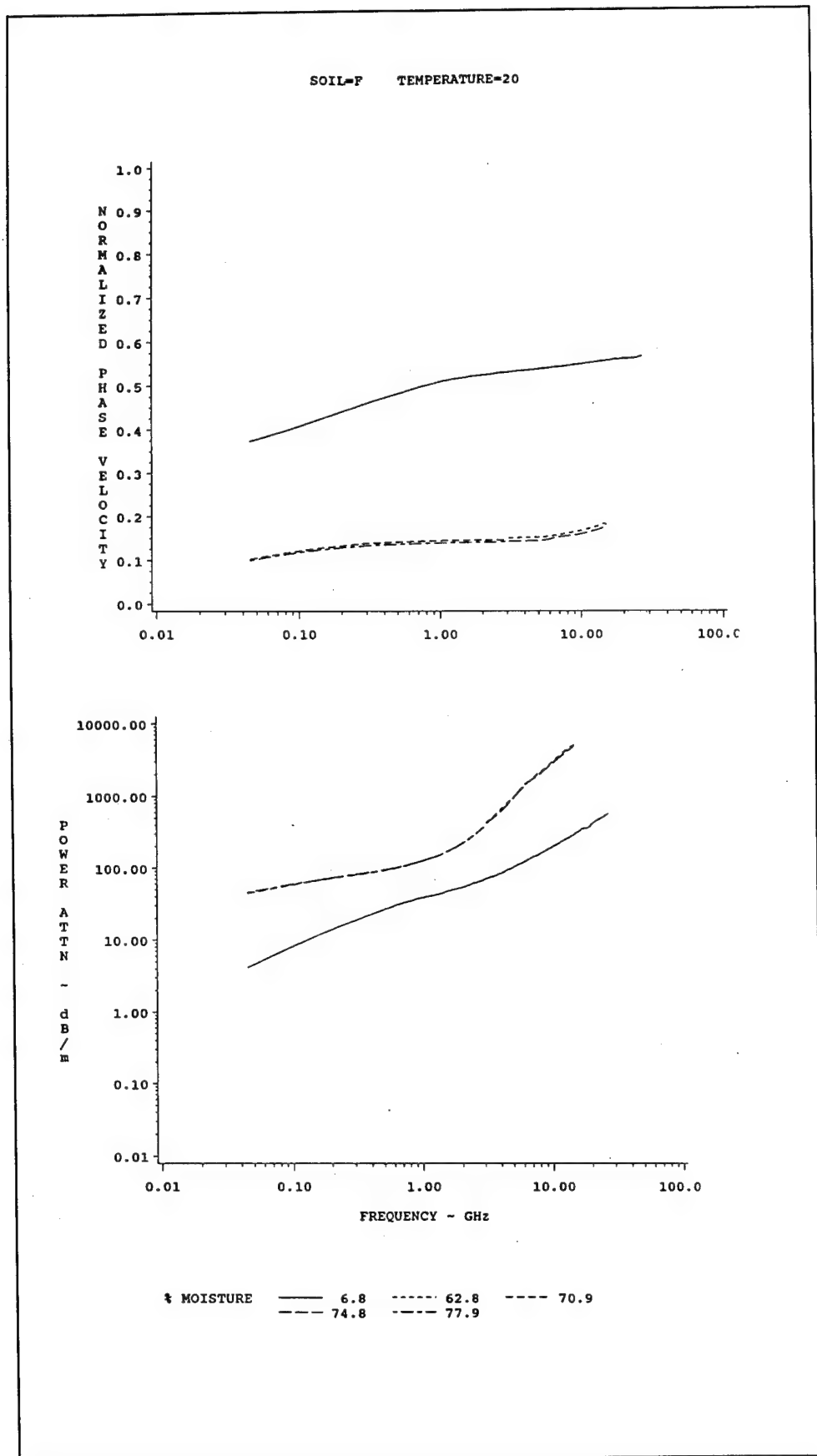


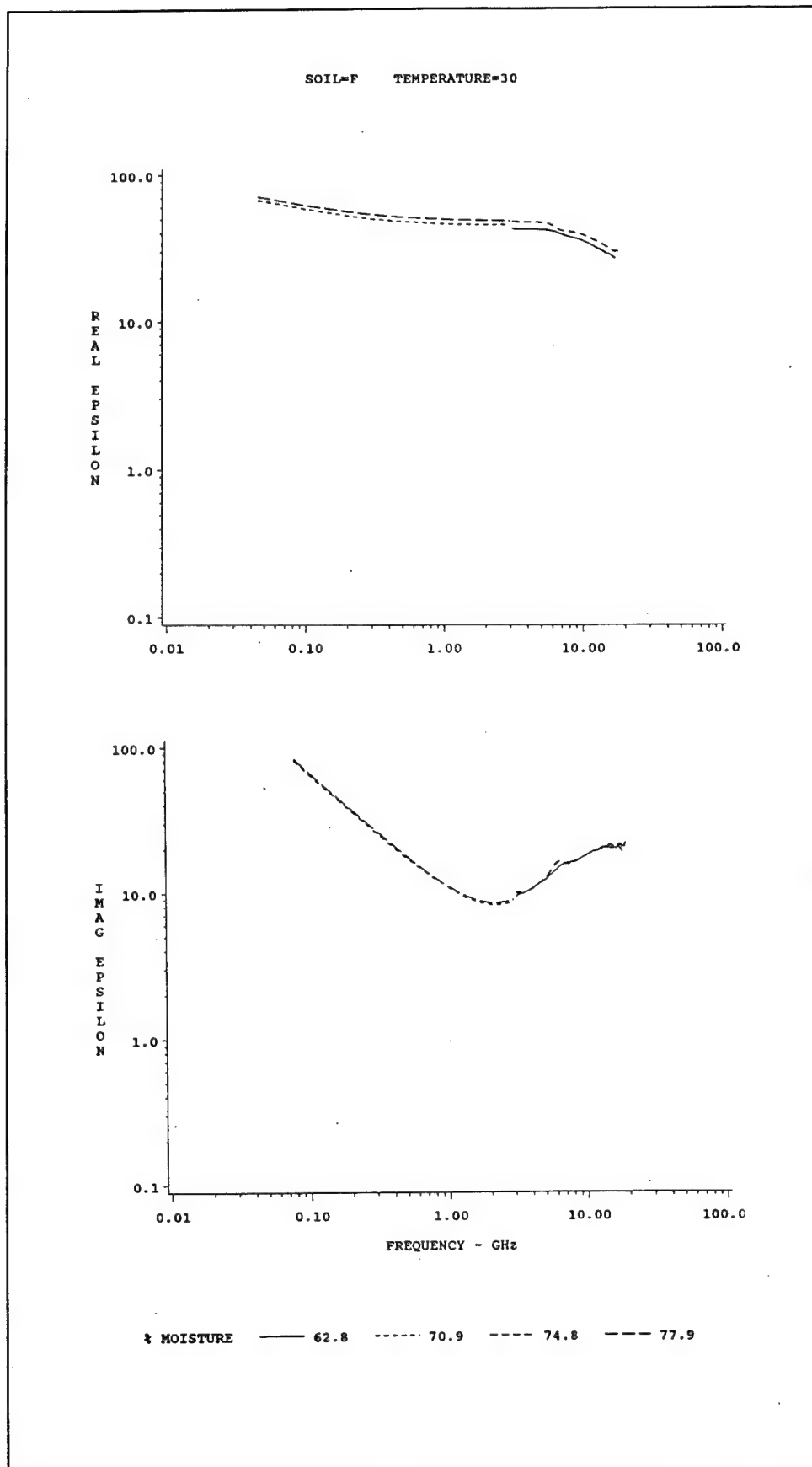


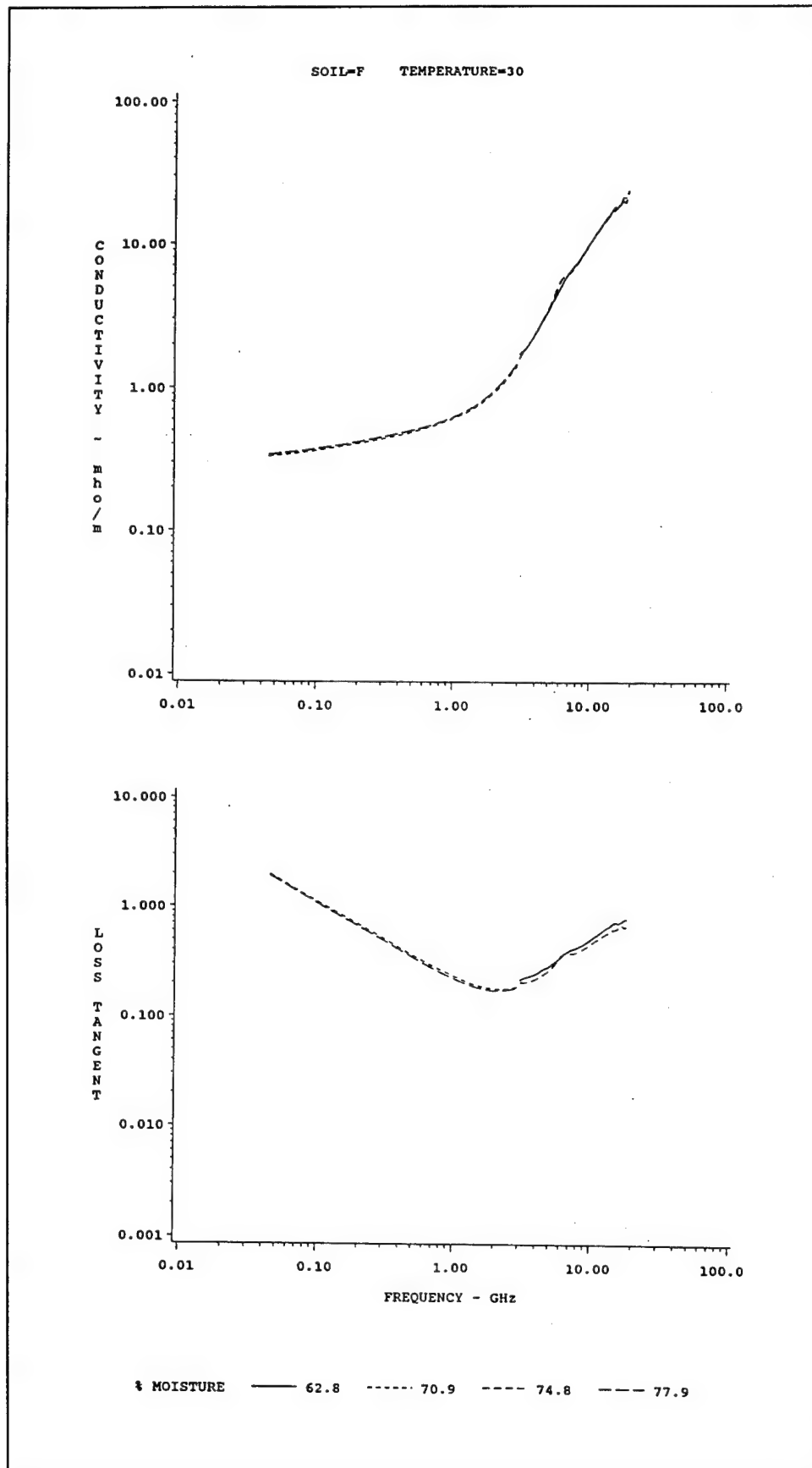


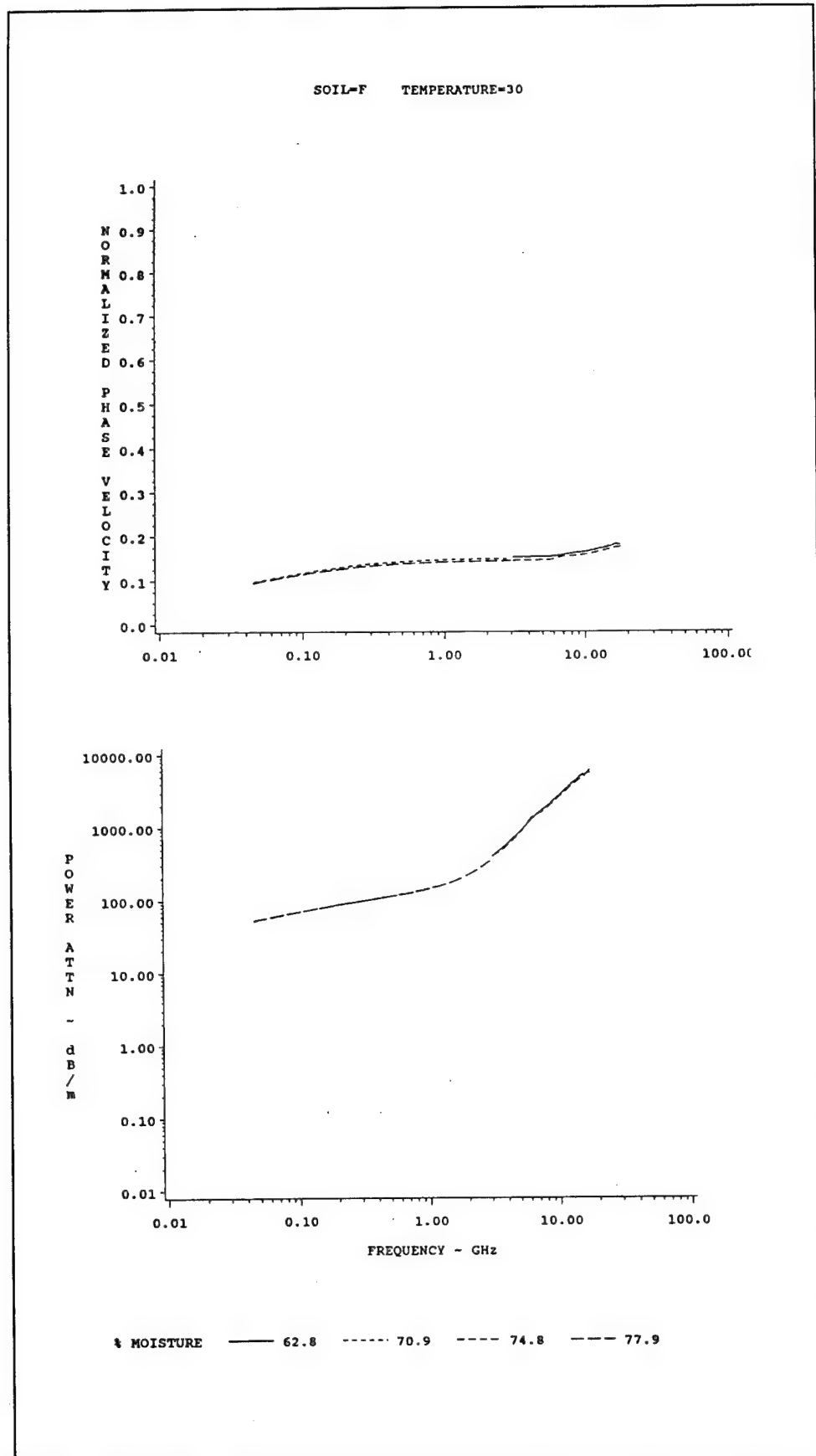


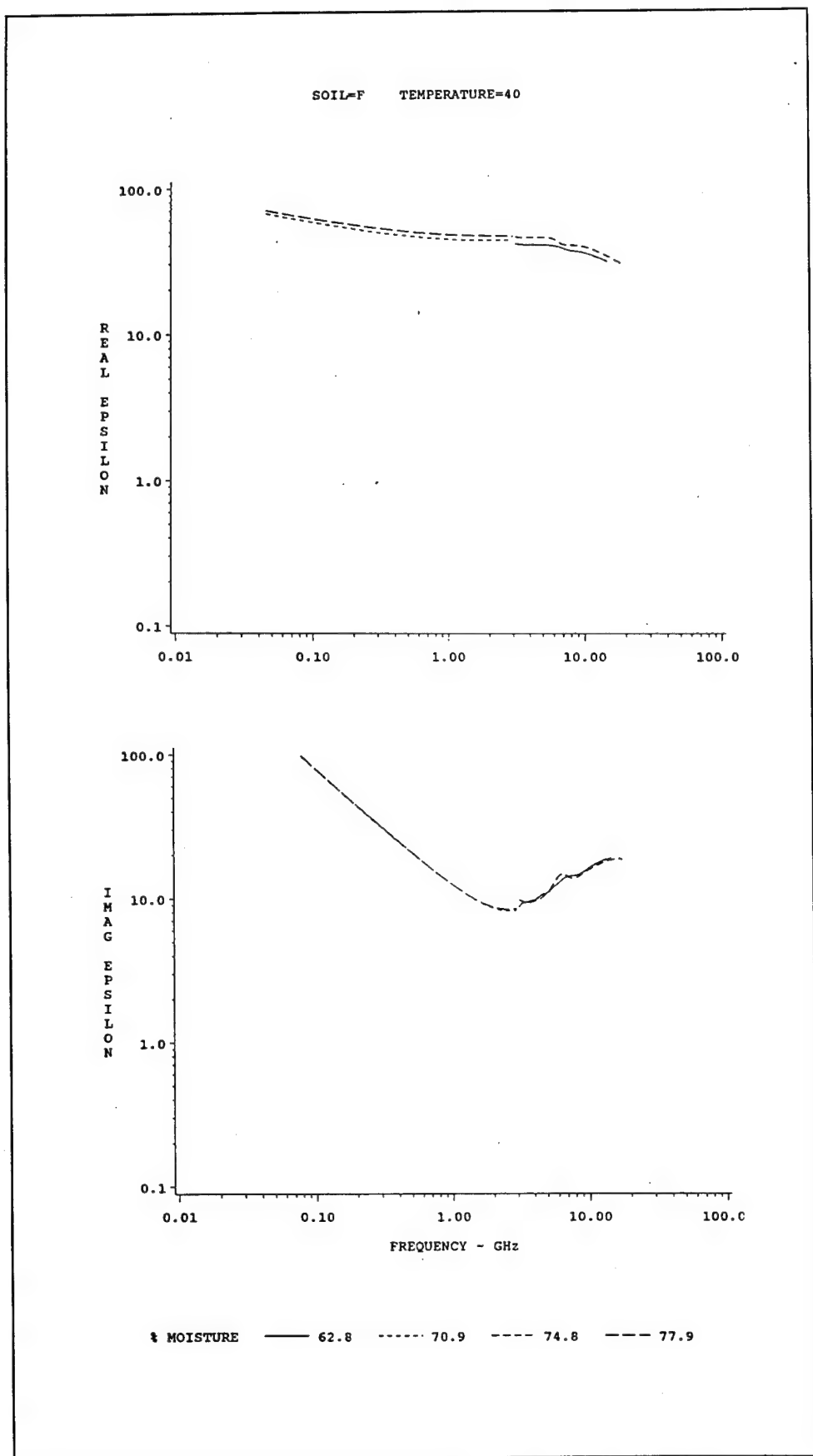


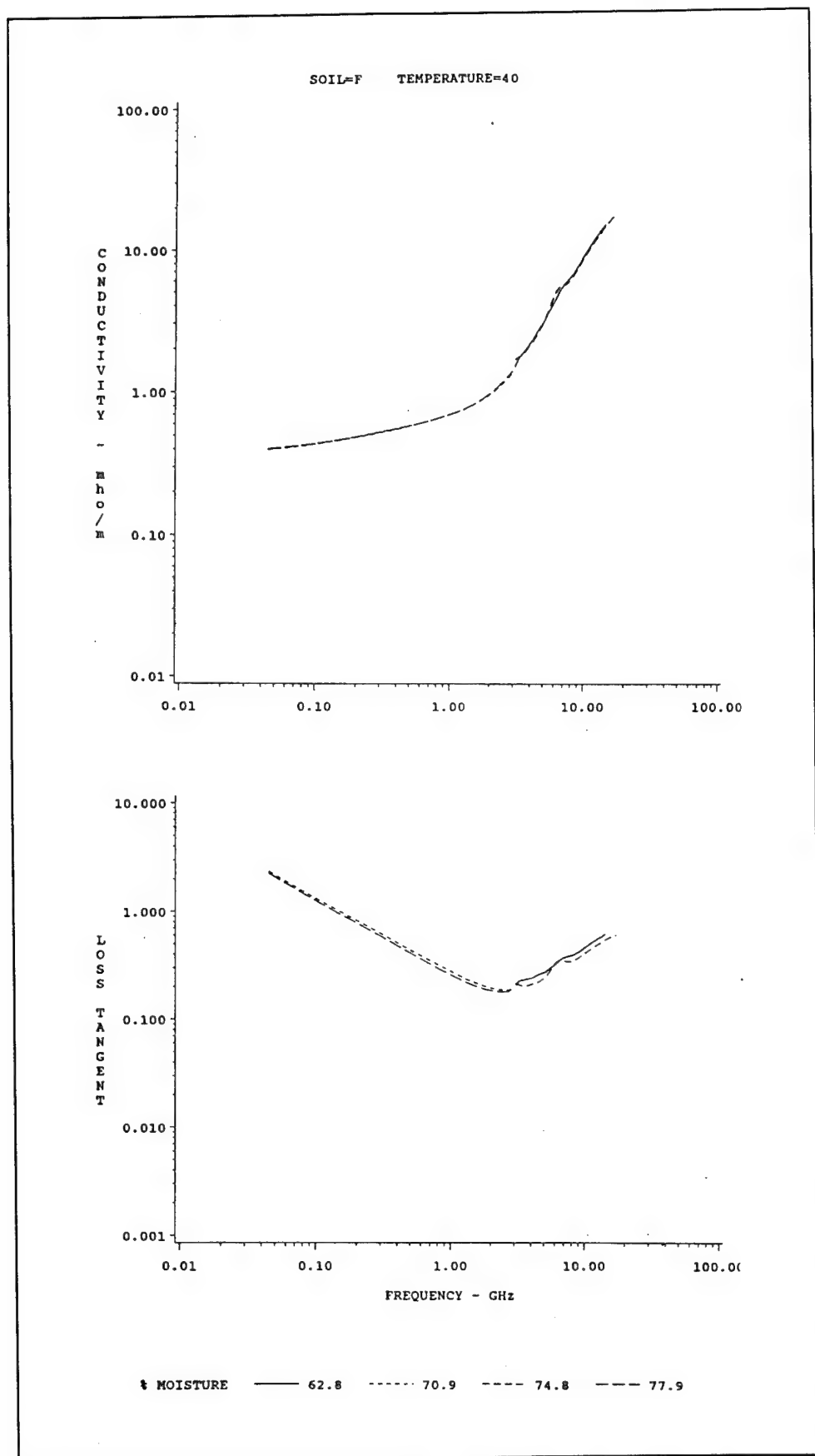


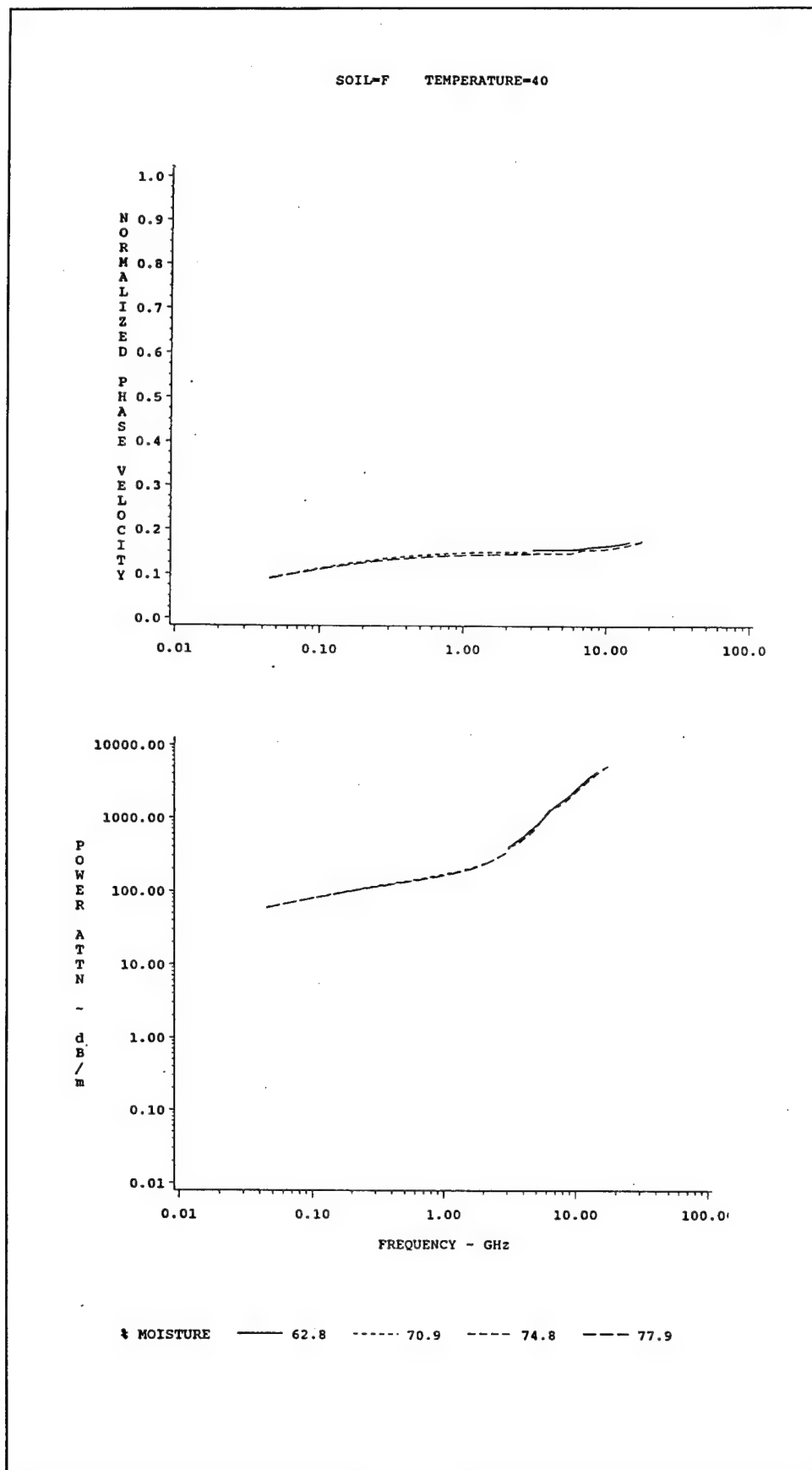


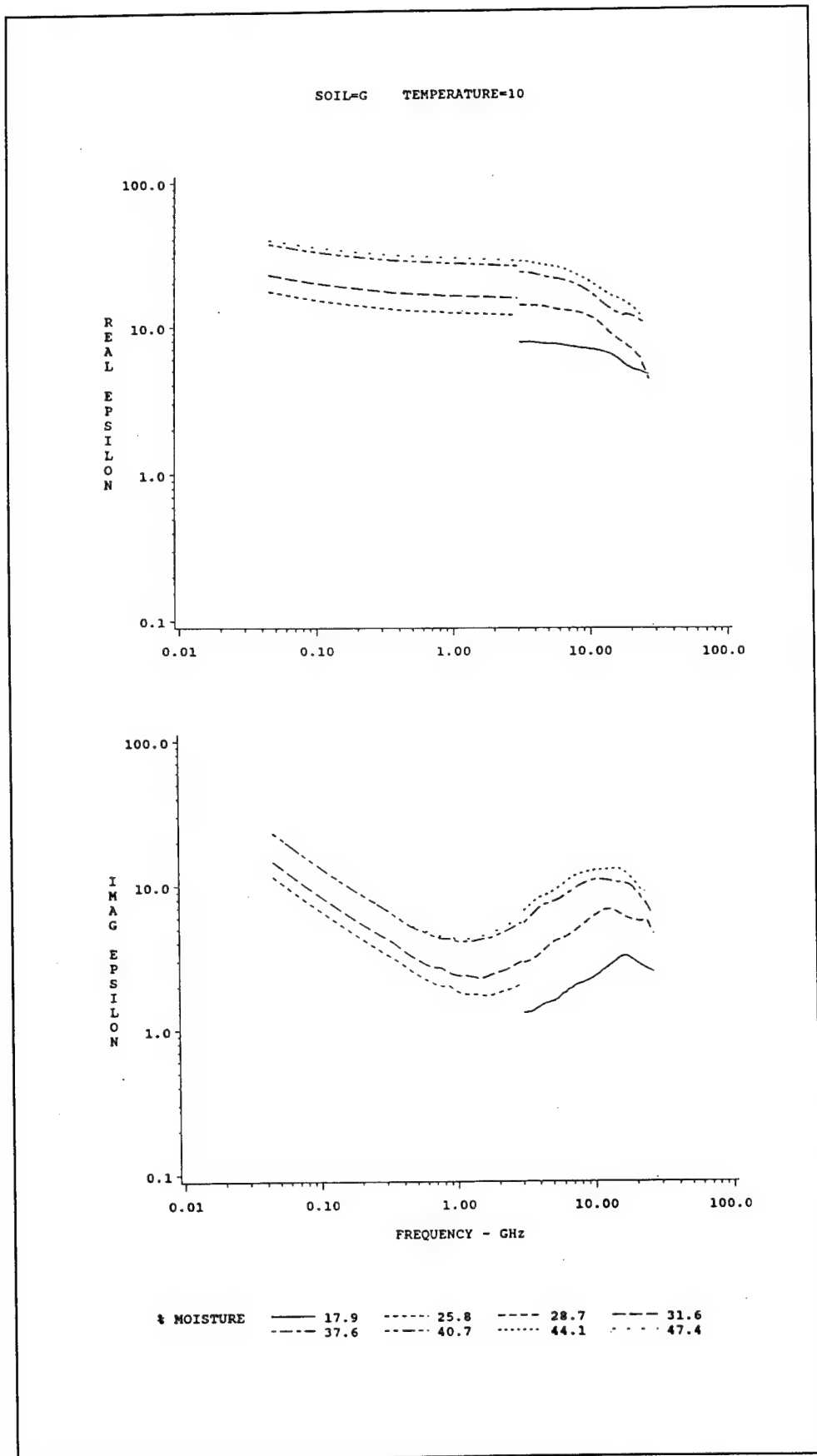


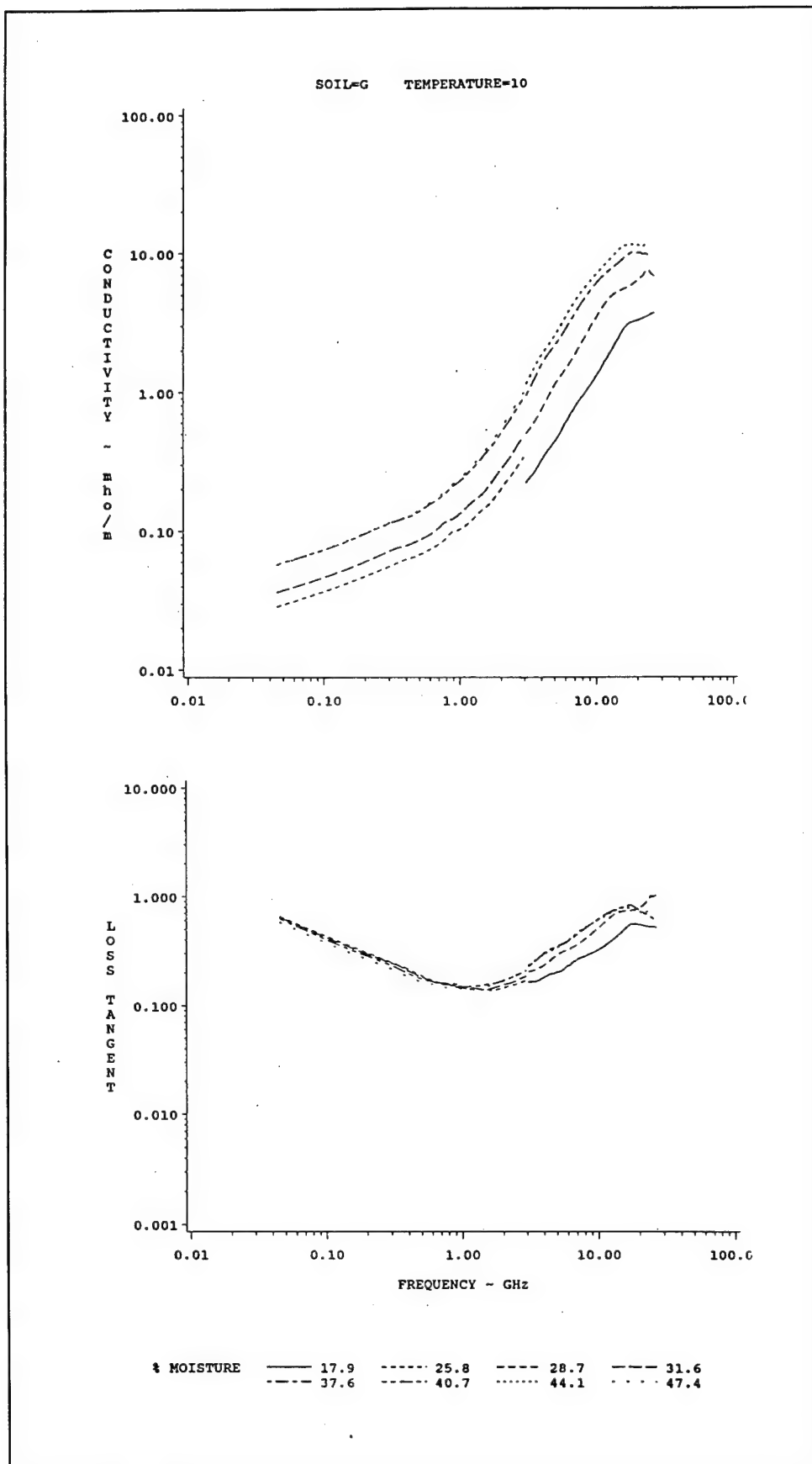


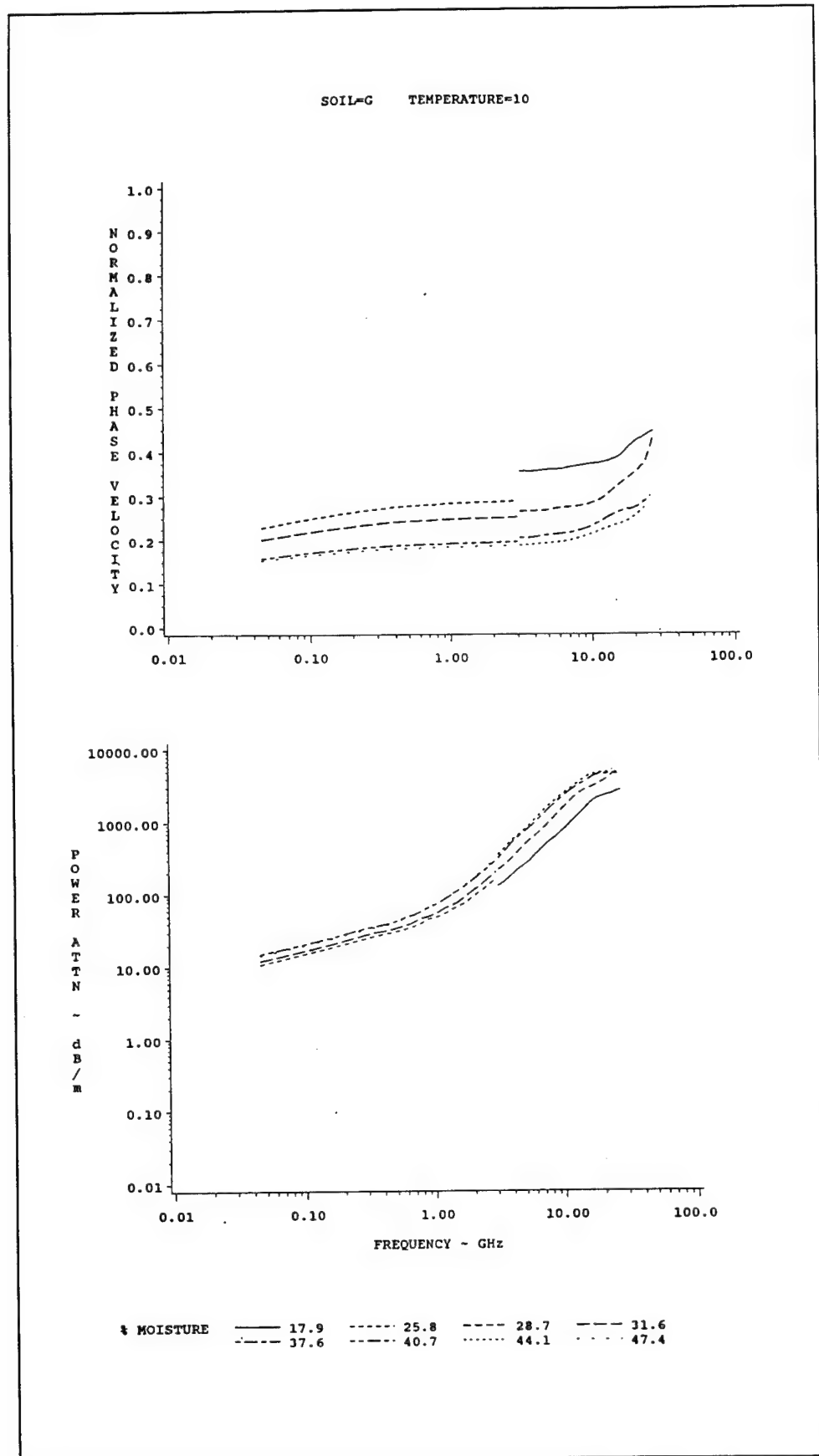


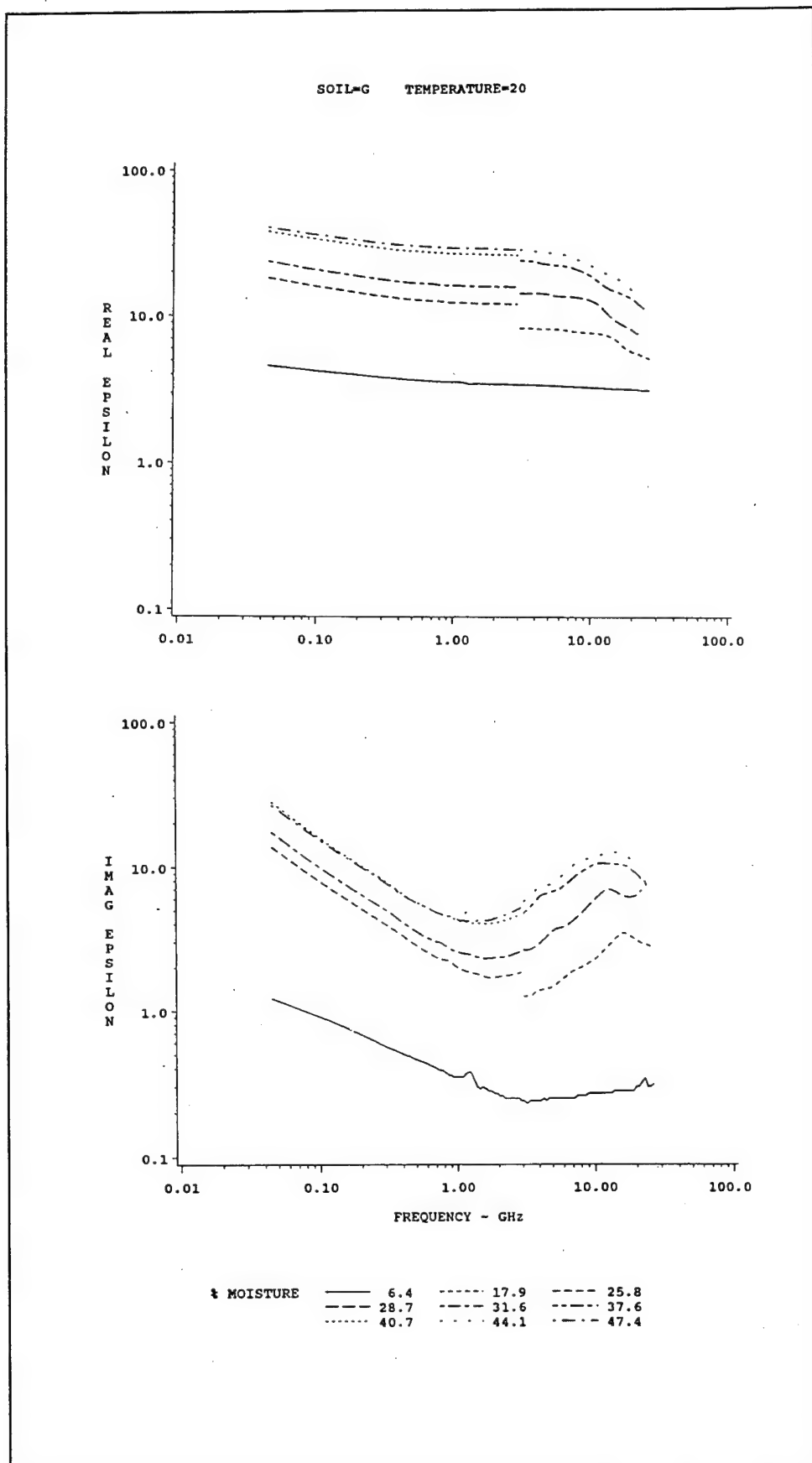


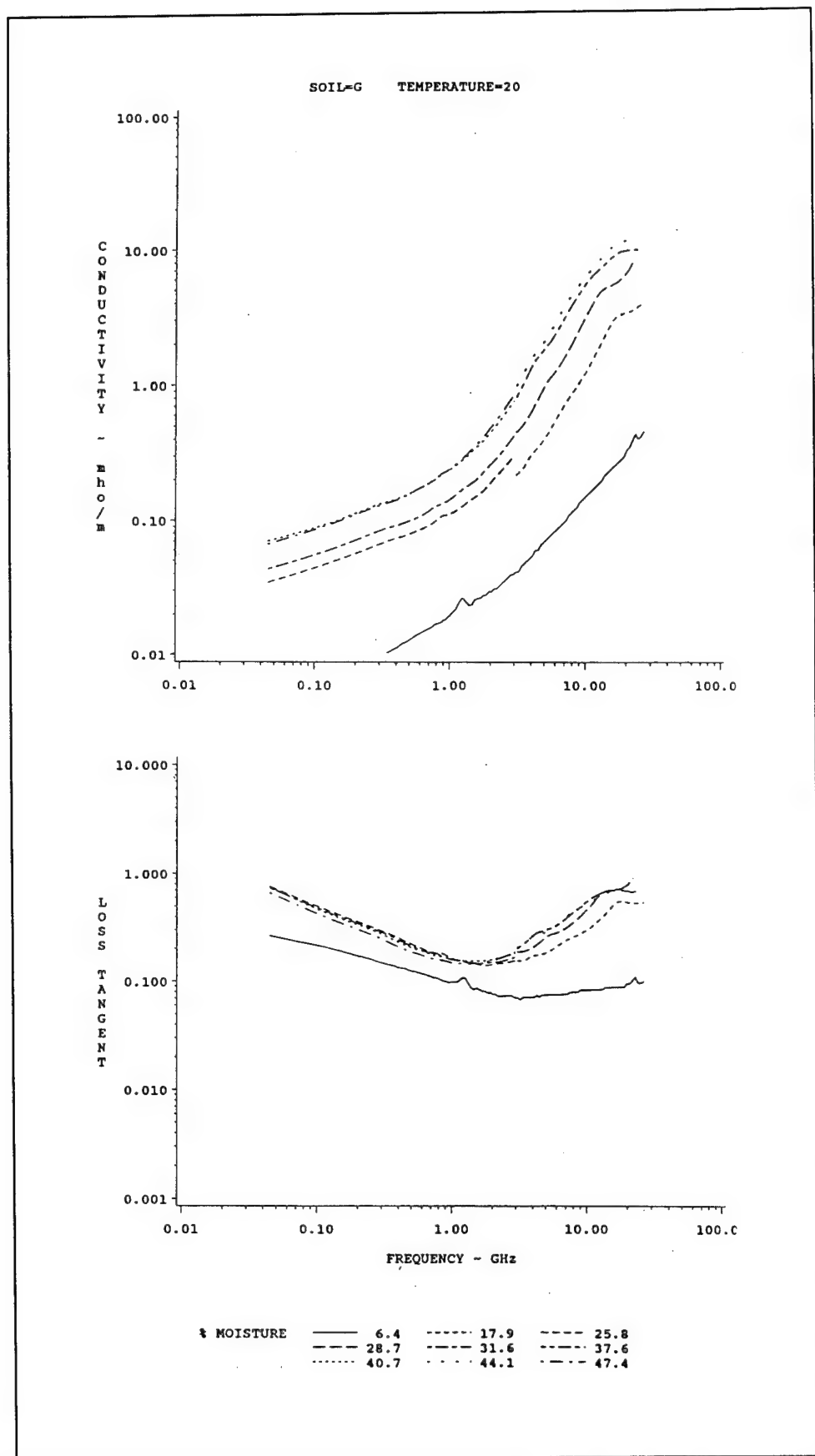


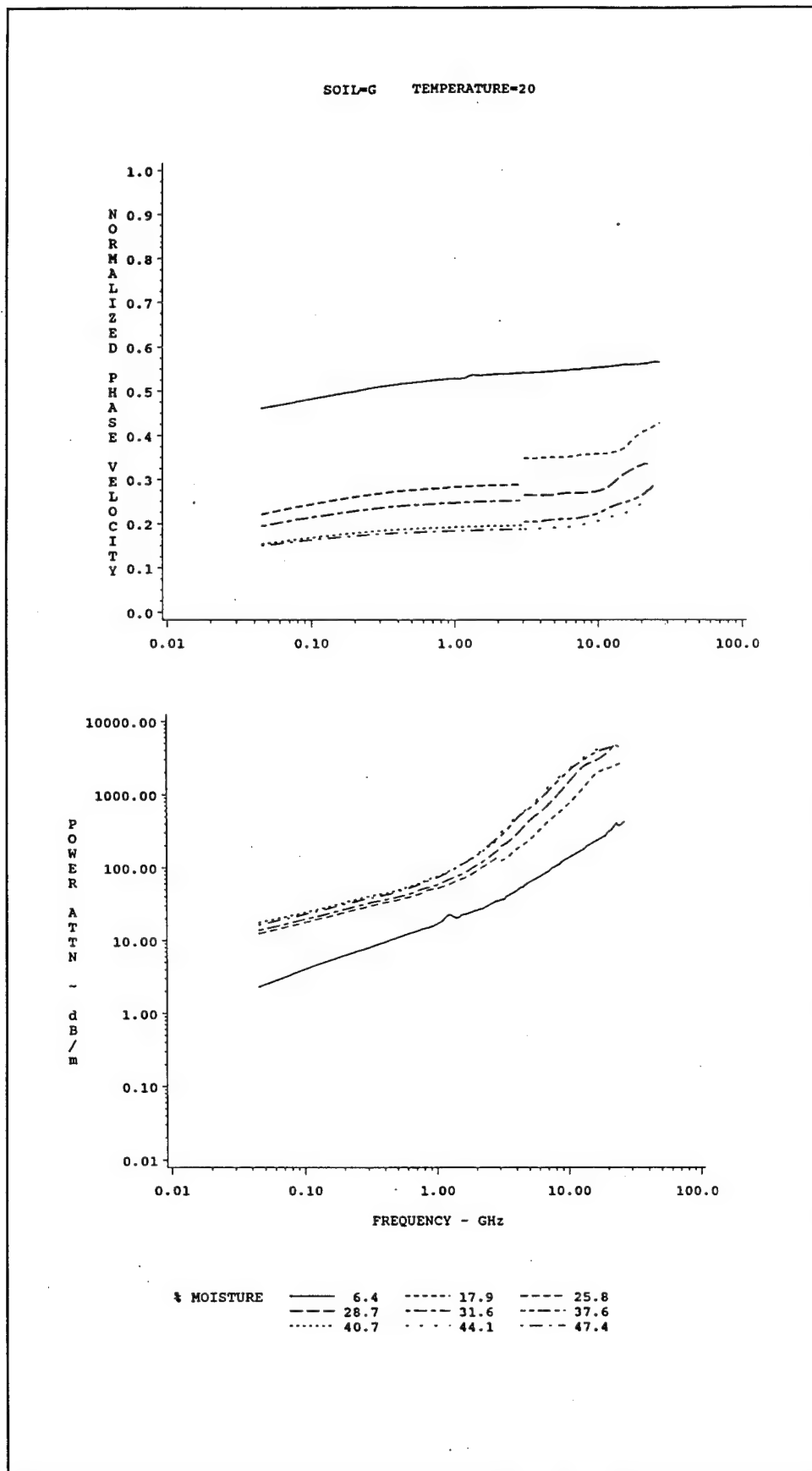


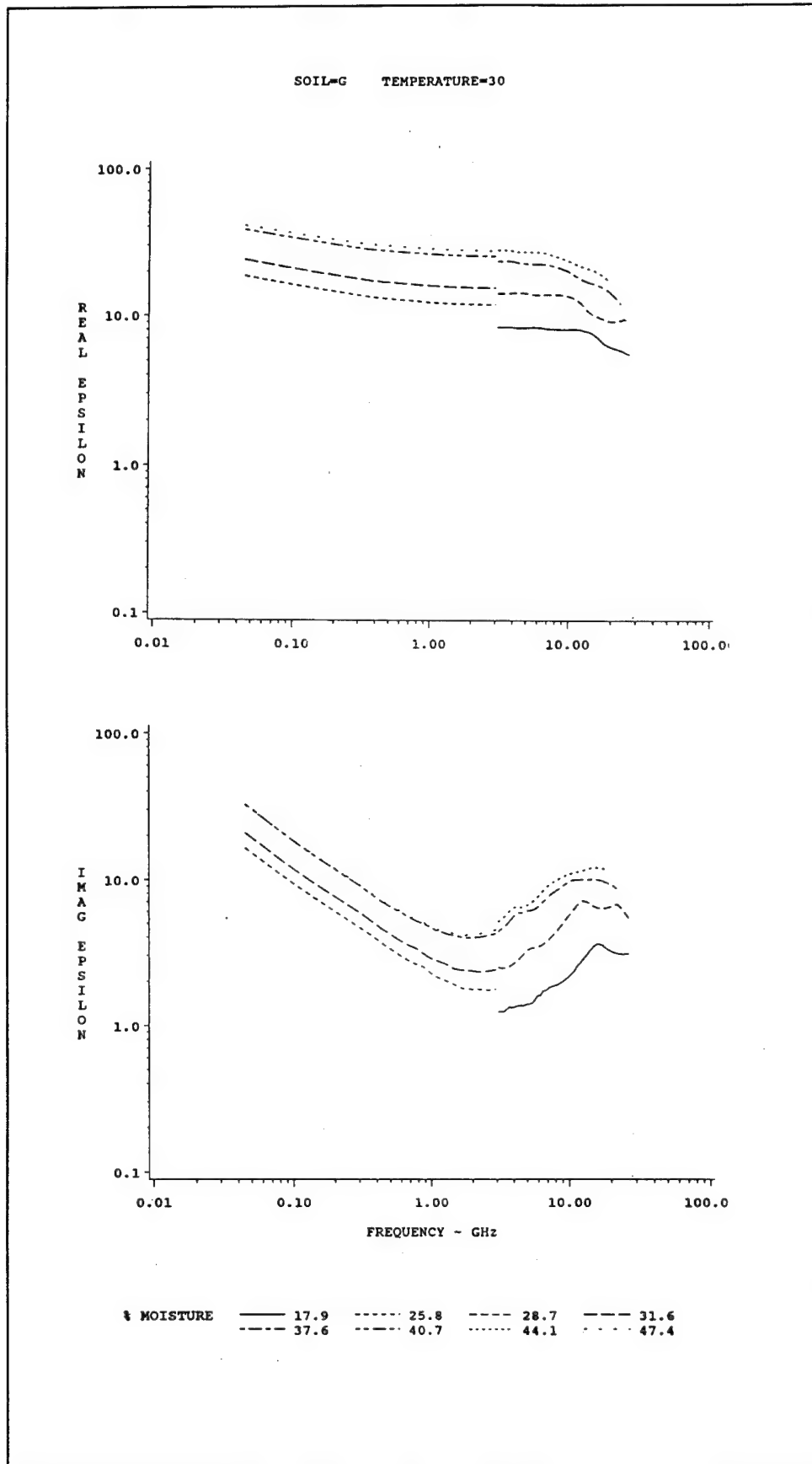


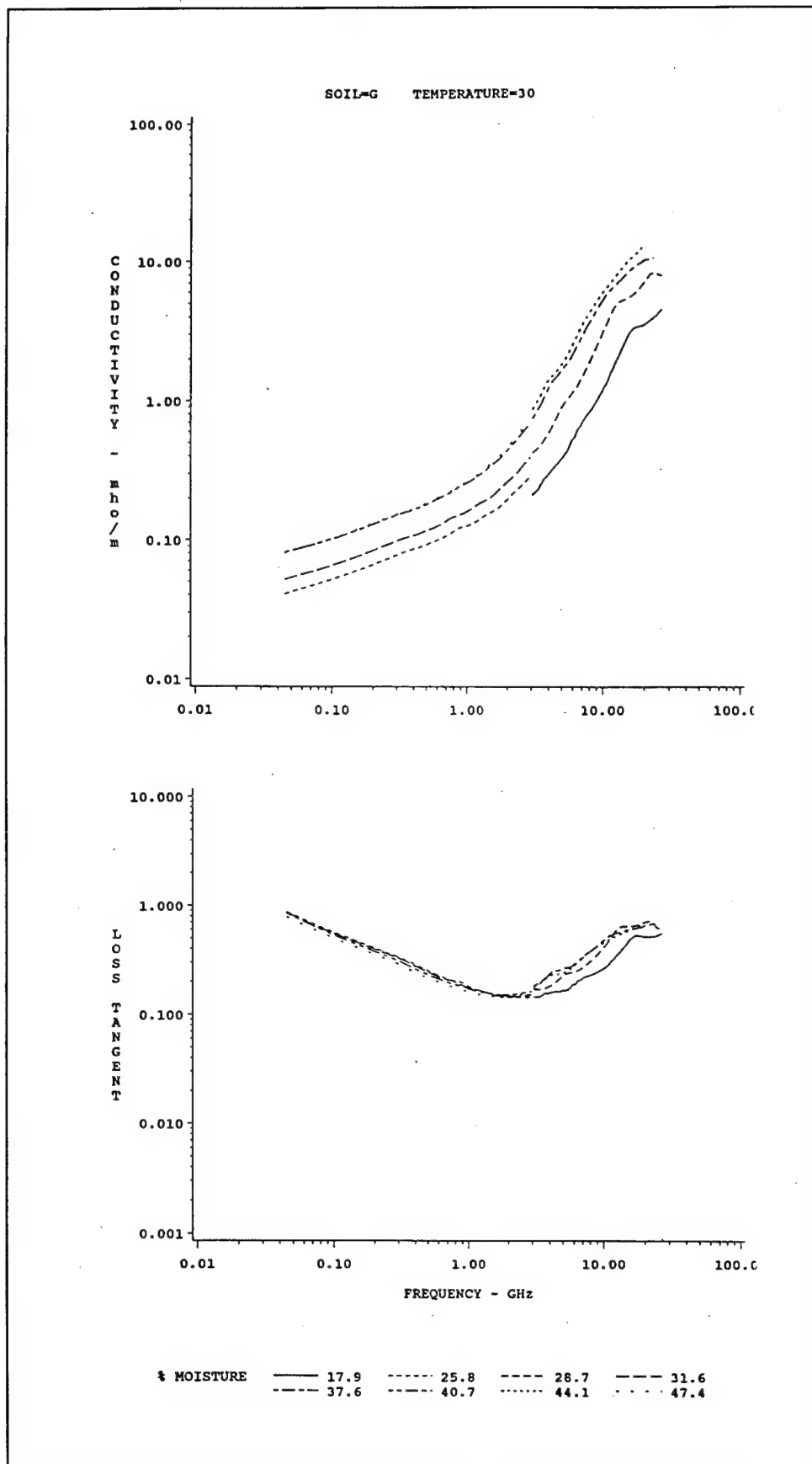


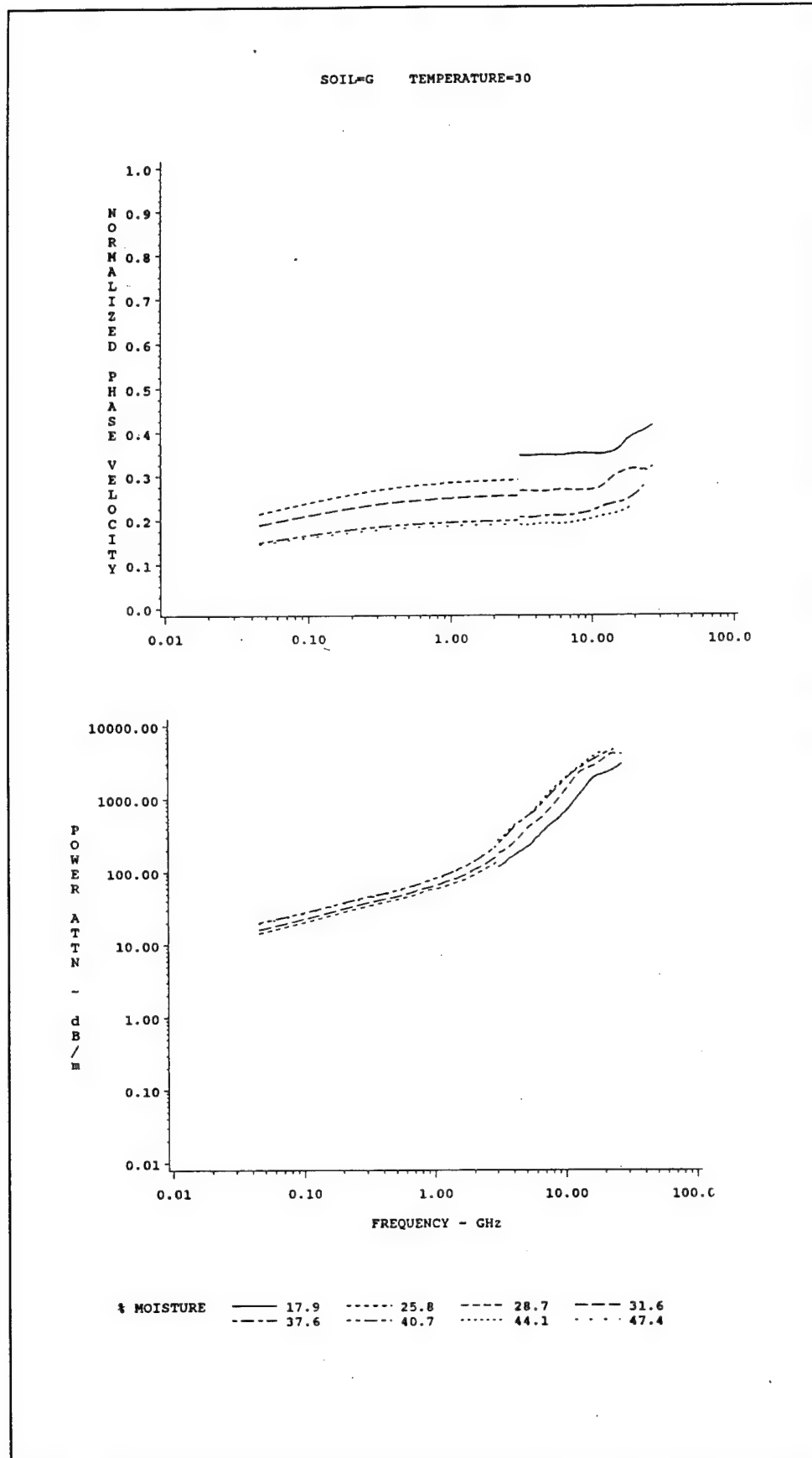


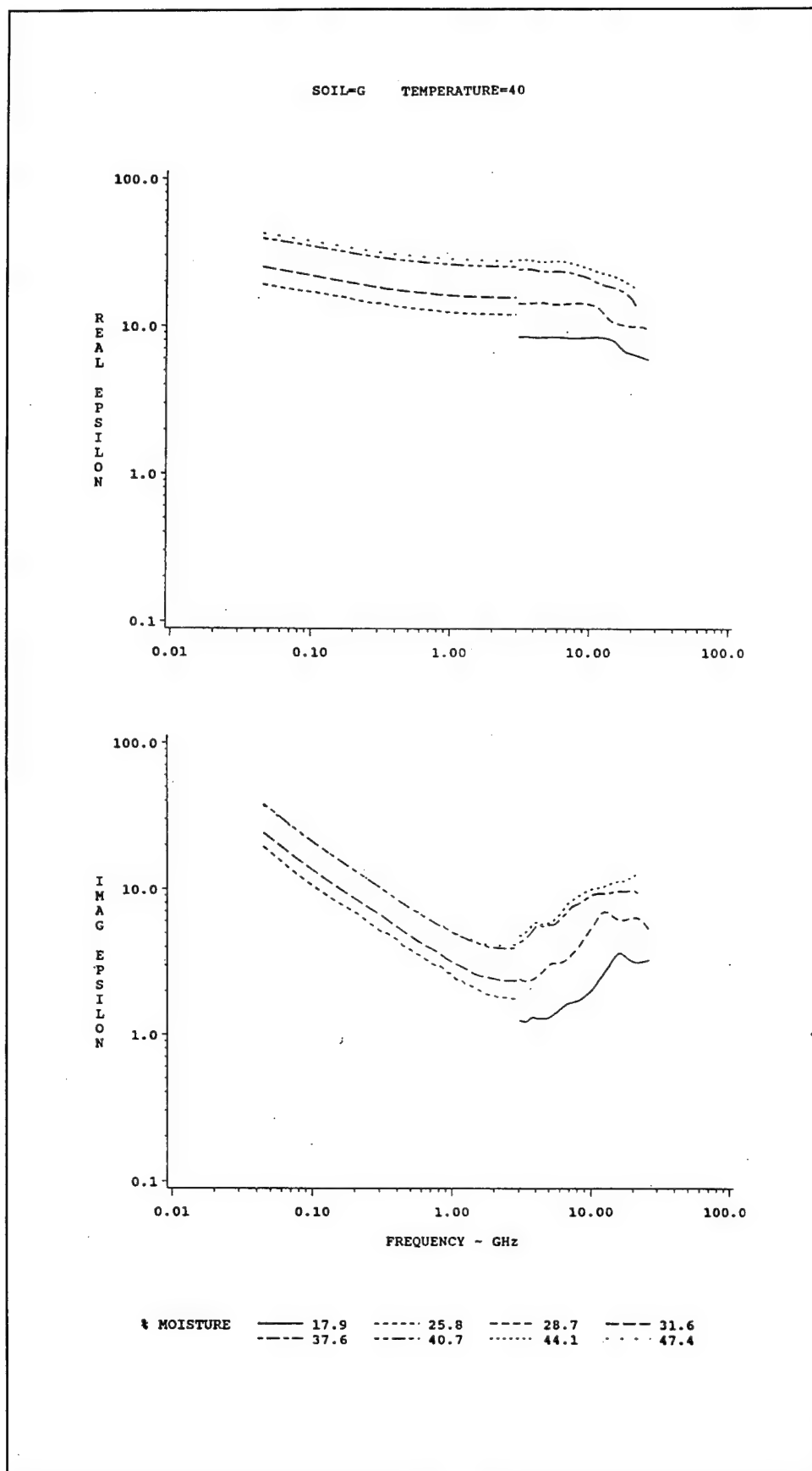


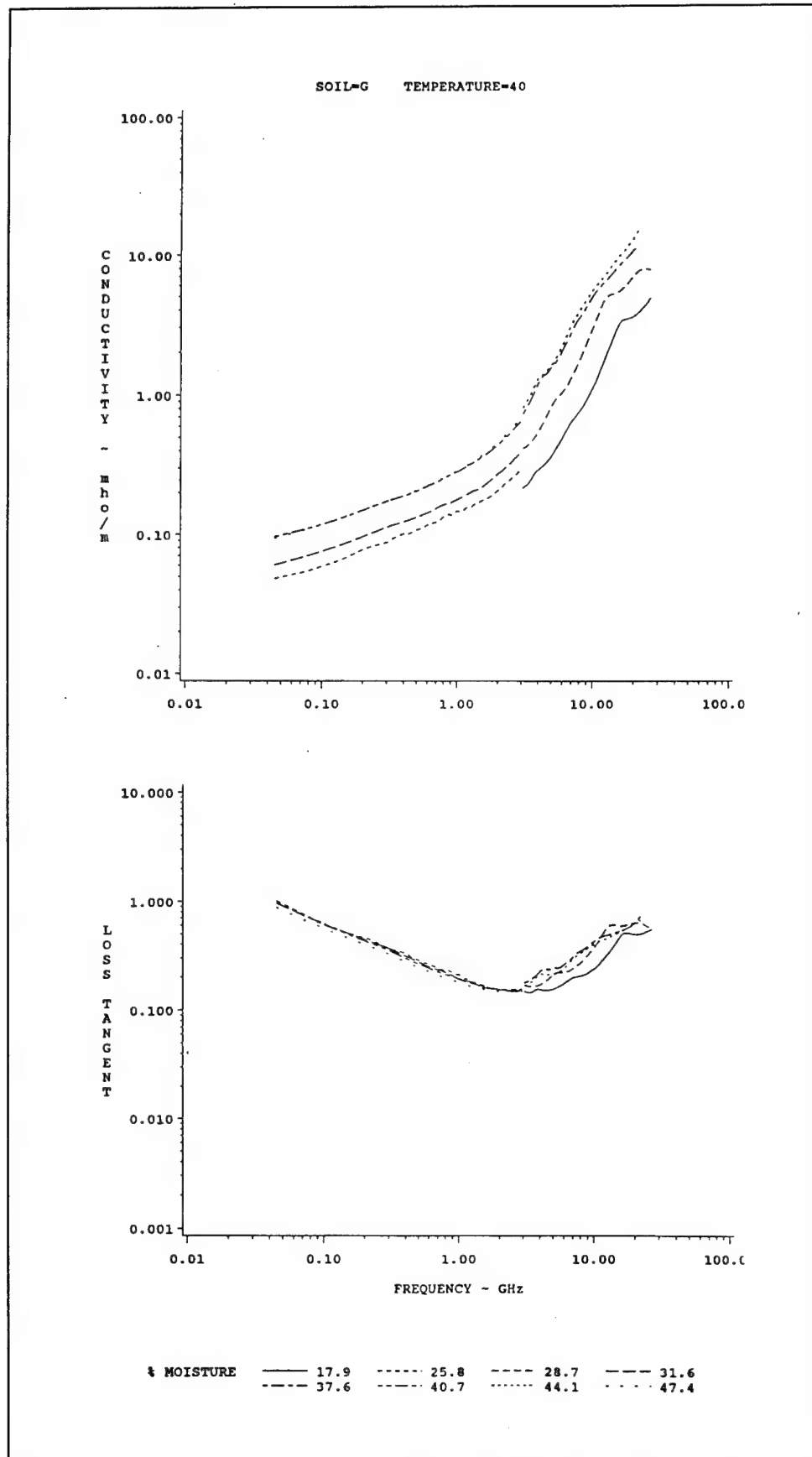




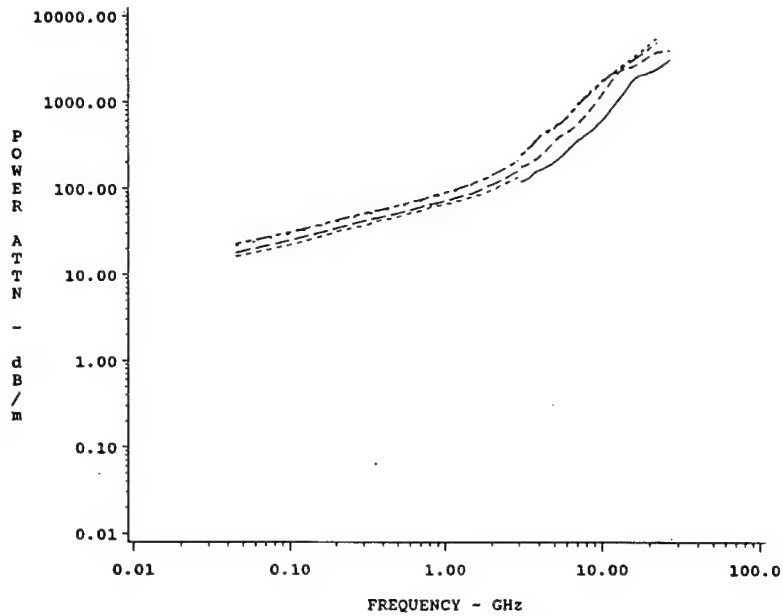
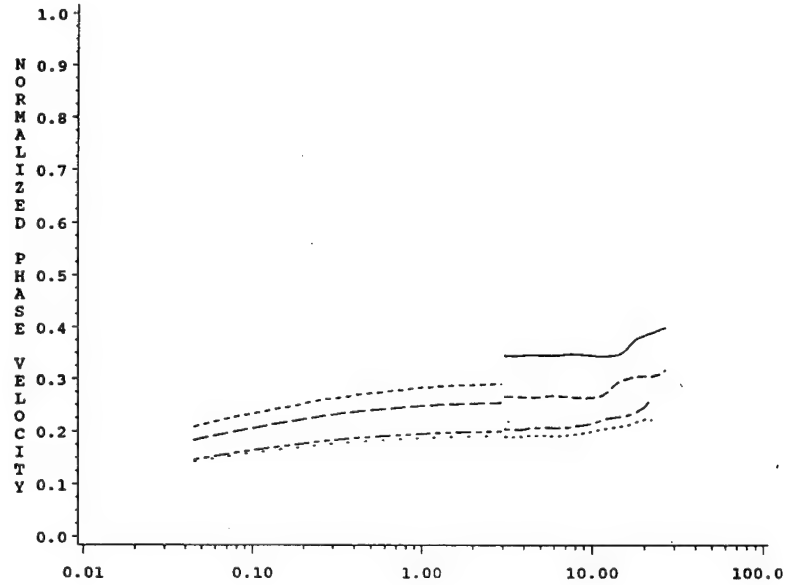




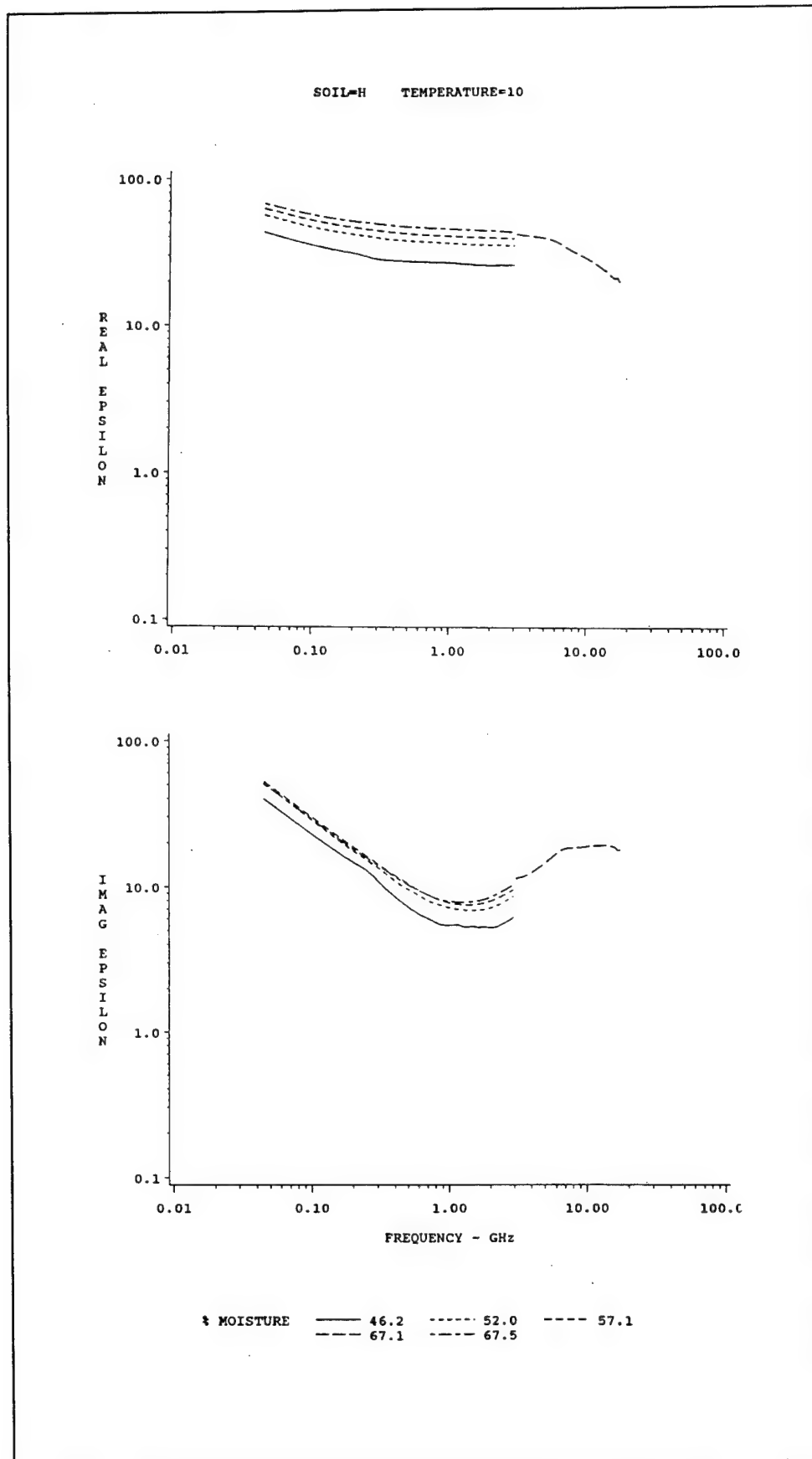


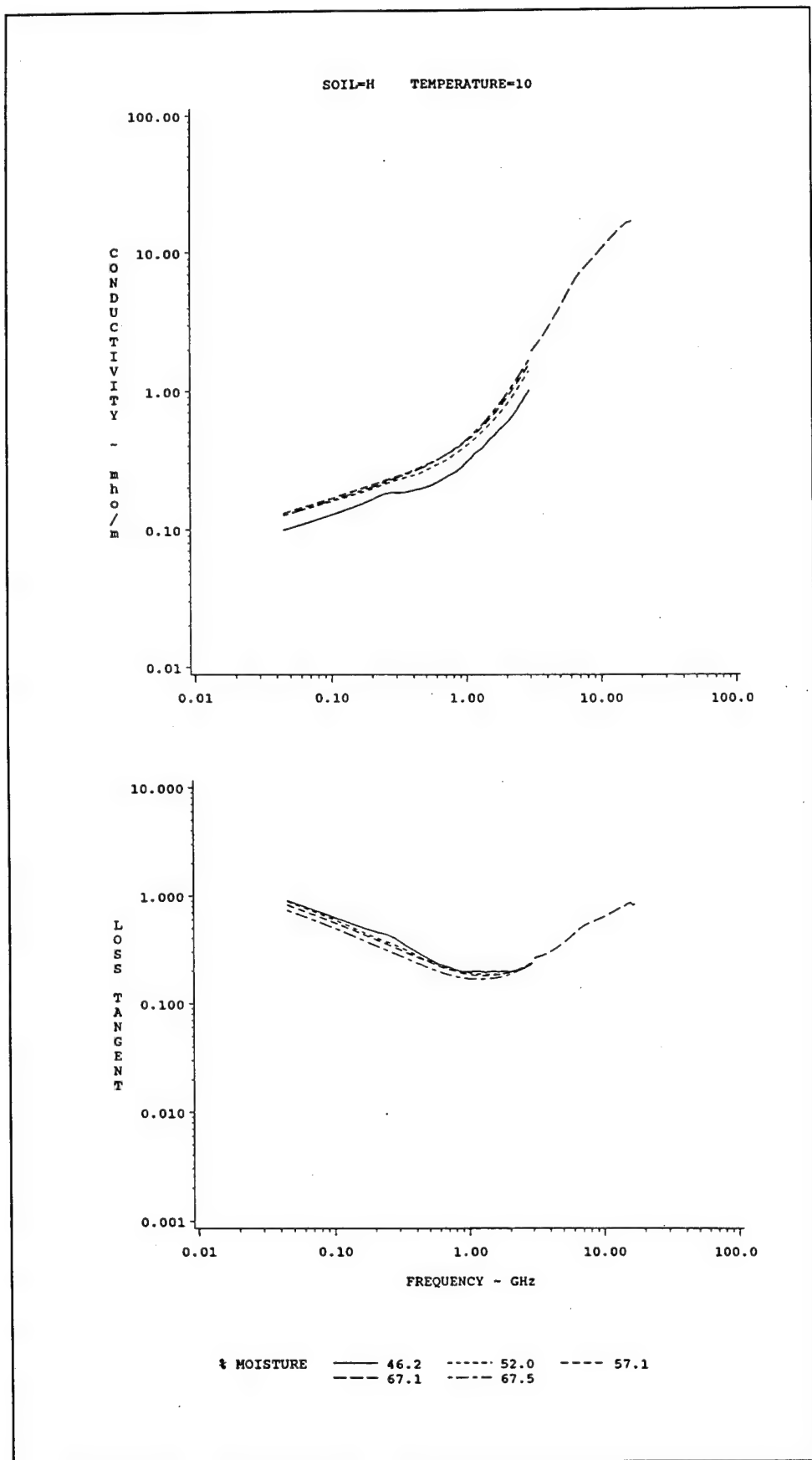


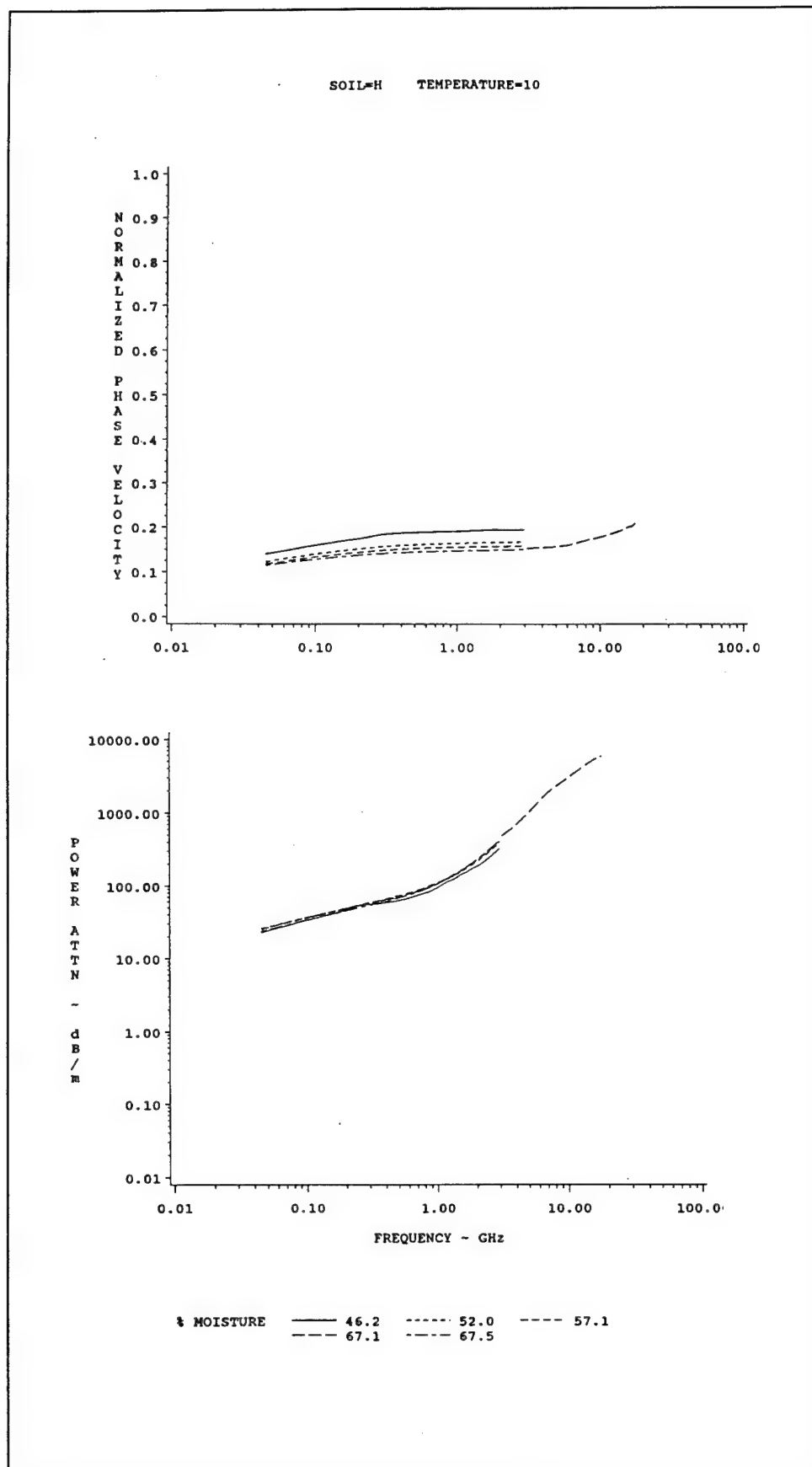
SOIL=G TEMPERATURE=40

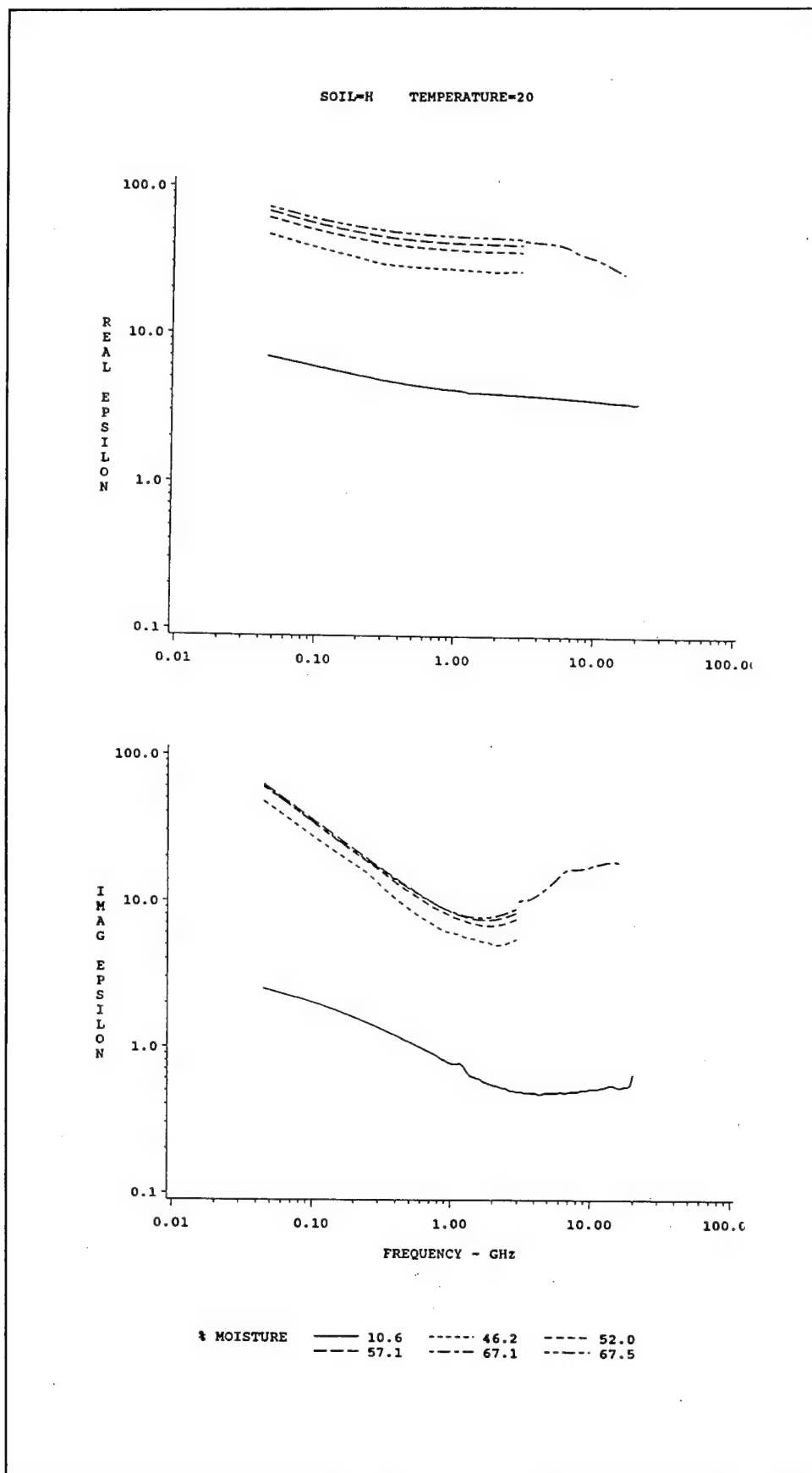


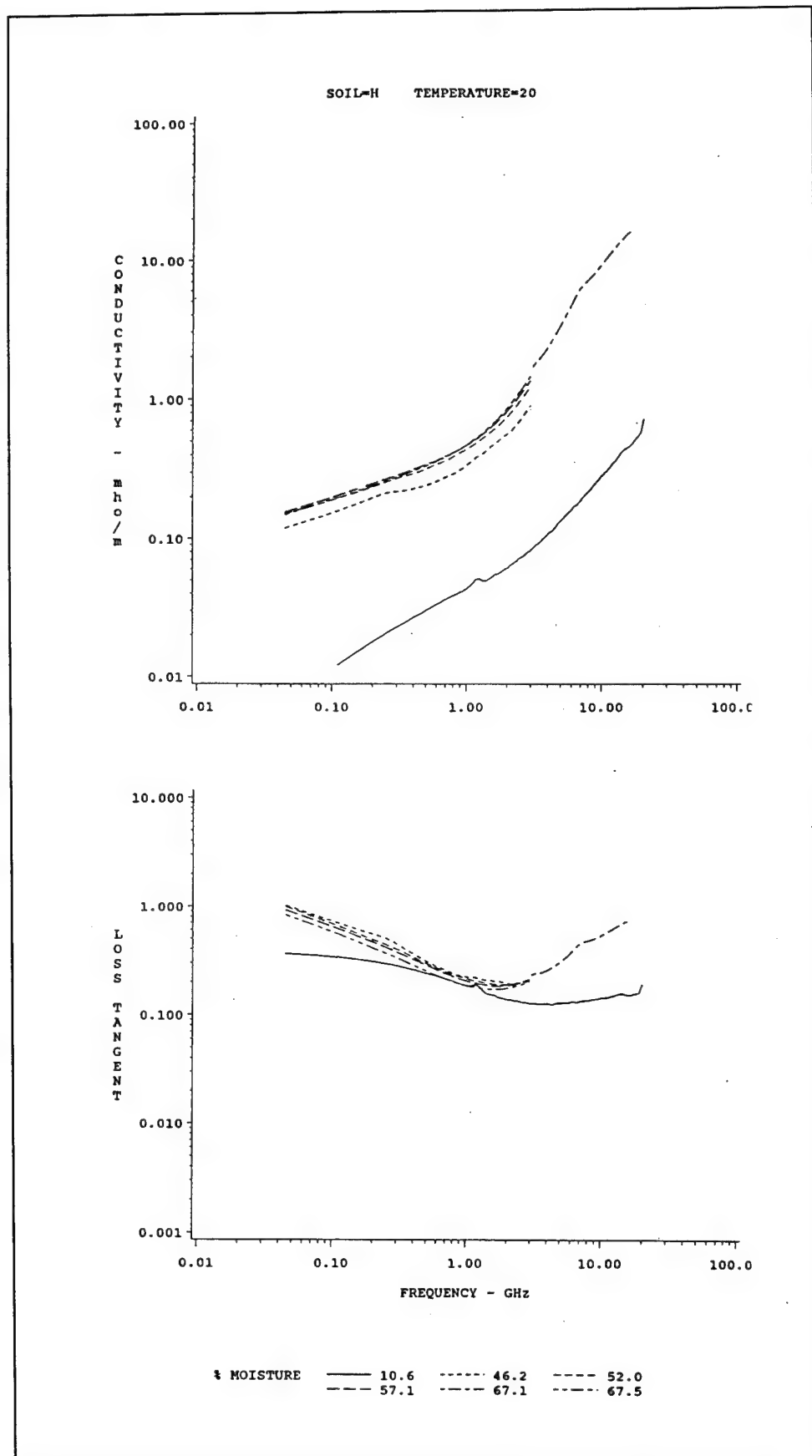
MOISTURE	17.9	25.8	28.7	31.6
	37.6	40.7	44.1	47.4

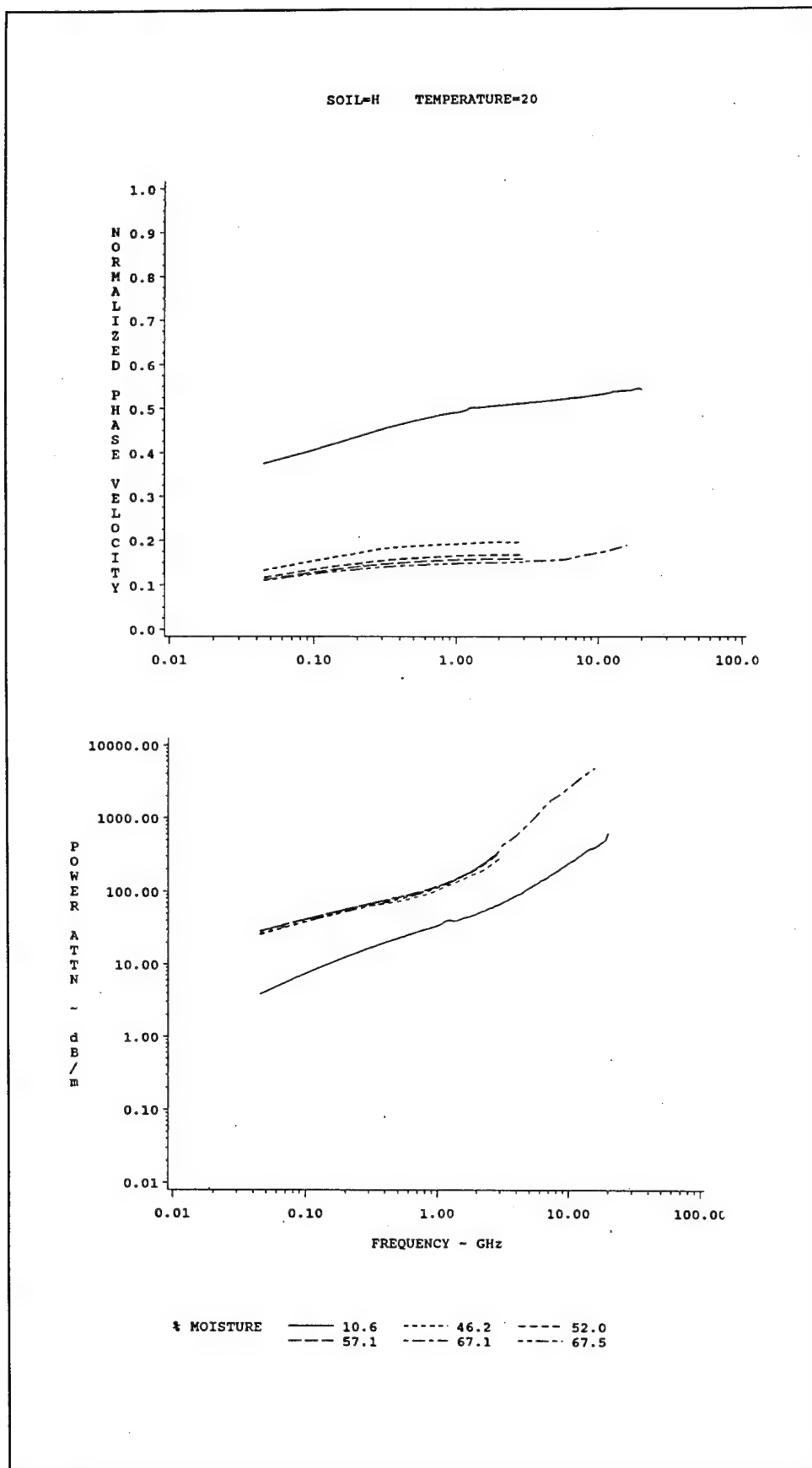


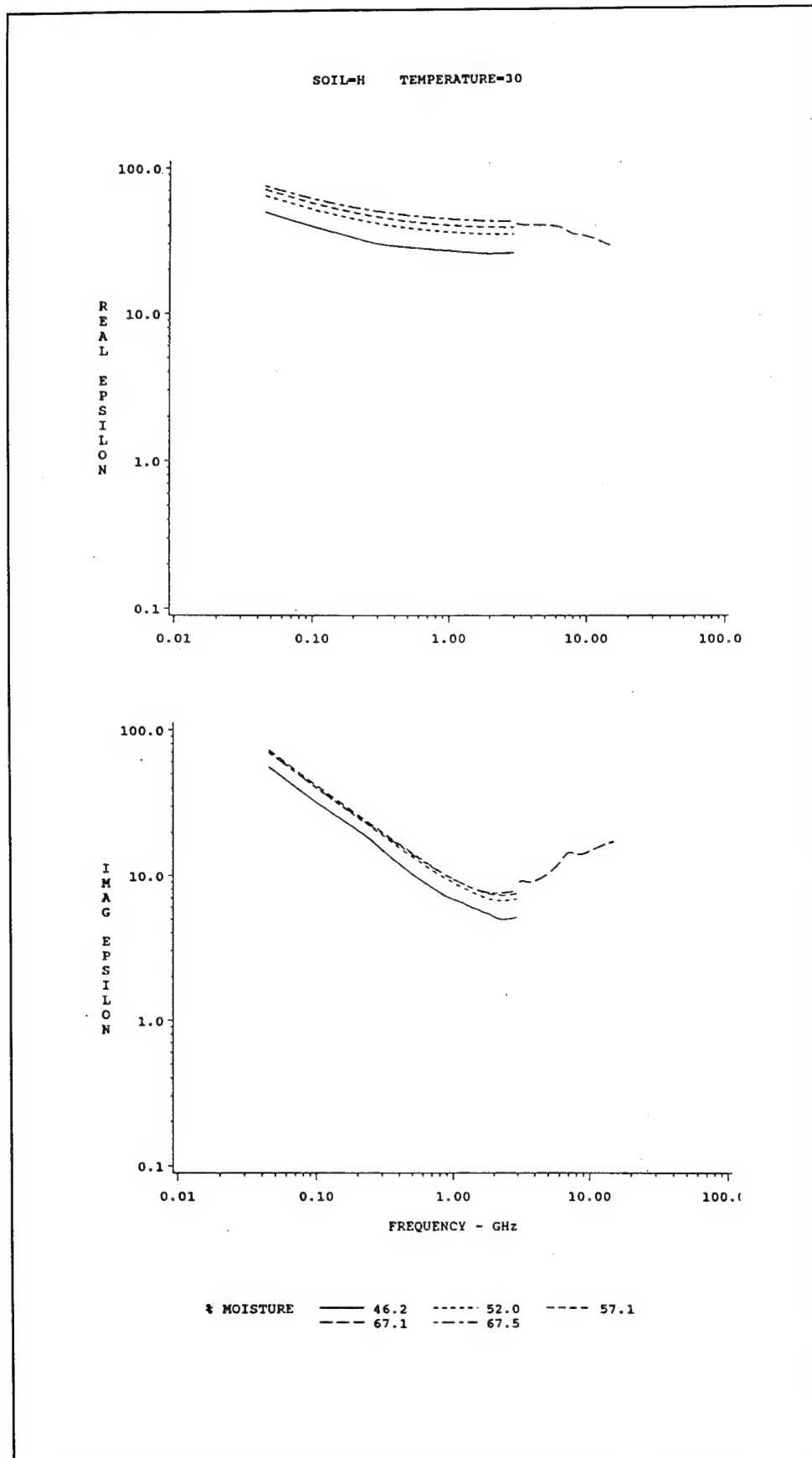


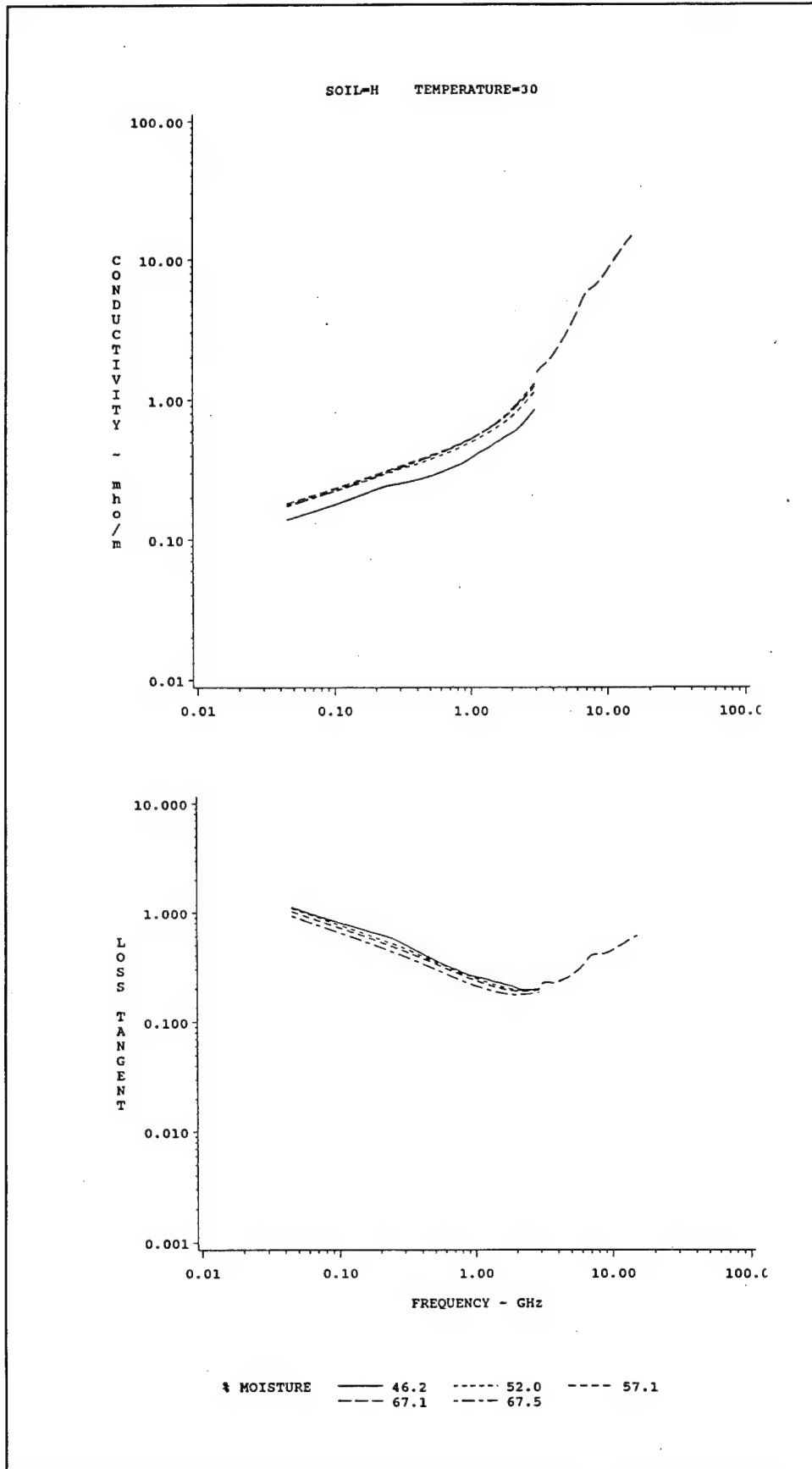




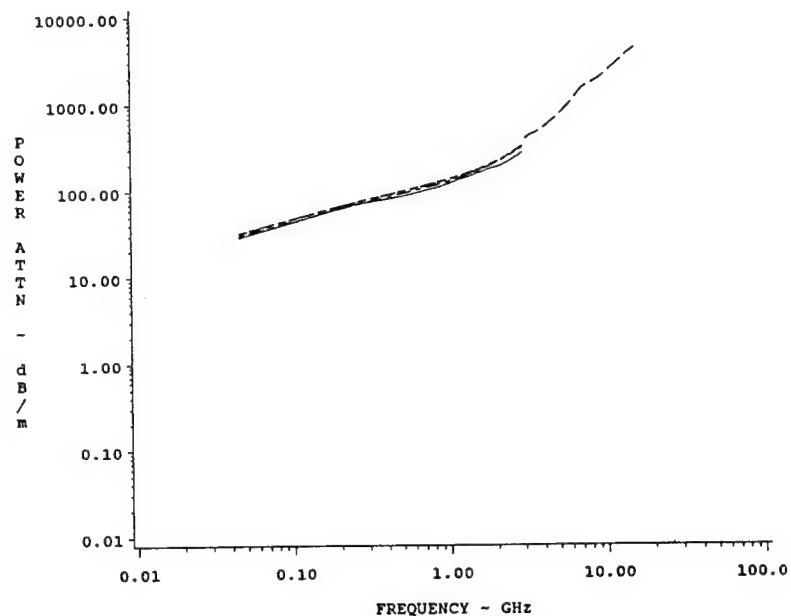
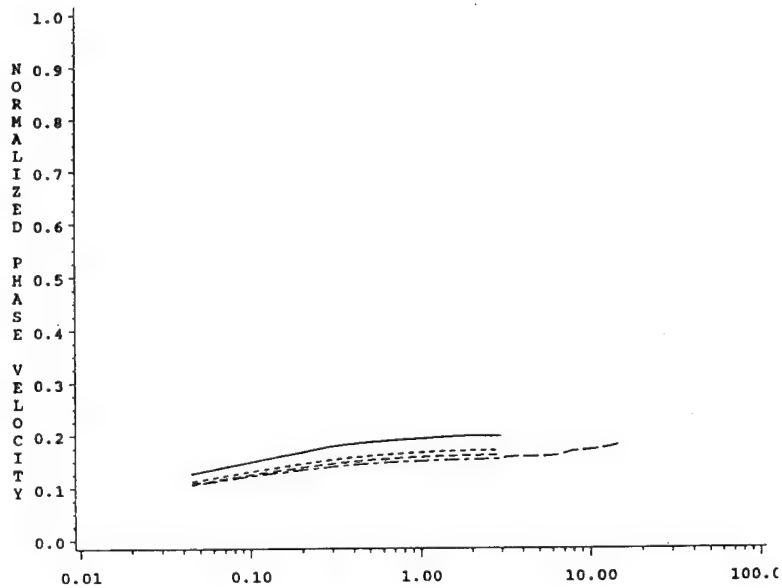




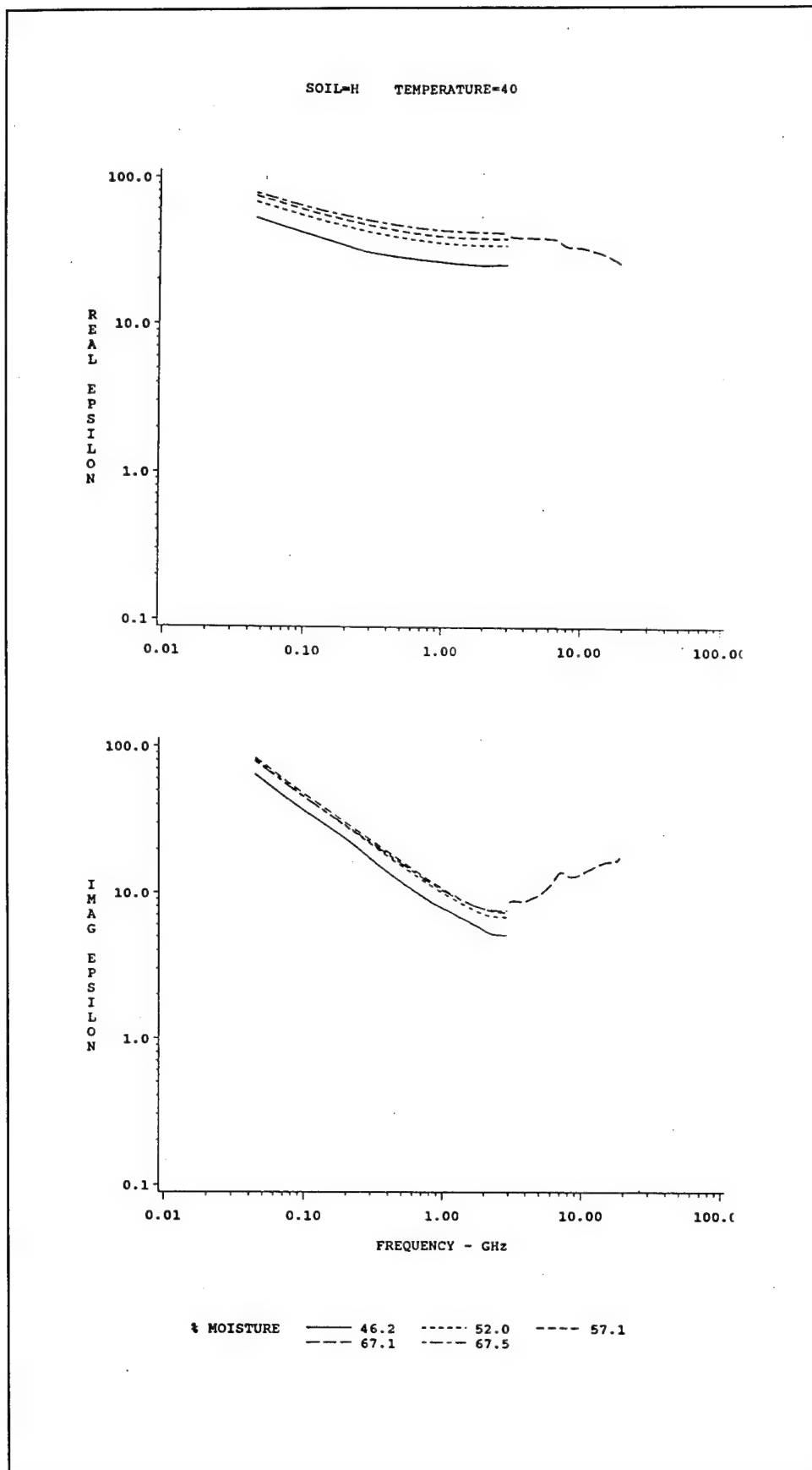


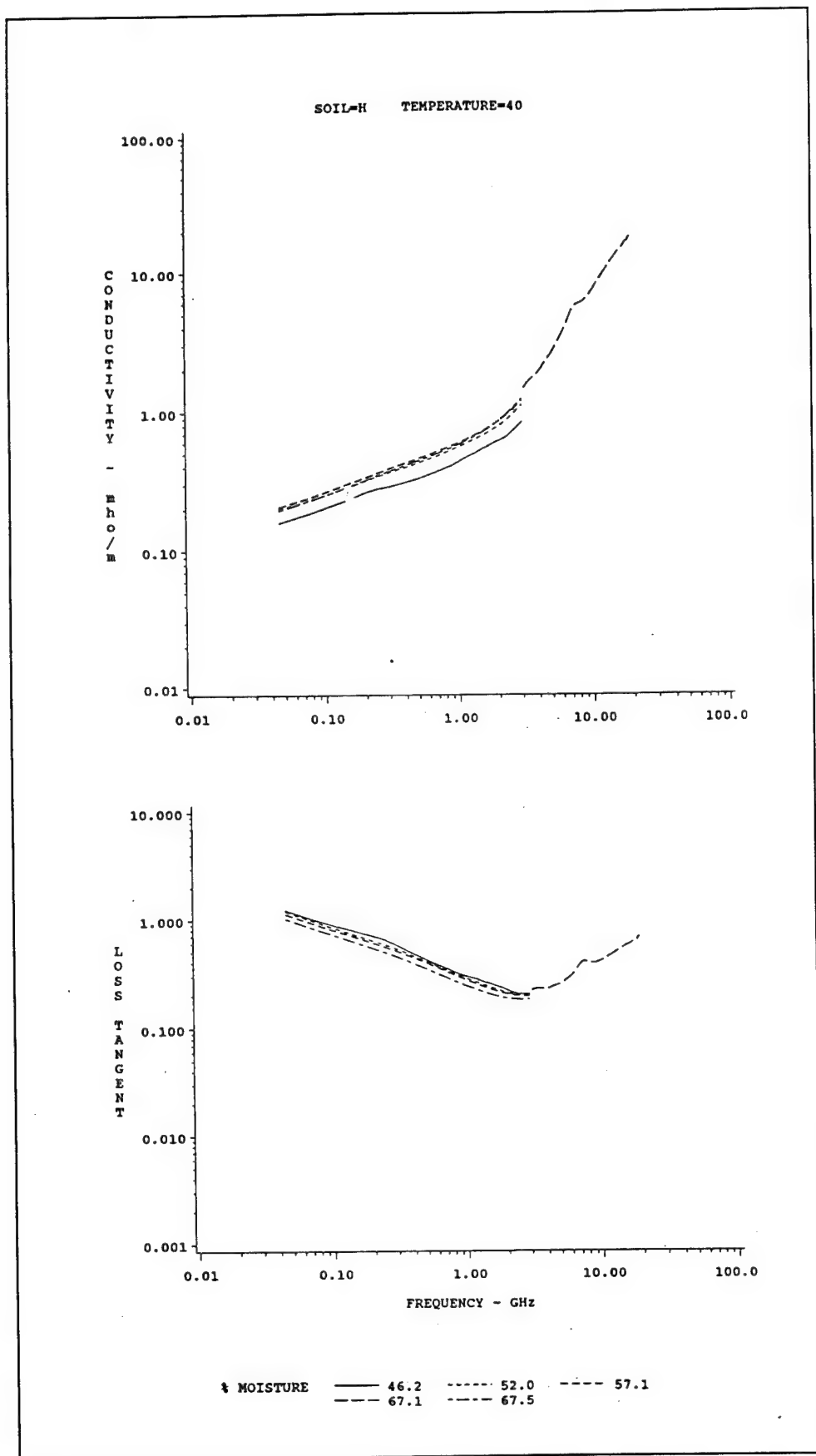


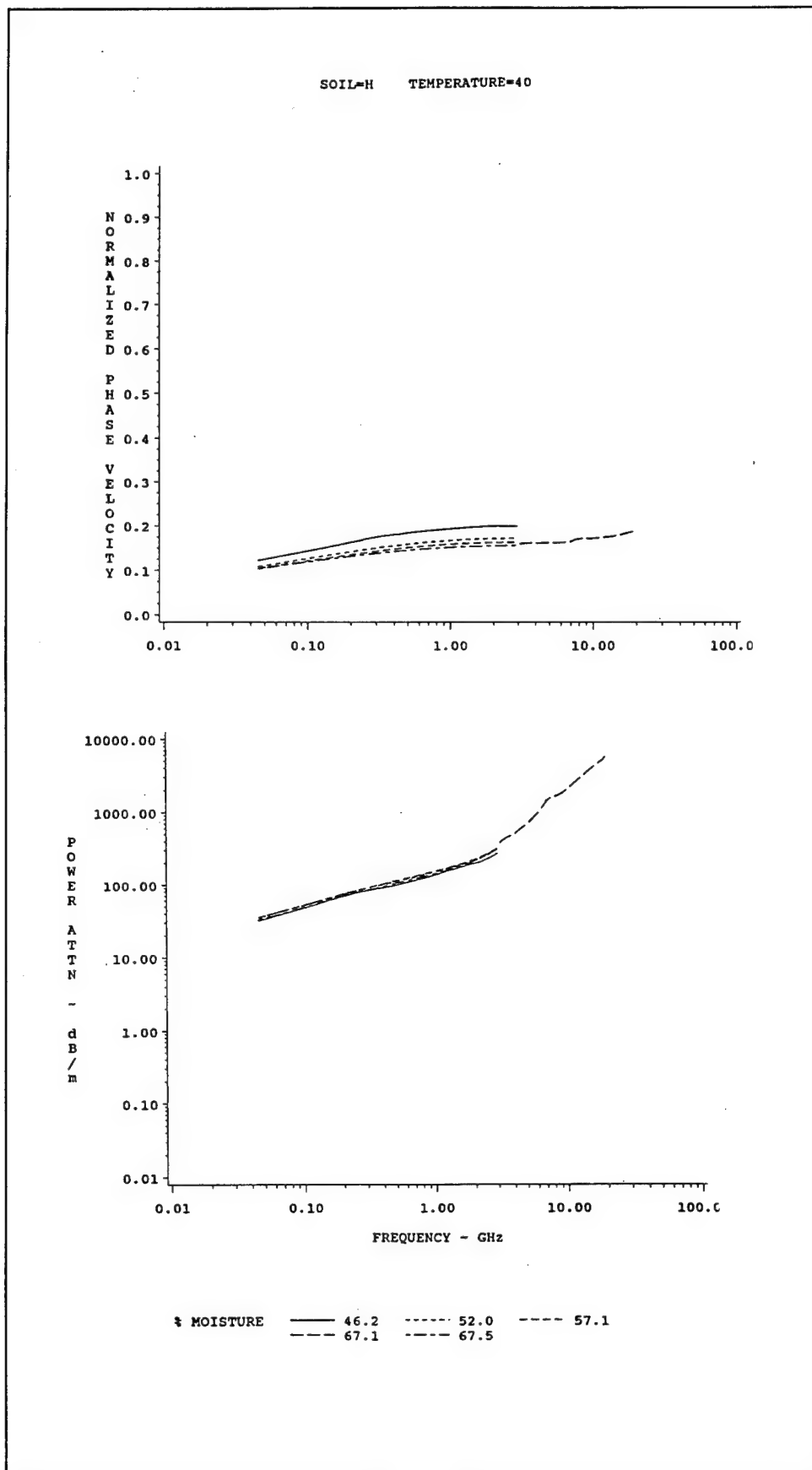
SOIL-H TEMPERATURE=30



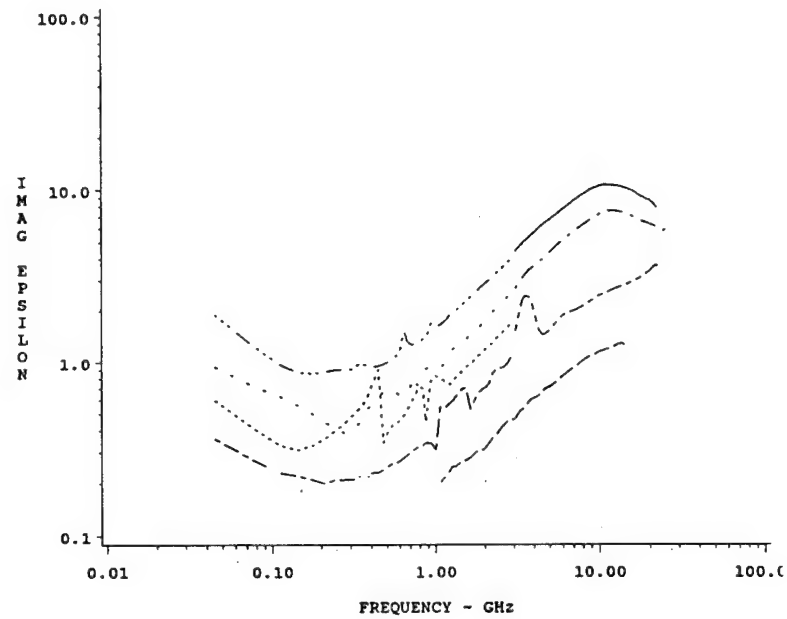
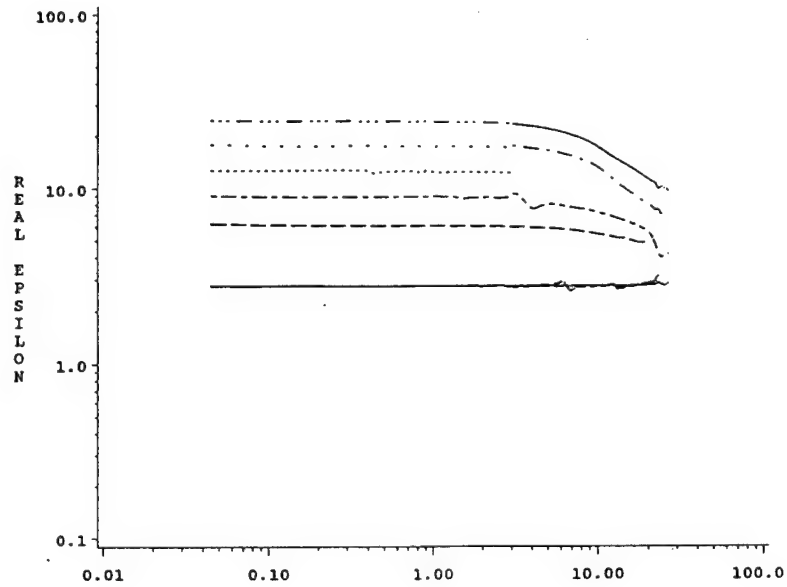
% MOISTURE ——— 46.2 - - - - 52.0 - . - . 57.1
 - - - 67.1 - - - 67.5



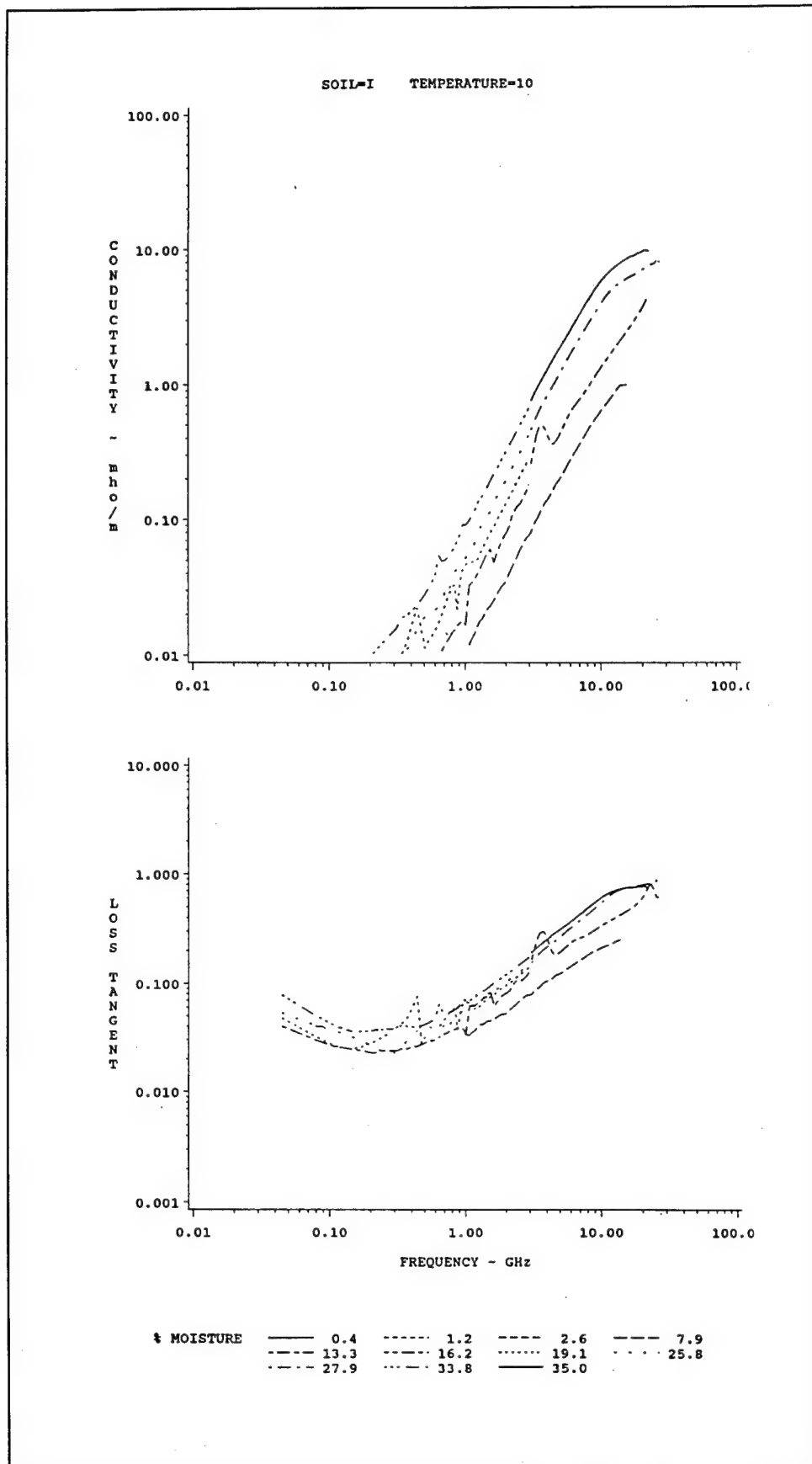


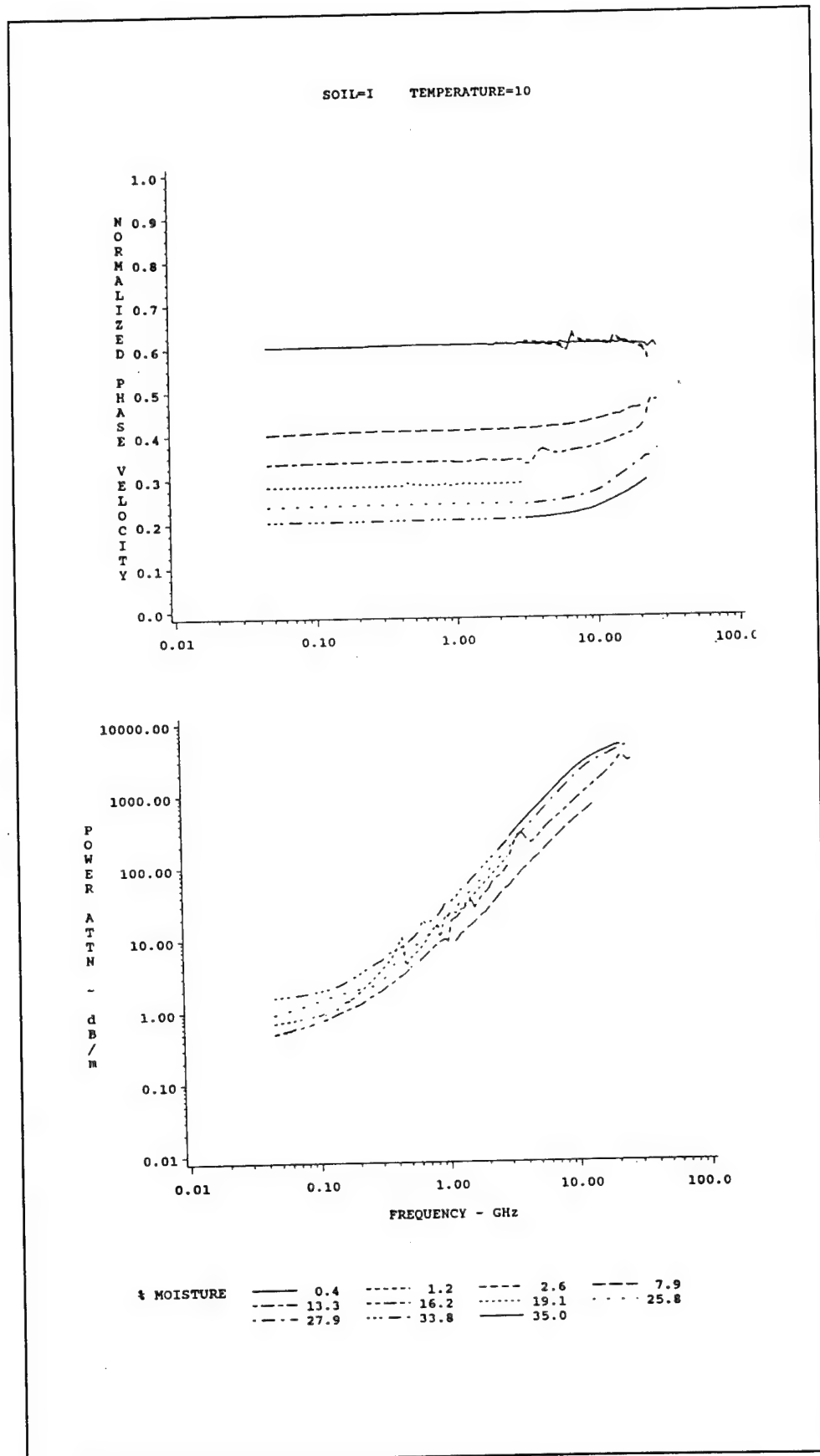


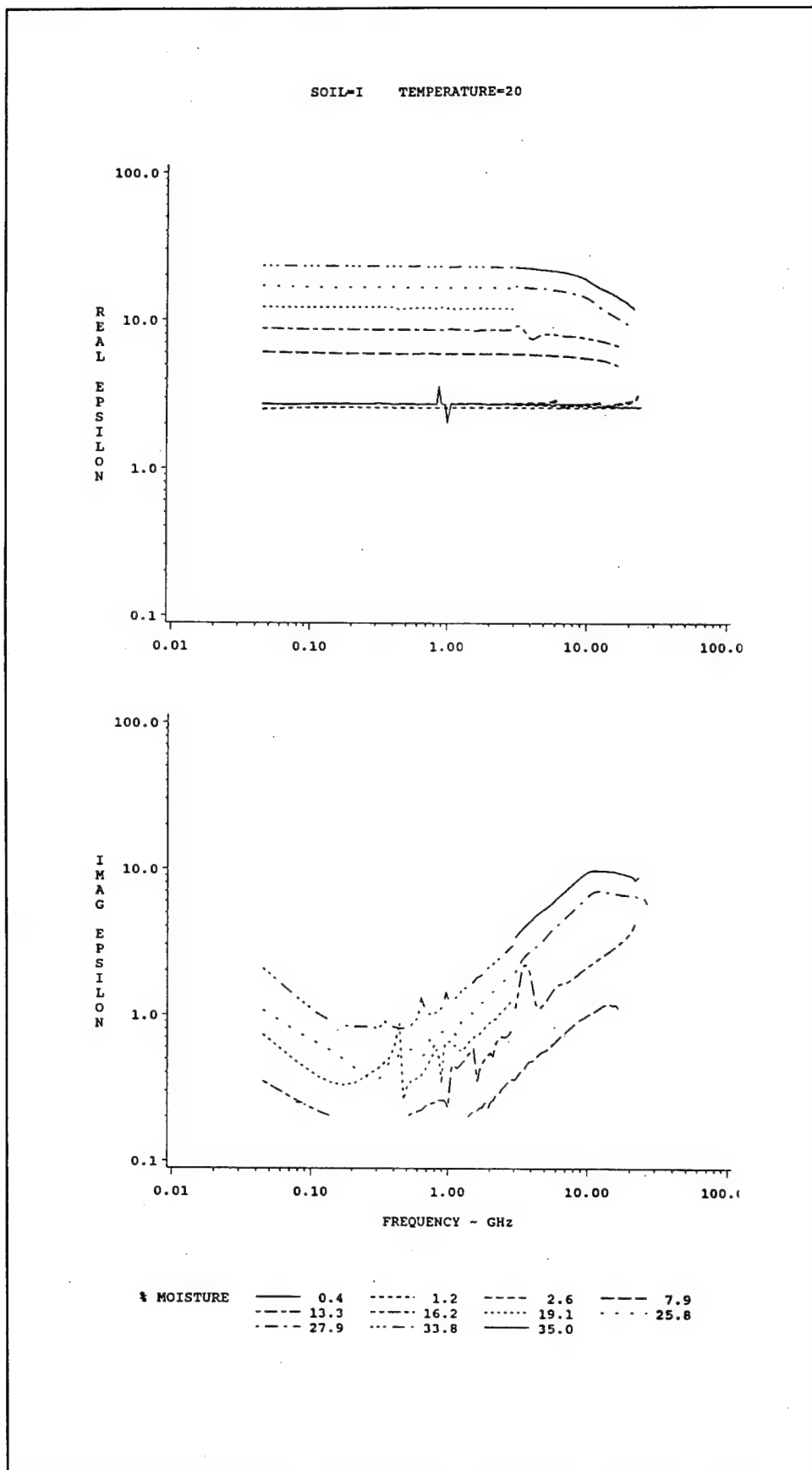
SOIL-I TEMPERATURE=10

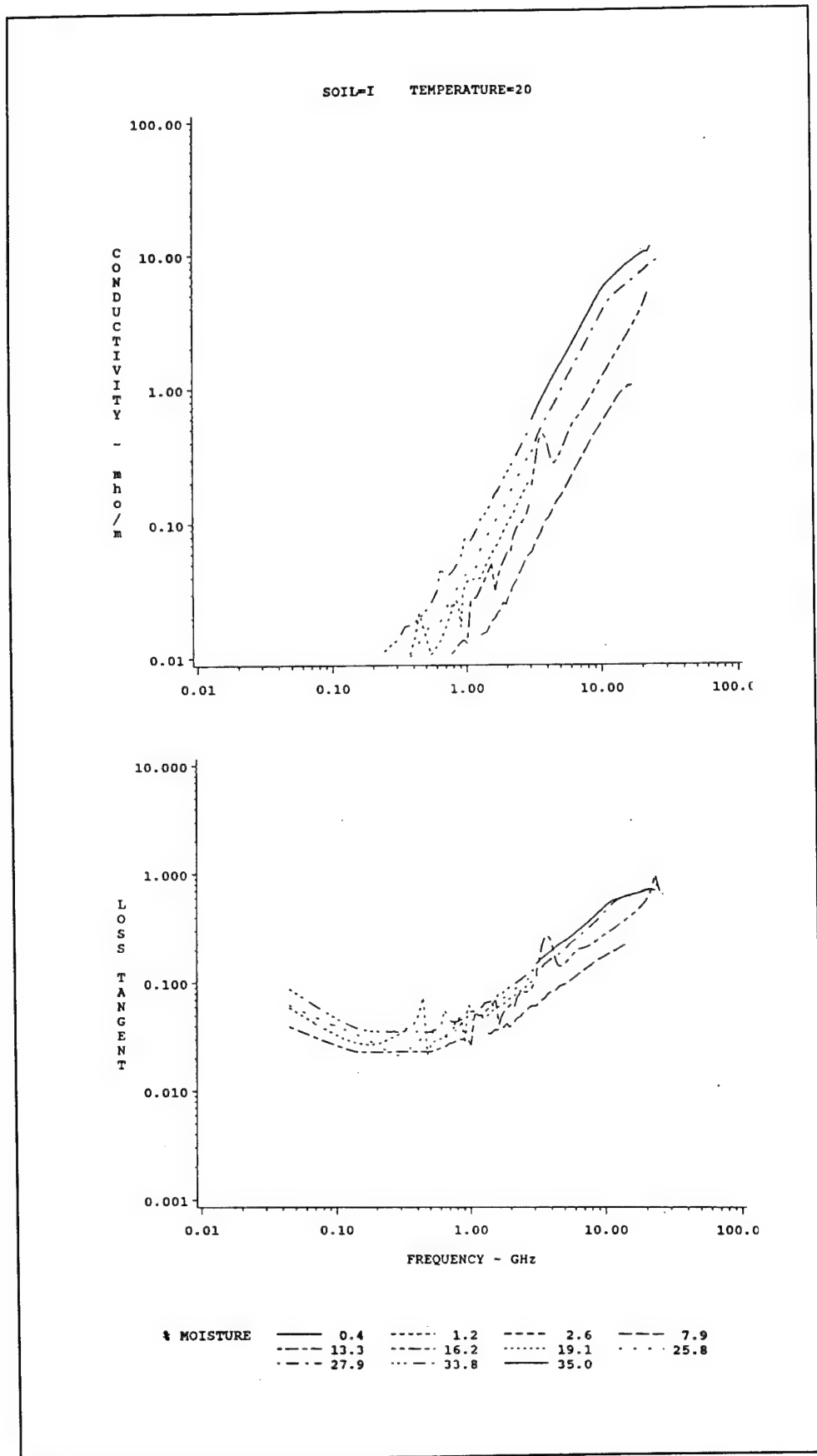


% MOISTURE	0.4	1.2	2.6	7.9
	13.3	16.2	19.1	25.8
	27.9	33.8	35.0	

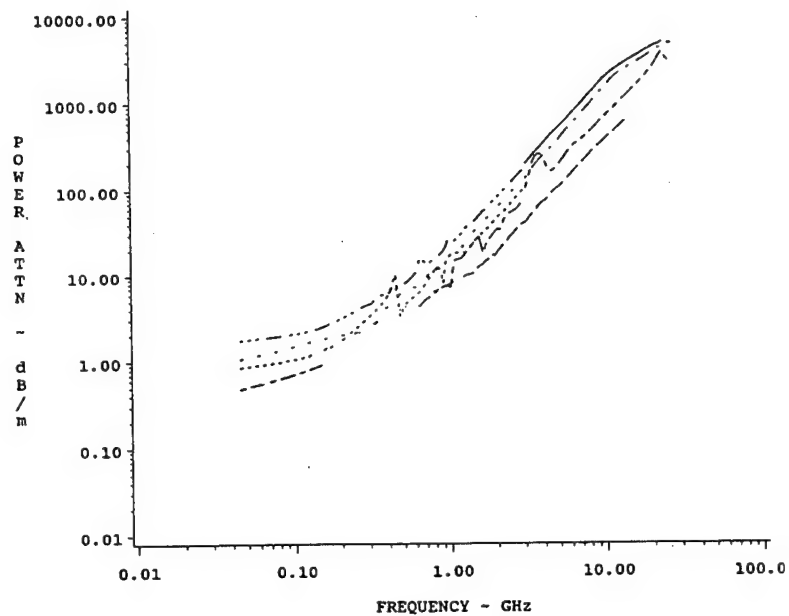
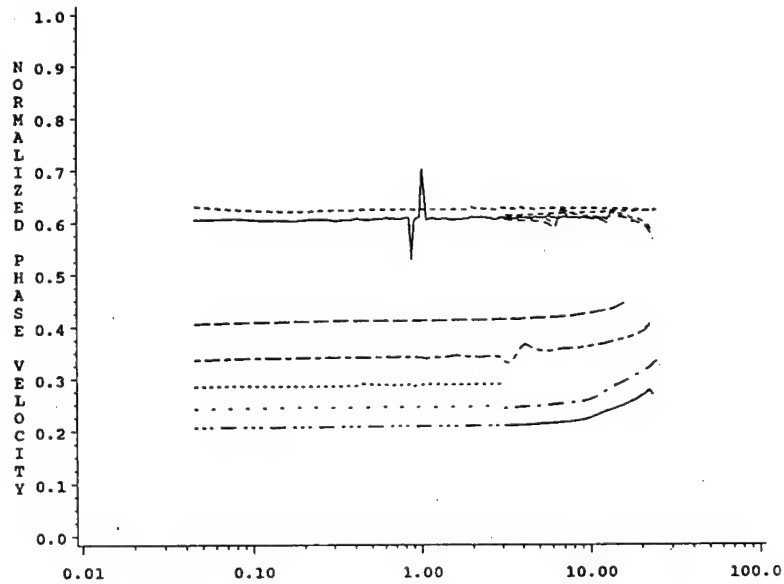




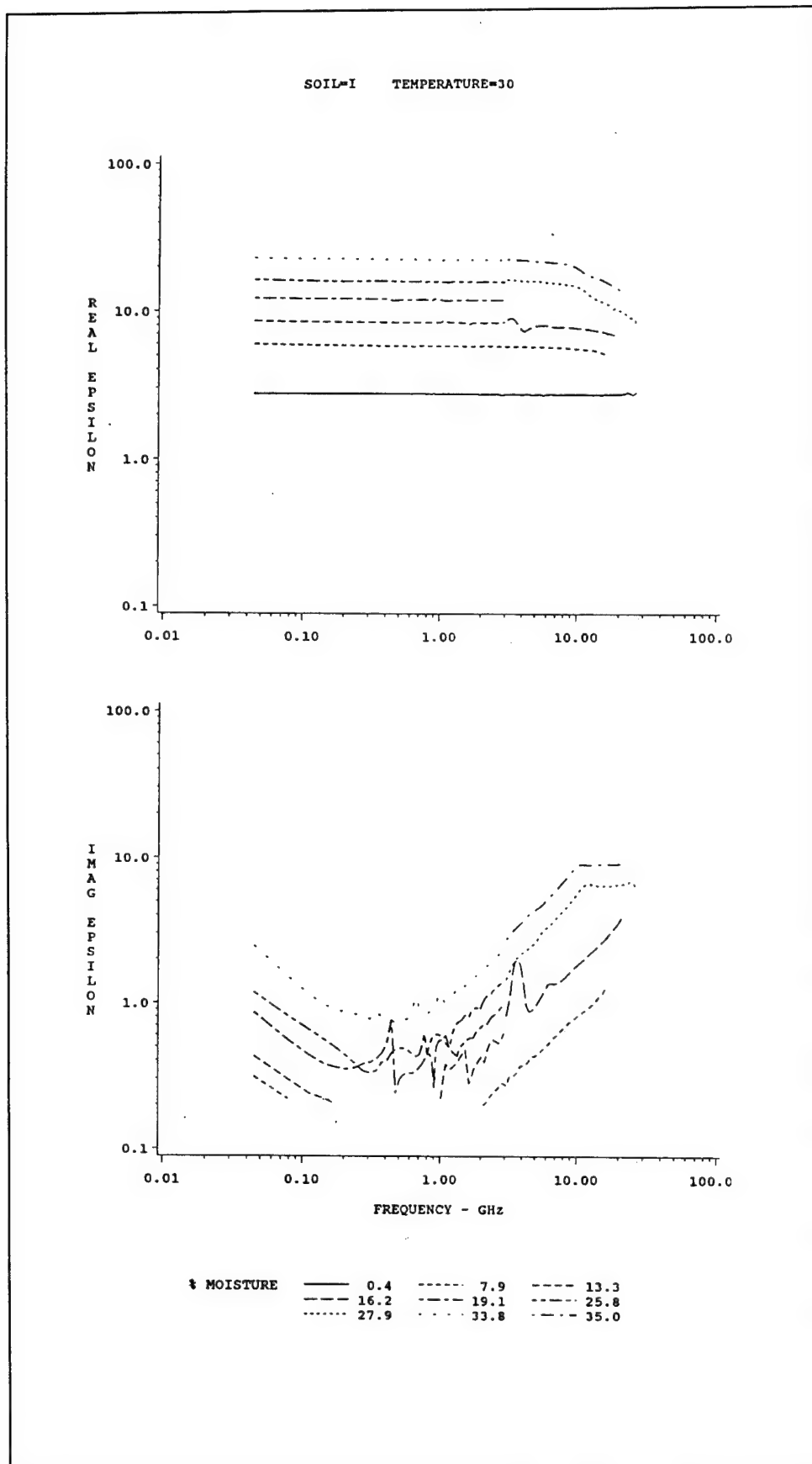


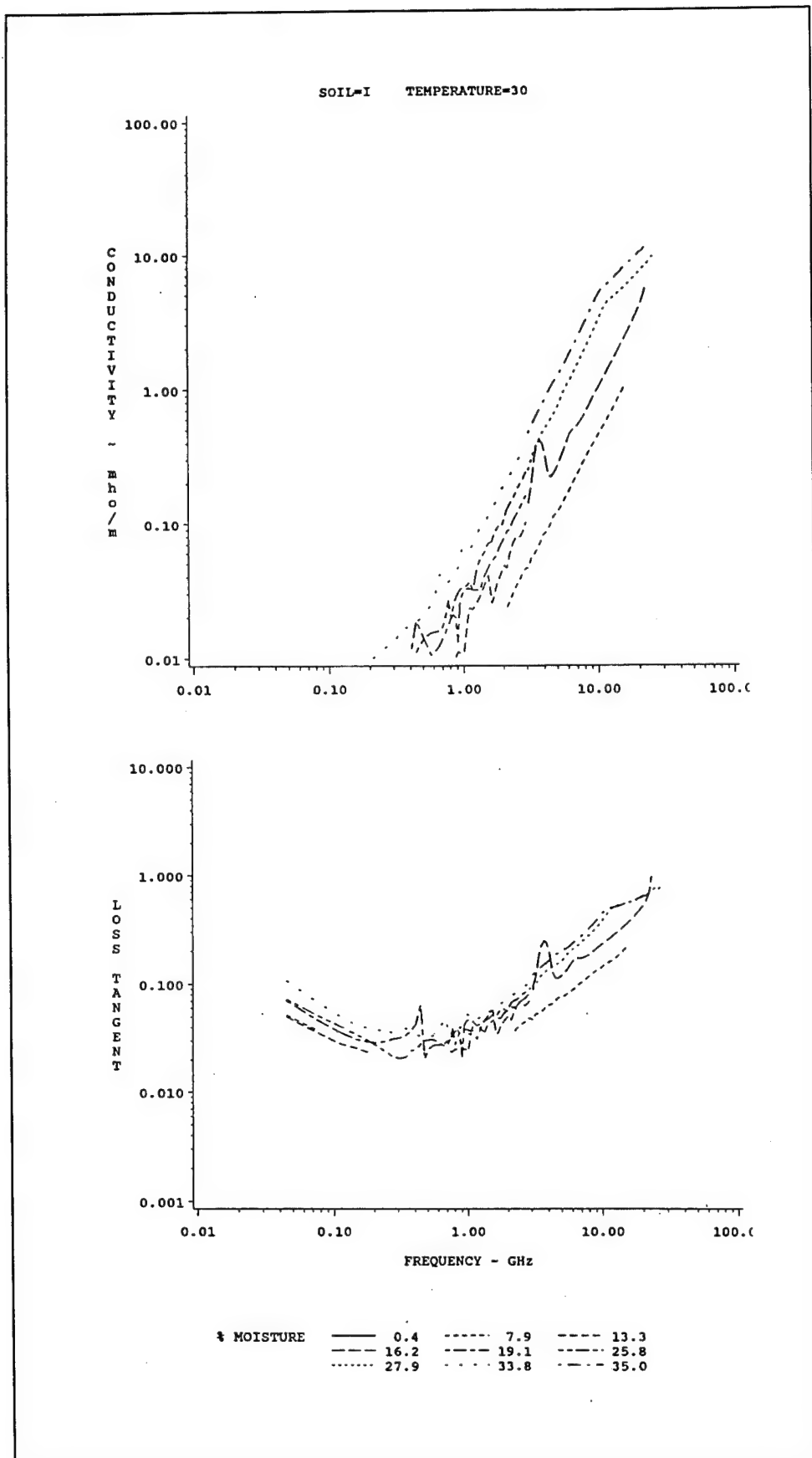


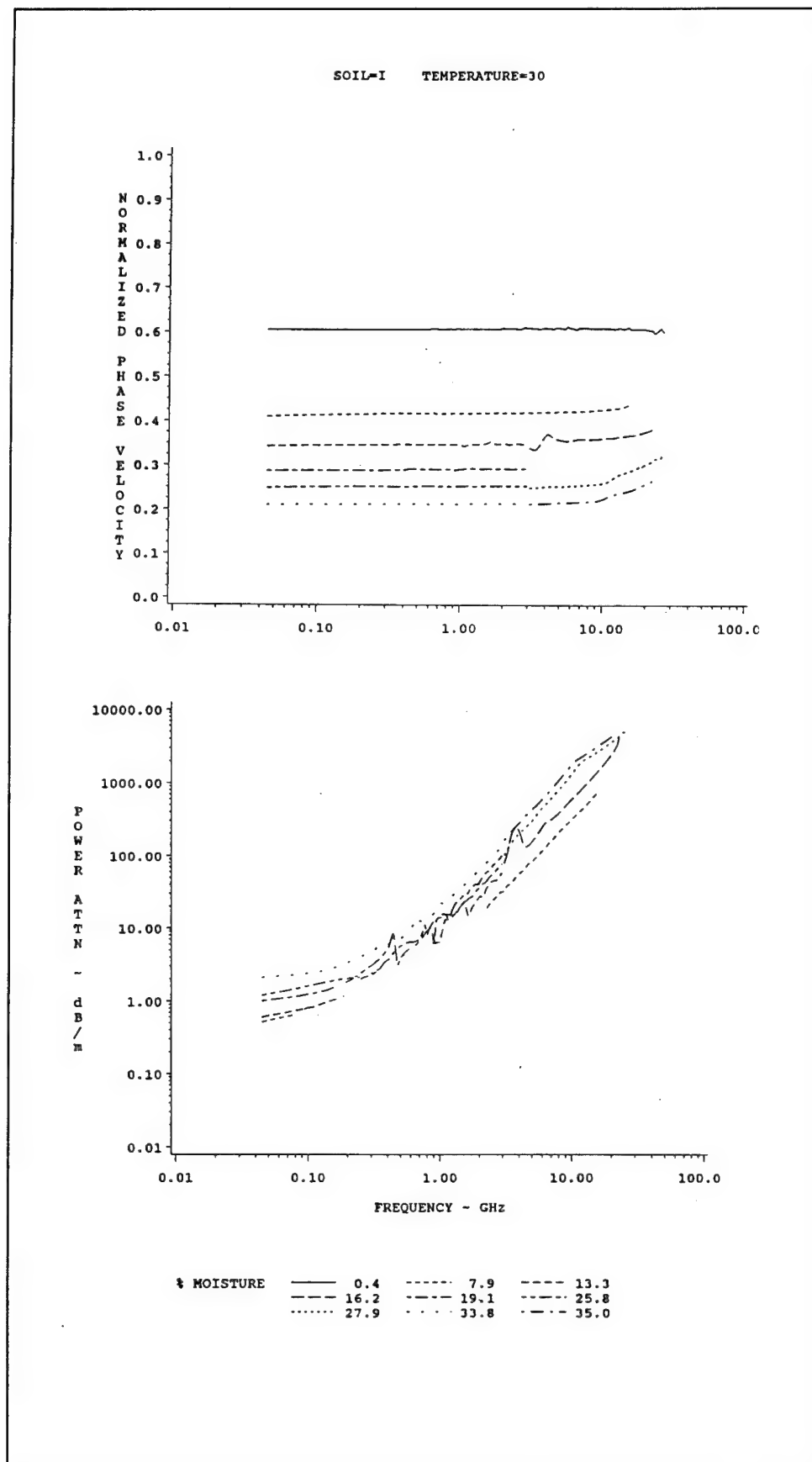
SOIL-I TEMPERATURE=20

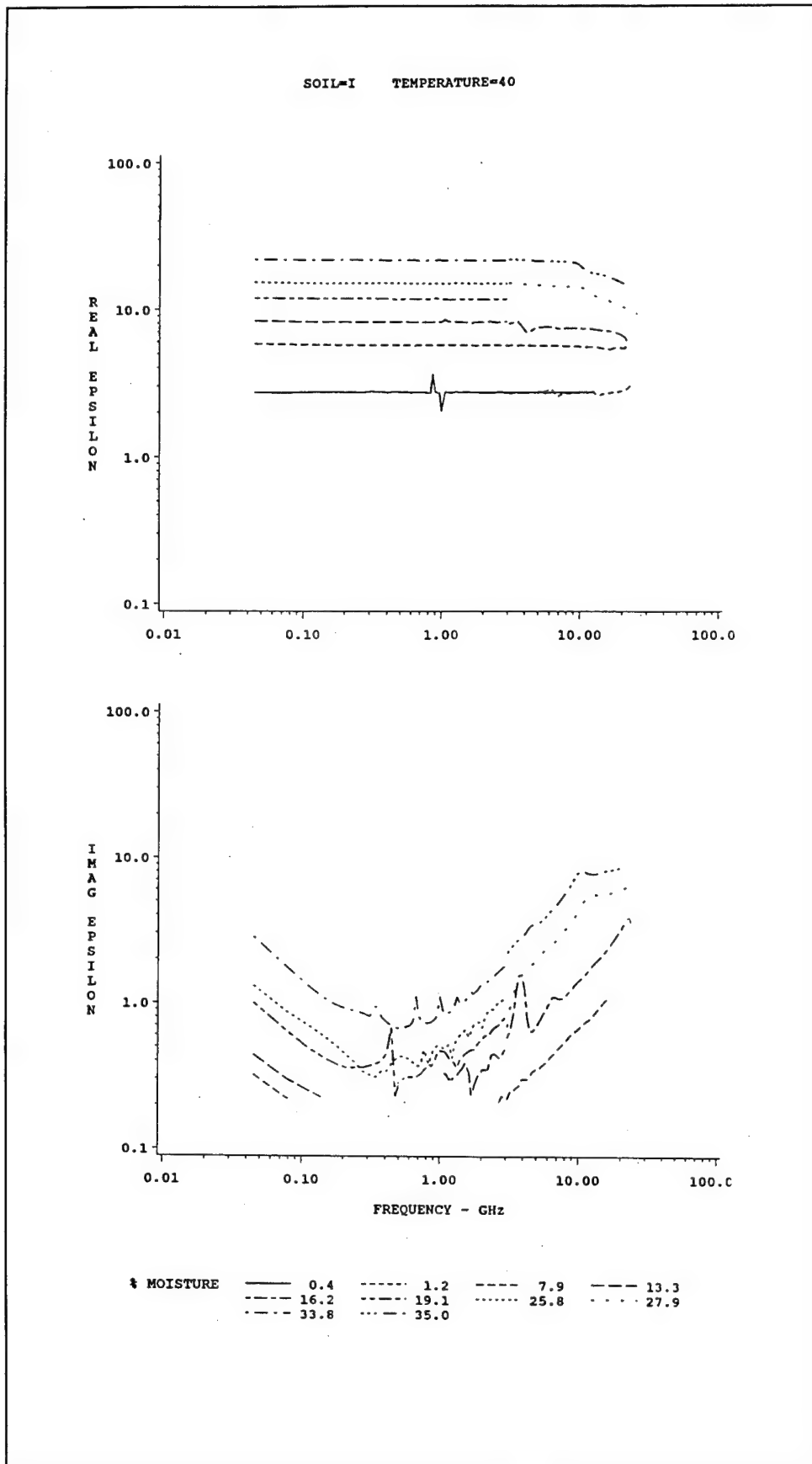


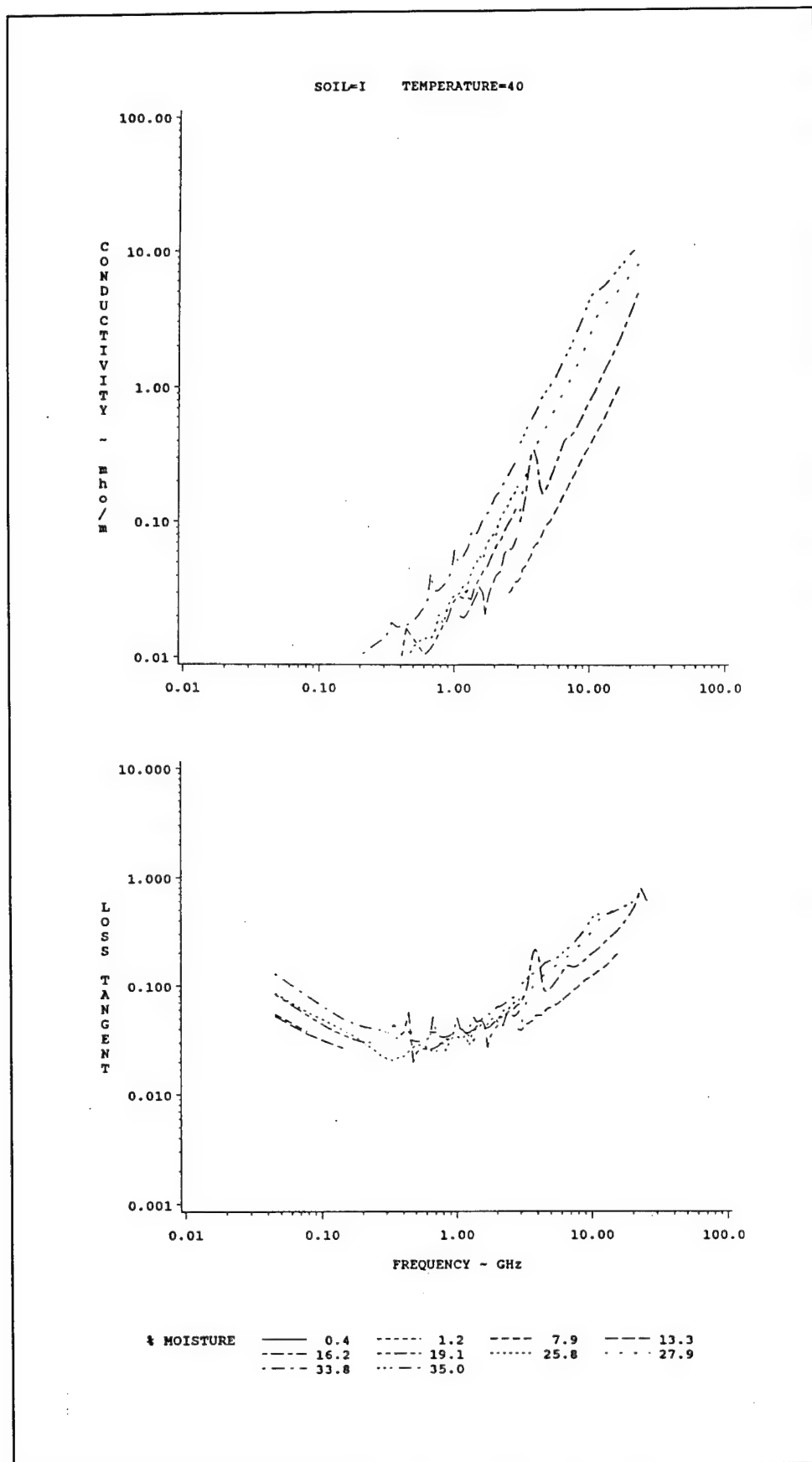
* MOISTURE	0.4	1.2	2.6	7.9
	13.3	16.2	19.1	25.8
	27.9	33.8	35.0	

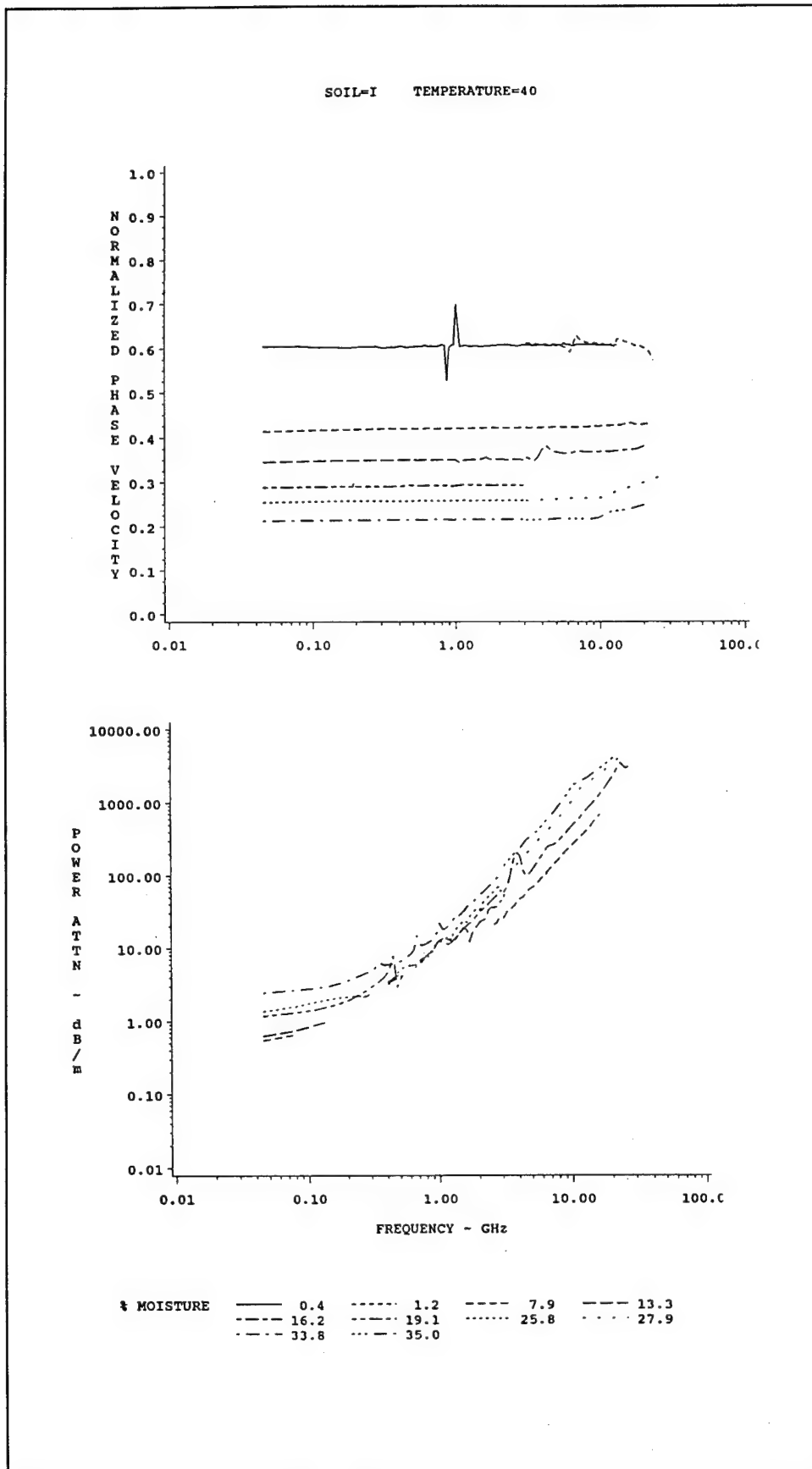


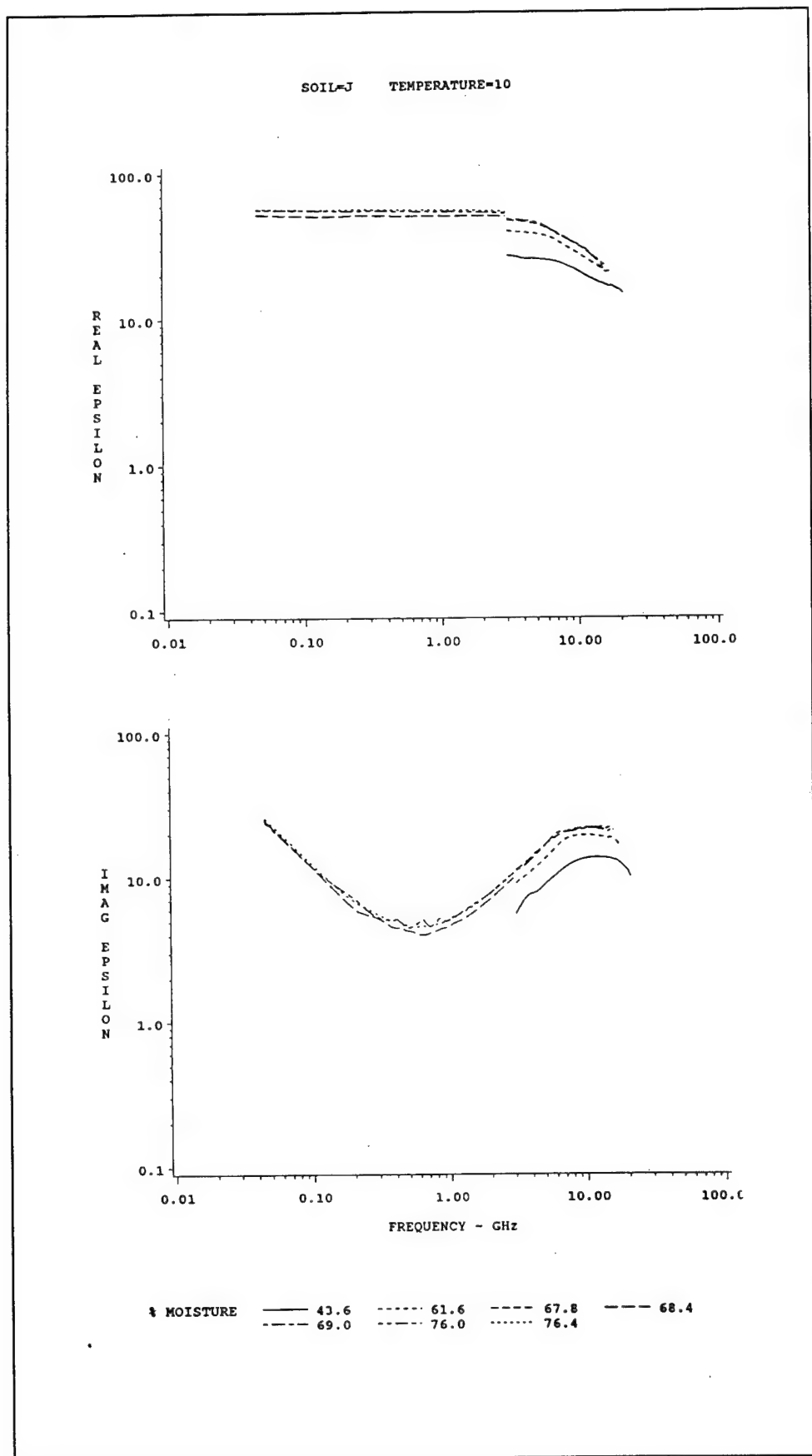


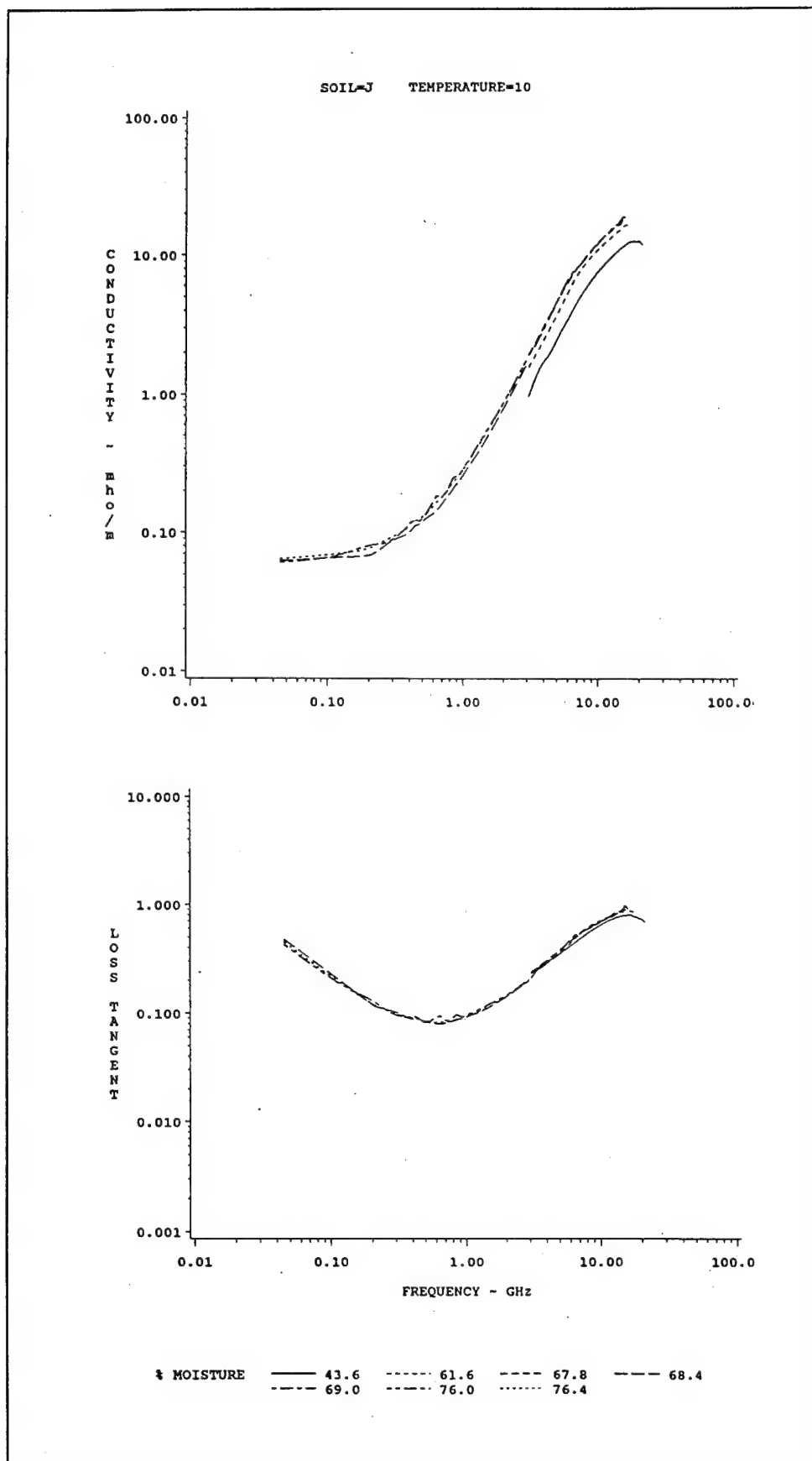


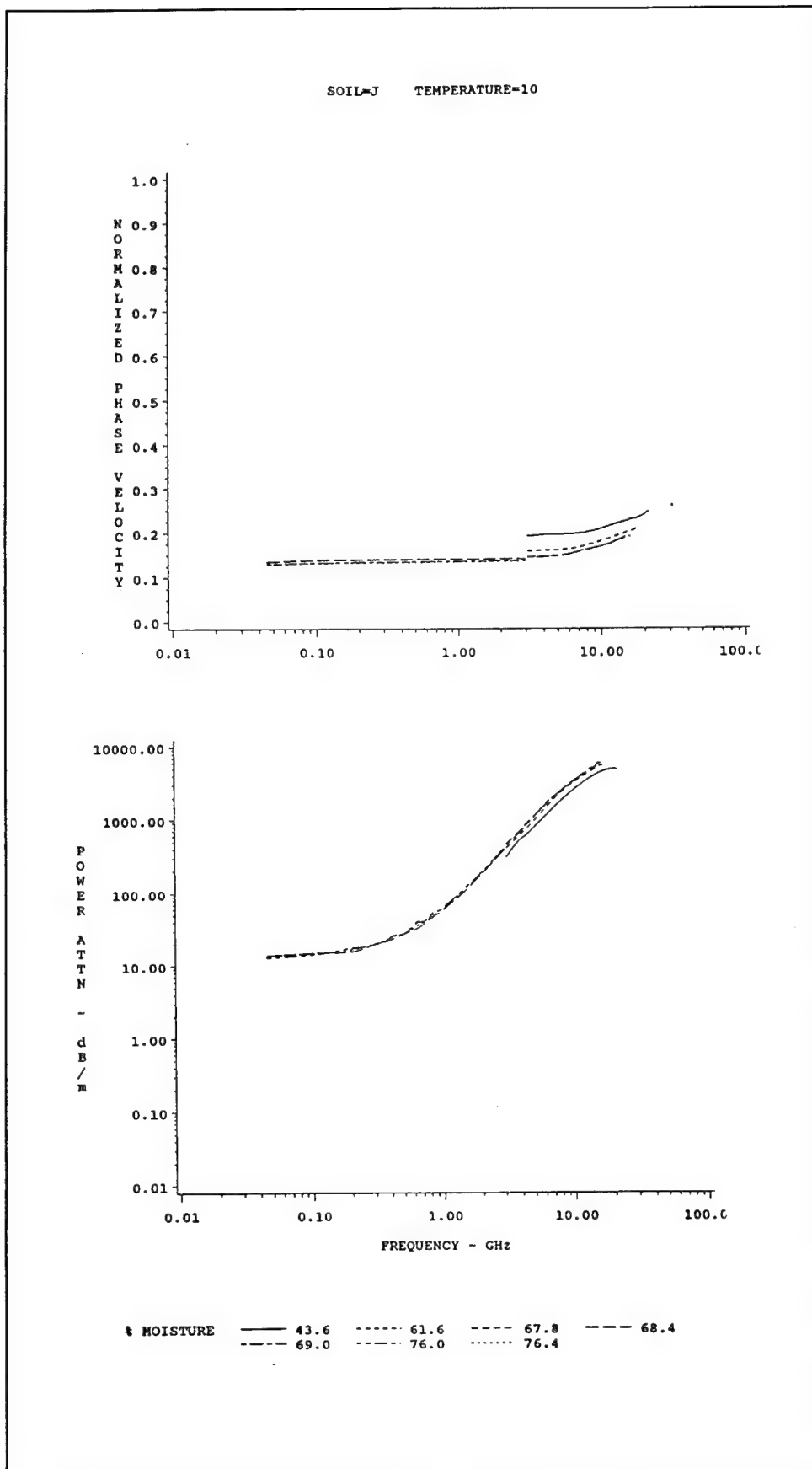


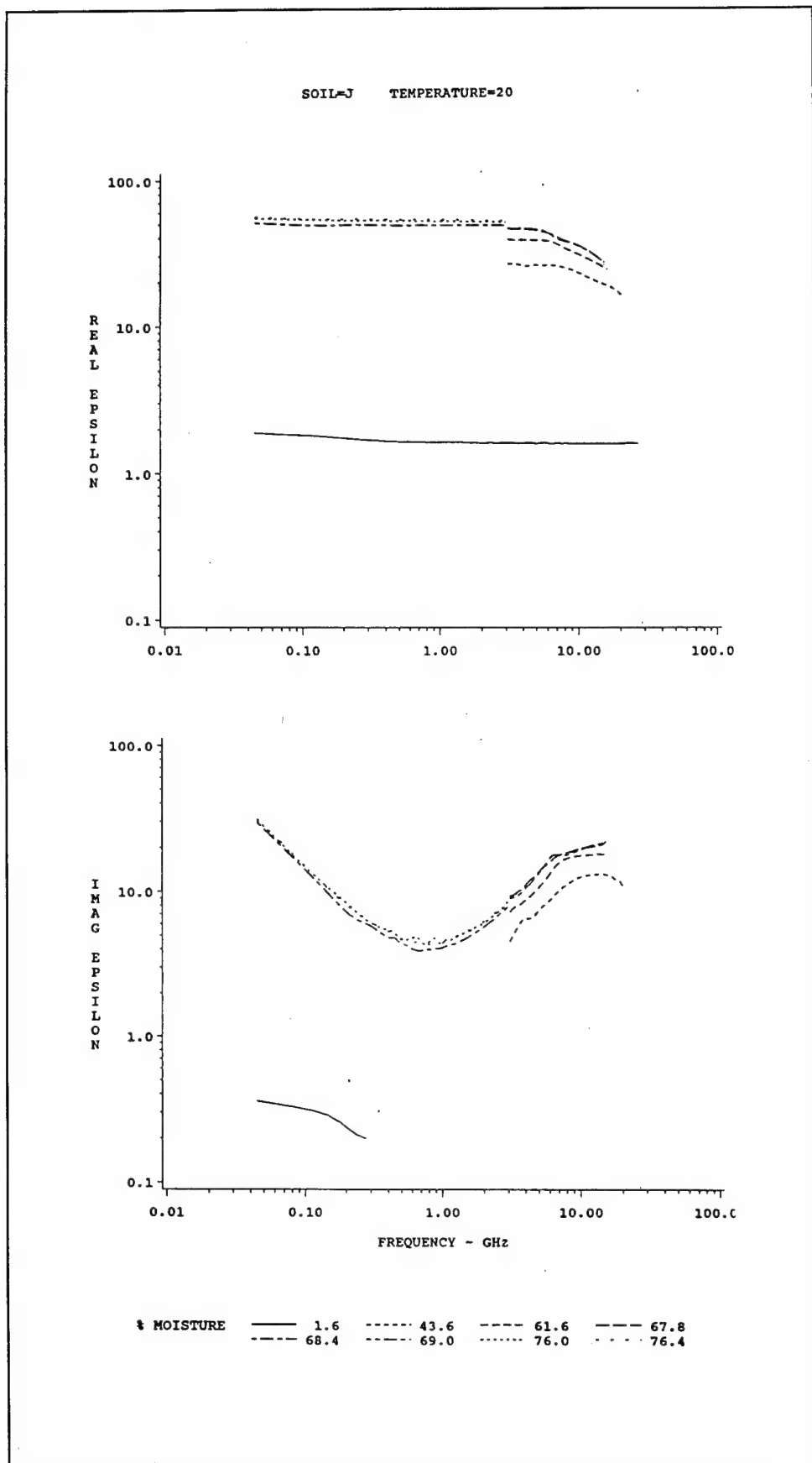


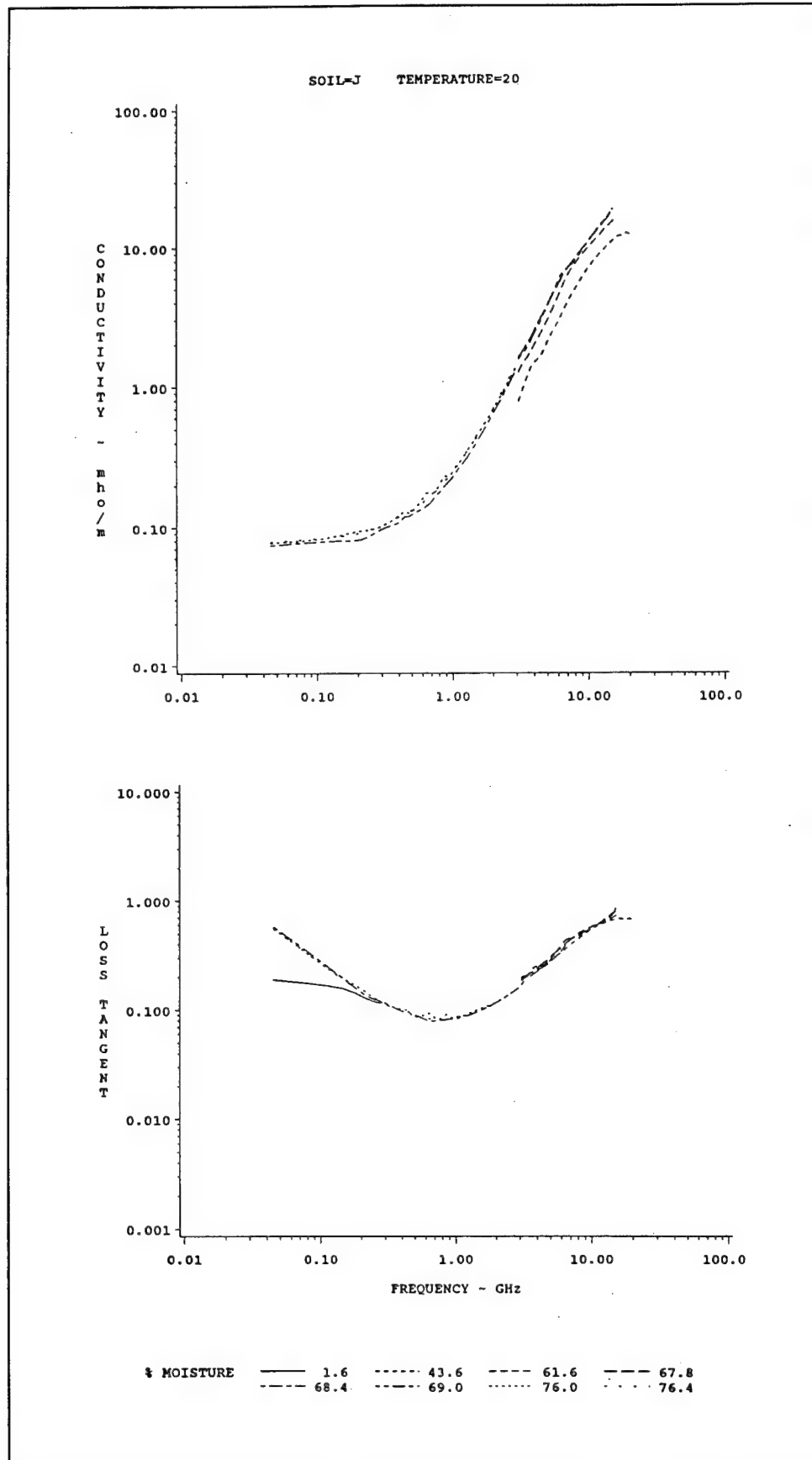


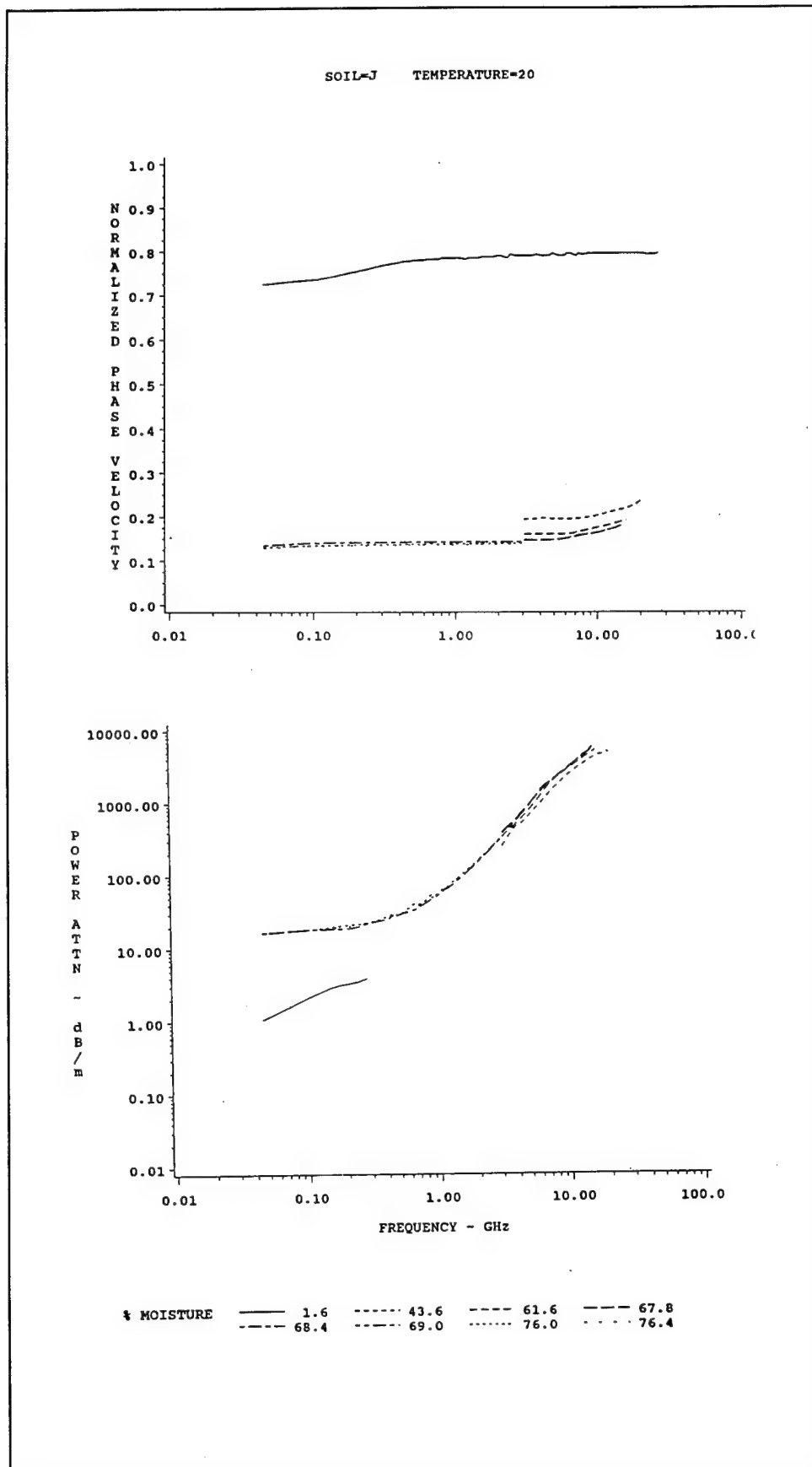


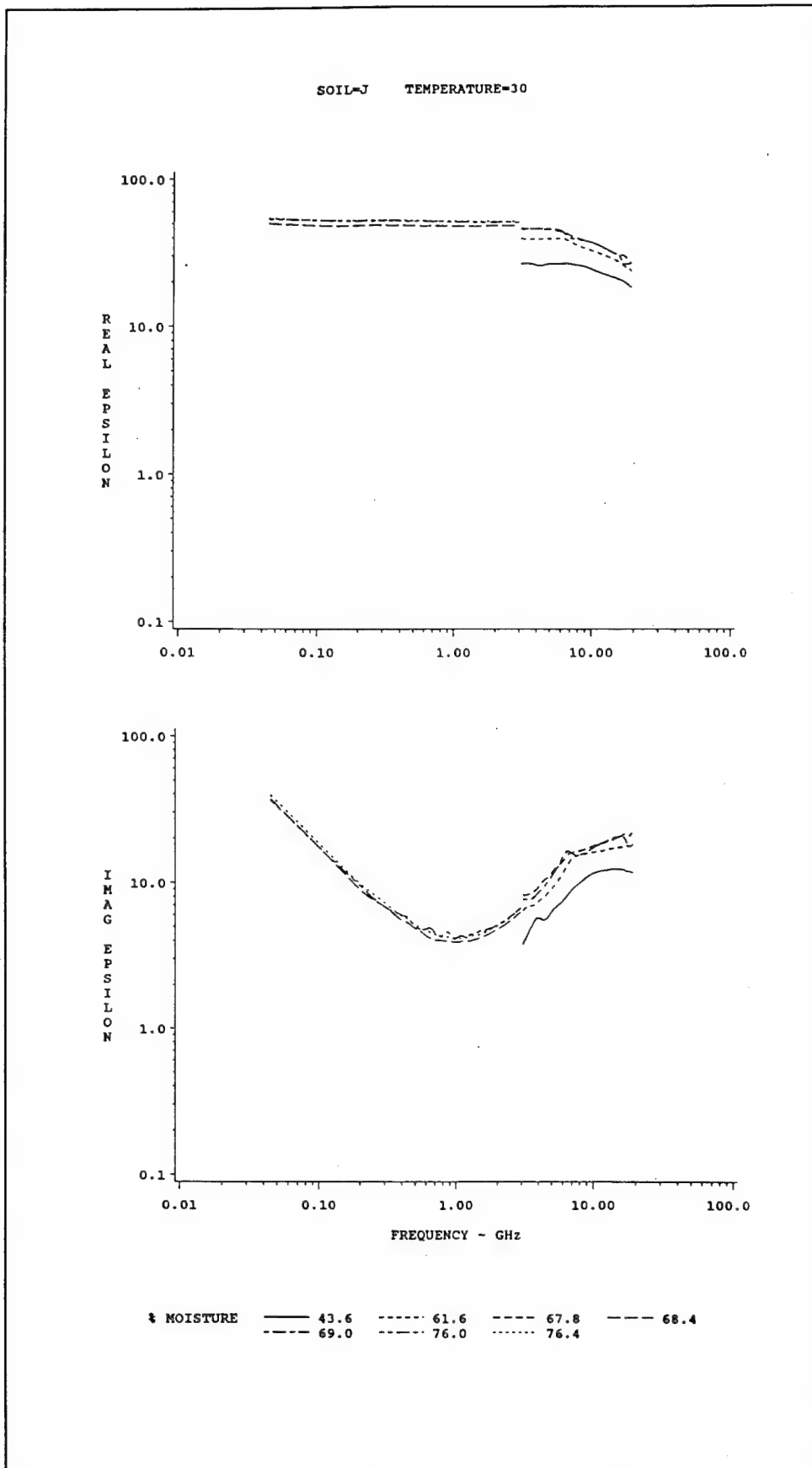


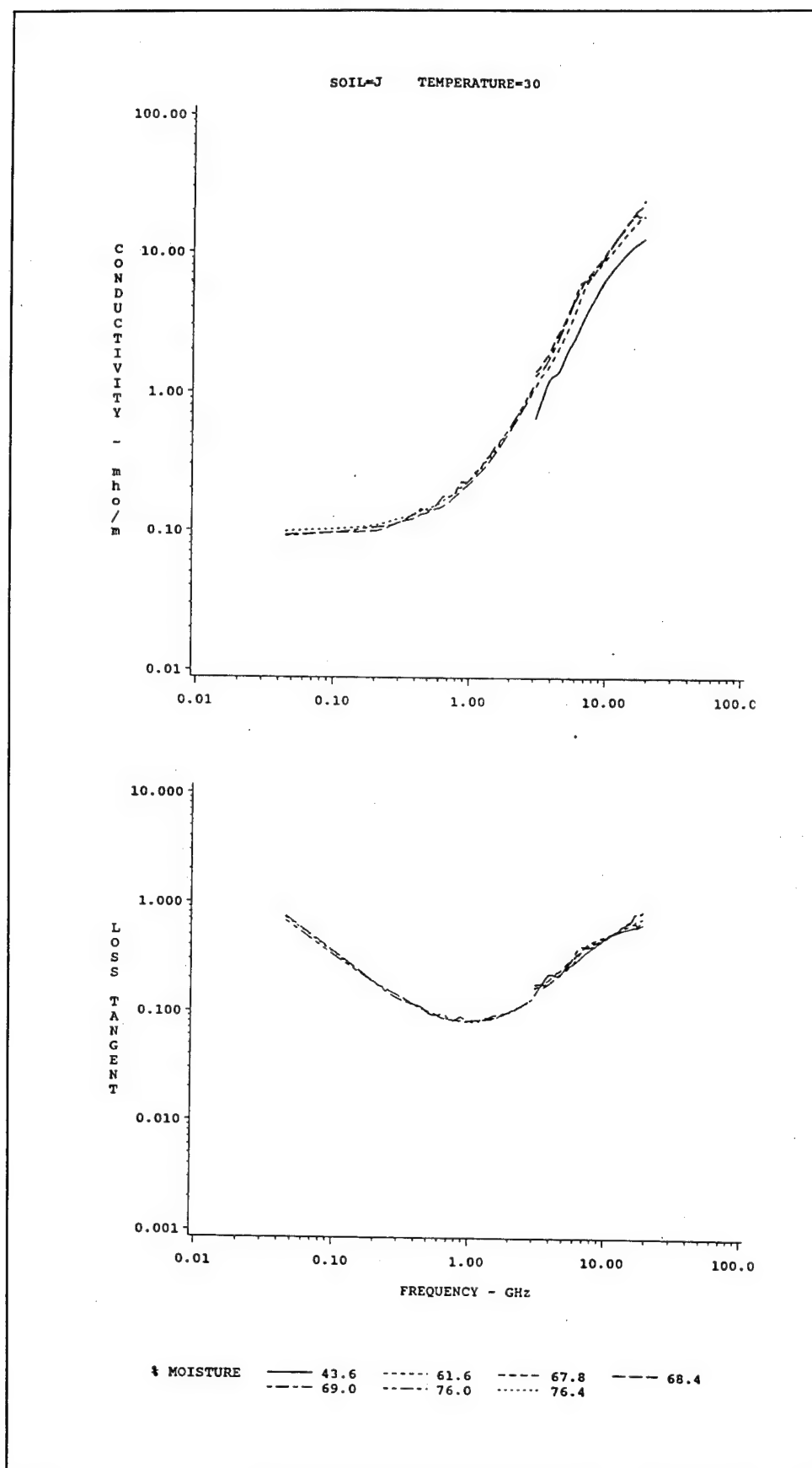


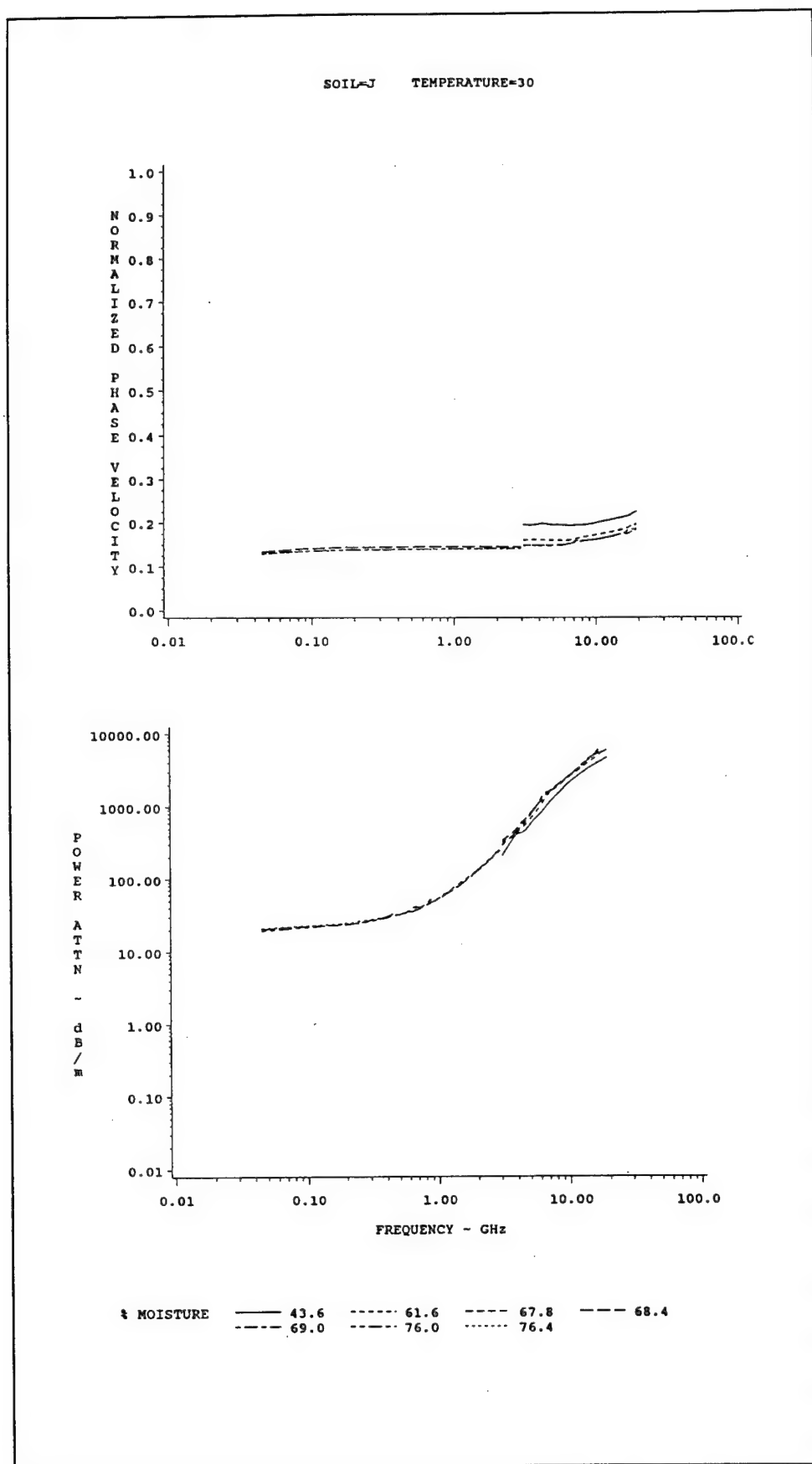


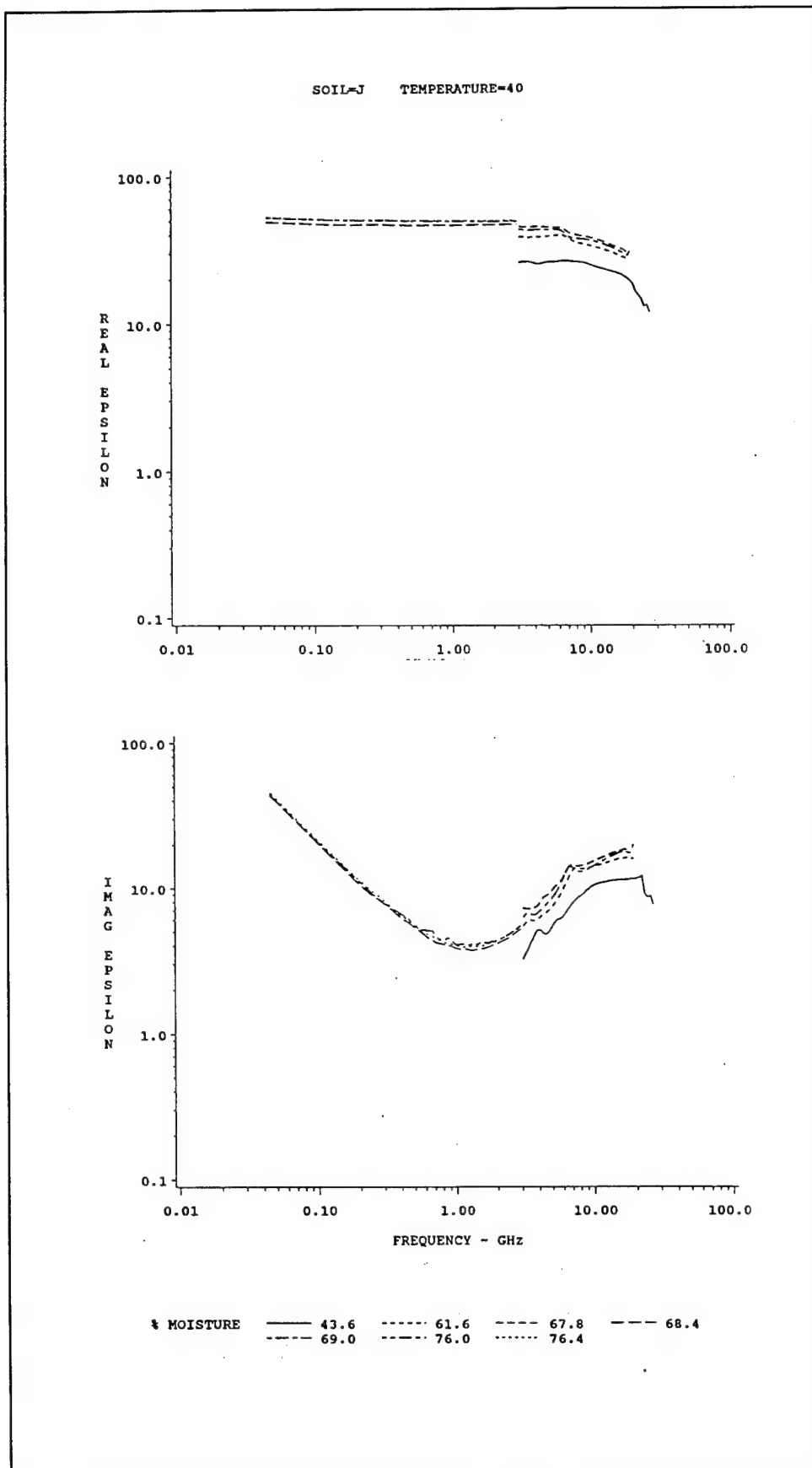


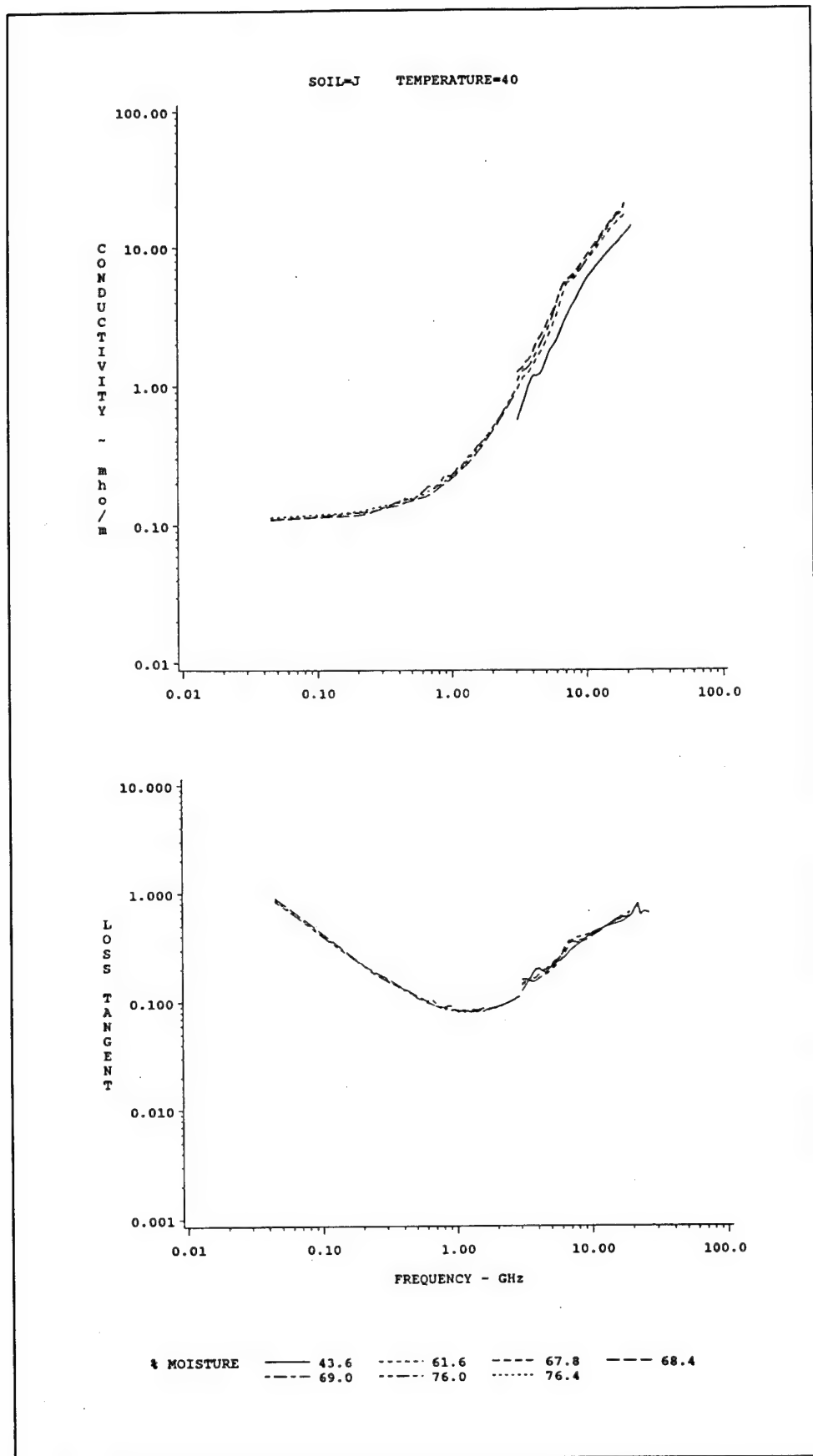


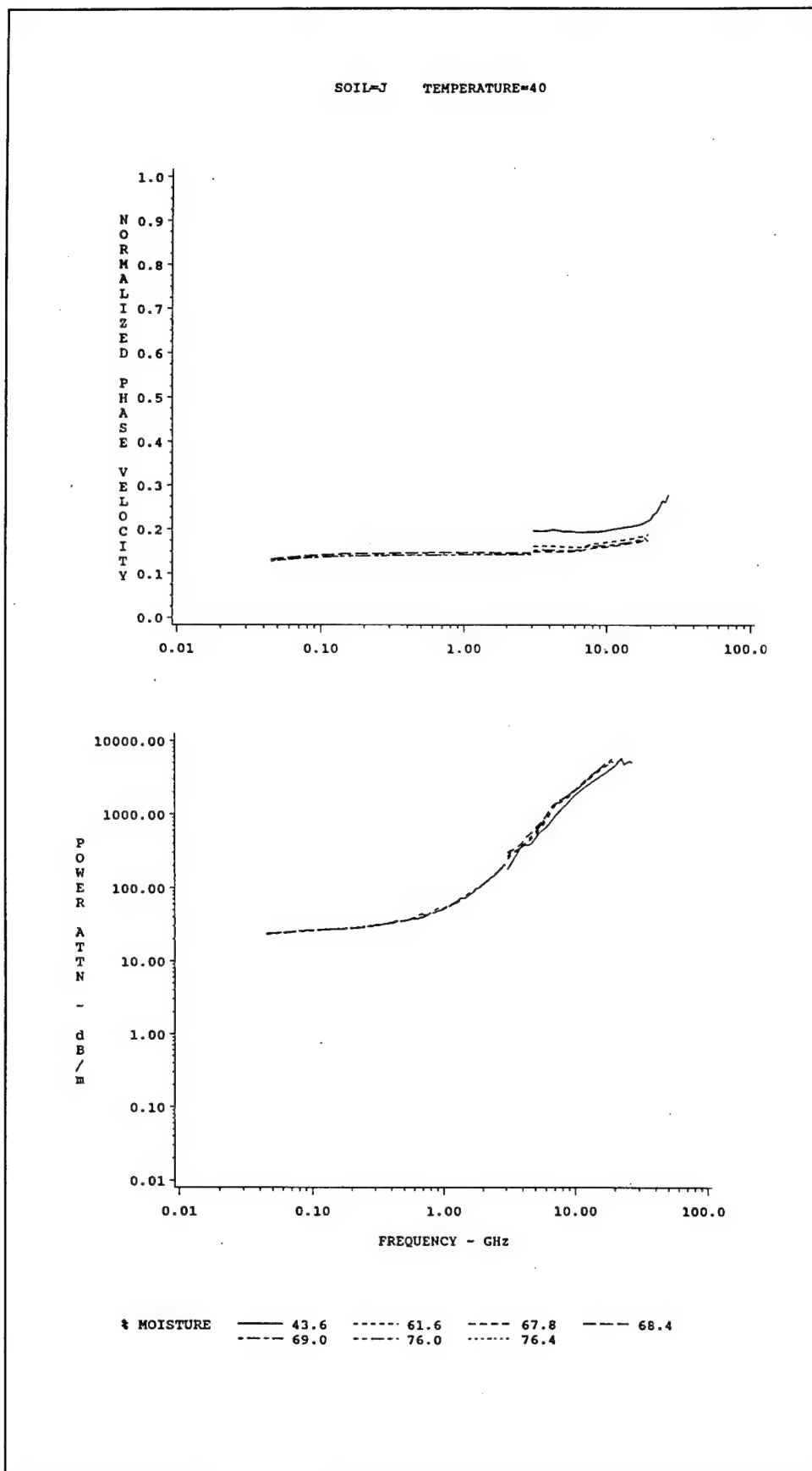


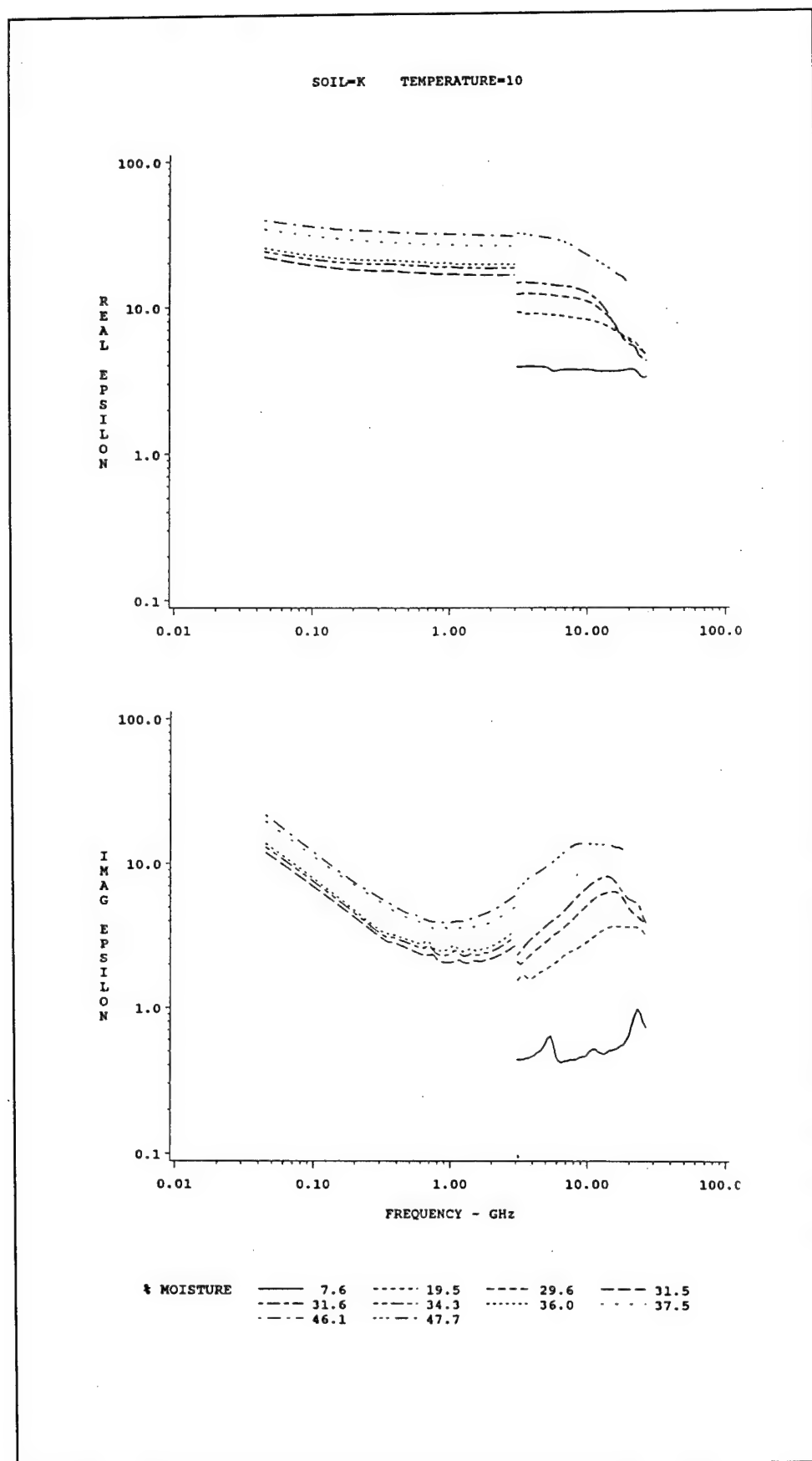


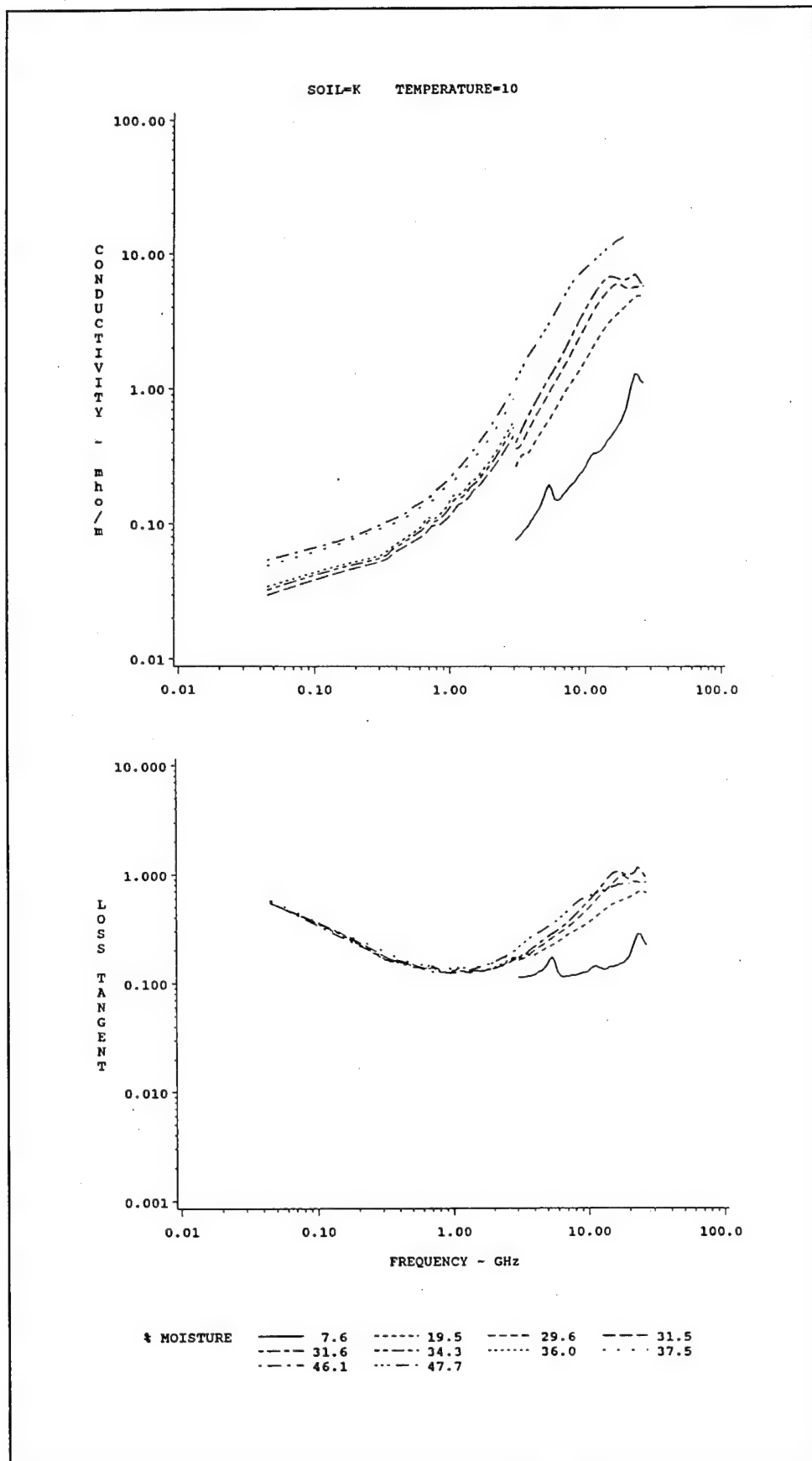


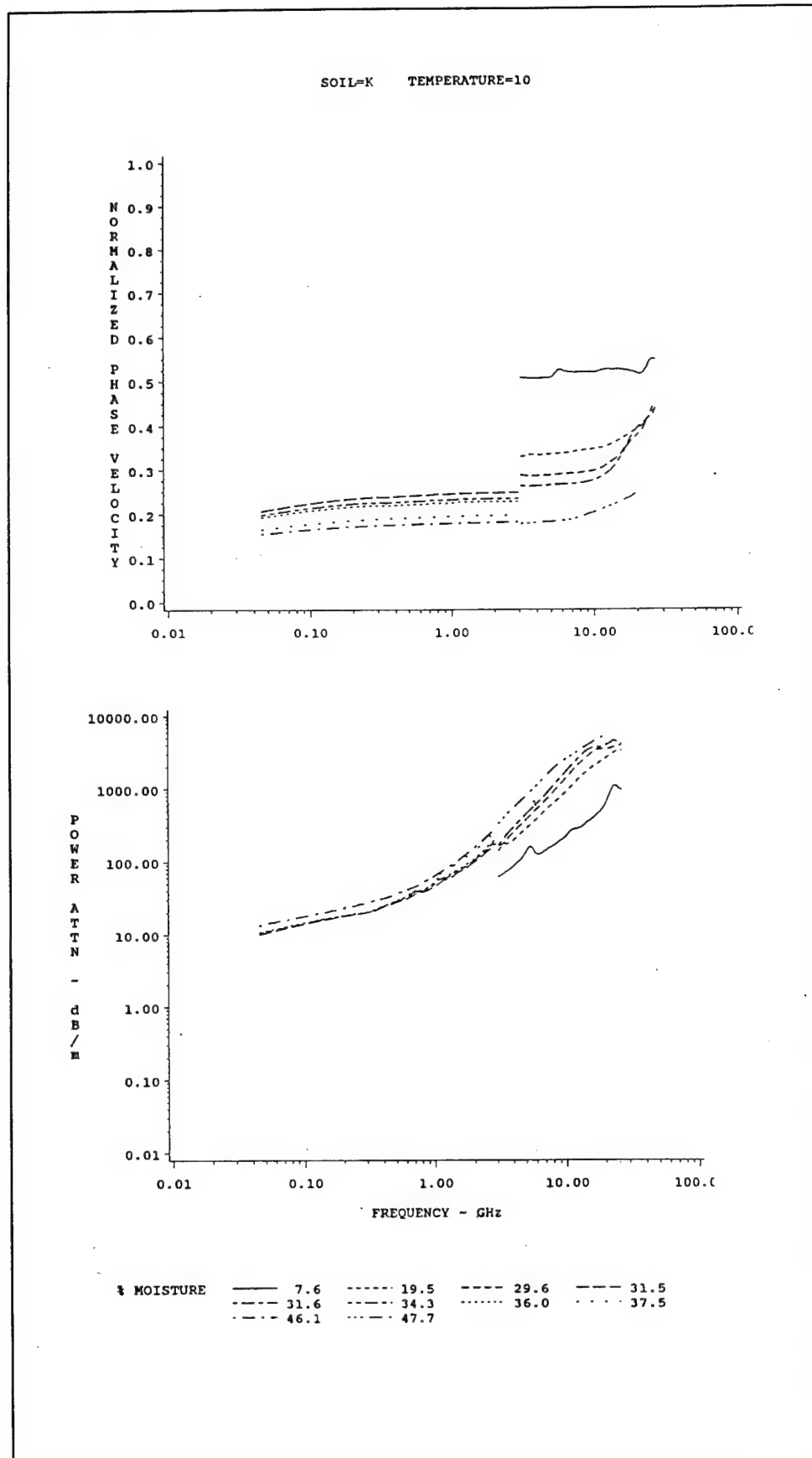


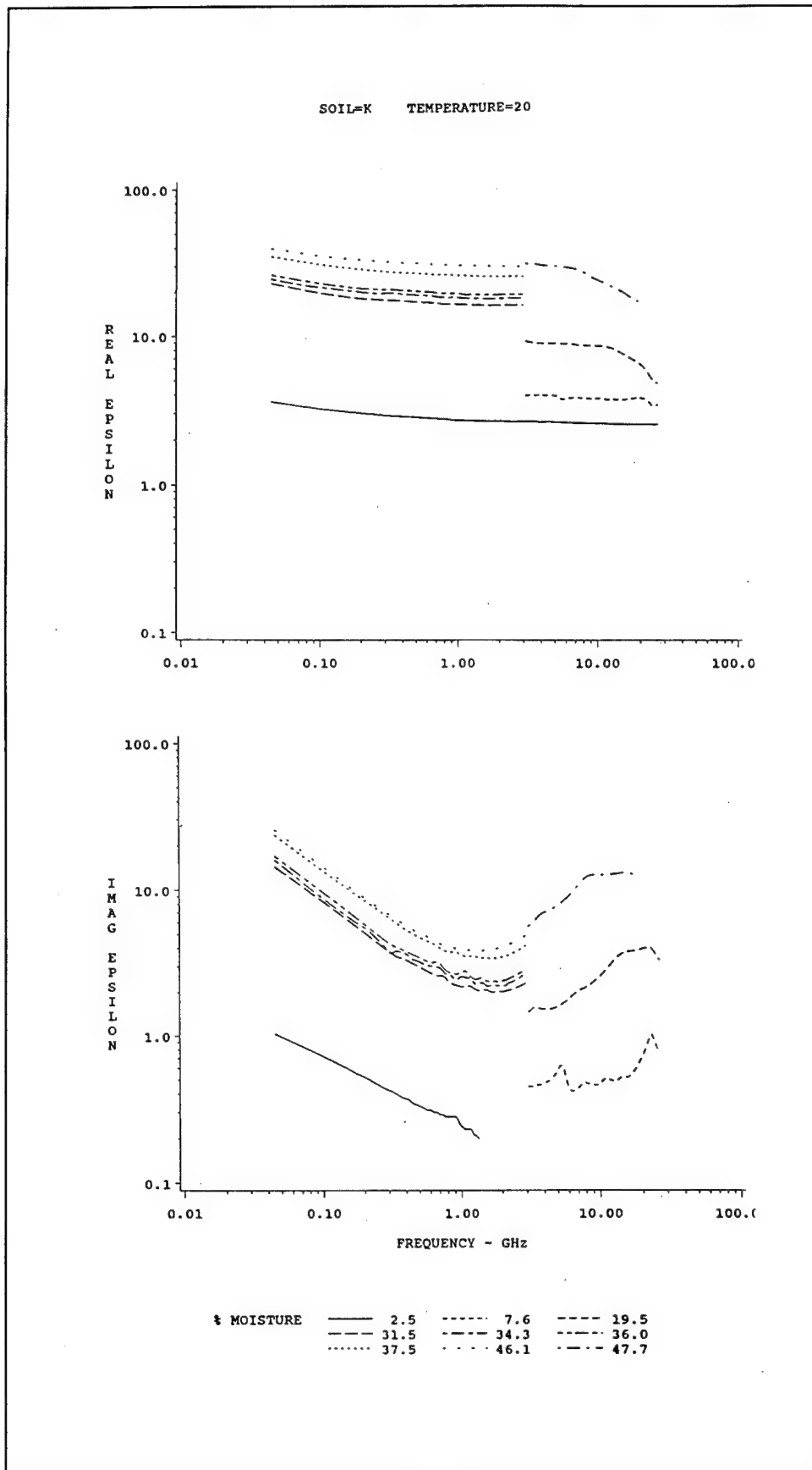


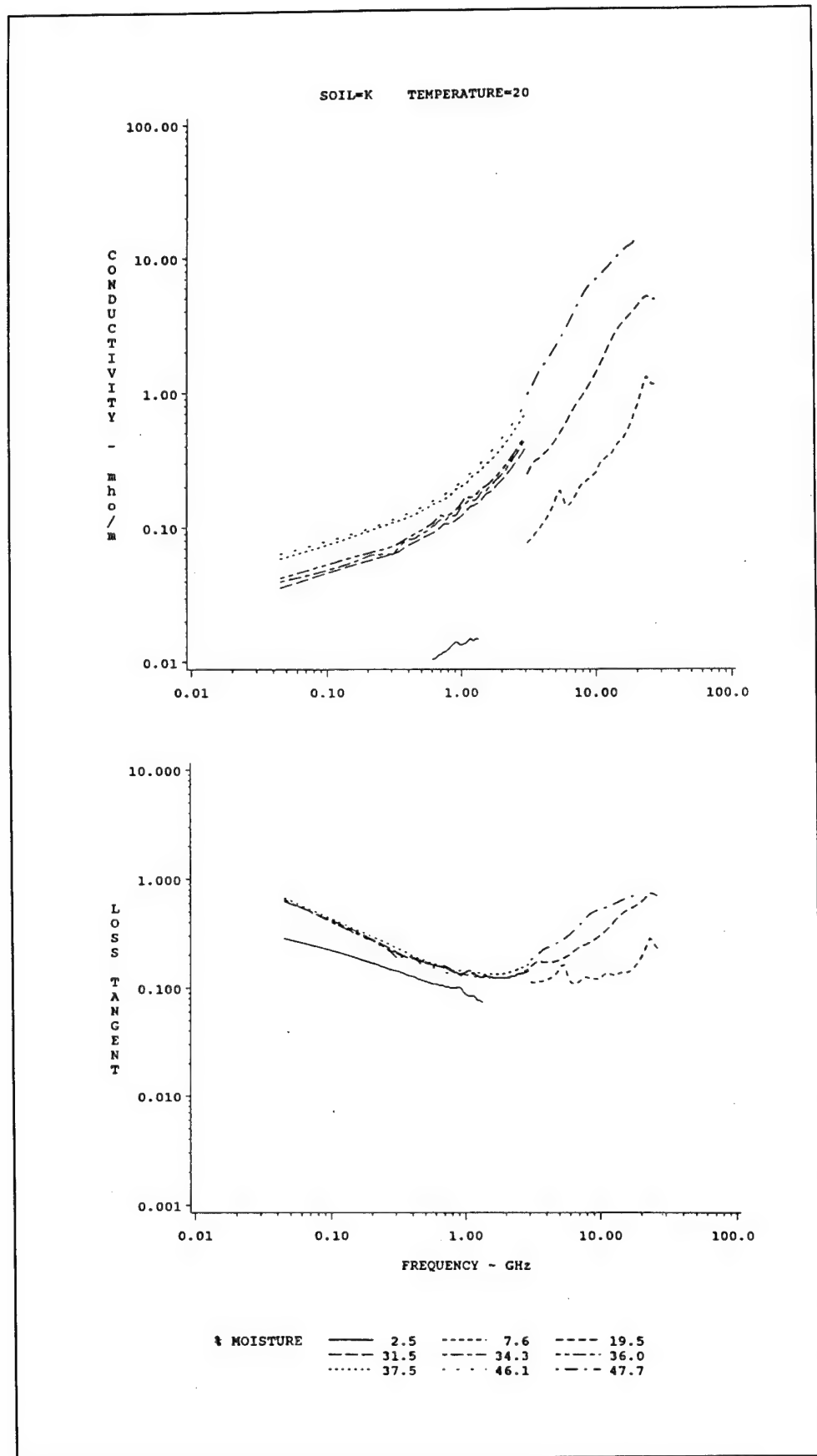


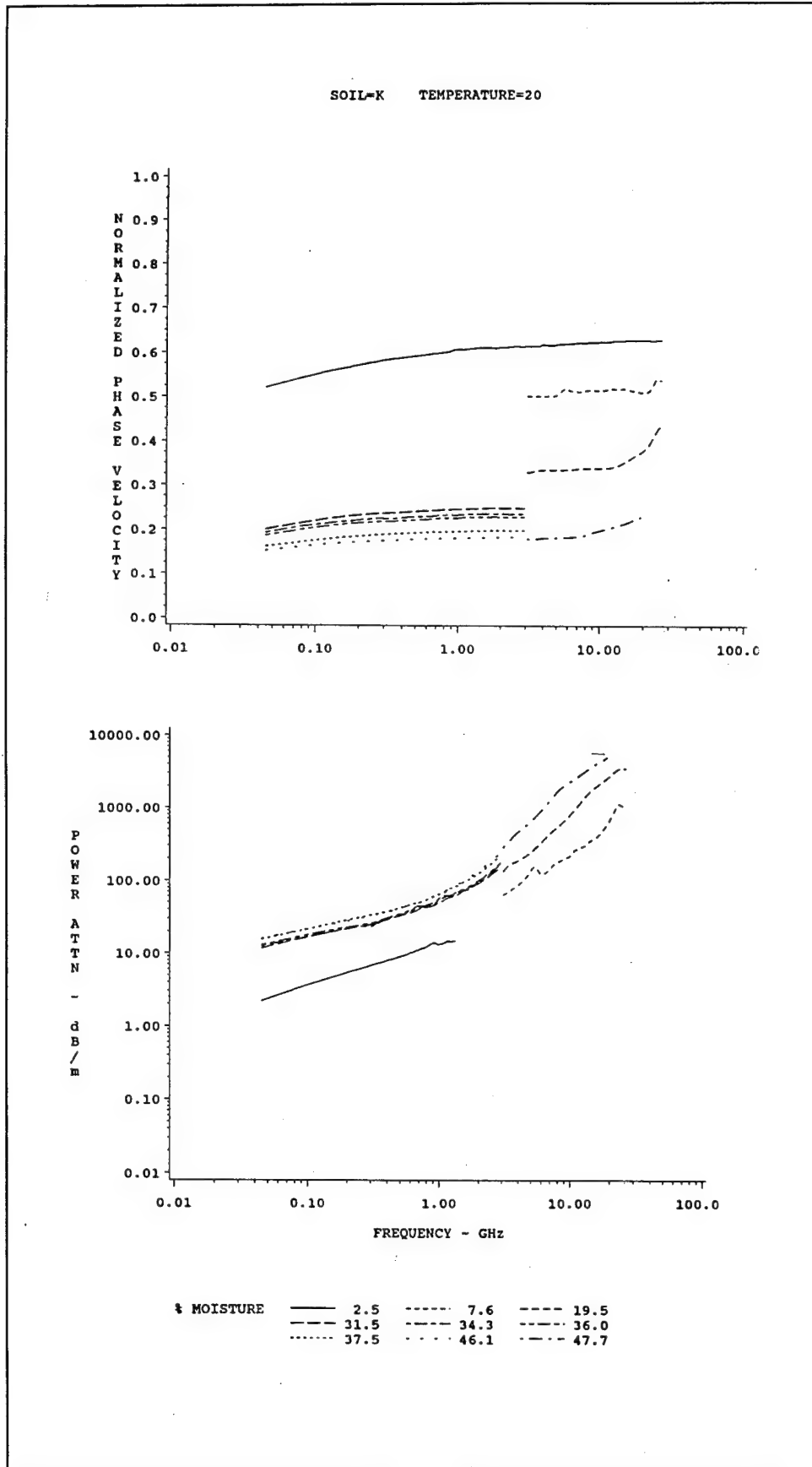


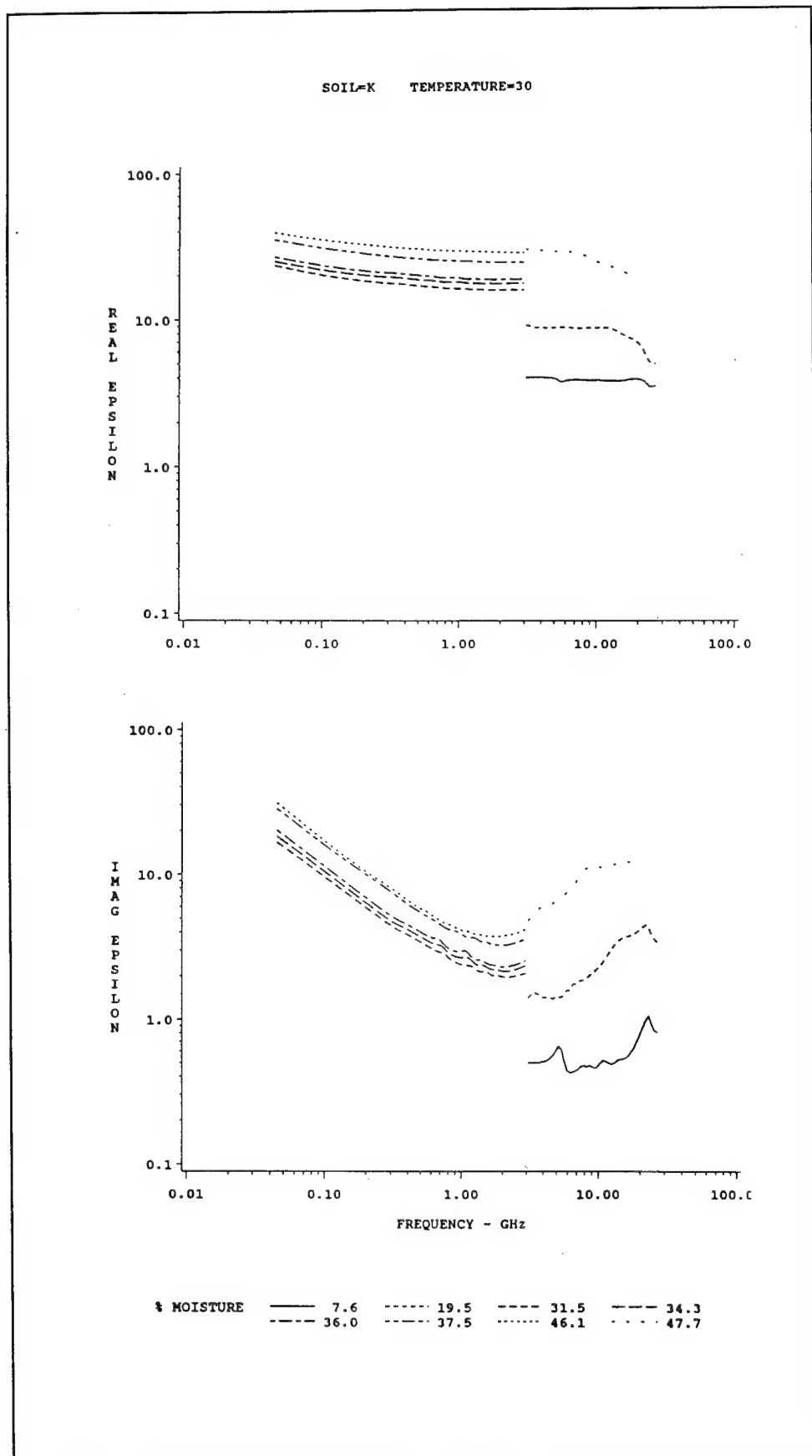


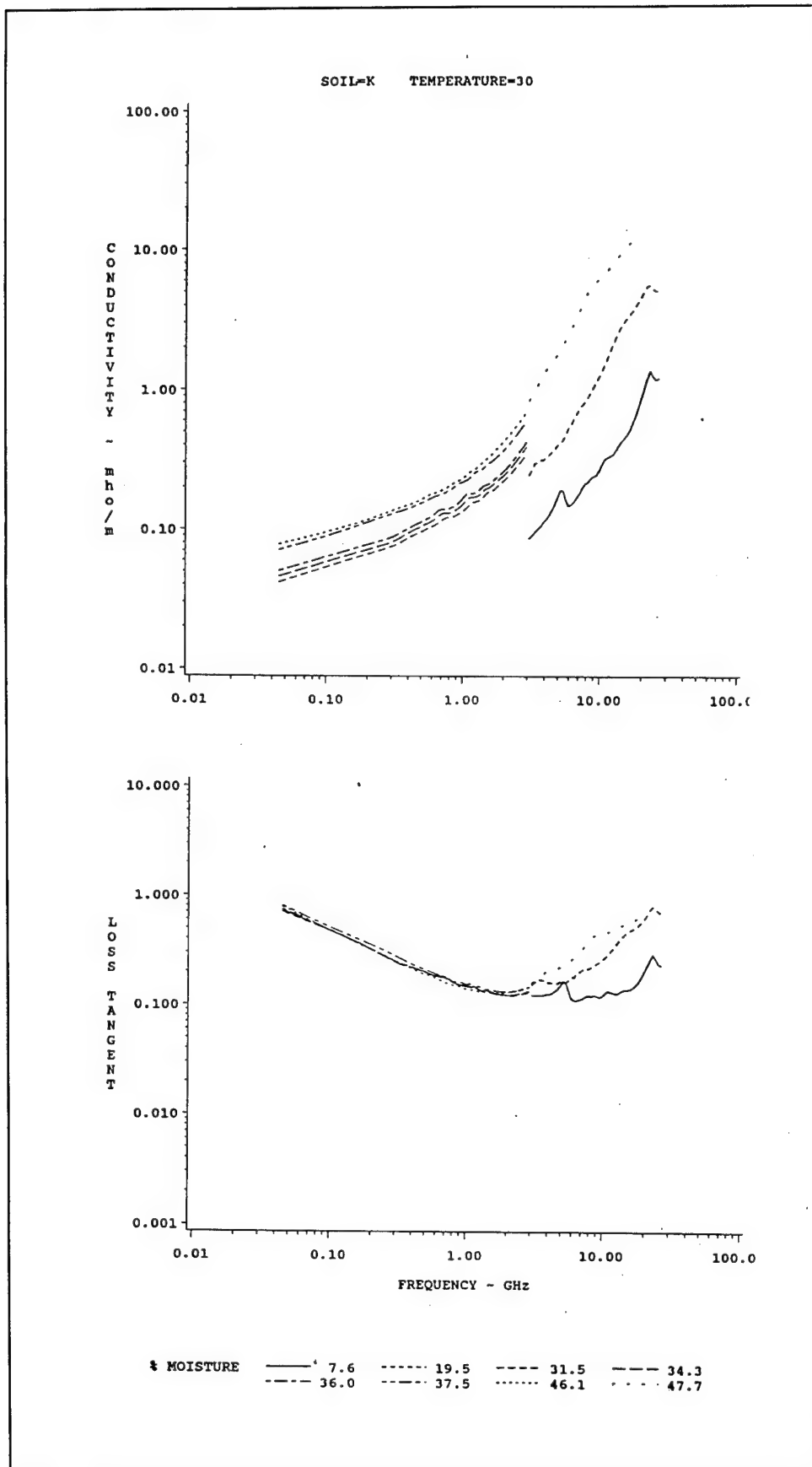




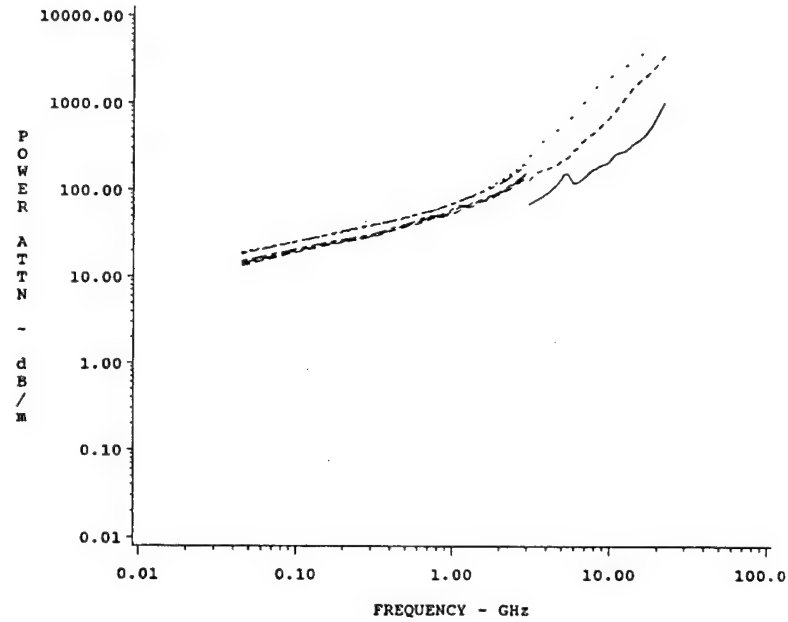
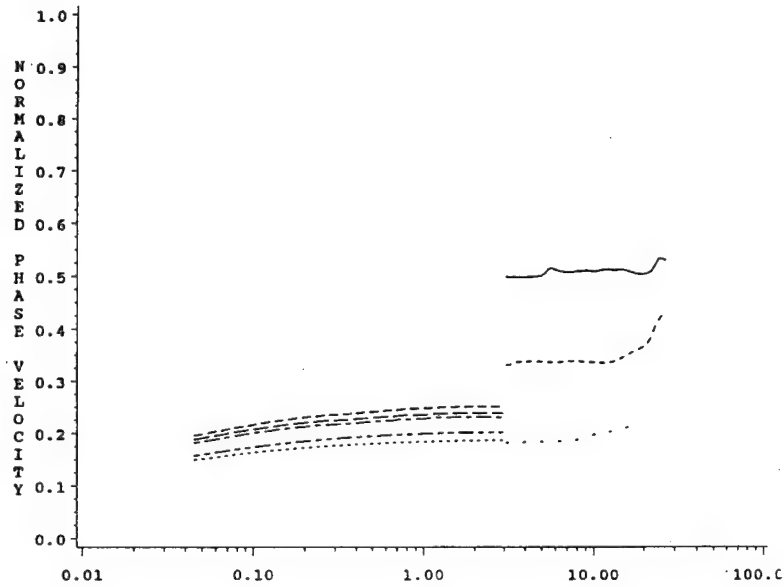




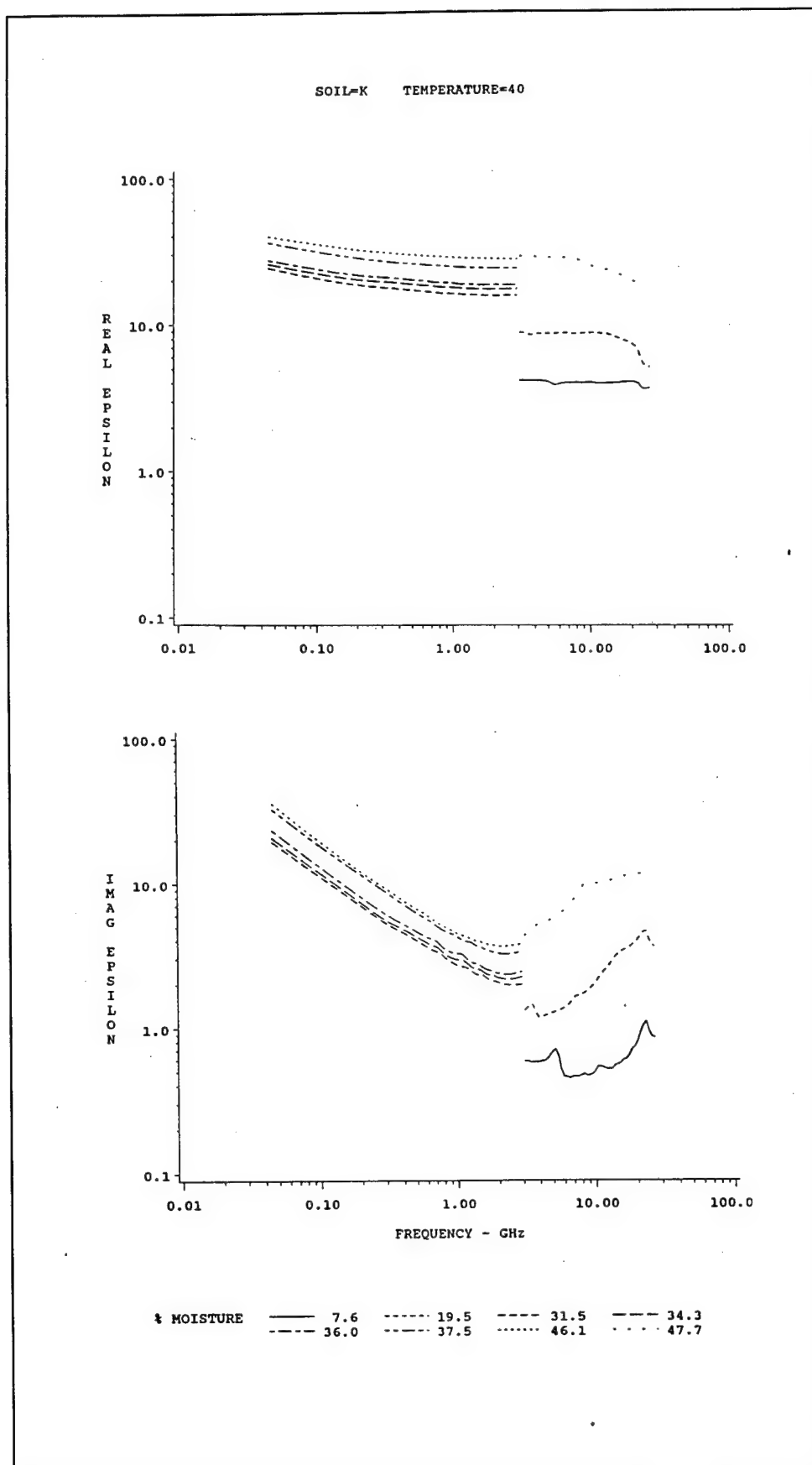


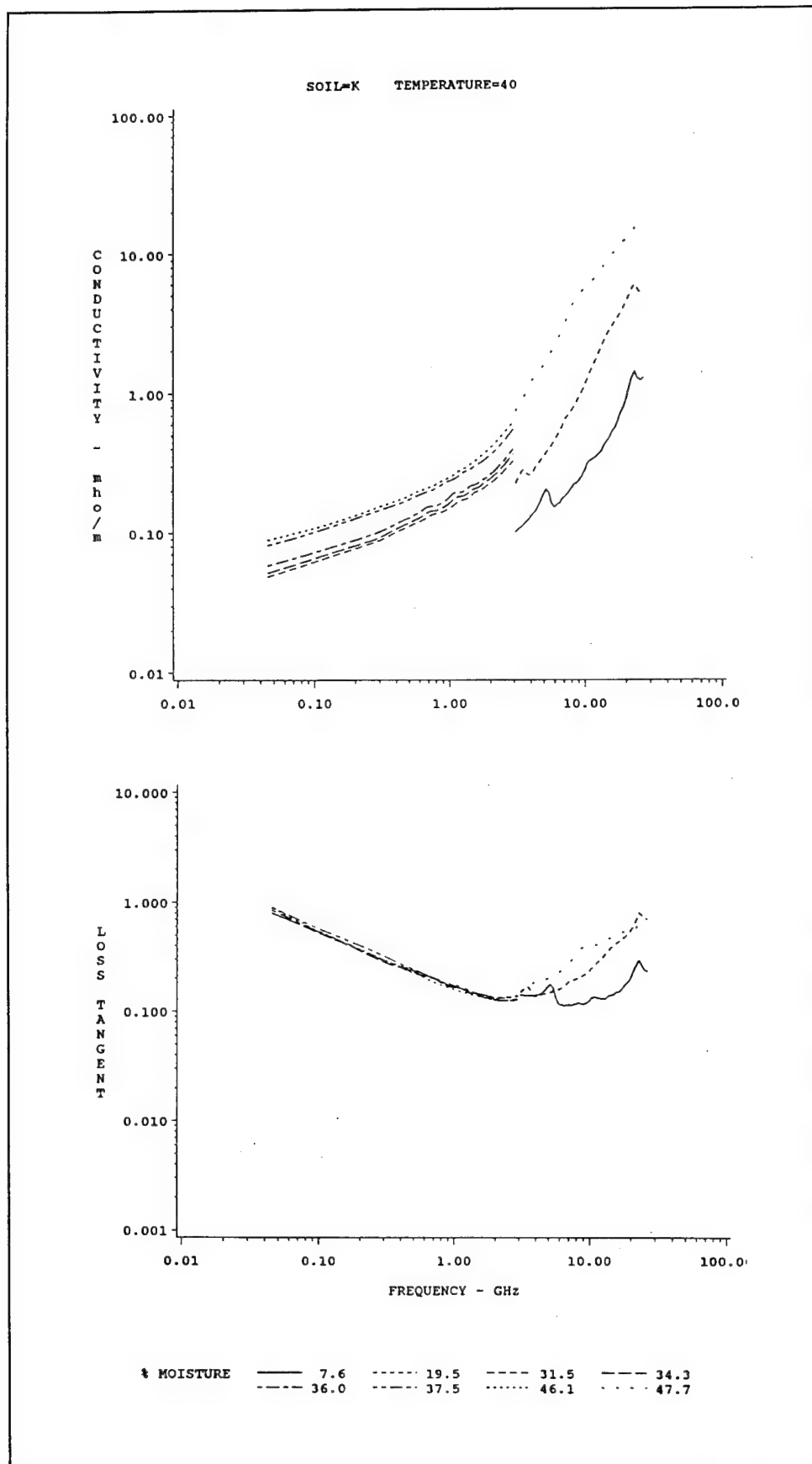


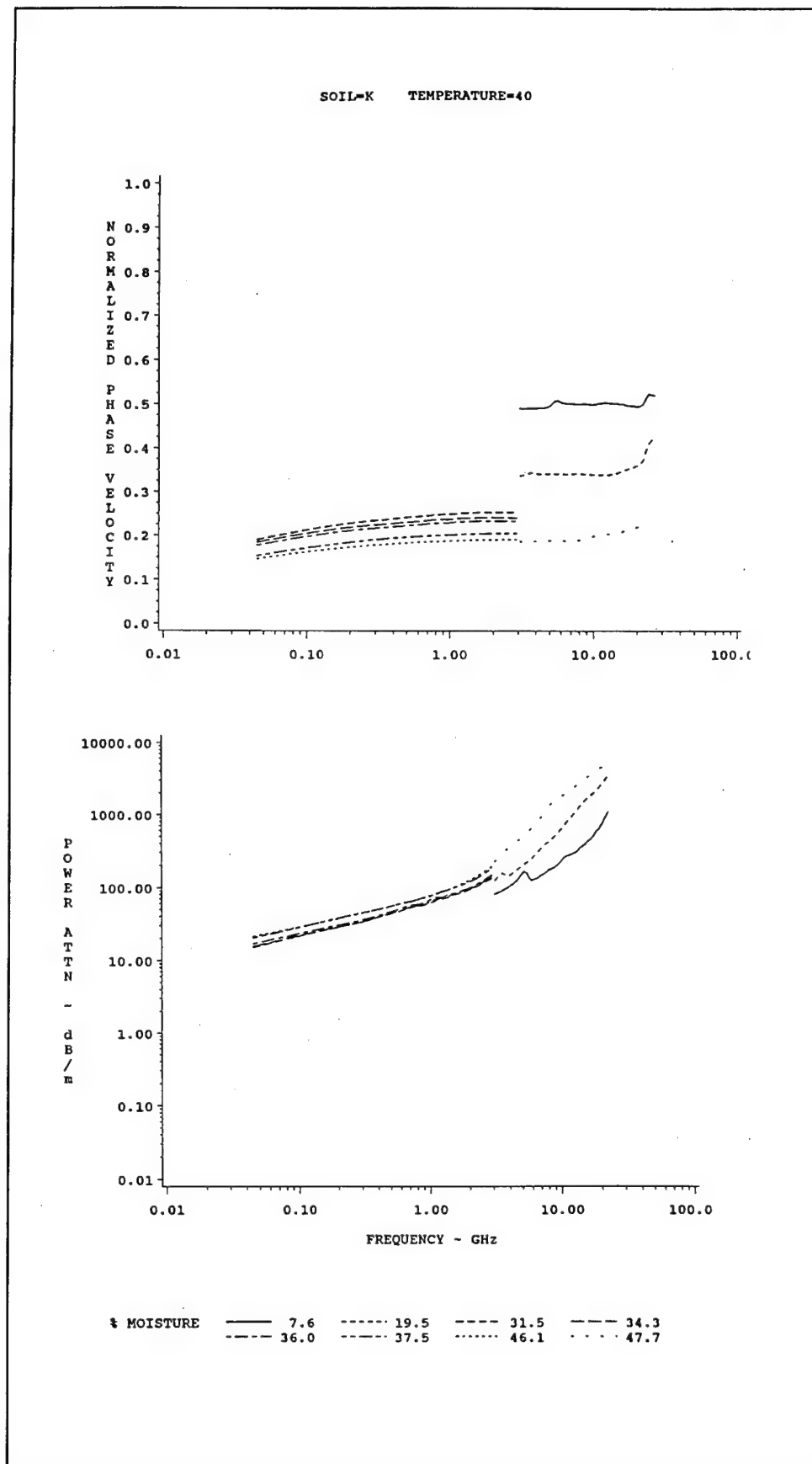
SOIL=K TEMPERATURE=30

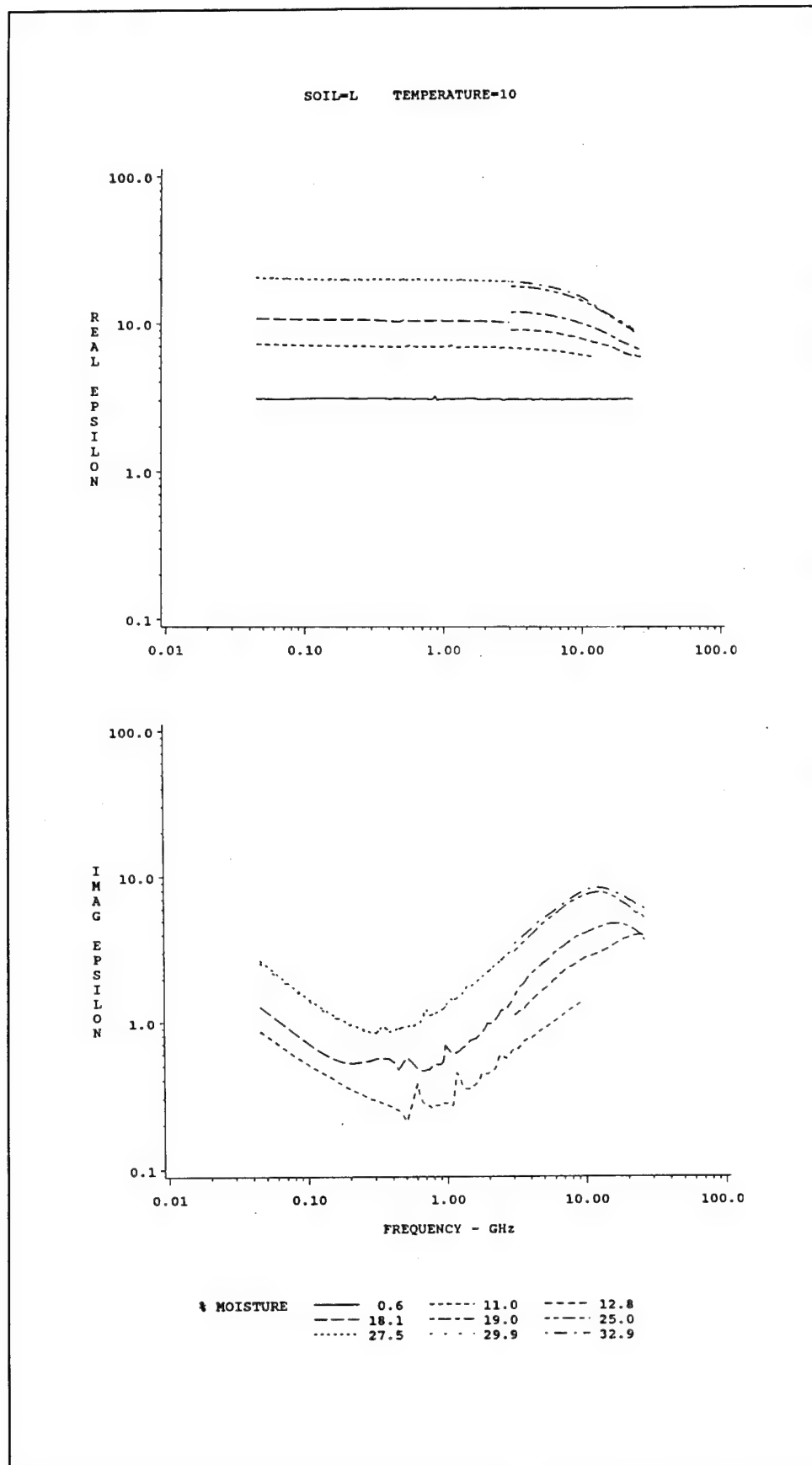


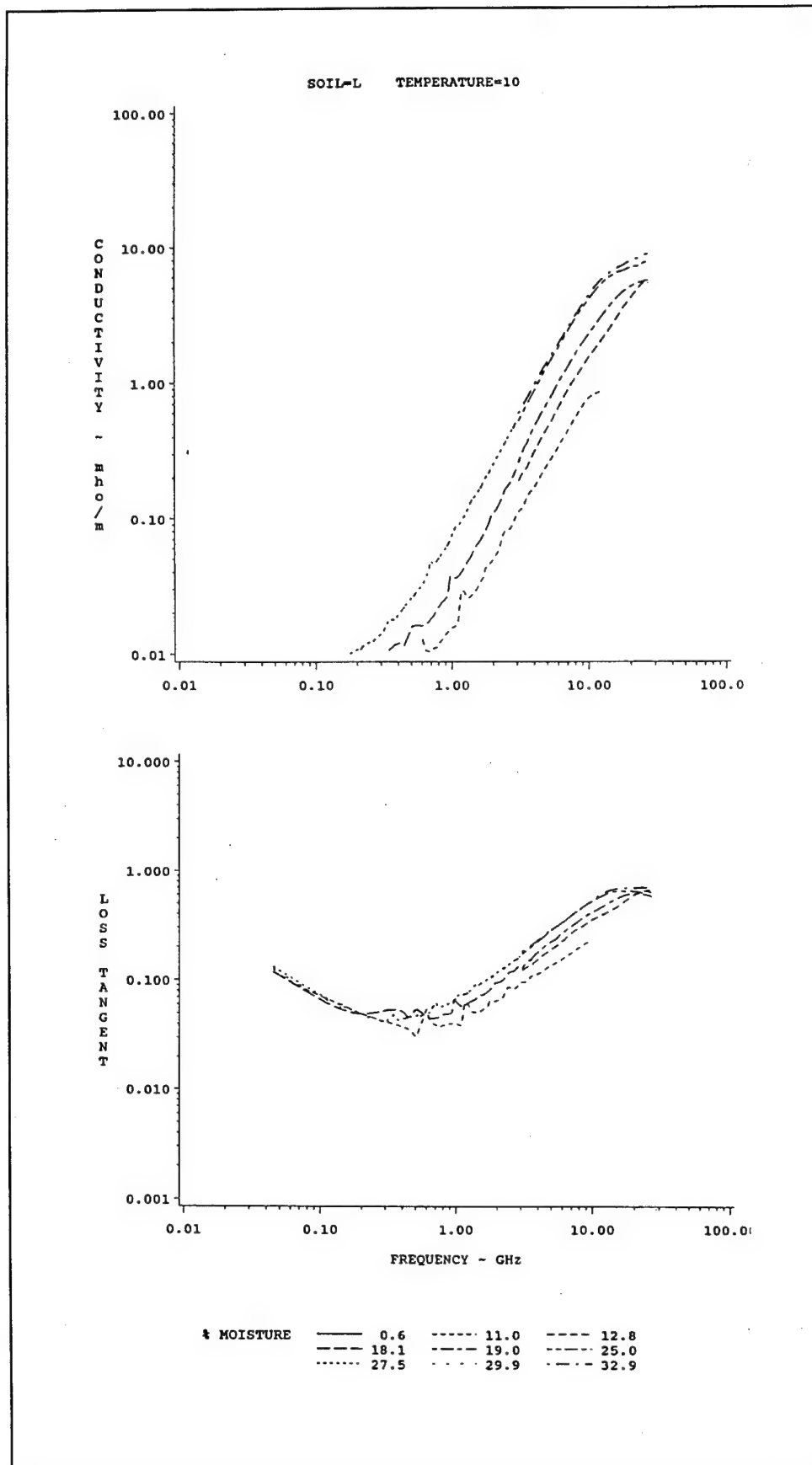
% MOISTURE ——— 7.6 - - - - 19.5 - - - - 31.5 - - - - 34.3
 - - - - 36.0 - - - - 37.5 ······ 46.1 ······ 47.7

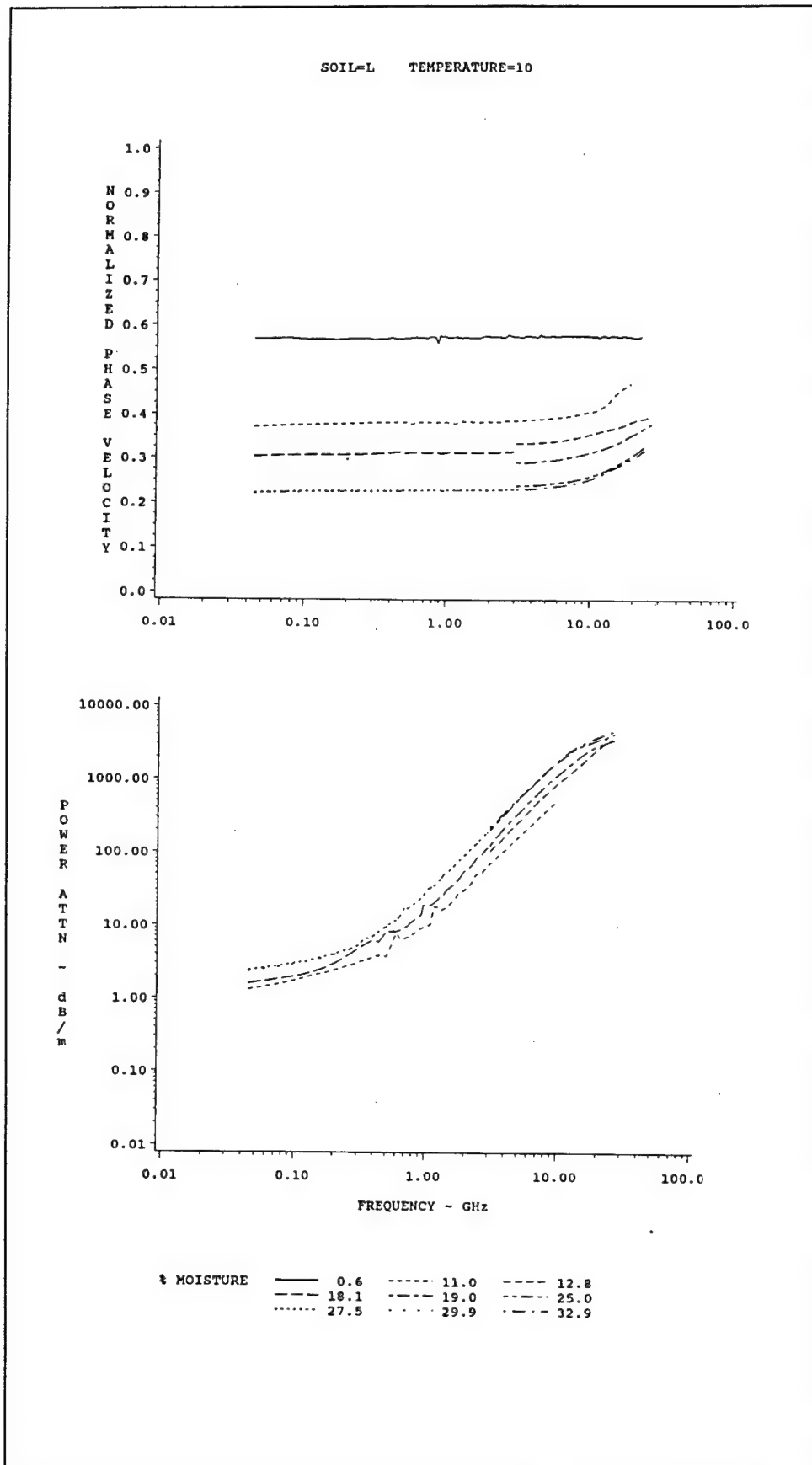


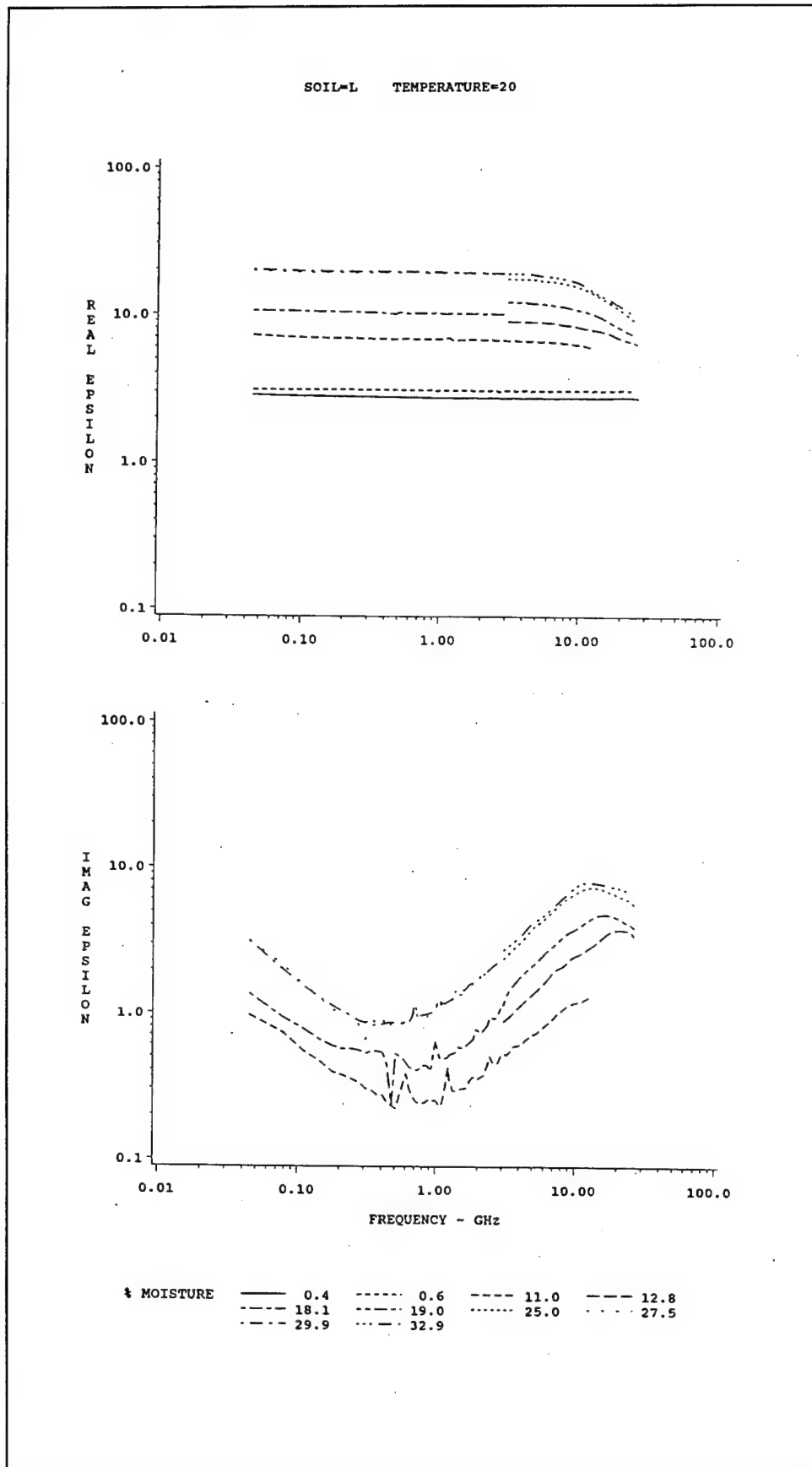


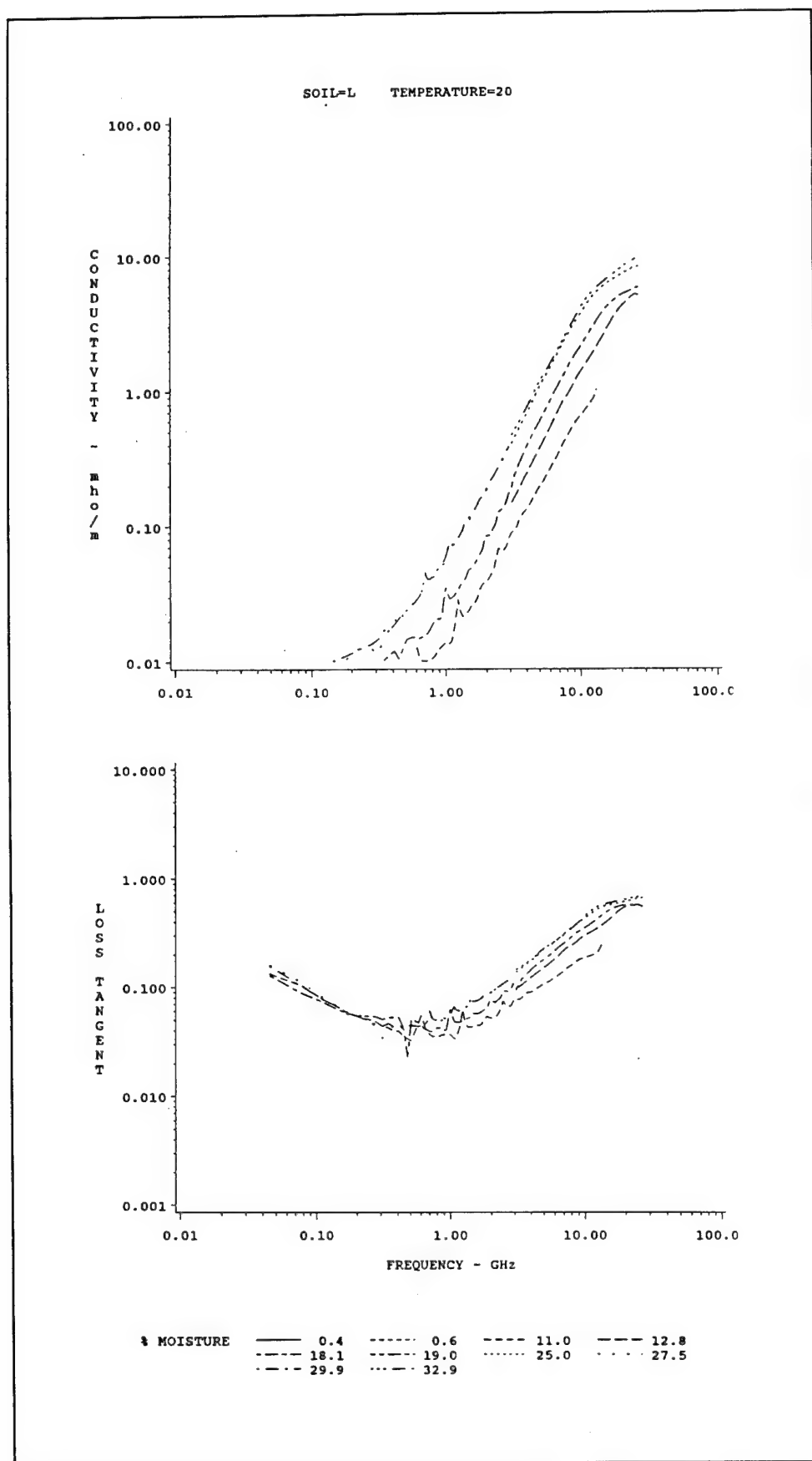


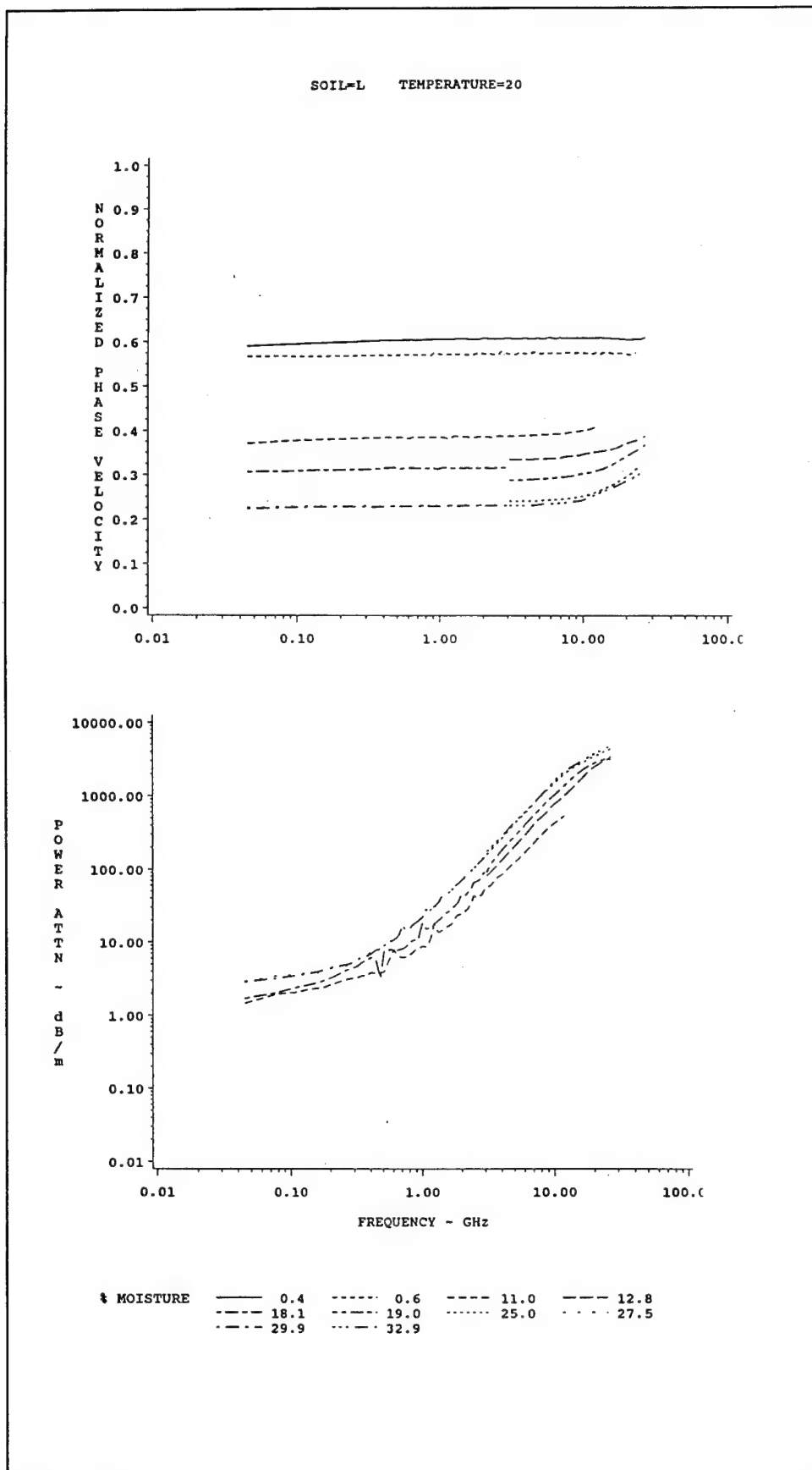


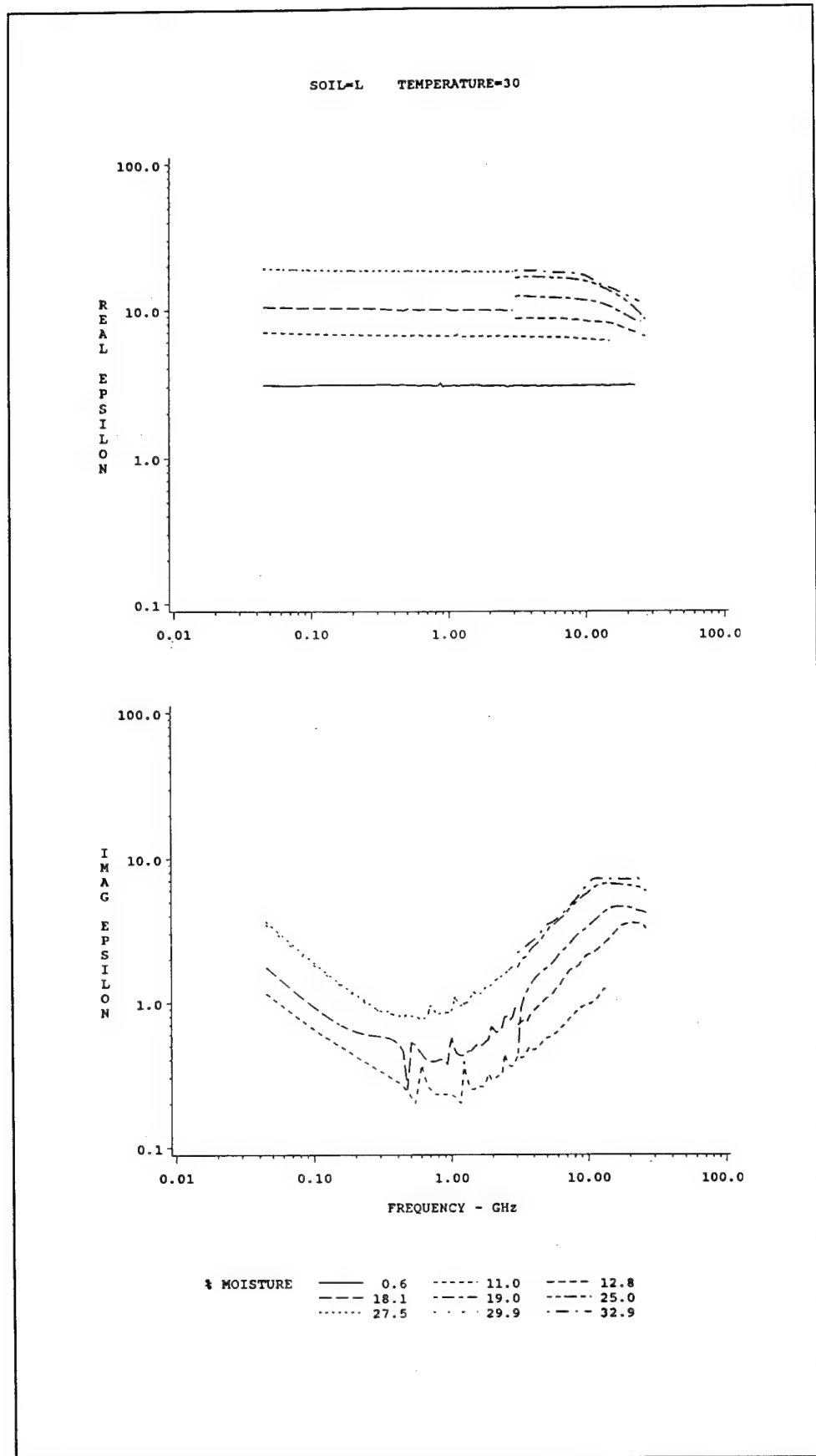


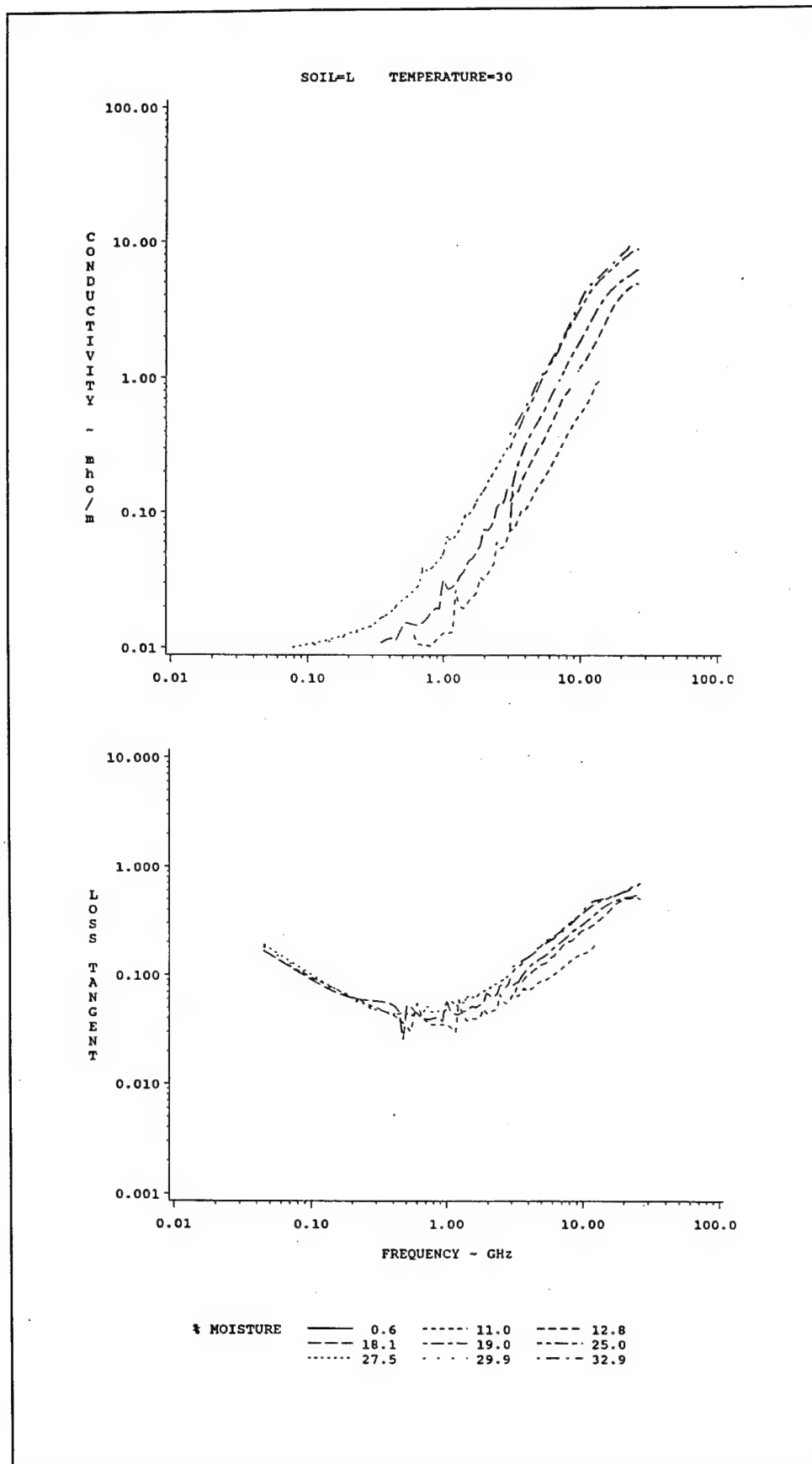


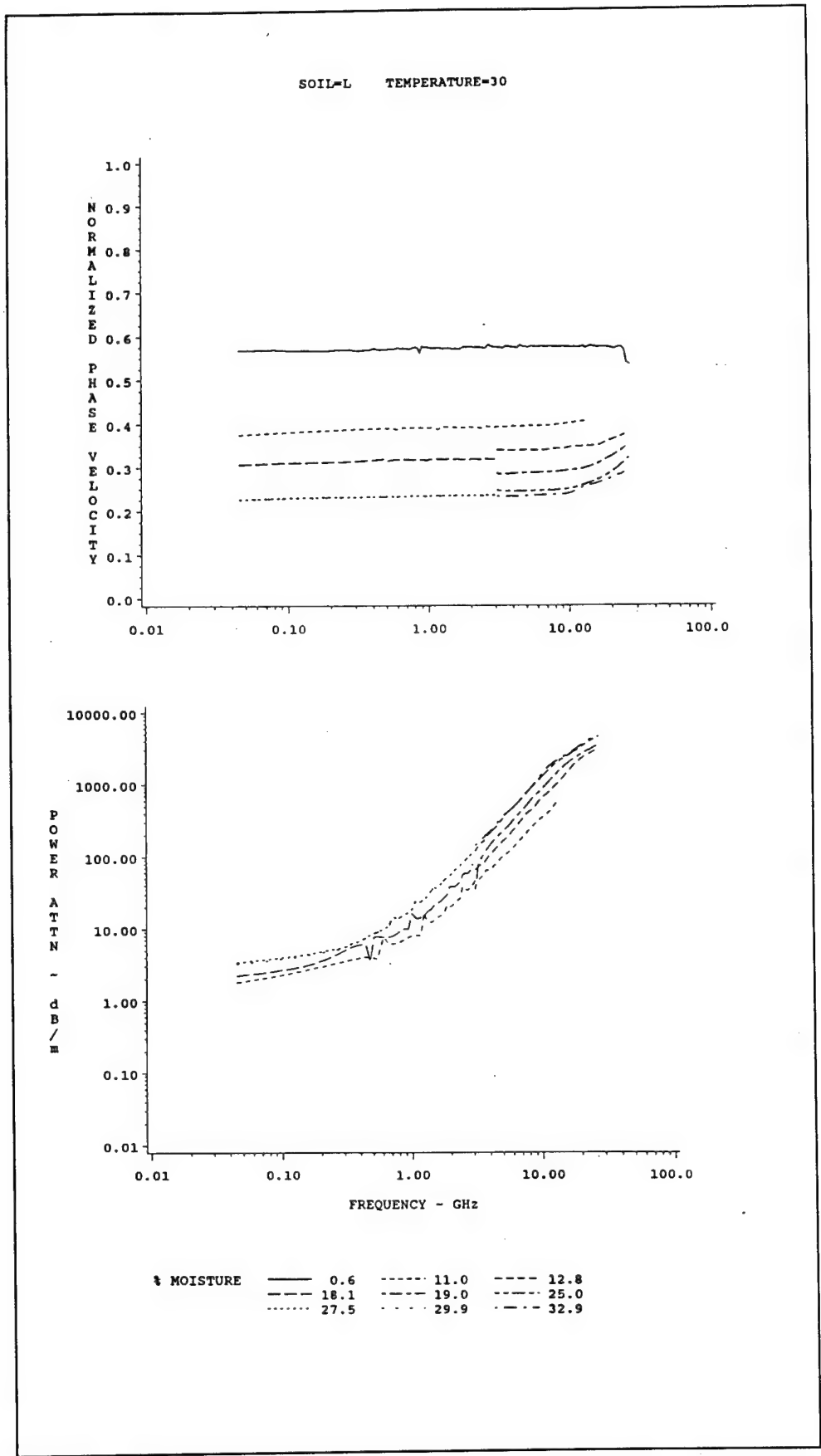




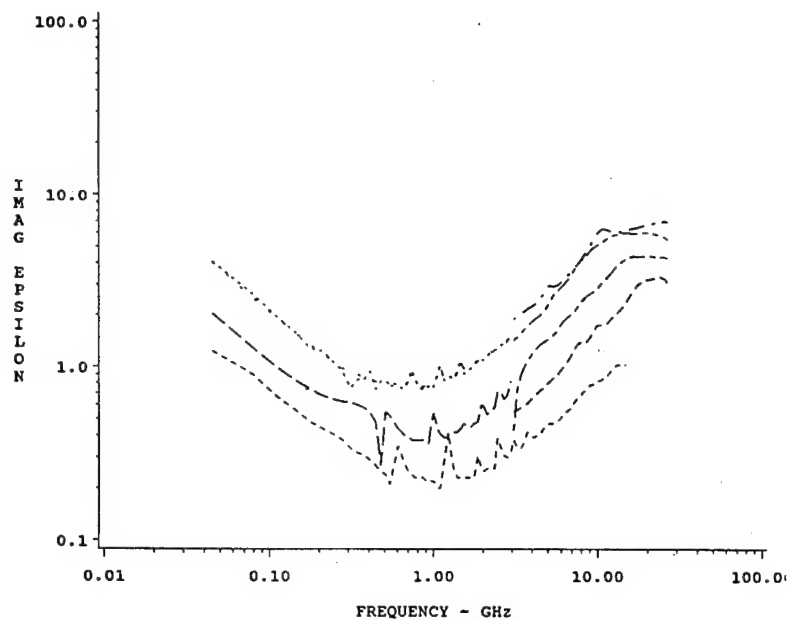
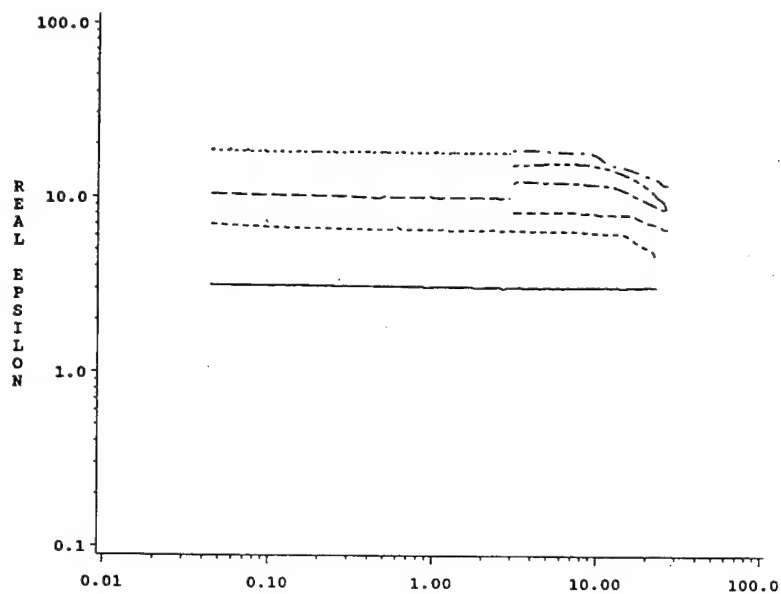




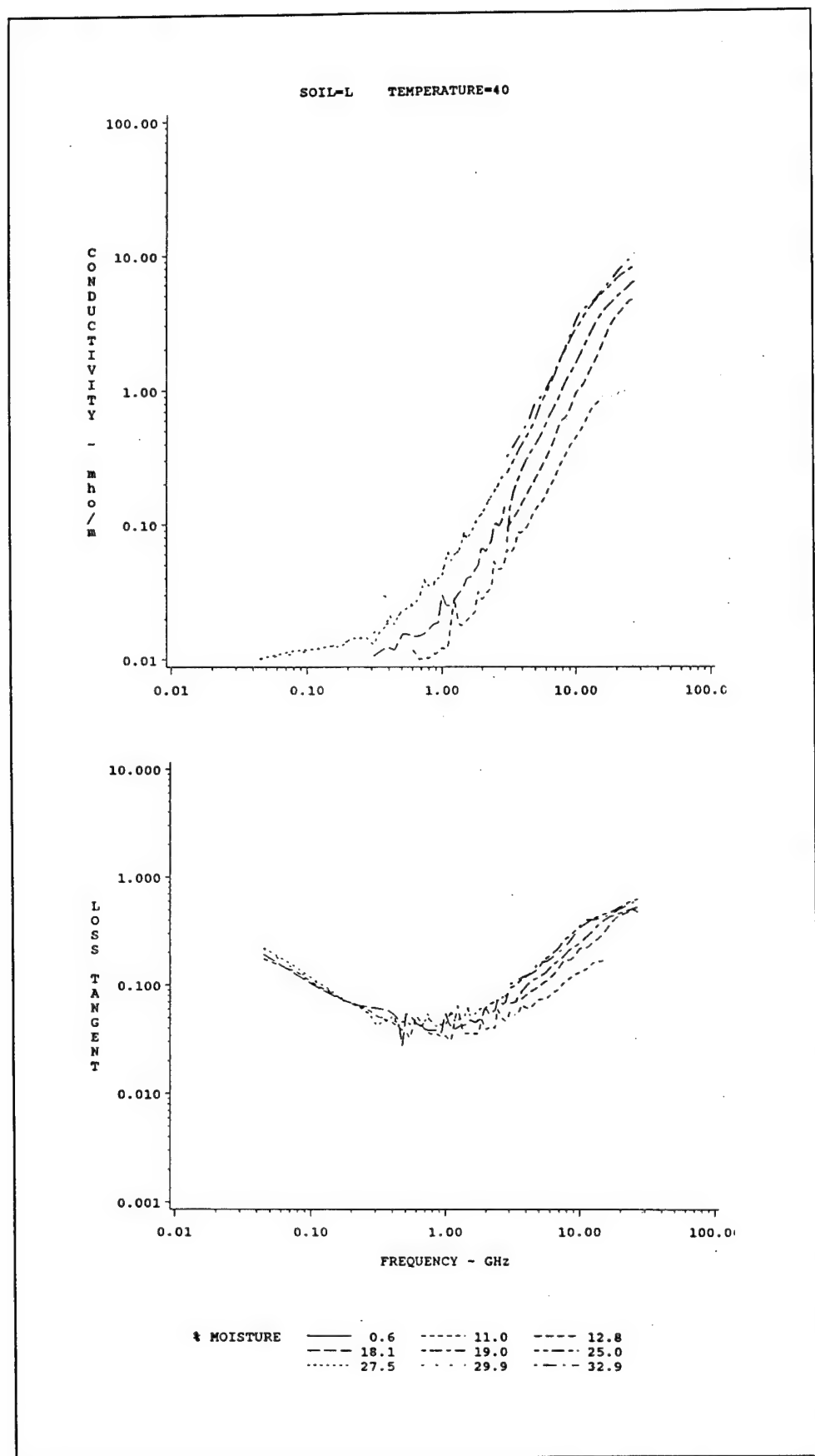


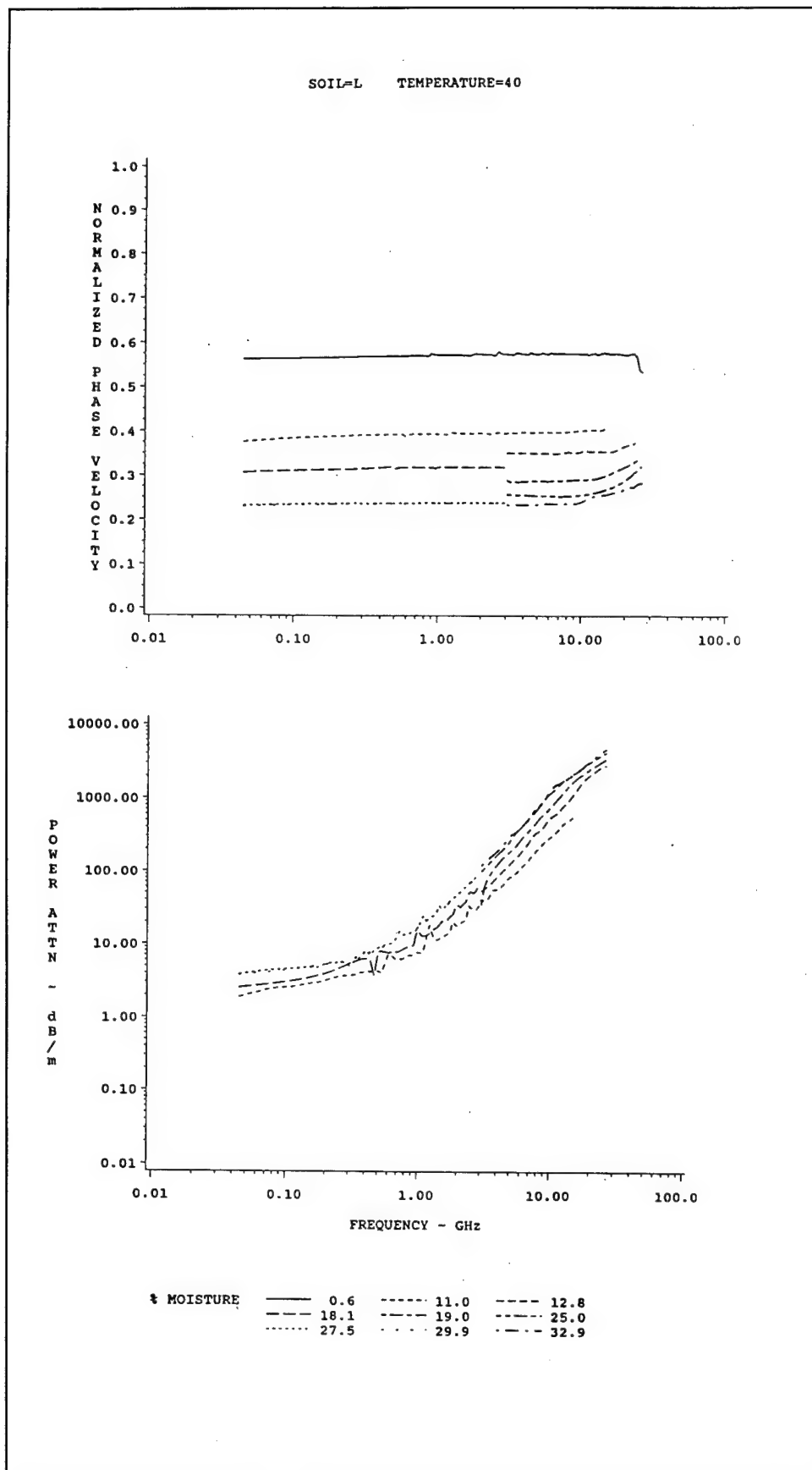


SOIL=L TEMPERATURE=40



% MOISTURE	0.6	11.0	12.8
	18.1	19.0	25.0
	27.5	29.9	32.9



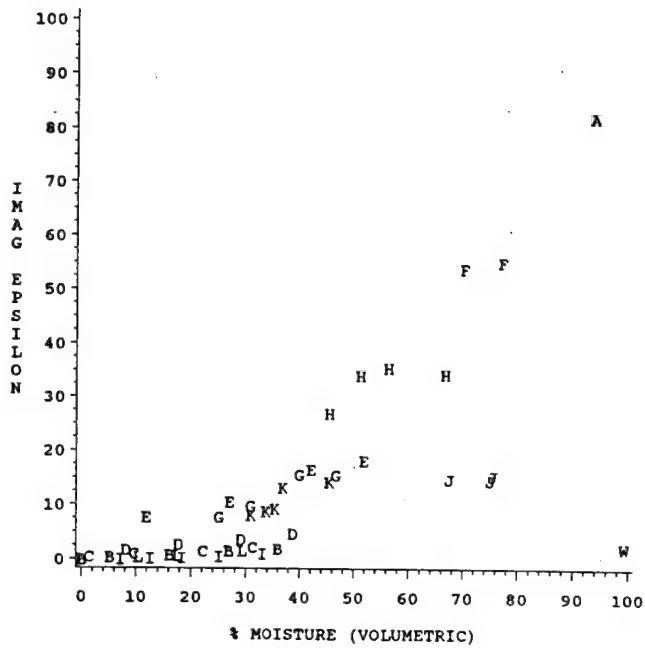
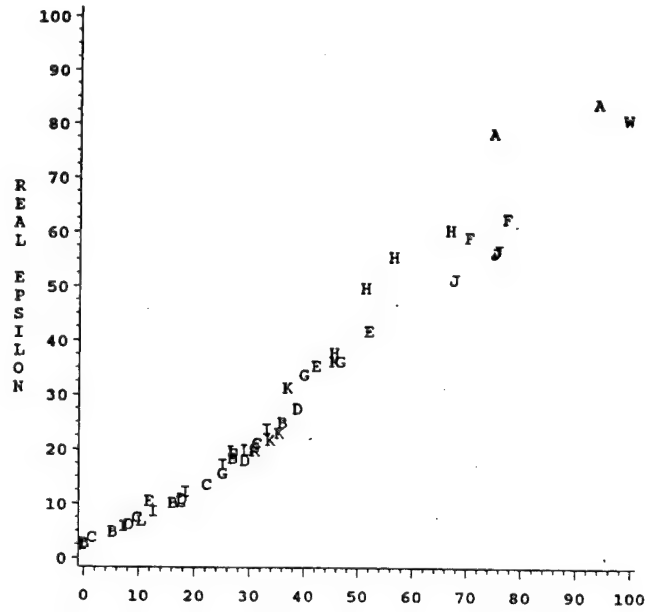


Appendix C

Electrical Properties of Soils Plotted Against Volumetric Moisture Content

78 MHz

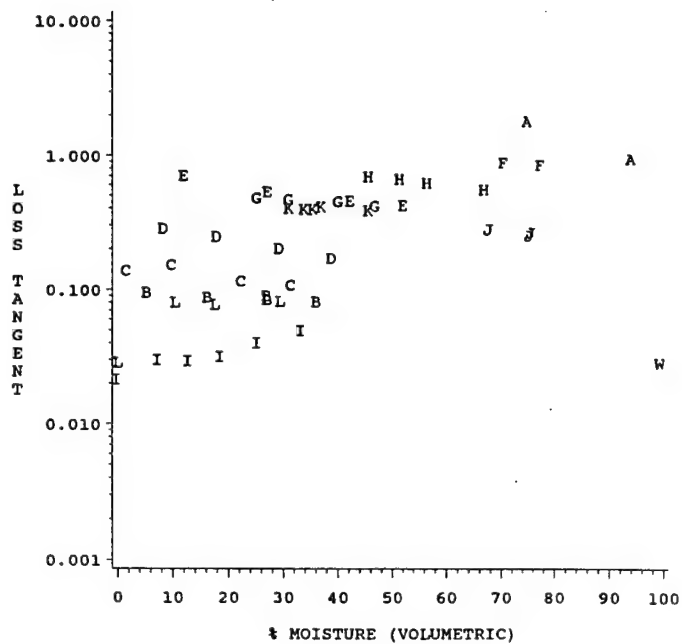
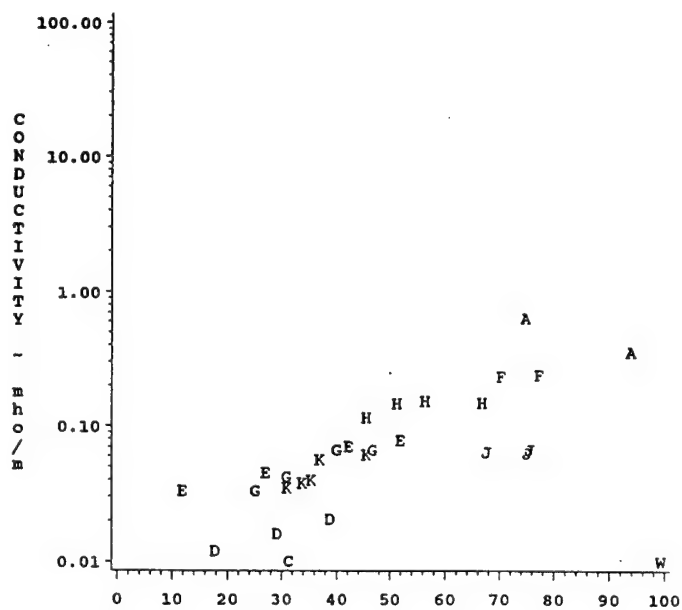
TMP=10



SOIL	A	A	A	A	B	B	B	B	B	C	C	C	C	C	D	D	D	D	D
	E	E	E	E	F	F	F	F	F	G	G	G	G	G	H	H	H	H	H
	I	I	I	I	J	J	J	J	J	K	K	K	K	K	L	L	L	L	L
	W	W	W	W	W	W	W	W	W	W	W	W	W	W	W	W	W	W	W

78 MHz

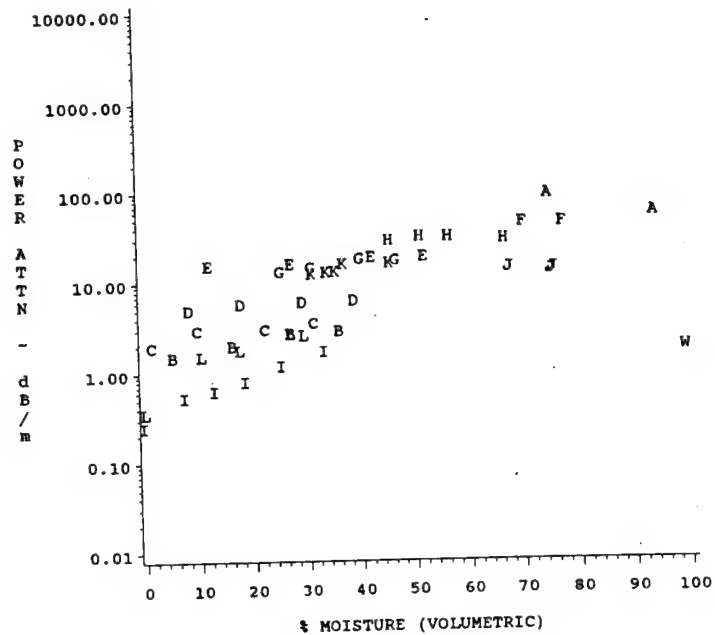
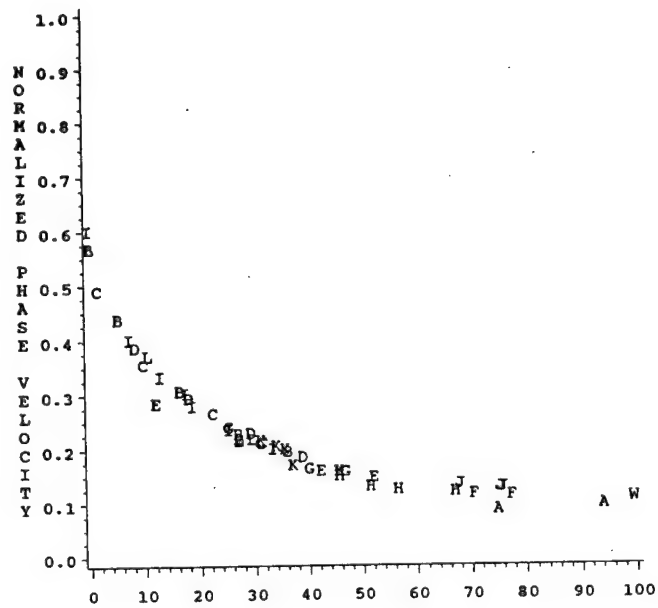
TMP=10



SOIL	A A A A	B B B B	C C C C	D D D D
	E E E E	F F F F	G G G G	H H H H
	I I I I	J J J J	K K K K	L L L L
	W W W WATER			

78 MHz

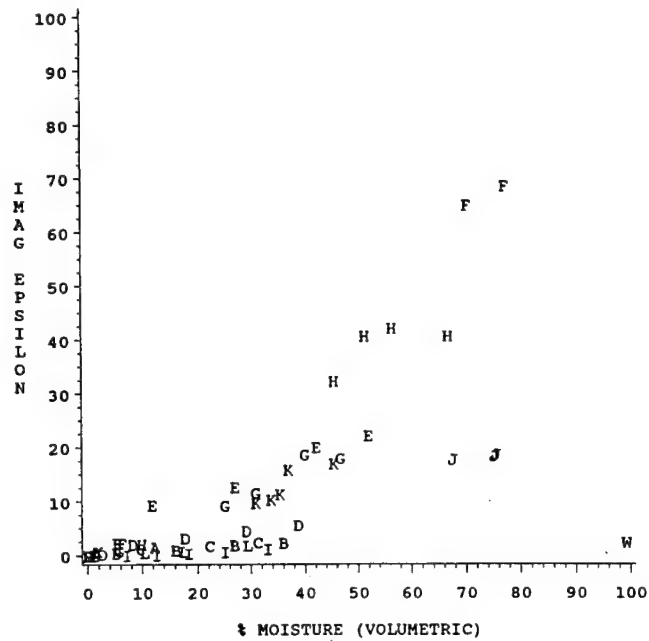
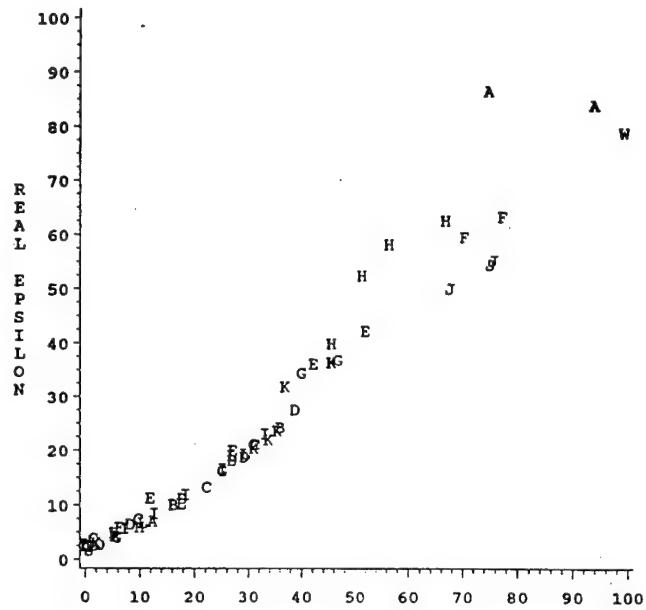
TMP=10



SOIL	A A A A	B B B B	C C C C	D D D D
	E E E E	F F F F	G G G G	H H H H
	I I I I	J J J J	K K K K	L L L L
	W W W WATER			

78 MHz

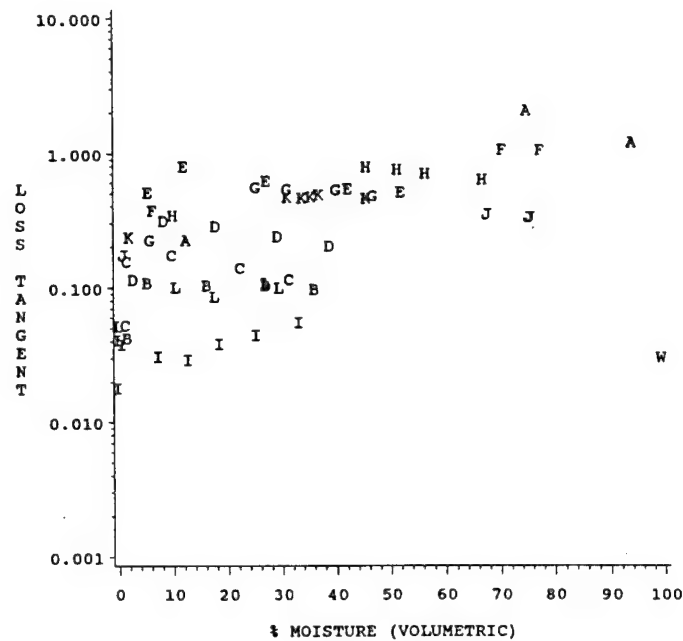
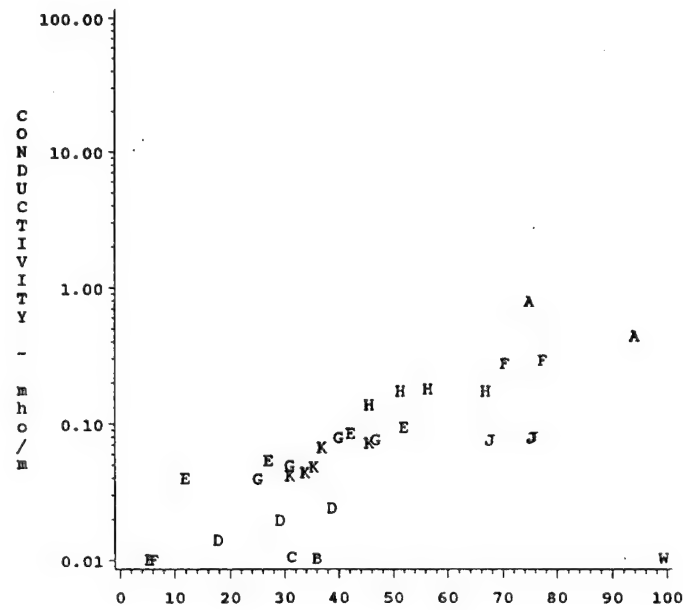
TMP=20



SOIL	A	A	A	A	B	B	B	B	B	C	C	C	C	C	D	D	D	D	D
	E	E	E	E	F	F	F	F	F	G	G	G	G	G	H	H	H	H	H
	I	I	I	I	J	J	J	J	J	K	K	K	K	K	L	L	L	L	L
	W	W	W	WATER															

78 MHz

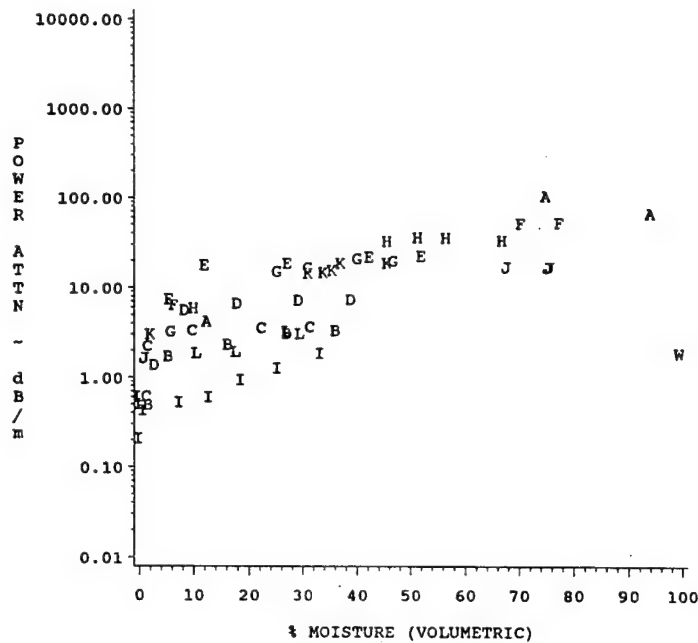
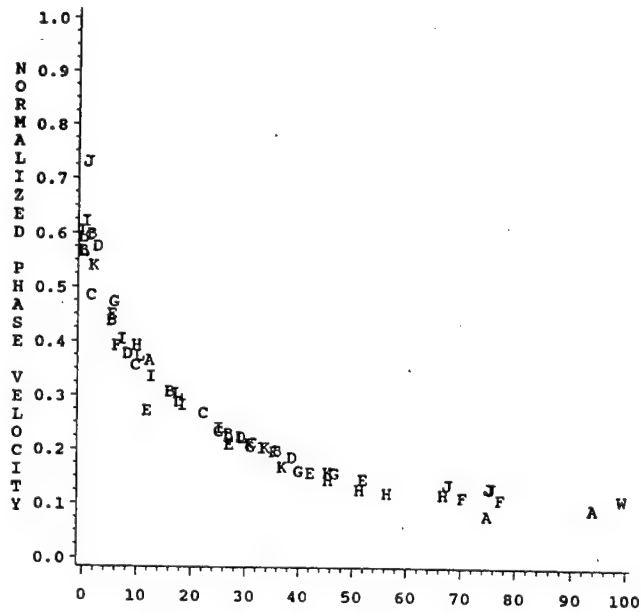
TMP=20



SOIL	A A A A	B B B B	C C C C	D D D D
	E E E E	F F F F	G G G G	H H H H
	I I I I	J J J J	K K K K	L L L L
	W W W	WATER		

78 MHz

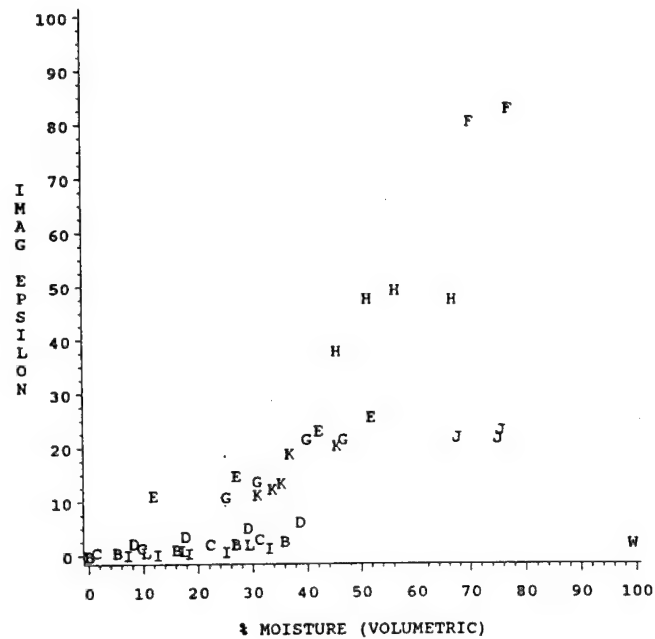
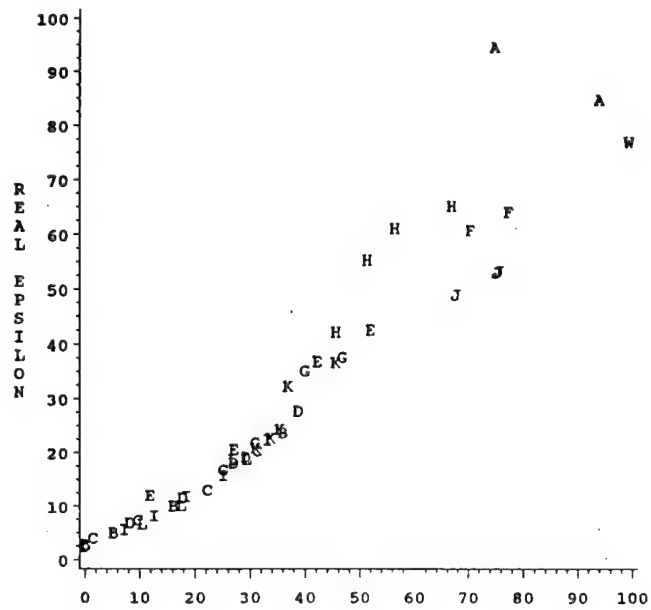
TMP=20



SOIL	A A A A	B B B B	C C C C	D D D D
	E E E E	F F F F	G G G G	H H H H
	I I I I	J J J J	K K K K	L L L L
	W W W	WATER		

78 MHz

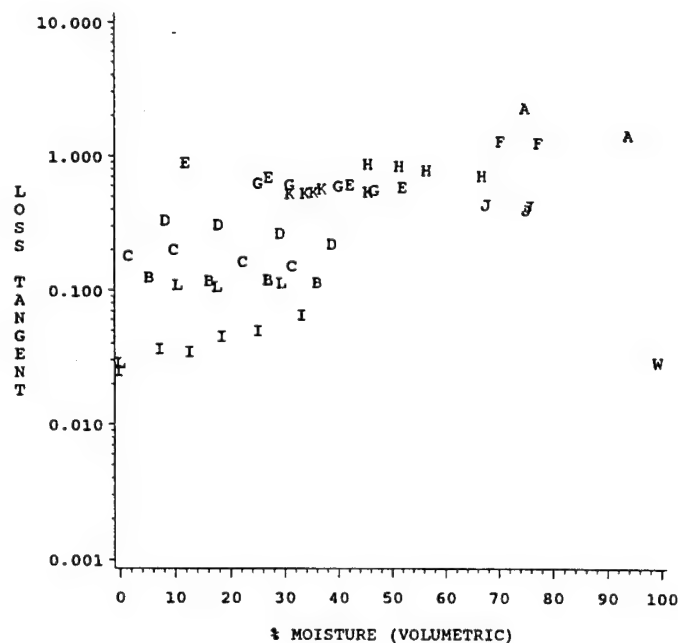
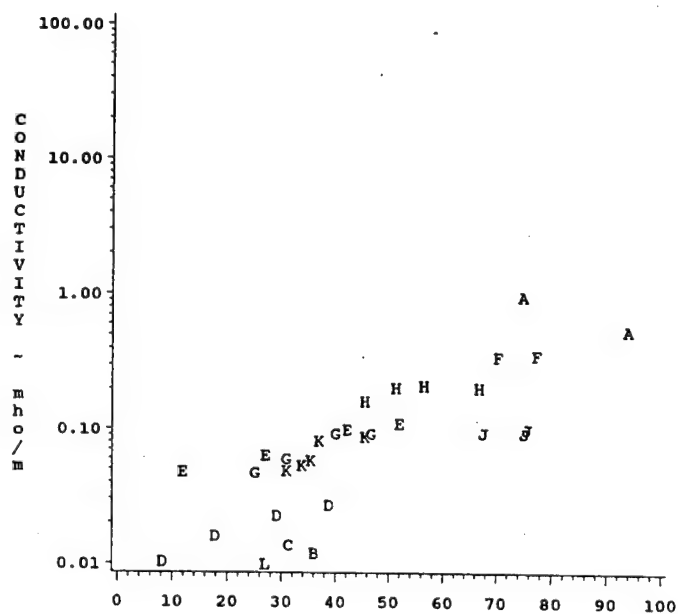
TMP=30



SOIL	A A A A	B B B B	C C C C	D D D D
	E E E E	F F F F	G G G G	H H H H
	I I I I	J J J J	K K K K	L L L L
	W W W WATER			

78 MHz

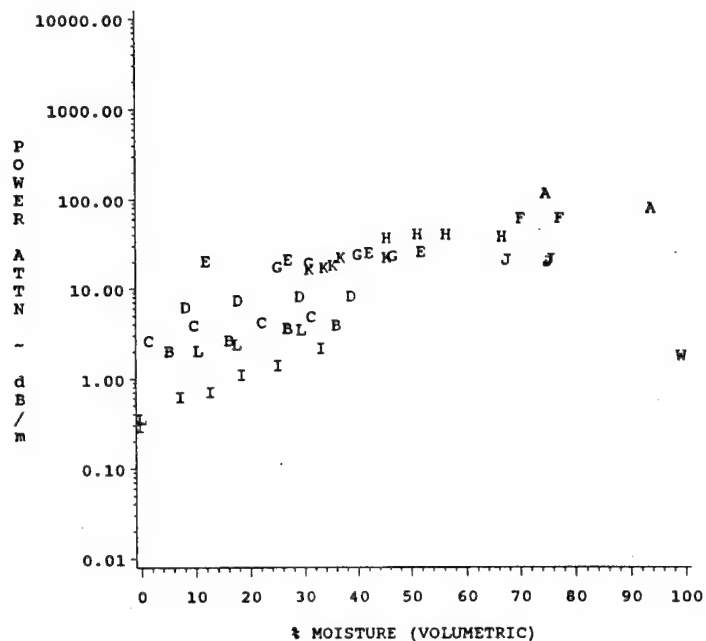
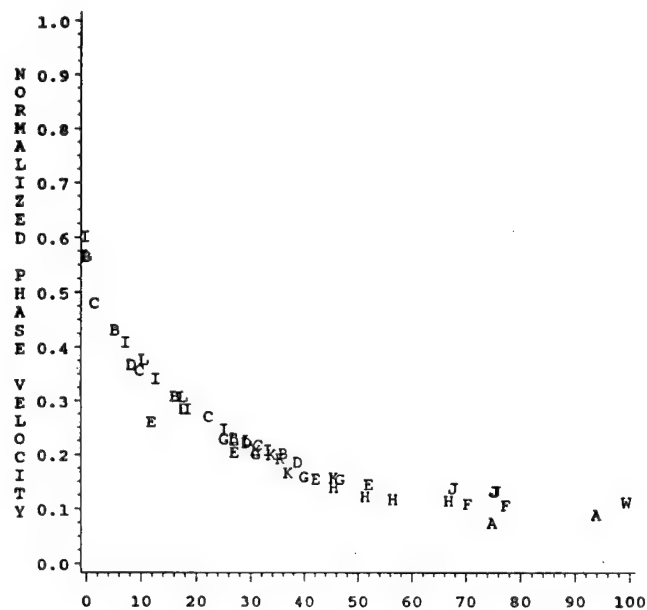
TMP=30



SOIL	A A A A	B B B B	C C C C	D D D D
	E E E E	F F F F	G G G G	H H H H
	I I I I	J J J J	K K K K	L L L L
	W W W WATER			

78 MHz

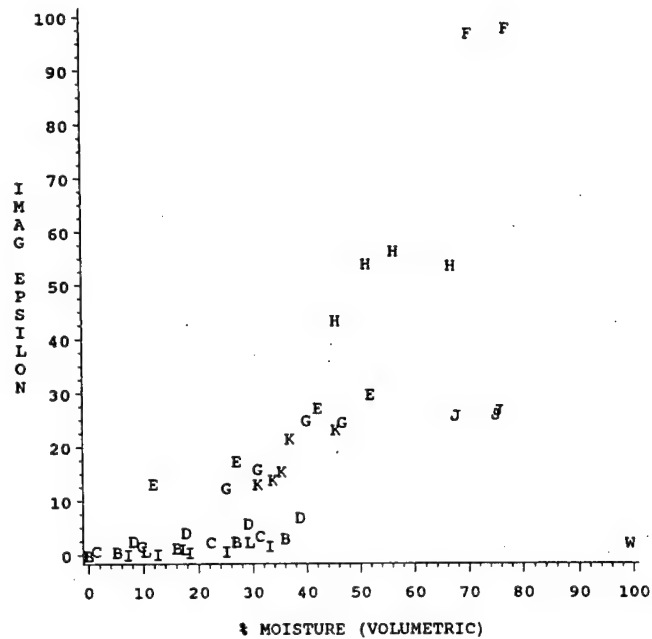
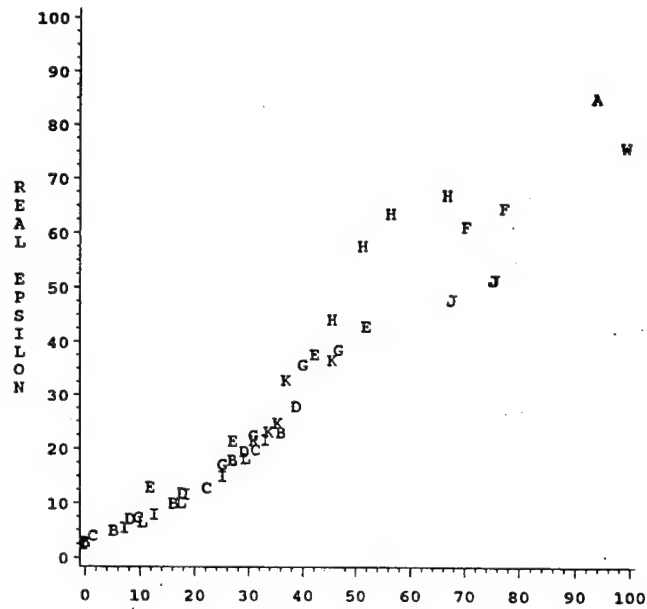
TMP=30



SOIL	A A A A	B B B B	C C C C	D D D D
	E E E E	F F F F	G G G G	H H H H
	I I I I	J J J J	K K K K	L L L L
	W W W WATER			

78 MHz

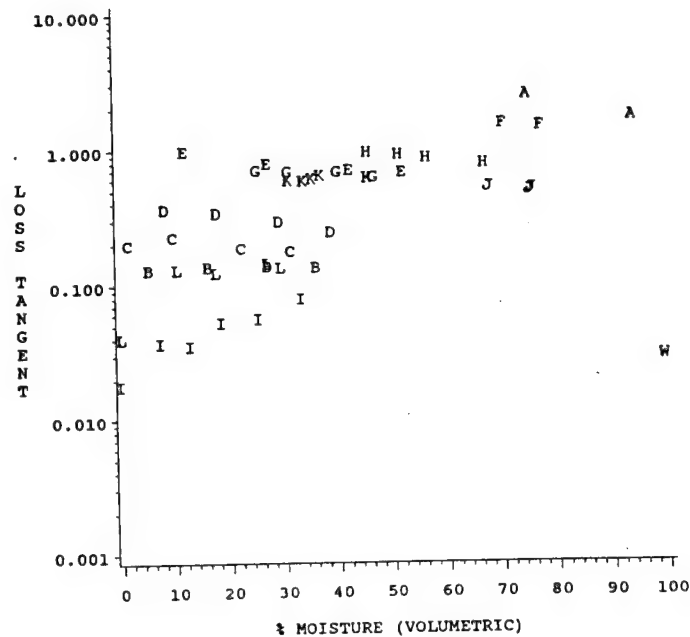
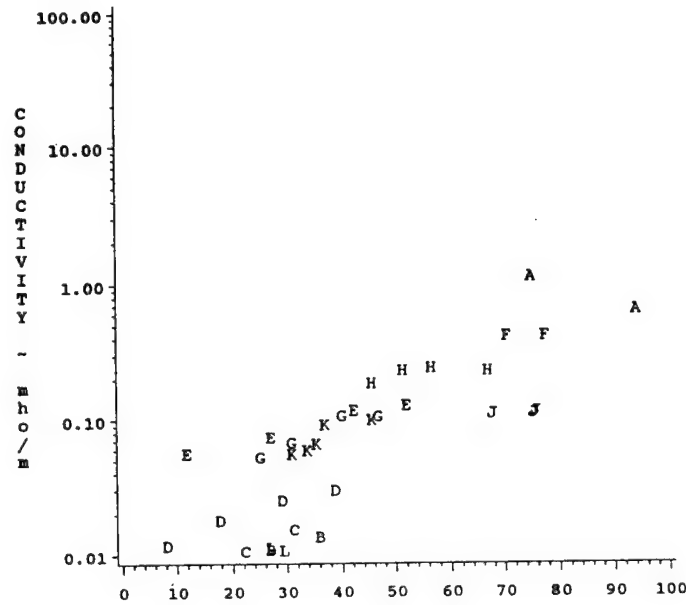
TMP=40



SOIL	A A A A	B B B B	C C C C	D D D D
	E E E E	F F F F	G G G G	H H H H
	I I I I	J J J J	K K K K	L L L L
	W W W WATER			

78 MHz

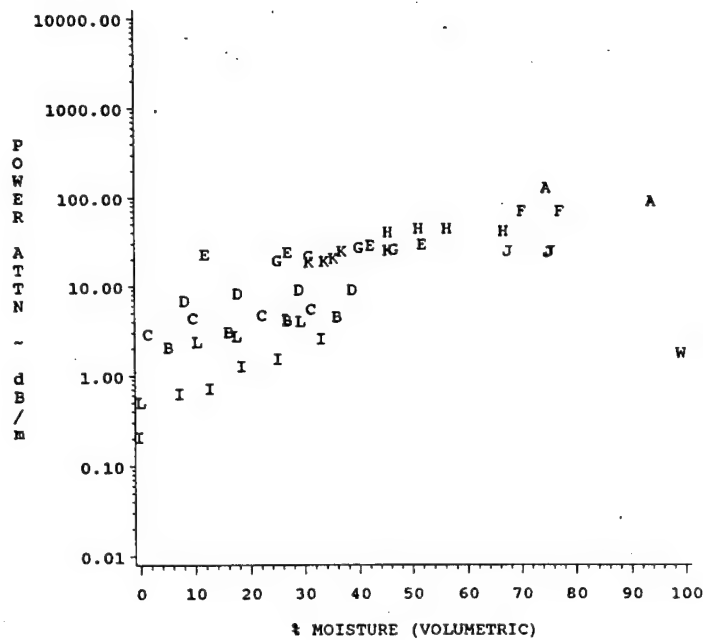
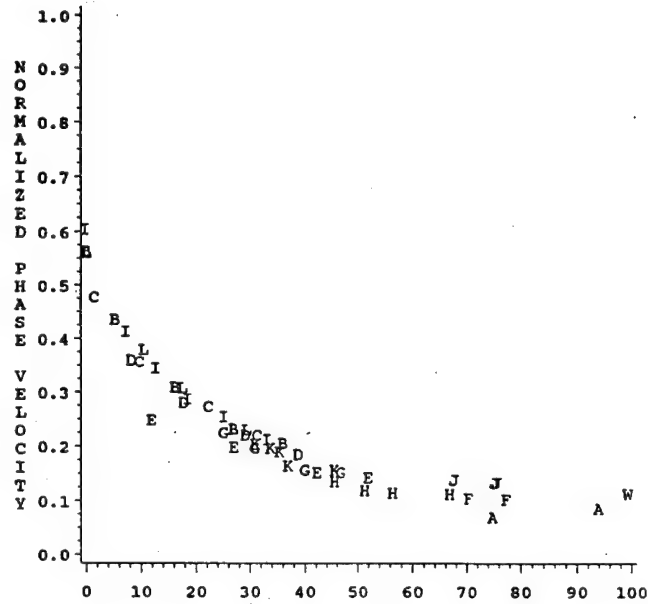
TMP=40



SOIL	A A A A	B B B B	C C C C	D D D D
	E E E E	F F F F	G G G G	H H H H
	I I I I	J J J J	K K K K	L L L L
	W W W WATER			

78 MHz

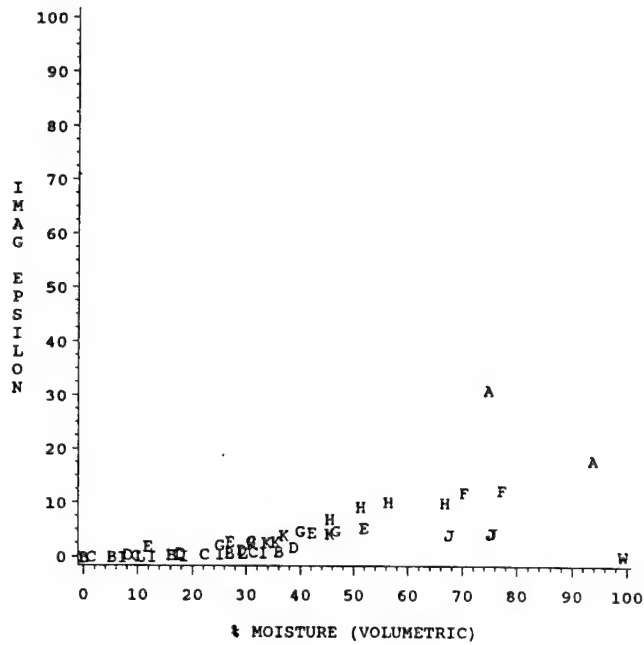
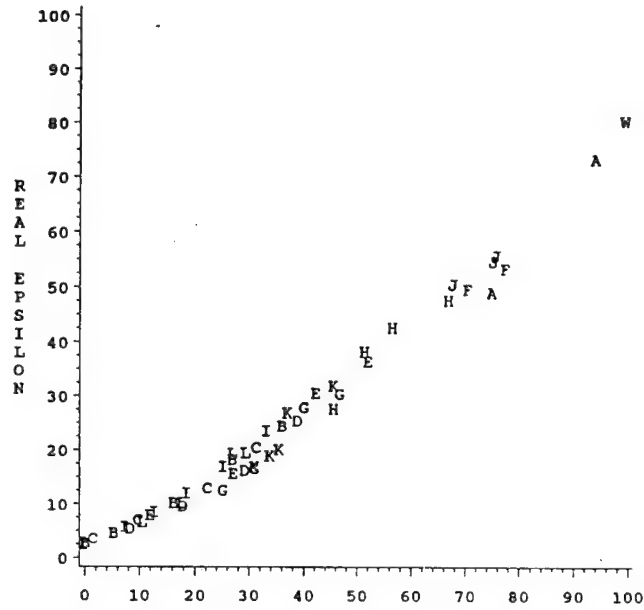
TMP=40



SOIL	A A A A	B B B B	C C C C	D D D D
	E E E E	F F F F	G G G G	H H H H
	I I I I	J J J J	K K K K	L L L L
	W W W WATER			

508 MHz

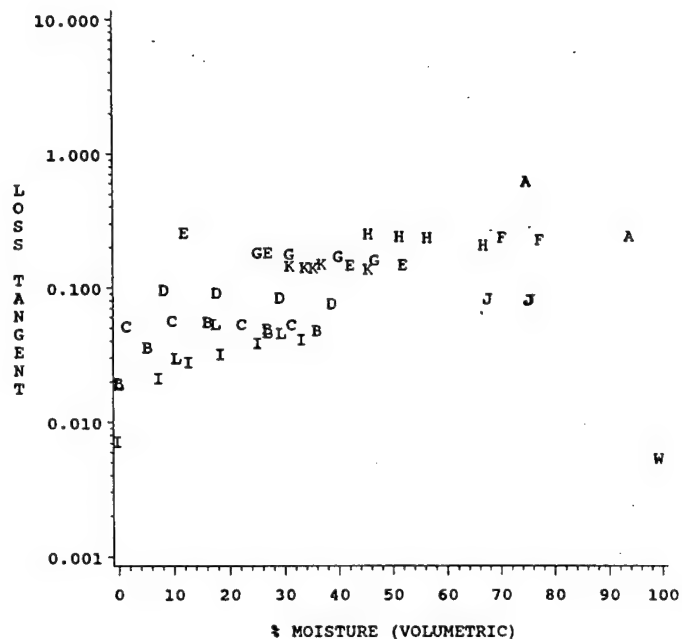
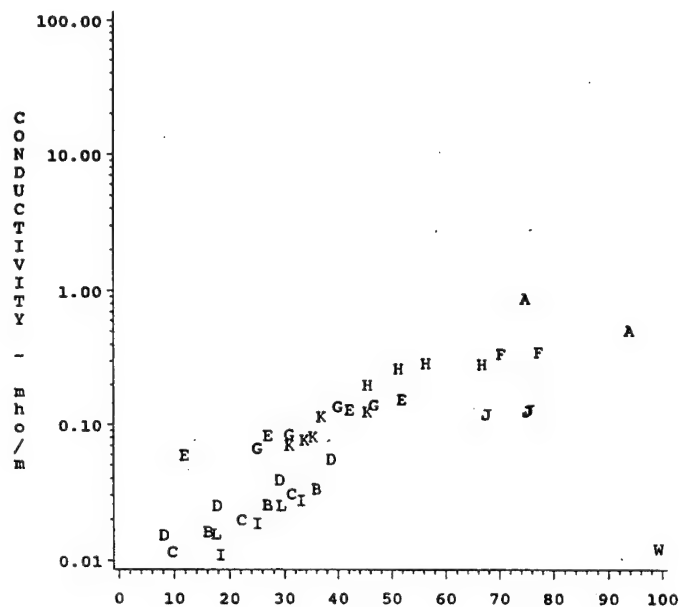
TMP=10



SOIL	A A A A	B B B B	C C C C	D D D D
	E E E E	F F F F	G G G G	H H H H
	I I I I	J J J J	K K K K	L L L L
	W W W WATER			

508 MHz

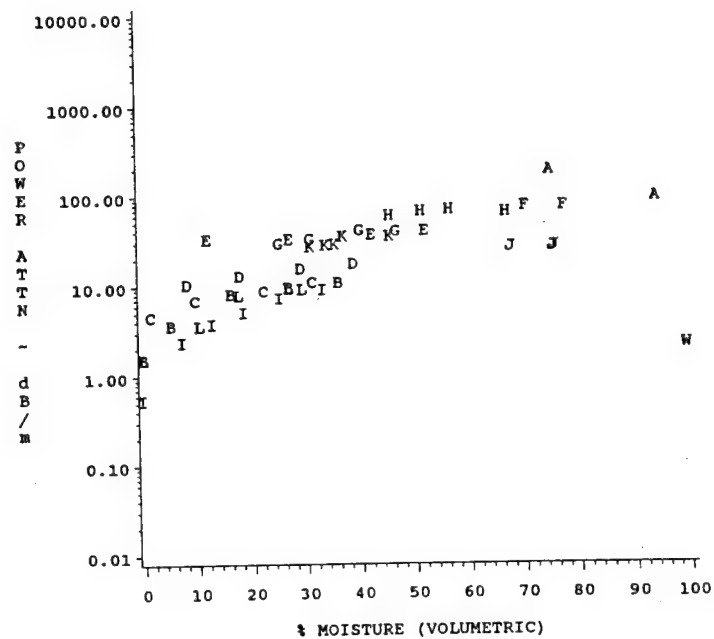
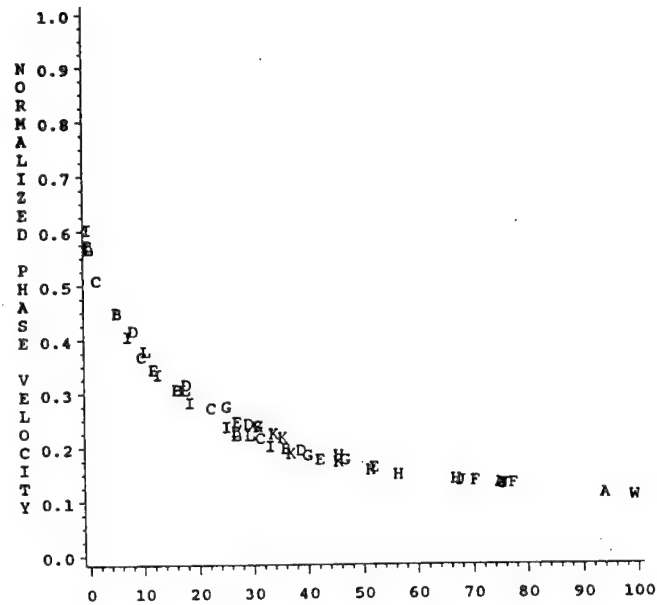
TMP=10



SOIL	A A A A	B B B B	C C C C	D D D D
	E E E E	F F F F	G G G G	H H H H
	I I I I	J J J J	K K K K	L L L L
	W W W WATER			

508 MHz

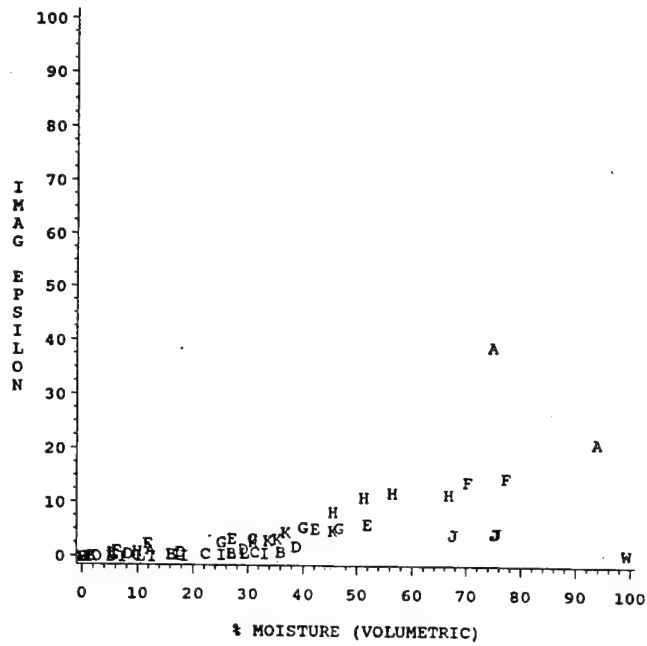
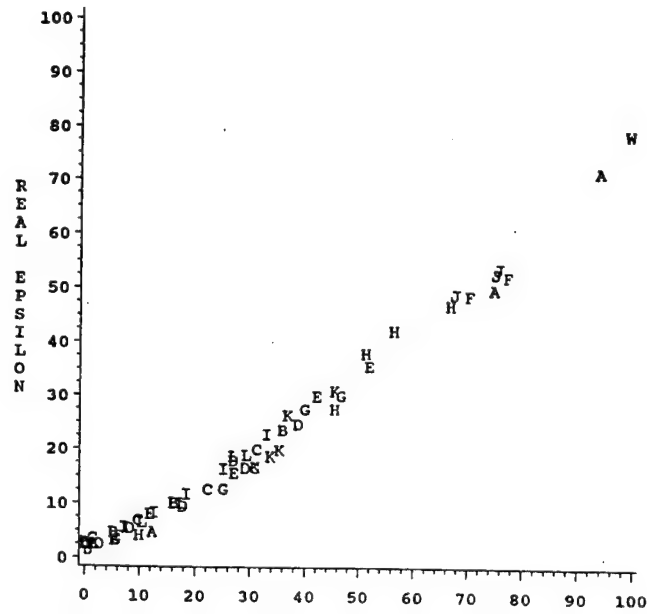
TMP=10



SOIL	A A A A	B B B B	C C C C	D D D D
	E E E E	F F F F	G G G G	H H H H
	I I I I	J J J J	K K K K	L L L L
	W W W WATER			

508 MHz

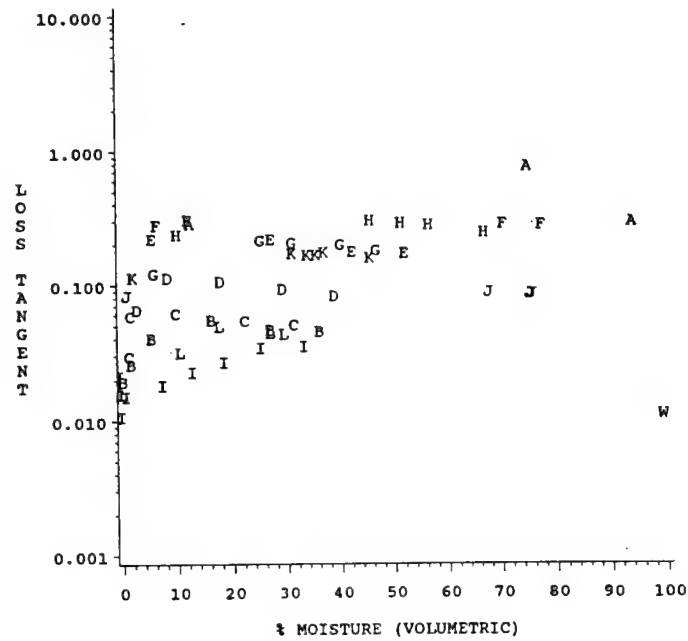
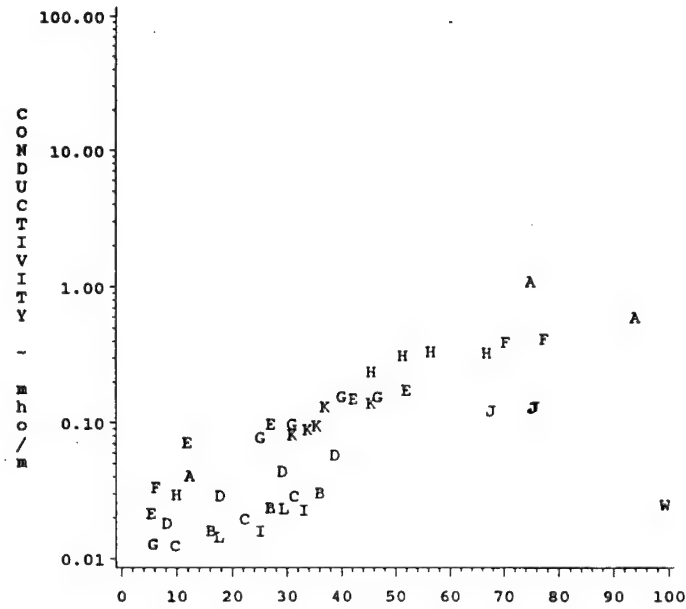
TMP=20



SOIL	A A A A	B B B B	C C C C	D D D D
	E E E E	F F F F	G G G G	H H H H
	I I I I	J J J J	K K K K	L L L L
	W W W WATER			

508 MHz

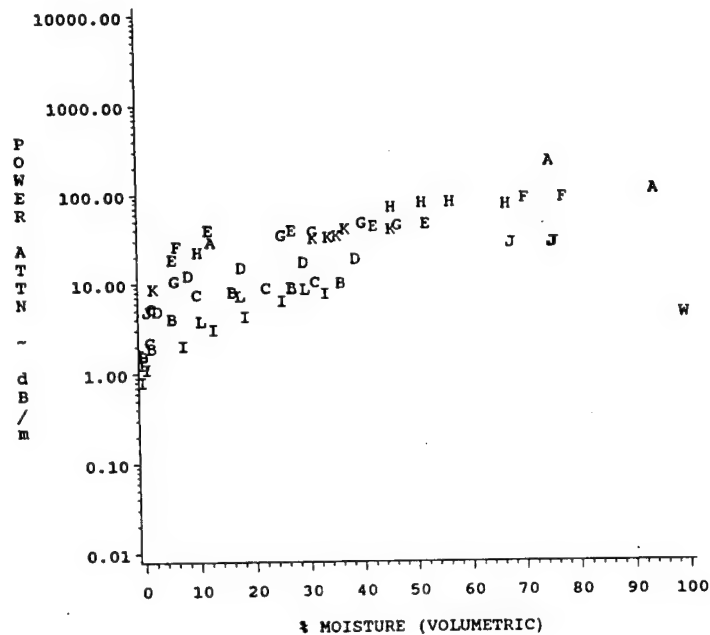
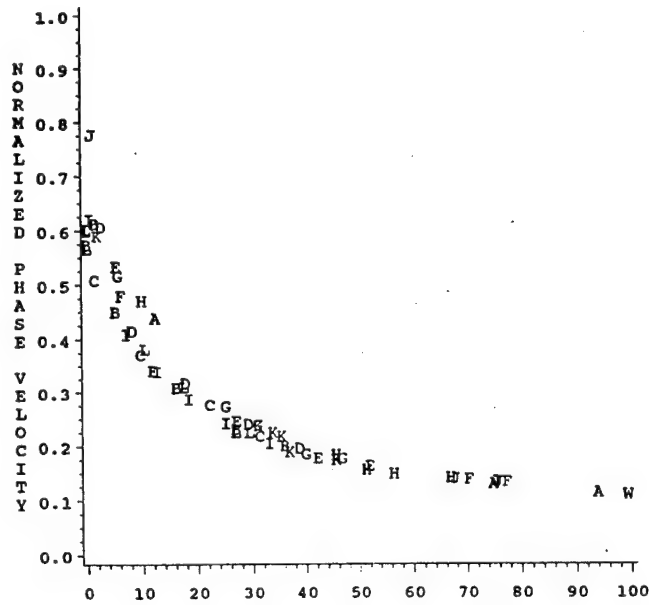
TMP=20



SOIL	A A A A	B B B B	C C C C	D D D D
	E E E E	F F F F	G G G G	H H H H
	I I I I	J J J J	K K K K	L L L L
	W W W WATER			

508 MHz

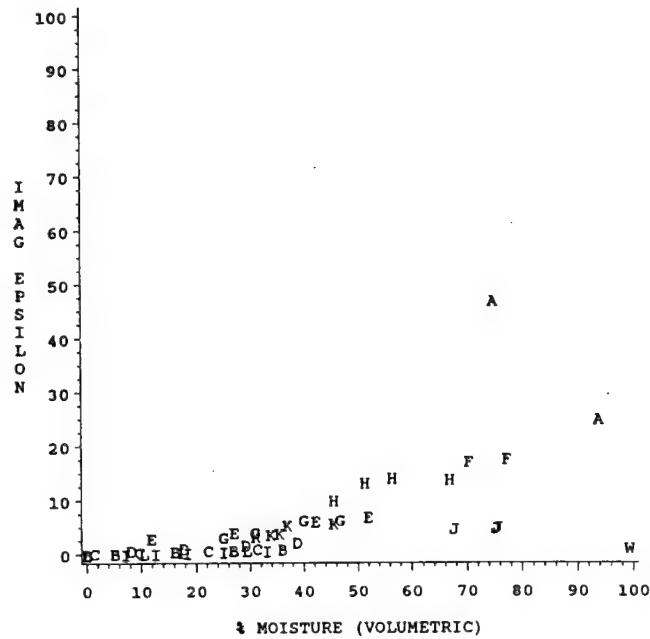
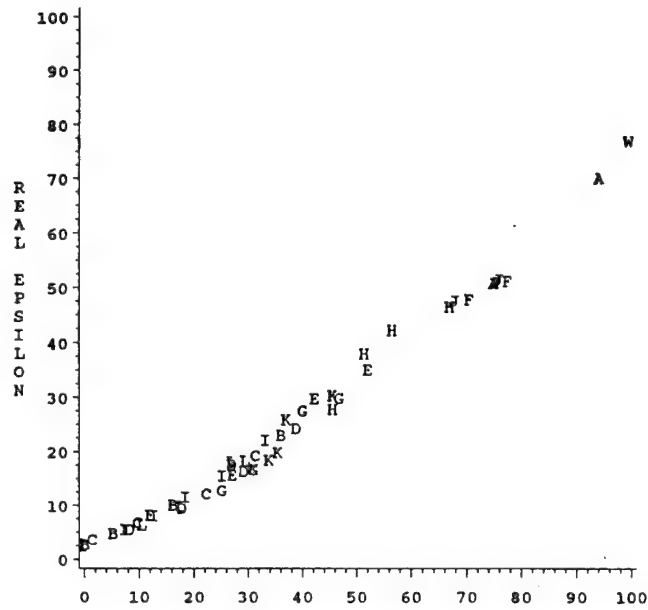
TMP=20



SOIL	A	A	A	A	B	B	B	B	C	C	C	C	D	D	D	D
	E	E	E	E	F	F	F	F	G	G	G	G	H	H	H	H
	I	I	I	I	J	J	J	J	K	K	K	K	L	L	L	L
	W	W	W	W												

508 MHz

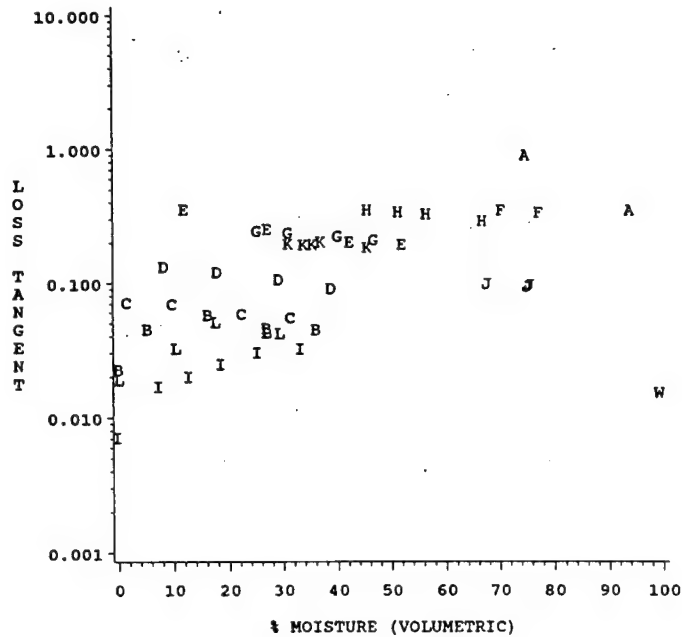
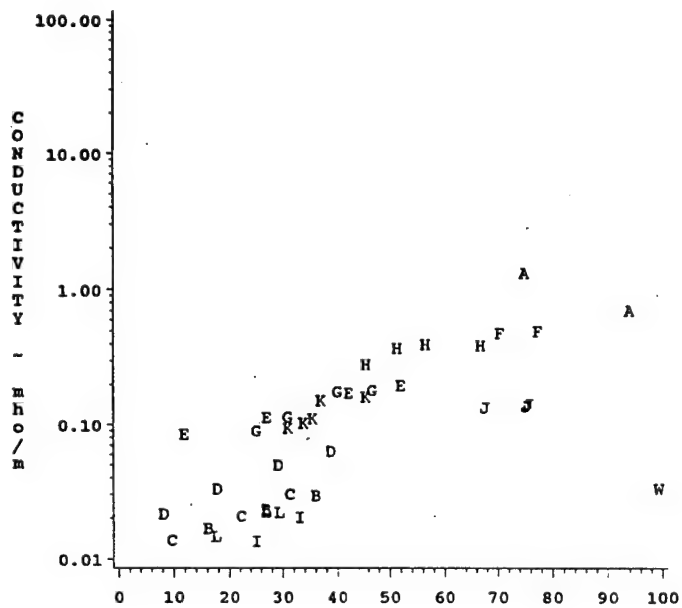
TMP=30



SOIL	A A A A	B B B B	C C C C	D D D D
	E E E E	F F F F	G G G G	H H H H
	I I I I	J J J J	K K K K	L L L L
	W W W WATER			

508 MHz

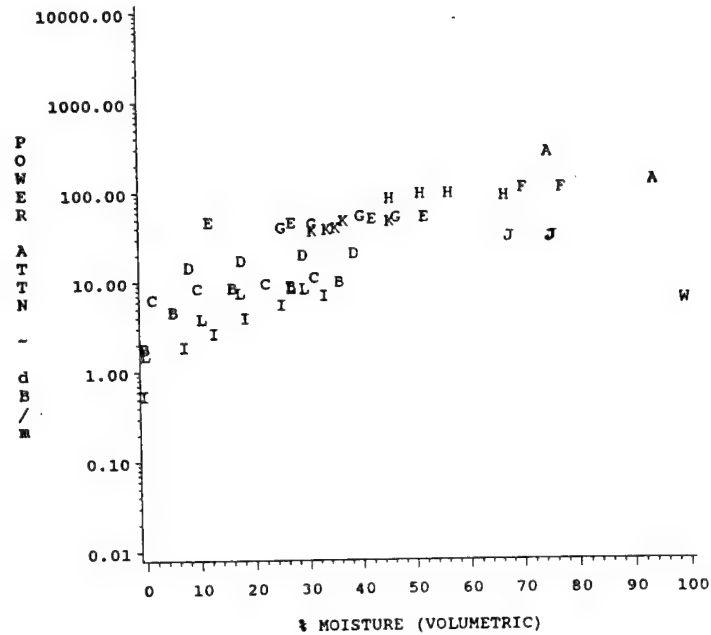
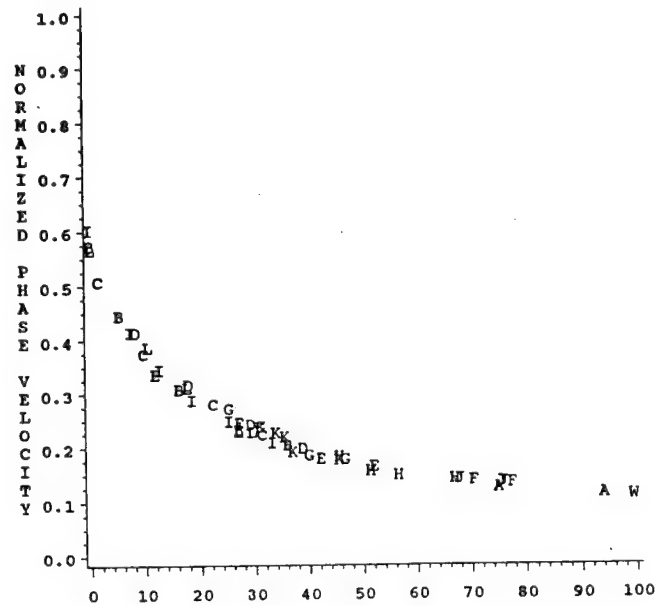
TMP=30



SOIL	A A A A	B B B B	C C C C	D D D D
	E E E E	F F F F	G G G G	H H H H
	I I I I	J J J J	K K K K	L L L L
	W W W	WATER		

508 MHz

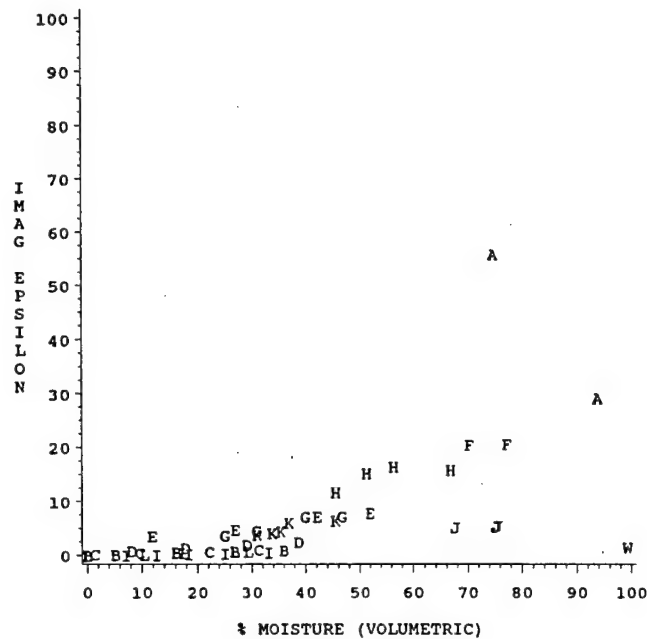
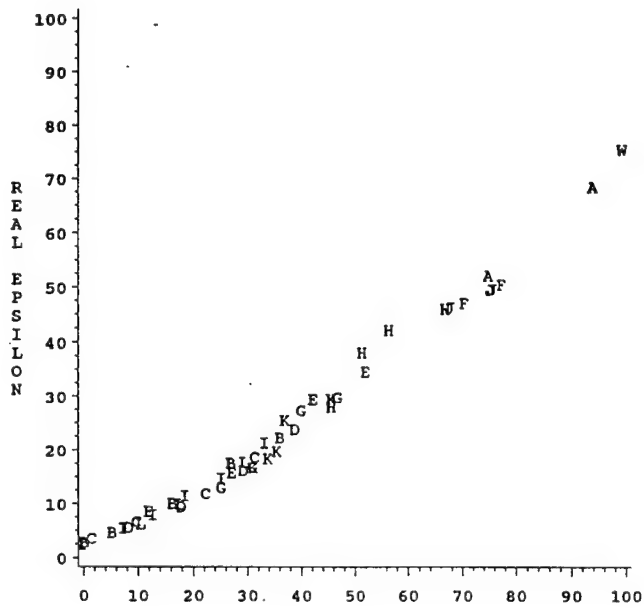
TMP=30



SOIL	A	A	A	A	B	B	B	B	C	C	C	C	D	D	D	D
	E	E	E	E	F	F	F	F	G	G	G	G	H	H	H	H
	I	I	I	I	J	J	J	J	K	K	K	K	L	L	L	L
	W	W	W	WATER												

508 MHz

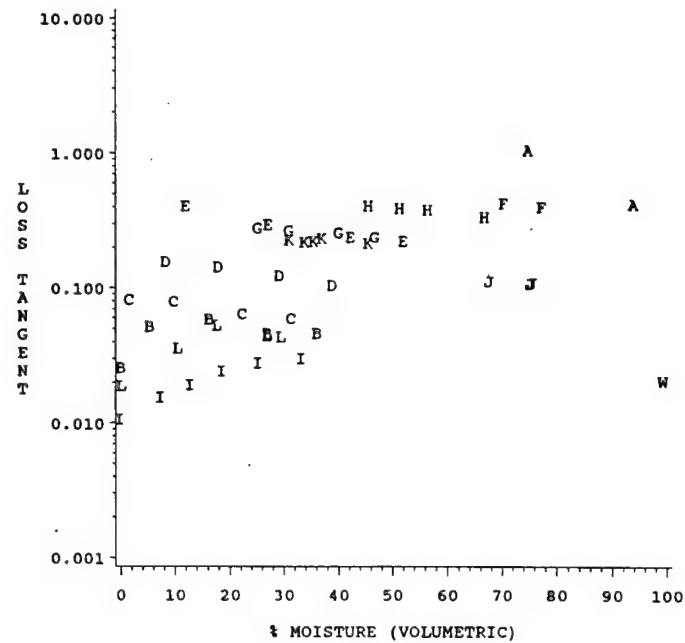
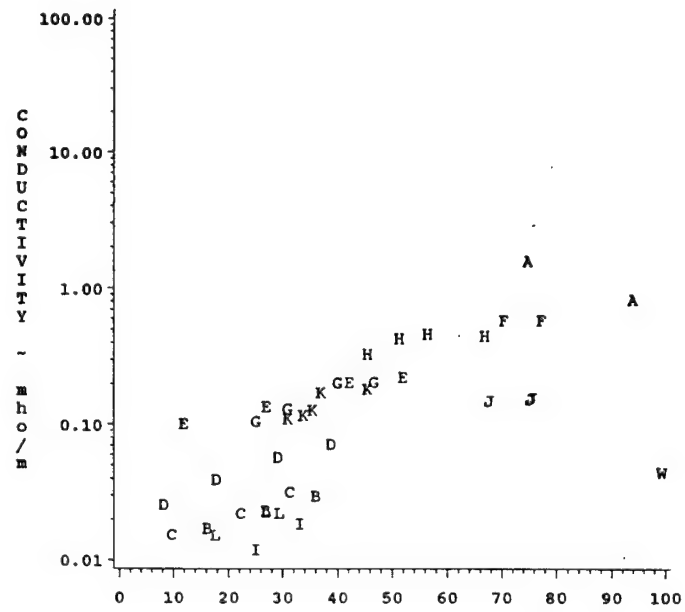
TMP=40



SOIL	A A A A	B B B B	C C C C	D D D D
	E E E E	F F F F	G G G G	H H H H
	I I I I	J J J J	K K K K	L L L L
	W W W WATER			

508 MHz

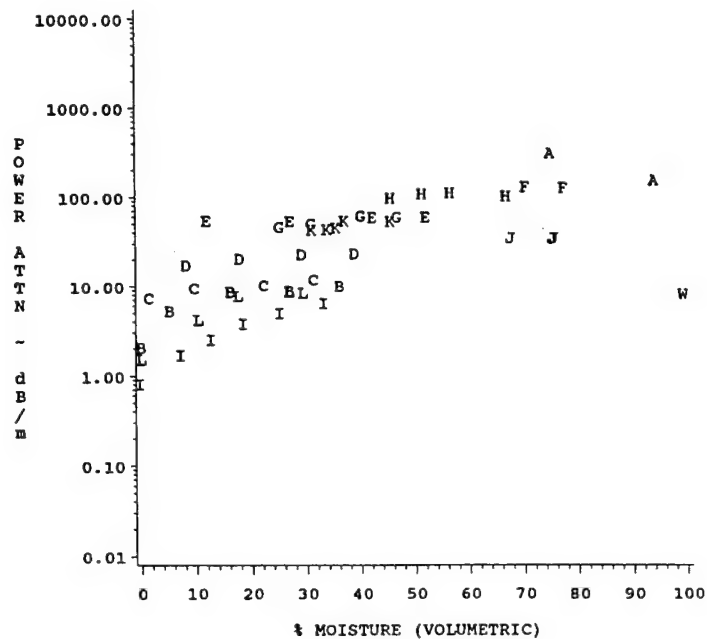
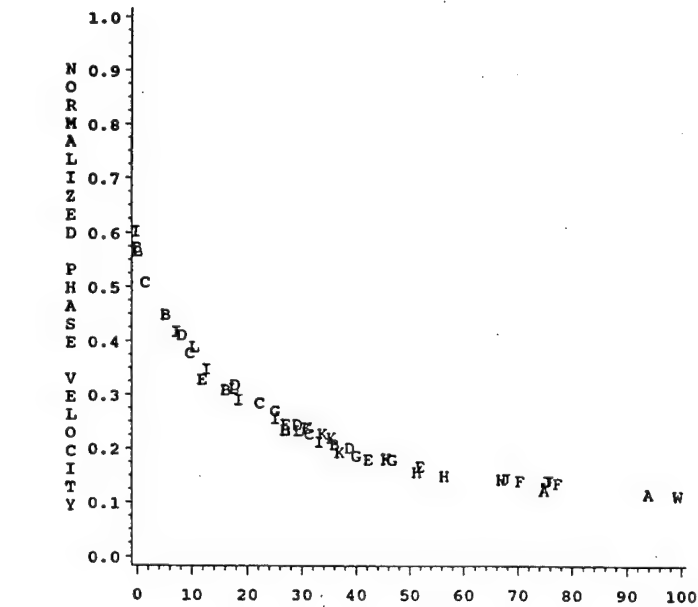
TMP=40



SOIL	A A A A	B B B B	C C C C	D D D D
	E E E E	F F F F	G G G G	H H H H
	I I I I	J J J J	K K K K	L L L L
	W W W	WATER		

508 MHz

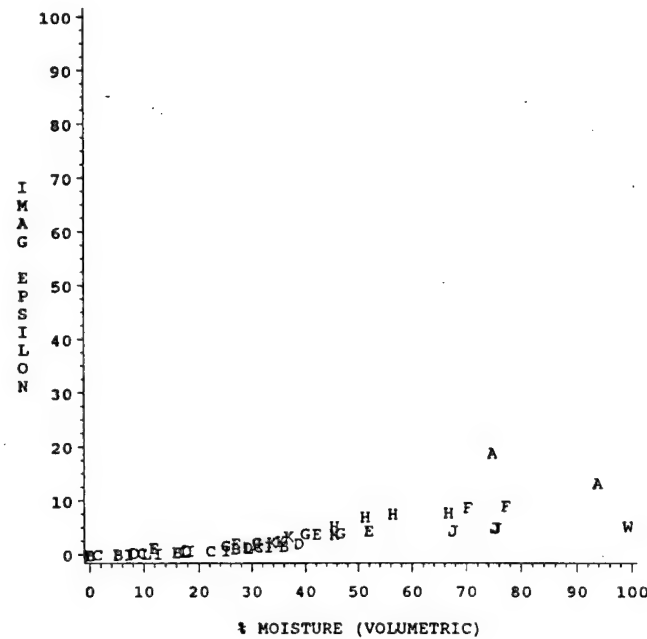
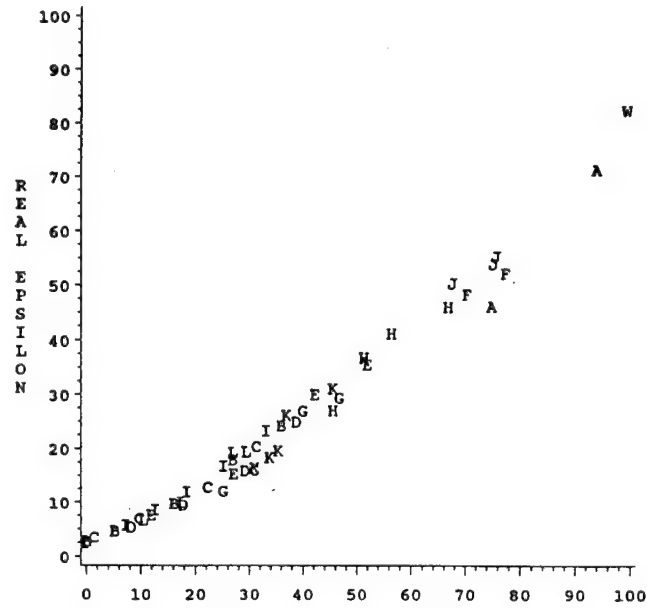
TMP=40



SOIL	A A A A	B B B B	C C C C	D D D D
	E E E E	F F F F	G G G G	H H H H
	I I I I	J J J J	K K K K	L L L L
	W W W	WATER		

1.004 GHz

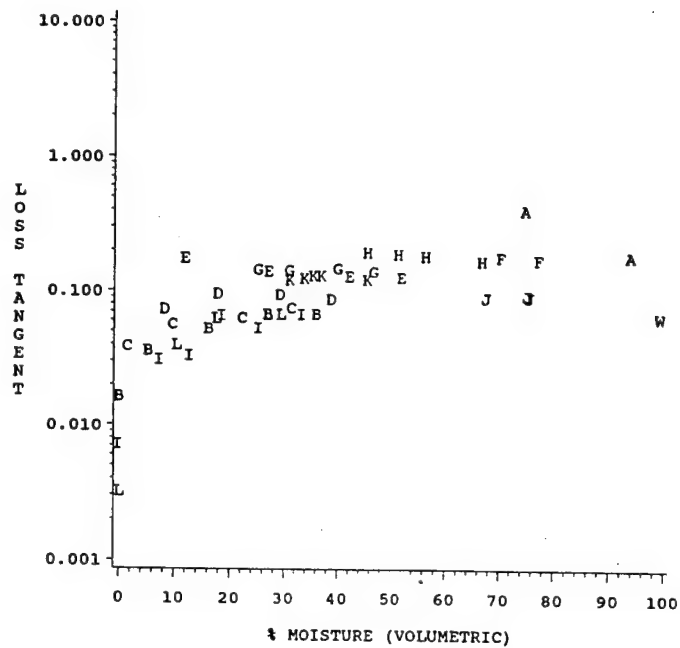
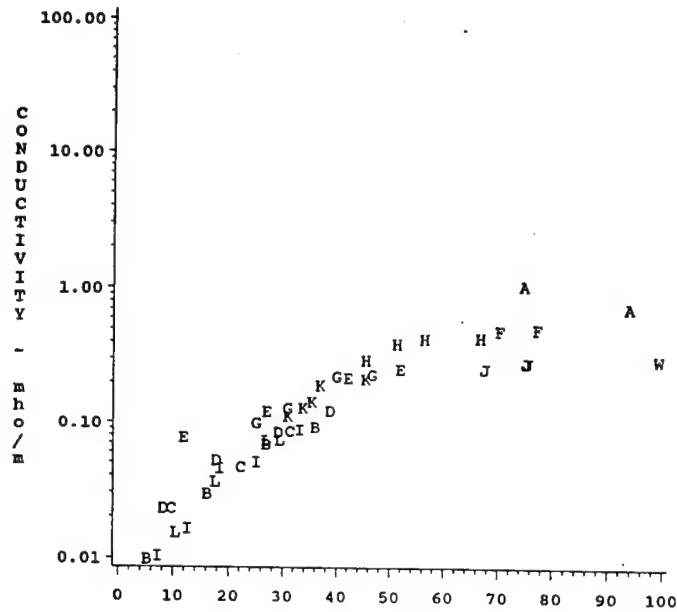
TMP=10



SOIL	A A A A	B B B B	C C C C	D D D D
	E E E E	F F F F	G G G G	H H H H
	I I I I	J J J J	K K K K	L L L L
	W W W WATER			

1.004 GHz

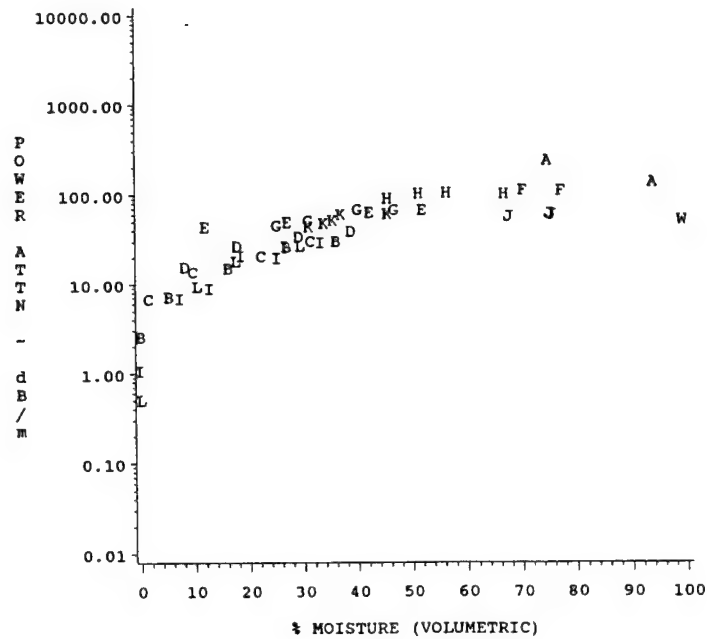
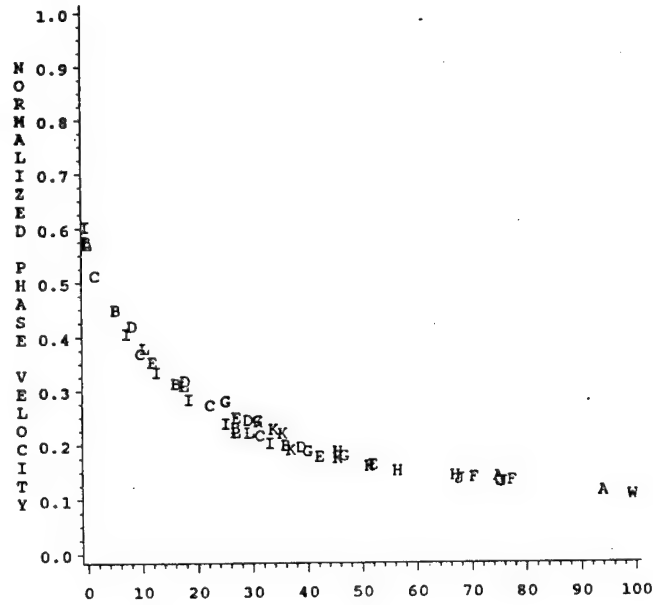
TMP=10



SOIL	A A A A	B B B B	C C C C	D D D D
	E E E E	F F F F	G G G G	H H H H
	I I I I	J J J J	K K K K	L L L L
	W W W WATER			

1.004 GHz

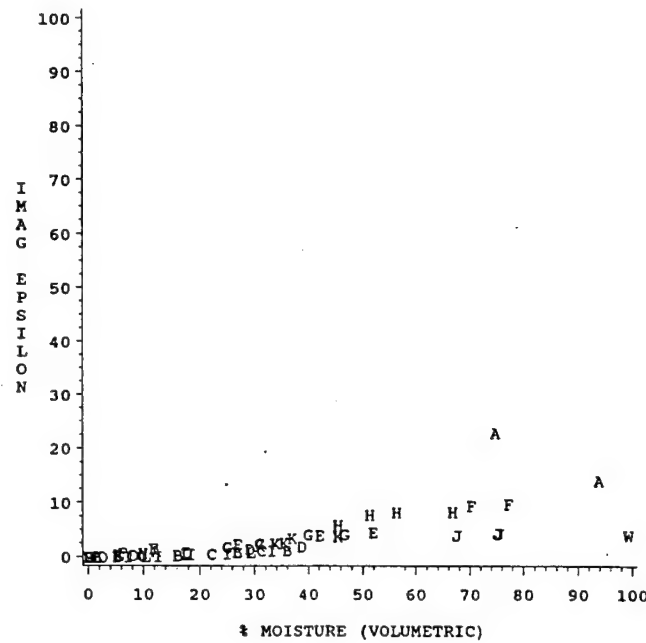
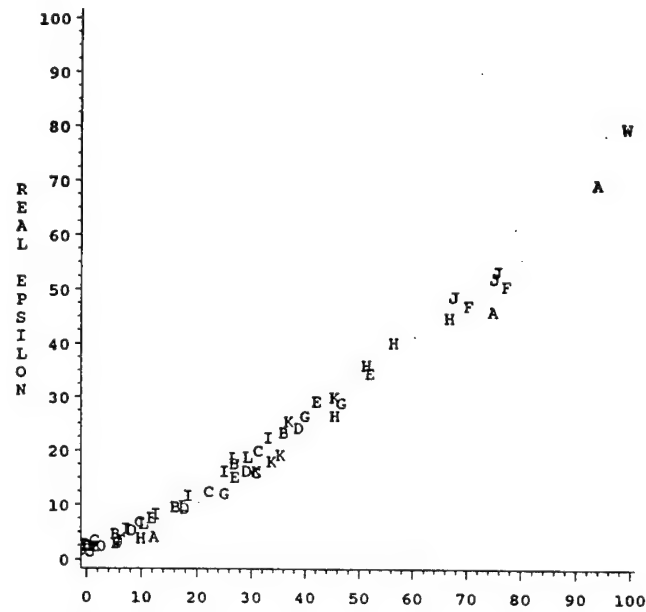
TMP=10



SOIL	A A A A	B B B B	C C C C	D D D D
	E E E E	F F F F	G G G G	H H H H
	I I I I	J J J J	K K K K	L L L L
	W W W WATER			

1.004 GHz

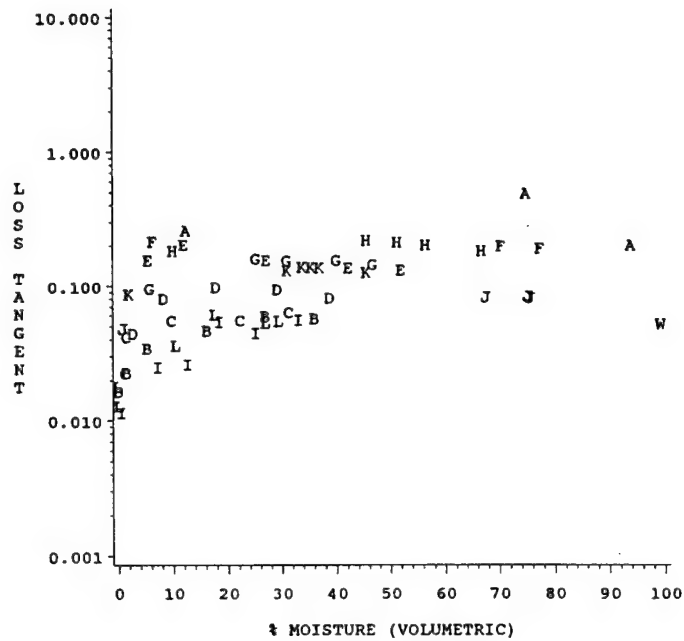
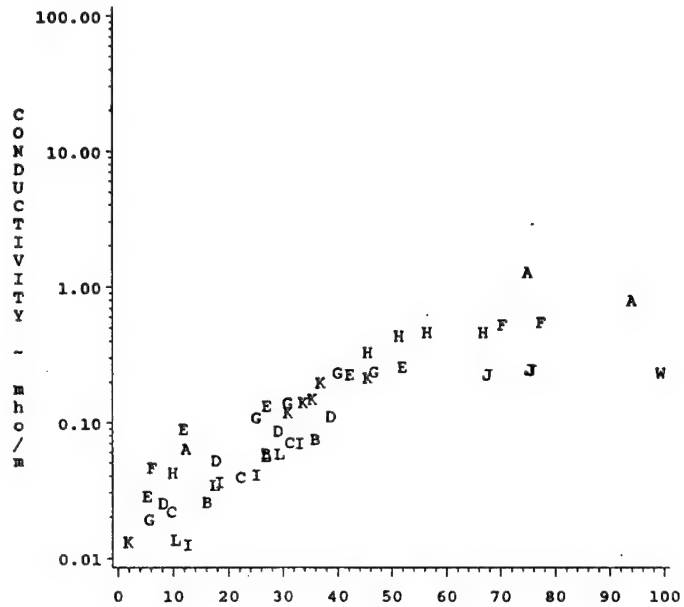
TMP=20



SOIL	A A A A	B B B B	C C C C	D D D D
	E E E E	F F F F	G G G G	H H H H
	I I I I	J J J J	K K K K	L L L L
	W W W WATER			

1.004 GHz

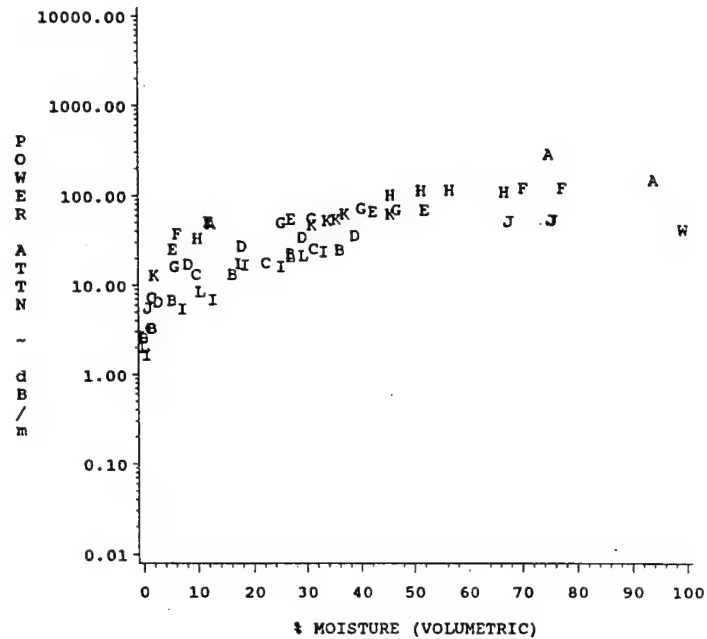
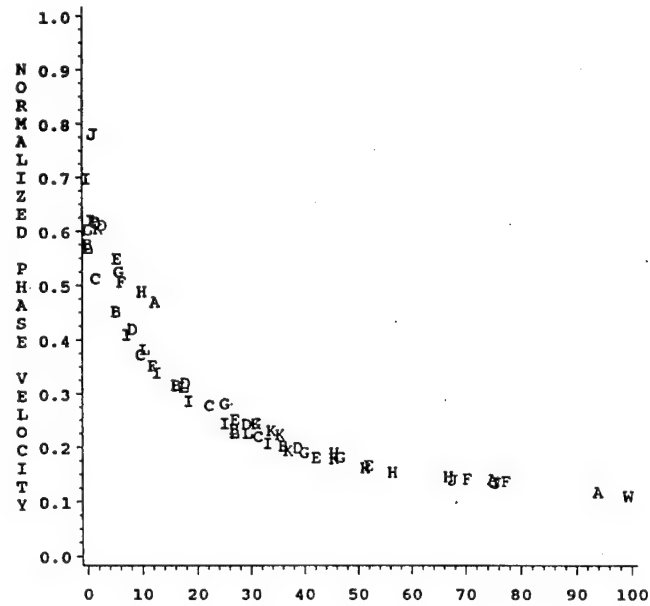
TMP=20



SOIL	A A A A	B B B B	C C C C	D D D D
	E E E E	F F F F	G G G G	H H H H
	I I I I	J J J J	K K K K	L L L L
	W W W	WATER		

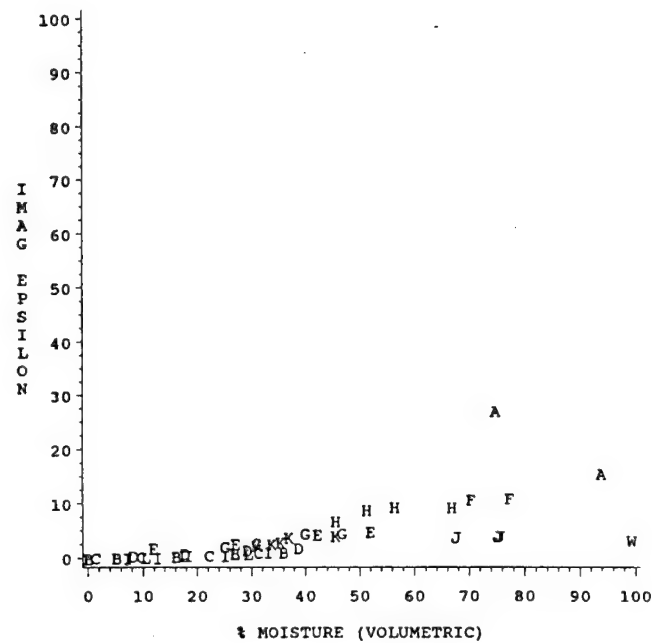
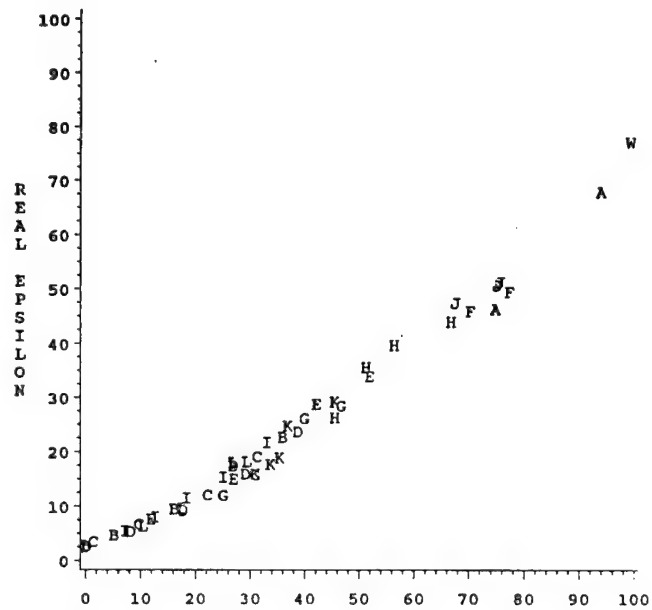
1.004 GHz

TMP=20

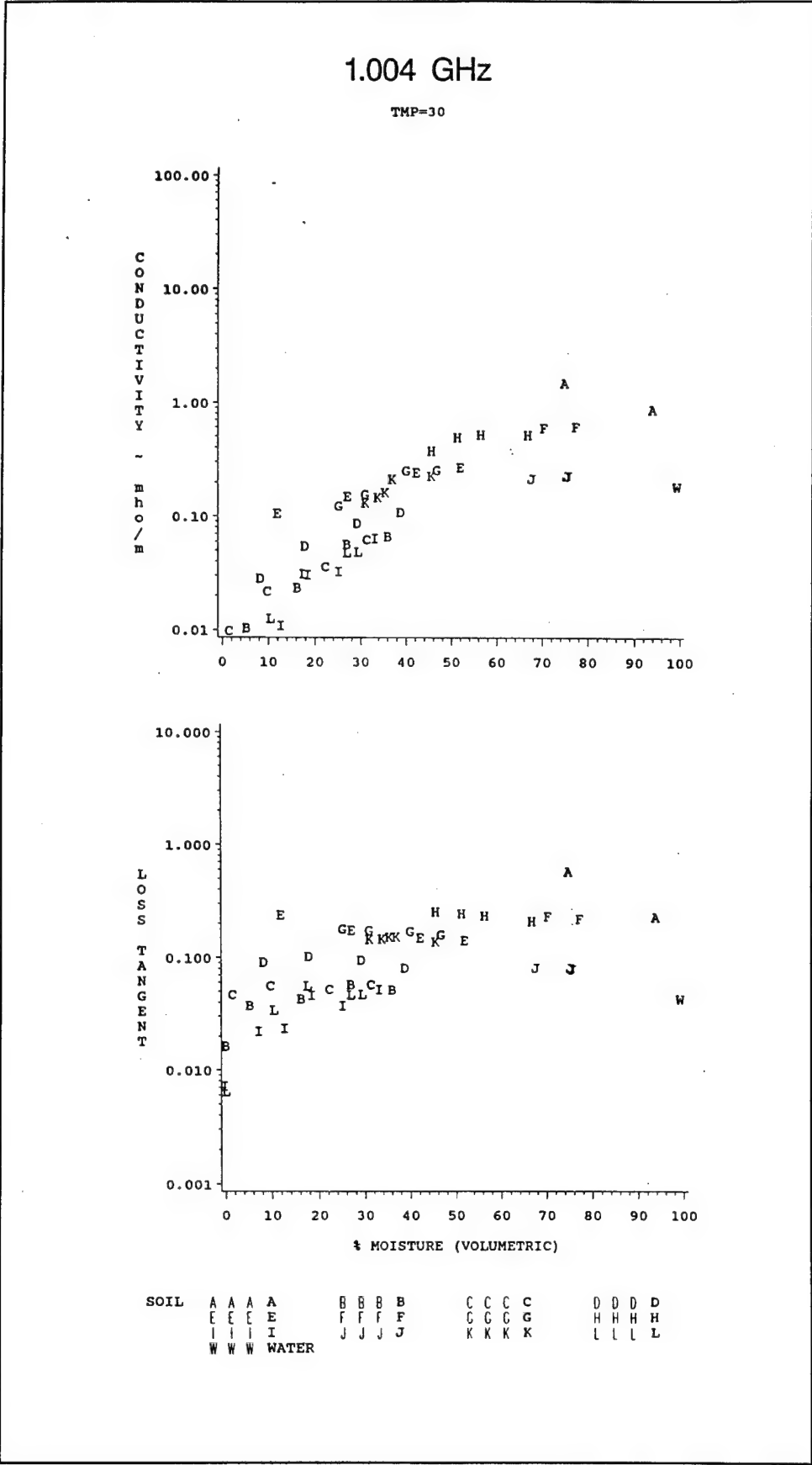


1.004 GHz

TMP=30

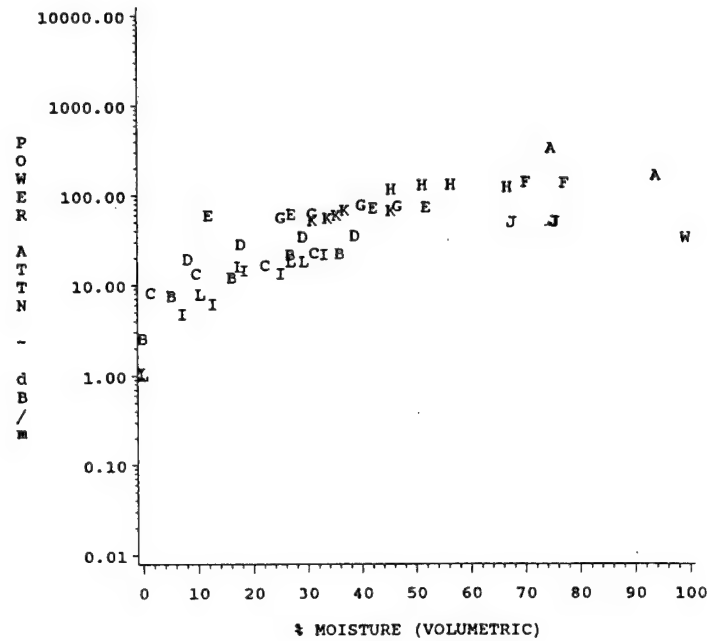
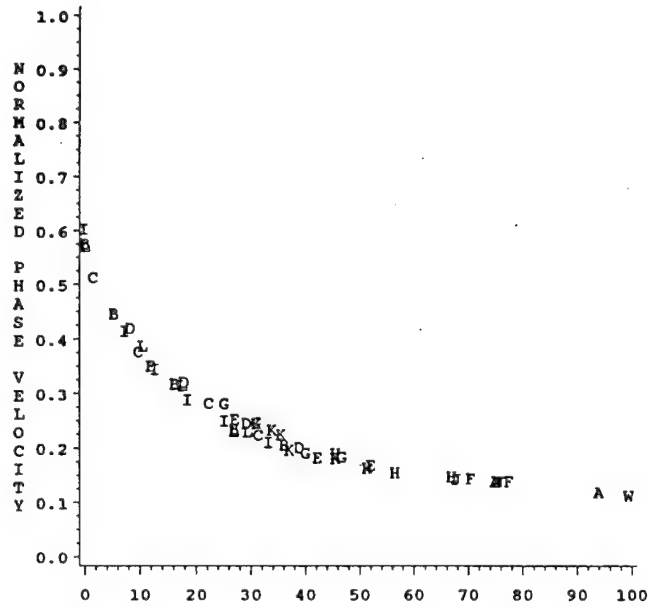


SOIL	A A A A	B B B B	C C C C	D D D D
	E E E E	F F F F	G G G G	H H H H
	I I I I	J J J J	K K K K	L L L L
	W W W WATER			



1.004 GHz

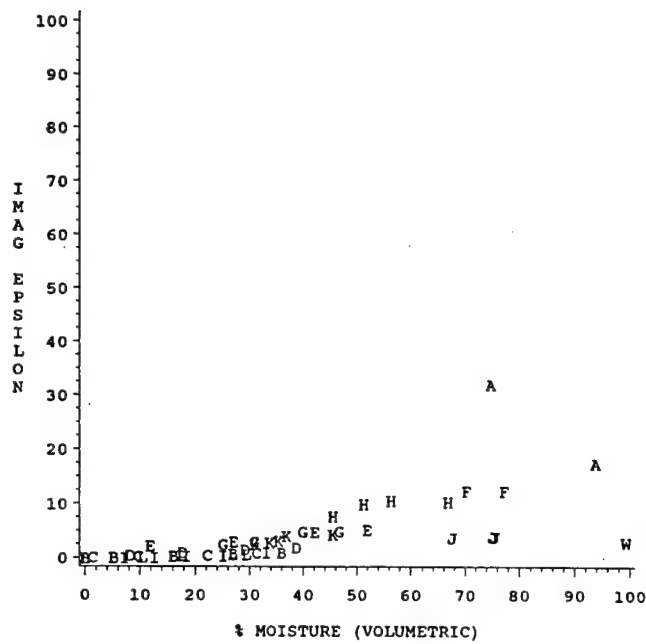
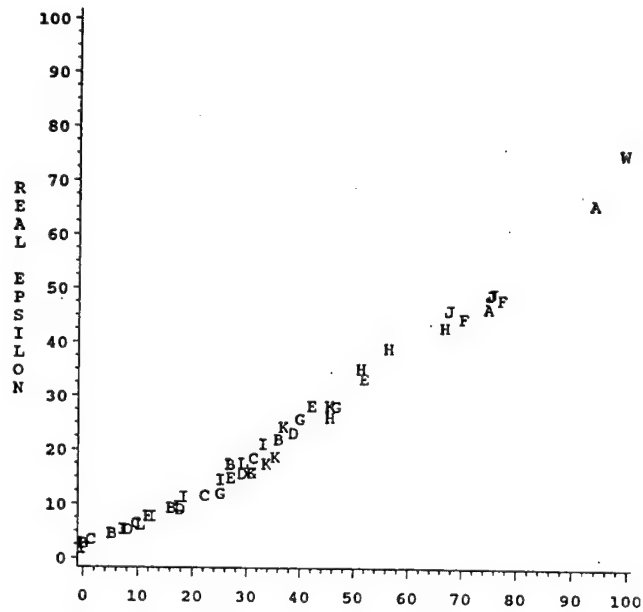
TMP=30



SOIL	A A A A	B B B B	C C C C	D D D D
	E E E E	F F F F	G G G G	H H H H
	I I I I	J J J J	K K K K	L L L L
	W W W WATER			

1.004 GHz

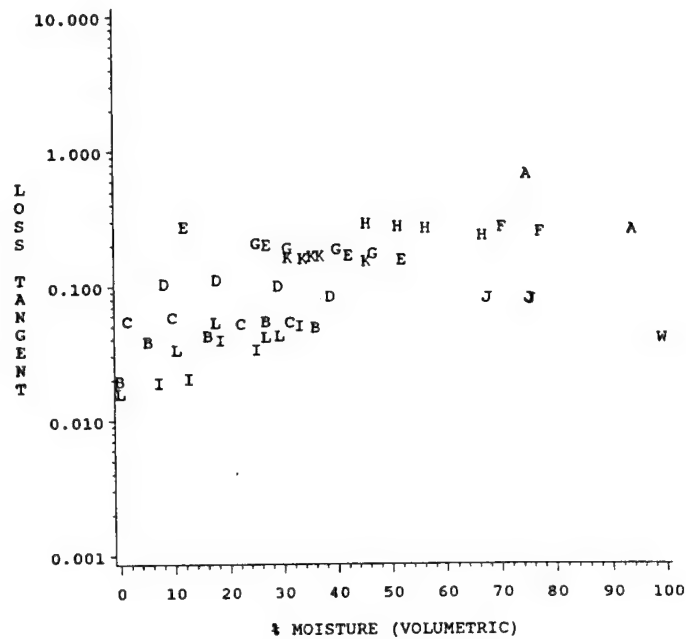
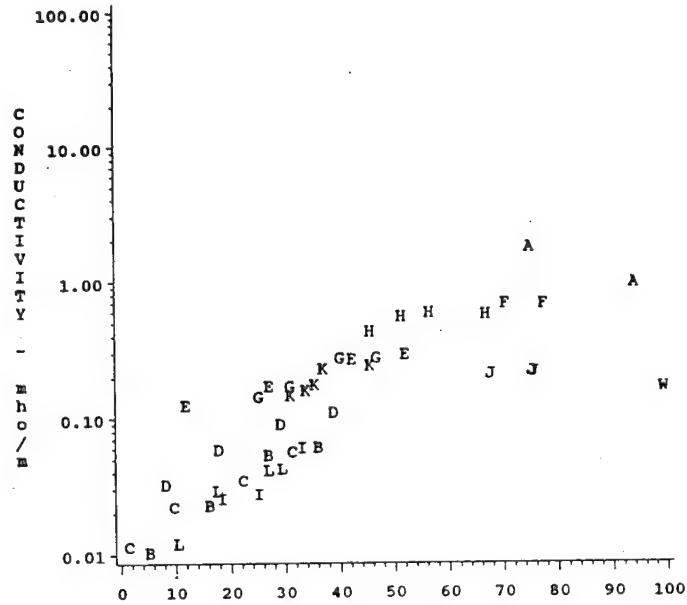
TMP=40



SOIL	A A A A	B B B B	C C C C	D D D D
	E E E E	F F F F	G G G G	H H H H
	I I I I	J J J J	K K K K	L L L L
	W W W WATER			

1.004 GHz

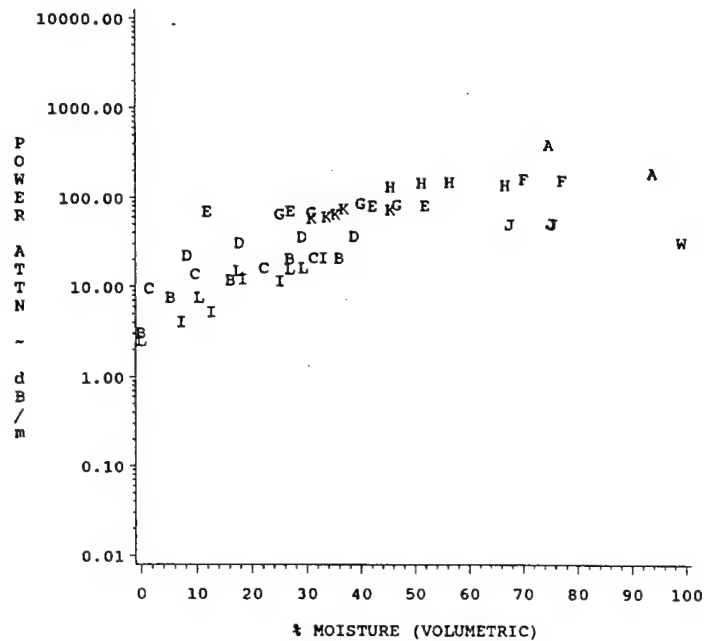
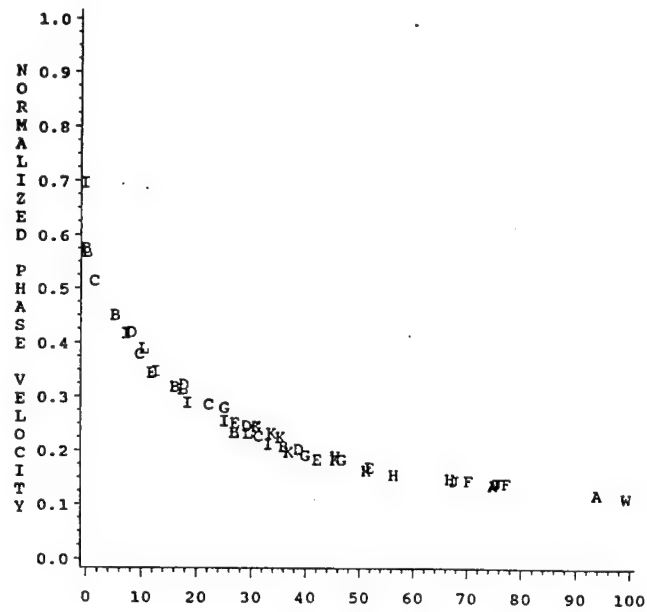
TMP=40



SOIL	A A A A	B B B B	C C C C	D D D D
	E E E E	F F F F	G G G G	H H H H
	I I I I	J J J J	K K K K	L L L L
	W W W WATER			

1.004 GHz

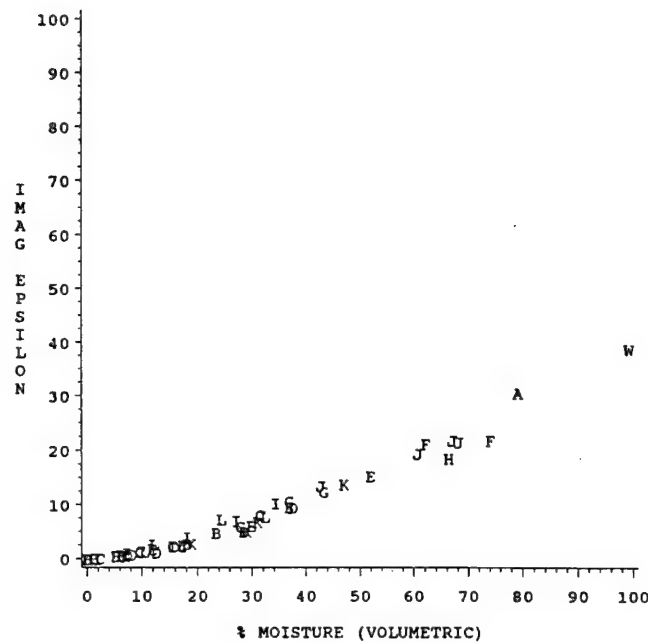
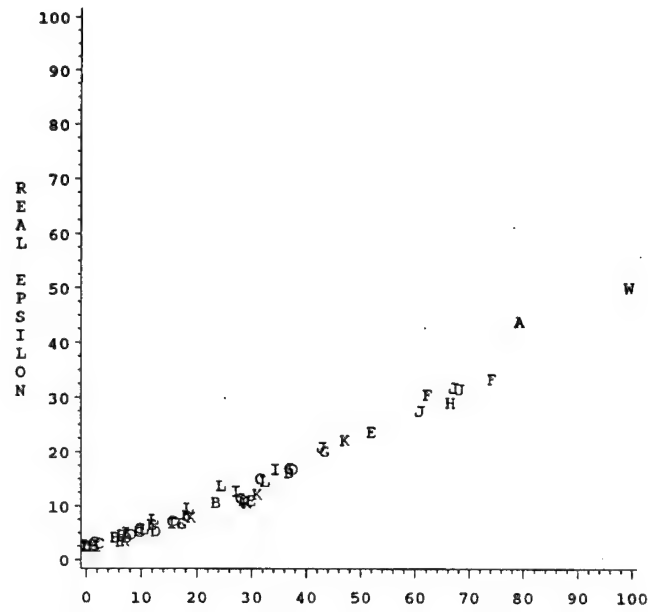
TMP=40



SOIL	A A A A	B B B B	C C C C	D D D D
	E E E E	F F F F	G G G G	H H H H
	I I I I	J J J J	K K K K	L L L L
	W W W WATER			

9.933 GHz

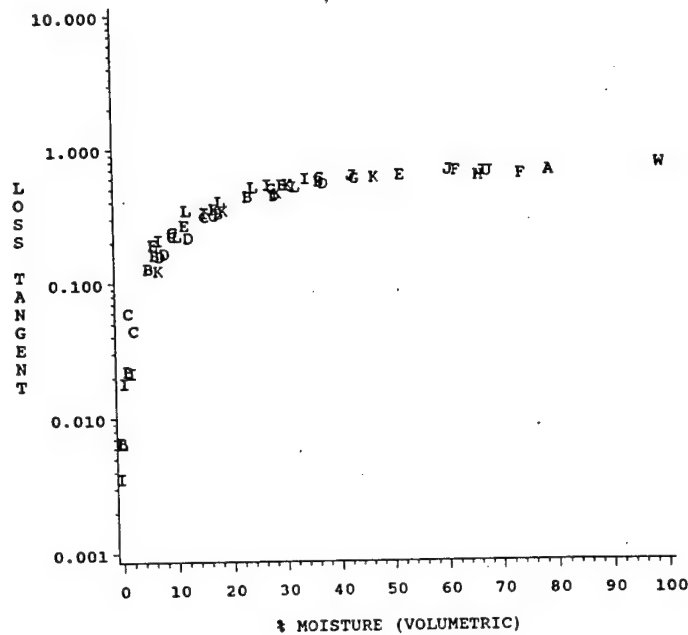
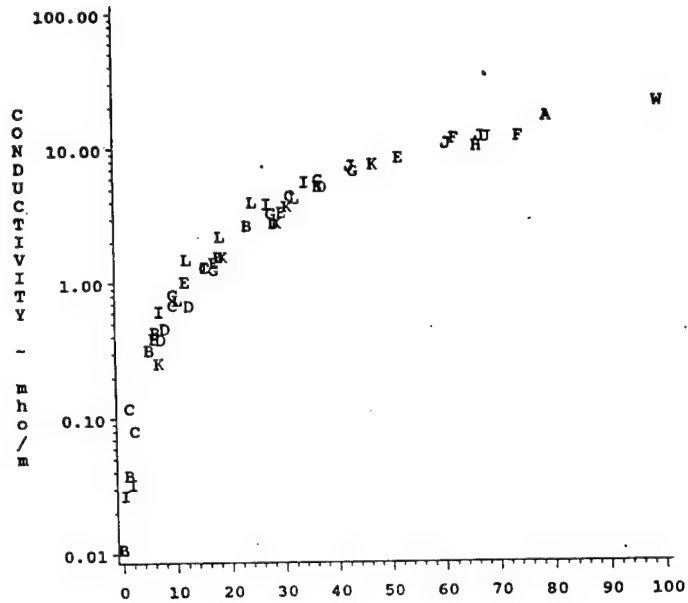
TMP=10



SOIL	A A A A	B B B B	C C C C	D D D D
	E E E E	F F F F	G G G G	H H H H
	I I I I	J J J J	K K K K	L L L L
	W W W WATER			

9.933 GHz

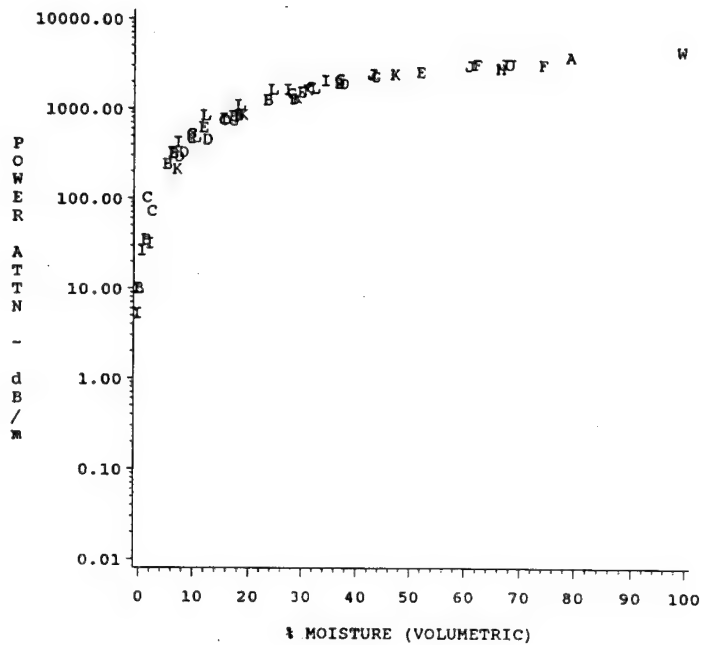
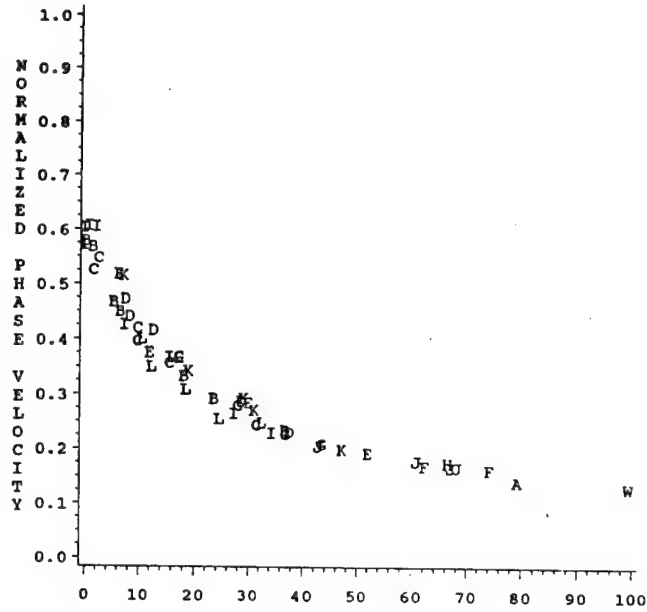
TMP=10



SOIL	A A A A	S S S S	C C C C	D D D D
	E E E E	F F F F	C C C C	H H H H
	I I I I	J J J J	K K K K	L L L L
	W W W	WATER		

9.933 GHz

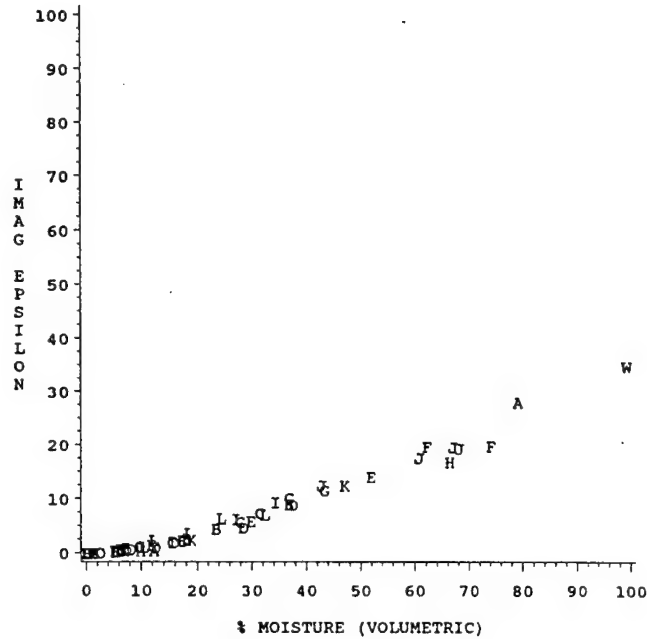
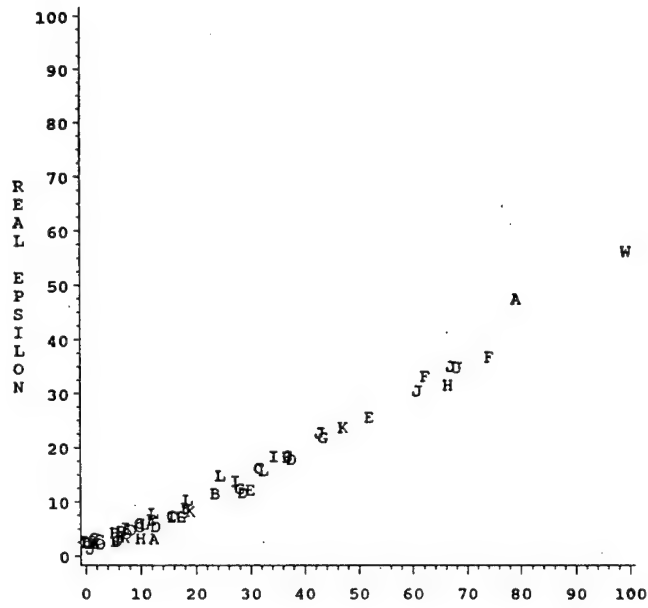
TMP=10



SOIL A A A A B B B B C C C C D D D D
 E E E E F F F F G G G G H H H H
 I I I I J J J J K K K K L L L L
 W W W WATER

9.933 GHz

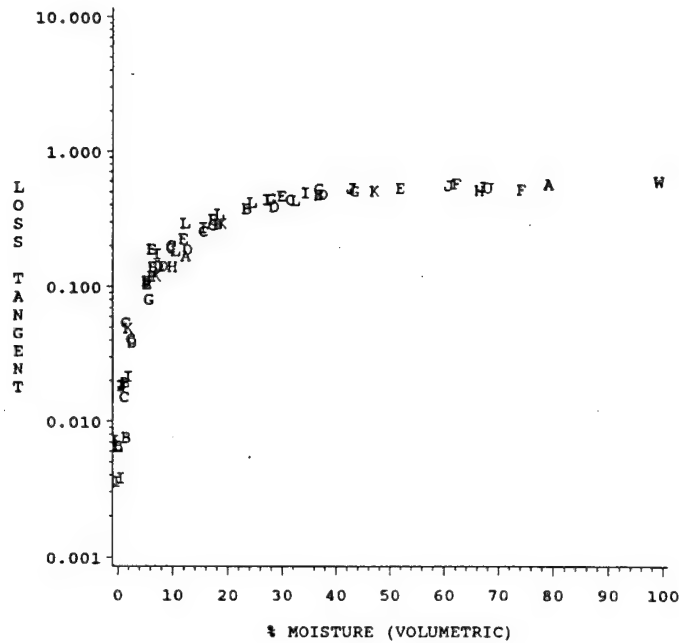
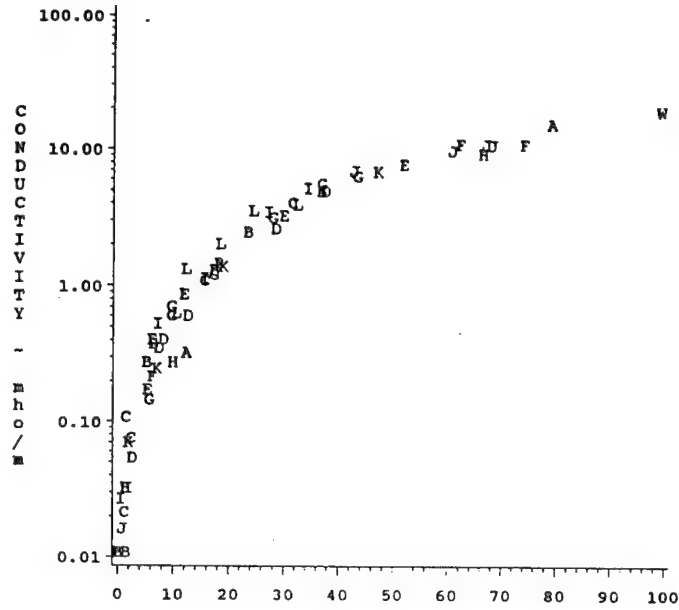
TMP=20



SOIL	A A A A	B B B B	C C C C	D D D D
	E E E E	F F F F	G G G G	H H H H
	I I I I	J J J J	K K K K	L L L L
	W W W WATER			

9.933 GHz

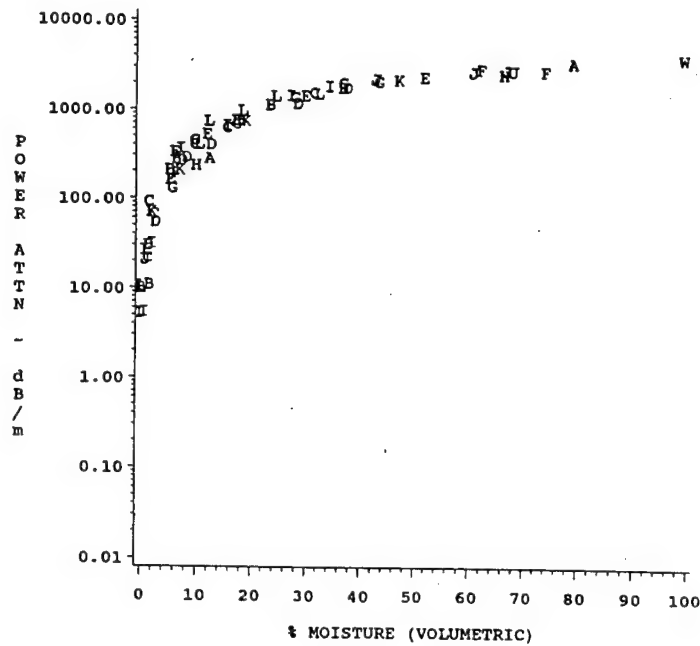
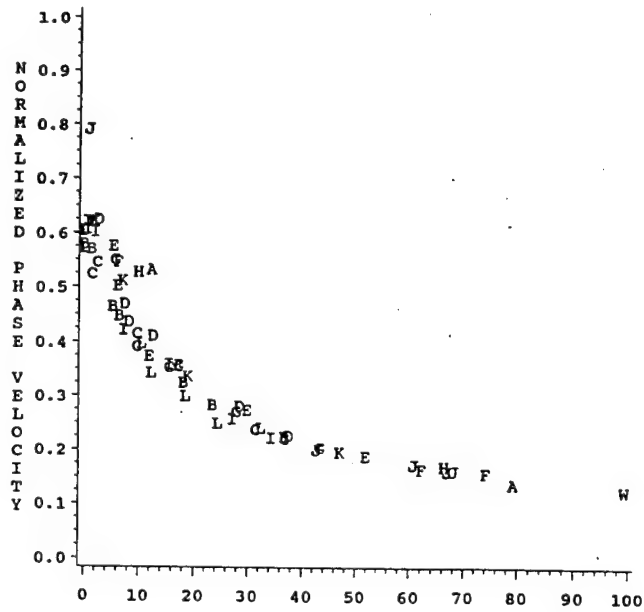
TMP=20



SOIL A A A A B B B B C C C C D D D D
 E E E E F F F F G G G G H H H H
 I I I I J J J J K K K K L L L L
 W W W WATER

9.933 GHz

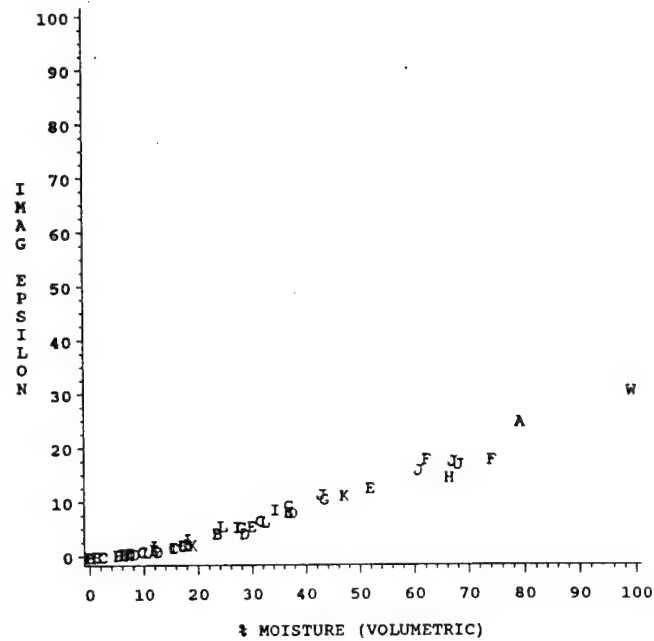
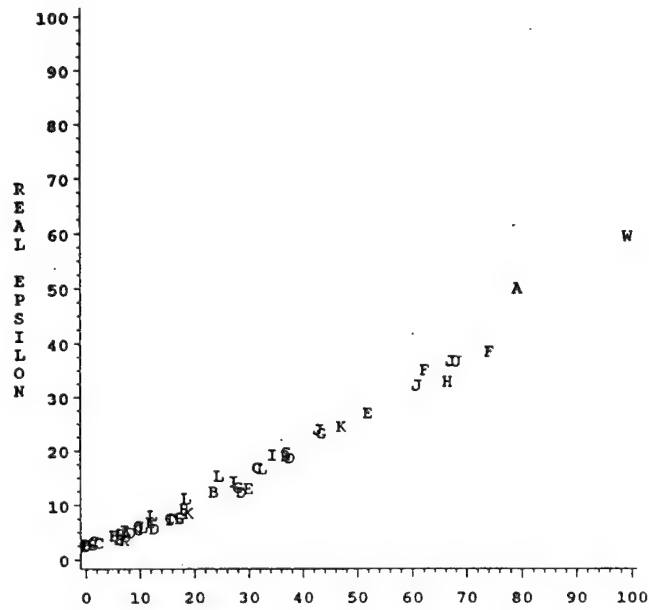
TMP=20



SOIL	A A A A	B B B B	C C C C	D D D D
	E E E E	F F F F	G G G G	H H H H
	I I I I	J J J J	K K K K	L L L L
	W W W WATER			

9.933 GHz

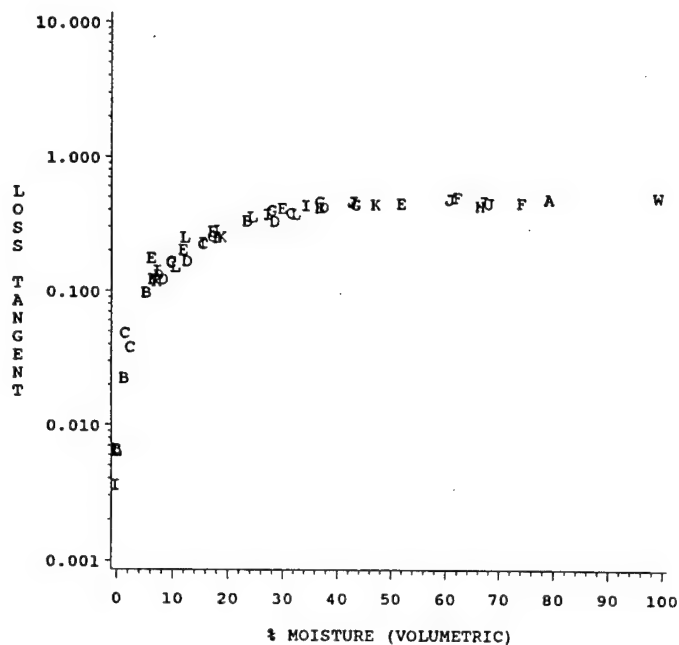
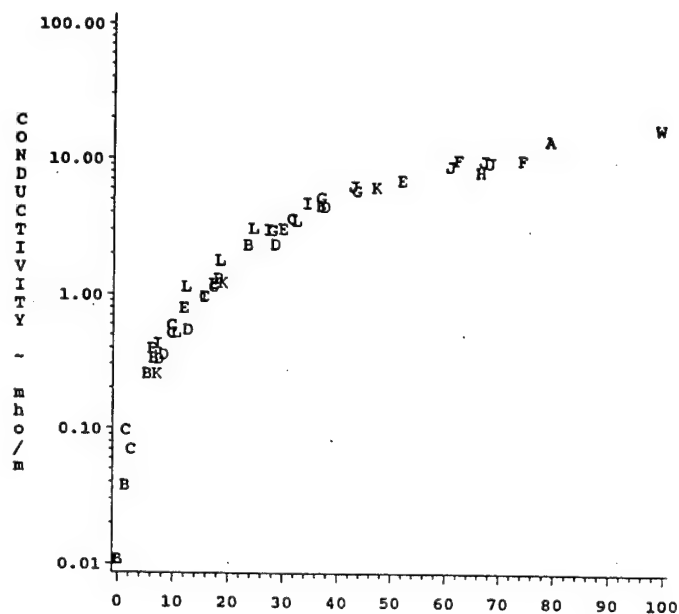
TMP=30



SOIL	A A A A	B B B B	C C C C	D D D D
	E E E E	F F F F	G G G G	H H H H
	I I I I	J J J J	K K K K	L L L L
	W W W WATER			

9.933 GHz

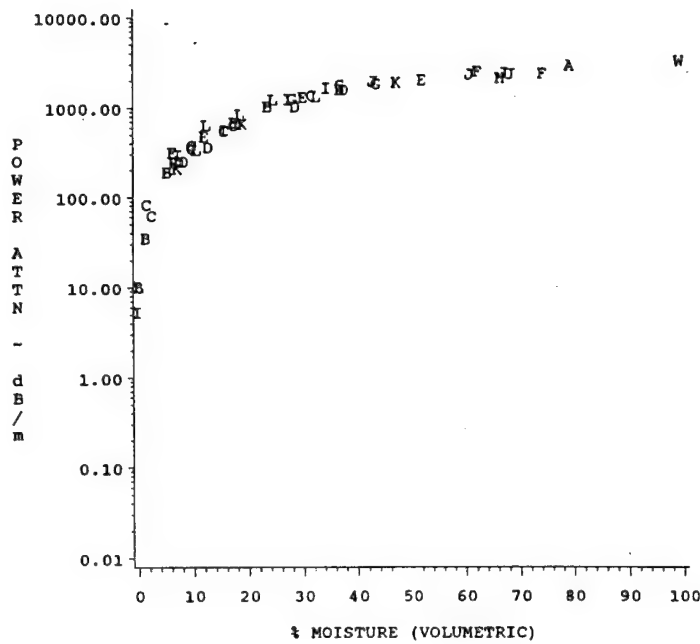
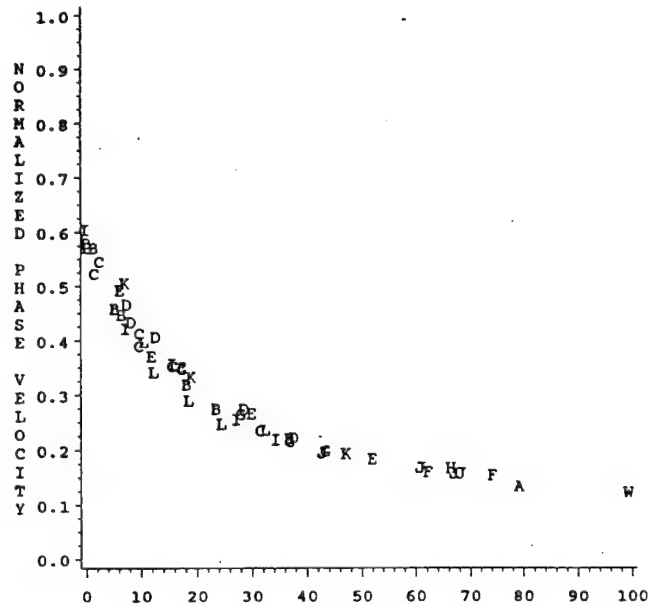
TMP=30



SOIL	A A A A	B B B B	C C C C	D D D D
	E E E E	F F F F	G G G G	H H H H
	I I I I	J J J J	K K K K	L L L L
	W W W	WATER		

9.933 GHz

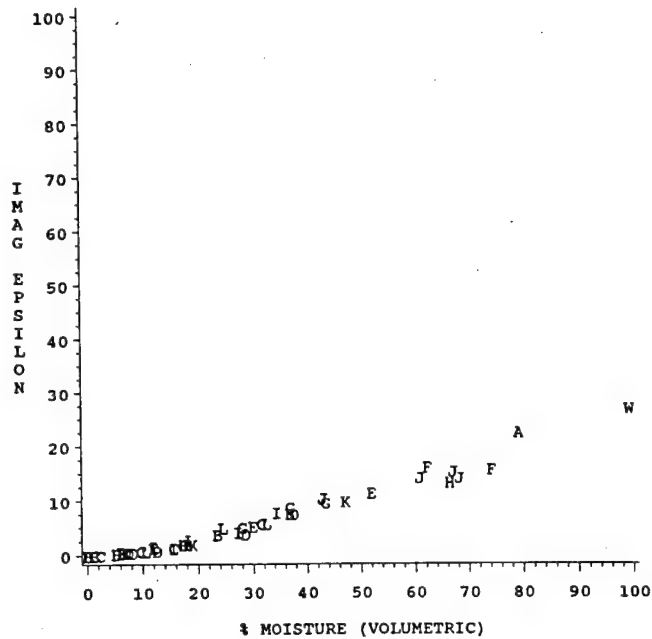
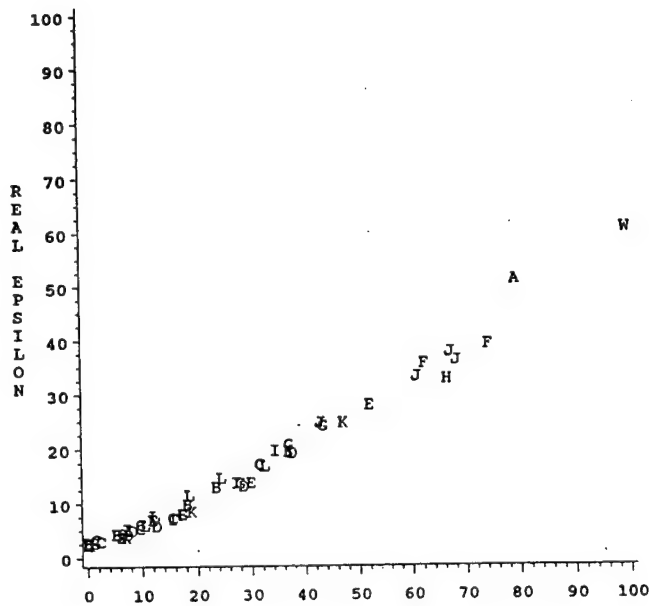
TMP=30



SOIL	A A A A	B B B B	C C C C	D D D D
	E E E E	F F F F	G G G G	H H H H
	I I I I	J J J J	K K K K	L L L L
	W W W	WATER		

9.933 GHz

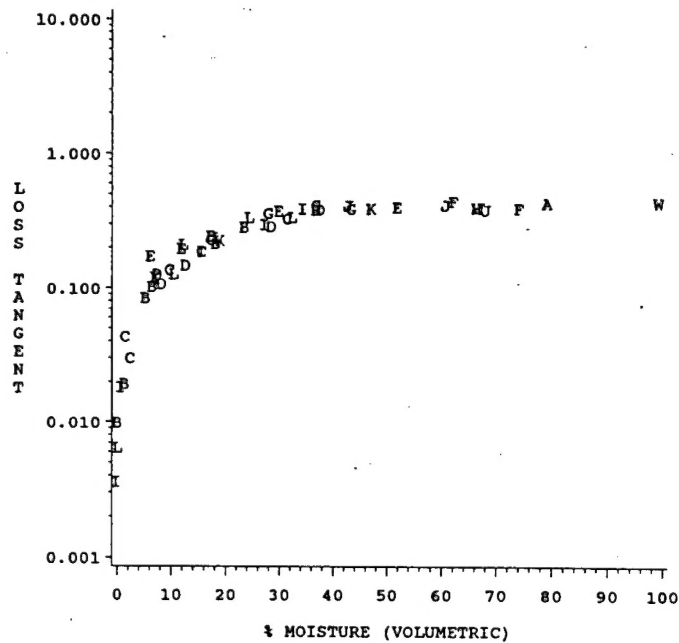
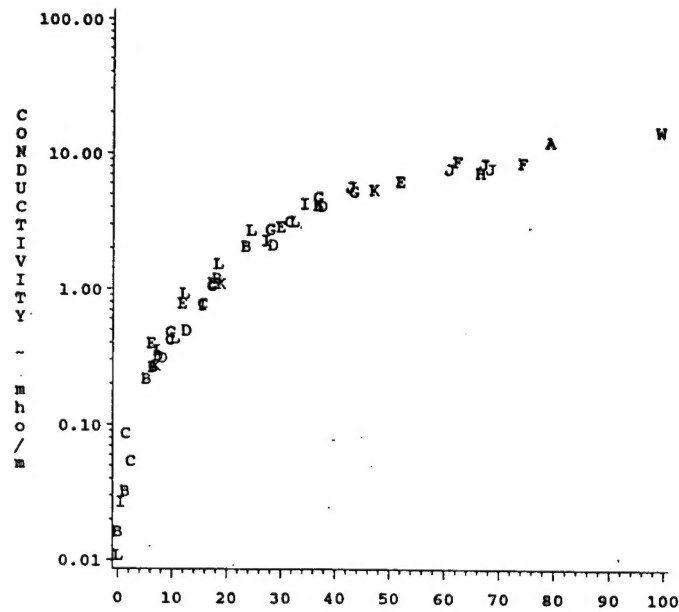
TMP=40



SOIL	A A A A	B B B B	C C C C	D D D D
	E E E E	F F F F	G G G G	H H H H
	I I I I	J J J J	K K K K	L L L L
	W W W WATER			

9.933 GHz

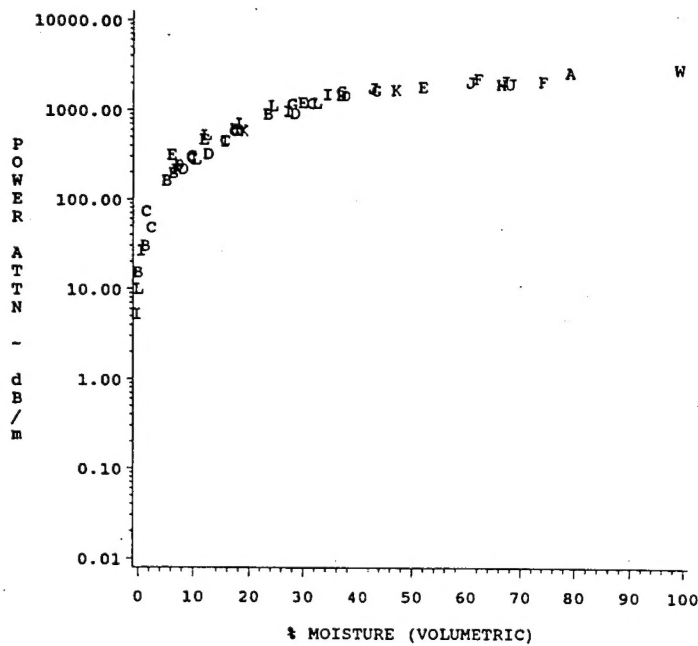
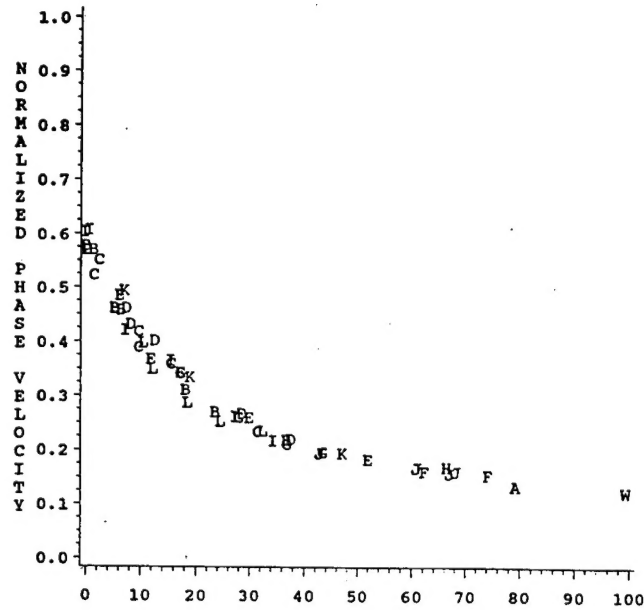
TMP=40



SOIL	A A A A	B B B B	C C C C	D D D D
	E E E E	F F F F	G G G G	H H H H
	I I I I	J J J J	K K K K	L L L L
	W W W WATER			

9.933 GHz

TMP=40



SOIL	A	A	A	A	B	B	B	B	C	C	C	C	D	D	D	D
	E	E	E	E	F	F	F	F	G	G	G	G	H	H	H	H
	I	I	I	I	J	J	J	J	K	K	K	K	L	L	L	L
	W	W	W	W	W	W	W	W	W	W	W	W	W	W	W	W

REPORT DOCUMENTATION PAGE			Form Approved OMB No. 0704-0188	
Public reporting burden for this collection of information is estimated to average 1 hour per response, including the time for reviewing instructions, searching existing data sources, gathering and maintaining the data needed, and completing and reviewing the collection of information. Send comments regarding this burden estimate or any other aspect of this collection of information, including suggestions for reducing this burden, to Washington Headquarters Services, Directorate for Information Operations and Reports, 1215 Jefferson Davis Highway, Suite 1204, Arlington, VA 22202-4302, and to the Office of Management and Budget, Paperwork Reduction Project (0704-0188), Washington, DC 20503.				
1. AGENCY USE ONLY (Leave blank)		2. REPORT DATE December 1995		3. REPORT TYPE AND DATES COVERED Final report
4. TITLE AND SUBTITLE Effect of Soil Composition on Complex Dielectric Properties			5. FUNDING NUMBERS	
6. AUTHOR(S) John O. Curtis, Charles A. Weiss, Jr., Joel B. Everett				
7. PERFORMING ORGANIZATION NAME(S) AND ADDRESS(ES) U.S. Army Engineer Waterways Experiment Station 3909 Halls Ferry Road Vicksburg, MS 39180-6199			8. PERFORMING ORGANIZATION REPORT NUMBER Technical Report EL-95-34	
9. SPONSORING/MONITORING AGENCY NAME(S) AND ADDRESS(ES) U.S. Army Corps of Engineers Research and Development Directorate Washington, DC 20314-1000			10. SPONSORING/MONITORING AGENCY REPORT NUMBER	
11. SUPPLEMENTARY NOTES Available from National Technical Information Service, 5285 Port Royal Road, Springfield, VA 22161.				
12a. DISTRIBUTION/AVAILABILITY STATEMENT Approved for public release; distribution is unlimited.			12b. DISTRIBUTION CODE	
13. ABSTRACT (Maximum 200 words) An industry-standard vector network analyzer system was used to measure the complex reflection and transmission coefficients of 12 different fine-grained soils over a frequency range of 45 MHz to 26.5 GHz. Measurement variables included sample temperature (10, 20, 30, and 40 °C), the amount of distilled, deionized water added to each soil sample, and the dry density of the soil in each sample holder (an uncontrolled parameter because of the sample preparation procedure). Data are presented both as a function of frequency at fixed temperatures and moisture content and as a function of moisture content at fixed temperatures and frequencies. Complex results are expressed in numerous ways, including the real and imaginary parts of the complex relative dielectric constant, loss tangent, electrical conductivity (through its relationship to the imaginary part of the dielectric constant), phase velocity normalized to the speed of light in a vacuum, and power attenuation in decibels/meter. Data support earlier models of a critical moisture content. Furthermore, for all but the very lowest frequencies, the data demonstrate that the permittivity of the soils, when considered as a function of volumetric moisture content, can be viewed as independent of soil type. Low-frequency losses in the soil/water/air mixtures are <div style="text-align: right;">(Continued)</div>				
14. SUBJECT TERMS Attenuation Conductivity Dielectric properties Soils			15. NUMBER OF PAGES 283 16. PRICE CODE	
17. SECURITY CLASSIFICATION OF REPORT UNCLASSIFIED	18. SECURITY CLASSIFICATION OF THIS PAGE UNCLASSIFIED	19. SECURITY CLASSIFICATION OF ABSTRACT	20. LIMITATION OF ABSTRACT	

13. (Concluded).

attributed to Maxwell-Wagner effects and ionic conductivity. Soils containing expandable clays demonstrate losses due to bound water of hydration. High-frequency losses are the result of free water molecular dipole relaxation.

While both bilinear and least-square polynomial fits to permittivity data for all soil types at selected frequencies are quite acceptable, exponential models do not fit the data well. Electrical analogue mixing models for predicting permittivity cannot be applied to the composite data and have limited applications to soils having neither salts nor expandable clay minerals.